Title

Site Characterization Plan Vol. I, part A, Chapter 1 & 2 (entire document) (DOE/RW-0199)

Author

DOE

101401

Document Date

12/30/88

ERC Index number

05.09.445

Document Type

Other Tech. Resource

Box Number

1720-1

Recipients

DOE & Participants

DOE/RW-0199 Vol 1

DOE/RW-0199 Vol 1

Nuclear Waste Policy Act
(Section 113)

Site Characterization Plan

Yucca Mountain Site, Nevada Research and Development Area, Nevada

Volume I, Part A

December 1988

Chapters 1 and 2

U. S. Department of Energy
Office of Civilian Radioactive Waste Management

DISCLAIMER

DOE/RW-0199

Nuclear Waste Policy Act
(Section 113)

Site Characterization Plan

Yucca Mountain Site, Nevada Research and Development Area, Nevada

Volume I, Part A

December 1988

Chapters 1 and 2

U. S. Department of Energy
Office of Civilian Radioactive Waste Management

FOREWORD

This site characterization plan (SCP) has been developed for the candidate repository site at Yucca Mountain in the State of Nevada. This site was one of three sites recommended by the Secretary of Energy and approved by the President, on May 27, 1986, for characterization under the provisions of the Nuclear Waste Policy Act (NWPA) of 1982. This site was subsequently designated by the Congress in the Nuclear Waste Policy Amendments Act (NWPAA) of 1987 as the only candidate site to be characterized at this time. This SCP has been developed to meet the requirements of Section 113(b)(1)(A)-(C) of the NWPA. It is being submitted to the U.S. Nuclear Regulatory Commission (NRC) and to the Governor and Legislature of the State of Nevada for review and comment, in accordance with Section 113(b)(1) of the NWPA as amended. The SCP is also being submitted to Clark, Lincoln, and Nye counties, which have been designated as affected units of local government, and is available to the public.

In accordance with the requirements of the NWPA and the regulations promulgated by the NRC in Title 10, Code of Federal Regulations, Part 60 (10 CFR Part 60), the SCP includes a description of the Yucca Mountain site (Chapters 1-5), a conceptual design for the repository (Chapter 6), a description of the packaging to be used for the waste to be emplaced in the repository (Chapter 7), and a description of the planned site characterization activities (Chapter 8). A consultation draft of the SCP (SCP/CD) was made available on January 8, 1988, in order to familiarize the NRC, the State of Nevada, and other interested parties with the contents of the document, and to promote interactions that would enhance the quality of the SCP that is now being issued. Comments received on the SCP/CD by the end of June 1988 have been considered in the preparation of this SCP. In addition, DOE, NRC, and State representatives participated in a number of technical meetings at which the major NRC concerns were discussed. The comments and the results of the meetings were reviewed and, where appropriate, an effort has been made to address these concerns in the SCP. Comments received subsequent to June 1988 and resulting in changes to site characterization will be addressed in semiannual progress reports.

The schedules and milestones presented in Sections 8.3 and 8.5 of the SCP were developed to be consistent with the June 1988 draft Amendment to the DOE's Mission Plan for the Civilian Radioactive Waste Management Program. The five month delay in the scheduled start of exploratory shaft construction that was announced recently is not reflected in these schedules. The DOE is currently evaluating the overall program schedule to determine what impacts this delay may have on the schedule for other program activities and milestones. Revisions to the overall program schedule and to the major program milestones will be addressed in the 1988 Mission Plan Amendment expected to be issued in the first quarter of calendar year 1989. Revisions to the schedules and milestones for site characterization activities will be provided in semiannual progress reports.

Consistent with the requirements of the NWPA, before proceeding to sink the exploratory shafts, the DOE will hold public hearings in the vicinity of the Yucca Mountain site to inform the residents of the plan and to receive their comments. These hearing are currently scheduled to be held during a

90-day comment period. In accordance with the requirements of *10 CFR Part 60*, the DOE will also defer sinking the exploratory shafts until there has been an opportunity to consider the NRC's comments on this activity. On the current schedule, the DOE will begin exploratory shaft construction in November 1989. Comments received on the SCP during the public comment period and subsequently from the NRC will be considered by the DOE in evaluating and revising its site characterization plans. Changes in the plans for site characterization activities will be noted in semiannual reports.

DOCUMENT ORGANIZATION

DOCUMENT ORGANIZATION (continued)

DOCUMENT ORGANIZATION (continued)

VOLUME IX

TABLE OF CONTENTS

Page

TABLE OF CONTENTS (continued)

TABLE OF CONTENTS (continued)

Page

TABLE OF CONTENTS (continued)

TABLE OF CONTENTS (continued)

TABLE OF CONTENTS (continued)

TABLE OF CONTENTS (continued)

TABLE OF CONTENTS (continued)

TABLE OF CONTENTS

VOLUME II

TABLE OF CONTENTS (continued)

TABLE OF CONTENTS (continued)

Page

TABLE OF CONTENTS (continued)

TABLE OF CONTENTS (continued)

TABLE OF CONTENTS (continued)

DECEMBER 1988

TABLE OF CONTENTS

VOLUME III

Page

TABLE OF CONTENTS (continued)

TABLE OF CONTENTS (continued)

TABLE OF CONTENTS (continued)

TABLE OF CONTENTS (continued)

Page

TABLE OF CONTENTS (continued)

TABLE OF CONTENTS (continued)

TABLE OF CONTENTS (continued)

TABLE OF CONTENTS

VOLUME IV

Page

TABLE OF CONTENTS (continued)

TABLE OF CONTENTS (continued)

TABLE OF CONTENTS (continued)

TABLE OF CONTENTS (continued)

TABLE OF CONTENTS (continued)

TABLE OF CONTENTS (continued)

TABLE OF CONTENTS (continued)

TABLE OF CONTENTS (continued)

TABLE OF CONTENTS

VOLUME V

TABLE OF CONTENTS (continued)

TABLE OF CONTENTS (continued)

TABLE OF CONTENTS (continued)

TABLE OF CONTENTS (continued)

TABLE OF CONTENTS (continued)

TABLE OF CONTENTS (continued)

TABLE OF CONTENTS (continued)

TABLE OF CONTENTS (continued)

TABLE OF CONTENTS (continued)

TABLE OF CONTENTS (continued)

TABLE OF CONTENTS (continued)

TABLE OF CONTENTS (continued)

TABLE OF CONTENTS (continued)

TABLE OF CONTENTS (continued)

TABLE OF CONTENTS (continued)

TABLE OF CONTENTS (continued)

TABLE OF CONTENTS (continued)

TABLE OF CONTENTS (continued)

TABLE OF CONTENTS (continued)

TABLE OF CONTENTS

VOLUME VI

TABLE OF CONTENTS (continued)

TABLE OF CONTENTS (continued)

TABLE OF CONTENTS (continued)

Page

TABLE OF CONTENTS (continued)

TABLE OF CONTENTS (continued)

TABLE OF CONTENTS (continued)

TABLE OF CONTENTS (continued)

TABLE OF CONTENTS (continued)

TABLE OF CONTENTS

VOLUME VII

TABLE OF CONTENTS (continued)

TABLE OF CONTENTS (continued)

TABLE OF CONTENTS (continued)

TABLE OF CONTENTS (continued)

TABLE OF CONTENTS (continued)

TABLE OF CONTENTS (continued)

TABLE OF CONTENTS (continued)

Page

TABLE OF CONTENTS (continued)

Page

TABLE OF CONTENTS (continued)

TABLE OF CONTENTS (continued)

TABLE OF CONTENTS (continued)

TABLE OF CONTENTS (continued)

TABLE OF CONTENTS (continued)

TABLE OF CONTENTS (continued)

TABLE OF CONTENTS (continued)

TABLE OF CONTENTS (continued)

TABLE OF CONTENTS

VOLUME VIII

Page

TABLE OF CONTENTS (continued)

TABLE OF CONTENTS (continued)

TABLE OF CONTENTS (continued)

TABLE OF CONTENTS (continued)

LIST OF FIGURES

VOLUME I

LIST OF FIGURES (continued)

LIST OF FIGURES (continued)

LIST OF FIGURES (continued)

LIST OF FIGURES (continued)

LIST OF FIGURES (continued)

LIST OF FIGURES (continued)

LIST OF FIGURES (continued)

LIST OF FIGURES (continued)

LIST OF FIGURES

VOLUME II

LIST OF FIGURES (continued)

LIST OF FIGURES (continued)

LIST OF FIGURES (continued)

LIST OF FIGURES (continued)

LIST OF FIGURES (continued)

LIST OF FIGURES (continued)

DECEMBER 1988

LIST OF FIGURES

VOLUME III

LIST OF FIGURES (continued)

LIST OF FIGURES (continued)

LIST OF FIGURES (continued)

LIST OF FIGURES (continued)

LIST OF FIGURES (continued)

LIST OF FIGURES (continued)

LIST OF FIGURES (continued)

LIST OF FIGURES (continued)

LIST OF FIGURES

VOLUME IV

LIST OF FIGURES (continued)

LIST OF FIGURES (continued)

LIST OF FIGURES (continued)

LIST OF FIGURES (continued)

DECEMBER 1988

[redacted]

LIST OF FIGURES

VOLUME V

LIST OF FIGURES (continued)

LIST OF FIGURES (continued)

LIST OF FIGURES (continued)

LIST OF FIGURES (continued)

LIST OF FIGURES

VOLUME VI

LIST OF FIGURES (continued)

LIST OF FIGURES (continued)

LIST OF FIGURES

VOLUME VII

LIST OF FIGURES (continued)

LIST OF FIGURES (continued)

LIST OF FIGURES (continued)

LIST OF FIGURES (continued)

LIST OF FIGURES

VOLUME VIII

LIST OF FIGURES (continued)

LIST OF FIGURES (continued)

LIST OF FIGURES (continued)

LIST OF FIGURES (continued)

LIST OF FIGURES (continued)

DECEMBER 1988

LIST OF TABLES

VOLUME I

LIST OF TABLES (continued)

LIST OF TABLES (continued)

LIST OF TABLES

VOLUME II

LIST OF TABLES (continued)

LIST OF TABLES (continued)

LIST OF TABLES (*continued*)

LIST OF TABLES (continued)

LIST OF TABLES

VOLUME III

LIST OF TABLES (continued)

LIST OF TABLES (continued)

LIST OF TABLES (continued)

LIST OF TABLES

VOLUME IV

LIST OF TABLES (continued)

LIST OF TABLES (continued)

LIST OF TABLES

VOLUME V

LIST OF TABLES (continued)

LIST OF TABLES (continued)

LIST OF TABLES (continued)

LIST OF TABLES (continued)

LIST OF TABLES (continued)

LIST OF TABLES

VOLUME VI

LIST OF TABLES (continued)

LIST OF TABLES (continued)

LIST OF TABLES (continued)

LIST OF TABLES (continued)

LIST OF TABLES (continued)

LIST OF TABLES

VOLUME VII

LIST OF TABLES (continued)

LIST OF TABLES (continued)

LIST OF TABLES (continued)

LIST OF TABLES (continued)

LIST OF TABLES (continued)

LIST OF TABLES (continued)

LIST OF TABLES (continued)

LIST OF TABLES (continued)

LIST OF TABLES (continued)

LIST OF TABLES

VOLUME VIII

LIST OF TABLES (continued)

LIST OF TABLES (continued)

DOE/RW-0199

Nuclear Waste Policy Act
(Section 113)

Site Characterization Plan

Yucca Mountain Site, Nevada Research and Development Area, Nevada

Volume I, Part A

Introduction

December 1988

U. S. Department of Energy
Office of Civilian Radioactive Waste Management

INTRODUCTION

The Nuclear Waste Policy Amendments Act of 1987 (the Amendments Act), which amended the Nuclear Waste Policy Act of 1982, has directed the U.S. Department of Energy (DOE) to characterize the Yucca Mountain site as a candidate site for the first geologic repository for radioactive waste. The characterization of a site is a program of studies directed at collecting the geologic information necessary to demonstrate the suitability of a site for development as a repository, to design the repository and the waste package, to prepare an environmental impact statement, and to obtain a construction authorization from the NRC. This program will be conducted in accordance with this site characterization plan (SCP), which has been prepared by the DOE in accordance with the requirements of Section 113(b)(1)(A) of the Nuclear Waste Policy Act, as amended. The purpose of the SCP is to summarize the information collected to date about the geologic conditions* at the site; to describe the conceptual designs for the repository and the waste package; and to present the plans for obtaining the geologic information necessary to demonstrate the suitability of the site for a repository, to design the repository and the waste package, to prepare an environmental impact statement, and to obtain from the U.S. Nuclear Regulatory Commission (NRC) an authorization to construct the repository.

This introduction begins with a brief section on the process for siting and developing a repository, followed by a discussion of the pertinent legislation and regulations. A description of site characterization is presented next; it describes the facilities to be constructed for the site characterization program and explains the principal activities to be conducted during the program. Finally, the purpose, content, organizing principles, and organization of this site characterization plan are outlined, and compliance with applicable regulations is discussed.

THE PROCESS OF REPOSITORY DEVELOPMENT

For the convenience of the reader, this section summarizes the process of repository siting, construction, operation, closure, and decommissioning. The discussion includes the types of waste to be received at the repository and the principal interactions with the NRC.

The siting of a repository

Yucca Mountain is one of three sites that had been selected for site characterization before the enactment of the Amendments Act. The other two sites were the Deaf Smith County site in Texas and the Hanford site in the state of Washington. These sites had been selected in a siting process that

---

*In this introduction, the term "geologic conditions" encompasses the geoengineering, hydrologic, geologic, geochemical, climatological, and meteorological conditions at the site, and the term "geologic information" is used in a general sense to refer to all the information that will be obtained from the site characterization program described in this plan.

had started in the late 1970s and culminated with the publication of environmental assessments that evaluated their suitability as potential sites for repositories. The Amendments Act directed the DOE to characterize only one of the sites--the Yucca Mountain site in Nevada--and to stop siting activities at the other two sites.

When site characterization has been completed, the DOE will determine whether the Yucca Mountain site is suitable for a repository. If the site is suitable, the Secretary of Energy will recommend to the President that the site be developed as a repository. This recommendation will be accompanied by an environmental impact statement prepared in accordance with the requirements of Section 114(f) of the Nuclear Waste Policy Act, the National Environmental Policy Act (NEPA), and DOE guidelines for NEPA implementation. If the President considers the site to be qualified for application for a construction authorization, the President will submit the recommendation to the Congress.

If the Yucca Mountain site is recommended to the Congress by the President, the State may submit, within 60 days, a notice of disapproval to the Congress. This disapproval prevents the use of the site for a repository unless the Congress passes a joint resolution of repository-siting approval within the next 90 days of continuous session. If no notice of disapproval is submitted or if a notice of disapproval is overturned by the joint resolution, then the site designation becomes effective. If the notice of disapproval is not overturned, then the disapproval stands, and the DOE will await further instructions from the Congress.

However, if the DOE determines at any time that the Yucca Mountain site is unsuitable for development as a repository, then the Secretary of Energy will terminate all site characterization activities at the site; notify the Congress, the Governor of Nevada, and the legislature of Nevada of the termination and the reasons therefore; and within 6 months, report to the Congress recommendations for further action to ensure permanent waste disposal, including the need for new legislative authority.

The Amendments Act also specifies that the State of Nevada is eligible to enter into a benefits agreement with the DOE, and this benefits agreement is to be negotiated in consultation with affected units of local government. If the benefits agreement is negotiated, the DOE will make payments to the State of Nevada in accordance with a specified schedule. However, the benefits must include the provision that the State of Nevada will waive its right to submit a notice of disapproval to the Congress.

In addition, the Amendments Act establishes the Office of the Nuclear Waste Negotiator, who is to attempt to find a State or Indian Tribe willing to host a repository at a technically qualified site on reasonable terms. The negotiator may seek to enter into negotiations with the State of Nevada.

The construction, operation, closure, and decommissioning of a repository

When the site designation becomes effective, the DOE will seek from the NRC authorization to construct the repository by submitting a license application. The Nuclear Waste Policy Act, as amended, requires that this license application be submitted not later than 90 days after the effective date of the site designation. The license application will contain a description of the site, a description of the design of the repository and the waste package, and an assessment of the performance of the entire mined geologic disposal system--that is, the site and the natural barriers at the site, the repository, and the waste package--with respect to applicable regulatory performance objectives. The NRC will review the application and decide whether to authorize the construction of the repository. When a construction authorization has been received from the NRC, the construction of the repository will begin.

When the repository is ready for operation, the DOE will submit an updated application to the NRC for a license to receive and possess radioactive material at the site. When this license has been received, the repository will begin to receive and emplace waste.

The Act specified that the waste accepted by the first repository cannot exceed the equivalent of 70,000 metric tons of heavy metal (MTHM) until a second repository becomes operational. Most of this waste (more than 60,000 MTHM) will consist of spent nuclear fuel from commercial power reactors. The remainder will consist of defense high-level waste and a small quantity of commercial high-level waste. Both the defense and the commercial high-level waste will be solidified into borosilicate glass before acceptance by the DOE.

After being filled to capacity, which is expected to take about 25 yr from the start of waste emplacement, the repository will be kept open for a period of time (up to 25 yr) in order to determine that the repository is performing as expected and the emplaced waste need not be retrieved. The DOE will then submit to the NRC an application for a license amendment that will allow it to permanently close the underground facilities of the repository and to decommission the surface facilities. When closure is completed, the DOE will apply for a license amendment to terminate the license.

REGULATIONS FOR GEOLOGIC DISPOSAL

As directed by the Nuclear Waste Policy Act, geologic repositories are subject to, and guided by, regulations promulgated by the U.S. Environmental Protection Agency (EPA), the NRC, and the DOE. More specifically, the scope and the content of the site characterization program are dictated by the information needed to demonstrate compliance with these regulations for site selection and licensing.

Primary standards and technical criteria

The primary standards for geologic repositories are concerned with protecting the health and safety of the public from the hazards of the waste to be emplaced in the repository; they have been promulgated by the EPA in 40 CFR Part 191. The key provisions of these standards are contained in Subpart B of 40 CFR 191. They specify (1) a limit on the amount of radioactivity that may enter the environment for 10,000 yr after disposal, (2) limits on

Subpart B of 40 CFR 191. Some of the plans described in this SCP were specifically designed to furnish data needed for demonstrating compliance with those standards as promulgated by the EPA in 1985. The basic information needed to demonstrate compliance with any disposal standards eventually promulgated by the EPA is expected to remain substantially the same, and therefore the approach to testing set forth in this SCP is expected to remain substantially the same. Nevertheless, any changes that may be made by the EPA to its standards will be evaluated by the DOE to ensure that the planned testing program will be adequate.

[redacted]

10 CFR Part 60. These regulations consist of (1) procedures for the licensing of geologic repositories and (2) technical criteria to be used in the evaluation of license applications under those procedural rules. The procedural portion of 10 CFR Part 60 provides specific requirements for a site characterization program and the associated site characterization plan. In addition to requiring that the EPA standards be met, the technical criteria of 10 CFR Part 60 provide a number of performance objectives. Among these requirements are the NRC radiation-protection standards contained in 10 CFR Part 20, design criteria for the surface and underground facilities of the repository, and three additional requirements: a minimum lifetime for the waste package, a limit on the release rate from the engineered barriers of the repository, and, for the natural system at the site, a minimum time of ground-water travel from the disturbed zone to the accessible environment.

<u>DOE siting guidelines</u>

As required by the Nuclear Waste Policy Act, the DOE has developed guidelines for nominating and recommending sites for characterization and selecting sites for the development of repositories. Promulgated as 10 CFR Part 960, they are referred to here as the "siting guidelines." The siting guidelines are based on both the EPA and the NRC regulations.

The siting guidelines are divided into implementation guidelines

The Nuclear Waste Policy Act defines site characterization as "activities, whether in the laboratory or in the field, undertaken to establish the geologic condition and the ranges of parameters of a candidate site relevant to the location of a repository, including borings, surface excavations, excavations of exploratory shafts, limited subsurface excavations and borings, and in situ testing needed to evaluate the suitability of a candidate site [redacted] geophysical testing needed to assess whether site characterization should be undertaken."

The activities planned for site characterization consist primarily of surface-based field studies, the construction of an exploratory shaft facility, and the tests conducted in that facility.

The field studies will be directed at obtaining information on the geologic, hydrologic, geochemical, climatologic, and engineering characteristics of the site and the surrounding area through exploratory drilling and testing, the testing of rock and water samples, geophysical surveys, and mapping.

To provide access for detailed study of the potential host rock as well as the overlying strata, the DOE will construct an exploratory shaft facility. The exploratory shaft facility will consist of (1) two exploratory shafts that will provide for access to the host rock, the transport of people and equipment, and ventilation; (2) underground testing areas; and (3) surface facilities needed to support construction and testing.

The exploratory shafts will be sunk to approximately the level where the underground facilities of a repository would be built. At this level they will be connected to one another and to underground testing areas. The shafts and the underground testing areas will be used to conduct tests and make observations and measurements of site conditions. The tests will be started during the construction of the exploratory shafts and will be continued in the exploratory shaft facility.

In conducting the site characterization program, care will be taken to reduce adverse environmental and socioeconomic impacts. As reported in the final environmental assessment (DOE, 1986b), no significant adverse impacts are expected to result from site characterization. Nonetheless, the DOE will monitor site characterization activities that might have significant environmental and socioeconomic impacts and, to the extent practicable, will impleand aquatic ecosystems, noise); archaeological, cultural, and historical resources; and the social and economic conditions in the area that could be affected by the repository. The environmental and socioeconomic studies to be conducted will be described in other planning documents.

THE SITE CHARACTERIZATION PLAN

Before beginning to sink the exploratory shafts, the DOE is required by the Nuclear Waste Policy Act (Section 113(b)(1)(A)) to prepare a site characterization plan (SCP). This plan is to be submitted to the NRC as well as the Governor and the legislature of the State of Nevada; it is also to be made available to the public. Furthermore, the DOE is required to hold public hearings in the vicinity of the Yucca Mountain site to inform the residents of the area about the SCP and to receive their comments.

Purpose and objectives

The basic purpose of the SCP is threefold:

1. To describe the site, the preliminary designs of a repository and a waste package appropriate to the site, and the waste-emplacement environment in sufficient detail that the basis for the planned site characterization program can be understood.

2. To identify the uncertainties and limitations on the site- and design-related information developed during site screening, to identify the issues to be resolved during site characterization and the information needed to resolve the issues, and to present the [illegible]

3. To describe general plans for the work, including performance confirmation, needed to (a) resolve outstanding issues and (b) reduce uncertainties in the data.

In this context, "issues" are defined as questions related to the performance of the geologic disposal system that must be resolved to demonstrate compliance with the applicable Federal regulations. The issues, which have been organized into a hierarchy, and the strategy for their resolution are discussed later in this section.

The SCP will provide the NRC, the State of Nevada, and the public with a vehicle for early input on the DOE's data-gathering and development work so as to avoid postponing issues to the point where modifications would entail major delays in, or disruptions of, the program. Early review of the plans presented in the SCP will provide an opportunity for the NRC to comment on strategy for resolving each issue. An understanding of these principles is helpful in following the discussions in the rest of this document; this section therefore discusses them briefly.

The issues hierarchy, which is described in more detail in a recent DOE report (DOE, 1986c), is a multitiered framework that lays out what must be known before a site can be selected and licensed. In providing this information, each tier contains progressively more detail than the tier above it. On the first, or highest, tier are the four "key issues." Stated as questions, they are derived from the system guidelines in the DOE siting guidelines; they therefore embody the principal requirements established by the regulations governing repositories. Affirmative answers to the key issues will be necessary if a site is to be selected and licensed.

Each of the key issues is followed, in the second tier, by two groups of issues related to performance and design. Also stated as questions, these issues expand on the requirement stated in the key issue they represent. When each group of issues was constructed, an effort was made to include in the group all the questions that must be answered to resolve the key issue.

The third tier consists of "information needs." Unlike the key issues and issues, the information needs are stated as requirements for technical information, rather than as questions. In constructing the information needs, the DOE attempted to list all the information necessary for resolving the issues. In principle, then, acquiring all the information called for at the third tier of the issues hierarchy will allow all the issues to be resolved through analyses and evaluations that use the information. If the issues are resolved affirmatively, the key issues will also have been resolved.

The issues hierarchy is useful in site characterization because it furnishes a framework for developing the test program and for explaining why the test program is adequate and necessary. In simple terms, the test program will be adequate if it adequately addresses all the information needs in the third tier of the issues hierarchy. And the necessity for any particular planned test can be established by determining its role in supplying an information need. For these reasons, the issues hierarchy is used as an organizing principle for Chapter 8 of this plan, which describes the site characterization program.

To use the issues hierarchy effectively, the DOE has adopted a formal strategy for resolving issues. This strategy, discussed in detail in Chapter 8, guides the development of specific plans for resolving each issue and provides the rationale for the associated site characterization activities.

The strategy begins with the identification of regulatory requirements, the development of the issues hierarchy from these requirements, and the preparation of a detailed description of the proposed geologic disposal system. The next part is a process called "performance allocation." It leads to detailed specifications of the information needed to resolve each issue and hence to plan for the investigations and studies that will produce the needed information. The issue resolution strategy then proceeds with the investigations and with analyses of their results until it is possible to show that the information needs have been satisfied. The collected information is used in a concluding set of analyses to resolve the issues, and the resolution is documented.

Scope

In accordance with Section 112(b)(2) of the Nuclear Waste Policy Act, scoping hearings were held in the State of Nevada in March 1983. The purpose of these hearings was to receive comments and recommendations with respect to the issues that should be addressed in the environmental assessment and the SCP.

The comments received from the public and the State were categorized in the report of the public hearings panel according to the document wherein the comments would be addressed. The comments from the public hearings were considered during the preparation of the SCP. The comments that are addressed in the SCP are tabulated in Section 8.2.1.2, Tables 8.2-3 and 8.2-4, and a correlation is provided to the appropriate SCP section where the technical concerns raised by the comments are addressed.

Regulatory requirements for the content of the SCP

The requirements of the Act. Section 113(b)(1)(A) of the Nuclear Waste Policy Act requires that the DOE prepare a general plan for site characterization activities. The plan is to include the following:

1. A description of the candidate site.

2. The extent of planned excavations during site characterization.

3. Plans for any onsite testing with radioactive or nonradioactive material.

4. Plans for any activities that may affect the capability of the candidate site to isolate the waste.

5. Plans to control any adverse, safety-related impacts from site characterization activities.

6. Plans for the decontamination and decommissioning of the candidate site and for the mitigation of any significant adverse environmental impacts caused by site characterization activities if the site is determined to be unsuitable for a repository.

7. Criteria to be used to determine the suitability of the candidate site for the location of a repository, developed pursuant to Section 112(a).

8. Any other information required by the NRC.

In addition, Section 113(b)(1)(B) requires a description of the waste package and relationship between the waste package and the site, and waste

[redacted]

below. Item 8 is included in the subsequent discussion of NRC requirements.

The extent of planned excavations (item 2 in the list above) is of interest for several reasons. First, some of the excavations at the site--that is, the exploratory shafts--will extend to the depth of the repository and, if not constructed properly, may adversely affect the waste-isolation potential of the site. Second, of the activities carried out during site characterization, the construction of shafts has the greatest potential for environmental impacts. In addition, the extent of planned excavations is related to the information about the host rock that can be collected in the exploratory shaft facility.

The use of radioactive materials (item 3) is of concern because of the [redacted] potential for releases to the environment. The DOE does not currently plan to use radioactive materials in site characterization except as follows. Some activities will use well-logging tools that contain radioactive materials and are commonly used in geologic and hydrologic exploration. After these tools have been removed, no radioactive material will be left behind at the site. The use of appropriate nonradioactive tracers will be evaluated during site characterization.

3. The description of plans for the use of radioactive materials is to include the use of radioactive tracers.

Regulatory Guide 4.17. To facilitate compliance with the requirements for the SCP, the NRC has prepared Regulatory Guide 4.17, Standard Format and Content of Site Characterization Plans for High-Level-Waste Geologic Repositories (NRC, 1987). The guide suggests the types of information to be provided in the SCP and establishes a uniform format for presenting the information. The DOE considered this guidance in developing the Annotated Outline for Site Characterization Plans (DOE, 1987), which has been reviewed by the NRC staff, who agreed that it was acceptable for the preparation of the SCP.

Organization of the site characterization plan and compliance with regulatory requirements

In preparing the SCP, the DOE made every effort to comply with the content requirements of the Nuclear Waste Policy Act and 10 CFR Part 60. The discussion that follows explains how the SCP is organized and how it meets the regulatory requirements discussed above. Table 1 presents the regulatory requirements and shows which sections of the SCP provide compliance with each particular requirement.

In preparing this SCP, the DOE has also made every effort to provide the detailed information that is identified in NRC Regulatory Guide 4.17 and that has been requested by NRC staff in a number of DOE-NRC meetings. As a result, this SCP provides considerably more information than the "general plan" required by the Act and by 10 CFR Part 60. The additional information has been provided to allow for a comprehensive review of DOE's site characterization program by the NRC, the State of Nevada, and the public.

The SCP is divided into two parts: Part A, which provides a description of the site, the waste package, and the design of the repository, and Part B, which presents the DOE's plans for the site characterization program.

Part A consists of an introduction and seven chapters. The introduction describes the geographic setting of the site and discusses sources of information and the history of site investigations. Chapters 1 through 5 discuss the available information about the site. Their objective is to comply with the requirements of Section 113(b)(1)(A)(i) and (v) of the Nuclear Waste Policy Act and 10 CFR 60.17(a)(1).*

In particular, Chapter 1 presents the data collected to date on the

Table 1. Compliance of the site characterization plan with regulatory requirements

Requirement	Section of the Act	Paragraph in 10 CFR 60	SCP chapter or section
1. Description of the candidate site	113(b)(1)(A)(i)	60.17(a)(1)	Chapters 1-5
2. Information on quality assurance programs that have been applied to the collection, recording, and retention of information used in preparing the description of the site	Not applicable	60.17(a)(1)	8.6.4.1
3. Description of site characterization activities, including--	113(b)(1)(A)(ii)	60.17(a)(2)	8.3, 8.4
3a. Description of the extent of planned excavations	113(b)(1)(A)(ii)	60.17(a)(2)(i)	8.4.2
3b. Plans for any onsite testing with radioactive material and nonradioactive material	113(b)(1)(A)(ii)	60.17(a)(2)(ii)	8.3.1.2.3[a]
3c. Plans for investigations that may affect the waste-isolation capability of the site	113(b)(1)(A)(ii)	60.17(a)(2)(iii)	8.4.2
3d. Plans to control adverse safety-related impacts	113(b)(1)(A)(ii)	60.17(a)(2)(iv)	8.4.2
3e. Plans to apply quality assurance to data collection, recording, and retention	Not applicable	60.17(a)(2)(v)	8.6.4.2

Table 1. Compliance of the site characterization plan with regulatory requirements (continued)

Requirement	Section of the Act	Paragraph in 10 CFR 60	SCP chapter or section
4. Plans for decontamination and decommissioning and the mitigation of significant adverse environmental impacts	113(b)(1)(A)(iii)	60.17(a)(3)	8.7
5. Criteria to be used to determine site suitability	113(b)(1)(A)(iv)	60.17(a)(4)	8.3.5.6, 8.3.5.7, 8.3.5.18
6. Description of the waste package and associated activities	113(b)(1)(B)	60.17(b)	Chapter 7, 8.3.4, 8.3.5
7. Conceptual repository design	113(b)(1)(C)	60.17(c)	Chapter 6, 8.3.2, 8.3.3

[a]No radioactive materials will be used in site characterization except as noted in the text. Nonradioactive materials are described in the referenced sections.

site characterization program presented in Part B. This summary, therefore, (1) summarizes the significant results, discussing, as appropriate, performance objectives, conceptual models and boundary conditions, and the quality of the data, including uncertainties; (2) describes how the data are related to the design of the repository and the waste package; and (3) identifies the information needs for the issues hierarchy (Part B). In addition, the summaries of Chapters 1 through 5 present a synopsis of the information that is requested by Regulatory Guide 4.17 but has not been shown to be relevant to the Yucca Mountain site. The uncertainties in the data presented in Chapters 1 through 5 were used in identifying the information needed to resolve the issues and in developing the plans presented in Part B.

The last two chapters in Part A are concerned with the conceptual design of the repository (Chapter 6) and the waste package (Chapter 7). Their objective is to comply with the requirements of Section 113(b)(1)(B) and (C) and 10 CFR 60.17(b). Each begins with an introduction that explains the purpose of the chapter, provides an overview of the current design concepts, and shows which SCP chapters contain the data on which the design is based and which chapters use or discuss the information presented in Chapter 6 or 7. Like the preceding chapters, Chapters 6 and 7 conclude with a summary section that links the design of the repository and the waste package, respectively, to the issues hierarchy and the site characterization program of Part B by providing a summary of design issues and related information needs. Chapter 6 presents the design basis for the repository, describes the conceptual design, discusses the information needed for the later phases of the design, and summarizes design issues. Chapter 7 describes what is currently known about the host rock in which the waste package will be emplaced, presents the design basis for the waste package, describes the current design and the alternatives that have been or are being considered, and discusses the status of research and development.

Part B, which consists of only one chapter (Chapter 8), describes the site characterization program. Its objective is to comply with the requirements of Sections 113(b)(1)(A)(ii), (iii), and (iv) of the Nuclear Waste Policy Act, Section 113 (b)(1)(B) of the Act, as well as 10 CFR 60.17(a)(2), (3), (4), and (5) and the quality assurance requirements of 10 CFR 60.17(a)(1) (see Table 1).

Part B begins with an introduction that provides an overview of the approach used in planning the site characterization program. The introduction is followed by the rationale for the site characterization program--namely, the issues hierarchy and the approach to issue resolution (Section 8.1). The next two sections are the most important components of Part B: Section 8.2 presents the site-specific issues hierarchy, whereas Section 8.3 presents the complete strategies for issue resolution and describes the investigations planned for the site; describes the design activities planned for the repository, the seals, and the waste-package programs; and describes the performance-assessment program. The purpose of the performance-assessment program is to determine whether the performance of the disposal system meets the requirements of the applicable Federal regulations. Section 8.4 presents the approach adopted by the DOE to guide the site characterization program, describes the characterization programs, and discusses the potential impacts of characterization activities on postclosure performance objectives. The remainder of Chapter 8 covers milestones, decision points, and schedules (Section 8.5); quality assurance (Section 8.6); and decontamination and decommissioning (Section 8.7).

Supporting documents

Numerous separate documents support the SCP by providing additional details concerning site data, design information, and plans for site characterization activities. The SCP, primarily in Chapters 1 through 7, presents relatively brief summaries of the data relevant to the site, much of which is obtained from organizational reports, professional papers, and other sources. Copies of the material that is summarized in Part A of the SCP will be made available in three locations. A full set of these references will be provided to the State of Nevada and to the NRC. The set of references will also be made available in the public reading room at the DOE Nevada Operations Office, located in Las Vegas, Nevada. One particular reference, the Site Characterization Plan-Conceptual Design Report (SCP-CDR) (SNL, 1987) merits specific discussion at this time. The Nuclear Waste Policy Act information on aspects of the design not strictly relevant to site characterization. This information is, however, of interest in understanding the functions of the repository. Copies of the complete SCP-CDR will be provided in the same manner as the other references.

Section 8.3.1 of Chapter 8 of the SCP describes the site investigations to be conducted to obtain site data. More-detailed descriptions of the individual studies comprising each investigation will be provided in study plans. Study plans will be made available to the NRC staff, and will typically reference more detailed technical procedures.

Periodic progress reports on site characterization

During site characterization at the Yucca Mountain site, the DOE will report not less than once every 6 months to the NRC as well as the Governor and the legislature of the State of Nevada on the nature and extent of such activities, the information developed from such activities, and the progress of waste-form and waste-package research and development. These reports will include the results of site characterization studies, the identification of new issues, plans for additional studies to resolve new issues, the elimination of planned studies no longer necessary, the identification of decision points reached, and modifications to schedules where appropriate. The reports will also describe progress in developing the repository design, noting when key design parameters or features that depend on the results of site characterization will be established.

DOE/RW-0199

Nuclear Waste Policy Act
(Section 113)

Site Characterization Plan

Yucca Mountain Site, Nevada Research and Development Area, Nevada

Volume I, Part A

Introduction References

December 1988

U. S. Department of Energy
Office of Civilian Radioactive Waste Management

REFERENCES FOR CHAPTER I

DOE (U.S. Department of Energy), 1986a. A Multiattribute Utility Analysis of [illegible] Repository--A Decision-Aiding Methodology, DOE/RW-0074, Washington, D.C.

DOE (U.S. Department of Energy), 1986b. Final Environmental Assessment: Yucca Mountain Site, Nevada Research and Development Area, Nevada, DOE/RW-0073, Washington, D.C.

DOE (U.S. Department of Energy), 1986c. Issues Hierarchy for a Mined Geologic Disposal System, OGR/B-10, OCRWM, Washington, D.C.

DOE (U.S. Department of Energy), 1987. Annotated Outline for Site Characterization Plans, DOE/RW-0142, Washington, D.C.

NRC (U.S. Nuclear Regulatory Commission), 1987. Standard Format and Content of Site Characterization Plans for High-Level-Waste Geological Repositories, Regulatory Guide 4.17, Washington, D.C.

SNL (Sandia National Laboratories), 1987. Site Characterization Plan Conceptual Design Report, SAND84-2641, 6 Vol., Sandia National Laboratories, Albuquerque, N. Mex.

CODES AND REGULATIONS

10 CFR Part 20 (Code of Federal Regulations), 1987. Title 10, "Energy," Part 20, "Standards for Protection Against Radiation," U.S. Government Printing Office, Washington, D.C., pp. 247-285.

DOE/RW-0199

DOE/RW-0199

Nuclear Waste Policy Act
(Section 113)

Site Characterization Plan

Yucca Mountain Site, Nevada Research
and Development Area, Nevada

Volume I, Part A

Part A, Mined Geologic Disposal System

December 1988

U. S. Department of Energy
Office of Civilian Radioactive Waste Management

INTRODUCTION

Part A of this site characterization plan (SCP) presents the research and exploration data compiled by the Yucca Mountain Project (formerly called the Nevada Nuclear Waste Storage Investigations Project) on the Yucca Mountain site during the site selection process. Conceptual designs for the proposed repository and waste package are also described. This information should be viewed as a preliminary step leading to, and providing a basis for, the site characterization investigations, studies, and design activities described in Part B. Performance assessment analyses discussed in Part B will determine whether a mined geologic disposal system can be constructed, operated, closed, and decommissioned to contain and isolate wastes without adverse effects to public health and safety.

Part A comprises seven chapters that provide information on the following topics:

1. Geologic, geomorphic, and geophysical characteristics of Yucca Mountain and the surrounding region.

2. Geomechanical and thermomechanical properties of the proposed host rock and its environment.

3. Hydrologic and hydrogeologic features of Yucca Mountain and the surrounding region.

4. Mineralogical, petrological, geochemical, and hydrochemical analyses of the Yucca Mountain area.

5. Present and past meteorological and climate data and analyses for the Yucca Mountain region.

6. Models and analyses used in previous and current site-investigation activities.

7. Preliminary conceptual repository and waste package designs appropriate for the present knowledge of the site.

Chapters 1 through 5 present the available data describing the physical characteristics of, and processes occurring at, the Yucca Mountain site and the surrounding region. Chapter 6 describes the preliminary conceptual design of the proposed repository, and Chapter 7 discusses investigations that have examined the expected waste-package environment and the proposed conceptual design for the waste package. The information in Part A is presented in sufficient detail to prepare the reader for the discussion of province (Figure A-1). The area is characterized by long, north to northwest-trending mountain ranges that are separated by intermontane sediment-filled structural basins. Yucca Mountain is an irregularly shaped

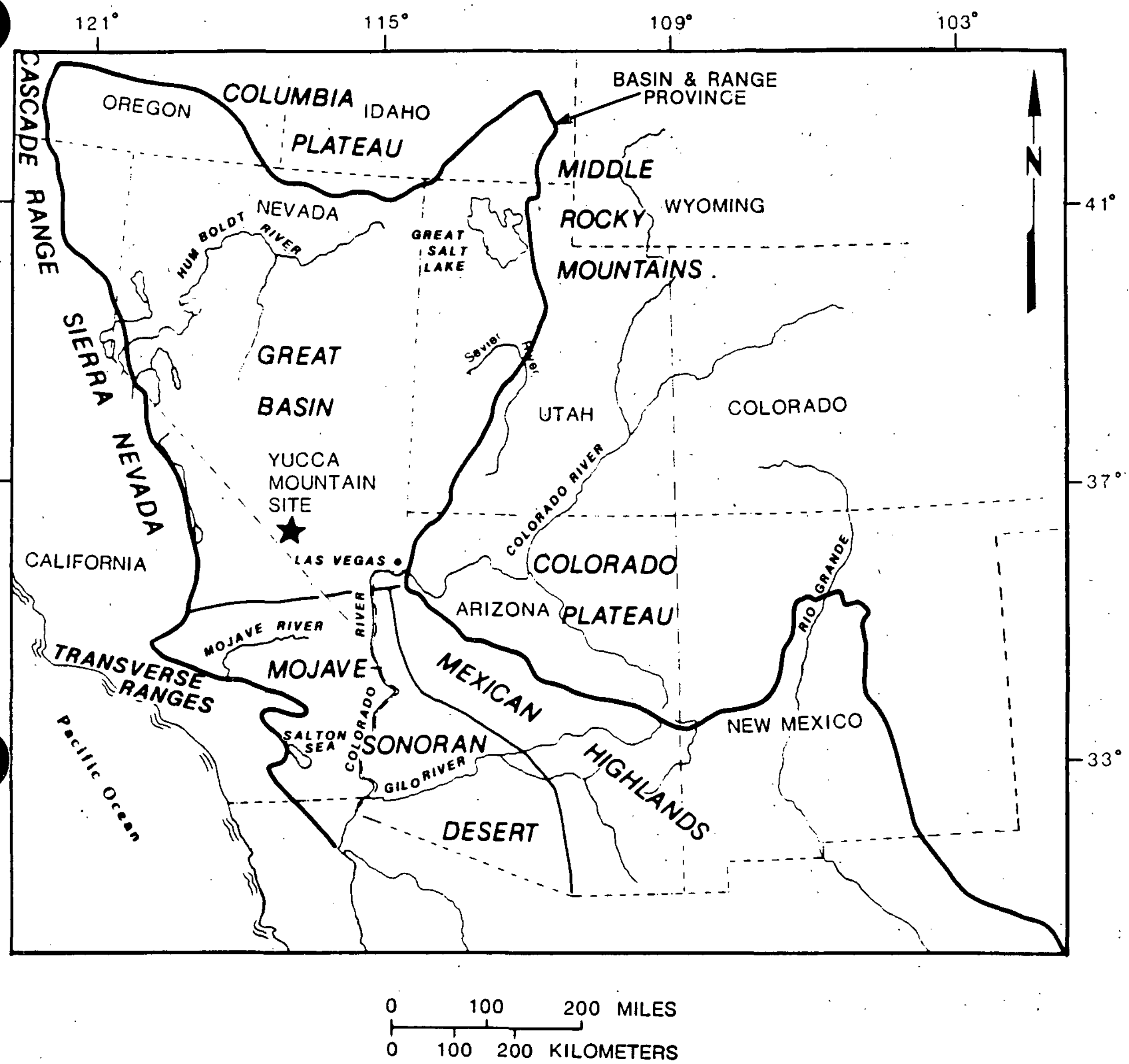

Figure A-1. Boundaries and larger subprovinces of the Basin and Range physiographic province (Hunt, 1974). Province boundary is indicated by heavy solid line. Salton Trough subprovince of southern California and Sacramento Mountains subprovince of central New Mexico are not shown.

DECEMBER 1988

The underground facility includes the underground structure, openings, and backfill materials, but excluding shafts, boreholes, and their seals.

The controlled area is a specific location, to be identified by passive institutional controls, that encompasses no more than 100 km^2 and extends no more than 5 km in any direction from the outer boundary of the original locations of the radioactive waste in a disposal system plus the subsurface underlying such a surface location. The term "site" is often used when referring to the controlled area, however, specific boundaries for the Yucca Mountain site have not been determined, and site boundaries shown on maps in this document should be considered preliminary and subject to change. The place, both at and below the surface, where the repository and ancillary facilities are constructed is called the repository site. This area includes the disturbed zone and the surrounding buffer zone, and has a surface area of several square kilometers. The atmosphere, the land surface, surface water, oceans, and all of the lithosphere that is beyond the controlled area is referred to as the accessible environment.

The candidate site is an area, within a geohydrologic setting, that is recommended for site characterization by the Secretary of Energy under Section 112 of the Nuclear Waste Policy Act of 1982, approved for characterization by the President under Section 112, or undergoing site characterization under Section 113 (NWPA, 1983). The hydrogeologic study area is delimited by the boundaries of the regional ground-water flow system that surrounds Yucca Mountain. The boundaries and subdivisions of this study area are shown in Figure A-3. The regional surface-water system that encompasses Yucca Mountain is called the hydrographic study area. Figure A-4 illustrates the boundaries of this study area.

SOURCES OF INFORMATION AND HISTORY OF SITE INVESTIGATIONS

Part A presents research and exploration data compiled during the site-selection process. The site-selection process is discussed in Chapter 2 of the Yucca Mountain environmental assessment (DOE, 1986). Part A contains information from research and exploration activities conducted directly by the Yucca Mountain Project, as well as data from other investigations of the characteristics of the Yucca Mountain region. The data and interpretations presented in Part A are available in separate program documents or data sets that have been released to the public.

Geologic investigations

During the past 80 years, the region surrounding Yucca Mountain has been the subject of numerous investigations. These studies have been conducted in support of mineral and energy resource exploration, nuclear-weapons testing, and other DOE activities at the Nevada Test Site. Studies of the Nevada Test Site region by the Yucca Mountain Project to aid the DOE in the site selec-

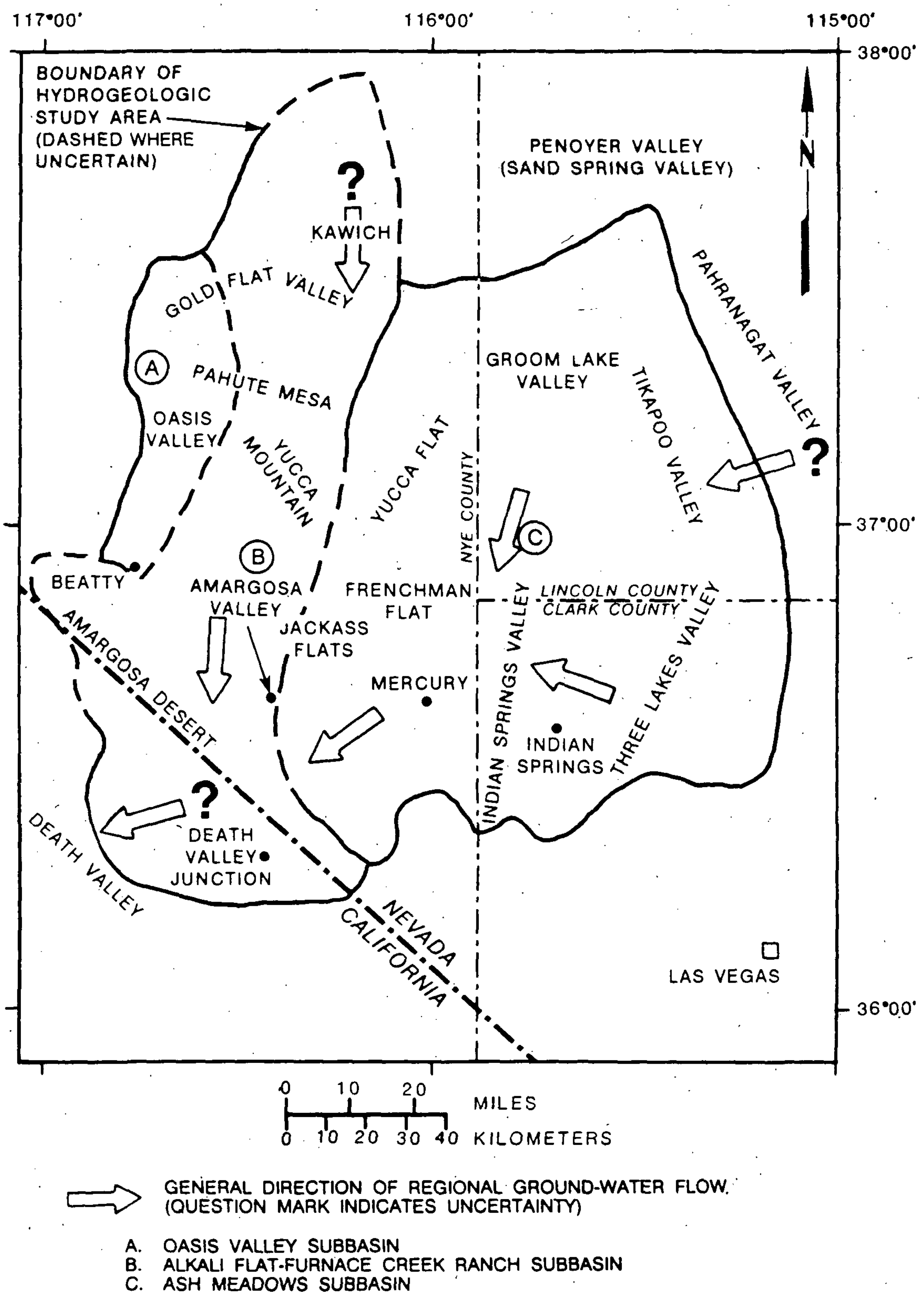

Figure A-3. Hydrogeologic study area, showing three ground-water subbasins. Modified from Rush (1970), Blankennagel and Weir (1973), Winograd and Thordarson (1975), Dudley and Larsen (1976), Waddell (1982), and Waddell et al. (1984).

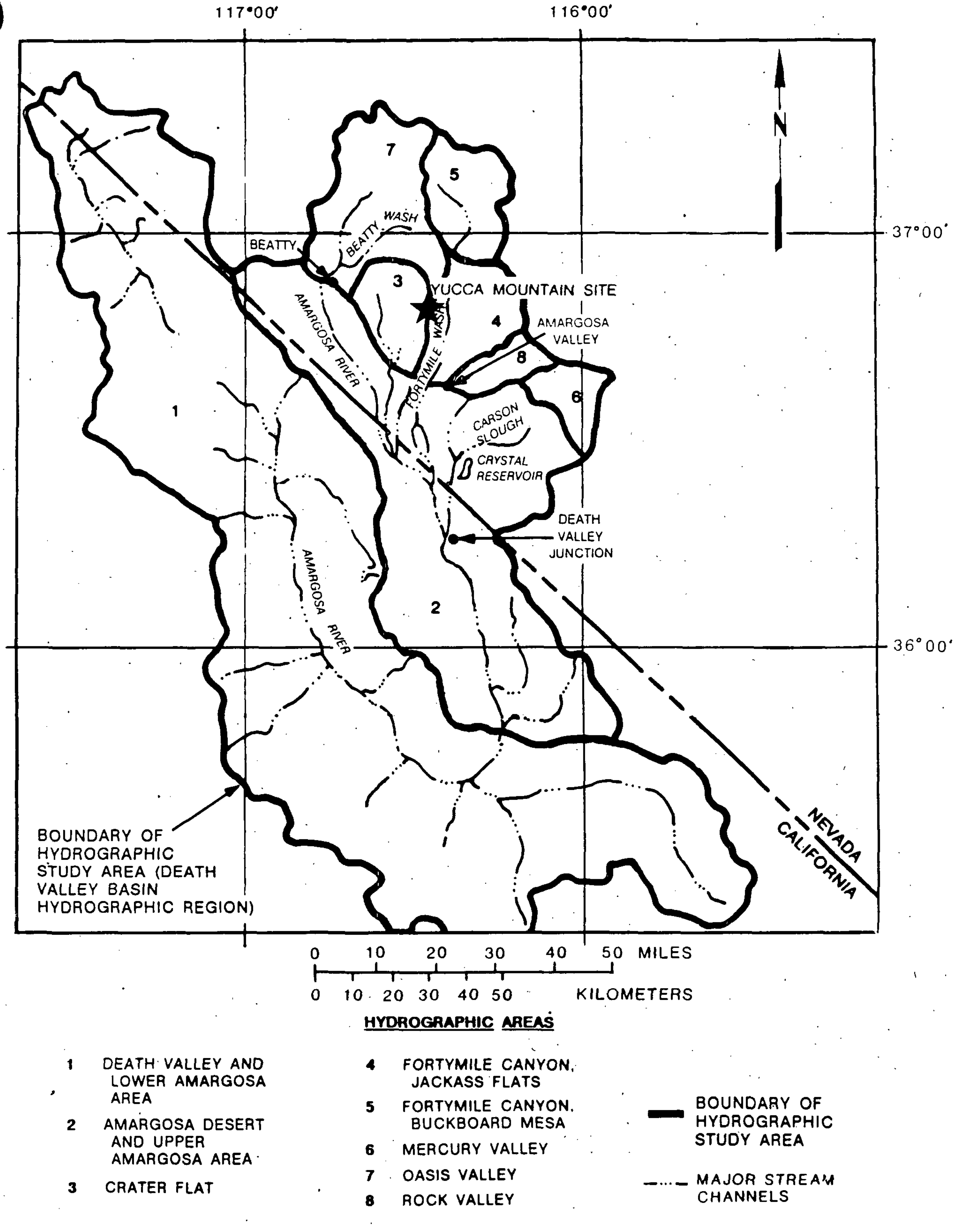

Figure A-4. Hydrographic study area, showing the eight hydrographic areas and major intermittent streams.

DECEMBER 1988

Geoengineering investigations

When the Yucca Mountain Project (formerly called Nevada Nuclear Waste Storage Investigations (NNWSI) Project) began, no site-specific samples were available for studying the effects of parameter variation on the mechanical properties of tuff. Laboratory data developed under the Yucca Mountain Project consist of test results on core samples from boreholes at Yucca Mountain, outcrops of the Topopah Spring Member (the proposed emplacement horizon), and an underground test facility in G-Tunnel at Rainier Mesa (Figure A-2) on the Nevada Test Site. The current data base was derived primarily from tests performed on relatively small-diameter core (approximately 6 cm). This data base consists of approximately 100 thermal-conductivity tests, 300 thermal-expansion tests, 75 mineralogical-petrological analyses, 700 bulk-property (porosity, density) measurements, and 350 mechanical-properties tests.

The field testing program in G-Tunnel has been a valuable part of the current design evaluation. The data and observations gathered from the Grouse Canyon Member of the Belted Range Tuff in G-Tunnel suggest this unit is a reasonable analog for the proposed emplacement horizon at Yucca Mountain in many aspects, including similar bulk, thermal, and mechanical properties; a similar degree and nature of fracturing; and a similar degree of saturation for geoengineering purposes; however, the hydrologic properties are substantially different. The overburden loading and openings dimensions are similar to those of the proposed repository.

Hydrologic investigations

Much of the preliminary data base is made up of regional hydrologic investigations performed since the 1960s for ground-water resource appraisals and evaluations of the hydrologic system at the Nevada Test Site done since saturation, potential, and flux in the rocks above, below, and within the proposed emplacement horizon.

Geochemical investigations

Geochemical information about the Nevada Test Site region has been collected for some time in support of the nuclear testing program. Much additional information has been collected since late 1977 for the Yucca Mountain Project. Information from sources other than the Yucca Mountain Project has been used primarily to aid interpretations or to confirm more recent data.

The geochemical data base compiled for the Yucca Mountain Project has been obtained from the examination of samples taken from the surface or at depth from Yucca Mountain and vicinity. Samples examined to determine mineralogy and petrology have come from drill cores, sidewall samples, drill cuttings, and surface outcrops. Ground-water samples have been taken from wells in the vicinity to characterize water chemistry. In addition to compiling a geochemical data base, laboratory experiments have been conducted to evaluate the stability of geochemical conditions and the effects of waste emplacement on geochemical conditions. Processes investigated include sorption, speciation, precipitation of waste elements, natural colloid formation, radiolysis, solubility, dissolution, diffusion, retardation, transport by both water and gas, hydrothermal alteration, and effects of the thermal pulse due to waste emplacement.

Climatological and meteorological investigations

Meteorological data have been collected in the Yucca Mountain region at Beatty since 1922 and at the town of Amargosa Valley since 1949. Meteorological data collection in support of the DOE activities at the Nevada Test Site has been ongoing since the late 1950s. Additional meteorological stations at different elevations near Yucca Mountain have been added since 1983 in support of the Yucca Mountain Project. Meteorological data that are currently being collected and calculated include wind speed and direction, standard deviation of wind direction, temperature and temperature difference due to elevation, net radiation, standard deviation of vertical wind speed, precipitation, relative humidity, and dew point.

Information regarding paleoclimatic conditions is required to evaluate the potential for future climate changes. Records of meteorological conditions for the Quaternary Period do not exist; however, climatological proxy data that give indications of the climatic conditions that existed in the Yucca Mountain region during the Quaternary have been collected and analyzed. These data include the analysis of packrat middens for information regarding past vegetation; the analyses of the chemistry, sediments, fossils, and fossil pollen from cores of lacustrine or paludal deposits; and the analysis of paleolake-level variations. These dated records can provide estimates of past climatic fluctuations and indications of potential future climatic changes can be obtained from these estimates.

DEFINITIONS OF DESIGN PHASES

The four design phases as used in this document have specific meanings. The conceptual design phase concentrates on the surface and underground system, structure, emplacement, and component designs that require site characterization data and provides the information to ensure that data-gathering plans related to design are adequately included in the SCP. Data-accuracy requirements are established and site-specific licensing issues related to site characterization are identified. This phase is called the SCP conceptual design in this report.

The advanced conceptual design phase presents the selected design alternatives and refines and fixes the design criteria and concepts to be made final in later design efforts. This design forms the basis for demonstrating project feasibility and estimating life-cycle costs. Preliminary drawings are prepared and a construction schedule developed as required by DOE Order 6410.1 (DOE, 1983).

The license application design presents the resolution of design and licensing issues identified and assessed in earlier design phases and develops the design of the items necessary to demonstrate compliance with the design requirements and performance objectives of 10 CFR Part 60.

The final procurement and construction design will develop the final (working) drawings and specifications for procurement and construction. The completion of this design phase will match the completion of the Title II design effort for the entire repository. This design phase will emphasize the completion of design and ancillary support items, final design refinement for the items necessary to demonstrate compliance with the design criteria and performance objectives of 10 CFR Part 60, the development of construction bid packages for all systems, and the development of final procurement and construction schedules.

SCOPE AND STATUS OF DESIGN WORK

As mentioned previously, Chapters 1 through 5 present the data and results of previous investigations and analyses concerning the geology, geoengineering, hydrology, geochemistry, and climatology and meteorology of the Yucca Mountain site. This information was instrumental in developing the conceptual designs for the repository and waste package discussed in Chapters 6 and 7. Studies discussed in Part B are planned to supplement and expand the current data base. As the data base is modified or expanded in the future, the conceptual designs found in Chapters 6 and 7 may be refined or changed after this report is released.

Site characteristics that have the principal effects on facility design are geology, geoengineering, hydrology, and geochemistry. Some information on meteorology was used in the siting of the surface facilities. The purpose of the conceptual design is to establish project feasibility, identify site characteristics that would be needed for future design efforts, and to obtain a preliminary cost estimate for facility construction and operation. The conceptual design is a preliminary design that serves as a basis for deciding whether to proceed to subsequent design phases and helps to guide the gathering of information for later design phases. Design concepts may be refined and design details will be provided in later phases of design.

The conceptual design phase produced a conceptual design report (SNL, 1987) that is summarized in this SCP. This design phase, concentrated on design features of the surface repository, underground repository, special waste-emplacement and retrieval equipment, waste-emplacement envelope, and waste package that require site characterization data. The conceptual design also provided input into the plans described in Part B to ensure that adequate information will be gathered to complete the remaining design phases. The conceptual designs described in Chapters 6 and 7 satisfy the requirements of the Nuclear Waste Policy Act of 1982, Section 113(b)(1)(C) (NWPA, 1983).

In establishing the basic characteristics and configurations of the repository engineered barriers, the conceptual design presented in Chapter 6 accomplished two purposes:

1. Delineation of those structures, systems, and components important to safety and isolation that are necessary to receive, process, transport, and permanently store radioactive waste in an underground facility.

2. Identification of needed information relative to both the design data base and the methods available for the engineering design of the repository.

Three overall capabilities must be considered in designing and operating the repository. The repository must be designed to safely emplace waste, retain the option to retrieve waste, and provide for the long-term containment and isolation of the waste.

Design elements of the repository shown in Figure A-5 include the following:

1. The main surface facilities that will be built on gently sloping terrain at the eastern base of Yucca Mountain. The surface facilities would be segregated into (a) the waste-receiving and inspection area, (b) the waste-operations area, and (c) the general support facilities area.

2. The shafts and ramps. Two exploratory shafts would initially be used for construction of the exploratory shaft facility. If the proposed repository is built, these shafts will be used as fresh air intakes, one for the waste emplacement area and one for the shops in the emplacement area and the decontamination area. Two 20-ft (6-m) diameter shafts would be constructed, one to provide access for men and materials and air intake for the development area and one to be the exhaust shaft for the emplacement area. Two ramps would be built: the waste ramp would allow transport of the waste packages to the underground facilities and the tuff ramp would be used for excavation of the underground facility and for removing excavated tuff.

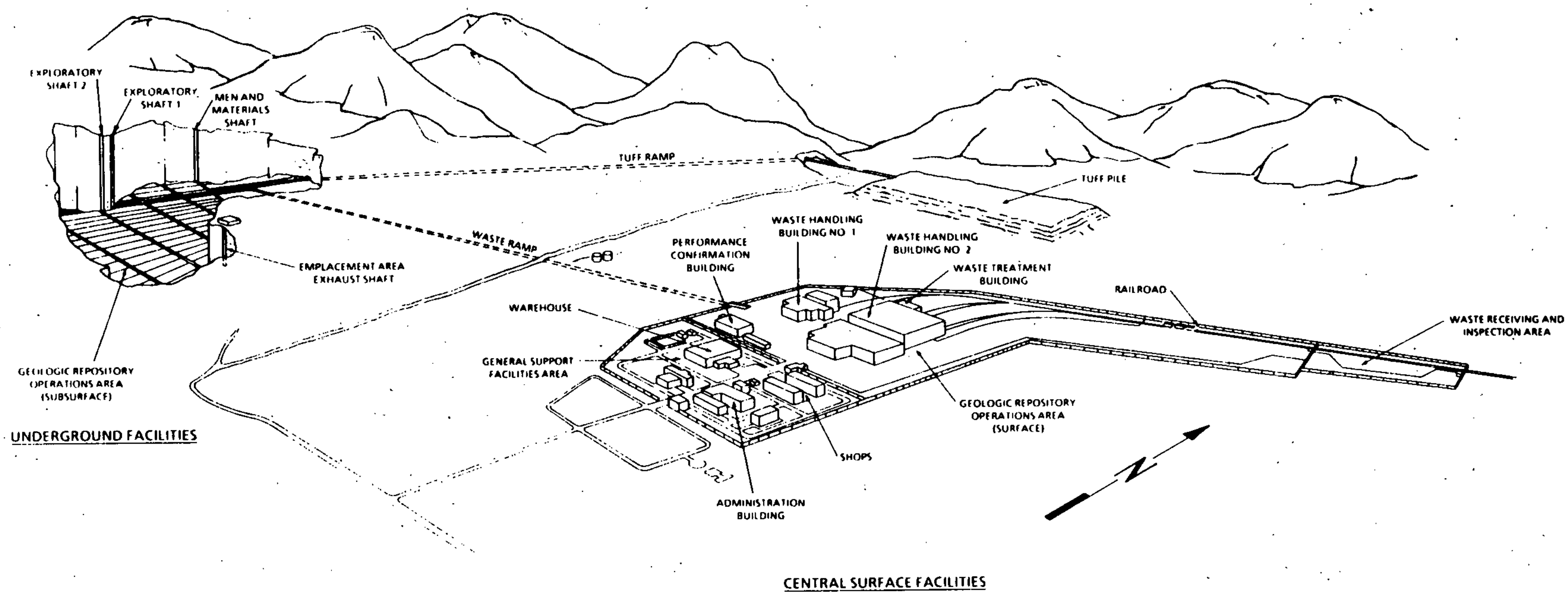

Figure A-5. Tuff repository perspective.

3. Underground facilities that will be located in the unsaturated zone in the Topopah Spring Member of the Paintbrush Tuff at least 657 ft (200 m) below ground level and will have an area of about 1,400 acres (570 hectares). Three parallel main entry drifts are planned to extend southwest through the underground facility to provide access to the emplacement panels during the development and emplacement phases. The 18 emplacement panels will be approximately rectangular and approximately 1,400 ft (430 m) wide, parallel to the main drifts, and 1,500 [illegible] with a midpanel drift to provide ventilation during development or retrieval.

Chapter 7 describes the conceptual design for the waste package. The purpose of the Yucca Mountain Project waste-package program is to develop a waste package for the disposal of spent fuel and high-level nuclear waste in a [illegible]

Design, analysis, fabrication, and prototype testing involves the development and testing of waste-package designs that are compatible with repository design.

Performance assessment involves development and validation of models for use in predicting waste-package performance. The development of advanced computer codes for modeling geochemical processes in the repository environment is a part of this activity.

SUMMARY

In addition to presenting the research and data gathered to date, Part A also briefly identifies information needed to satisfy regulatory guidelines or to fully characterize the site. The absence or sparseness of site-specific data in certain technical areas results in varying degrees of uncertainties on the current data base. Site characterization activities are planned to help decrease these uncertainties and to improve the data base for the resolution of issues. Part B presents the detailed identification of the needed information, deriving the needs from the regulatory requirements, which are embodied in a formal hierarchy of issues. Part B also discusses the currently planned studies, tests, analyses, and design work needed to characterize the site. Part A identifies the applicable sections in Part B that discuss the planned work.

DOE/RW-0199

Nuclear Waste Policy Act
(Section 113)

Site Characterization Plan

Yucca Mountain Site, Nevada Research and Development Area, Nevada

Volume I, Part A

Part A References

December 1988

U. S. Department of Energy
Office of Civilian Radioactive Waste Management

REFERENCES FOR CHAPTER A

Blankennagel, R. K., and J. E. Weir, Jr., 1973. Geohydrology of the Eastern Part of Pahute Mesa, Nevada Test Site, Nye County, Nevada, U.S. Geological Survey Professional Paper 712-B, U.S. Goverment Printing Office, Washington, D.C.

DOE (U.S. Department of Energy), 1983. "Management of Construction Projects," DOE Order 6410.1, Washington, D.C.

DOE (U.S. Department of Energy), 1986. Final Environmental Assessment: Yucca Mountain Site, Nevada Research and Development Area, Nevada, DOE/RW-0073, Washington, D.C.

Dudley, W. W., Jr., and J. D. Larson, 1976. Effect of Irrigation Pumping on Desert Pupfish Habitats in Ash Meadows, Nye County, Nevada, U.S. Geological Survey Professional Paper 927, U.S. Goverment Printing Office, Washington, D.C.

Hunt, C. B., 1974. Natural Regions of the United States and Canada, W. H. Freeman & Co., San Francisco, Calif.

NWPA (Nuclear Waste Policy Act), 1983. "Nuclear Waste Policy Act of 1982," Public Law 97-425, 42 USC 10101-10226, Washington, D.C.

Rush, F. E., 1970. Regional Ground-Water Systems in the Nevada Test Site Area, Nye, Lincoln, and Clark Counties, Nevada, Department of Conservation and Natural Resources, Water Resources Reconnaissance Series Report 54, State of Nevada, Carson City.

SNL (Sandia National Laboratories), 1987. Site Characterization Plan Conceptual Design Report, SAND84-2641, 6 Vol., Sandia National Laboratories, Albuquerque, N. Mex.

Waddell, R. K., 1982. Two-Dimensional, Steady-State Model of Ground-Water Flow, Nevada Test Site and Vicinity, Nevada-California, USGS-WRI-82-4085, Water-Resources Investigations Report, U.S. Geological Survey.

Waddell, R. K., J. H. Robison, and R. K. Blankennagel, 1984. Hydrology of Yucca Mountain and Vicinity, Nevada-California--Investigative Results Through Mid-1983, USGS-WRI-84-4267, Water-Resources Investigations Report, U.S. Geological Survey.

Winograd, I. J., and W. Thordarson, 1975. Hydrogeologic and Hydrochemical Framework, South-Central Great Basin, Nevada-California, with Special Reference to the Nevada Test Site, U.S. Geological Survey Professional Paper 712-C, U.S. Geological Survey, pp. C1-C126.

CODES AND REGULATIONS

10 CFR Part 60 (Code of Federal Regulations), 1987. Title 10, "Energy," Part 60, "Disposal of High-Level Radioactive Wastes in Geologic Repositories," U.S. Government Printing Office, Washington, D.C., pp. 627-658.

DOE/RW-0199

Nuclear Waste Policy Act
(Section 113)

Site Characterization Plan

Yucca Mountain Site, Nevada Research and Development Area, Nevada

Volume I, Part A

Chapter 1, Geology

December 1988

U. S. Department of Energy
Office of Civilian Radioactive Waste Management

Chapter 1

GEOLOGY

INTRODUCTION

Chapter 1 describes the geology of Yucca Mountain and the pertinent parts of the southern Great Basin in which the site is located. Figure 1-1 shows the location of the Yucca Mountain site in southwestern Nevada. The chapter provides a geologic basis for, and complement to, the discussions in the chapters that follow. Similarly, it provides a basis for the studies planned to characterize the candidate site and ultimately for the design of a waste container and repository that would comply with regulations. The emphasis in Chapter 1 is on the geologic characteristics that would affect the performance of the controlled area, as they are known from studies of the area immediately surrounding the proposed repository and from studies of the surrounding region. The chapter also emphasizes Quaternary geologic processes in the region surrounding Yucca Mountain, as a basis for anticipating future processes that would affect the controlled area during operation of the repository and during the subsequent isolation period.

In lieu of the term "candidate area," the word "region" has generally been used. For most of the discussion in Chapter 1, a geologically meaningful region has proved to be the southern Great Basin. But the specific region considered varies by topic. For each topic discussed in Chapter 1, the largest region in which specific geologic patterns consistently represent the patterns in the prospective controlled area have been considered. The intent of this approach was to include all relevant information, thereby allowing for the greatest possible confidence in the interpretations of the geologic characteristics of the controlled area and of the processes that have affected the region in the geologically recent past and, thus, are likely to affect the controlled area during the 10,000-yr isolation period.

SOURCES OF INFORMATION IN CHAPTER 1

The information in this chapter is drawn from the literature (references are listed at the end of the chapter). The information comes from field and laboratory studies of Yucca Mountain and the surrounding region, notably, studies done since the late 1970s in anticipation of possible site characterization. Additional geologic information has been collected in studies that are in progress, or that have been completed, but have not yet been published. Because such unpublished information is not available for review, it is not discussed in this chapter. It is, however, one of the bases for the further studies planned for site characterization (Section 8.3.1).

Geologic studies in the Yucca Mountain area date back to 1907. Early work is summarized by Eckel (1968); more recent work by Sinnock (1982) and the U.S. Geological Survey (USGS, 1984). Bibliographies of reports providing geologic data on the Yucca Mountain area have been prepared by the U.S. Department of Energy (DOE, 1986) and Glanzman (1979, 1980, 1981, 1983, 1984, 1985). Concentrated research in the area began in the late 1950s, in

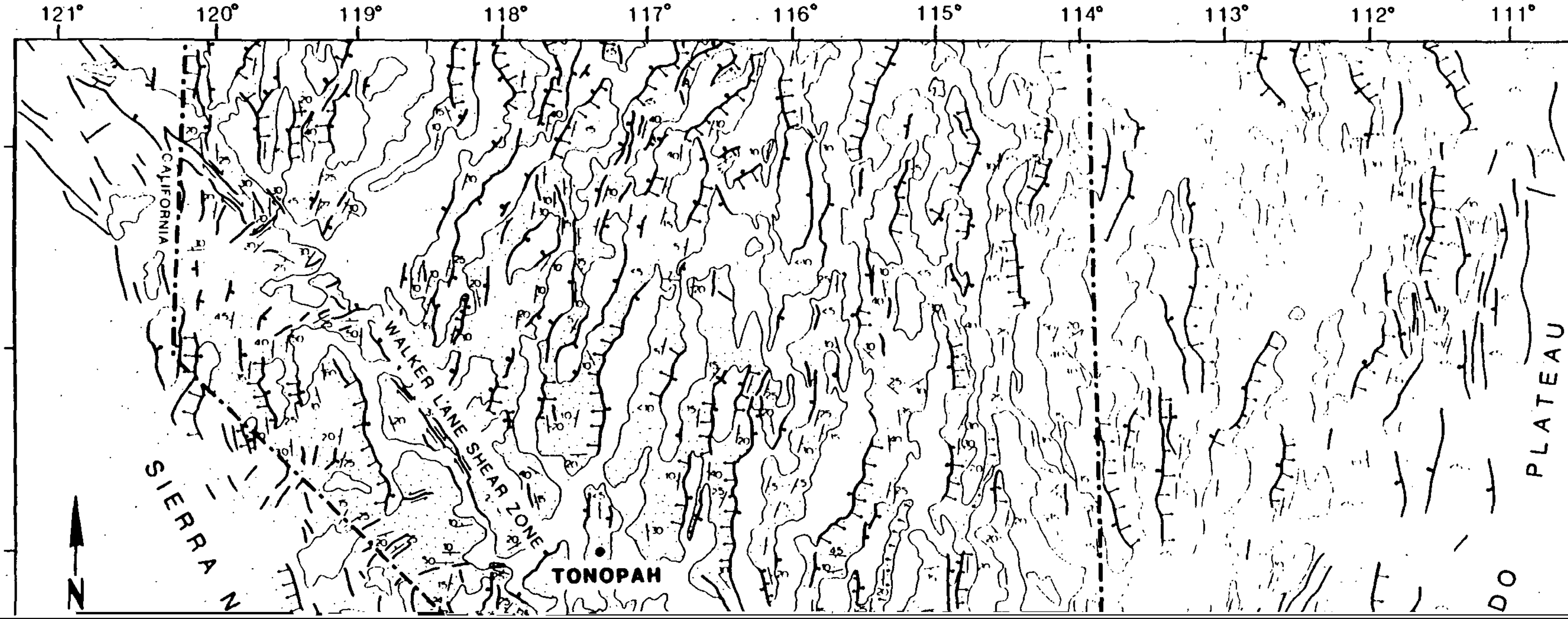
121°
120°
119°
118°
117°
116°
115°
114°
113°
112°
111°
40°
39°
38°
CALIFORNIA
WALKER LANE SHEAR ZONE
TONOPAH
SIERRA N
PLATEAU
DO
N

connection with underground testing of nuclear weapons at the Nevada Test Site (NTS), adjacent to Yucca Mountain. Geologic mapping at 1:24,000-scale of the test site and of Yucca Mountain itself was largely completed during the 1960s. Many detailed studies concerned with nuclear testing also have been completed.

Since late 1977, Yucca Mountain has been studied as a potential site for a geologic repository (DOE, 1986). Subsurface exploration, begun in late 1978, has demonstrated the presence of a sequence of ash-flow tuff units more than 1,000 m thick. Since 1978, 182 holes (approximately 40 of which are more than 100 m deep) have been drilled and 23 trenches excavated within 10 km of the repository boundary. In 1978 and 1979, 47 seismic stations were installed within 160 km of the proposed repository, and in 1981 six additional stations were installed at Yucca Mountain. Geologic mapping has been supplemented by trenching, drilling, analysis of remote-sensing imagery, electrical resistivity studies, low-altitude aeromagnetic studies, and seismic refraction and reflection studies. These studies have aided in the location of concealed faults, the assessment of fault and fracture patterns, and the mapping and interpretation of the rocks beneath the volcanic sequence at Yucca Mountain.

The geology of Nevada was summarized by Stewart (1980a), and the stratigraphy, structure, and mineral deposits of the area around Yucca Mountain (southern Nye County) by Cornwall (1972). The geology of the region surrounding Yucca Mountain is shown on the 1:500,000-scale geologic map of Nevada (Stewart and Carlson, 1978) and on the 1:750,000-scale geologic map of California (Jennings, 1977). An index to more detailed geologic mapping in the region was compiled by Fouty (1984). A 1:1,000,000-scale aeromagnetic map of Nevada was compiled by Zietz et al. (1978). Isostatic residual gravity data for the region are shown at 1:500,000 scale in USGS (1984).

A 1:48,000-scale geologic map (USGS, 1984) shows the local geologic setting of Yucca Mountain. A 1:48,000-scale aeromagnetic map also is available for Yucca Mountain and the surrounding area (Kane and Bracken, 1983). A 1:24,000-scale geologic map (Lipman and McKay, 1965) encompasses Yucca Mountain and a 1:12,000-scale geologic map (Scott and Bonk, 1984) encompasses the central part of Yucca Mountain, which includes the location of the proposed repository.

USES OF GEOLOGIC INFORMATION

Chapter 1 summarizes published information on the geology of the Yucca Mountain site and various alternate models that can be used to predict site behavior and are consistent with the presently available data. The chapter provides a geologic basis for, and complement to, the discussions in the chapters that follow. The information in this chapter provides a data base for the studies planned to characterize the Yucca Mountain site and provides a basis to determine what further studies (Section 8.3.1) are needed. Additionally, geologic information provides one basis for the design of the repository and the waste container that would meet the performance objectives of 10 CFR 60.111 through 60.113.

Related discussions of issues and information needs are in Sections 1.8

Information on the long-term stability with respect to tectonic and geologic processes (Section 1.5) will provide a basis for determining if tectonic disruptive-event scenarios are significant.

The location of mines and drillholes (Section 1.6) and the resource potential of the site (Section 1.7) bear on the ability of the site to isolate waste. Drillholes could be pathways for radionuclide travel, and the resource potential of the site bears on the likelihood of future human interference at the site, a potential postclosure disruptive event.

QUALITY AND UNCERTAINTY OF DATA AND RELIABILITY OF INTERPRETATIONS

The quality and extent of information contained in Sections 1.1 through 1.7 provide an adequate foundation for the planned site characterization activities presented in Chapter 8.

Chapter 1 draws on published information only. Accordingly, it does not cite studies if, at the time of writing, it appeared that the results of those studies would not be published by mid-1987. Such studies include uncompleted or unpublished geologic studies focused expressly on Yucca Mountain as a proposed repository. Thus, the data presented here are somewhat incomplete and the information for the most part is insufficient for fully addressing the qualifying conditions of 10 CFR Part 960 and performance objectives of 10 CFR Part 60. The planned investigations described in Chapter 8 (Section 8.3.1) are designed to supply the information required to

To adequately design the repository and assess its ultimate performance, a tectonic model or models must be developed that incorporate and logically relate all pertinent geologic and seismologic observations that have a tectonic implication. The parameters for such a model (e.g., magnitude and orientation of principal stresses in the region, structural controls on stresses, fault slip rates, subsurface fault configurations, and focal plane solutions) are incompletely developed at this time.

1.1 GEOMORPHOLOGY

Desert geomorphic processes acting in conjunction with extensional tectonism have molded the present topography of the Yucca Mountain area, and these processes continue to change the landscape. Future tectonism, climatic change (Section 1.1.3.1.2), or complex threshold-related changes (Section 1.1.3.3.2) could alter the intensity and the distribution of these processes, thereby changing present patterns and rates of erosion and deposition. Such changes could, in turn, affect erosion, surface drainage, ground-water recharge, and subsurface water flow. Thus, the geomorphic processes that have operated in the Yucca Mountain area during the Quaternary and changes in these processes through time are important to several aspects of waste isolation at Yucca Mountain (e.g., the design and construction of surface facilities; assessment of rapid mass wasting or flooding hazards to surface facilities before closure; the evaluation of possible degradation of monuments

1.1.1 PHYSIOGRAPHY

Yucca Mountain is in the southern part of the Great Basin, the northernmost subprovince of the Basin and Range physiographic province (Figure 1-2). Generally defined, the Basin and Range province is that area of southwestern North America that is characterized by more or less regularly spaced subparallel mountain ranges and intervening alluviated basins formed by extensional faulting. Within the United States, the province describes an irregular arc that curves around the western and southern margins of the Colorado Plateau. As shown in Figures 1-2 and 1-3, the western boundary is defined by the Transverse Ranges, the Sierra Nevada, and the southern Cascade Range; the northern boundary by the Columbia Plateau; and the northeast boundary by the Wasatch Range of the middle Rocky Mountains (Hunt, 1974). The geology of the province can be generalized as a late Precambrian and Paleozoic continental margin assemblage, grading from miogeoclinal strata on the east to eugeoclinal strata on the west, that was complexly deformed by late Paleozoic and Mesozoic orogenies. Western portions of the province were subsequently intruded by Mesozoic granitic rocks, broadly overlain by Cenozoic volcanic rocks, and extensively deformed by at least two phases of middle to late Cenozoic extensional faulting (Stewart, 1978, 1980a; Sections 1.2 and 1.3). The distinctive physiography of the province is largely the product of the most recent extensional phase of deformation.

Within a region as large and structurally complex as the Basin and Range province, physiographic variability is to be expected. In central Nevada, imposing mountain ranges as much as 80 km long and 25 km wide locally rise to altitudes above 3,500 m. Altitudes average more than 2,600 m along range crests and nearly 1,700 m along the axes of the intervening basins. The ranges are consistently aligned along north-to-northwest trends and comprise more than 40 percent of the total surface area of the region (Tables 1-1a and 1-1b). In contrast, the ranges of the Mojave Desert in southeastern California are significantly smaller and lower. Range areas average 170 km^2 and altitudes along range crests average 1,550 m, which is 140 m less than average basin altitudes in central Nevada. Range trends are variable, and ranges account for generally less than 30 percent of the total area as shown in Table 1-1a and Table 1-1b. Because of such contrasts, the Basin and Range province was subdivided into five subprovinces by Fenneman (1931). Portions of two of these subprovinces, the Great Basin and the Mojave-Sonoran Desert, make up the region surrounding Yucca Mountain.

1.1.1.1 The Great Basin and Mojave-Sonoran Desert subprovinces

The Great Basin, largest of the Basin and Range subprovinces, includes all of the Basin and Range province north of the Garlock fault and the eastward extension of this major structure across the southern tip of Nevada (Figures 1-2 and 1-3, Section 1.1.1). The eastern and western boundaries of the subprovince also coincide with major structural boundaries, the high Colorado Plateau on the east and the Sierra Nevada on the west. The Great Basin is not, as its name suggests, a large regional depression. Rather, it can be more accurately described as a great bulge consisting of a central area of elevated basins and ranges that is flanked on three sides by large areas of significantly lower terrain: the Bonneville Basin on the east, the

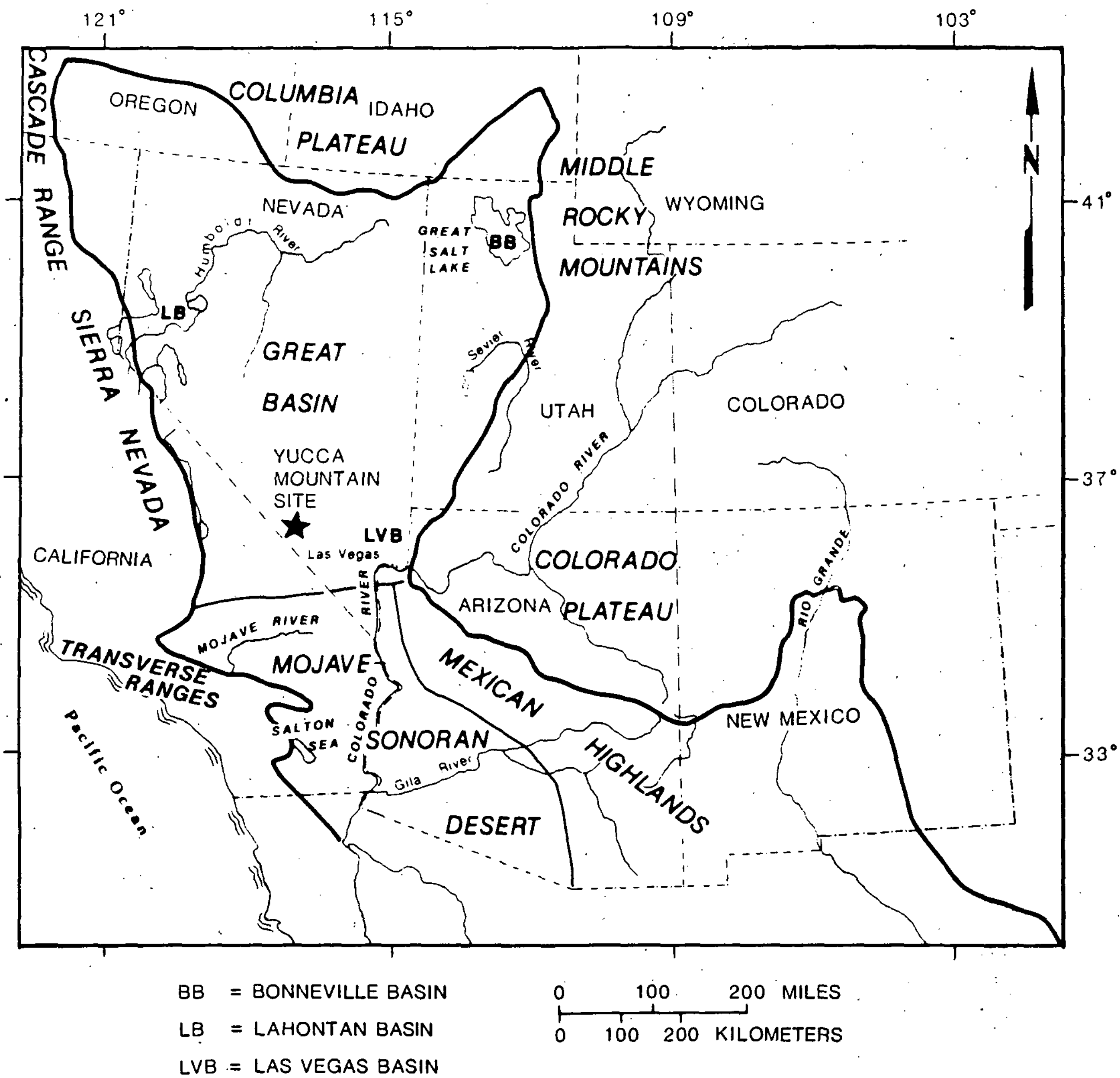

Figure 1-2. Boundaries and larger subprovinces of the Basin and Range physiographic province (Hunt, 1974) Province boundary is indicated by heavy solid line. Salton Trough subprovince of southern California and Sacramento Mountains subprovince of central New Mexico are not shown.

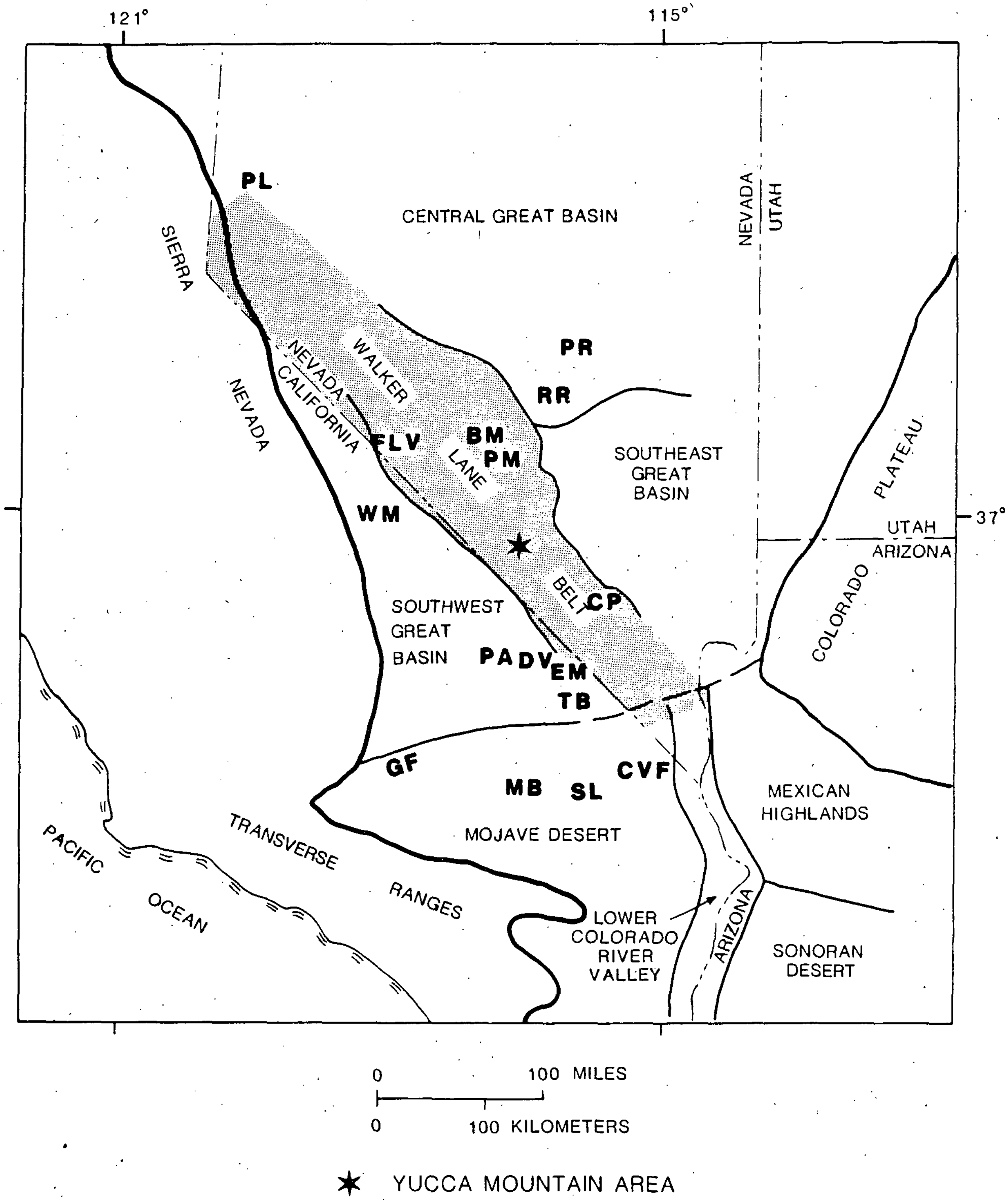

Figure 1-3. Generalized map showing approximate locations of the physiographic subdivisions of the west-central and southern Great Basin discussed in the text. Stippled pattern indicates the general location of the Walker Lane belt (Carr, 1984; Stewart, 1986). Key: BM, Black Mountain; CP, Charleston Peak; CVF, Cima Volcanic Field; DV, Death Valley; EM, Eagle Mountain; FLV, Fish Lake Valley; GF, Garlock fault; MB, Manix Basin; PA, Panamint Range; PL, Pyramid Lake; PM, Pahute Mesa; PR, Pancake Range; RR, Reveille Range; SL, Soda Lake; TB, Tecopa Basin; WM, White Mountains.

Table 1-1a. Morphometric characteristics of physiographic areas in the southern Great Basin

Physiographic area	Total area (km^2)	Total range area km^2	Total range area %	Total piedmont area km^2	Total piedmont area %	Total basin area km^2	Total basin area %	Basin closure[a] (m)	Average basin elevation (m)	Average range elevation (m)
Central Great Basin	24,850	10,525	42.3	11,825	47.6	2,520	10.1	170	1,695	2,625
Southeast Great Basin	22,650	8,350	36.9	12,040	53.1	2,260	10.0	205	1,265	2,135
Southwest Great Basin	25,630	13,595	53.0	9,825	38.4	2,210	8.6	635	395	2,090
Northeast Mojave Desert	19,710	5,600	28.4	12,625	64.1	1,485	7.5	135	765	1,550
Walker Lane belt										
Northwest Goldfield block	7,310	2,935	40.2	3,420	46.8	955	13.0	130	1,390	2,290
Northeast Goldfield block	8,105	1,565	19.3	4,425	54.6	2,115	26.1	90	1,320	2,245
Spotted Range-Mine Mountain block	1,940	560	28.8	1,270	65.3	114	5.9	100	1,065	1,645
Spring Mountains block	4,675	2,335	50.0	2,340	50.0	NA[b]	NA	NA	690	2,390

[a]Average for the five largest closed basins in each physiographic area.
[b]NA = not applicable.

Table 1-1b. Morphometric characteristics of physiographic areas in the southern Great Basin

Physiographic area	Total relief (m)	Range relief (m)	Piedmont relief (m)	Piedmont width (km)	Average piedmont slope (%)	Average range area (km^2)	Range spacing (km)
Central Great Basin	930	725	205	5.9	3.6	1,446	26.2
Southeast Great Basin	870	630	240	6.0	4.0	388	20.0
Southwest Great Basin	1,670	1,380	290	4.9	6.3	1,130	23.0
Northeast Mojave Desert	785	485	300	8.2	3.7	160	19.6
Walker Lane belt							
Northwest Goldfield block	900	635	265	6.1	4.4	244	17.5
Northeast Goldfield block	725	490	235	7.7	3.0	147	30.9
Spotted Range-Mine Mountain block	580	390	190	4.5	4.3	71	9.5
Spring Mountains block	1,700	1,190	510	11.9	4.3	2,332	NA[a]

[a]Data not applicable.

Lahontan Basin on the west, and the southern area including the Las Vegas Basin on the south (Hunt, 1974). With the exception of limited areas along its northern, northwestern, and southeastern margins, all drainage is internal. Closed basins are common, and many of these basins supported perennial lakes at one time or another during the Pleistocene (Sections 3.7.4 and 5.2.1).

South of the Great Basin, the Mojave-Sonoran Desert subprovince forms a broad east-west-trending belt of desert terrain that extends eastward from the Transverse Ranges of southern California to the Mexican Highlands of central and eastern Arizona (Figure 1-2). This subprovince includes three physiographically distinct areas: the Mojave Desert, the lower Colorado River valley, and the Sonoran Desert. Although morphometrically similar, these three areas contrast strongly in drainage integration and basin dissection. Drainage within the Mojave Desert is predominantly internal, and most of the closed basins of the region are undissected except in proximal piedmont areas. Drainage within the Sonoran Desert has been largely integrated, and basin dissection is more continuous and widespread than in the Mojave. Within the valley of the lower Colorado River, piedmonts are deeply and pervasively dissected in response to base-level lowering along that major drainage.

Elongate mountain ranges and intermontane sedimentary basins are the principal landscape elements of both the Great Basin and the Mojave-Sonoran Desert subprovinces. The ranges are as much as 150 km long, 25 km wide, and linear to curvilinear in overall plan. Locally, they rise more than 3,000 m above the intervening basins (Dohrenwend, 1987). These mountain ranges are mostly fault-bounded blocks. Both range flanks may be faulted, but more commonly only one flank is bounded by a major fault and the range is tilted. In the Great Basin, range tilting averages about 15 to 20 degrees (Stewart, 1980b). Tilted ranges are asymmetrical in cross profile with steep, fault-bounded range fronts and relatively gentle dip slopes along the back-tilted flank. The morphologic characteristics of a fault-bounded range front reflect its general level of tectonic activity. Active range fronts are characterized by conspicuous faceted spurs with locally preserved slickensided remnants of the original fault surface, steep undissected alluvial fans, low range-front sinuosities, and low ratios of valley-floor width to valley depth. Inactive range fronts are characterized by highly sinuous, deeply embayed range fronts with broad, gently sloping pediments and (or) by streams. The floors of most open basins are moderately to deeply dissected, locally exposing basin-fill deposits that record thousands to millions of years of late Tertiary and Quaternary history (Mulhern, 1982, Dohrenwend, 1985; Jefferson, 1985).

The piedmonts are made up of complex associations of coalescing alluvial fans (bajadas) and pediments. Piedmont slopes average between 3.0 and 4.5 percent in most areas (Tables 1-1a and 1-1b, Section 1.1.1) and are generally less than 15 percent, although slopes as steep as 35 percent occur locally in piedmont areas proximal to some of the more active range fronts. Most piedmonts are segmented into complex mosaics of dissected and undissected surfaces (Peterson, 1981). Surfaces of active alluvial transport or deposition, or both, and surfaces recently abandoned by drainage originating in the range are characteristically undissected to slightly dissected but may possess as much as 1 to 3 m of local constructional relief where dominated by debris flow and sieve deposits. Late Pleistocene surfaces are typically slightly to moderately dissected. Remnants of these surfaces are usually flat and smooth and are commonly veneered with eolian fine sand and silt armored by interlocking stone pavements. Older surfaces are commonly highly degraded and deeply dissected by piedmont-source drainage (Dickey et al., 1980; Dohrenwend, 1982; Wells et al., 1985b).

1.1.1.2 The region surrounding Yucca Mountain

The region surrounding Yucca Mountain can be subdivided into several clearly defined physiographic areas that reflect regional variations in structure, lithology, and late Cenozoic tectonism (Carr, 1984; Stewart, 1986; Figure 1-3). These physiographic areas include (1) the large north-northeast-trending basins and ranges of the central Great Basin; (2) the somewhat smaller, more arcuate, and more closely spaced basins and ranges of the southeast Great Basin; (3) the massive ranges and deep basins of the southwest Great Basin; (4) the small, irregularly shaped ranges and basins of the northeast Mojave Desert; and (5) the highly variable terrain of the northwest-trending Walker Lane belt (a broad zone of diverse topography between the Sierra Nevada and the southwest Great Basin) on the west and the region of typical basin-and-range topography on the east (i.e., the central and southeast Great Basin) (Stewart, 1986). The general morphometric characteristics of these physiographically distinct areas are summarized in Tables 1-1a and 1-1b.

1.1.1.2.1 Central Great Basin

The north-northeast-trending basins and ranges of the central Great Basin extend across the elevated central portion of the Great Basin. Basin altitudes in the southern part of the area average 1,690 m, and range crest altitudes average approximately 2,625 m. The ranges, averaging 860 km^2 in area and more than 900 m in total relief, are among the largest in the region and occupy more than 40 percent of the area of the central Great Basin (Tables 1-1a and 1-1b). These ranges are mostly tilted fault blocks that are linear to curvilinear in overall form. Many of the range fronts display abundant morphologic indications of active range-front faulting. Although closed basins are common, many of the basins are connected by integrated drainage that feeds the two major drainage systems of the subprovince, the Humboldt River to the north and the White River to the southeast.

1.1.1.2.2 Southeast Great Basin

The southeast Great Basin presents a distinct contrast with the central Great Basin to the north. The basins and ranges of the southeast Great Basin are significantly smaller than those farther north. On average, the ranges are slightly lower and less than 50 percent as large, and the basins show a comparable decrease in size (Tables 1-1a and 1-1b). Also, the ranges are significantly narrower, more closely spaced, and distinctly curvilinear in overall plan. Although part of the area is drained by the White River-Muddy River system, flowing southward into Lake Mead, tributary drainage to this open system is limited and most of the basins are closed.

1.1.1.2.3 Southwest Great Basin

The southwest Great Basin (the Mono-Inyo block of the Walker Lane belt as defined by Carr (1984) and Stewart (1986)) is a large triangular area of about 25,000 km^2 located almost entirely in southeastern California. It is bounded on the west by the Sierra Nevada, on the south by the Garlock fault, and on the northeast by the Walker Lane belt. The morphologic and morphometric characteristics of this block indicate that it is tectonically the most active area in the region surrounding Yucca Mountain. Ranges occupy about 53 percent of this area, and range relief averages nearly 1,400 m. The 3,454 m separating the axis of Death Valley from the crest of the Panamint Range represents the greatest amount of local relief in the Basin and Range province. The piedmonts are narrower (less than 5 km on the average) and steeper (more than 6 percent on the average), and the larger basins are more than three times deeper (average depth of closure of about 635 m) than in any other part of the region (Tables 1-1a and 1-1b). Moreover, range fronts commonly exhibit morphologic characteristics diagnostic of relatively rapid vertical tectonic movement (Bull and McFadden, 1977) shallow. The Mojave River, originating in the Transverse Ranges, is the only significant interbasin drainage system in this region.

1.1.1.2.5 Walker Lane belt

The Walker Lane belt is a complex zone of strike-slip displacement that subparallels the western margin of the Great Basin from the area of Pyramid Lake in northwest Nevada to the Mojave Desert (Carr, 1984; Stewart, 1986) (Figure 1-3). This northwest-trending zone, 80 to 150 km wide and about 700 km long, is made up of at least eight major geomorphically distinct structural blocks, each of which is characterized by different topographic and structural trends (Stewart, 1986). Three of these blocks are in the region surrounding Yucca Mountain. These are the Spotted Range-Mine Mountain, the Spring Mountains, and the Goldfield blocks (Figure 1-4). The four sections of the Goldfield block (the northwest, northeast, Amargosa Desert, and volcanic plateaus sections) are also shown on Figure 1-4.

Spotted Range-Mine Mountain block. The Spotted Range-Mine Mountain block is a zone of northeast-trending faults that occupies a roughly triangular area of nearly 2,000 km^2 between the volcanic plateaus of the Goldfield block (to the north and west), the southeast Great Basin (to the northeast and east), and the Spring Mountains (to the south). The faults locally cut Quaternary alluvial deposits (Carr, 1984). The physiography of this small block contrasts sharply with that of the surrounding region. The ranges (including the Striped Hills, Skull Mountain, the Specter Range, and Mercury Ridge) are small (70 km^2 average area), low, discontinuous, highly elongate, and closely spaced, and their east-to-northeast orientations are at sharp angles to the north-to-northwest physiographic and structural trends of the region (Figure 1-5).

Spring Mountains block. The Spring Mountains (Figure 1-4) are also both geologically and physiographically distinct within the southern Great Basin. This range is underlain by upper Proterozoic and Paleozoic sedimentary rocks that have been relatively undeformed during the Cenozoic (Longwell et al., 1965; Stewart, 1986). Among the largest ranges in the southern Great Basin, the Spring Mountains form a high-standing, generally northwest trending upland mass that, together with contiguous piedmont slopes, occupies an area of nearly 4,700 km^2. The average range relief exceeds 1,200 m and the average piedmont width exceeds 11 km. The 3,633-m Charleston Peak, high point of the range, is the only area in southern Nevada believed to have experienced late Pleistocene alpine glaciation (Porter et al., 1983). Because of its height and relatively uneventful Cenozoic tectonic history, the range is deeply embayed by large canyons. The perennial streams that occupy the uppermost reaches of these drainages are unique in the southern Great Basin.

Goldfield block. The Goldfield block (Figure 1-4) occupies an elongate area of approximately 22,000 km^2 north and west of Yucca Mountain. This portion of the Walker Lane belt is unusual in that it lacks major northwest-trending strike-slip faults and major basin-and-range faults (Stewart, 1986). The topography of the Goldfield block is variable, and the block can be divided into four physiographically distinct sections: (1) irregular basins

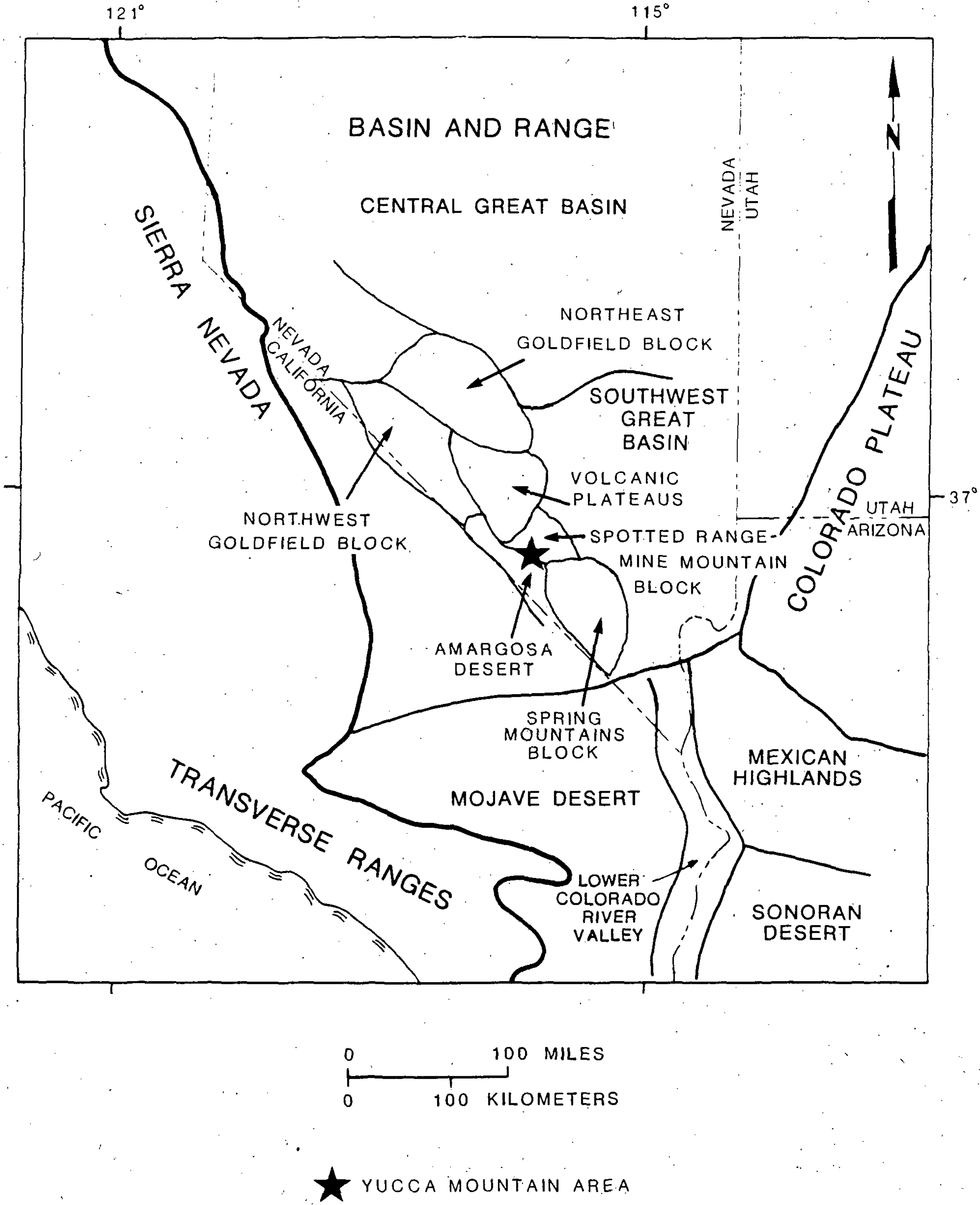

Figure 1-4. Physiographic subdivisions of the west-central and southern Great Basin.

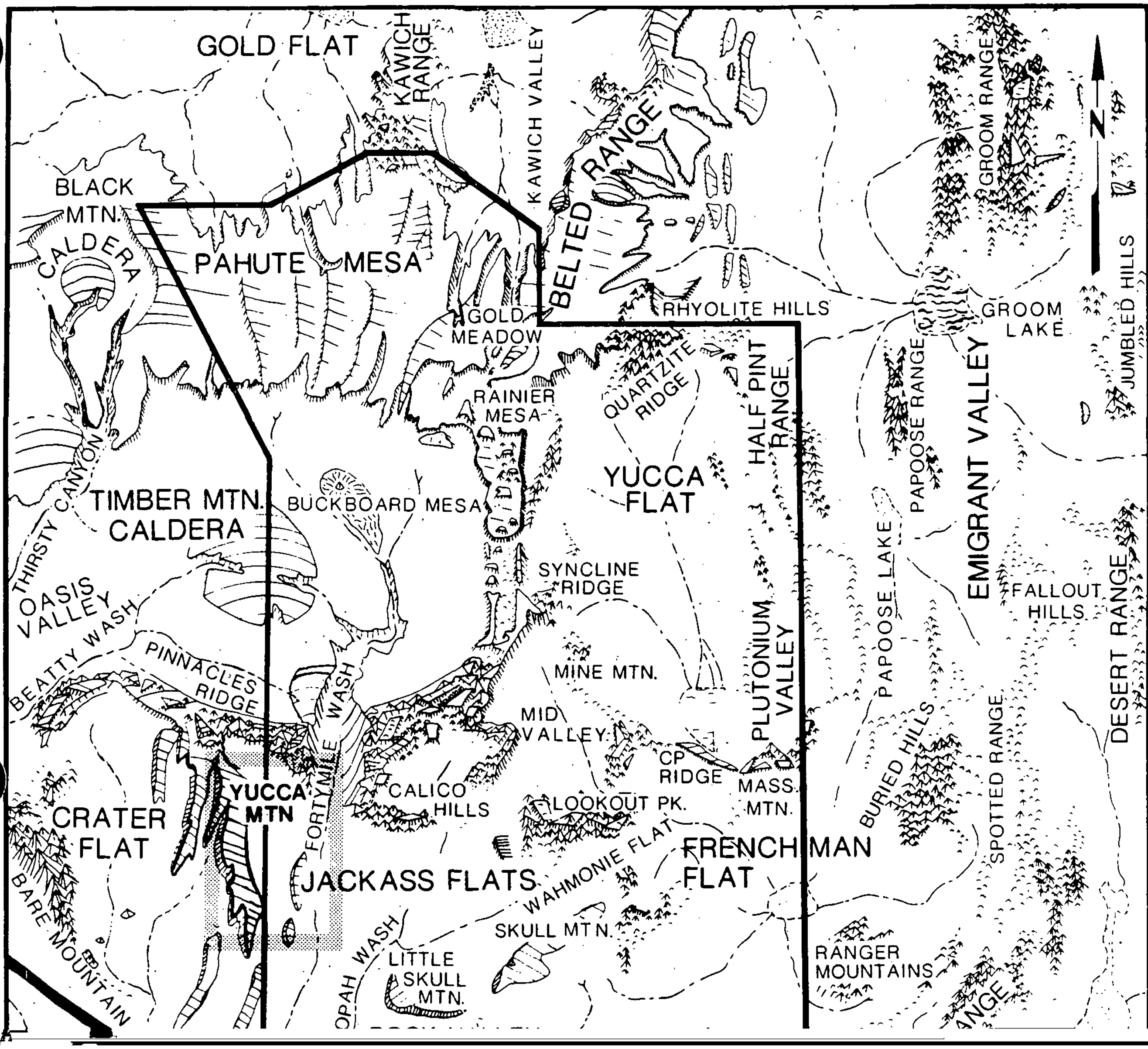
GOLD FLAT
KAWICH RANGE
KAWICH VALLEY
BELTED RANGE
GROOM RANGE
BLACK MTN.
CALDERA
PAHUTE MESA
JUMBLED HILLS
GOLD MEADOW
RHYOLITE HILLS
GROOM LAKE
RAINIER MESA
QUARTZITE RIDGE
HALF PINT RANGE
PAPOOSE RANGE
EMIGRANT VALLEY
THIRSTY CANYON
TIMBER MTN. CALDERA
BUCKBOARD MESA
YUCCA FLAT
PAPOOSE LAKE
OASIS VALLEY
SYNCLINE RIDGE
FALLOUT HILLS
DESERT RANGE
BEATTY WASH
PINNACLES RIDGE
MINE MTN.
PLUTONIUM VALLEY
FORTYMILE WASH
MID VALLEY
BURIED HILLS
SPOTTED RANGE
YUCCA MTN
CALICO HILLS
CP RIDGE
MASS. MTN.
CRATER FLAT
LOOKOUT PK.
FRENCHMAN FLAT
JACKASS FLATS
WAHMONIE FLAT
BARE MOUNTAIN
SKULL MTN.
TOPAH WASH
LITTLE SKULL MTN.
RANGER MOUNTAINS

and ranges of the northwest part; (2) broad, irregular basins and low discontinuous ranges of the northeast part; (3) the broad, northwest-trending basin of the Amargosa Desert; and (4) the irregularly shaped volcanic plateaus of the Pahute Mesa-Timber Mountain-Yucca Mountain area.

The northwest part of the Goldfield block is a highly elongate, northwest-trending area, 40 to 60 km wide, that lies northeast of Fish Lake Valley and northern Death Valley along the California-Nevada border. This area is in many ways similar to the southeast Great Basin; mean values of range relief, area, and spacing, and of piedmont width and slope are approximately the same for both areas. However, the ranges of the northwest Goldfield block are variable in trend and highly irregular in overall plan, and the area lacks the pervasive generally north trending structural grain that characterizes most of the Great Basin.

The northeastern part of the Goldfield block is characterized by the most subdued physiography in the southern part of the Great Basin. The physiography of this area more closely resembles the Mojave Desert than the southern Great Basin. Mean values of range relief and area and of pediment width and slope for the northeast Goldfield block and the northeast Mojave Desert are nearly identical. Ranges are small, low, and discontinuous, and the irregular range fronts suggest an almost complete lack (or at most, a very low level) of vertical range-front faulting. Moreover, the relative proportions of ranges, basins, and piedmonts also suggest a low level of differential vertical tectonic movement. Ranges make up less than 20 percent and basin flats more than 25 percent of the northeastern part of the Goldfield block, and average range spacing is nearly 31 km. These values represent extremes for any area in the southern Great Basin or northern Mojave Desert.

The broad northwest-trending basin of the Amargosa Desert occupies the southwestern corner of the Goldfield block. This basin, approximately 80 km long and as much as 30 km wide, is one of the largest in the southern Great Basin. It slopes gently southeastward along the course of the Amargosa River from an elevation of about 975 m on the south piedmont of the Bullfrog Hills, near Beatty, to an altitude of about 600 m at Eagle Mountain, 8 km south of Death Valley Junction (Figure 1-5). Large areas of this gently sloping basin flat are veneered with sheets of fluvially reworked eolian sand (Swadley, 1983).

Contiguous volcanic uplands occupy most of the southern part of the Goldfield block. These flat-topped uplands and their associated calderas make up a roughly triangular area of about 5,000 km^2 that includes Pahute Mesa, Black Mountain, Timber Mountain, Shoshone Mountain, and Yucca Mountain (Figure 1-5). This area is underlain by gently dipping, faulted tuffs and flow rocks of the late Tertiary southwestern Nevada volcanic field (Carr, 1984). Summit surfaces are broad and relatively flat with minor constructional relief. In many areas, these summit surfaces end abruptly at steep, caprock-protected slopes partly armored with discontinuous aprons of blocky talus. Generally radial, but locally structurally controlled, drainage systems have deeply dissected the flanks of these uplands. Two of these deeply incised drainages, Beatty Wash and Fortymile Wash, flank the north and east margins of Yucca Mountain.

1.1.2 GEOMORPHIC UNITS

1.1.2.1 Physiographic subdivisions

The Yucca Mountain area can be subdivided into eight clearly defined physiographic areas: Bare Mountain, Crater Flat, Yucca Mountain, Fortymile Wash, Jackass Flats, the valley of Beatty Wash, Pinnacles Ridge, and the northeast margin of the Amargosa Desert. These areas are shown in Figures 1-6, 1-7a, 1-7b, 1-8a, and 1-8b and discussed in the following paragraphs.

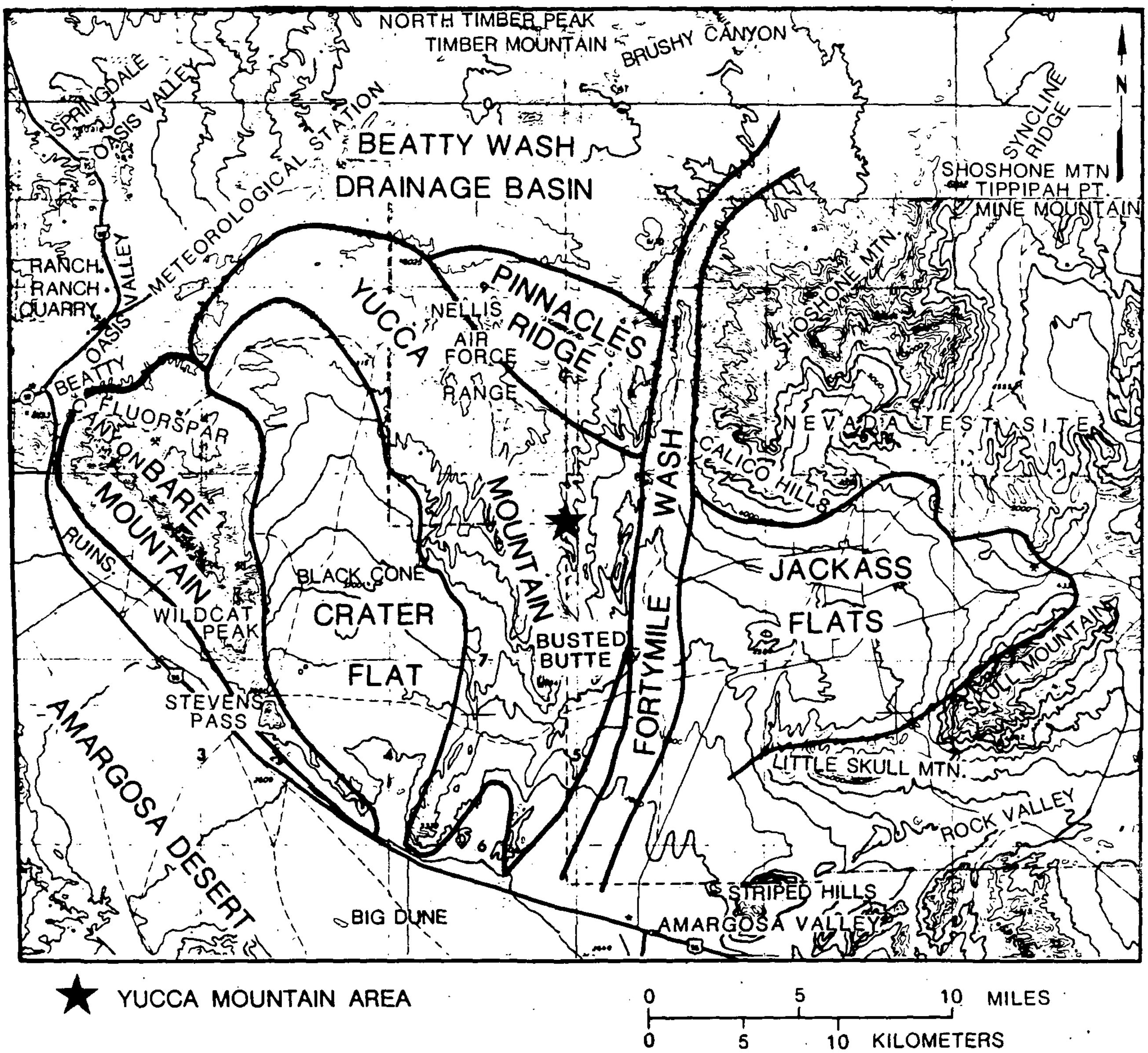

Figure 1-6. Topography and physiographic subdivisions of the Yucca Mountain area.

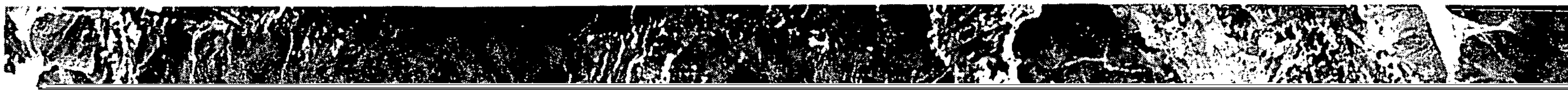

DECE

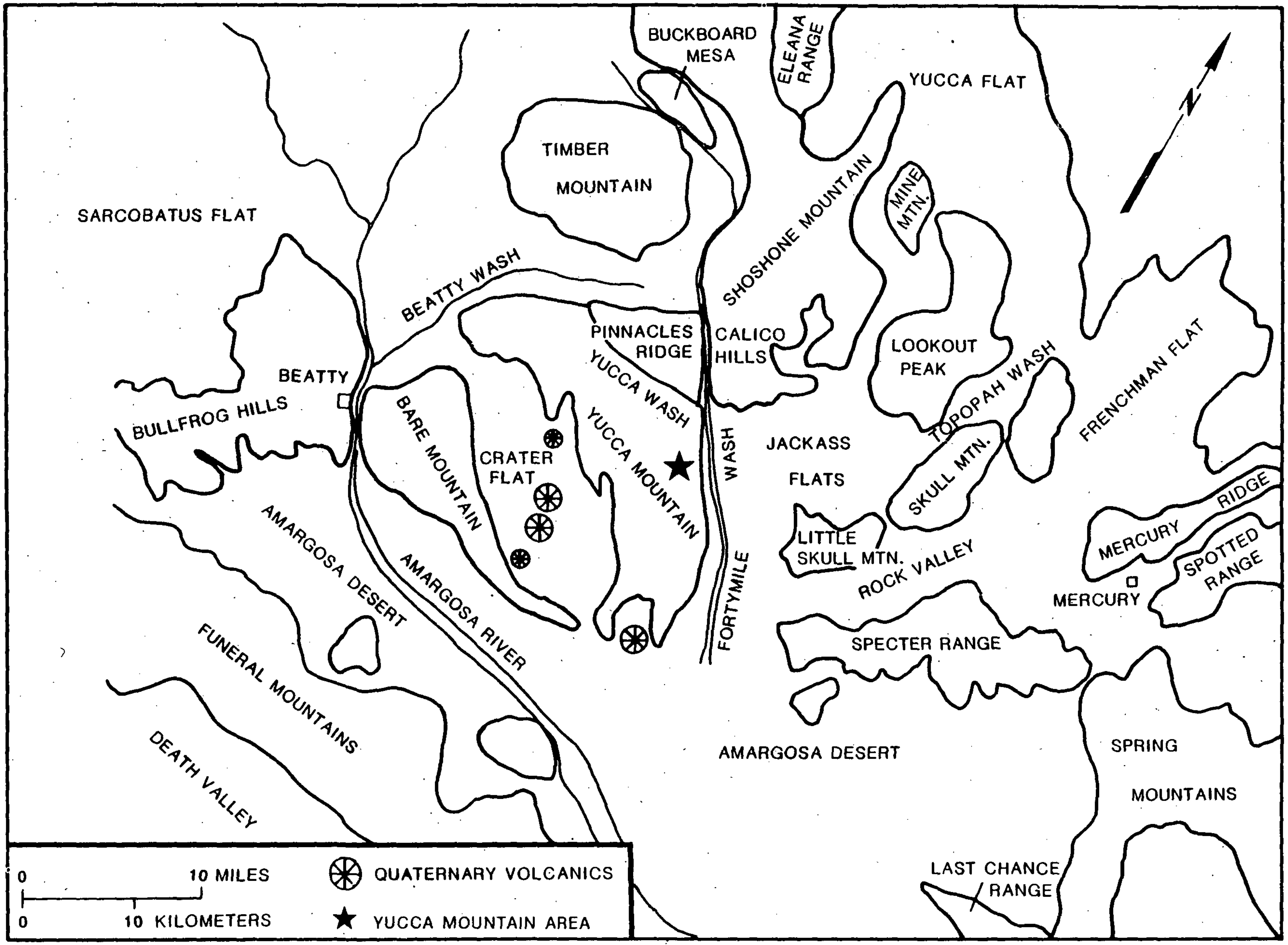

Figure 1-7b. Overlay for Landsat image no 2299-17404, scene 043/034 (Figure 1-7a)

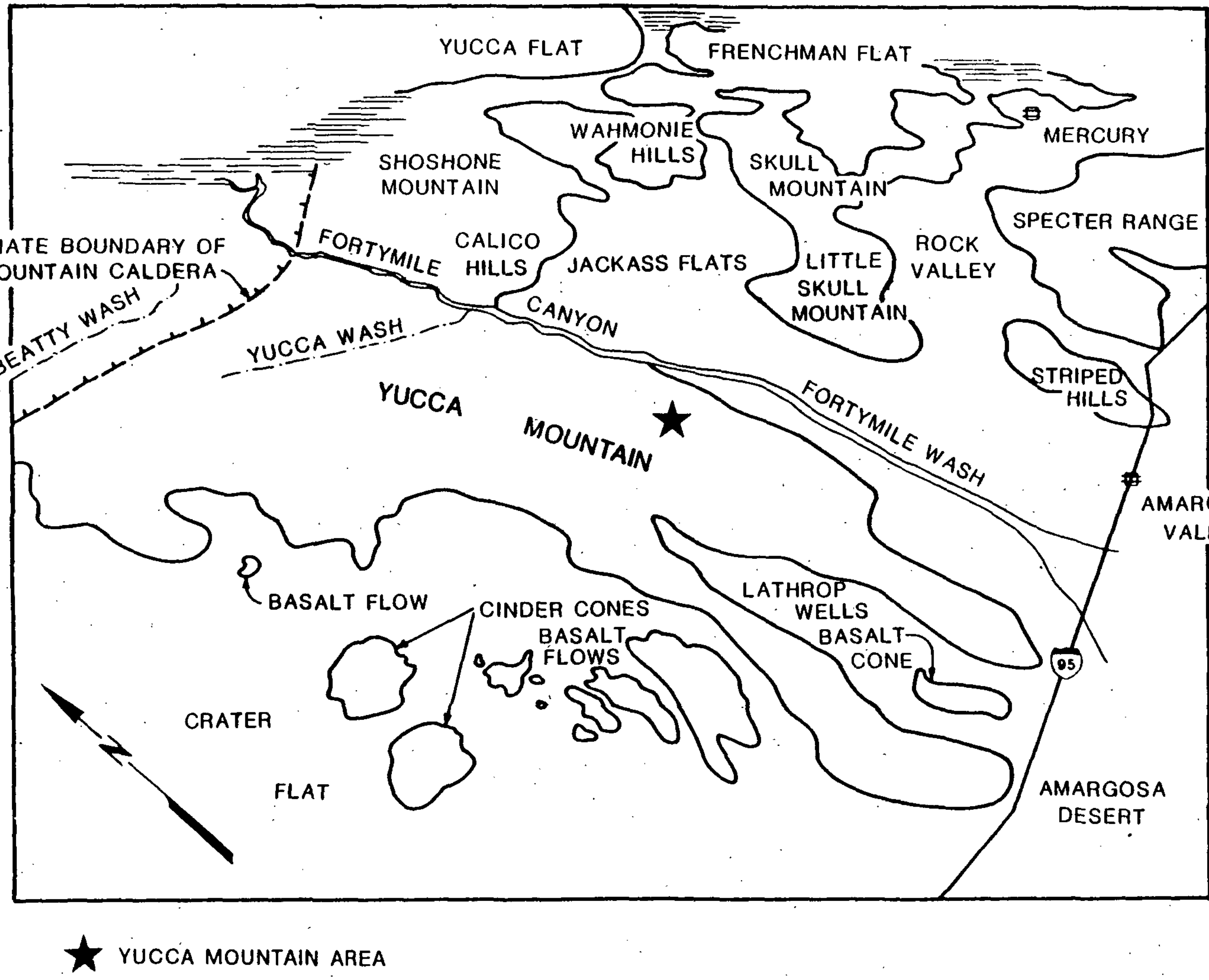

Figure 1-8b. Overlay for high-altitude oblique aerial photograph shown in Figure 1-8a.

basaltic flows measured by Walker (1973). The heights of the main scoria cones in the Crater Flat area range from 27 to 140 m (Crowe et al., 1983b).

Yucca Mountain and its contiguous piedmont slopes. Yucca Mountain, an irregularly shaped volcanic upland, 6 to 10 km wide and about 40 km long, extends from the valley of Beatty Wash on the northern to the northeastern side of the Amargosa Desert on the south. The crest of the mountain ranges between altitudes of 1,500 and 1,930 m, about 650 m higher than the floor of Crater Flat. The mountain is dominated by a subparallel series of en echelon, north-trending ridges and valleys controlled by high-angle faults (Figure 1-8a). These fault blocks are tilted eastward (Scott and Bonk, 1984) so that the fault-bounded west-facing slopes are generally high, steep, and straight, whereas the east-facing slopes are more gentle and deeply dissected by subparallel systems of linear valleys. The upper slopes of the mountain are striped by elongate lobes of darkly varnished rock flows and talus. The narrow valleys and ravines high on the east-facing slopes are floored by bedrock; downstream reaches of these valleys widen and are floored by the terraced alluvial deposits of intermittent streams. Drainage from the west flank of the mountain flows down fault-controlled canyons and across the slightly dissected western piedmont into Crater Flat; drainage from the east flank flows down Yucca, Drill Hole, and Dune washes into Fortymile Wash.

The general topography of Yucca Mountain is mapped on parts of five U.S. Geological Survey topographic maps:

Bare Mountain, Nevada--1:62,500 scale, 40-foot contour interval (USGS, 1954);

Big Dune, Nevada--1:62,500 scale, 80-foot contour interval (USGS, 1952a);

Busted Butte, Nevada--1:24,000 scale, 20-foot contour interval (USGS, 1983);

Lathrop Wells, Nevada--1:24,000 scale, 20-foot contour interval (USGS, 1961a); and

Topopah Spring NW, Nevada--1:24,000 scale, 20-foot contour interval (USGS, 1961c).

Fortymile Wash. Fortymile Wash drains an area of approximately 620 km^2 north and east of Timber Mountain and south of Pahute Mesa; it then flows almost directly southward through Fortymile Canyon, which lies between Pinnacles Ridge and Shoshone Mountain. After leaving the mouth of Fortymile Canyon, the wash continues southward down the south-sloping piedmont that forms the west end of Jackass Flats. Along this latter reach, the wash has cut a nearly linear trench, 150 to 600 m wide and as much as 25 m deep, into the Quaternary alluvial deposits of the piedmont (Swadley et al., 1984). This entrenchment gradually decreases downslope until the wash merges with the general level of the piedmont near the northeastern margin of the Amargosa basin. As discussed in Section 8.3.1.6, additional study is under way to determine the age and cause of this entrenchment. This information will provide, in addition to site specific incision rates, an understanding of the unusual depth of Fortymile Wash as compared with other canyons in the region and the factors contributing to the development of Fortymile Wash. Most of the larger tributaries to the lower reaches of Fortymile Wash originate on the eastern flank of Yucca Mountain.

Jackass Flats. Jackass Flats is an asymmetrical alluviated basin, 8 to 10 km wide and nearly 20 km long, that extends eastward from Yucca Mountain. It is bounded on the north by the Calico Hills, on the east by Lookout Peak, and on the south by Little Skull and Skull Mountains. The surface of the flats is made up of the south-sloping piedmont of the Calico Hills and the predominantly northwest-sloping piedmonts of Lookout Peak and Skull Mountain. Topopah Wash, the major axial drainage, diagonally bisects the basin near the intersection of these two piedmonts. Proximal piedmont areas are moderately dissected, with shallow (5 to 10 m deep) arroyos and rounded interfluves; distal piedmont areas are largely undissected. Along the western edge of the basin near Fortymile Wash, the depth of basin fill is approximately 130 m (Byers and Warren, 1983).

The valley of Beatty Wash. Beatty Wash, one of the larger tributaries of the upper Amargosa River, drains an irregularly shaped area of about 250 km^2 along the southern margin of the Timber Mountain-Oasis Valley caldera (Carr, 1984). This area includes the southwestern flank of Timber Mountain and the northern flanks of Yucca Mountain and Pinnacles Ridge. The basin topography is generally steep and irregular. Valley depths range from about 200 to 790 m, and the total relief from the mouth of the basin to the crest of Timber Mountain exceeds 1,200 m.

Pinnacles Ridge. Pinnacles Ridge is a roughly triangular upland, about 11 km long and 6 km wide, that is bounded on the north by Beatty Wash, on the east by Fortymile Wash, and on the southwest by Yucca Wash. The ridge is contiguous with and extends southeastward from the northeastern flank of Yucca Mountain. Its south flank is structurally and lithologically similar to Yucca Mountain, and its crest is the eroded southern margin of the Timber Mountain caldera (Carr, 1984). The ridge crest varies from about 250 to 670 m above the large washes that surround it, and tributaries to these washes have cut a radial system of deep, linear valleys into its flanks.

The northeast margin of the Amargosa Desert. The Amargosa Desert is described as part of the Goldfield block in Section 1.1.1.2.5.

1.1.2.2 Landforms

The type and distribution of landforms in the Yucca Mountain area are typical of ranges and open basins in the southern part of the Great Basin. The topography of the area was initially created by the relative uplift of the ranges and subsidence of the basins and was subsequently modified by erosion of the ranges and alluviation in the basins. This topography can be divided into two general categories of landforms: upland landforms in the mountain ranges and piedmont slopes in the adjacent basins. Level basin floors or basin flats are not present in the open basins immediately surrounding Yucca Mountain.

The uplands of the Yucca Mountain area are composed of three general landform types: (1) ridge crests, (2) valley bottoms, and (3) the intervening hillslopes. With the exception of the caprock-protected dip slopes that characterize the crestal areas of Yucca Mountain, the ridge crests are mostly angular and rugged. The valleys are generally narrow and V-shaped along their upper and middle reaches but locally contain flat, alluviated floors in their lower reaches. Valley morphology ranges from shallow, straight, steeply sloping gullies and ravines to relatively deep, bifurcating, gently sloping valleys and canyons. The hillslopes between ridge crests and valley bottoms typically include at least three general forms: (1) narrow upper convexities, (2) extensive straight segments, and (3) broad lower concavities. Free faces or cliffs are also common. Bedrock outcrops are most common on the upper slopes, particularly along the free faces. The straight segments are discontinuously veneered with mantles of blocky talus and lobes of poorly sorted colluvium. Numerous gullies and small ravines locally cut these colluvial veneers and expose the underlying bedrock. The concave lower slopes are typically mantled with variable thicknesses of wash deposits (including debris cones and steep, poorly sorted alluvial fans). Locally, particularly along the western flanks of Busted Butte and Fran Ridge, these lower slopes are deeply buried beneath wedge-shaped ramps of eolian sand.

The open basins surrounding Yucca Mountain, including Crater Flat and Jackass Flats, are floored almost entirely by gentle piedmont slopes. These piedmonts are complex mosaics of dissected Pleistocene surfaces juxtaposed against slightly dissected to undissected Holocene surfaces. They can be divided into three general areas: (1) proximal slopes adjacent to the range fronts, (2) intermediate slopes, and (3) distal slopes along and adjacent to the basin axes. Remnants of older surfaces are generally most common in proximal areas where they are typically dissected to a ridge and ravine topography. Ridge interfluves in these dissected areas are typically rounded and highly degraded, and the intervening ravines are mostly steep sided and v-shaped. Such dissection is particularly common in areas that have been abandoned by mountain-fed drainage. Intermediate piedmont slopes typically include the intersection points of the piedmont drainages (i.e., the points of transition from net erosion to net aggradation). Consequently, individual depositional units are typically thin (less than a few meters thick), and surfaces of all ages lie at approximately the same level. As a result, the spatial relations among the various ages of surfaces and their associated deposits are commonly highly complex. For example, it is not unusual for older surfaces to be both overlain by younger deposits and incised by younger channels. In contrast, distal piedmont slopes are substantially less complex. Younger deposits typically bury older deposits in these areas, and distal slopes are dominated by the conspicuous bar-and-swale microtopography

It briefly reviews determinants of the types and the rates of geomorphic processes operating in the region surrounding Yucca Mountain, summarizes the average late Tertiary and Quaternary erosion rates in the southern Great Basin and adjacent areas, and discusses the more significant geomorphic processes presently active in the Yucca Mountain area. Together with predictions of future tectonic activity and climatic change, this information is necessary for estimating the magnitude and the distribution of erosion and deposition on Yucca Mountain and the contiguous piedmonts during the next 10,000 yr.

1.1.3.1 Determinants of geomorphic processes

Geomorphic processes in the southern Great Basin and the northern Mojave Desert are determined largely by climate, existing topography, and tectonic activity, as well as by the spatial and temporal relations between these determinants. Late Cenozoic extensional tectonism, related volcanism, and a history of predominantly semiarid to arid climate have combined to produce a structurally dominated landscape of high relief, with rugged uplands separated by gently sloping lowland basins. Within this landscape, erosion and erosional processes are concentrated in the high, steep, and relatively wet uplands, whereas deposition and depositional processes are generally concentrated in the low, gently sloping, and relatively arid lowlands. The intervening piedmonts serve primarily as surfaces of transport between the eroding uplands and the aggrading basins.

1.1.3.1.1 Influence of tectonism on geomorphic processes

Thus, it is unlikely that vertical tectonic movement will significantly affect the types and the rates of geomorphic processes in the Yucca Mountain area during the next 10,000 yr.

1.1.3.1.2 Influence of climate on geomorphic processes

Yucca Mountain is one of the warmest and driest regions of the United States. The present climate is characterized by hot summers, mild winters, and little precipitation (Section 5.1.1). At Beatty, 24 km west and 420 to 880 m below the crest of Yucca Mountain, maximum July temperatures average 37.5°C, and the mean annual temperature is almost 25°C. Precipitation averages about 110 mm/yr, and the average relative humidity ranges from approximately 25 percent during June and July to about 55 percent during December. Inferences of full-glacial late Pleistocene climates in the southern Great Basin vary widely; however, most studies indicate that semi-arid climates persisted in the basins and lower ranges, although subhumid climates may have existed in the highest mountains (Section 5.2.1). Recent research indicates that mean annual temperatures were approximately 7 to 10°C colder than present temperatures (Porter et al., 1983; Spaulding et al., 1983; Spaulding, 1985; Section 5.2.1). Neotoma (pack rat) midden assemblages indicate reductions in summer precipitation and increases in winter precipitation, but less than a 25-percent increase in the average annual precipitation in the southern Great Basin (Spaulding et al., 1983). These paleohydrologic conditions failed to produce large pluvial lakes like those that existed north of latitude 37°N. (Mifflin and Wheat, 1979; Smith and Street-Perrott, 1983). Moreover, equilibrium-line elevations of mountain glaciers exceeded 3,300 m in most areas (Porter et al., 1983) and the elevation threshold for significant nivation exceeded 2,700 m (Dohrenwend, 1984). Thus, glacial and periglacial processes have probably not been active in the Yucca Mountain area during most, or perhaps all, of middle and late Quaternary time. Thus lacustrine processes were, at most, confined to limited basin areas (Section 5.2.1).

The predominantly semiarid to arid climates of the past and present have tended to preserve the landscape of the region surrounding Yucca Mountain. Weathering in arid environments proceeds more slowly than in more humid environments, and weathering appears limited on most of the bedrock slopes of the mountain. The flow of surface water is intermittent and subject to flash flood episodes, typically occurring in response to small, intense storms of brief duration. Because of a lack of perennial streams, sediment transport also is intermittent and, in the long term, slow. Sediment storage between upland slope and basin floor is manifested in a variety of constructional landforms, including colluvial wedges, talus cones, alluviated valley floors, and alluvial fan segments. The late and middle Pleistocene ages of many of these landforms (as indicated by soil development, rock-varnish development, and radiometric ages (Swadley et al., 1984; Rosholt et al., 1985; Reheis, 1986)) attest to the slow and discontinuous nature of sediment transport throughout the region.

1.1.3.2 Average erosion rates in the region surrounding Yucca Mountain

Average late Tertiary and Quaternary erosion rates for local areas of the southern Great Basin and the northern Mojave Desert can be inferred from differences in height between active and relict basalt-capped erosion surfaces (Marchand, 1971; Dohrenwend et al., 1984, 1985; Turrin and Dohrenwend, 1984). Estimates based on this approach for several widely separated upland areas are compiled in Table 1-2. The average downwasting rates in these areas range between 0.8 and 4.7 cm per 1,000 yr for periods of 0.67 to 10.8 million years. The differences in these average rates show no apparent relation to regional variations in late Tertiary and Quaternary vertical tectonic activity. Thus, it would appear that the general degradation of upland areas in the region surrounding Yucca Mountain is proceeding relatively slowly. However, it should be emphasized that the rates compiled in Table 1-2 are long-term (millions to tens of millions of years) averages that understate the potential significance of the short-term (tens of thousands to hundreds of thousands of years) episodes of intense erosion that occur locally whenever critical-process thresholds are crossed.

On the other hand, examples of local erosion during individual storm events substantially overstate even the short-term effects of threshold-related erosion episodes. The instantaneous (relative to geologic time) erosion that may occur during an individual storm cannot be meaningfully extrapolated to even short-term erosion rates without detailed knowledge of (1) the local occurrence of similar storm events and (2) the complex temporal and spatial relations between erosion and deposition in intermittent drainage systems.

1.1.3.3 Significant late Quaternary geomorphic processes in the Yucca Mountain area

1.1.3.3.1 Tectonic and volcanic processes

During the Quaternary, tectonic and volcanic processes in the Yucca Mountain area have included (1) slow (less than 3 cm/1,000 yr) relative vertical tectonic adjustment (vertical fault displacement or burial of dated basalt flows) (Carr, 1984); (2) local surface faulting along the eastern and possibly the western flank of Bare Mountain, along the eastern and western flanks of Yucca Mountain, and in Crater Flat (Carr, 1984; Swadley et al., 1984; USGS, 1984; Section 1.3.2); (3) horizontal movement on these fault systems (Reheis, 1986; Whitney et al., 1986; Yount et al., 1987); and (4) local Strombolian volcanic activity from seven basaltic centers located 8 to 40 km from the proposed repository (Vaniman and Crowe, 1981; Section 1.3.2.1.2). The effect of these intermittent and localized constructional processes on the late Quaternary landscape of the Yucca Mountain area has been limited, and their impact on the magnitude and the distribution of degradational processes in the area is limited to areas in the immediate vicinity of these fault zones and volcanic centers. Comparable tectonic and volcanic activity over the next 10,000 yr would likely induce a comparably limited effect on the (late Quaternary) landscape of the Yucca Mountain area.

Table 1-2. Erosion rates in upland areas of the southwestern Basin and Range Province inferred from height differences between active and relict basalt-capped erosion surfaces

Location	Minimum age of relict erosion surface (my)[a]	Maximum average downwasting rate (cm/10^3 yr)	Reference
Buckboard Mesa volcanic plateaus, Goldfield block	2.82	4.7	Carr, 1984
Cima volcanic field, Mojave Desert	3.88 3.64	2.8 2.5	Dohrenwend et al., 1984
	0.85 0.67	3.8 3.0	
Lunar Crater volcanic field central Great Basin	1.08 2.86	1.1 0.8	Dohrenwend, 1987
Reveille Range, central Great Basin	5.7 3.8	3.1 1.6	Dohrenwend et al., 1985
White Mountains east flank, Mono-Inyo block	10.8 10.8	2.4 2.0	Marchand, 1971

[a]my = million years.

1.1.3.3.2 Surficial processes

Estimates of latest Tertiary and Quaternary vertical tectonic movement (Carr, 1984; Section 1.3.2.4), estimates of late Quaternary climatic history (Section 5.2.1), and the general geomorphic characteristics of the Yucca Mountain area (Section 1.1.2) indicate that only a limited number of geomorphic processes involving the significant movement of surficial materials have been operating in the Yucca Mountain area during the late Quaternary. These processes are (1) degradation of upper upland slopes by weathering, talus formation, colluviation, and surface-wash processes; (2) degradation of lower upland slopes by colluviation and gully formation on interfluves and by intermittent streamflow in gullies and valleys; (3) alternating degradation and aggradation by intermittent streamflow in lower valley and upper piedmont areas; (4) net aggradation by intermittent streamflow in lower piedmont and basin areas; and (5) eolian deposition on piedmonts and, locally, on lower upland slopes.

Landscape degradation in the southwest Basin and Range Province is dominated by a general pattern of upland erosion, piedmont transport, and basin deposition. Erosion is generally most rapid in upland areas of concentrated fluvial activity; however, erosion is relatively slow in caprock-protected areas, where surface materials are either too permeable or too resistant to permit the integration of drainage lines. In the specific case of Yucca Mountain, crestal areas and upper slopes are effectively protected by the quartz-latitic upper part of the Tiva Canyon Member of the Paintbrush Tuff (Scott and Bonk, 1984). Dip-slope drainage lines are broad, shallow, and widely spaced and, where preserved, dip-slope surfaces are generally only slightly dissected. The upper slopes of the mountain immediately beneath these caprock-protected surfaces are relatively smooth and little dissected. The long-term stability of these slopes is indicated by discontinuous mantles of darkly varnished blocky talus.

Similarly varnished talus slopes in the northern Mojave Desert are at least late-middle Pleistocene or early-late Pleistocene in age. For example,

in the area of the Cima volcanic field, such slopes support well-developed soils with thick Bk horizons (B horizons impregnated with pedogenic carbonate) containing abundant clay films and stage III carbonate accumulations (continuous carbonate cement and fillings) (Dohrenwend et al., 1984). In the Tecopa Basin (near southern Death Valley), such slopes locally preserve high shorelines of late-middle or early-late Pleistocene Lake Tecopa (Dohrenwend, 1985). The widespread occurrence of darkly varnished talus on the upper slopes of Yucca Mountain and adjacent buttes suggests the general long term erosional stability of this entire upland area. Additionally, a detailed and comprehensive analysis of the rock varnish on these talus deposits (including age estimates based on the relative abundance of soluble and insoluble cations within the varnish) is planned (Section 8.3.1.17.4). Additional evidence indicating the long-term stability of hillslopes in the Yucca Mountain area is provided by the preservation of late Pleistocene Neotoma (pack rat) middens in small caves and rock overhangs on steep slopes

Breccia is common, as are small, closely spaced faults. The other three slide blocks, also situated in steep midslope areas, are located on the steep west-facing scarp of Yucca Mountain. These blocks are very small, ranging from 0.01 to 0.03 km^2 in area. All of these blocks were identified on the basis of offset bedrock stratigraphy; none displays morphologic characteristics suggestive of recent movement.

The lower upland slopes and piedmonts of the Yucca Mountain area also are generally stable. The average downwasting rates over the past 1 to 5 million years have been 0.5 to 2.0 cm/1,000 yr on lower range flanks and proximal piedmont areas and less than 0.5 cm/1,000 yr in middle and distal piedmont areas. These rates are documented by relations between relict erosion surfaces buried by lava flows (dated by the potassium-argon method) and modern erosion surfaces in the Cima volcanic field of the northern Mojave Desert and the Pancake and Reveille Ranges of the central Great Basin (Dohrenwend et al., 1984, 1985). In the immediate vicinity of Yucca Mountain, slightly to moderately dissected piedmont surfaces underlain by middle to late Pleistocene alluvial deposits dominate proximal piedmont areas in the eastern and northern part of Crater Flat, in the northern part of Jackass Flats, and in Rock Valley (Swadley et al., 1984). Moreover, the presence of four basaltic centers dated by the potassium-argon method and associated flows within a few meters of the modern surface of Crater Flat demonstrates that this gently sloping alluvial plain has remained in a state of approximate erosional-depositional equilibrium along at least half of its 24-km length for the past 1.1 million years (Vaniman and Crowe, 1981; Swadley et al., 1984).

Eolian processes have further reduced the generally slow rates of landscape degradation in many areas of the southwest Basin and Range province. Silt and fine sand deflated from basin and distal piedmont areas have been

redeposited as loess blankets and sand sheets across large areas of adjacent piedmonts. Piedmont surfaces mantled with sand sheets can be highly stable. In northern Jackass Flats, a sand sheet veneering the south-sloping piedmont of the Calico Hills has been dated by uranium-trend analysis at 160,000 $\pm$90,000 yr (Rosholt et al., 1985). Although the average deposition rate of these eolian veneers is generally low (even in the ideal traps afforded by the rough, permeable surfaces of basaltic lava flows (Wells et al., 1985a)), these deposits significantly slow degradational processes on piedmont surfaces. The permeable sand sheets limit surface runoff, and the nearly ubiquitous desert loess (the silt-rich vesicular A horizon of most piedmont soils) plays a crucial role in the formation of the stone pavements that armor most abandoned piedmont surfaces (McFadden et al., 1985). Moreover, in areas of concentrated eolian activity, climbing and falling dunes locally form sand ramps as much as 6 km long and 150 m high that almost completely bury the lower flanks of the smaller ranges (H.T.U. Smith, 1967; R.S.U. Smith, 1982). On the eastern side of Yucca Mountain, the west flanks of Fran

Although the Yucca Mountain area has generally been geomorphically stable, episodes of rapid erosion have occurred locally in areas of concentrated fluvial activity (e.g., the ravines, valleys, and washes of the mountain and its adjacent piedmonts). In these areas, the rates of stream incision, averaged over the past 0.15 to 0.3 million yr range from 5.3 to 37.5 cm/1,000 yr (Table 1-3). Within environments characterized by arid climates and low rates of vertical tectonic activity, geomorphic processes operate intermittently over the short as well as the long term, and episodes of rapid erosion and deposition are generally restricted in both time and space. At any given time, a variety of climatic, physiographic, and geologic factors may combine in local areas to exceed a critical process threshold, thereby inducing a rapid, short-term geomorphic change that slows asymptotically as the landscape adjusts to a new condition of relative stability.

Table 1-3. Average rates of stream incision in the Yucca Mountain area

Location	Geomorphic setting	Approximate age of the incised surface (my)[a]	Average rate of incision ($cm/10^3$ yr)	Age reference
Busted Butte, west flank	Valleys and ravines incising eolian sand ramps	0.24	37.5	Whitney et al., 1985
Fortymile Wash	Entrenched wash on proximal piedmont	0.16 0.30	5.3 8.5	Swadley et al., 1984
Yucca Mountain east valleys	Consequent valleys incising caprock-protected dip slopes	10.0	1.2-1.9	Scott and Bonk, 1984

[a]my = million yr.

A particularly [illegible] example of threshold-controlled erosion in arid drainage has become well established, incision proceeds rapidly but then quickly slows as equilibrium with the surrounding upland-source drainage is asymptotically approached.

Applying this general scenario to the specific case of fluvial degradation on Yucca Mountain suggests (1) that the consequent valleys that incise the east-facing dip slopes of the mountain may have been formed by relatively short lived episodes of intense erosion and (2) that the subsequent degradation of these valleys has been modest relative to the initial period of incision. This interpretation is consistent with the documented stability of the surrounding piedmonts and the apparent stability of the upper slopes of the mountain. Whatever the case, whether these valleys were formed gradually over the 10-million-year degradational history of the mountain or rapidly during a short-lived interval of intense erosion, the possibility of a sustained period of rapid valley incision in the future appears to be remote.

1.2 STRATIGRAPHY AND LITHOLOGY

This section describes the stratigraphic framework and characteristic lithologies of rocks and surficial deposits in the Yucca Mountain area and in the surrounding southern part of the Great Basin (Figure 1-9). Specifically, this section provides stratigraphic and lithologic information characterizing the rock sequence and the surficial deposits at the Yucca Mountain site. The descriptions given here respond to investigations in characterization programs 8.3.1.4 (rock characteristics), 8.3.1.14 (surface characteristics), and 8.3.1.15 (thermal and mechanical properties).

This section also provides a basis for further discussion of the physical (Chapter 2), geochemical/alteration (Chapter 4), and hydrologic (Chapter 3) properties of the host rock sequence in the controlled area. These properties are the basis for design and performance assessment.

To adequately establish the stratigraphic relationships and characterize the lithology of rocks in the Yucca Mountain area, the stratigraphic sequence is considered here at both local and regional scales. Descriptions of rocks proceed from oldest to youngest unless otherwise noted.

The proposed host rock for the proposed repository is the welded and devitrified part of the Topopah Spring Member of the middle Miocene Paintbrush Tuff, one of several thick ash-flow tuffs of middle to late Tertiary age in the upper part of the stratigraphic sequence at Yucca Mountain. The Topopah Spring Member was selected as the proposed host rock because of its lateral continuity, dense welding, and stratigraphic setting above a major aquitard (Chapter 3) (Johnstone et al., 1984). The host rock lies in the upper part of a thick volcanic sequence, which is as much as 3,000 m thick in the Yucca Mountain area. Volcanic rocks, present over much of the southern Great Basin, are described here as the Cenozoic part of the sequence. Rocks below the volcanic sequence in the Yucca Mountain area and the surrounding southern Great Basin consist mainly of carbonate and detrital rocks of Proterozoic, Paleozoic, and Mesozoic age. These rocks, described here as the pre-Cenozoic part of the sequence, form regional aquifers and aquitards (Section 3.6).

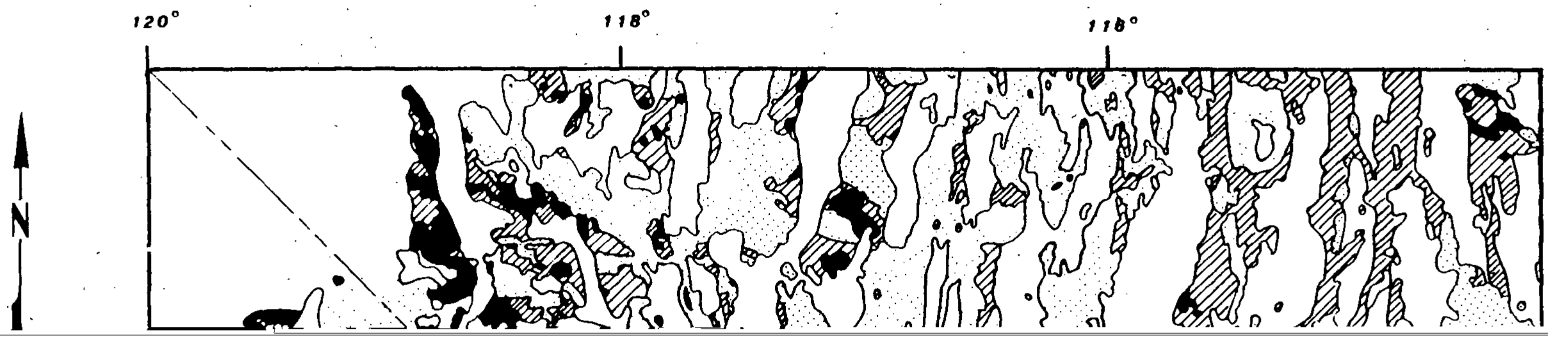
120°
118°
118°
N

Also included are descriptions of a variety of surficial deposits that flank Yucca Mountain and are locally present over much of the region. Surficial deposits include soil, alluvial, eolian, and lacustrine deposits formed in present-day topographic and structural basins. These surficial deposits will be considered in designing the surface facilities and in assessing the ages of movement on Quaternary faults with respect to the long-term performance of the repository.

1.2.1 STRATIGRAPHY AND LITHOLOGY OF ROCKS AND SURFICIAL DEPOSITS IN THE SOUTHERN GREAT BASIN

Geologic formations, hydrogeologic units, and the lithologic character of pre-Cenozoic and Cenozoic rocks in the southern part of the Great Basin are shown on Figure 1-10. The sequence ranges from early Proterozoic to Quaternary in age and consists of igneous, metamorphic, and sedimentary rock, as well as a thin veneer of unconsolidated surficial material. Not including early Proterozoic crystalline basement rocks, the combined thickness of the

pre-Cenozoic and Cenozoic parts of the sequence in the southern part of the Great Basin may extend over 18,000 m locally. The pre-Cenozoic and Cenozoic parts of the sequence are separated by a regionally significant unconformity, which is easily recognized in outcrop and drillholes, and is commonly discernible in the subsurface by geophysical means. The unconformity is a major regional stratigraphic marker that delineates the base of the Tertiary sequence throughout the southern part of the Great Basin. The boundary is distinctive because of the significant difference in lithology and mode of origin of rocks above and below the boundary. Surficial deposits rest on a

extensive.

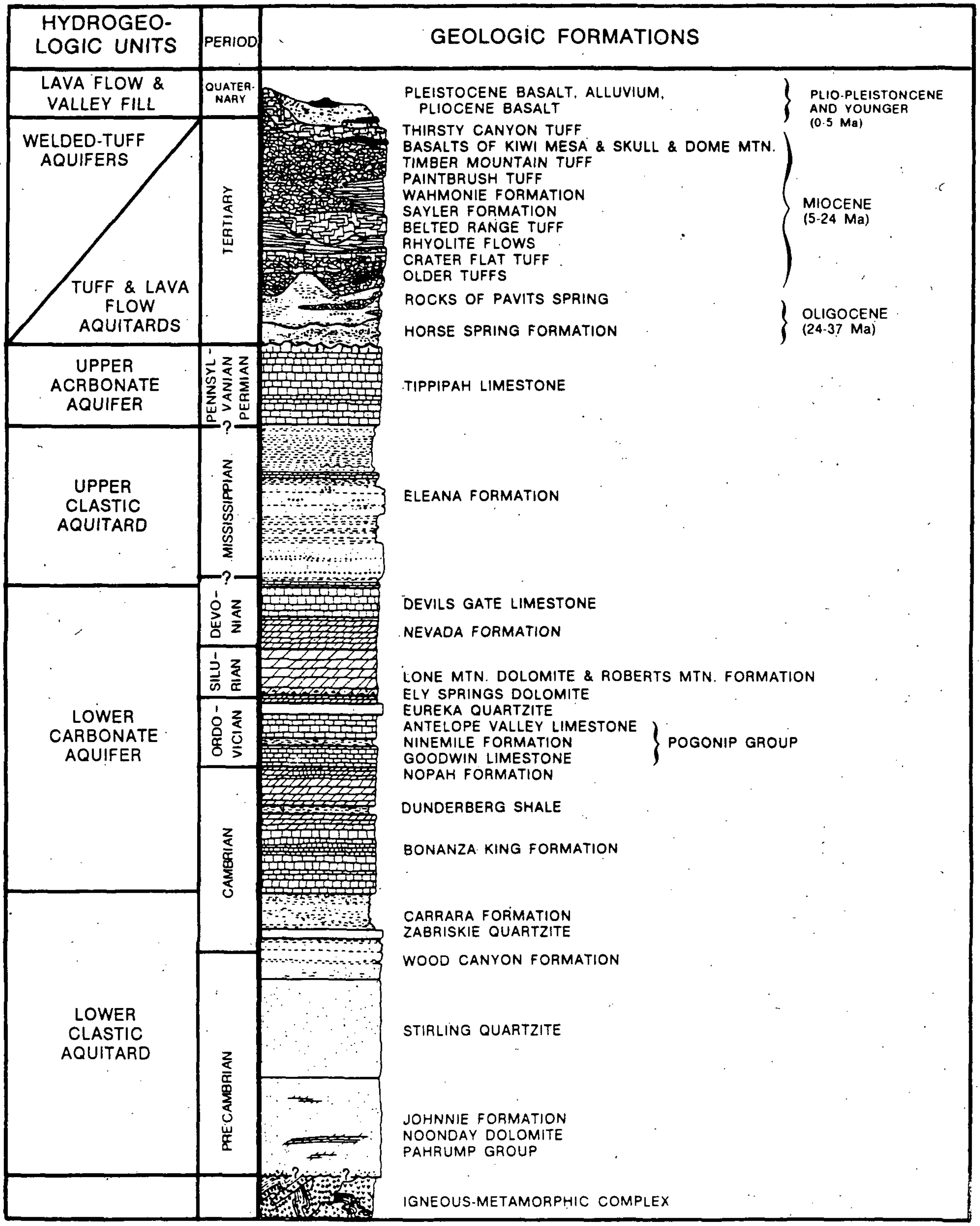

Figure 1-10. Generalized regional stratigraphic column showing geologic formations and hydrogeologic units in the Nevada Test Site area. Modified from Sinnock (1982) and Carr et al. (1986).

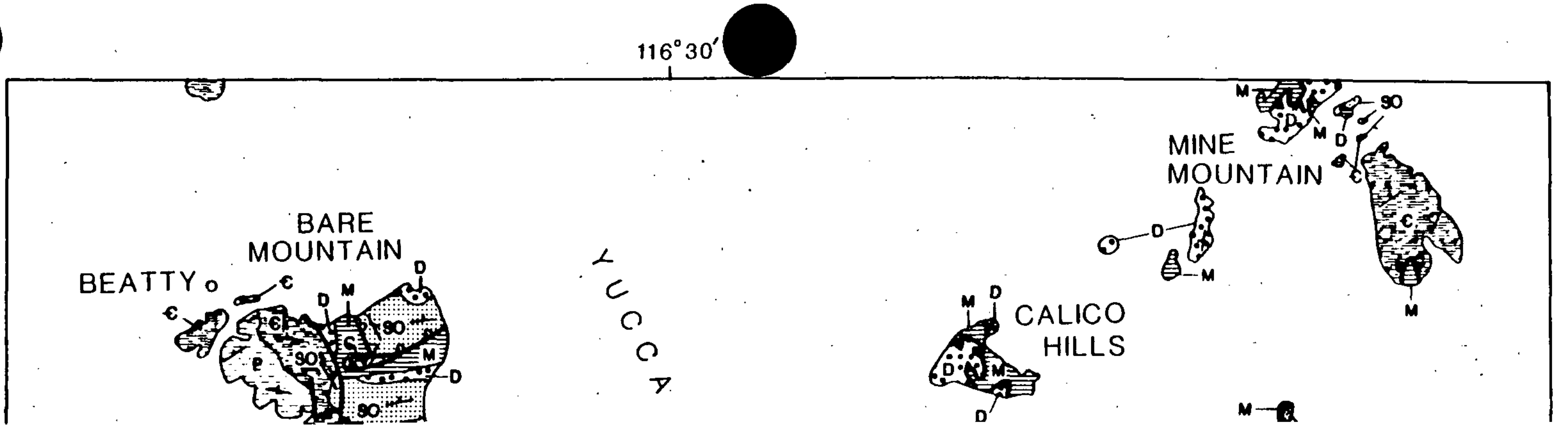
116°30′
BEATTY
BARE MOUNTAIN
YUCCA
CALICO HILLS
MINE MOUNTAIN
SO
D
M

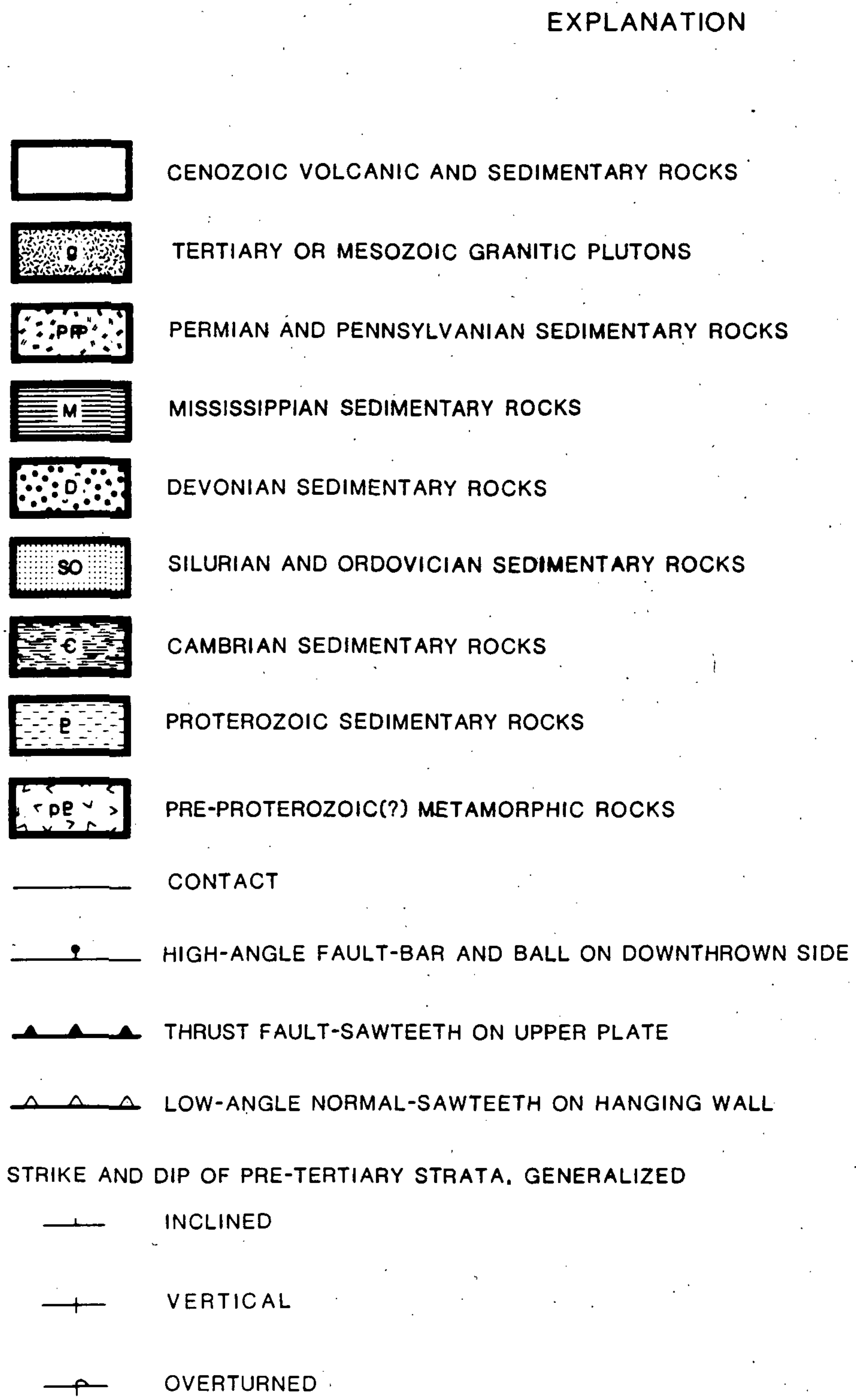

Figure 1-11b. Legend for index map showing the location and extent of pre-Cenozoic rock outcrops in the area surrounding Yucca Mountain. Modified from Robinson (1985).

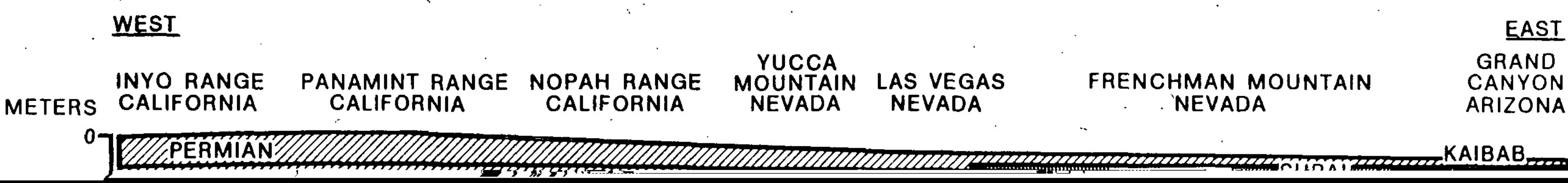
WEST
EAST
METERS
0
INYO RANGE CALIFORNIA
PANAMINT RANGE CALIFORNIA
NOPAH RANGE CALIFORNIA
YUCCA MOUNTAIN NEVADA
LAS VEGAS NEVADA
FRENCHMAN MOUNTAIN NEVADA
GRAND CANYON ARIZONA
PERMIAN
KAIBAB

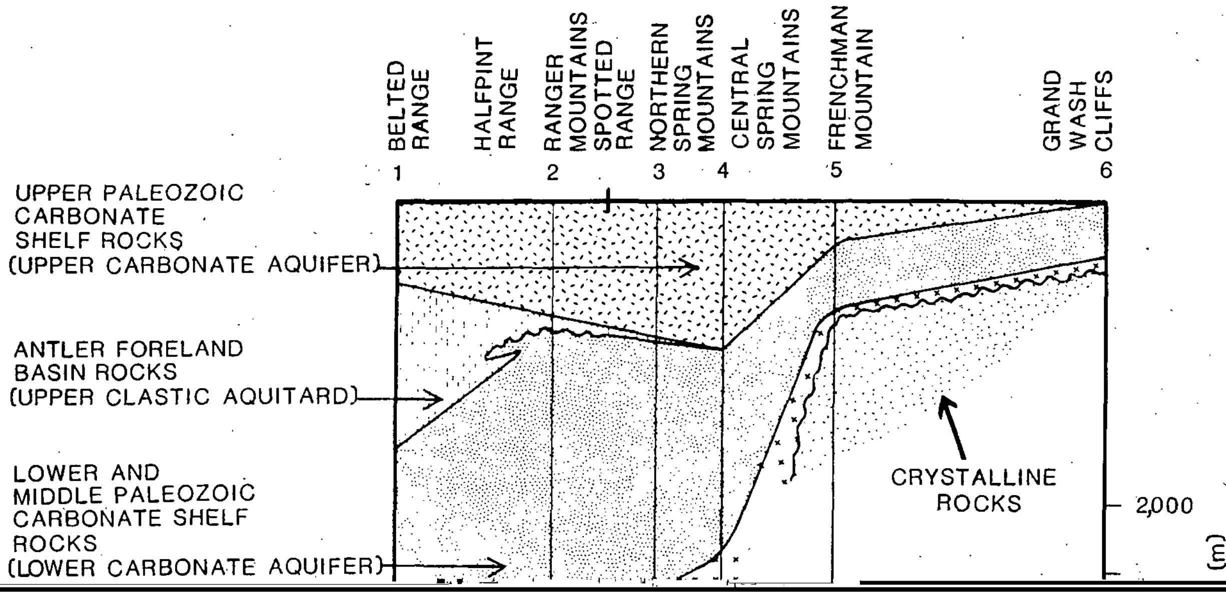
BELTED RANGE
HALFPINT RANGE
RANGER MOUNTAINS SPOTTED RANGE
NORTHERN SPRING MOUNTAINS
CENTRAL SPRING MOUNTAINS
FRENCHMAN MOUNTAIN
GRAND WASH CLIFFS
1
2
3
4
5
6
UPPER PALEOZOIC CARBONATE SHELF ROCKS (UPPER CARBONATE AQUIFER)
ANTLER FORELAND BASIN ROCKS (UPPER CLASTIC AQUITARD)
LOWER AND MIDDLE PALEOZOIC CARBONATE SHELF ROCKS (LOWER CARBONATE AQUIFER)
CRYSTALLINE ROCKS
2,000
(m)

southwest of Yucca Mountain (Jennings, 1977). Similar gneiss and schist of equivalent or younger age also crop out north and northwest of Yucca Mountain in the Bullfrog and Trappman Hills (Stewart and Carlson, 1978) and in the Grand Canyon region approximately 375 km southeast of Yucca Mountain (Figure 1-14). Although unconfirmed by drilling, rocks of similar lithology and equivalent age also are probable at depth in the Yucca Mountain area.

Younger Precambrian rocks (middle to late Proterozoic) rest unconformably on the early Proterozoic gneiss and schist and are divided, in ascending order, into the Pahrump Group and the Noonday Dolomite. Pahrump rocks locally attain a thickness of about 2 km and consist of sandstone, conglom-

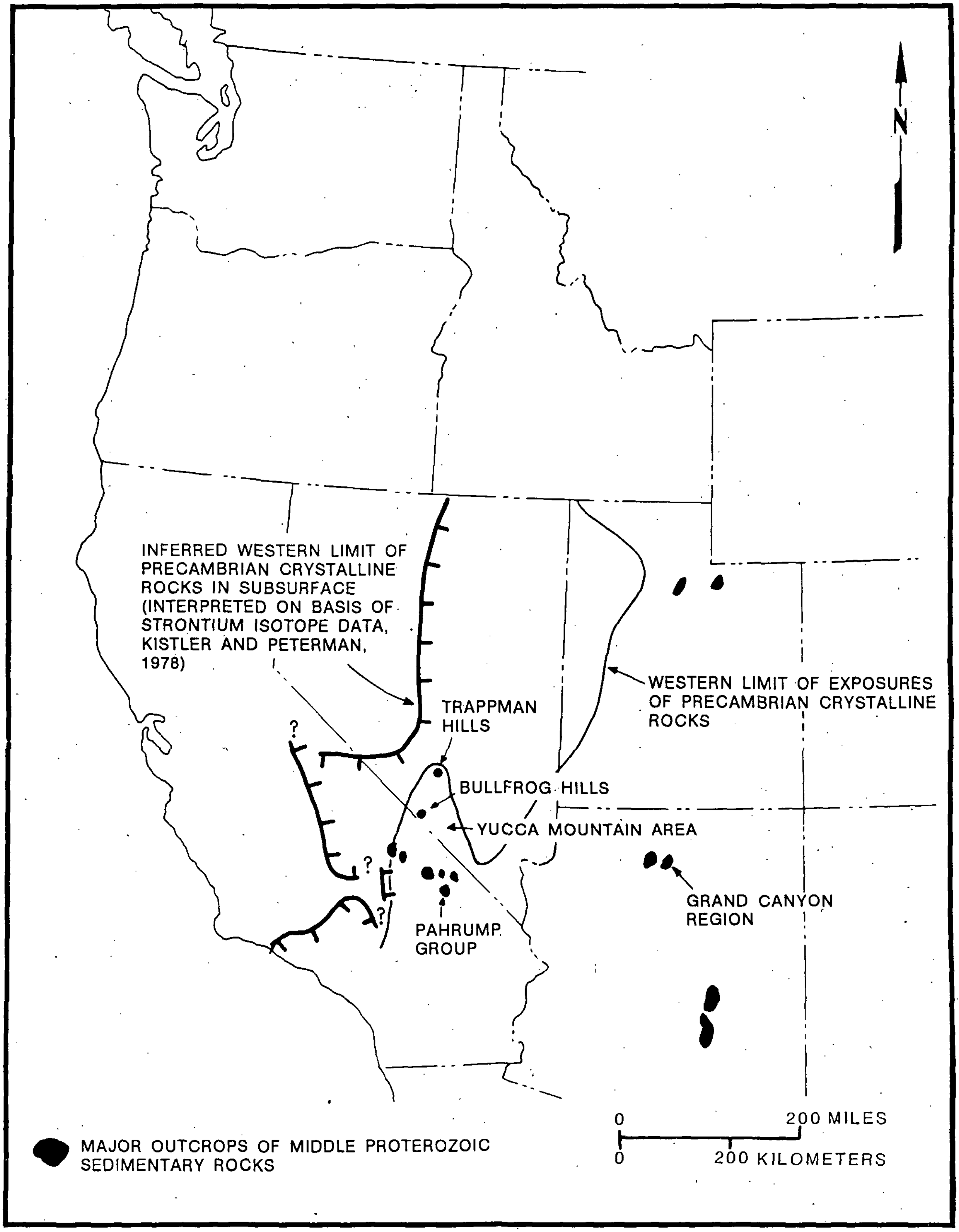

Figure 1-14. Distribution of Lower and Middle Proterozoic crystalline rocks and Middle and Upper Proterozoic restricted basin deposits in the Great Basin. Modified from USGS (1984).

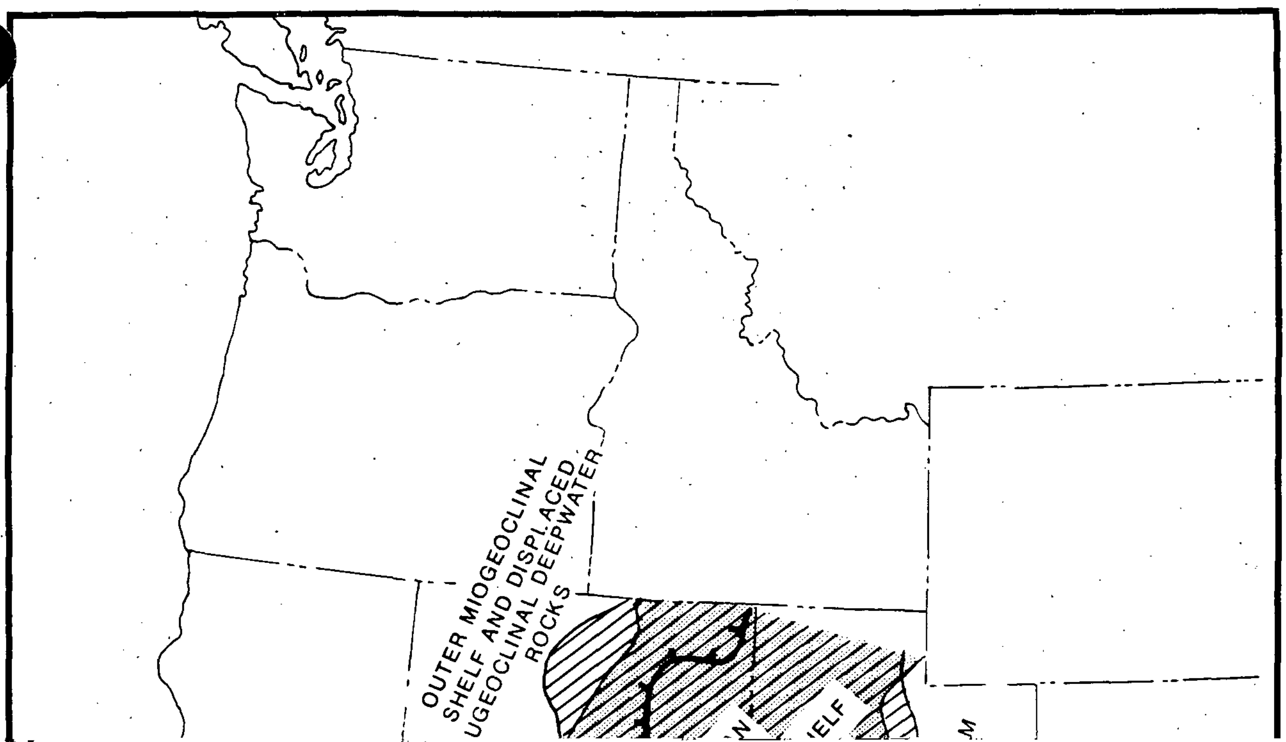
OUTER MIOGEOCLINAL
SHELF AND DISPLACED
UGEOCLINAL DEEPWATER
ROCKS

In Late-Devonian and Early Mississippian time an orogenic highland (Antler orogenic belt) is interpreted to have formed in the area of the outer [illegible]

in the upper part of the continental shelf in the vicinity of the southern Great Basin (Figure 1-16). The trough has been described as the Antler foreland flysch basin (Poole, 1974). The Upper Devonian and Mississippian Eleana Formation, a sequence of argillite, quartzite, conglomerate, and limestone more than 2,300 m thick, was deposited in the trough. This and other associated clastic units comprise the upper of two regionally important aquitards in the Paleozoic rock sequence (Figure 1-13). The foreland flysch basin deposits thin and become finer grained toward the east, where the basin shallowed against the western flank of the continental craton. In the southern and eastern parts of the Great Basin, clastic basin deposits grade into continental shelf carbonate rocks equivalent to the Eleana Formation.

Carbonate platform-facies rocks, including the Tippipah Limestone (more than 1,000 m thick), were deposited on top of the Mississippian flysch basin deposits during the Pennsylvanian and Early Permian. These upper Paleozoic carbonate rocks comprise the upper aquifer in the eastern part of the area. According to Winograd and Thordarson (1975), the upper carbonate aquifer is probably not present in the Yucca Mountain area.

1.2.1.1.2 Mesozoic rocks

Sedimentary and igneous rocks of Triassic, Jurassic, and Cretaceous age are locally present in the southern part of the Great Basin. Mesozoic rocks unconformably overlie older Paleozoic and Proterozoic rocks. Sedimentary rocks include marine and nonmarine sequences. Triassic and Jurassic rocks include sandstone, shale, and limestone of the Moenkopi Formation; sandstone, siltstone, and shale of the Chinle Formation; and sandstone of the Aztec Sandstone (Longwell et al., 1965). Mesozoic sedimentary rocks crop out in the Spring Mountains, about 80 km southeast of Yucca Mountain (Stewart and

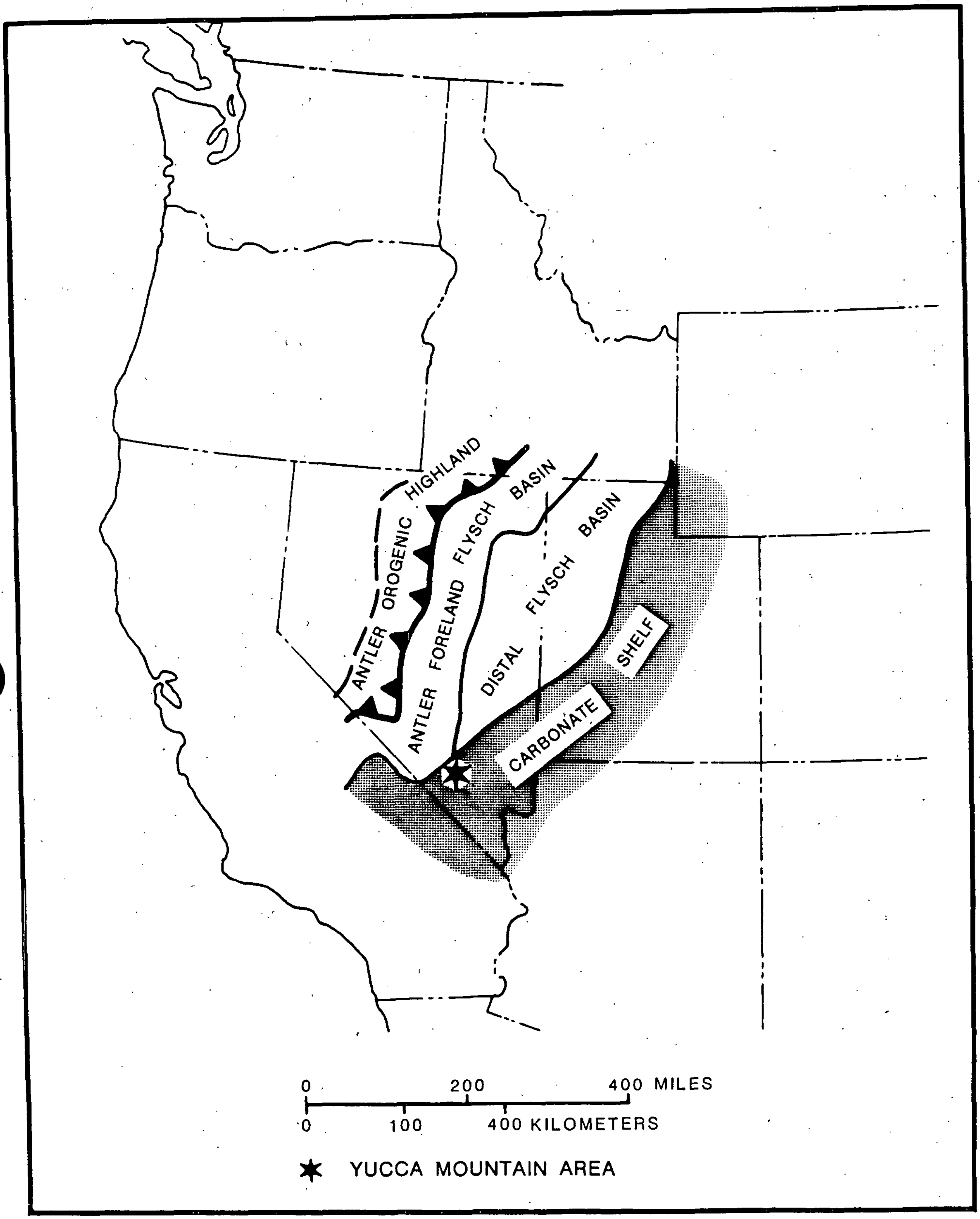

Figure 1-16. Late Devonian and Mississippian paleogeography of the Great Basin. Modified from USGS (1984).

1.2.1.2 Cenozoic rocks

Cenozoic rocks of the southern part of the Great Basin are both sedimentary and volcanic. Most are extrusive volcanic rocks of late Eocene to Holocene age. The Eocene and Miocene volcanic sequence is dominantly silicic, accounts for most of the bedrock exposed in the region (including all the exposure at Yucca Mountain), and is over 3,000 m thick. The Pliocene to Holocene volcanic rocks are basaltic and relatively thin.

[illegible]

sequences near the base of the Cenozoic sequence, range locally from 1,500 to 3,000 m in thickness and consist of breccia, conglomerate, sandstone, shale, and thin limestone beds deposited locally in intermontane basins and calderas. These deposits commonly originated as alluvial fans in fluvial systems and in lacustrine environments which occupied some of the basins and inactive caldera complexes. Many local formation names have been used to name these rocks throughout the region. In the vicinity of Yucca Mountain, these rocks are included in the Titus Canyon and Pavits Spring Formations. Elsewhere in the region, they are included in the Esmerelda, Horse Spring (Figure 1-10), Muddy Creek, Artist Drive, Furnace Creek, and the Nova Formations (Grose and Smith, 1984).

1.2.1.2.1 Late Eocene to late Miocene volcanic rocks

Voluminous quartz-latite and rhyolite ash-flow sheets were erupted between 32 and 16 million years ago from large caldera complexes in central and southern Nevada (Marvin et al., 1970, 1973; Ekren et al., 1971, 1973, 1974a; Gromme et al., 1972; Stewart and Carlson, 1976). The distal ash-flow deposits of some of these ash-flow sheets reached the northern part of the southern Great Basin. Large volumes of rhyolite ash and lava were erupted intermittently between about 16 and 8 million years ago from numerous coalesced caldera centers north of Yucca Mountain (Byers et al., 1976a; Christiansen et al., 1977). The volcanic rocks that underlie Yucca Mountain were emplaced about 14 to 11 million years ago during the culminating phases of this episode of caldera eruptions. During the past 10 to 8 million years, most volcanism has been confined to southern Death Valley (12 to 4 million years) and the region to the west (i.e., Owens Valley, Argus Range, and Coso and involved bimodal basalt-rhyolite eruption during the latter stages of silicic volcanism, which dominated the region in early to middle Miocene time in the southern Great Basin. This episode involved the discharge of large volumes of basaltic and rhyolitic lava. The second episode of basaltic eruption, known as the older rift basalt episode (Crowe et al., 1986), gradually replaced the initial episode. During the second episode, the volume of lava drastically decreased. These basalts range in age from 9 to 6.5 million years. The third and least voluminous episode of basaltic eruption occurred after a pause in volcanic activity (from 6.5 to 3.7 million years ago). This episode occurred from 3.7 to perhaps as recently as 0.1 million years before present (Sinnock and Easterling, 1983) and has been called the younger rift basalt episode by Crowe et al. (1986). Additional data on the age of the third episode of basaltic activity will be collected during site characterization (Section 8.3.1.8). No rhyolitic deposits less than 6 million years old are known to have originated from volcanic centers in the southern Great Basin; however, rhyolitic cones as young as 10,000 yr old occur along the western margin of the southern Great Basin in the Long Valley-Mono Basin and Coso area of eastern California.

1.2.1.3 Surficial deposits

Surficial deposits of late Tertiary and Quaternary age veneer the volcanic bedrock sequence over most of the region (Figure 1-9,). These deposits become quite thick locally and consist of fluvial deposits associated with alluvial fans, playa deposits, lacustrine deposits (formed locally in some closed intermontane basins), colluvium, and eolian deposits. The character and type of most surficial deposits depend mainly on the composition of bedrock, the tectonic setting (Section 1.3), the topography

(Section 1.1), and the climatic patterns (Chapter 5) that have developed.

Surficial deposits are mainly alluvial fan deposits eroded from tectonically developing highlands and deposited on adjacent piedmont slopes. These deposits, in turn, commonly merge with floodplain deposits and eolian sand sheets and dunes on the basin floors. Scattered spring, pond, and lacustrine deposits occur in some intermontane basins.

1.2.2 STRATIGRAPHY AND LITHOLOGY OF ROCKS AND SURFICIAL DEPOSITS AT YUCCA MOUNTAIN

The rocks at Yucca Mountain (Figure 1-17) comprise a gently dipping sequence of Miocene ash-flow tuffs, lavas, and volcanic breccias more than 1,800 m thick, intercalated with relatively thin units of volcaniclastic rocks and flanked by younger alluvial deposits. Surface mapping (Christiansen and Lipman, 1965; Lipman and McKay, 1965; USGS, 1984), supplemented by data from core and drillholes as deep as 1,800 m (Figures 1-18, 1-19, and 1-20), provides excellent stratigraphic data on the upper part of the Yucca Mountain sequence. These data indicate that individual units in the upper part of the volcanic sequence are laterally continuous in the vicinity of

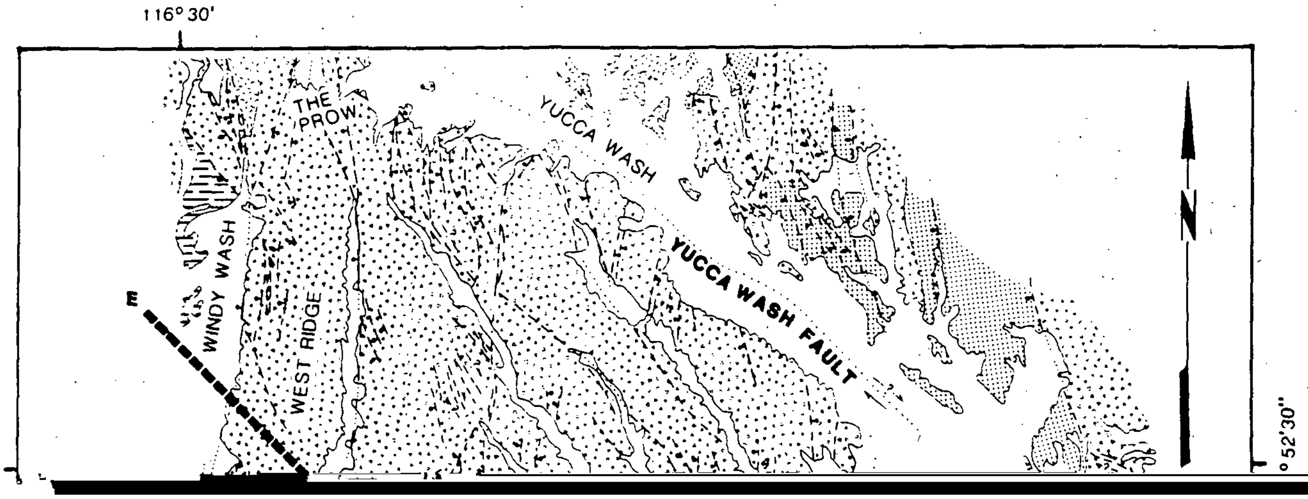
116° 30'
THE PROW
YUCCA WASH
WINDY WASH
WEST RIDGE
YUCCA WASH FAULT
N
° 52'30"

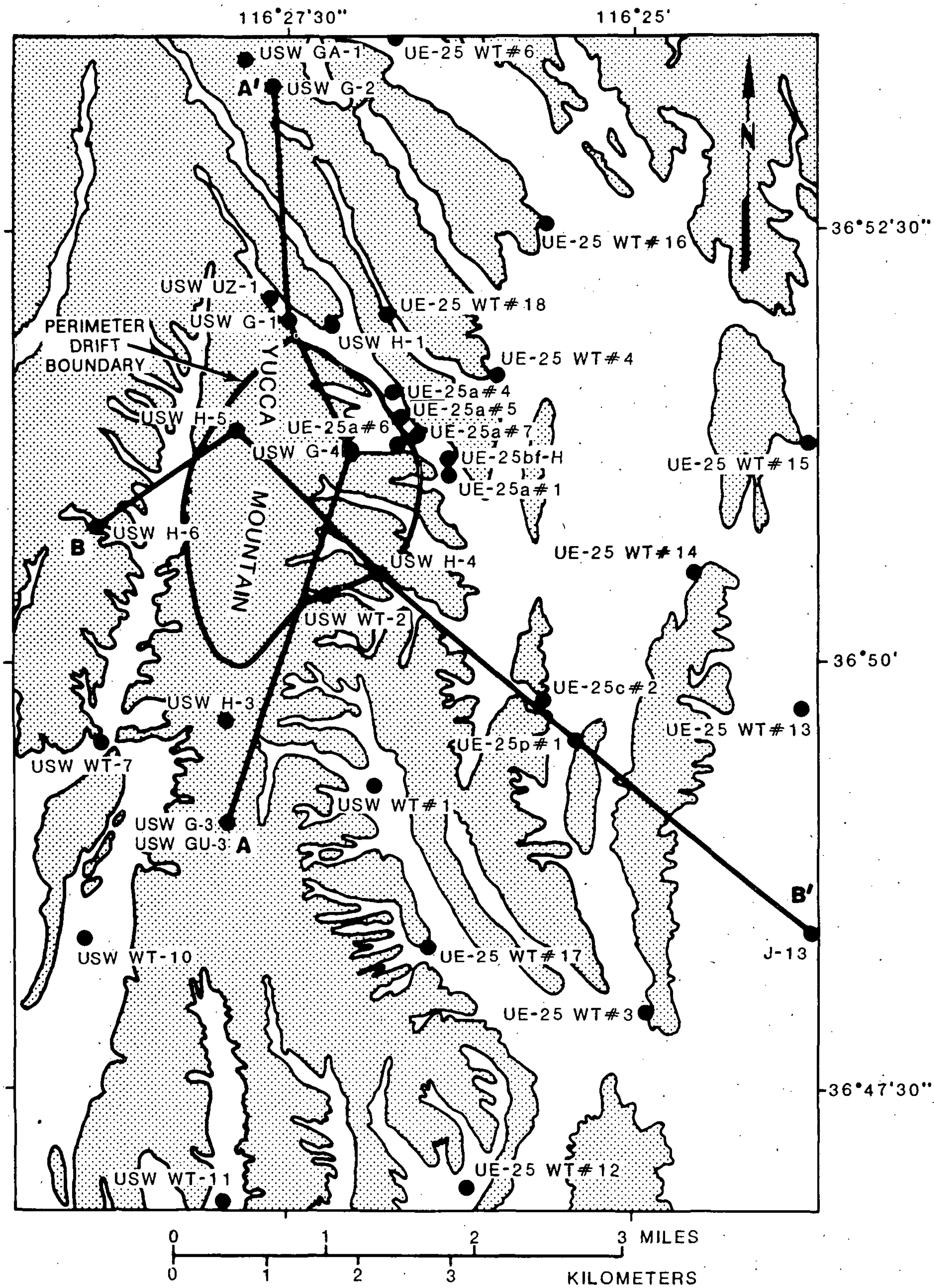

Figure 1-18. Index map showing the locations of selected drillholes in the vicinity of Yucca Mountain and the locations of cross sections shown on Figures 1-19 and 1-20. Modified from USGS (1984).

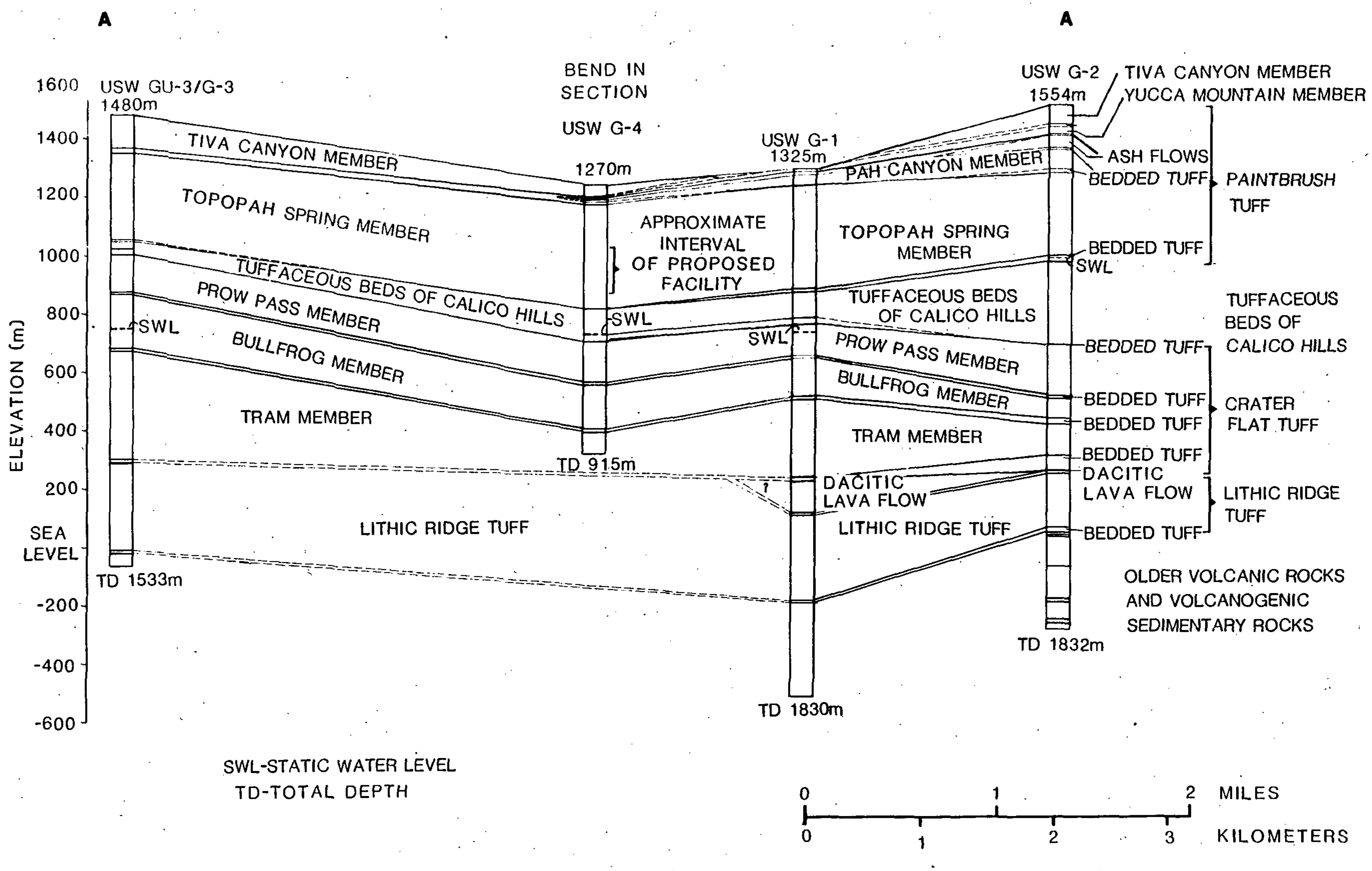

Figure 1-19. North-south stratigraphic correlation between selected drillholes at Yucca Mountain. Modified from USGS (1984).

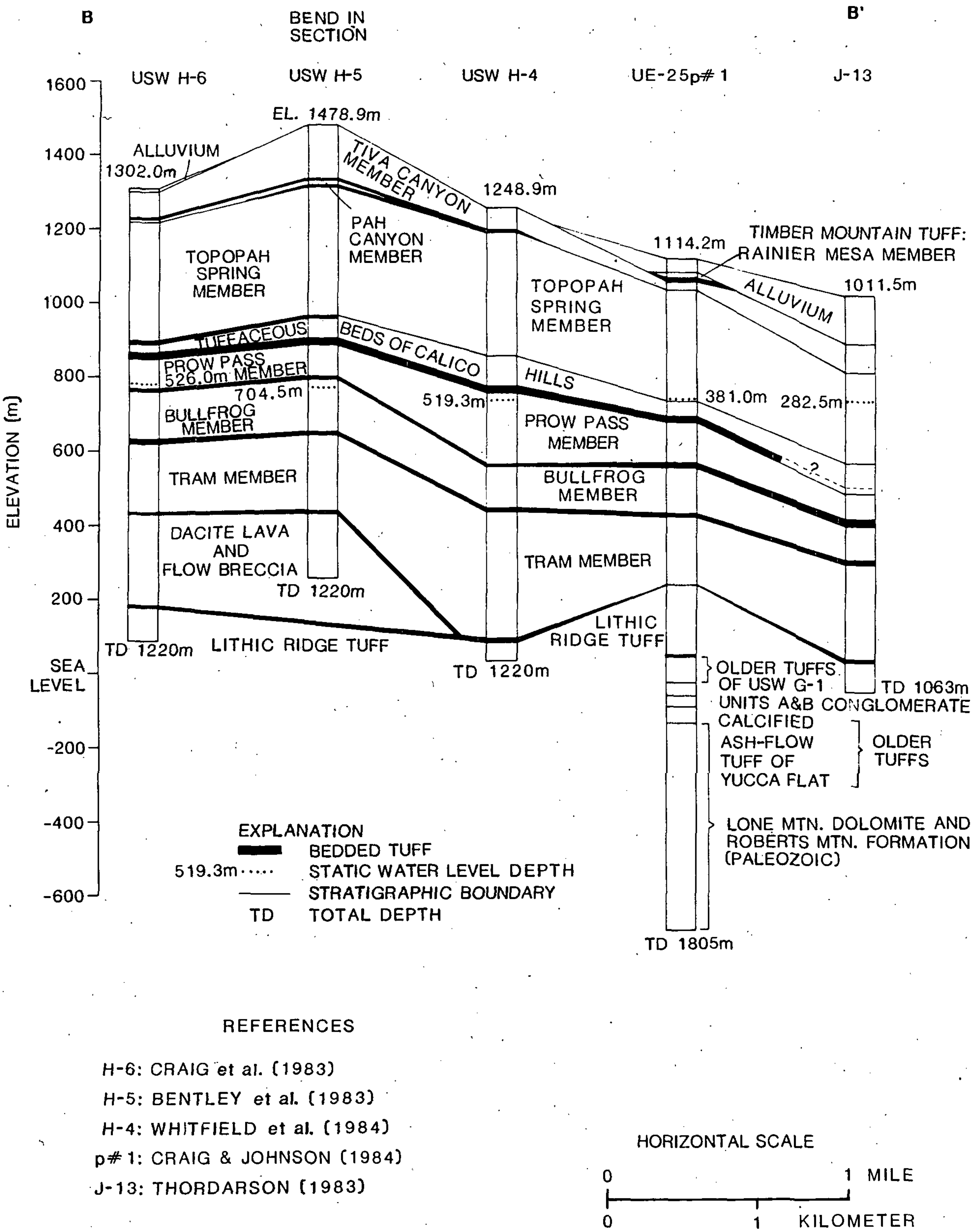

Figure 1-20. East-west stratigraphic correlation between selected drillholes at Yucca Mountain.

drillhole data. Only one drillhole in the Yucca Mountain area penetrates pre-Cenozoic rocks. The character of rocks below about 1,800 m is mainly inferred from geophysical data and the interpolation and extrapolation of data from the surrounding region.

Estimates based on borehole and geophysical data indicate that the depth to the subvolcanic surface (the contact between Cenozoic and pre-Cenozoic units) ranges from 1,000 m beneath the southeastern part of Yucca Mountain (drillhole UE-25p#1) to more than 3,500 m beneath the northwestern part (USGS, 1984).

1.2.2.1 Pre-Cenozoic rocks

Because of the sparsity of drillhole information with regard to the pre-Cenozoic rocks in the Yucca Mountain area, the regional stratigraphic column shown in Figure 1-10 must be viewed as an approximation of the Yucca Mountain pre-Cenozoic stratigraphic sequence. Figure 1-11 (Section 1.2.1.1), modified from Robinson (1985), shows the distribution of pre-Cenozoic rocks exposed in the vicinity of Yucca Mountain.

Drillhole UE-25p#1 (Figures 1-18 and 1-20) penetrates pre-Cenozoic rocks on the eastern flank of Yucca Mountain. This exploratory drillhole intersected dolomite at a depth of 1,244 m below the surface and continued in carbonate rocks to a total depth of 1,805 m. Rocks within the interval are assigned to the Lone Mountain Dolomite and the Roberts Mountain Formation (Muller and Kibler, 1984) of Silurian age. It is clear on the basis of data collected at this drillhole that at least part of Yucca Mountain is underlain by Silurian carbonate rocks, which are part of the lower carbonate aquifer of Winograd and Thordarson (1975) and USGS (1984).

Gravity data suggest that pre-Cenozoic rocks are at least 3,000 m beneath the surface under much of Yucca Mountain. Geophysical data and models that allow for this interpretation are discussed by Snyder and Carr (1982). Using only geophysical data Snyder and Carr (1982) were not able to determine whether the pre-Cenozoic rocks beneath Yucca Mountain are entirely upper Proterozoic and Paleozoic strata or if they also include younger intrusive rocks.

Beneath the northern part of Yucca Mountain, the Mississippian Eleana Formation may occur 2,200 to 2,400 m below the surface. Bath and Jahren (1984) interpreted relatively high intermediate-altitude aeromagnetic values at Yucca Mountain as signatures of a magnetized tabular body of slightly metamorphosed Eleana Formation, which may extend westward into the Yucca Mountain area from surface exposures in the Calico Hills 15 km to the northeast, where similar aeromagnetic values have been observed. It is further suggested by the data of Bath and Jahren (1984) that the subvolcanic basement at Yucca Mountain may contain deep-seated granitic rocks that provided a heat source for metamorphism of the Eleana Formation and adjacent pre-Cenozoic rocks that may be present.

1.2.2.2 Cenozoic rocks

The rock being considered as host for the repository is densely welded ash-flow tuff of the Topopah Spring Member of the middle Miocene Paintbrush Tuff. This volcanic unit is part of a 1,000- to 3,000-m-thick silicic volcanic sequence that consists of a series of welded and nonwelded ash-flow and ash-fall tuffs and lavas, and volcanic breccias derived from nearby calderas and volcanos about 14 to 11 million yr ago (Byers et al., 1976a; Christiansen et al., 1977; Carr et al., 1984). The volcanic rocks at Yucca Mountain and the adjacent region comprise seven formations (Figure 1-20, Table 1-4), some of which contain several members differentiated on the basis of lithologic or physical and chemical properties or both. Individual volcanic units at Yucca Mountain are laterally continuous and range in thickness from approximately 70 to approximately 370 m. Lava and flow breccias are fairly common in the subsurface in the northern part of Yucca Mountain but are rare in the southern part.

The stratigraphic framework of Tertiary volcanic rocks at Yucca Mountain has been determined by geologic mapping and the analysis of cores from several of the 36 drillholes that penetrate the upper part of the sequence (Figure 1-18). Table 1-4 shows the ages, magnetic polarities, and thickness of Tertiary rock units in the vicinity of Yucca Mountain, and Figures 1-19 and 1-20 show north-south and east-west cross sections. Intervals of bedded tuff generally only a few meters thick, but in places as much as 50 m thick, separate the welded tuff and other flow rock units. Poorly exposed and too thin to map at customary scales, the bedded tuff is nevertheless important to site characterization because its physical and chemical properties differ markedly from those of the flow rocks. Otherwise, the stratigraphic nomenclature essentially conforms to that originally applied by Christiansen and Lipman (1965), Lipman and McKay (1965), Orkild (1965), Byers et al. (1976a), and Carr (1984). Stratigraphic data obtained from the drillholes shown in Figure 1-18 are presented in detail by Spengler et al. (1979, 1981), Spengler and Rosenbaum (1980), Maldonado and Koether (1983), Rush et al. (1983), Scott and Castellanos (1984), and Spengler and Chornack (1984). The principal characteristics of the rocks are described below.

The physical properties of representative core samples of the Paintbrush Tuff, the tuffaceous beds of Calico Hills, and the Crater Flat Tuff have been described by a number of authors (Chapters 2 and 4). Anderson (1981, 1984) has measured bulk density, porosity, resistivity, induced polarization, compressional sonic velocity, hydraulic conductivity, magnetic susceptibility, and remnant magnetization of core samples from drillholes UE-25a#1, USW G-3, USW GU-3, and USW G-4. The geophysical characteristics of stratigraphic units in drillholes UE-25a#1, USW G-1, UE-25p#1, and USW G-4 have been reported in Spengler et al. (1979), Muller and Kibler (1983, 1984), and Spengler and Chornack (1984), respectively. Paleomagnetic and magnetic-property data from drillholes USW G-1, USW G-2, USW GU-3, USW G-3, and USW VH-1 also have been interpreted by Rosenbaum and Snyder (1985).

Rock being considered for a repository at Yucca Mountain is densely welded ash-flow tuff of the Topopah Spring Member of the Paintbrush Tuff. The genesis, emplacement, and crystallization history of an ash-flow cooling unit are briefly described here (see Smith (1960) for detailed discussion). Ash flows are hot pyroclastic deposits that generally were erupted from

Table 1-4. Stratigraphy, age, and magnetic polarity of Tertiary volcanic rocks at Yucca Mountain[a]

K-Ar age (my)[b]	Magnetic polarity[c]	Rock unit[d]	Thickness (m)
10.2		Basalt dikes	
		* Timber Mountain Tuff	
		* Rainier Mesa Member	0-46
		Bedded tuff	0-61
		* Paintbrush Tuff	
12.5	R	* Tiva Canyon Member	69-148
		Bedded tuff	1-15
	R	* Yucca Mountain Member	0-29
		Bedded tuff	0-47
	R	* Pah Canyon Member	0-71
		Bedded tuff	0-9
13.1	N	* Topopah Spring Member	287-369
		Bedded tuff	1-17
13.4[e]		Tuffaceous beds of Calico Hills	27-289
		Bedded tuff	0-21
		* Crater Flat Tuff	
	N	* Prow Pass Member	80-193
		Bedded tuff	2-10
13.5	N	* Bullfrog Member	68-187
		Bedded tuff	6-22
	R	* Tram Member	190-369
		Bedded tuff	3-50
	N	Dacite lava and flow breccia	0-249
		Bedded tuff	0-14
	I	* Lithic Ridge Tuff	3-7
13.9		Older volcanic rocks and volcanogenic sedimentary rocks	345+

[a]Source: USGS (1984).

[illegible]

[c]Magnetic polarity: N = normal; R = reversed; I = intermediate.

[d]Names and rankings of some units do not conform to USGS usage. Formally recognized names are preceded by *.

[e]Age determined on associated lava flow.

relatively shallow magma chambers. The eruptions are rapid and consist of a series of closely spaced pulses in which very hot, highly gas-charged, [illegible] pumice and ash fragments are flattened by the weight of the overlying material. The thicker or hotter ash flows may become densely welded, attaining densities of as much as 2.5 g/cm^3 with less than 10-percent porosity; colder or thinner flows may be nonwelded or only partially welded, with densities as low as 1.5 g/cm^3 and porosities as high as 40 percent. Nonwelded ash-fall tuff generally forms from the accumulation of glassy ash settling out of ash clouds. However, some ash falls are hot enough to become welded also. A [illegible] ary overprint of crystallization zones. Bedded tuffs typically form as a result of reworking of nonwelded tuff deposits. Further alteration to secondary minerals like clays and zeolites may result from interactions with ground water, particularly in zones that are glassy and less welded.

1.2.2.2.1 Pre-Lithic Ridge volcanic and volcanogenic rocks

Rocks beneath the Lithic Ridge Tuff are difficult to correlate because of their heterogeneity and varied degree of alteration; they are not known to crop out in the Yucca Mountain area. Drillhole USW G-1 (Figures 1-19 and 1-20, Section 1.2.2) penetrated 323 m of ash-flow tuff interbedded with ash-fall tuff and reworked tuffaceous sediments. Most of the tuff is partially to moderately welded, and the tuffaceous sediments are moderately indurated. These rocks are altered and contain smectite (montmorillonite and related clays), analcime, and clinoptilolite, as well as traces of calcite and chlorite as alteration products (Spengler et al., 1981). Three subunits have been defined in drillhole USW G-1 on the basis of the relative abundance of major minerals.

In drillhole USW G-2, a 345 m thickness of altered volcanic and volcanogenic rocks was penetrated below the bedded tuff that lies beneath the Lithic Ridge Tuff. In ascending order, the sequence includes (1) 19 m of ash-flow tuff; (2) 17 m of bedded tuff, conglomerate, and ash-flow tuff; (3) 66 m of dacitic lava and flow breccia; (4) 10 m of bedded and ash-flow tuff; (5) 132 m of quartz latitic lava and flow breccia; and (6) 101 m of rhyolitic lava and flow breccia.

In drillhole USW G-3, 45 m of ash-flow tuff were penetrated below the bedded tuff underlying the Lithic Ridge Tuff. This tuff unit, whose base was

1.2.2.2.2 Lithic Ridge Tuff

A thick section of massive ash-flow tuff overlying the older ash-flow and bedded tuff has been named the Lithic Ridge Tuff (Carr et al., 1984). Its thickness ranges from 185 m, north of the proposed repository (at drillhole USW G-2), to 304 m at the south end of the repository (at drillholes USW GU-3 and USW G-3). The unit is nonwelded to moderately welded and has been extensively altered to smectites and zeolites.

The Lithic Ridge Tuff is distinguished by a relatively low volume percentage of quartz phenocrysts (3 to 11 percent of the total phenocrysts), notable amounts of sphene, and an abundance of lithic fragments, including fragments of distinctive spherulitic rhyolite lava. Many slight variations in the degree of welding, phenocryst ratios, and lithic fragment content suggest that the unit is the result of several eruptive surges.

The Lithic Ridge Tuff is separated from the overlying dacitic lava and flow breccia (where present) by as much as 14 m of bedded tuff. At the south end of the repository (drillhole USW G-3), this layer consists of a moderately to well-indurated bedded tuff composed mainly of pyroclastic-fall material 8.5 m thick.

1.2.2.2.3 Dacitic lava and flow breccia

Dacitic lava and autoclastic flow breccia overlie the Lithic Ridge Tuff in deep drillholes in the northern and western parts of Yucca Mountain, but are absent elsewhere (Figure 1-20, Section 1.2.2). The thickness of the unit is 22 m in drillhole USW G-2, 112 m in drillhole USW H-1, and 249 m in drillhole USW H-6. In drillhole USW G-1, most of the unit is flow breccia made up of angular to subangular fragments of dacite, commonly from 2 to 10 cm long. The breccia is intercalated with a few lava flows ranging from 1 to more than 17 m thick. In contrast, the unit in drillhole USW G-2 consists largely of lava with flow breccia confined to the uppermost and lowermost parts.

The phenocryst content is variable, but mafic minerals, mostly horn-

The Crater Flat Tuff is distinguished from other units in the vicinity of Yucca Mountain by the relative abundance of quartz and biotite phenocrysts. In addition, the Prow Pass Member and, to a lesser degree, the

The ash-flow tuff part, of the Tram Member, ranges in thickness from 104 m (drillhole USW G-2) to 370 m (drillholes USW GU-3 and USW G-3), is moderately welded to nonwelded, and is underlain by 3 to 50 m of reworked and bedded tuff. The average phenocryst content is approximately 11 percent, of which approximately 30 percent is quartz. This unit is distinguished from many other tuffs by its reversed remnant magnetization (Table 1-4, Section 1.2.2.2).

Two subunits are distinguished within the Tram Member on the basis of the relative abundance of lithic fragments; the lower subunit is rich in these fragments and the upper subunit is poor (Spengler et al., 1981). South and east of drillhole USW G-1, more than two-thirds of the basal part of the lower subunit characteristically contains zeolite minerals, including clinoptilolite, mordenite, and analcime. Other alteration products are illite-smectite, calcite, kaolinite, and, in places, albite and pyrite. The upper 20 m (drillhole UE-25b#1) to 65 m (drillhole USW G-1) of the lower subunit have less secondary alteration but approximately the same lithic content as the basal part. In drillhole USW G-1, the upper part of the lower subunit contains 10 to 15 percent smectite and 10 to 15 percent zeolites, including clinoptilolite, mordenite, and analcime. Inclusions of lava fragments constitute as much as 33 percent of the rock volume.

The upper subunit of the Tram, from 126 to 171 m thick, is partially welded and has a microcrystalline groundmass. Zeolite and clay minerals are scarce or absent. However, in drillhole USW G-4 the uppermost 20 m contain some 40 percent clinoptilolite and mordenite (Spengler and Chornack, 1984).

welded core, but in the south (drillholes USW GU-3, USW G-3, and USW G-4) it is compound, composed of two welded zones separated by a 1-m-thick bed of welded ash-fall tuff. Most of the upper part of the member is devitrified or shows evidence of vapor-phase crystallization. The total phenocryst content falls from 12 to 17 percent above the ash-fall layer to 9 to 11 percent below [illegible] 1984). The percentage of quartz likewise decreases [illegible]

whereas alkali feldspars remain constant and plagioclase increases. In drillholes USW G-1, USW G-2, and USW G-4, the upper part of the Bullfrog is partially altered to zeolites or clay or both; in drillhole UE-25b#1, only the lower 21 m have been slightly altered to clay; in drillholes USW GU-3 and USW G-3, little to no alteration has occurred.

The Bullfrog Member is separated from the overlying Prow Pass Member by as much as 10 m of ash-fall tuff and tuffaceous sediments, which are commonly zeolitized.

The ash-flow tuff of the Prow Pass Member, from 80 m (drillhole USW H-6) to 193 m (drillhole USW G-2) thick, is similar in appearance and petrologic characteristics to the Bullfrog, but the two members are distinguished because (1) mudstone fragments in the Bullfrog are fewer and smaller than in [illegible]

Tuffaceous beds of the Calico Hills at drillhole USW GU-3 are characterized by having an uppermost part that is relatively rich in mafic phenocrysts (8 percent of the phenocrysts consist of biotite, hornblende, orthopyroxene, and opaque phases with plagioclase as the dominant feldspar), a middle part that has an intermediate phenocryst assemblage, and a lowest part that is relatively rich in felsic phenocrysts (only a trace of biotite and orthopyroxene is present, and sanidine is the dominant feldspar). Also, the lowest part of these tuffs contains larger and more abundant lithic fragments than do the two upper parts. This sequence probably represents at least three separate magmatic pulses that tapped different portions of one chemically zoned magma chamber.

Several lines of evidence suggest that the sequence of tuffs found in the core from drillhole USW GU-3 may differ from the tuffaceous beds of Calico Hills at drillholes USW G-2 and USW G-1:

1. The hornblende and the orthopyroxene found in the upper part of drillhole USW G-3 are not found in other cores.

2. In drillhole USW GU-3, the upper part of these tuffs is characterized by a higher phenocryst content, a higher mafic phenocryst content, and a plagioclase/sanidine ratio greater than one: the lower part is characterized by a lower phenocryst content, a very low mafic phenocryst content, and a plagioclase/sanidine ratio less than one. This sequence of changes in phenocryst ratios is the inverse of that observed at drillhole USW G-2 (Maldonado and Koether, 1983).

3. The tuffaceous beds of Calico Hills thin from 290 m at drillhole USWG-2 to 95 m at drillhole USW G-1 over a distance of only 2.5 km. At drillhole USW GU-3, almost 4.5 km farther south, these tuffaceous beds are less than 30 m thick, close to the distal ends of these tuffs (Scott and Castellanos, 1984).

Ash-fall-tuff and reworked-tuff beds from 1 to 17 m thick separate the tuffaceous beds of Calico Hills from the overlying Paintbrush Tuff.

1.2.2.2.6 Paintbrush Tuff

The Paintbrush Tuff, more than 460 m thick, makes up nearly all of the exposed rocks at Yucca Mountain, as shown in Figure 1-17 (Section 1.2.2) (Lipman and Christiansen, 1964; Orkild, 1965; Lipman et al., 1966; Byers et al., 1976a). The Paintbrush Tuff was erupted from 13.1 to 12.5 million years ago (Marvin et al., 1970).

In ascending order, the four members of the Paintbrush Tuff are (1) Topopah Spring, (2) Pah Canyon, (3) Yucca Mountain, and (4) Tiva Canyon. The Topopah Spring and Tiva Canyon members consist predominantly of densely welded, devitrified ash-flow tuffs that enclose between them a sequence of nonwelded to partially welded ash-flow tuff and tuffaceous sediments, including the Pah Canyon and the Yucca Mountain members. The Pah Canyon and Yucca

Mountain members are thickest in the northwestern part of Yucca Mountain and thin to the southeastward.

The ash-flow tuff of the Topopah Spring Member, from 287 m (drillhole USW G-2) to 369 m (drillhole USW H-1) thick, is the thickest and most extensive member of the Paintbrush Tuff at Yucca Mountain. As this unit is the potential host rock for a repository it is discussed in some detail.

Topopah Spring Member

The Topopah Spring Member of the Paintbrush Tuff is a multiple-flow compound cooling unit (Lipman et al., 1966). The description presented here

is based mainly on reports by Spengler and Chornack (1984), Scott and Castellanos (1984), Scott and Bonk (1984), and Byers (1985) and applies to Yucca Mountain as shown in Figure 1-18. A nonwelded to partially welded glassy basal zone, from 10 to 20 m thick, grades upward by increased welding into a densely welded basal vitrophyre, from 10 to 25 m thick. The basal vitrophyre grades abruptly upward into a densely welded, devitrified, unvesiculated zone, the lower nonlithophysal zone, from 27 to 56 m thick. This zone grades upward into the lower lithophysal zone, from 43 to 117 m thick. Overlying the lower lithophysal zone is the middle nonlithophysal zone, from 20 to 50 m thick; this zone represents a second eruptive pulse, as it is slightly chilled at the base (the groundmass at the base is finer grained than the groundmass elsewhere in the zone). The upper lithophysal zone, from 54 to 96 m thick, represents the vesiculated portion of the second eruptive phase. Finally, a third eruptive pulse of quartz-latitic ash-flow tuff forms the caprock zone, from 39 to 62 m thick. A thin (approximately 1 m) vitrophyre, occurring in most places in the uppermost part of the caprock, resulted from chilling at the upper surface of the ash flow.

On the basis of potential radionuclide isolation time, allowable gross thermal loading, excavation stability, and relative economics, the densely welded, devitrified part of the Topopah Spring Member (the lower non-lithophysal zone described below) has been selected as the primary target unit for the proposed repository (Johnstone et al., 1984). More specific-ally, the proposed repository horizon lies within the lower nonlithophysal zone in the lower part of the member.

Thickness data from drillholes USW G-1, USW G-3, UE-25a#1, USWH-3, USW H-4, and USW H-5 (Spengler et al., 1979; Spengler et al., 1981; Bentley, et al., 1983; Scott and Castellanos, 1984; Thordasson et al., 1984; and Whitfield et al., 1984) and rock descriptions by Scott and Bonk (1984) have been used to compile the following composite descriptions of zones and subzones from base to top of the Topopah Spring:

1. Lower nonwelded to moderately welded zone. This zone, 13 to 42 m thick, is rhyolitic, glassy, nonwelded to partially welded, moderate-orange-pink (Munsell color designation 5YR 8/4), with black (N1) to brownish-gray (5YR 4/1) shards. Phenocrysts of plagioclase and alkali feldspar account for less than 2 percent of the rock.

2. Basal vitrophyre zone. This zone, 10 to 25 m thick, is rhyolitic, glassy, moderately to densely welded, and dark-gray (N3) to brownish-black (5YR 2/1). Phenocrysts of plagioclase and alkali

feldspar form less than 2 percent of the rock; locally, the vitrophyre is poorly developed. The lower vitrophyre is generally unaltered, with the exception of smectites and zeolites that fill fractures in the upper part.

3. Lower nonlithophysal zone. The probable host rock for the proposed repository. This zone, 27 to 56 m thick, is rhyolitic, devitrified, moderately to densely welded, and mottled pale red (10R 6/2) and moderate orange pink (10R 7/4). Phenocrysts of plagioclase and alkali feldspar form less than 2 percent of the rock. The percentage of lithophysae ranges from 0 to 2 percent.

4. Lower lithophysal zone and laterally equivalent subzones. This zone, 43 to 117 m thick, is rhyolitic, devitrified, moderately to densely welded. Its color is pale red (10R 6/2); lithophysae have grayish-orange-pink (10R 8/2) margins. Phenocrysts account for about 2 percent of the rock and consist largely of alkali feldspar and plagioclase. Lithophysae accounts for 10 to 15 percent of the rock, are from 5 to 15 cm in diameter, and have oblate spheroidal shapes. Exfoliated weathered surfaces are common. The orangish-red lithophysal subzone is distinguished by a moderate-orange-pink (10R 7/4) to moderate-reddish-orange (10R 6/6) color. The mottled lithophysal subzone is distinguished by a mottling of pale-red (10R 6/2) and moderate-orange-pink (10R 7/4) colors. The purplish-brown lithophysal and reddish-brown-brick and brownish-orange lithophysal subzones are distinguished by a grayish-red-purple (5RP 4/2) to light-brownish-gray (5YR 6/1) color, a lithophysal content of less than 2 percent, and a grayish-orange (10YR 7/4) to pale-brown (5YR 5/2) color, respectively.

5. Middle nonlithophysal zone and laterally equivalent subzones. This zone, 20 to 50 m thick, is rhyolitic, devitrified, and moderately to densely welded and is distinguished by an absence of lithophysae and conchoidal-fractured weathered surfaces. Phenocrysts of plagioclase, alkali feldspar, and biotite form less than 5 percent of the rock. The gray nonlithophysal subzone is distinguished by a light-gray (N7) color. The orange subzone is distinguished by a grayish-orange (10YR 7/4) color. The brick and orange-brick subzones are distinguished from one another by a pale-red (5R 6/2) color and a grayish-orange (10YR 7/4) color. The orange-brick lithophysal subzone is distinguished from the orange-brick subzone by the presence of 2 percent lithophysae. The brownish-orange-brick zone is distinguished by a grayish-orange-pink (5YR 7/2) color.

6. Upper lithophysal zone. This zone, 54 to 96 m thick, is rhyolitic, devitrified, moderately to densely welded. Laterally equivalent zones are the same as the overlying rounded zone, except for a pale-red (5R 6/2) color and from 5 to 15 percent convolute and oblate lithophysae that are 5 to 20 cm in diameter, with pinkish-gray (5YR 8/1) margins. The upper and lower subzones are distinguished by a light-gray (N7) color in each and by lithophysae that are of smaller diameter (less than 10 cm) and more spherical in

the lower zone. This zone is distinguished by the absence of the rounded exfoliation slopes that are characteristic elsewhere.

7. Caprock zone. This zone, 39 to 62 m thick, is the quartz-latitic upper part of the Topopah Spring Member. The caprock consists of four subzones; in descending order these are; a nonwelded to partially welded, light-brown (5YR 6/4) to brownish-gray (5YR 4/1) pumiceous tuff; a densely welded, black (N1) vitrophyre with moderate-red (5YR 4/2) lenses; a pale-red (5R 6/2) devitrified densely welded tuff; and a rounded subzone. Phenocrysts form about 15 percent of the vitrophyre and the devitrified subzones; alkali-feldspar phenocrysts are common, and some plagioclase and biotite are present. These subzones form cliffs. The glass of the thin

devitrification and authigenic crystallization to smectite. The rounded subzone is rhyolitic, devitrified, and moderately to densely welded. Its color is light-gray (N7) to light-brownish gray (5YR 6/1). Very light-gray (N8), well-flattened cognate pumice fragments are common. Phenocrysts form 10 percent of the rock and consist primarily of alkali feldspar, plagioclase, and rare biotite. The zone weathers to form rounded exfoliated slopes. A thin lithophysal subzone is locally present as a lateral equivalent of the uppermost rounded subzone and is distinguished by the presence of lobate lithophysae that are 1 to 3 cm in the long dimension and account for 10 to 20 percent of the rock volume.

Petrology of the Topopah Spring Member. The Topopah Spring Member of the Paintbrush Tuff is petrologically complex because it is a thick, compound cooling unit with greatly varying phenocryst compositions and abundances. In the lower three-fourths of the member, within the proposed host rock, phenocryst abundances are less than 2 percent (typically 0.5 percent) and the

phenocrysts include sanidine, plagioclase of andesine to oligoclase composi-

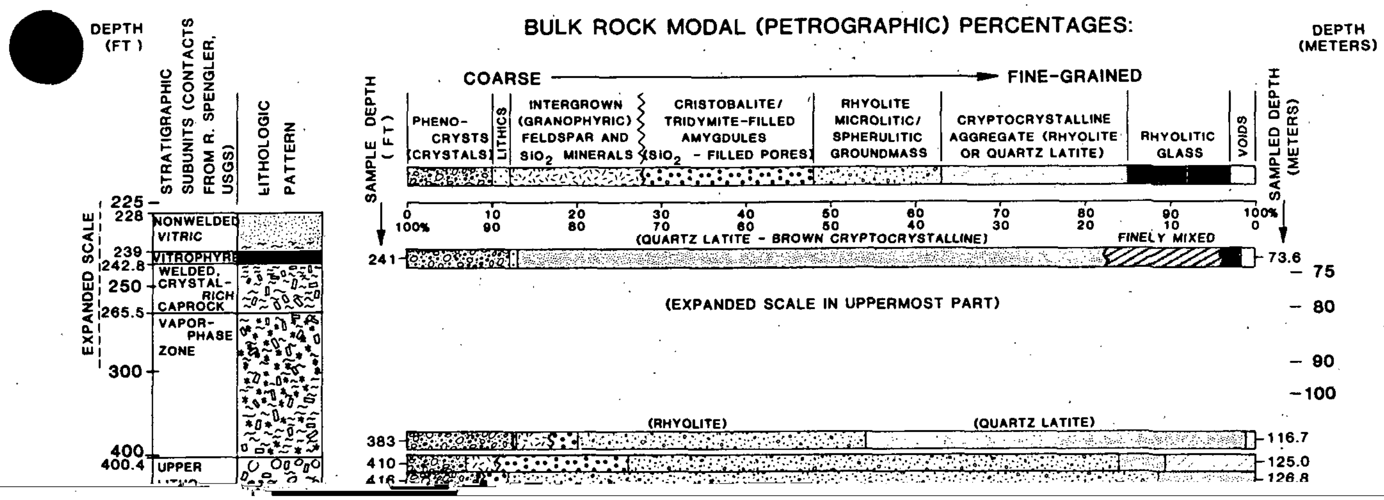

BULK ROCK MODAL (PETROGRAPHIC) PERCENTAGES:
DEPTH (FT)
DEPTH (METERS)
STRATIGRAPHIC SUBUNITS (CONTACTS FROM R. SPENGLER, USGS)
LITHOLOGIC PATTERN
EXPANDED SCALE
COARSE
FINE-GRAINED
SAMPLE DEPTH (FT)
SAMPLED DEPTH (METERS)
PHENO-CRYSTS (CRYSTALS)
LITHICS
INTERGROWN (GRANOPHYRIC) FELDSPAR AND SIO2 MINERALS
CRISTOBALITE/TRIDYMITE-FILLED AMYGDULES (SIO2 - FILLED PORES)
RHYOLITE MICROLITIC/SPHERULITIC GROUNDMASS
CRYPTOCRYSTALLINE AGGREGATE (RHYOLITE OR QUARTZ LATITE)
RHYOLITIC GLASS
VOIDS
NONWELDED VITRIC
VITROPHYRE
WELDED, CRYSTAL-RICH CAPROCK
VAPOR-PHASE ZONE
UPPER
(QUARTZ LATITE - BROWN CRYPTOCRYSTALLINE)
FINELY MIXED
(EXPANDED SCALE IN UPPERMOST PART)
(RHYOLITE)
(QUARTZ LATITE)

Figure 1-21 show rock textures at various stratigraphic levels, starting with the coarsest (crystals and lithic fragments) at the left and ending with the finest (cryptocrystalline, glass, and voids) at the right.

Figure 1-22 shows the percentages of phenocrysts that crystallized from the Topopah Spring magma at depth before eruption. The Topopah Spring magma was compositionally zoned within the magma chamber from high-silica rhyolite (approximately 77 weight percent SiO_2) downward to quartz latite (approximately 70 weight percent SiO_2) or even less silicic compositions at greater depth. This sequence was inverted during eruption (Lipman et al., 1966). The changing, upward-increasing phenocryst assemblage may be a guide to stratigraphic position in the Topopah Spring Member. One difficulty is that the lower three-fourths of the Topopah Spring is high-silica rhyolite with commonly less than 2 percent phenocrysts, yielding poor data on crystal abundances. This difficulty is being overcome by counting phenocrysts separately on 0.5-mm traverses and by relying on additional thin sections (Byers, 1985).

Byers (1985) reaches three preliminary conclusions about the petrographic stratigraphy of the Topopah Spring Member (Figures 1-21 and 1-22).

First, the lower nonlithophysal zone (the candidate host rock) can be distinguished from the middle nonlithophysal zone by three criteria.

1. The lower nonlithophysal zone contains 1.5 to 3.2 percent foreign lithic fragments (xenoliths), whereas the middle nonlithophysal zone has only a fraction of a percent. This is understandable because the earlier pulse of the Topopah Spring eruption would be expected to contain more foreign fragments from both the vent walls and the ground surface over which it traveled.

2. Quartz microphenocrysts are common in the middle nonlithophysal zone but are absent or nearly absent in the lower nonlithophysal zone.

3. The lower nonlithophysal zone is densely welded, whereas the middle lithophysal zone is moderately welded.

Second, the similarity of the cryptocrystalline texture of the middle nonlithophysal zone to that of the lower zone suggests that the middle nonlithophysal zone was also formed by chilling, probably caused by a brief hiatus between eruption pulses. This break allowed the lower lithophysal zone to form by vapor-phase action, which cooled the upper surface on which the next eruptive pulse (represented by the middle nonlithophysal zone) was deposited. The middle nonlithophysal zone was chilled, as indicated by the increased cryptocrystallinity toward the lower contact (Figure 1-21), but was not chilled by a sufficiently high temperature gradient to form a medial vitrophyre, as may be found in some thick ash-flow tuffs.

Third, stratigraphic position in the two lithophysal zones is not well indicated by any petrographic trends observed to date. However, stratigraphic position within the upper lithophysal zone can be partially determined from the increase of total phenocrysts and alkali feldspar upward in the upper half of the zone (Figures 1-21 and 1-22) and from the occurrence of

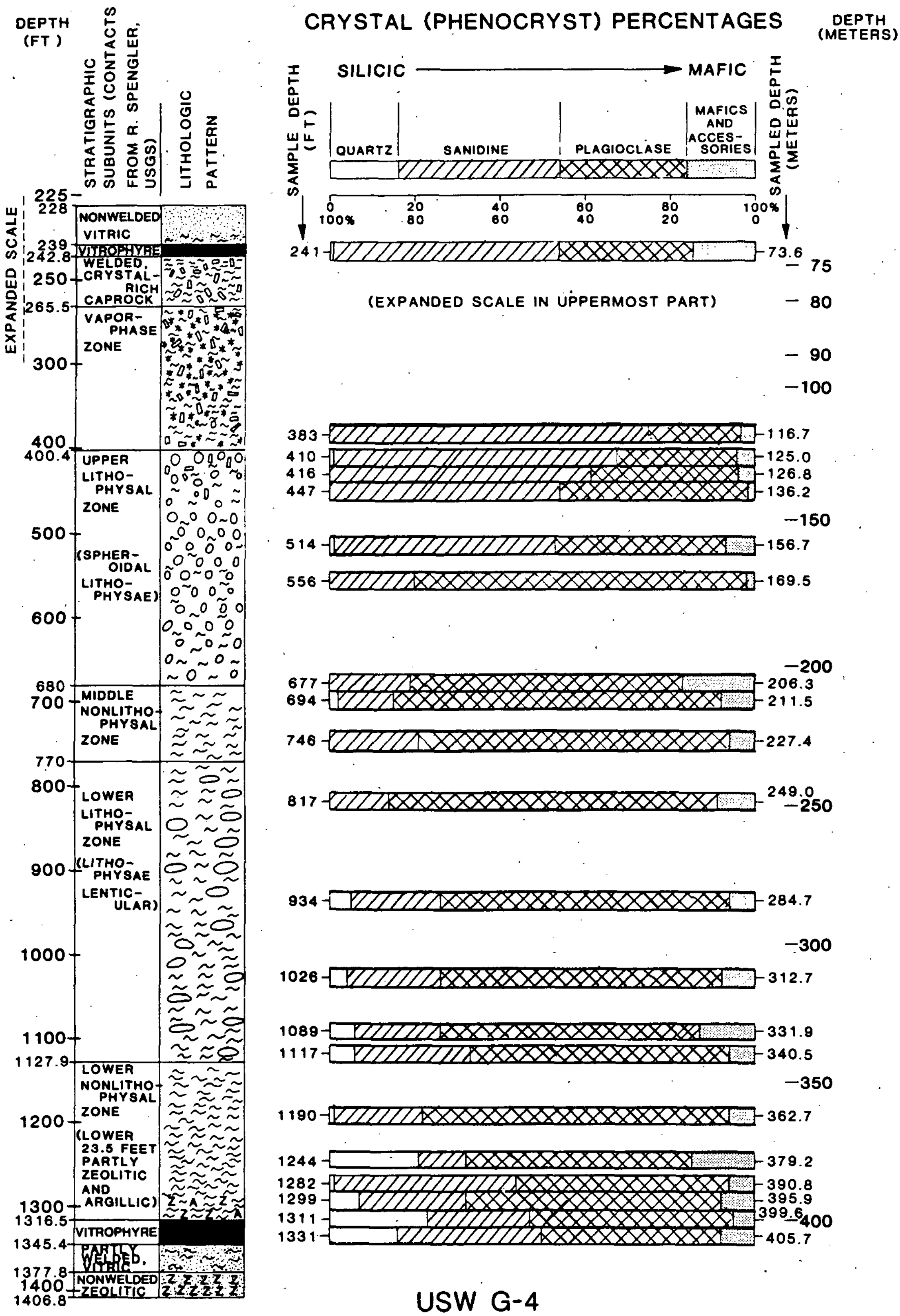

Figure 1-22. Phenocryst assemblages in selected samples, Topopah Spring Member, drillhole USW G-4. Modified from Byers (1985).

chilled cryptocrystalline quartz latite lenticles in the upper one-fifth of the upper lithophysal zone (Figure 1-21).

These modal petrographic distinctions are being supplemented by electron microprobe data for feldspar phenocrysts and for bulk-rock and groundmass samples with a glassy or cryptocrystalline texture. In Table 1-5 several groundmass analyses are compared with the bulk-rock x-ray fluorescence (XRF) analyses of the Topopah Spring Member reported by Zielinski (1983). Even though two different drillholes are compared, and two different analytical methods were used, there is little difference between the groundmass and the bulk-rock analyses. The somewhat higher iron contents of the bulk-rock XRF analyses are expected because Byers (1985) did not use the iron-titanium oxide phenocrysts during this groundmass analyses.

Studies planned and in progress will use new samples from drillholes, excavation, and test construction in the exploration block to define the limits of mineralogic variability in the host rock. These data will be important for assessing the results of in situ experiments to be performed in the exploratory shaft facility where the mineralogy surrounding the experiments must be considered. The mineralogic variability of the host rock may also help determine stratigraphic position during repository construction. Plans to conduct statistical analyses of the mineralogic variability of the host rock are be provided in Section 8.3.1.3.

Pah Canyon, Yucca Mountain, and Tiva Canyon members

The Pah Canyon and the Yucca Mountain members are relatively thin, nonwelded ash-flow tuffs, which are the distal edges of flow sheets that thicken to the northwest (Lipman and Christiansen, 1964; Orkild, 1965). The Pah Canyon attains a maximum thickness of 71 m; the Yucca Mountain, 29 m. The Pah Canyon contains 5 to 15 percent phenocrysts, mainly alkali feldspar, plagioclase, and biotite. In contrast, the overlying Yucca Mountain Member is a distinctively uniform, shard-rich tuff containing small amounts of pumice, phenocrysts, and lithic fragments.

The uppermost unit of the Paintbrush Tuff at Yucca Mountain, the Tiva Canyon Member, is from 90 to 140 m thick in outcrop. It is a multiple-flow, compound cooling unit made up of ash flows that erupted approximately 12.5 million yr ago from the Claim Canyon caldera segment north of Yucca Mountain (Lipman et al., 1966; Byers et al., 1976b). The Tiva Canyon is almost entirely densely welded and caps most of the surface of Yucca Mountain. The mineral composition of the Tiva Canyon phenocrysts is similar to that of the Topopah Spring, with the notable exception that sphene is present as a phenocryst mineral in the Tiva Canyon. The Tiva Canyon has a compositional zoning that is similar to that of the Topopah Spring. Ten mappable units are distinguished in the Tiva Canyon (Scott et al., 1983; Scott and Bonk, 1984). In ascending order, these units are informally designated as (1) columnar, (2) hackly, (3) lower lithophysal, (4) red clinkstone, (5) gray clinkstone, (6) rounded step, (7) lower cliff, (8) upper lithophysal, (9) upper cliff, and (10) caprock. The rounded step subunit is laterally equivalent to the combined red and gray clinkstone subunit.

The Tiva Canyon thickens southward from approximately 90 m to nearly 140 m, then thins again to 125 m in the southernmost part of Yucca Mountain.

Table 1-5. Average whole rock and groundmass analyses in weight percent of rhyolitic devitrified tuff and underlying vitrophyre, Topopah Spring Member, Paintbrush Tuff[a]

Subject analyzed (groundmasses are indicated; others are whole rock)	Number of analyses	SiO_2	Al_2O_3	Fe as Fe_2O_3	MgO	CaO	Na_2O	K_2O	TiO_2	P_2O_5	MnO	BaO	Analytical method
Middle nonlithophysal groundmass (USW G-4, Byers, 1985)	34	76.48 ±2.49	12.45 ±1.33	0.76 ±0.28	0.04 ±0.05	0.23 ±0.07	3.28 ±0.43	6.56 ±0.96	0.07 ±0.03	ND[b]	0.09 ±0.06	10.04 ±0.16	Electron microprobe of cryptocrystalline groundmass
Middle nonlithophysal zone (USW G-1; Zielinski, 1983)	2	76.55 ±0.21	12.50 ±0.00	1.97 ±0.17	0.16 ±0.01	0.45 ±0.00	3.26 ±0.01	4.96 ±0.02	0.08 ±0.00	<0.05	0.06 ±0.01	ND	X-ray fluorescence
Lower lithophysal zone (USW G-1; Zielinski, 1983)	2	76.65 ±0.07	12.65 ±0.07	1.80 ±0.11	0.25 ±0.11	0.48 ±0.02	3.12 ±0.13	4.96 ±0.04	0.08 ±0.00	<0.05	0.06 ±0.00	ND	X-ray fluorescence
Lower nonlithophysal zone (USW G-1; Zielinski, 1983)	1	76.6	12.6	1.83	0.23	0.52	3.17	4.84	0.08	<0.05	0.06	ND	X-ray fluorescence
Lower nonlithophysal groundmass (USW G-4; Byers, 1985)	33	78.03 ±1.91	11.86 ±0.89	0.84 ±0.30	0.05 ±0.03	0.44 ±0.34	3.61 ±0.83	4.99 ±2.00	0.07 ±0.03	ND	0.07 ±0.05	0.05 ±0.07	Electron microprobe of cryptocrystalline groundmass
Densely welded crystallized tuff (Outcrop; Lipman et al., 1966)	5	76.84 ±0.38	12.72 ±0.25	0.94 ±0.13	0.18 ±0.07	0.55 ±0.09	3.60 ±0.09	4.98 ±0.12	0.10 ±0.00	0.01 ±0.01	0.07 ±0.01	0.009 ±0.002	Wet; Ba, spectrographic, calculated as BaO
Lower vitrophyre (Outcrop, Lipman et al., 1966)	2	76.75 ±0.21	12.85 ±0.21	0.96 ±0.04	0.36 ±0.18	0.58 ±0.04	3.45 ±0.07	4.90 ±0.28	0.10 ±0.01	0.02 ±0.00	0.06 ±0.00	0.007 ±0.001	Wet; Ba, spectrographic, calculated as BaO
Lower vitrophyre groundmass[c] (USW G-4; Byers, 1985)	8	77.45 ±0.32	12.68 ±0.20	0.65[c] ±0.28	0.01 ±0.01	0.42 ±0.04	3.49 ±0.09	5.16 ±0.05	0.06 ±0.04	ND	0.06 ±0.05	0.01 ±0.02	Electron microprobe of glass
Lower vitrophyre (USW G-1; Zielinski, 1983)	3	76.77 ±0.12	13.00 ±0.10	1.17 ±0.11	0.11 ±0.02	0.58 ±0.05	3.47 ±0.05	4.77 ±0.03	±0.08 ±0.00	<0.05	0.06 ±0.00	ND	X-ray fluorescence

[a]Upper figure is arithmetic mean, plus or minus; lower figure is sample standard deviation. Data are normalized to 100 percent total (volatile-free) for purposes of comparison (for original data, see references cited).

[b]ND = no data.

[c]Brown glass analyses (6) pooled with colorless glass analyses (2); brown glass, 0.08 ± 0.07 percent Fe_2O_3; colorless glass, 0.02 ± 0.01 percent Fe_2O_3. Only significant difference between glasses is in percent of iron.

Within the Tiva Canyon, the relative proportion of the total unit represented by the thicknesses of the two lithophysal subunits decreases southward from approximately 30 to 10 percent. As the lithophysal zones thin, the nonlithophysal zones thicken.

1.2.2.2.7 Post-Paintbrush ash-flow tuffs at Yucca Mountain

Petrochemical work by Warren and Byers (1986) has identified a nonwelded ash-flow and ash-fall tuff sequence between the top of the Tiva Canyon Member of the Paintbrush Tuff and the base of the overlying Rainier Mesa Member of the Timber Mountain Tuff in the vicinity of Yucca Mountain (Table 1-4, Section 1.2.2.2). The sequence is present in the subsurface beneath alluvial deposits on the eastern flank of Yucca Mountain in the area proposed for the surface facilities of the repository. The sequence ranges in thickness from zero to 61 m and is intermediate in composition between that of the underlying Tiva Canyon and the overlying Rainier Mesa units. The sequence is a possible lateral stratigraphic equivalent of the Pinyon Pass(?) and tuff of Chocolate Mountain located north of Yucca Mountain in the vicinity of the Claim Canyon cauldron segment (Byers et al., 1976a).

1.2.2.2.8 Timber Mountain Tuff

The 11.3-million-year-old Rainier Mesa Member of the Timber Mountain Tuff (Marvin et al., 1970) is locally present in valleys on the flanks of Yucca Mountain (USGS, 1984). It is a series of ash flows and ash falls that unconformably overlies down-faulted blocks of the Paintbrush Tuff, but it either was not deposited on, or was removed by erosion from, the top of the higher standing fault blocks that form most of Yucca Mountain.

At Yucca Mountain, the Rainier Mesa Member has a maximum thickness of approximately 46 m. It is nonwelded and glassy at the base, grading upward into partly welded devitrified tuff near the interior. Its phenocrysts (10 to 25 percent) are mainly quartz and alkali feldspar, with some plagioclase and biotite (Lipman and McKay, 1965).

1.2.2.2.9 Basalt

The youngest volcanic rocks at Yucca Mountain (10 million years old) are basalt dikes less than 1 m thick that intrude a fault and nearby fracture in the northwest part of Yucca Mountain at the head of Solitario Canyon near Little Prow (USGS, 1984). The basalt is very fine grained and locally vesicular, with sparse microphenocrysts of olivine, plagioclase, and rare clinopyroxine grading into an intergranular groundmass. The basalt was brecciated near its margins by later movement along the fault (Section 1.5.1.2.2). Younger basaltic flows and cones are present in the area around Yucca Mountain (Sections 1.3.2.1.2 and 1.8.1.3.1).

1.2.2.2.10 Calcite deposits along faults, fractures, and at the surface

Deposits of calcite, with subordinate amounts of opaline silica, and minor sepiolite are associated with Late Cenozoic faults and Late Pliocene to Holocene surficial deposits in the vicinity of Yucca Mountain (Swadley et al., 1984; Voegele, 1986a,b). The deposits described will hereafter be referred to as calcite deposits. The faults with associated calcite deposits include the Bare Mountain fault (Swadley et al., 1984; Reheis, 1986), the Paintbrush Canyon fault (Swadley et al., 1984), the Bow Ridge fault (Trench 14, Figure 1-23); (Voegele, 1986a,b; Taylor and Huckins, 1986; Vaniman et al., 1988), the Solitario Canyon fault (Swadley et al., 1984), the Windy Wash fault (Swadley and Hoover, 1983; Whitney et al., 1986), and a N-S trending fault on the west side of Busted Butte (Grant, 1986). Ages and rates of fault movements are discussed in Section 1.3.2.2.2 and faulting recurrences are discussed in Section 1.3.2.2.1. A discussion of the available petrologic, geochemical, and age data is presented below along with a summary of the possible origins of the calcite deposits.

The calcite deposits occur along fault planes in unconsolidated alluvium and in bedrock. The calcite deposits exhibit several generations of deposition. They may exhibit laminations that are subhorizontal to nearly vertical in orientation or appear in a massive form (Voegele, 1986a). In Trench 14, where the Bow Ridge fault can be observed to displace alluvium and bedrock, the calcite deposit contains angular blocks of the bedrock (Voegele, 1986a,b). Stringer veins of the calcite occur within the soil surrounding the faults in Trench 14 (Taylor and Huckins, 1986). In soil horizons, the calcite deposits occur as coatings, which may be laminated, on stones and as finely disseminated matrix material; these soil deposits may or may not be associated with faults (Vaniman et al., 1984b; Taylor and Huckins, 1986; Taylor and Shroba, 1986). Vaniman et al. (1984b) reports a close textural and mineralogical similarity between pedogenic material in weathered alluvium and material deposited along faults.

Various origins for the calcite deposits have been proposed including precipitation from low temperature descending water and from low to high temperature ascending water. The deposits may have formed by multiple proc-

esses involving deep-seated ground-water flow, perched ground-water flow, hydrothermal activity, surficial runoff water or water flow induced by seismic activity (Voegele, 1986a,b). Descending water models include deposition by a process where surface water moved carbonate and silica in solution down into the fault zone and deposited carbonate and opaline silica (Reheis, 1986; Taylor and Huckins, 1986). The various models of origin have the potential to impact several regulatory concerns including 10 CFR 60.112

DECEMBER 1988

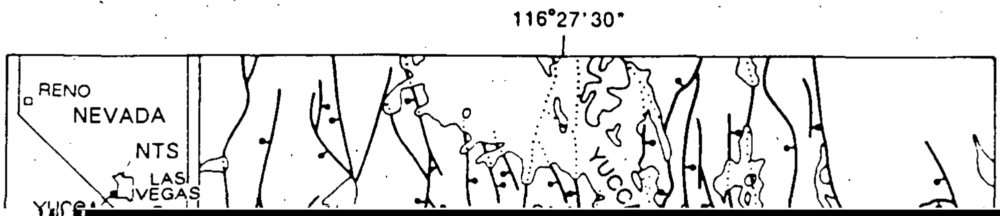

(Szabo and O'Malley, 1985). The field location of the samples are discussed in Swadley et al. (1984). The three samples (two opals and an opal residue from acid leaching) yield ages of greater than 400,000 yr ago, and the fourth is greater than 350,000 yr ago (Szabo and O'Malley, 1985). Studies are planned (Section 8.3.1.5) to determine the genetic relationship of these soil samples to the calcite vein fillings in fault zones. The calcite vein material in Trench 14 has not been dated. However, the vein material in Trench 14 will be dated and information concerning the origin of these materials obtained (Section 8.3.1.5). Additional age information on the age of the calcite deposits is inferred by other methods.

Calcite deposits within the Bow Ridge and Windy Wash fault zones contain undated basaltic ash that is believed to correlate with one of two basaltic eruptions from Crater Flat (Crowe and Vaniman, 1985; Taylor and Huckins, 1986; Whitney et al., 1986).

These basaltic eruptions have been dated at approximately 1.2 and possibly less than 0.1 million yr ago (Vaniman et al., 1982). A correlation with even the younger ash is consistent with a relatively old age for the calcite deposits. Ages for other carbonate and opaline vein fillings and surface deposits range from 26,000 to more than 400,000 yr ago (Szabo et al., 1981; Szabo and Kyser, 1985; Szabo and O'Malley, 1985). Plans for age determinations and other information regarding the origin of the calcite deposits in Trench 14 and other locations are discussed in Section 8.3.1.5.

Stable isotope studies on the calcite deposits

Carbon and oxygen isotope work on fault-associated calcite and opaline silica samples from Trench 14 indicates that the deposits may have formed at or near surface temperatures (<15°C) (O'Neil, 1984, 1985). Low temperatures of formation may also be supported by the presence of similar mineral assemblages of calcite, opal-CT, and sepiolite in soil deposits (Taylor and Huckins, 1986).

Carbon and oxygen isotope work on calcite-filled fractures from drill-holes in Yucca Mountain yield temperatures that increase with depth and range from 20 to 46°C (Szabo and Kyser, 1985). Fractures are discussed in Sections 1.3.2.2.2, 2.2.2.2, 2.2.2.3, 2.2.2.4, and 2.2.2.5. A maximum geothermal gradient of 43°C/km has been estimated from these data. The gradient represents an upper limit because the calculated temperature does not take into account the isotopic fractionation due to other processes. These results compare well with estimated thermal gradients of 36 to 45°C/km derived from stable isotope studies of calcite from drill core (Sass et al., 1980). Stable isotopic work is further discussed in Section 8.3.1.5.

Fluid inclusion studies on the calcite deposits

Limited fluid inclusion data also tend to support a low-temperature origin for the calcite and opaline silica deposits in Trench 14 because the inclusions are single phase as opposed to two- and three-phase inclusions that are typical of high-temperature deposits; however, these inclusions are extremely small and optical data alone do not provide definitive conclusions (Vaniman et al., 1984b). Further work will include optical fluid inclusion analysis but will center on the fluid chemistry of the inclusions in order to provide additional data on the petrogenesis of the calcite deposits in Trench 14 (Section 8.3.1.5).

Paleontological studies on the calcite deposits

Paleontological studies of three carbonate samples from Trench 14 are consistent with pedogenic origin of the calcite-silica deposits. These studies identified charophytes in two samples but no ostracodes (Forester, written communication, 1985). Ostracodes are indigenous to all modern spring-fed pools near the Nevada Test Site, and ostracodes are ubiquitous in the fossil record of springs (Stuckless, 1986). The absence of ostracodes and the presence of rare charophytes may indicate the introduction of biological material as windblown debris rather than by in situ growth associated with spring activity. Future paleontological studies are described in Section 8.3.1.5.

Possible analogs for the calcite deposits

Laminated calcite vein material along fractures in the Amargosa Desert of Nevada and Death Valley in California has been interpreted to represent feeders from springs (Winograd et al., 1983) in a Plio-Pleistocene marsh environment (Hay et al., 1986). The veins are thought to have originated by low-temperature (<50°C) precipitation from calcite-saturated artesian ground water rising along tensional fractures in Pliocene and Pleistocene alluvium, fanglomerate, and lake beds (Winograd et al., 1983). On the basis of this interpretation, the distribution of these veins indicates that the water table was higher during the Pliocene and early to middle Pleistocene (Winograd and Szabo, 1986). Winograd and Szabo (1986) suggest that the regional water table has declined tens to hundreds of meters in response to tectonics and increased aridity. Changes in the water table level and potential effects of these changes on the nuclear waste repository are discussed in Sections 3.9.8 and 3.7.4. Although no marsh deposits are known at Yucca Mountain, the calcite deposits have some mineralogical similarity to the marsh deposits in the Amargosa Desert (Hay et al., 1986; Taylor and Huckins, 1986). The origin of the Yucca Mountain deposits will be evaluated during site characterization (Section 8.3.1.5.2).

Samples of possible spring deposits described as tufa or nodular tufa deposits from the southern end of Crater Flat near Yucca Mountain yield preliminary uranium-thorium dates of 78,000 ± 5,000 yr and approximately 30,000 yr, respectively (SCP Section 1.2.2.3; Szabo et al., 1981). Further work on these deposits may reveal information about the level of the water table and the possibility of perched ground water in the Yucca Mountain vicinity, as well as provide a better understanding of the reported tufa deposits and pedogenic processes in this area. The deposits will be investigated with respect to their mineralogy, morphology, and origin. Additional dates will be generated on these deposits located at the southern end of Crater Flat (Section 8.3.1.5.2).

Future work will focus on the age, mineralogy, isotopic composition, temperature of formation, and distribution of the calcite deposits that emphasizes the potential impact on waste isolation and containment. Analog environment will be compared with the calcite deposits.

1.2.2.3 Surficial deposits

The late Tertiary and Quaternary surficial sedimentary deposits of the Yucca Mountain area consist of colluvium; fan alluvium; eolian sand sheets, ramps, and dunes; lacustrine sediments; and playa deposits. These range in age from late Pliocene for some of the lacustrine sediments to modern for the youngest alluvial deposits (Swadley et al., 1984). Hoover et al. (1981) described the stratigraphy of these deposits, and the following brief descriptions of map units (Figures 1-24a and 1-24b) are based mainly on their work. The deposits are grouped into five major units: (1) late Pliocene and early Pleistocene lacustrine deposits, (2) late Pliocene(?) and early Pleistocene alluvial deposits, (3) middle-to-late Pleistocene alluvial and eolian deposits, (4) Holocene alluvial and eolian deposits, and (5) spring and marsh deposits. The distribution of these units is shown on a generalized surficial deposit map in Figure 1-24a.

Late Pliocene and early Pleistocene deposits are the oldest surficial deposits in the area. They consist of lacustrine deposits of unconsolidated to moderately indurated marl and silt that locally contain beds of limestone,

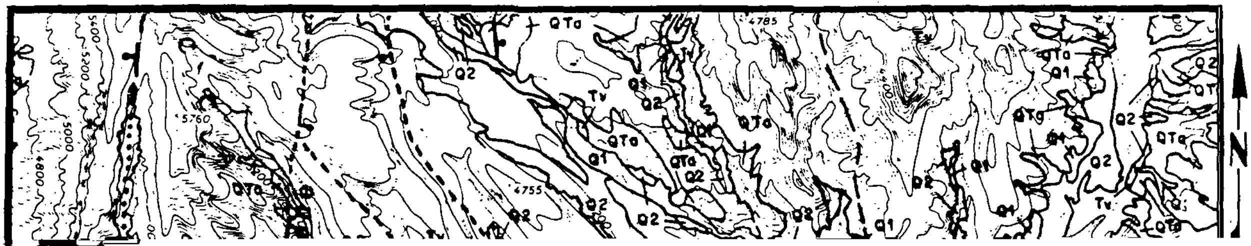
QTa
Q2
Q1
Tv
5760
4755
4785
N

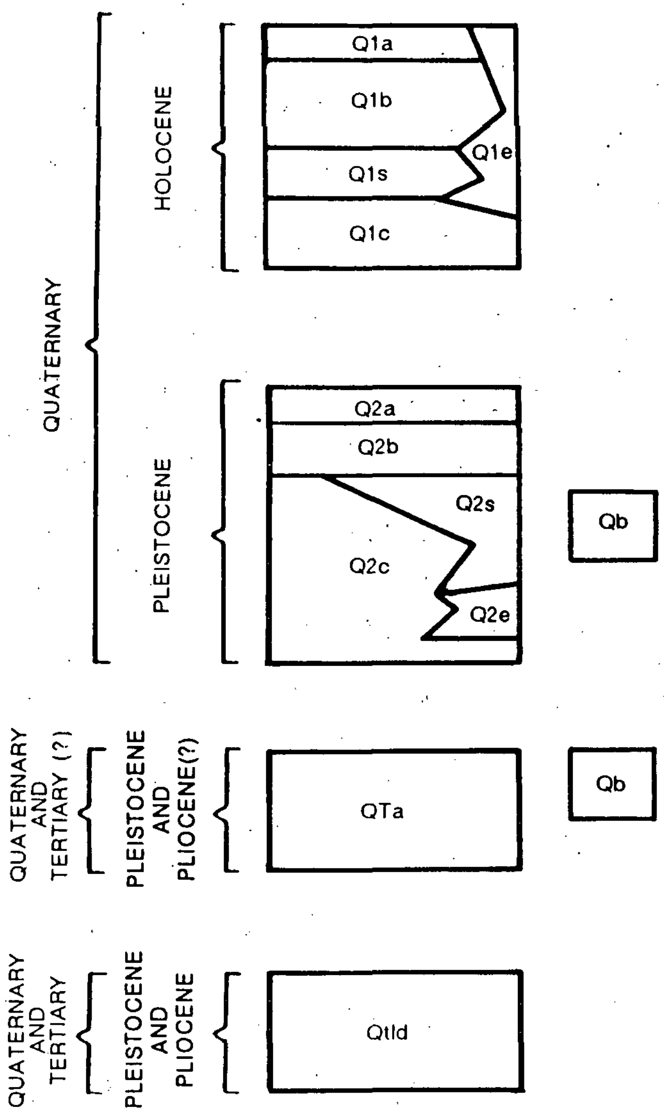

UNIT	ESTIMATED AGE RANGE (IN YEARS)
HOLOCENE DEPOSITS	
Q1a - FLUVIAL DEPOSITS	PRESENT TO 150
Q1b - FLUVIAL DEPOSITS AND DEBRIS FLOWS	150 TO 4,000
Q1e - EOLIAN DUNES AND SAND SHEETS	PRESENT TO 8,000
Q1s - FLUVIAL SAND SHEETS	4,000 TO 7,000
Q1c - COARSE FLUVIAL DEPOSITS	7,000 TO 9,000
MIDDLE AND LATE PLEISTOCENE-PLIOCENE (?) DEPOSITS	
Q2a - LOCAL DEBRIS FLOWS	≈40,000
Q2b - FLUVIAL DEPOSITS	160,000 TO 250,000
Q2s - FLUVIAL SAND SHEETS	270,000 TO 700,000
Qb - BASALT FLOWS AND CINDERS	100,000 TO 300,000
Q2e - EOLIAN DUNES AND SHEETS	700,000 TO 750,000
Q2c - COARSE FLUVIAL DEPOSITS	270,000 TO 800,000
EARLY PLEISTOCENE (?) DEPOSITS	
QTa - DEBRIS FLOWS, MINOR FLUVIAL DEPOSITS	1.1×10^6 TO 2×10^6
Qb - BASALT FLOWS AND CINDERS	1.1×10^6 TO 1.3×10^6
PLIOCENE-PLEISTOCENE DEPOSITS	
QTld - LACUSTRINE DEPOSITS	$< 2 \times 10^6$ TO 4×10^6

Figure 1-24b. Quaternary units present in the Yucca Mountain area and mapped on Figure 1-24a. Modified from Swadley et al. (1984).

Eolian sand deposits consist of well-sorted, fine sand that occurs as small dunes and irregularly shaped sheets over much of the Amargosa Valley. Eolian deposits commonly overlie all other units.

Soils formed in alluvium, colluvium, and eolian sand at Yucca Mountain display distinctive trends in the accumulation of calcium carbonate and opaline silica. These trends correspond to the ages of the surficial deposits, which range from Holocene to early Pleistocene or late Pliocene(?) (Taylor, 1986; Taylor and Shroba, 1986).

Soils formed on Quaternary deposits of Q1a, Q1b, Q1s, and Q1e (Figures 1-24a and 1-24b) are very weakly developed and contain little or no secondary calcium carbonate or opaline silica. Soils formed on Q1c and Q2a have a weakly developed horizon of calcium carbonate accumulation (Bk

horizon) about 20 to 50 cm thick. The undersides of stones in the Bk horizon commonly have thin, discontinuous coatings of calcium carbonate or silica or both.

Soils formed in deposits of Q2b commonly have a silica-enriched duripan (Bqm horizon) about 50 cm thick; this typically overlies a moderately developed horizon of secondary calcium carbonate accumulation (Bk/k horizon) about 50 to 70 cm thick. Secondary silica in the duripan typically occurs as finely disseminated matrix cement and as coatings and pendants on stones. Secondary calcium carbonate in the Bk/k horizon typically occurs as coatings on stones, bridges between some of the stones, and locally as a finely disseminated matrix cement.

Soils formed in deposits of Q2c, Q2e, and Q2s commonly have a silica-indurated Kqm horizon that is cemented with calcium carbonate and is about 50 cm thick. The Kqm horizon typically overlies a Bk/k horizon that is enriched in calcium carbonate and is about 40 to 50 cm thick.

Soils formed in QTa deposits are distinguished from younger soils by their prominent Kqm horizons, which are usually more than 1 m thick. The upper part of the Kqm horizon commonly consists of thin layers enriched in calcium carbonate and cemented by thin laminae of opaline silica.

1.3 STRUCTURAL GEOLOGY AND TECTONICS

This section discusses the tectonic and structural setting of Yucca Mountain. Although the discussion focuses on the southern Great Basin, it considers the plate tectonic setting of Yucca Mountain in the context of western North America to provide a tectonic framework for the more local structural configuration at Yucca Mountain. The regional structures related to the tectonic setting that are important to repository siting are also defined.

The structures, stresses, and thermal conditions at Yucca Mountain are among the factors that influence the design of the proposed repository. Additionally, the geologic processes that have occurred in the past give a basis for predicting future processes that could affect the long-term isolation of waste. At Yucca Mountain, possible future processes include faulting and volcanism (Section 1.5) and seismicity (Section 1.4). The data in Section 1.3 address data needs of investigations in the site program as follows. Section 1.3.2.2.2 addresses the structure necessary to locate the underground facility for Characterization Program 8.3.1.4 (rock characteristics). Sections 1.3.2.3 and 1.3.2.5 address spatial distribution of ambient stress and thermal conditions for Characterization Programs 8.3.1.2 (Geohydrology), 8.3.1.8 (postclosure tectonics), 8.3.1.9 (natural resources), and 8.3.1.15 (thermal and mechanical properties). Sections 1.3.2 and 1.3.2.4 address nature and rates of tectonic processes for Characterization Programs 8.3.1.8 (postclosure tectonics) and 8.3.1.17 (preclosure tectonics).

Information that will be obtained to satisfy the above information requirements, as well as information on seismicity discussed in Section 1.4, will serve as the data base for seismic hazard evaluations for the Yucca Mountain site. A description of the approach utilized to identify and resolve performance and design issues associated with significant seismic and tectonic events is included in Sections 8.3.1.8 and 8.3.1.17. Significant seismic and tectonic events are the events that, in light of tectonic history and other characteristics of the site, must be considered in evaluating the compliance of the repository with the performance objectives of 10 CFR Part 60.

1.3.1 TECTONIC FRAMEWORK

This section describes the regional tectonic setting of Yucca Mountain, including its relationship to intraplate faulting in terms of current plate tectonic theories. Yucca Mountain is in a broad belt of highly deformed continental crust that comprises most of western North America (Cordilleran Orogenic belt), and which has been subjected to numerous episodes of tectonism as a result of the interaction of major continental and oceanic plates, particularly during the last 200 million years.

1.3.1.1 Modern plate tectonic setting

The present configuration of the crustal plates that have affected the tectonic history of Yucca Mountain is shown in Figure 1-25. Three large oceanic plates, the Pacific, the Juan de Fluca, and the Cocos, are in contact with the North American continent along its west coast. The Juan de Fuca and Cocos plates have convergent (subduction) boundaries in common with the North American plate. The Pacific-North American plate boundary is a conservative one (transform fault) north of the Gulf of California, where it presently corresponds to the right-slip San Andreas fault system: It has conservative and accretionary (sea floor spreading ridge) elements within the Gulf. The three oceanic plates share accretionary boundaries along the East Pacific Rise (Cocos-Pacific) and the Gorda and Juan de Fuca Ridges (Juan de Fuca-Pacific), but the ridges are offset on several large transform faults, such as the Blanco and the Medocino fracture zones. The Cocos and Juan de Fuca plates are the remnants of a larger plate, the Farallon, that has been largely consumed since the Cretaceous (Atwater, 1970; Minster and Jordan, 1978; Engebretson et al., 1985).

The western half of the North American continental plate, the Cordilleran Orogenic belt, was subjected to numerous tectonic episodes from the Late Cretaceous to the present. It is defined by the interplate boundary in the west and extends to the Rocky Mountain front in the east. Yucca Mountain lies in the Basin and Range structural province, which comprises a large, central part of the deformed half of the plate.

Relative motion between the plates is the direct and indirect cause of the deformation of the continental crust of western North America. Quaternary deformation in California and Nevada is due to the northward rotation of the Pacific plate relative to the North American plate, about a pole near 50°N. and 70°W. (Morgan, 1968; Atwater, 1970; Minster and Jordan, 1978; Engebretson et al., 1985). Right-lateral displacement along the San Andreas fault system, at rates of 2 to 5 cm/yr and totaling 300 to 600 km (Crowell, 1973, 1975), and recent sea-floor spreading in the Gulf of California attest to the plate rotation during the last 10 million years.

Large parts of western North America have undergone crustal extension during the Neogene (Hamilton, 1978; Davis, et al., 1982; see Section 1.3.2 for additional discussion of crustal extension). Mechanical extension of the

lithosphere results in its thinning by an amount equivalent to the inverse of the extension (McKenzie, 1978). The Mohorovocic discontinuity (Moho) beneath the extended parts of the western United States is observed to be at a depth of approximately 30 km (Smith, 1978; Klemperer et al., 1986), in contrast to its 40-km depth beneath the unextended parts (Keller et al., 1979). This suggests that plate motions have also resulted in widespread mantle up-

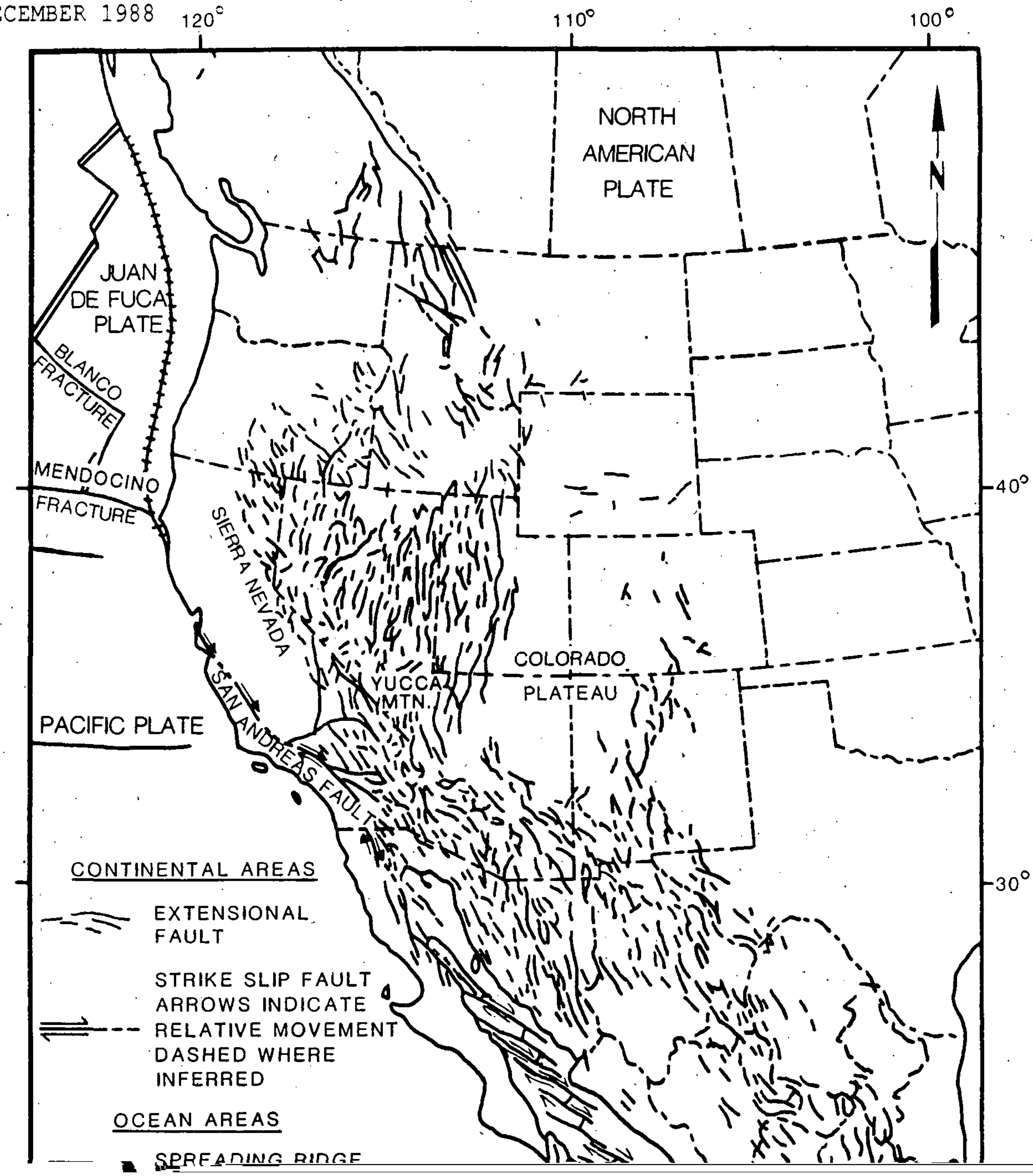
120°
110°
100°
40°
30°
N
NORTH AMERICAN PLATE
JUAN DE FUCA PLATE
BLANCO FRACTURE
MENDOCINO FRACTURE
SIERRA NEVADA
YUCCA MTN.
COLORADO PLATEAU
PACIFIC PLATE
SAN ANDREAS FAULT
CONTINENTAL AREAS
EXTENSIONAL FAULT
STRIKE SLIP FAULT ARROWS INDICATE RELATIVE MOVEMENT DASHED WHERE INFERRED
OCEAN AREAS

1.3.1.2 Structural provinces and subprovinces

The Basin and Range structural province includes Nevada and western Utah and extends from southeastern California to southern New Mexico and into Mexico. It is geologically diverse, but is structurally characterized by Miocene to Holocene range-front faulting with associated horsts and grabens. In Nevada, the structural province corresponds to the Great Basin physiographic subprovince (Section 1.1), which, at its southern end, lies between broad uplifted terranes that have experienced less significant internal deformation during the Tertiary. These are the Colorado Plateau province to the east and the Sierra Nevada Range to the west (Figure 1-25, Section1.3.1.1). The Colorado Plateau consists chiefly of Paleozoic and Mesozoic platform sedimentary rocks that have flat to gentle dips and rest nonconformably on various Proterozoic crystalline rocks. The Sierra Nevada Range is mainly a batholith, chiefly of late Mesozoic plutonic rocks; it has a gentle westerly tilt and a steep eastern escarpment.

The southeastern part of the Great Basin, including Yucca Mountain, is distinct from the southwestern part in east-central California, forming two physiographic areas (Section 1.1). Both of these areas are characterized by

horsts and grabens or tilted block ranges, but in the southeastern area the valleys are nearly filled with sediment and the ranges are deeply eroded. By contrast, the southwestern area, which includes Death Valley, has high relief and contains numerous Quaternary faults. The southwestern area terminates to the south against the Mojave Desert province, an uplifted region of subdued topography where the Tertiary tectonic features are characterized by numerous right-lateral faults with northwestern trends. To the south, the southeastern area merges with the Sonoran Desert section of the Basin and Range province in western Arizona and southeastern California (Section 1.1).

Province and subprovince boundaries typically coincide with large strike-slip faults (Figure 1-26). The Garlock fault, with 48 to 65 km of left slip (Smith, 1962; Smith and Ketner, 1970), separates the basins and ranges of the Death Valley-Sierran region from the Mojave Desert. The Death Valley and Furnace Creek faults (Figure 1-26) are en echelon components of a right-lateral fault system across which there has been 10 to 80 km of displacement (Stewart et al., 1968). This fault system and other large right-lateral faults with northwest trends in the Walker Lane (Albers, 1967; Stewart, 1967, 1978) separate the southeastern and southwestern areas. The Las Vegas Valley shear zone, with at least 40 (and probably 65) km of right-

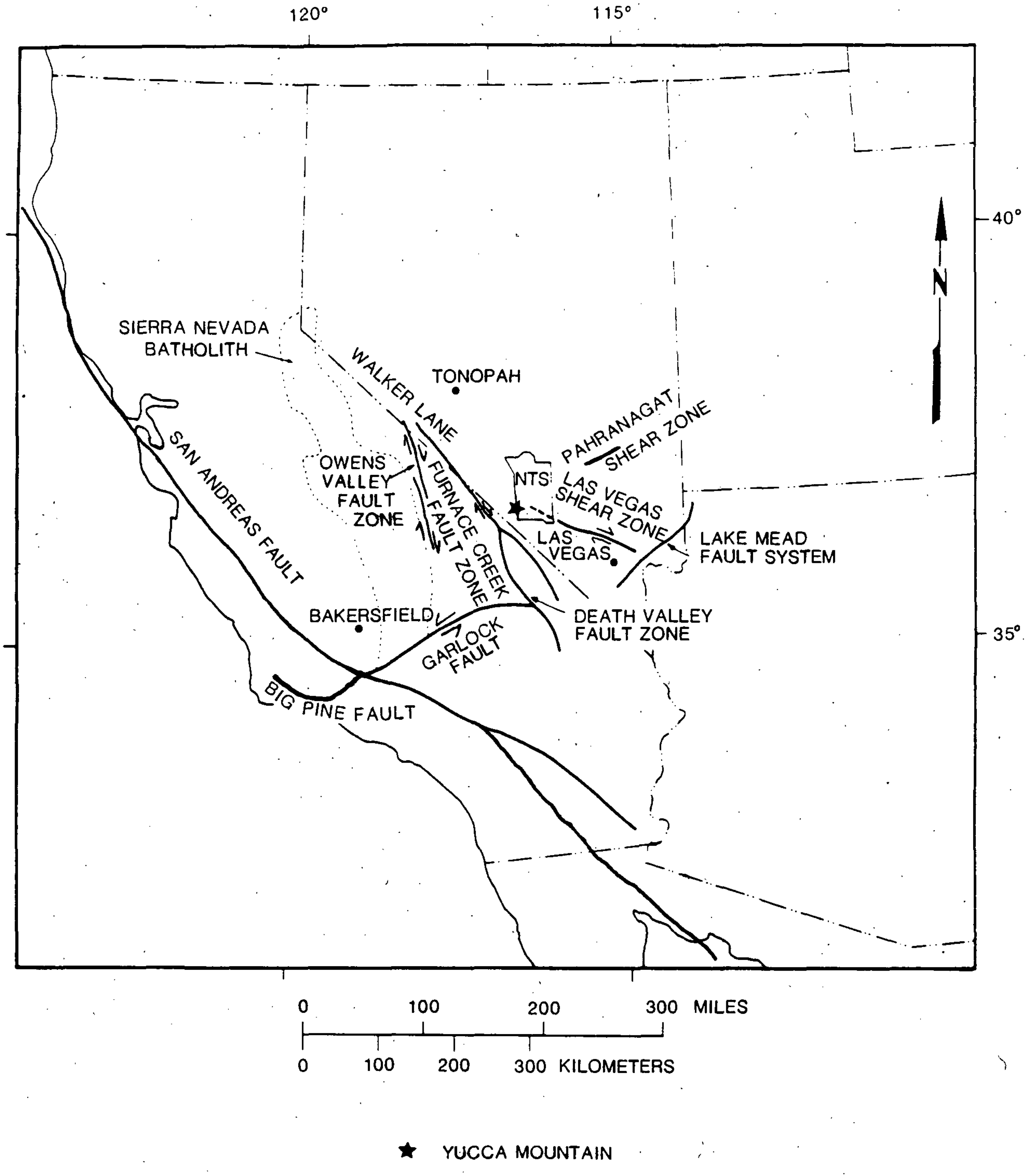

Figure 1-26. Major strike-slip faults of the southern Great Basin and vicinity. Right-lateral faults include the San Andreas, Walker Lane, Death Valley, Furnace Creek, and Las Vegas Valley. Left-lateral faults are the Big Pine, Garlock, Lake Mead, and Pahranagat. Modified from Sinnock (1982).

Parts of the province boundaries are expressed seismically (Section 1.4). The southwestern boundary of the Basin and Range province corresponds to the southern segment of the Nevada-California seismic belt, along which the 1872 Owens Valley earthquake occurred (Section 1.4). A diffuse zone of epicenters marks the west-central edge of the Basin and Range province, and the Intermountain seismic belt corresponds to the northeastern border of the Basin and Range province (Section 1.4). The Mojave and Sierran subprovinces meet along the seismically active part of the Garlock fault.

Other boundaries are not seismically expressed. The boundary between the southern Great Basin and the Mojave Desert is along an inactive stretch of the Garlock fault, and the diffuse East-West seismic belt is well north of the geomorphic transition between the southern Great Basin and the Sonoran sections of the Basin and Range province (Section 1.4). However, Christiansen and McKee (1978) observed that the East-West seismic belt and geophysical gradients distinguish the northern Great Basin from the Sonoran section at about the latitude of Yucca Mountain. Other geologically important, but seismically inactive, boundaries occur at the northwestern edge of the Basin and Range province, along the Colorado Plateau-Basin and Range transition, and along the Walker Lane between the southwestern and the southeastern portions of the Great Basin.

1.3.1.3 Yucca Mountain area

Yucca Mountain is in the southern part of the Great Basin physiographic province, near the border between its western and eastern parts (Section 1.1). It also lies along the boundary, described by Christiansen and McKee (1978), between the southern and the northern parts of the Basin and Range structural province. Thus, its structural history is closely tied with the regional history of the Basin and Range province. The major tectonic features near Yucca Mountain include (1) strike-slip faults like the Las Vegas Valley shear zone and the Death Valley Furnace Creek zone, (2) many large Basin and Range normal faults and other extensional structures, and (3) the seismic and geophysical contrasts between the southern and northern parts of the province described by Christiansen and McKee (1978).

1.3.2 TECTONIC HISTORY

This section discusses the tectonic history of the western United States as a basis for discussing the volcanic (Section 1.3.2.1) and structural (Section 1.3.2.2) history of the southern Great Basin (i.e., the region surrounding Yucca Mountain). Also discussed are regional stress (Section 1.3.2.3), crustal movement (Section 1.3.2.4), and regional geothermal patterns (Section 1.3.2.5).

Before 200 million years ago, what is now the western United States underwent events of rifting, passive margin formation, and crustal collision. The oldest rocks of eastern California, Montana, and Arizona show evidence of a period of Proterozoic rifting that resulted in the breakup of a large continent and in the formation of an ocean basin to the west of North America

(Stewart, 1972). The passive continental margin that formed after the breakup extended from the Death Valley area to western Montana and slowly subsided during most of the early Paleozoic (Burchfiel and Davis, 1975). Overthrust Paleozoic oceanic assemblages in the Antler and the Sonoma orogens of northeastern Nevada and in the El Paso Mountains of southern California record episodes of oceanic closure and crustal collision (Dickinson, 1977; Dickey et al., 1980) during the middle and late Paleozoic. Fossiliferous Permian rocks from various latitudes and different island-arc, oceanic-crust, and melange terranes are now welded to western North America. These juxtapositions of different paleoclimatic and paleobiogeographic provinces indicate the subduction of vast amounts of oceanic crust during Triassic and Jurassic time (Hamilton, 1978). Gentle subsidence continued east of these collisional zones.

During much of Cretaceous and early Tertiary time, western North America was bordered on the west by two oceanic plates, Kula on the northwest and Farallon on the southwest (Engebretson et al., 1985). The boundary between the North American plate and the Kula plate was probably a convergent transform fault, whereas the boundary between the Farallon plate and the North American plate was a subduction zone. Magmatism related to this subduction zone formed the Sierra Nevada batholith as a magmatic arc over a period of 60 million yr during the Late Jurassic and the Cretaceous. Tectonism and sedimentation in and adjacent to the offshore trench resulted in the formation of the Franciscan complex and the Great Valley sequence in coastal California (Bailey and Blake, 1969; Dickinson, 1970). A continuous belt of east-directed thrust faults, the Sevier orogenic zone (Armstrong, 1968), formed in southeastern Nevada, western Utah, eastern Idaho, western Wyoming, and western Montana. Major changes of motion between the North American, Pacific, and African plates and the consequent reconfiguration of the composite subduction zone-transform fault boundary of western North America during the Late Cretaceous and early Tertiary resulted in a broadening of the belt of deformation to include the Rocky Mountain region during the Laramide Orogeny (Coney, 1978; Hamilton, 1978). After the orogeny, magmatism occurred in two large belts from northern and central Nevada to southwestern Colorado and from southeastern California to southwestern New Mexico between 20 and 40 million years ago (Eaton, 1979).

The east Pacific Rise came in contact with the North American plate shortly after 28 million years ago at about latitude 30°N. (Engebretson et al., 1985). A transform-transform-trench triple junction (McKenzie and Morgan, 1969) migrated northwest from the point of contact. The junction was offshore at about the latitude of Yucca Mountain by 12 to 16 million years ago, and continued migrating to its present position at latitude 40°N. (Engebretson et al., 1985). At all times, a subduction zone lay to the north of the junction and a transform fault to the south. Widespread extensional tectonism in the Basin and Range structural province, most of which occurred between 20 million years ago and the present, coincided with the triple-junction migration. Thus, the extensional tectonism was clearly related to the change in plate boundaries, but the relations are poorly understood. Several theories have been proposed to explain the extensional tectonics and the associated high heat flow and crustal thinning of the Basin and Range province during the late Tertiary. These theories basically fall into two groups: those that are based on strike-slip tectonics related to the counterclockwise rotation of the North American plate relative to the Pacific plate (Atwater, 1970) and those that are based on the subduction of the Farallon plate beneath the continent (Eaton, 1982). Right-lateral strike slip on faults forming the transform boundary between the Pacific and North American plates began shortly after 28 million years ago. That boundary evidently lengthened and jumped inland (eastward) as the triple junction forming its northern termination migrated northwestward (Fox et al., 1985). Right-lateral strike slip on the San Andreas fault, the present boundary, probably began sometime around 10 to 12 million years ago (Crowell, 1975), and it is possible that the tectonic regime may have changed from extension, related to subduction, to oblique extension related to the San Andreas fault (Hamilton, 1982) at that time. As summarized by Stewart (1978), in this view western North America is within a broad belt of right-lateral movement related to differential motion between the North American and the Pacific plates. Some of the right-lateral movement is now taken up on the San Andreas fault and related zones of right-lateral shear, such as the Walker Lane in the western Great Basin. The movement is also thought to produce distributed extension and tensional crustal fragmentation (including basin and range structure) along trends oriented obliquely to the trend of the San Andreas fault.

Theories that have been called upon to explain the tectonic features and timing of tectonic events in the Basin and Range province typically center around mechanical plate interaction and mantle upwelling models. Hot, low-density material in the mantle rises up to the mantle-crust boundary and has the effect of raising the temperature of the lower crust, placing extensional stresses on the crust, and initiating magmatism that intrudes and passes through the crust. Eaton (1979) has proposed that subduction of the Farallon plate initiated these mantle upwelling processes as a result of back-arc spreading processes.

In Eaton's (1979) model, extensional failure first occurred about 30

million years ago in southeastern California, southwestern Arizona, and in the Rio Grande rift in a calc-alkalic volcanic arc that had formed east of the convergent plate boundary between the Farallon and the North American plates. A new area of extension began behind the arc about 17 million years ago in the Great Basin as the rise that separated the Farallon and the Pacific plates grew closer to the trench west of the North American plate. As a result, the subducted Farallon plate became progressively warmer and thinner as younger parts of it were consumed by subduction. Extension might have taken place by basaltic diking and by solid state flowage of the deep lithosphere, possibly driven by hydrodynamically forced convective motions in the asthenosphere as a result of steepened subduction of the Farallon plate.

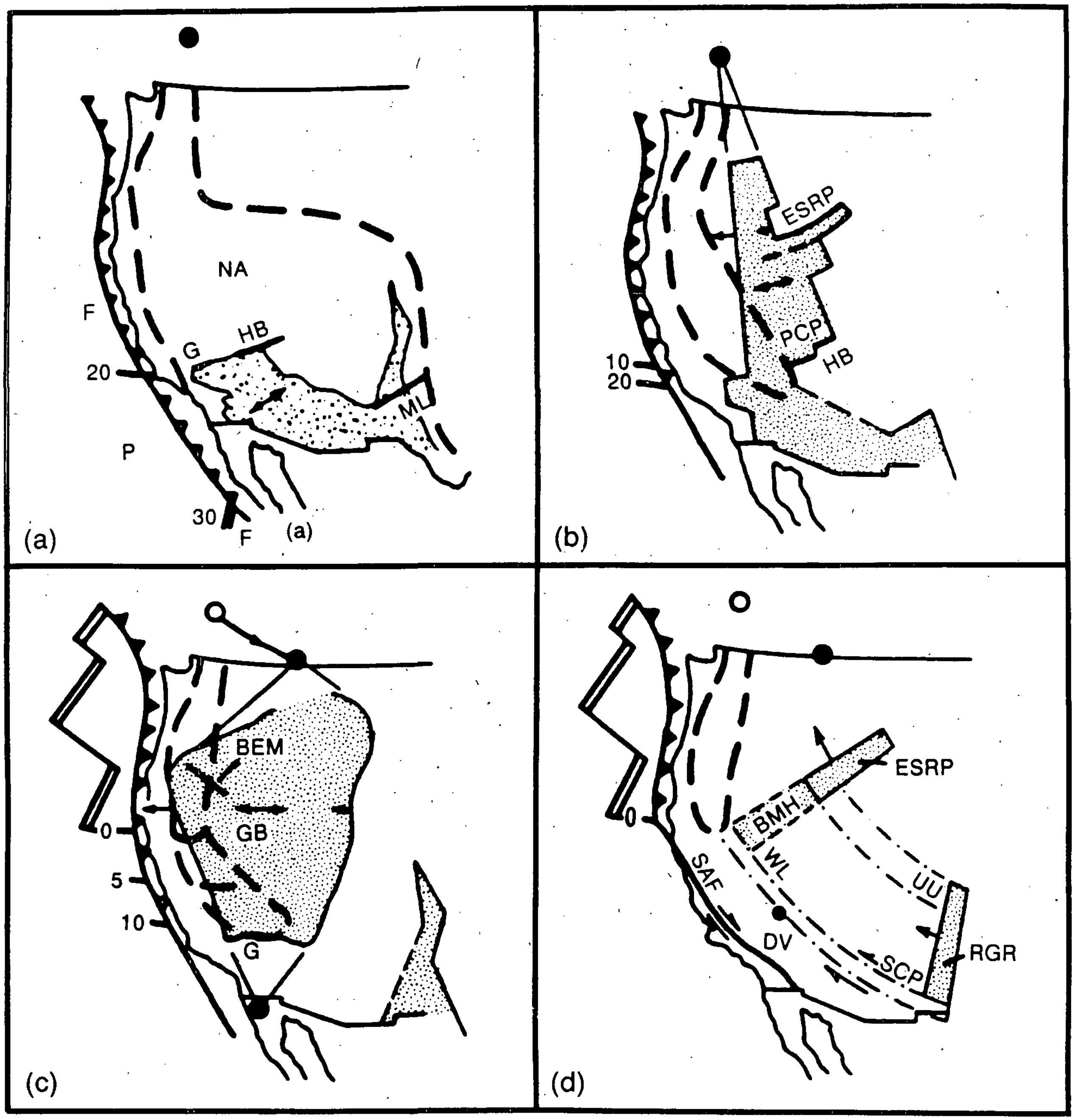

Figure 1-27. Schematic diagram showing tectonic evolution of extension in the continental western United States. Individual figures represent the following blocks of time: a, 30 to 20 million yr ago; b, 20 to 10 million yr ago; c, 10 million yr ago to the present, and d, 7 million yr ago to present. Toothed lines identify convergent plate boundaries and dashed lines, boundaries of volcanic arcs. The Mendocino triple junction is located at the intersection of the trench and the short, solid lines labelled 20, 10, 5, and 0 million yr. Stippling identifies approximate areas of active extension for each period; that of the period 30 to 20 million yr ago was characterized by plastic stretching of the middle crust, hence the use of different stipple pattern. Labelled lines are postulated transform structures. Rifts and other features are also labelled: GB identifies the north-central Great Basin; SA, the San Andreas fault; RGR, the Rio Grande rift; BMH, The Battle Mountain High, and DV, th Death Valley, California, region. Doubled-headed arrows show interpreted directions of quasi-rigid or stiff-plastic subplate rotations. Long arrows qualitatively indicate relatively greater total movement than short ones in diagrams b, c, and d. Solid dots mark locations of interpreted poles of opening. The open circle marks an abandoned pole location.

Las Vegas Valley shear zone, and the southern margin of the Colorado Plateau to the Rio Grande rift (part d of Figure 1-27).

Tectonism caused by the active boundary between the Pacific and the North American plates has continued to dominate the framework of western North America in Quaternary time. Large strike-slip faults, like the San Andreas and Garlock faults (Figure 1-26, Section 1.3.1.2), have records of Pleistocene and Holocene activity (Smith, 1978), indicating that the northward motion of the Pacific plate relative to the American plate continues. Quaternary arc magmatism, related to subduction of the Juan de Fuca plate beneath North America, is evident in the Cascade Mountains, notably at Mount St. Helens, where recent eruptions have occurred (Lipman and Mullineaux, 1981). Young volcanism in the Great Basin and on the Colorado Plateau is characterized chiefly by basaltic eruptions, with documented Quaternary flows and cones in southeast and east-central California, southwestern Utah, northern Arizona, southern Idaho, northwestern Wyoming, and parts of Nevada (Christiansen and McKee, 1978). Quaternary silicic to intermediate magmatism, possibly related to Basin and Range extension, has occurred (1) in the Long Valley area of California (250 km northwest of Yucca Mountain), where recent shallow seismicity suggests the migration of magma and the potential of a future eruption (Hill et al., 1985); (2) in the Mono Basin (250 km northwest of Yucca Mountain) where flows are less than 10,000 yr old (Miller, 1985); and (3) in the Coso field (150 km southwest of Yucca Mountain) with 40,000-yr-old flows (Duffield et al., 1980).

1.3.2.1 Volcanic history

This section discusses the igneous history of the southern Great Basin and Yucca Mountain. It emphasizes the history of Tertiary volcanism to provide a basis for related discussions of the proposed repository host rock in other sections of this document. Specific topics include the stratigraphy and lithology of the host rock and surrounding units (Section 1.2.2), the mechanical properties of the tuffs (Section 2.1), the thermal properties of the tuffs (Sections 2.4 and 2.5), jointing and fracturing in the volcanic sequence (Section 1.3.2.2.2), faulting associated with volcanism (Section 1.3.2.2.2), the hydraulic characteristics of the tuffs (Section 3.9.2), and the geochemical characteristics of the tuffs (Section 4.1). This section also emphasizes the history of Quaternary volcanism as a basis for assessing the likelihood of future igneous activity that could affect the repository (Section 1.5).

Arc magmatism, associated with the formation of the Sierra Nevada batholith, affected parts of Nevada until about 80 million years ago (Crowder et al., 1973; Lanphere and Reed, 1973). Several Cretaceous plutons crop out near Yucca Mountain (Bath et al., 1983; Carr, 1984); the closest being Fluorspar Canyon, at the north end of Bare Mountain, approximately 18 km west of the candidate site. Magmatism shifted east to the Rocky Mountain region between 72 and 55 million years ago, during the Laramide Orogeny [illegible]

Yucca Mountain region. The magmatic gap started to close about 40 million years ago, as fields of silicic to intermediate igneous activity migrated south and southwestward out of northern Nevada (Figures 1-28a through 1-28d), and northward from northern Mexico into southern Arizona (Cross and Pilger, 1978). The southward transgression ended near Yucca Mountain about 15 to 20 million years ago (Stewart and Carlson, 1978). Volcanism also had transgressed northward from Mexico as far as Lake Mead by about 14 million years ago (Anderson, 1971), leaving a small amagmatic gap in southern Nevada (Figure 1-28c). Volcanism shifted toward the margins of the Great Basin (Christiansen and McKee, 1978) and the composition of the magma changed at about that time. In the early, transgressive phase of volcanism, the magma was chiefly of andesitic to rhyolitic; the subsequent change was to basaltic and bimodal rhyolitic- basaltic composition (Christiansen and Lipman, 1972; Lipman et al., 1972). Near Yucca Mountain, the change in magma composition occurred approximately 9 million years ago (Crowe et al., 1983a).

1.3.2.1.1 Middle Tertiary volcanism

This section summarizes the history of middle Tertiary volcanism in the Great Basin and the Sonoran Desert of Arizona. Most of the volcanic rocks at and near Yucca Mountain formed during this time. The rocks are mainly silicic volcanic and volcaniclastic rocks derived from the Timber Mountain-Oasis Valley caldera complex (Figure 1-29) 9.5 to 16 million years ago (Christiansen et al., 1977).

Middle Tertiary silicic and intermediate volcanic rocks in Nevada and western Utah occur in arcuate east-trending belts that decrease in age to the south (Stewart et al., 1977). The nearest volcanic activity was 250 km north of Yucca Mountain 43 to 34 million years ago, and it left no record in southern Nevada. By 20 to 28 million years ago, volcanism had migrated far enough south that silicic ash flows and tuffs, formed during nearby caldera eruptions to the north, were deposited near Yucca Mountain (Figure 1-28b).

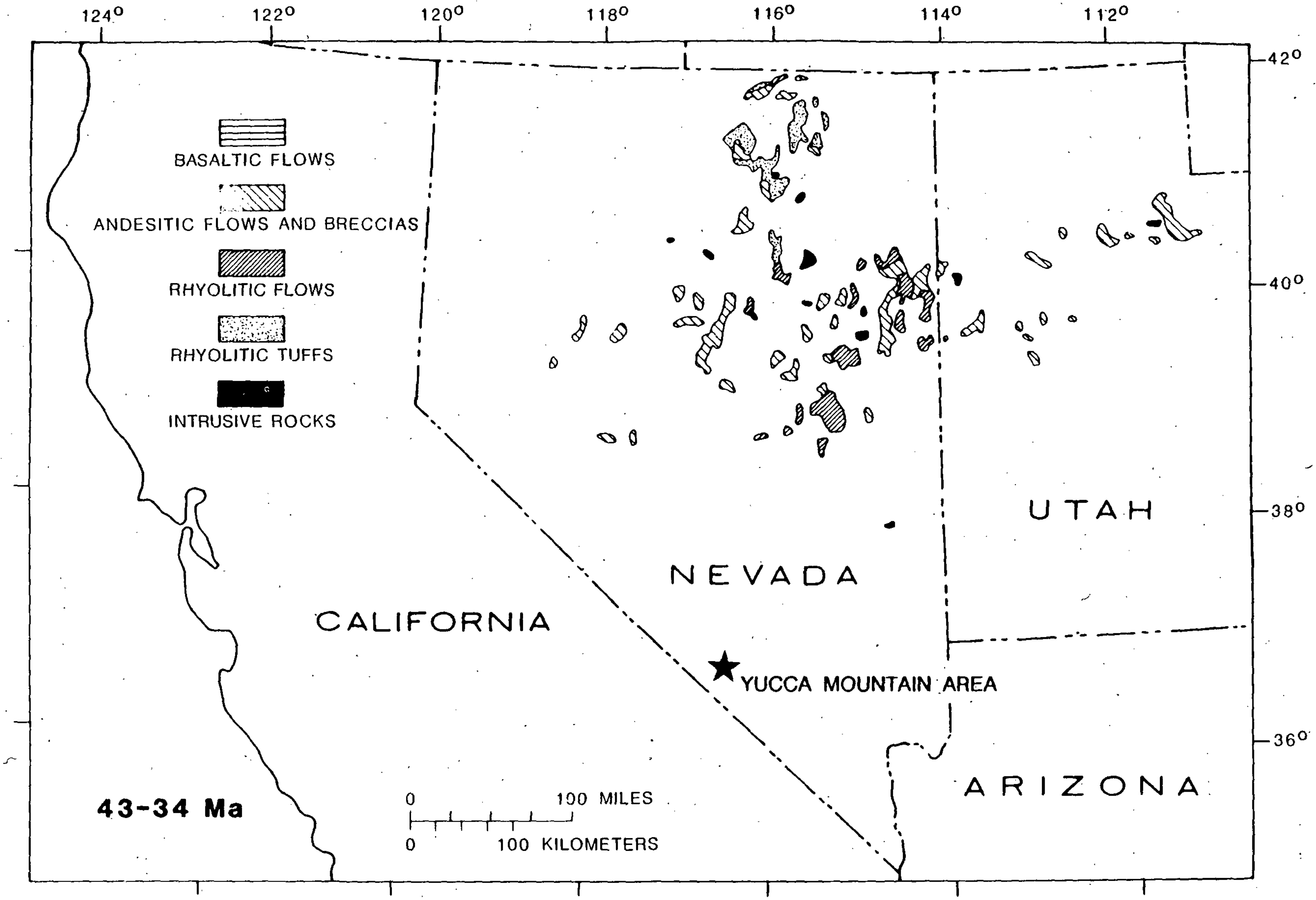

Figure 1-28a. Distribution of the Cenozoic volcanic rocks in the southern Great Basin. Time periods shown are 43-34 Ma (map a), 34-17 Ma (map b), 17-6 Ma (map c), and 6-0 Ma (map d). Ma = million years ago. Modified from Stewart et al. (1977).

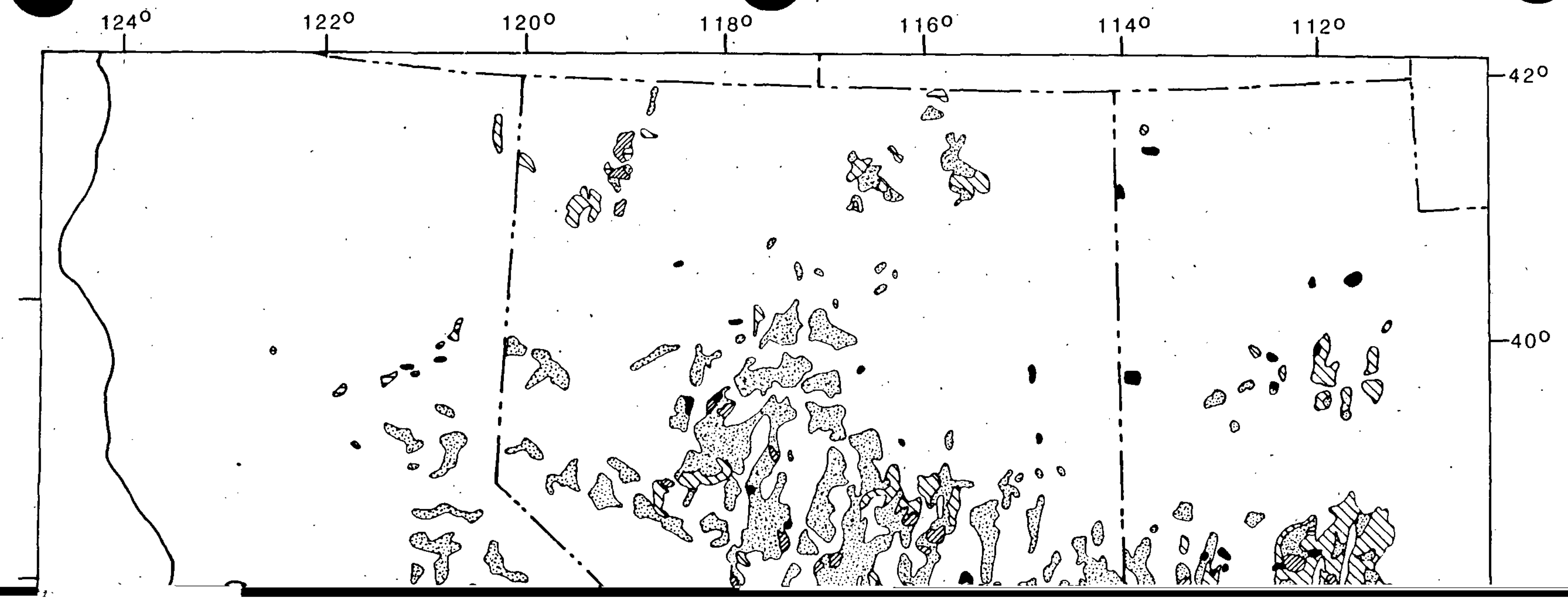
124°
122°
120°
118°
116°
114°
112°
42°
40°

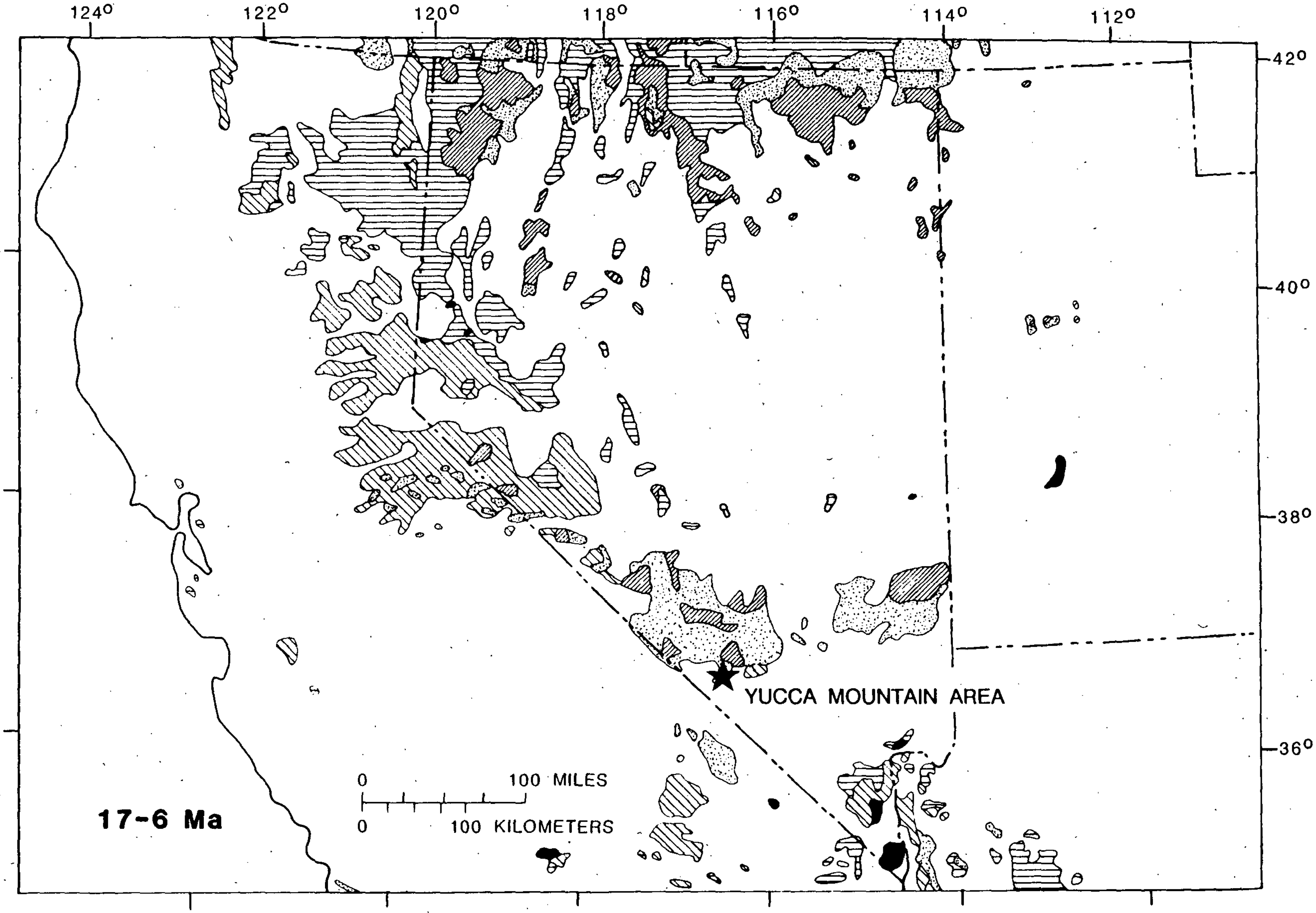

Figure 1-28c. Distribution of the Cenozoic volcanic rocks in the southern Great Basin. Time periods shown are 43-34 Ma (map a), 34-17 Ma (map b), 17-6 Ma (map c), and 6-0 Ma (map d). Ma = million years ago. Modified from Stewart et al. (1977).

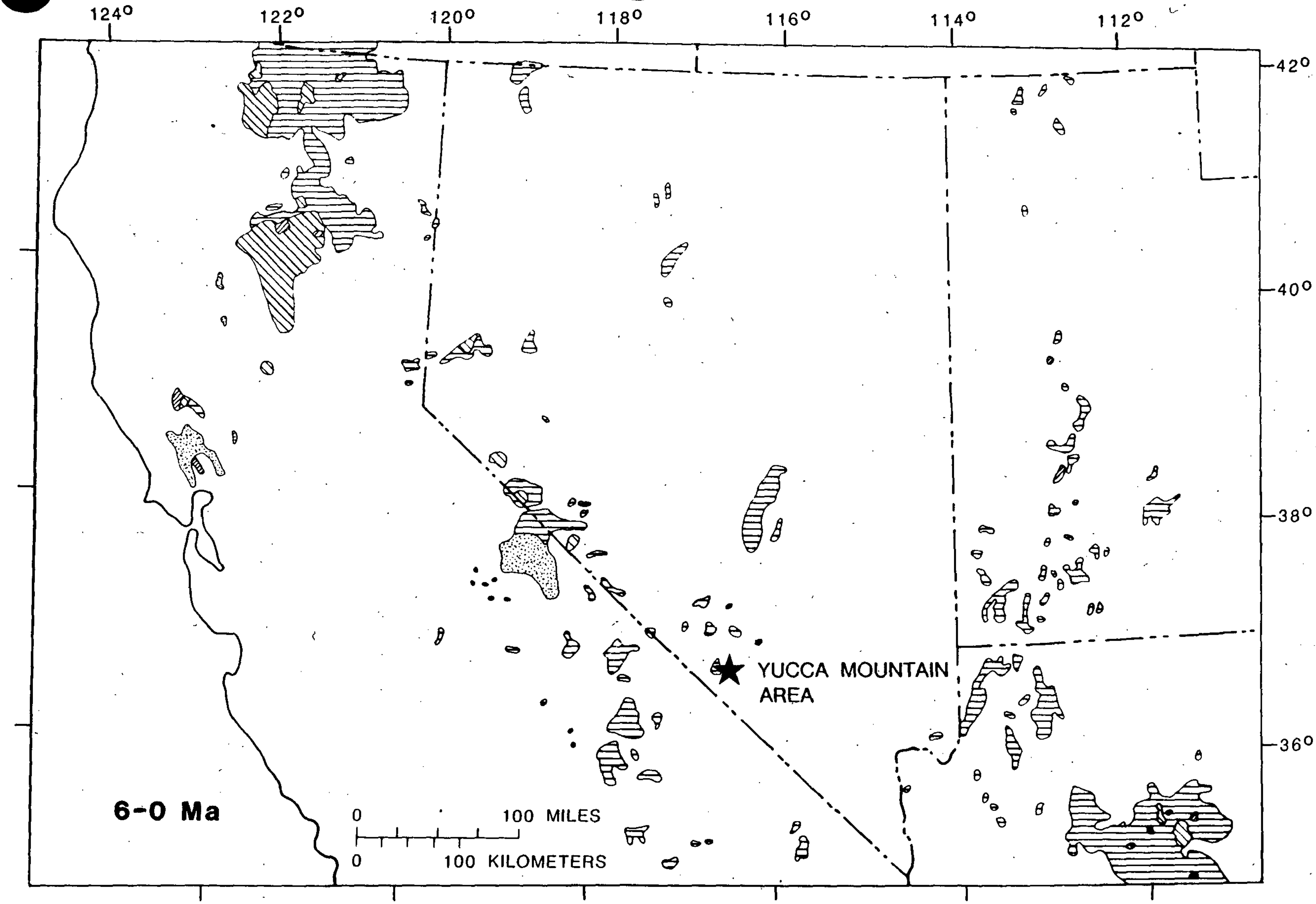

Figure 1-28d. Distribution of the Cenozoic volcanic rocks in the southern Great Basin. Time periods shown are 43-34 Ma (map a), 34-17 Ma (map b), 17-6 Ma (map c), and 6-0 Ma (map d). Ma = million years ago. Modified from Stewart et al. (1977).

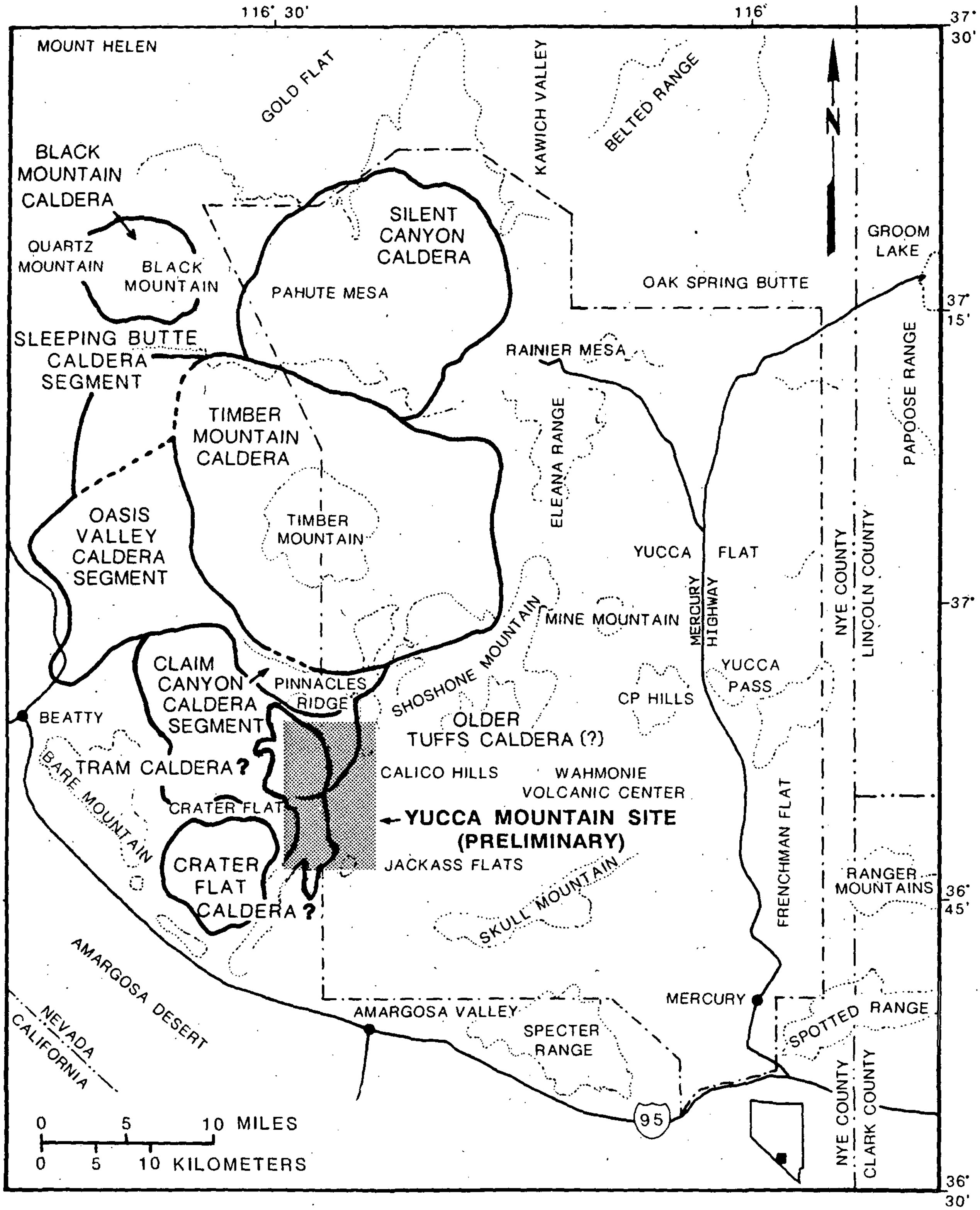

Figure 1-29. Calderas of the southwest Nevada volcanic field near Yucca Mountain. Modified from Maldonado and Koether (1983).

An older center at Crater Flat has been postulated by Carr et al. 1984; it was apparently buried beneath voluminous flows from the Timber Mountain-Oasis Valley center. The center could include two cauldrons, the Crater Flat and the Prospector Pass segment of the Tram Caldera, and it was possibly active approximately 13.9 million years ago (Carr et al., 1984). These buried calderas may reflect volcano-tectonic subsidence that included the entire area west and north of Yucca Mountain (Carr, 1984). However, Scott et al. (1984b) and Broxton et al. (1985) present evidence that the Crater Flat tuff may have come from the Timber Mountain-Oasis Valley complex, which would indicate that Crater Flat was not the site of a caldera. The subvolcanic rocks beneath Crater Flat are more than 3,000 m deep (Snyder and Carr, 1982).

Middle Tertiary volcanic centers in southern Nevada seem to be conbelt is perpendicular to the inferred least principal stress (Zoback et al., 1981; Section 1.3.2.3); thus, it is parallel to the most likely direction of dike injection.

Some basalt fields in the Death Valley-Pancake Range zone contain a large volume (more than 3 km^3) of rock, were relatively long-lived (active for several million years), bimodal, and consist mainly of various types of basalt (Table 1-6). Locally, minor amounts of rock in these fields are extremely silicic (high-silica rhyolite). Other fields contain a small volume (typically 0.1 km^3) and consist of scoria cones or clusters of cones and associated basaltic lavas (Table 1-6).

The basalt centers of the Death Valley-Pancake Range zone occur in three structural settings (Crowe and Carr, 1980). Some coincide with north-northeast trending zones of extension between active or formerly active northwest trending strike-slip faults. Many erupted near the ring-fracture zones of inactive cauldrons, and others are associated with normal faults.

The oldest basalts of the Death Valley-Pancake Range zone occur near the earlier silicic volcanic centers. They were erupted during the waning stages of large-volume silicic volcanism, and they range in composition from basalt to basaltic andesite or latite. Younger basalts show no relation to the silicic volcanic centers. They were erupted during episodes of extensional faulting, and they are alkaline basalt and hawaiite (Vaniman et al., 1982). Rift basalts older than 6.5 million years old have trace-element abundances typical of alkali basalt throughout the Great Basin (Crowe et al., 1983b). Those younger than 6.5 million years are enriched in incompatible trace elements other than rubidium; they occur near Yucca Mountain and in southern Death Valley (Crowe, et al. 1983b).

Crowe et al. (1986) suggest that the trace-element enrichment in the basalts might indicate that they underwent (1) mantle metasomatic enrichment, (2) a decrease in the degree of mantle partial melt with time, or (3) contamination with enriched crustal rocks. He favors the first possibility and concludes that the alteration in the mantle predated the derivation of the basalts. Table 1-6 indicates that the basalts near Yucca Mountain erupted near, or in association with, faults, rifts, and fracture zones, which strongly suggests structural control of the volcanism.

The style of eruption of the youngest rift basalt was Strombolian, a style characterized by isolated small-volume and short-duration eruptions that formed scoria cones and lava flows. Strombolian eruptions range in duration from 1 day to 15 yr with a median value of 30 days (Wood, 1980). Volcanoes of this type may occur singly or in large fields of many cones. Fields may be the site of intermittent eruptions from newly formed cones over a period of millions of years. The cones resulting from Strombolian eruptions range in size from a diameter of 0.25 to 2.5 km with a mean of about 0.9 km. Cone heights are about 0.18 of the basal cone diameter (Wood, 1980). The volumes of lava flows associated with this type of

Table 1-6. Characteristics of basaltic volcanism fields in the Yucca Mountain area[a] (page 1 of 2)

Field	Description	Tectonic setting	Age (million years)
Death Valley	A. Southern Death Valley--single scoria cone, no lavas B. Older lavas of Shoreline Butte	Close to Southern Death Valley fault, near its intersection with north-northeast trending faults	2 to 0.5
Greenwater-Black Mountain	Three cycles of bimodal activity from south to north and older to younger: Quartz bearing basalts, olivine basalts, and mafic andesite	General "pull-apart" or spreading area between Furnace Creek and Death Valley fault zones. Vents along north to north-northeast trending fault zones	8 to 4
NTS[b] region--silicic cycle basalts (e.g., basalts of Basalt Ridge, Dome Mountain, Kiwi Mesa, and Skull Mountain)	Large volume lava sheets and shields	Ring fracture zones or Basin and Range faults within or near rhyolite caldera complexes	11 to 8
NTS region--"rift" cycle basalts (e.g., basalts of Silent Canyon, Nye Canyon, Paiute Ridge, Buckboard Mesa, Sleeping Butte, and Crater Flat)	Small volume scoria cones with minor lava erupted during distinct pulses of activity throughout the NTS region	Basin and Range faults in general but including (1) their intersection with caldera ring zones and (2) north-northeast trending rifts possibly related to right-stepping offsets in strike-slip shear zones of Walker Lane belt	8 to 0.3

Table 1-6. Characteristics of basaltic volcanism fields in the Yucca Mountain area[a] (page 2 of 2)

Field	Description	Tectonic setting	Age (million years)
Kawich Valley	Isolated scoria cones, lavas and small plugs	Basin and Range faults	10 to 8
Reveille Range	Sheets and local shields of scoria cones and large volume lavas including local trachy-andesite and trachyte plugs or domes	North-northeast trending rifts between northwest trending strike-slip faults and north-south trending Basin and Range faults	5.9 to 3.8
Lunar Crater (Pancake Range)	Numerous single or coalesced Strombolian and Surtseyan centers with small to large volume lavas	Localized along major north-northeast trending rift zone that crosses a much older (20-30 million years) caldera complex (Ekren et al., 1974b). Older basalts are mostly related to caldera ring fracture, younger to north-northeast trending rifts.	<0.13

[a]Modified from USGS (1984).
[b]NTS = Nevada Test Site.

The rates of volcanic activity during the last 8 million years, expressed as a function of the number of cones per given area and time period, are consistently low. For example, Crowe et al. (1982) calculated the Quaternary rate in the NTS region as 3.9 x 10^{-9} cones/km^2/yr. The youngest centers near Yucca Mountain are in southern and northern Death Valley; near Crater Flat, immediately west of Yucca Mountain; and north of Beatty, Nevada. The Lathrop Wells cinder cone, at the southern edge of Crater Flat, is the youngest volcanic feature in the Yucca Mountain area. Crowe and Carr (1980) give the age of this cone as being between 200,000 and 300,000 yr based on potassium-argon dating. Sinnock and Easterling (1983) provide 18 additional potassium-argon dates for this cone (dated by 3 independent laboratories). They report an average age estimate of 460,000 yr with uncertainty ranges of several hundred thousand yr. Some of the uncertainty in the dating is probably the result of the use of the potassium-argon method on materials that are at the younger limits of the technique. Recent geomorphic studies of the Lathrop Wells cone indicate that more than one volcanic event may have occurred at this site. The lava flows at the base of the cone (the source of the potassium-argon samples) may be the result of an older event while the cone may represent a much younger event than previously thought. According to Wells et al. (1988) and Crowe et al. (1988), comparison of the geomorphic characteristic of the cone with dated cones in the Cima volcanic field indicate that the age of the cone could be approximately 15,000 yr. Planned studies (Section 8.3.1.8.1) will refine the dating of such young basalts, because the dating may be important in preparing postclosure release scenarios. The probability of future volcanic activity in the site region is discussed in Section 1.5.1.

1.3.2.2 Structural history

This section discusses the structures and the structural history of the southern Great Basin (Section 1.3.2.2.1) and of Yucca Mountain and its immediate surroundings (Section 1.3.2.2.2). The discussion here is based on the geographically broader treatment of tectonic history in Section 1.3.1. The discussion emphasizes the history and characteristics of the Tertiary and Quaternary faults and fractures of Yucca Mountain; (i.e., it emphasizes the geologic structures that may affect the construction of the proposed repository and its effectiveness in isolating the waste). This discussion also considers faults and fractures that might provide hydrologic pathways to the accessible environment (Section 3.9.3.1). Finally, the discussion provides a basis for assessing the potential for the repository being disrupted by a fault (Section 1.5.2). Related topics discussed elsewhere in Chapter 1 are the seismicity of the region (Section 1.4) and the likelihood of faulting during the 10,000 yr isolation period (Section 1.5.2).

1.3.2.2.1 Structures and structural history of the southern Great Basin

The tectonic episodes that were dominant during Proterozoic time in the southern Great Basin were (1) the tectonic, metamorphic, and intrusive activity that produced the Precambrian crystalline basement rocks in the southwestern Great Basin and (2) the tectonic activity that established a late Precambrian continental margin in western Nevada (Stewart, 1980a). Most of the exposed crystalline basement is concentrated in the Lake Mead area and south of Las Vegas in an area that was uplifted possibly as a Laramide arch (Bohannon, 1984). A small exposure occurs in the Bullfrog Hills west of Yucca Mountain (Stewart, 1980a), so these rocks probably underlie Yucca Mountain at depth. Structures associated with the formation of the Proterozoic continental margin are exposed near Death Valley (Burchfiel and Davis, 1975), but any possible correlative structures are deeply buried at Yucca Mountain.

The Paleozoic was a time of slow subsidence and deposition throughout southern Nevada. Middle and late Paleozoic orogenic events, such as the Antler, that are recorded in other parts of Nevada occurred west and north of Yucca Mountain and were not felt there. General references like Fiero (1986) and Stewart (1980a) provide discussions of pre-Mesozoic tectonic activity in the Great Basin. Folding in the region around Yucca Mountain has generally been the result of low angle thrust or detachment faulting or high angle normal or strike-slip faulting and is discussed as part of the faulting process rather than being considered separately.

Mesozoic structures

Mesozoic thrust faults, which superimpose older rocks on younger rocks, are exposed in a north-trending belt in west-central Nevada, in a northeast trending belt in southeastern Nevada, and in short segments near Yucca Mountain (Stewart, 1980a; Figure 1-30). Triassic and Jurassic rocks in west-central Nevada locally occur in complex imbricate thrust slices,

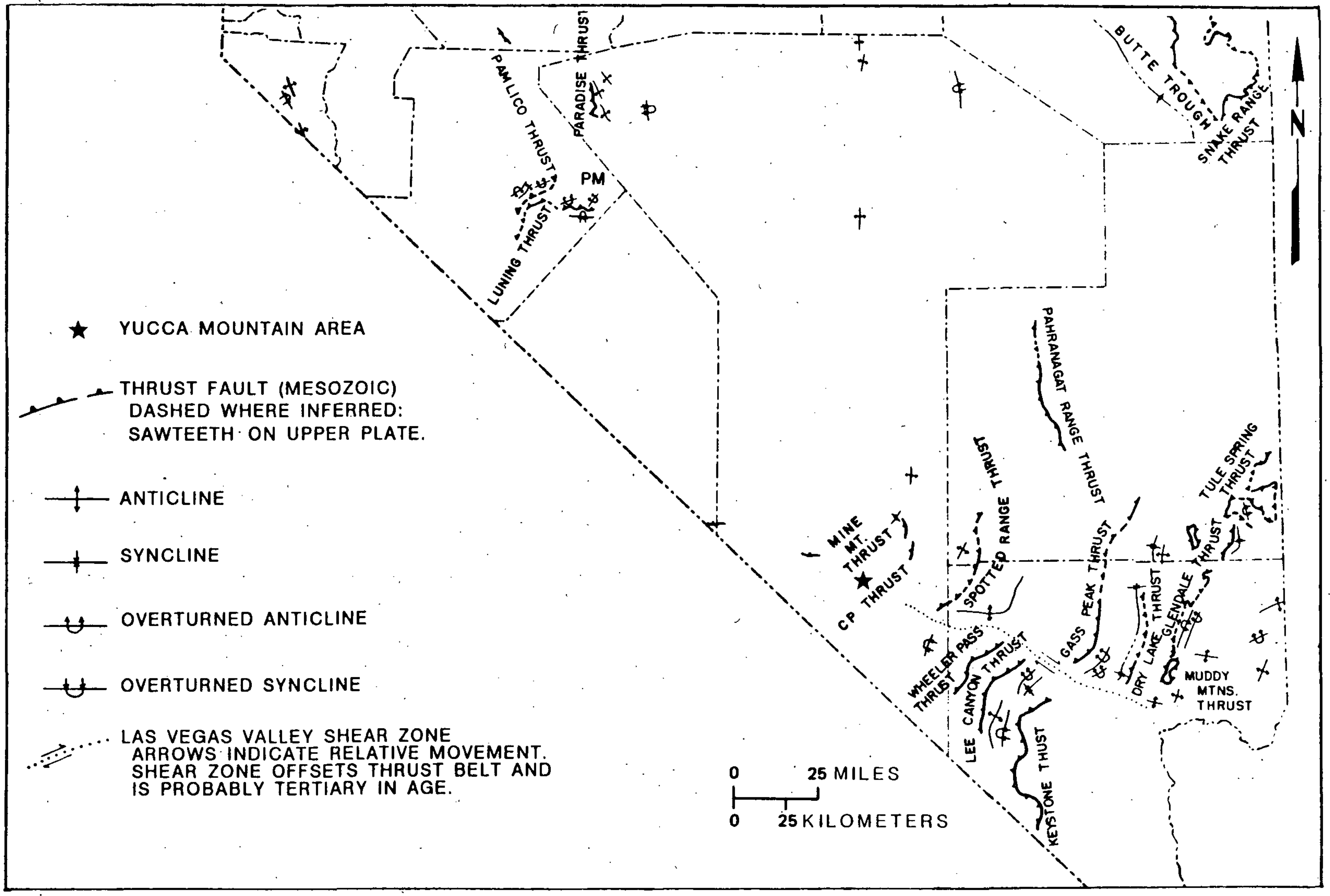

Figure 1-30. Major Mesozoic thrust faults in southern Nevada. Modified from Stewart (1980a).

Nevada (Barnes and Poole, 1968; Figure 1-30). The surface traces of several thrusts have been mapped and are called the CP, the Mine Mountain, and the Spotted Range thrusts (Stewart, 1980a). The CP thrust, the easternmost, roots in the west and climbs stratigraphically from the postulated root until it reaches the Eleana Formation in the Eleana Range where it flattens and is folded in a series of large-amplitude folds (Carr, 1984). The CP thrust dips to the east beneath Yucca Flat, so the Paleozoic rocks exposed southeast of there are allochthonous, and the Mine Mountain thrust is probably a secondary fault in the upper plate of the CP thrust (Carr, 1984). The CP thrust may surface to the southeast as the Spotted Range thrust (Carr, 1984). The age of the thrusting near Yucca Mountain is poorly defined as occurring pre-middle Miocene and post-late Paleozoic.

Mesozoic folds in southern Nevada are chiefly large overturned folds in rocks caught between thrust faults. Rare open and overturned folds in the autochthon of the Sevier belt (Longwell et al., 1965) are demonstrably Tertiary in age (Bohannon, 1983, 1984), indicating that Mesozoic deformation was gentle beneath the thrusts. Large folds occur between the Willow Tank and the Muddy Mountain thrusts (Bohannon, 1983), between the Keystone and the Lee Canyon thrusts (Burchfiel et al., 1974), and between the Dry Lake and the Gass Peak thrusts (Longwell et al., 1965) in the Sevier belt. At Bare Mountain, 15 km west of Yucca Mountain, upper Precambrian and Paleozoic beds are steeply dipping to overturned below the CP thrust, which is also broadly folded. Carr (1984) mapped large, open folds beneath the CP thrust in the Eleana Range and these may also occur under Tertiary rocks at Yucca Mountain. It is not known, when this folding occurred in relation to the thrust faulting.

Ductile folds several meters in amplitude are common in metamorphosed rocks in the northwest part of Bare Mountain, but these small folds have no effect on the distribution of major stratigraphic sequences.

Tertiary structures

Oligocene conglomerate and breccia in the Titus Canyon Formation of the northeast Grapevine Mountains, 30 to 40 km southwest of Yucca Mountain, show evidence of early Oligocene normal faulting (Reynolds, 1969), but the extent of tectonism of that age is not known. The only other early Tertiary rocks described from the southern Great Basin are the Oligocene volcanic rocks of central Nevada (Cornwall and Kleinhampl, 1964). The absence of early Tertiary deposits suggests that much of the area was then elevated and undergoing erosion (Stewart, 1980a).

The late Tertiary structural history of the Great Basin was dominated by normal and strike-slip faults. The normal faults resulted from regional extension of the crust, which has been estimated at as low as 10 to 15 percent (Stewart, 1971) and as high as 100 percent (Hamilton and Myers, 1966, Hamilton, 1987; Wernicke et al., 1982). Low estimates result from geometric constraints created by assuming that the normal faults are steep and penetrate deep into the crust. Some of the high estimates were derived from regional tectonic reconstructions and are thus independent of fault geometry, but they require mechanisms of crustal extension capable of producing the large crustal distortions. Other high estimates rely on large displacements across strike-slip faults that operated in conjunction with the normal faults

(Wise, 1963). Detachment faults, with listric faults and closely spaced planar normal faults that change from a steep to a gentle dip with time (through block rotation), offer mechanisms to extend the crust beyond 100 percent (Wernicke and Burchfiel, 1982). The relative roles of strike-slip, normal, and detachment faulting in deforming the Basin and Range province is uncertain.

All three types of Tertiary faults occur at or near Yucca Mountain. Although the following discussions of extensional tectonism (normal and detachment faults) and of strike-slip faulting (and related detachments) are separate, the evolving tectonic rationale for faults at the site should explain, in so far as possible, the complex relations among all types of faults observed.

Extensional tectonism. Extensional tectonism has occurred in one part or another of the Basin and Range province since possibly the late Eocene, but Zoback et al. (1981) observed that it changed in orientation and possibly in style during that time. Two overlapping phases have been identified: (1) older extensional faulting, associated with voluminous silicic volcanism, from late Eocene to middle Miocene time (Crowe, 1978; Dickinson and Snyder, 1979), and (2) basin-and-range faulting, middle Miocene and younger, which controls the present-day topography of the Basin and Range Province (Stewart, 1978). Zoback et al. (1981) noted that the apparent least principal stress orientation has changed from west-southwest to west-northwest (Section 1.3.2.3). Rogers et al. (1983) and Stock et al. (1985) confirm that the present orientation of the least principal stress is N.60°W. at Yucca Mountain.

Many geometries have been proposed for the subsurface configuration of the normal faults in the Great Basin. They include high-angle planar faults that form classic horst-and-graben structures (Stewart, 1978), listric faults whose dips flatten with depth to form large rotated blocks and detachment faults that form a shallowly dipping surface into which the basin-and-range normal faults merge at depth (Bartly and Wernicke, 1984; Hamilton, 1987). These fault geometries are illustrated on Figure 1-31. Each of these types of faulting is hypothesized to eventually merge into a zone of decoupling at the transition between brittle and ductile behavior that occurs at a depth of approximately 15 km in the Great Basin (Eaton, 1982). Below this zone, extension probably occurs by ductile stretching, thinning or intrusions of basaltic material from below or by a combination of these processes. Earthquakes generally do not occur below depths of about 15 km in the Great Basin (Smith, 1978).

Zoback et al. (1981) and Anderson et al. (1983) have found evidence of all three types of fault geometry in the Great Basin. To date, all of the large, historical earthquakes in the region, such as the 1954 Dixie Valley-Fairview Peak earthquake, the 1959 Hebgen Lake earthquake, and the 1983 Borah Peak earthquake have occurred on planar, high-angle faults that show little or no evidence of flattening to depths of about 15 km (Anderson et al., 1983; Doser, 1985; Okaya and Thompson, 1985; Richins et al., 1985; Stein and Barrientos, 1985; Thompson, 1985). Anderson et al. (1983) suggest that areas of high-angle faulting and seismicity may be controlled by localized linear

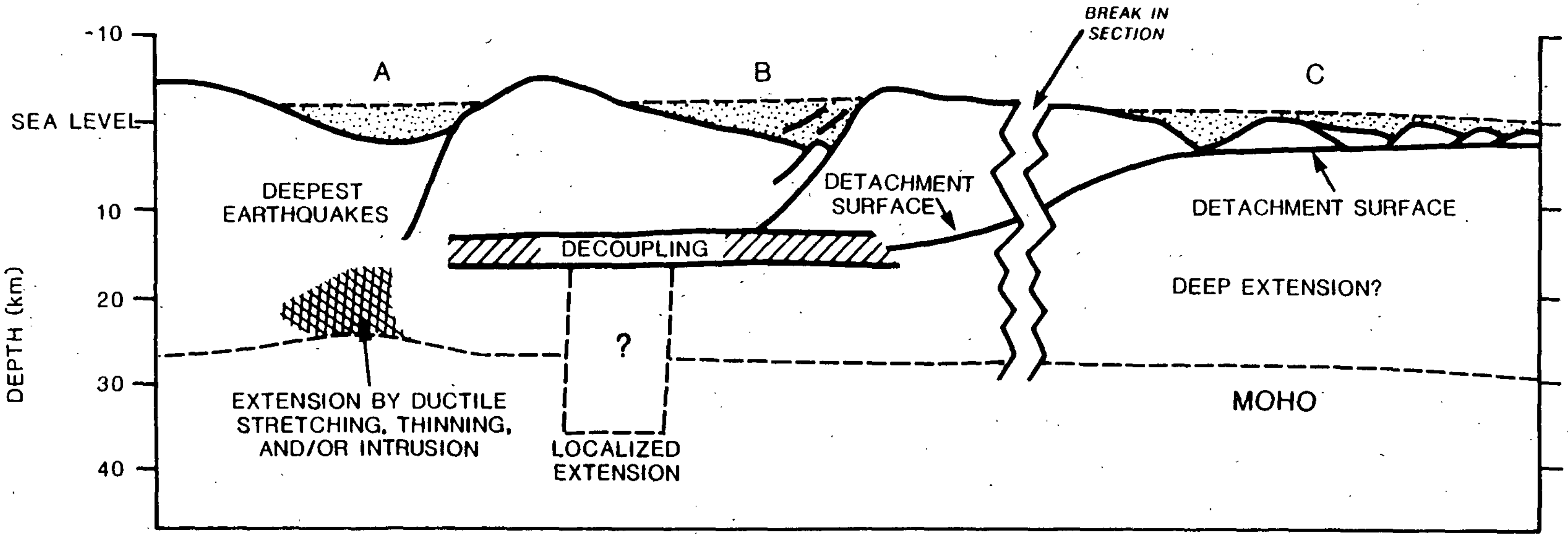

Figure 1-31. Diagrammatic cross section showing three contrasting modes of basin formation that may exist in the Basin and Range Province. Although subsurface data indicate that each basin has some unique properties, the planar faulting in mode A could represent basins such as those beneath Dixie, northern Diamond, and Railroad valleys; the listric faulting in mode B could represent basins beneath Goshute and Marys River valleys; and the detachment faulting in mode C could represent basins beneath Raft River Valley and the Sevier Desert. The distance separated by the break in the section could range from a few kilometers to several tens of kilometers, depending on the dip of the detachment surface. Stipple pattern indicates basin-fill sediments. Modified from Anderson et al. (1983).

zones of extension in the region below the zone of brittle behavior. However, Quaternary fault scarps have been found on faults occurring above detachment faults, which indicate that this type of faulting may also have seismogenic potential (Crone and Harding, 1984). The differing geometry of the fault types may also indicate that the seismic hazard differs between high-angle and low-angle faulting (Anderson et al., 1983). Stewart (1978) observed that most tilted blocks are not rigid and uplifted solely by vertical movement along discrete range-front faults, but are broken to varied [illegible]

block (Figure 1-32).

Detachment faults are an integral part of many recent models of extensional tectonism (Davis et al., 1980; Wernicke, 1981; Hamilton, 1987). Seismic data and drilling in the Sevier Desert basin show horst and graben or tilted block structures that truncate downward at a postulated large detachment fault (McDonald, 1976; Mitchell, 1979; Anderson et al., 1983). Other Tertiary detachment faults have been inferred in east-central Nevada (Bartley and Wernicke, 1984), in the Mormon Mountains (Wernicke, 1981), in the Sheep Range (Guth, 1981), in the Muddy Mountains (Bohannon, 1983), throughout western Arizona and southeastern California (Davis et al., 1982), in the Death Valley area (Stewart, 1983), in the Bullfrog Hills (Maldonado, 1985b), and in the Gabbs and Gillis Ranges (Hardyman, 1980; Hardyman, 1984; Ekren and Byers, 1986). The location of these faults are shown on Figure 1-33. Detachment faults in the Gillis and Gabbs Valley Ranges (location 8, Figure 1-33) have been interpreted to be kinematically related to strike-slip faulting as the primary process of deformation and that associated normal faulting is a consequence of strike-slip faulting and detachment (Hardyman et al., 1975; Hardyman, 1978).

On the basis of the regional tectonic framework, local structural geometry, and magnetic declination studies, Scott (1986) and Scott and Rosenbaum (1986) suggest that a detachment fault may occur beneath Yucca Mountain. The remanent magnetic declinations in the welded Tiva Canyon Member of the Paintbrush Tuff, corrected for structural tilt about horizontal axes, display progressively greater clockwise declinations from north to south. Relative to the northern end of Yucca Mountain, the southern end appears to be rotated clockwise 30 degrees about a vertical axis. The postulated detachment structures are thought to form the surfaces on which the structural rotation took place. At several places near Yucca Mountain, gently dipping faults separate younger rocks above from older rocks below;

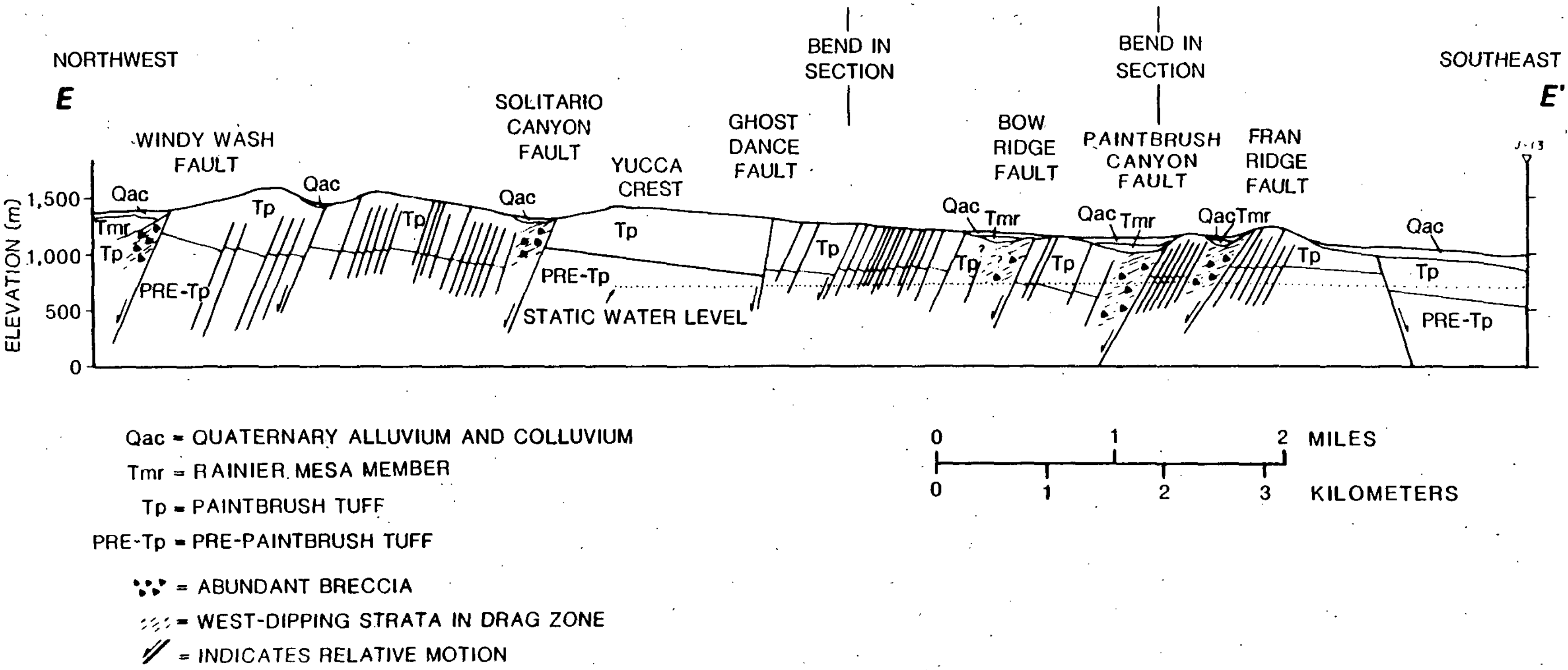

Figure 1-32. Schematic geologic cross section E-E' at Yucca Mountain. See Figure 1-17, (Section 1.2.2) for location of cross section E-E'. Modified from Scott and Bonk (1984).

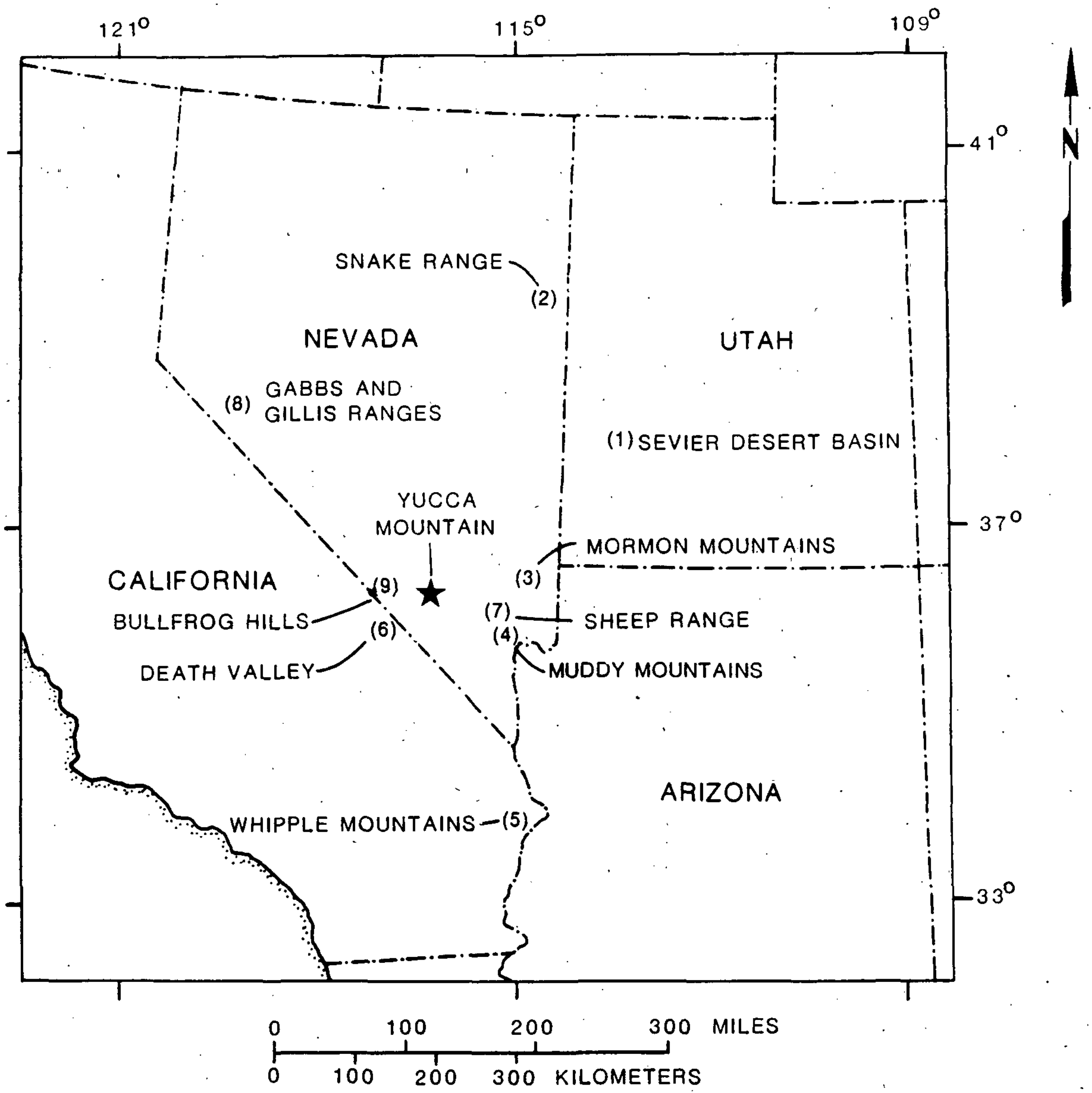

REFERENCES

(1) ANDERSON ET AL. (1983); MCDONALD (1976); MITCHELL (1979)

(2) BARTLEY AND WERNICKE (1984)

(3) WERNICKE (1981)

(4) BOHANNAN (1983)

(5) DAVIS ET AL. (1982)

(6) STEWART (1983)

(7) GUTH (1981)

(8) EKREN AND BYERS (1986)

(9) MALDONADO (1985b)

Figure 1-33. Locations of postulated detachment faults in the southern Great Basin.

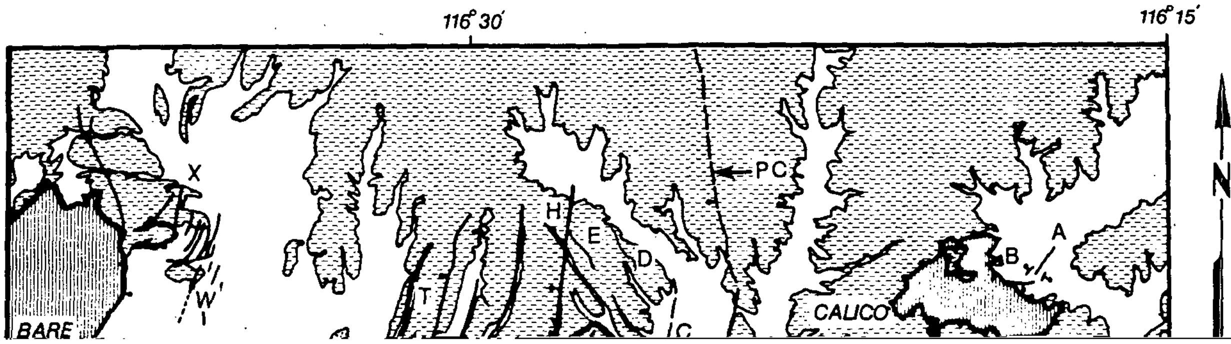
116° 30′
116° 15′
N
PC
X
W
H
E
D
C
T
A
B
CALICO
BARE

Both east and west of Yucca Mountain, the inferred detachment appears to be between Tertiary and older rocks, which suggests that the uppermost detachment beneath Yucca Mountain is at the base of the Tertiary section. The geometry of the base of the Tertiary section near Yucca Mountain is suggested by gravity data. East of Yucca Mountain, a distinct northeast trending gravity high between Busted Butte and the Calico Hills has been interpreted as a structural high in the pre-Tertiary rocks or, alternatively, as an eroded northwest facing escarpment on pre-Tertiary rocks (Snyder and Carr, 1982). Beneath the southern part of Yucca Mountain (between Busted Butte and Crater Flat), structural relief in the pre-Cenozoic rocks is at least 2,000 m (Snyder and Carr, 1982); along the west flank of Yucca Mountain, pre-Cenozoic rocks are at least 3,000 m beneath the surface (Hoffman and Mooney, 1983).

Structural analysis of deformed and faulted Miocene ash flows suggests that the entire area of Yucca Mountain, including the area of the proposed repository, might be underlain at unknown depth by one or more detachment faults (Scott, 1986). This possibility has not been confirmed, nor have the depth, attitude, and total extent of the postulated detachment(s) been determined. Conjecturing that the uppermost detachment fault corresponds to the contact between Miocene volcanic rocks and subjacent Paleozoic rocks, preliminary reinterpretation of published gravity data (Snyder and Carr, 1984) indicates that the postulated detachment slopes moderately to N.60W. in the direction of least horizontal stress (Stock et al., 1985). The pre-Tertiary surface, or a high-angle fault offsetting it, was intersected in drillhole UE25p#1 at a depth of about 1,000 m (Carr et al., 1986). The detachment hypothesis differs from that of Snyder and Carr (1982), who previously interpreted the Crater Flat area as a structural depression resulting from a combination of graben structures and old calderas.

Detachment faults are well documented in the geologic record (Davis et al. 1982) of the Basin and Range province. Arabasz (1986) studied the microseismicity of a portion of Utah, where detachment geometry and upper plate faulting have been suggested from surface mapping, and postulated that mapped structures had little to do with seismicity. It is possible that detachment faults do not produce microearthquakes, or perhaps none are active. The short time span available to study seismic trends may be insufficient to delineate detachment activity.

It has been suggested by Gans et al. (1985) that the northern Snake Range decollement (NSRD) originated during the Oligocene as a detachment occurring at the transition between brittle and ductile behavior, with localized ductile stretching below and more widely distributed, high-angle normal faulting above. Younger east-dipping normal faults cut the NSRD, forming tilted fault blocks and highly asymmetrical grabens, and folded the

The timing of extensional tectonism in the Basin and Range province is not well documented. Late Eocene to Oligocene metamorphism and detachment faulting occurred in northeastern Nevada (Compton et al., 1977), but extension started later, about 15 million years ago, in southeastern Nevada (Bohannon, 1983, 1984). It probably did not begin until about 13 million [redacted] southeastern Nevada (Bohannon, 1983, 1984), but it continues between Death Valley and the Sierra Nevada Range (Roquemore and Zellmer, 1986; Schweig, 1986). In northeastern Death Valley, north- and northeast-trending faults formed between 20 and 16 million years ago and between about 14 and 13 million yr ago (Reynolds, 1974a,b). Doming, folding, and faulting along north-trending faults occurred between 11 and 7 million years ago (Reynolds, 1974a). Faulting has been nearly continuous since about 7 million years ago, forming the present-day topographic relief, the largest in the southwest United States. Late Pleistocene and Holocene fault scarps are common along the length of the Death Valley-Furnace Creek fault zone (Hunt and Mabey, 1966; Reynolds, 1969). Ongoing studies are providing data on the timing of extension in southern Nevada.

(Wise, 1963; Atwater, 1970; Stewart, 1978), strike slip is viewed as the

Yucca Mountain is in the Walker Lane (Figure 1-26), a northwest-trending belt of right-lateral faults that disrupts the regional structural grain in the southwestern part of the Great Basin along the California-Nevada border (Gianella and Callaghan, 1934; Locke et al., 1940; Longwell, 1960; Stewart, 1967; 1978). Many north-trending structures and ranges curve markedly near this belt (Albers, 1967). Displacement along the Walker Lane occurs in part as right-lateral slip and in part as bending (Figure 1-35); total displacement may be 130 to 190 km (Stewart et al., 1968). Faulting may have begun as early as the Jurassic (Albers, 1967) or not until after the deposition of the 29-million-year-old Horse Spring Formation (Ekren et al., 1968). Some faults in the Walker Lane are covered by undeformed upper Miocene or Pliocene volcanic rocks, while others displace Pliocene and Quaternary deposits (Albers, 1967).

The Las Vegas Valley shear zone (Figure 1-26) is a concealed zone of

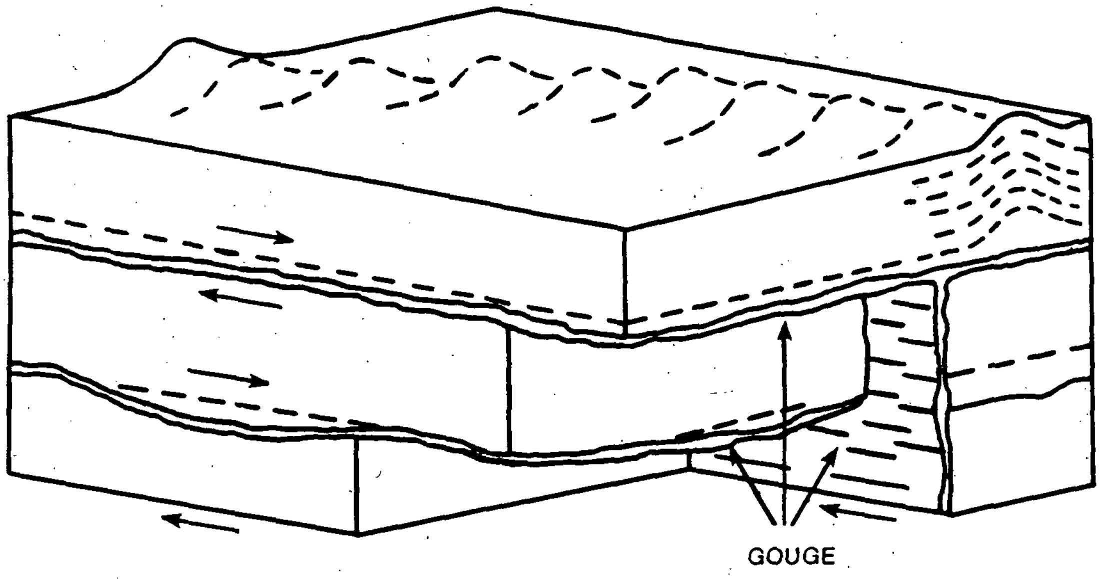

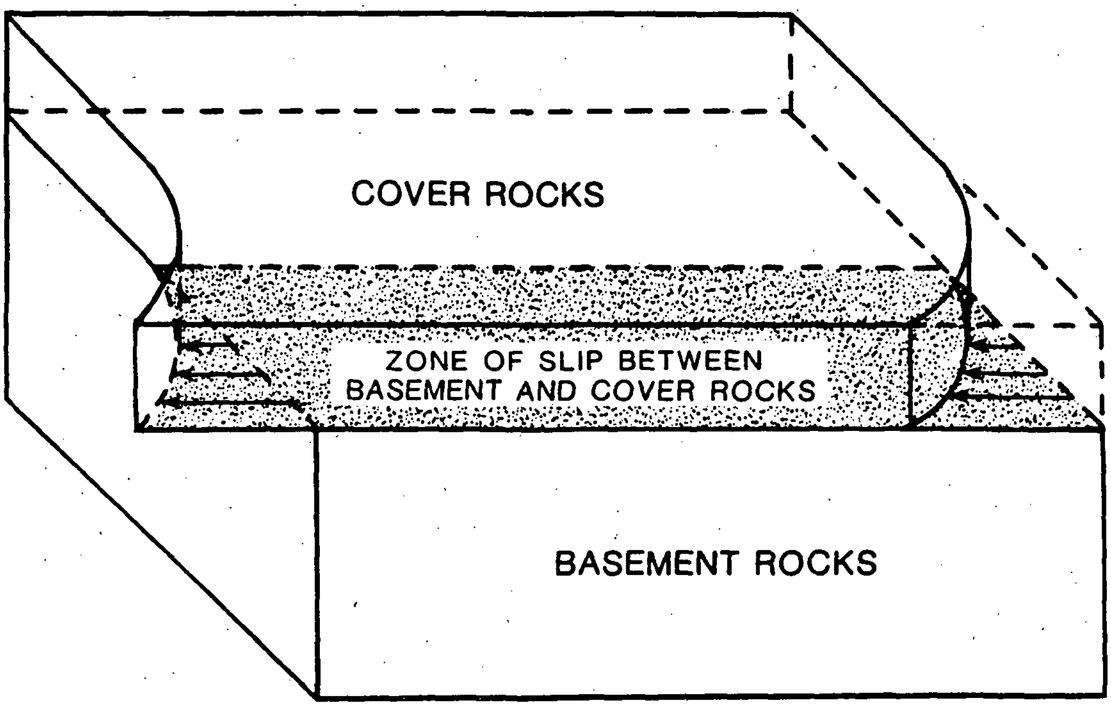

Figure 1-35. Idealized models of upper crustal deformation involving right-lateral shear on through-going wrench fault and displacement on an overlying detachment fault. The upper diagram shows model proposed by Molinari (1984) to explain the broad zone of short surface ruptures observed after the 1932 Cedar Mountain earthquake. The lower diagram shows the model proposed by Burchfiel (1965) to explain large scale bending that is observed along faults such as the Las Vegas shear zone.

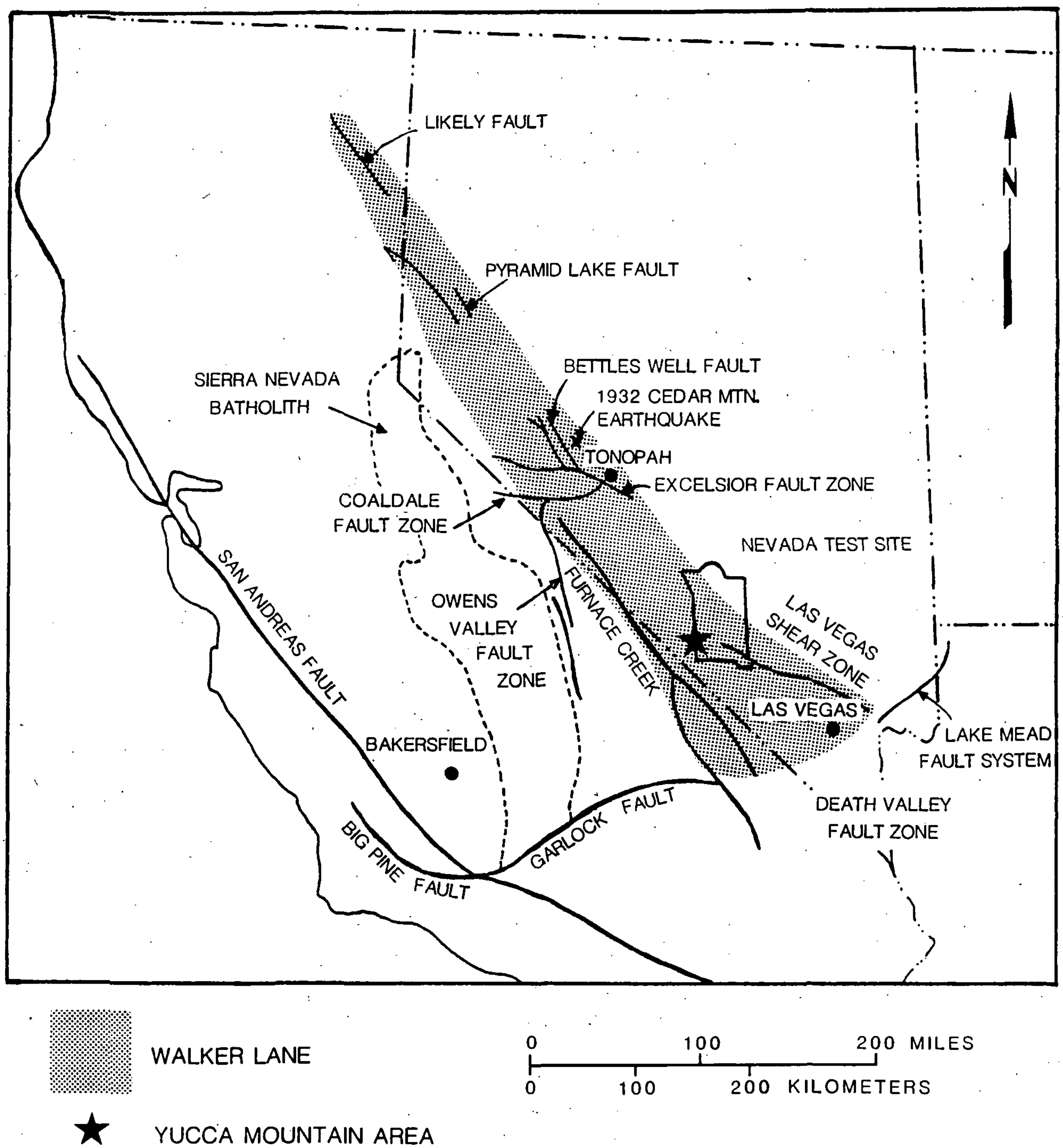

Figure 1-36. The Walker Lane and major associated faults. Modified from Stewart (1985).

The northern part of the Walker Lane is also known to be active with abundant evidence of Holocene activity in the vicinity of Pyramid Lake (Bell and Slemmons, 1979; Anderson and Hawkins, 1984). Stewart (1985) has postulated two major east-trending strike-slip faults, named the Excelsior and Coaldale faults, that cut across the trend of Walker Lane faulting just south of the Monte Cristo Valley area. These faults had most of their offset in the late Mesozoic, but some reactivation in the Cenozoic is also indicated. Stewart (1985) notes that major strike-slip faults like the Owens Valley-White Mountain fault system and the Furnace Creek fault zone have their northern terminus at these faults and that infers major strike-slip faults in the northern segment of the Walker Lane, such as the Bettles Well fault, also have their southern terminus against these faults. Stewart suggests that, although these northwest-trending faults may be mostly late Cenozoic in age, they may have been initiated before, and been offset by, the Excelsior and the Coaldale faults. In any case, the geometry of the fault pattern in the Walker Lane (Figure 1-36) suggests that the displacement occurring along the northern Walker Lane at Monte Cristo Valley and Pyramid

Lake is being distributed at this break in the northwest trend to the Owens Valley-White Mountain, Furnace Creek, and southern Walker Lane zones with the western zones being the most active.

Burchfiel (1965) and Ekren (1968) proposed that the Las Vegas Valley shear zone is continuous in the subsurface beneath the southern NTS and Yucca Mountain and that it connects with the southern part of the Walker Lane systems join east of Las Vegas, and they were active at the same time; however, the details of the join and the kinematics of their interaction are poorly understood (Bohannon, 1983).

In the vicinity of Yucca Mountain, the Walker Lane is composed of a broad zone (100 km wide) of relatively short (about 40 km long) northwest trending right-lateral shear zones like the Yucca-Frenchman shear (Carr, 1984). These shears are similar to transform type faults in that they may display greater extension on one side of the fault than the other. These shear zones are expressed in the Miocene tuffs as small northwest-striking faults but are mainly expressed as right-lateral flexure of the tuffs and short north-northwest trending faults (Carr, 1984). These northwest trending shears typically end abruptly at north- to northeast-striking shear zones that are contained within the Walker Lane and have small amounts of left-lateral displacement. The most significant of these zones is the Spotted Range-Mine Mountain zone which passes just east and south of Yucca Mountain (Figure 1-37). This zone is composed of several parallel fault segments that are 30 to 40 km long. Total displacements are on the order of 1 to 2 km on individual faults (Carr, 1984). An example occurs along the Mine Mountain fault south of Mine Mountain, where the Paintbrush and the Timber Mountain tuffs are displaced about 1 km in a left-lateral sense. Seismicity occurs in the zone and Quaternary displacements have been found along faults in the zone, especially in Rock Valley (Carr, 1984). The Spotted Range-Mine Mountain zone has been included in an alignment of northeast-trending features that extends from the Garlock fault to the Pahranagat shear zone to the east (Greensfelder et al., 1980). However, in spite of this alignment, there is no evidence of a through-going structural feature exposed in the Paleozoic rocks that occur in the 70 km separating the Spotted Range-Mine Mountain zone from the Pahranagat shear zone (Carr, 1984).

In addition to the change in orientation of basins and ranges in the Walker Lane belt, the structural grain of certain structural blocks in the belt is sharply deflected from the regional trend. These blocks appear to have been rotated about a vertical axis (Albers, 1967). Recent paleomagnetic and structural studies of Miocene ash flows indicate that Yucca Mountain has been rotated 30 degrees clockwise since the middle Miocene time (Scott and Rosenbaum, 1986), and thus, it appears to have been deformed within a right lateral couple, as do other parts of the Walker Lane belt. The rotation of structural blocks in a zone of strike-slip faulting has been modeled by Ron et al. (1984) and found to agree with paleomagnetic data for a strike-slip zone in northern Israel. Nur et al. (1986) and Ron et al. (1986) have found similar evidence of rotated blocks in strike-slip settings in the Yerington and the Lake Mead areas of Nevada.

Quaternary structures

This section considers faults with Pleistocene and Holocene offset in the region surrounding Yucca Mountain (Section 1.3.2.2.2 considers faults and fractures in Yucca Mountain itself). Quaternary offset has been documented on many faults in the region surrounding Yucca Mountain, and late Pleistocene and Holocene movement has been documented on several faults; however, late

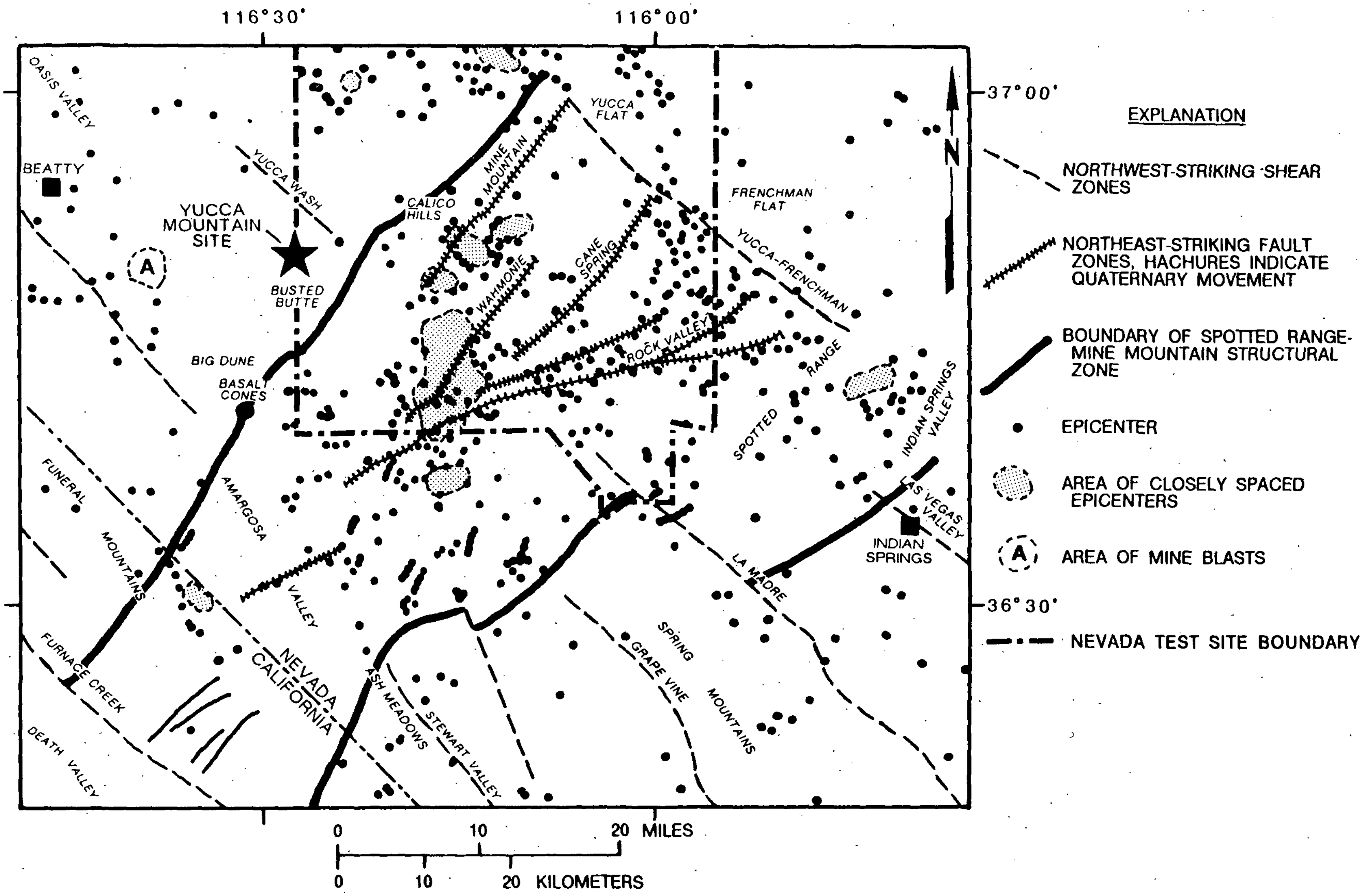

Figure 1-37. Spotted Range-Mine Mountain structural zone and included Quaternary fault zones, showing the relationship to seismicity of the southern Nevada Test Site area, August 1978 through May 1984. Modified from Carr (1984).

Pleistocene and Holocene deposits that would document late Quaternary faulting are often absent from the fault zone of interest. Faults with Quaternary offset are a basis for assessing the seismic hazard to the proposed repository.

In the area surrounding Yucca Mountain, faults showing evidence of Quaternary movement are associated with distinct scarps, steep linear to curvilinear mountain fronts, and lineaments across surficial deposits (USGS, 1984). Prominent mountain fronts and surface lineaments that probably represent late Pliocene Quaternary faults are shown on a preliminary map (USGS, 1984) and generalized on Figure 1-38.

A zone of faults having demonstrable Pleistocene displacement extends southward from the Sand Spring Valley, 120 km northeast of Yucca Mountain, through Yucca Flat and curves southwestward into the Amargosa Desert (Figure 1-38) (USGS, 1984). A set of surface faults in the Pahrump Valley is inferred to be a continuation of this zone (Carr, 1984).

West of Yucca Mountain, in the Death Valley and the Panamint Valley areas, late Quaternary fault scarps are numerous (Figure 1-38). At least one scarp in Death Valley was interpreted as about 2,000 yr old on the basis of archaeological evidence (Hunt and Mabey, 1966). In Panamint Valley, about 90 km west of Yucca Mountain, there are numerous youthful fault scarps, with as much as 20m of right-lateral strike-slip displacement (Smith, 1979). Holocene faulting is known at Yucca Flat, 50 km northeast of Yucca Mountain, and in the southwest Great Basin, about 50 km to the west. Local surface rupture related to underground weapon testing is also common at the Nevada Test Site (Section 1.5.2.3). In Yucca Flat, the latest natural movement on the Yucca fault system was estimated to be early to middle Holocene; other fault scarps in Yucca Flat appear to be pre-Holocene (Carr, 1974). However, at several times during approximately the last 50 yr, large cracks have formed at the south end of the Yucca Flat playa and at several other playas in the area. Carr (1974) considered most of the linear cracks in these playas to be tectonic, and resistivity soundings suggested that there are faults beneath the playa deposits with the same trend and location as some of the cracks (Zohdy and Bisdorf, 1979).

Holocene faulting also is likely in the eastern range-front fault zone at Bare Mountain, 15 km west of Yucca Mountain, and on the Windy Wash fault, on the western flank of Yucca Mountain (Section 1.3.2.2.2).

1.3.2.2.2 Structures and structural history of Yucca Mountain

This section describes the structure of central Yucca Mountain within a few kilometers of the proposed repository, considering the faults that cut Yucca Mountain, the structural blocks defined by the major faults, the history of fault movement, and the fractures in the host rocks. Those structures are described in the context of relevant structures immediately surrounding Yucca Mountain, from Bare Mountain, about 15 km to the west, to the Calico Hills, about 10 km to the east (Figure 1-34). This discussion provides a description of the geologic structure in which the proposed

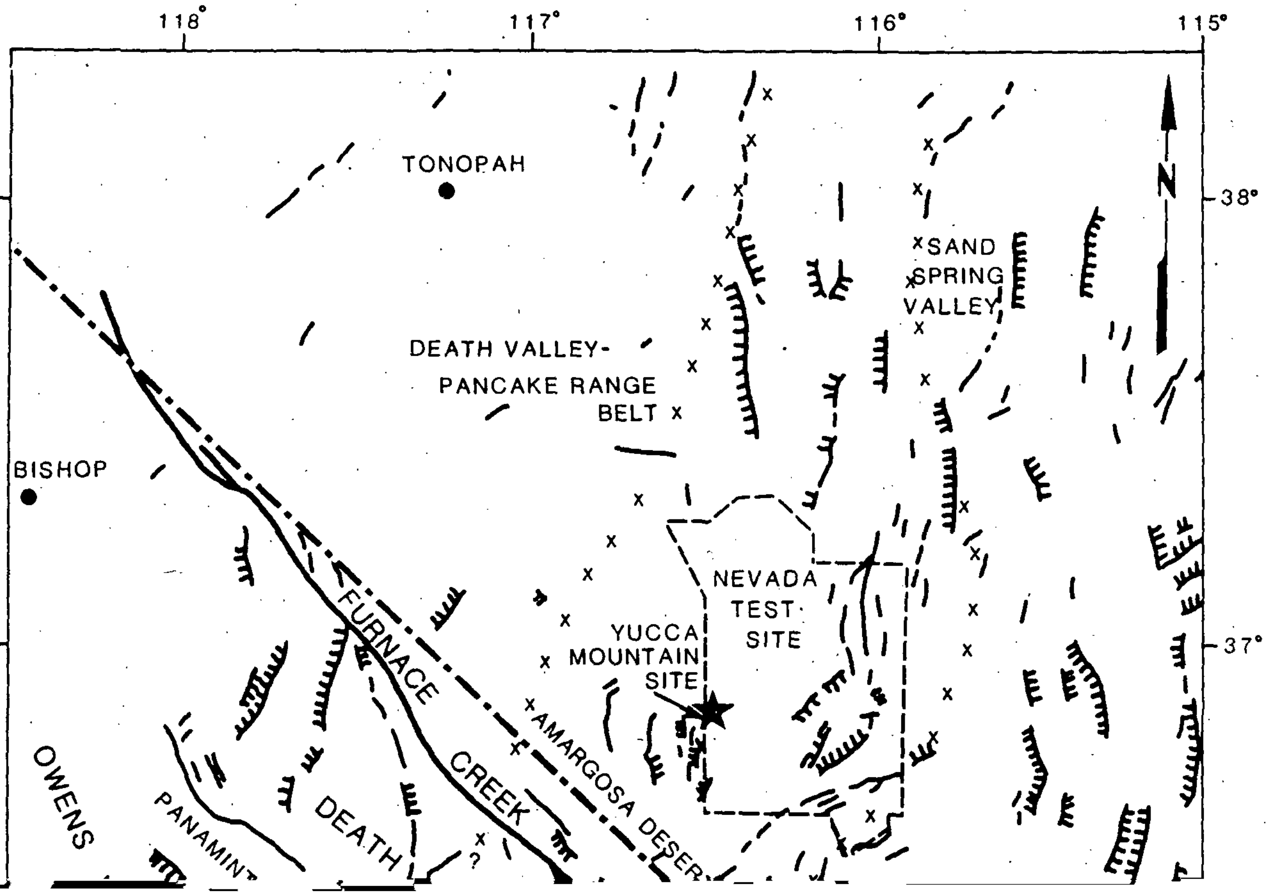
118°
117°
116°
115°
38°
37°
N
TONOPAH
SAND SPRING VALLEY
DEATH VALLEY-PANCAKE RANGE BELT
BISHOP
NEVADA TEST SITE
YUCCA MOUNTAIN SITE
FURNACE CREEK
AMARGOSA DESERT
OWENS
PANAMINT
DEATH

repository would be constructed and provides a basis for assessing the potential for fault disruption of the proposed repository (discussed in Sections 1.5.2, 8.3.1.8.2, and 8.3.1.17.2), and the potential for seismic activity that might affect the isolation of waste or the construction and operation of the repository (discussed in Sections 1.4, 8.3.1.8.2, and 8.3.1.17.3).

Yucca Mountain is the erosional remnant of a volcanic plateau; it consists of a series of north-trending structural blocks that have been tilted eastward along major west-dipping, high-angle normal faults (Scott and Bonk, 1984). Current data suggest that those blocks may be imbricate fault slices overlying one or more detachment faults (Section 1.3.2.2.1). The normal faults that bound the blocks may be planar or listric faults that displace any detachment faults that may exist or these faults may merge with or abut against the detachment surface. Tertiary and Quaternary offset on individual normal faults at Yucca Mountain has been small relative to offsets on major normal faults elsewhere in the southern Great Basin (Anderson et al., 1983). The major normal faults bounding the structural blocks at Yucca Mountain, however, are typically only 1 to 2 km apart, whereas those bounding mountain ranges elsewhere in the Great Basin are typically some tens of kilometers apart. The component of strike-slip fault offset at Yucca Mountain is unknown; seismic-reflection profiles suggest an unknown component of strike-slip offset on the Windy Wash fault (Whitney et al., 1986).

At Yucca Mountain, the structural blocks and the west-dipping normal faults that define them have been delineated by geologic mapping and by resistivity and low-altitude aeromagnetic surveys (Figures 1-32, 1-39, 1-40, 1-41) (Section 1.3.2.2.1). Major normal faults that bound the structural blocks generally strike north and dip steeply west (Figures 1-32 and 1-41). The faults are typically 1 to 2 km apart and generally have vertical offsets of more than 100 m. These faults control the basic geomorphic features of Yucca Mountain (Figure 1-40). They decrease in both offset and abundance northward throughout Yucca Mountain. The pattern of north-trending blocks appears to extend westward from Yucca Mountain beneath the alluvial fill of Crater Flat to Bare Mountain where bounding faults dip eastward as well as westward (USGS, 1984).

On the major normal faults in central Yucca Mountain, most offset occurred between 12.9 and 11.6 million years ago; the 12.9-million-year-old Tiva Canyon Member of the Paintbrush Tuff is offset more than the 11.6-million-year old Rainier Mesa Member of the Timber Mountain Tuff. But offset has continued into the Pliocene and Quaternary on the Bow Ridge, Paintbrush Canyon, and Solitario Canyon faults and into the Holocene on the Bare Mountain and Windy Wash faults (Table 1-7). Planned studies of known and suspected Quaternary faults will focus on characterizing significant Quaternary faults within about 5 km of the repository and particularly at Bow Ridge and Busted Butte, where multiple episodes of Quaternary movement are suspected (Section 8.3.1.8).

Within each structural block are numerous steep, west-dipping normal faults of a second type. These faults generally strike north to north-northwest; they are closely spaced and typically have less than 3 m of offset, forming an imbricate pattern (Figure 1-42). Between these faults,

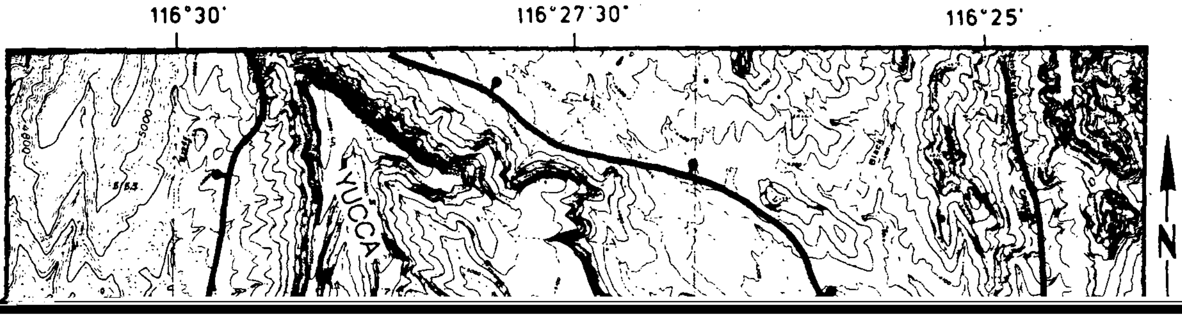
116°30'
116°27'30"
116°25'
YUCCA
N

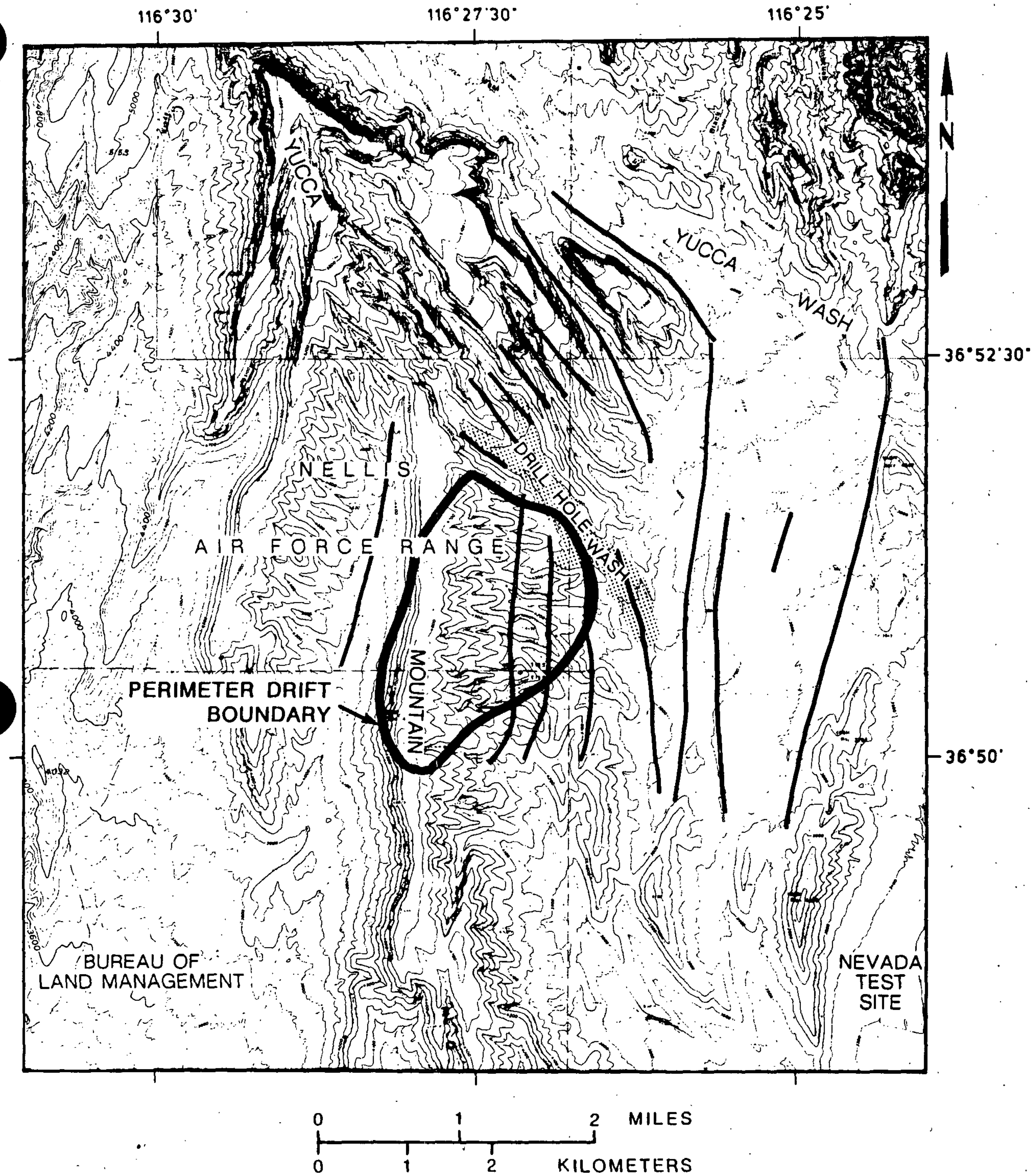

Figure 1-40. Faults and fractures at Yucca Mountain interpreted from electrical resistivity data. Stippling shows zone of inferred fracturing and faulting along Drill Hole Wash; fault trends appear to change abruptly across this zone. Modified from USGS (1984).

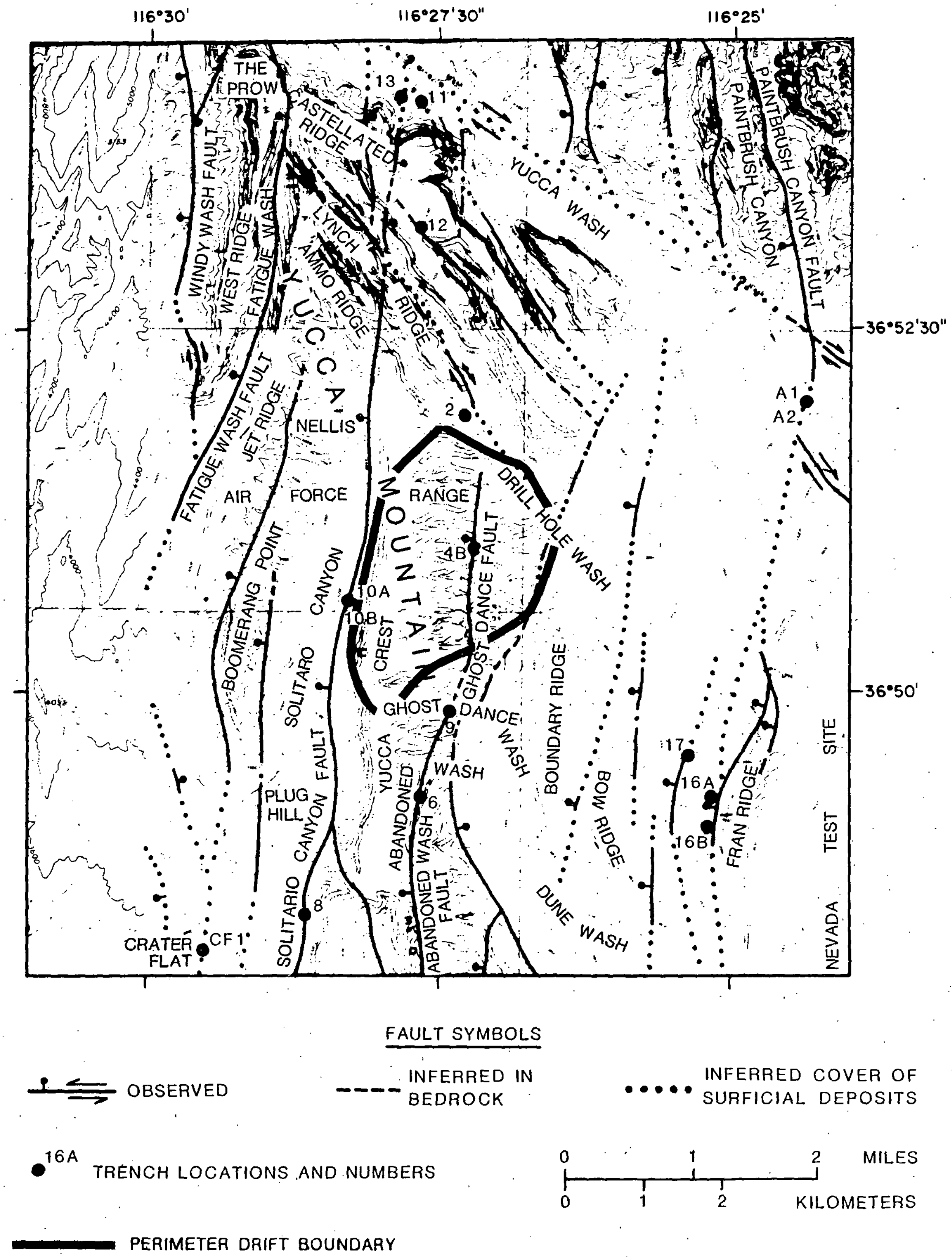

Figure 1-41. Faults at Yucca Mountain interpreted from geologic mapping. Modified from USGS (1984).

Table 1-7. Summary of Quaternary faulting at and near Yucca Mountain[a] (page 1 of 3)

Fault or fault group[b,c]	Trench number[d]	Youngest unit faulted or fractured[e]	Oldest unit not faulted or fractured	Inferred age of last movement (yr)	Method of dating	Remarks
A (4)	Not trenched	QTa	Q1c	< 2 x 10^6 > 7,000	Correlation of stratigraphic units	
B	Not trenched	Q2c	Unknown	< 270,000	Correlation of stratigraphic units	No mimimum age determined
Paintbrush Canyon fault	A1, A2, 16, 16B	Q2e (fractures in trench A2)	Q2c soil (in trench A1)	< 700,000 > 270,000	Correlation of stratigraphic units	
Bow Ridge fault (C)	14	Q2s (fractures in trench 14)	Q2a	< 270 ± 90 x 10^3 > 38 ± 10 x 10^3	Uranium trend	
D	11	No Quaternary offset found	QTa	NA[f]	NA	No evidence of Quaternary offset
E	12	No Quaternary offset found	Q2 soil	NA	NA	No evidence of Quaternary offset
F	4, 6, 9	No Quaternary offset found	Q2c	NA	NA	No evidence of Quaternary offset
G	2	No Quaternary offset found	Q2c	NA	NA	No evidence of Quaternary offset
Solitario Canyon fault zone	8, 10, 108	QTa	QTa soil	1.2 x 10^6	Petrographic correlation of basalt ash; correlation of stratigraphic units	
H	13, GA1A, GA1B	No Quaternary offset found	Q2c	NA	NA	
I	Not trenched	QTa	Q2e	< 2 x 10^6 > 700,000	Correlation of stratigraphic units	

Table 1-7. Summary of Quaternary faulting at and near Yucca Mountain[a] (page 2 of 3)

Fault or fault group[b,c]	Trench number[d]	Youngest unit faulted or fractured[e]	Oldest unit not faulted or fractured	Inferred age of last movement (yr)	Method of dating	Remarks
J	Not trenched	QTa	Unknown	$< 2 \times 10^6$	Correlation of stratigraphic units	> 1.2 million years ago inferred from lack of scarp
K	Not trenched	QTa	Q1c	$< 2 \times 10^6$ > 7,000	Correlation of stratigraphic units	> 1.2 million years ago inferred from lack of scarp
L	Not trenched	QTa	Unknown	$< 2 \times 10^6$	Correlation of stratigraphic units	> 1.2 million years ago inferred from lack of scarp
M	CF1	QTa	Q2 soil	1.2×10^6	Petrographic correlation of basalt ash; correlation of stratigraphic units	
N	Not trenched	QTa	Q1c	$< 2 \times 10^6$ > 7,000	Correlation of stratigraphic units	> 1.2 million years ago inferred from from lack of scarp
O	Not trenched	QTa	Q2c(?)	$< 2 \times 10^6$ > 270,000(?)	Correlation of stratigraphic units	> 1.2 million years ago inferred from lack of scarp
P	Not trenched	QTa	Q2c(?)	$< 2 \times 10^6$ > 160,000(?)	Correlation of stratigraphic units	> 1.2 million years ago inferred from lack of scarp
Windy Wash fault (Q)	CF2, CF2.5 CF3	Holocene silt[g]	--	<6,500[g]	Thermoluminescence[g]	At least seven episodes of Quaternary faulting
R	Not trenched	QTa	Q2b(?)	$< 2 \times 10^6$ > 160,000(?)	Correlation of stratigraphic units	
S	Not trenched	QTa	Q2c	$< 2 \times 10^6$ > 270,000	Correlation of stratigraphic units	

Table 1-7. Summary of Quaternary faulting at and near Yucca Mountain[a] (page 3 of 3)

Fault or fault group[b,c]	Trench number[d]	Youngest unit faulted or fractured[e]	Oldest unit not faulted or fractured	Inferred age of last movement (yr)	Method of dating	Remarks
T	Not trenched	QTa	Unknown	$< 2 \times 10^6$	Correlation of stratigraphic units	1 million years ago or younger inferred from scarp
U	Not trenched	QTa	Q1c	$< 2 \times 10^6$ > 7,000	Correlation of stratigraphic units	> 1.2 million years ago inferred from lack of scarp
V	Not trenched	QTa	Q2c(?)	$< 2 \times 10^6$ > 270,000(?)	Correlation of stratigraphic units	> 1.2 million years ago inferred from lack of scarp
W (7)	Not trenched	QTa	Unknown	$< 2 \times 10^6$ > 270,000	Correlation of stratigraphic units	> 1.2 million years ago inferred from lack of scarp
X	Not trenched	QTa	Unknown	$< 2 \times 10^6$	Correlation of stratigraphic units	> 1.2 million years ago inferred from lack of scarp
Y	Not trenched	QTa	Q2c	$< 2 \times 10^6$ > 270,000	Correlation of stratigraphic units	> 1.2 million years ago inferred from lack of scarp
Bare Mountain Fault Zone	Not trenched	Q1c	--	Holocene[h]	Correlation of stratigraphic units and geomorphic evidence	Recurrent Quaternary faulting[h]

[a]Source: Swadley et al. (1984) and as noted in other footnotes.
[b]Number of faults in group shown in parentheses.
[c]Location of faults shown on Figure 1-34.
[d]Location of trenches near site shown on Figure 1-41.
[e]Unit shown is faulted except where fractures are indicated. Unit definitions are given on Figure 1-26.
[f]NA = not applicable.
[g]Data from Whitney et al. (1986).
[h]Data from Reheis (1986).

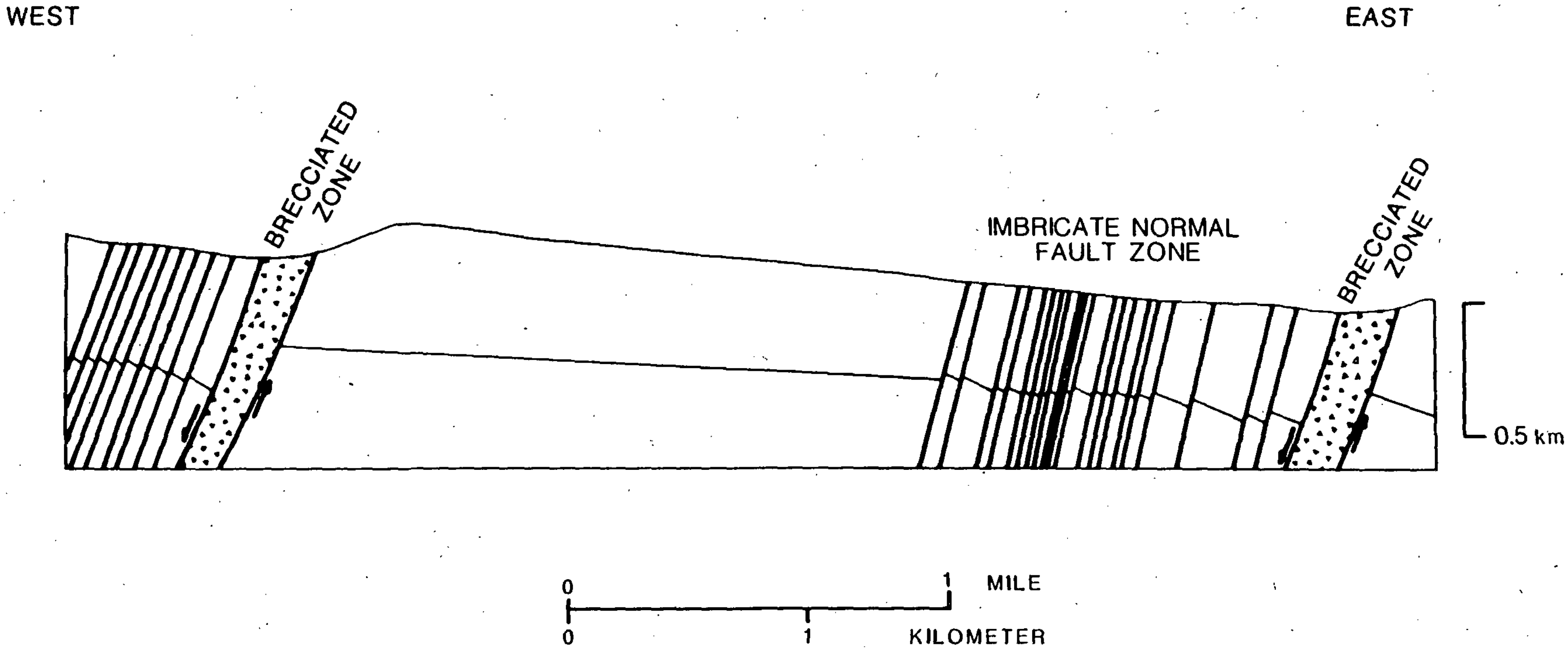

Figure 1-42. Schematic cross section of typical structural block in Yucca Mountain, showing widely spaced major normal faults and closely spaced imbricate normal faults.

foliation planes (defined by flattened pumice) in the tuffs have been rotated as much as 50 degrees eastward. The faults are more abundant in the eastern part of each structural block and more common in the southern part of Yucca Mountain than in the northern part (Scott, 1984).

Northwest-trending washes and strike-slip faults characterize the area between Drill Hole Wash and Yucca Wash (Figure 1-41). Geological and geophysical data indicate that the fault planes are nearly vertical, have less than 100 m of right-lateral offset, and may have brecciated zones 20 m or more wide (Scott et al., 1984a). These faults could transect the structural blocks or, alternatively, the faults could be upper plate transforms to greater extension to the south. Several strike-slip faults have been mapped in upper Drill Hole Wash (Figure 1-41), and similar faults may exist under alluvium in lower Drill Hole Wash. In oriented core from drillhole UE-25a#4, in the middle part of the wash, numerous steeply dipping fractures parallel the wash (Spengler and Rosenbaum, 1980). In drillhole UE-25a#1, in the lower part of the wash, fractures also are numerous and dip steeply but their orientation is unknown (Spengler et al., 1979). Striations within two fault zones in drillhole UE-25a#1 suggest a component of lateral movement. Surface mapping and drillhole information limit maximum vertical offset on faults in the wash to less than 4 m (Scott et al., 1984a).

On the northwest-striking right-lateral faults, cross-cutting relationships suggest that most offset also occurred between 12.5 and 11.3 million years ago. The 12.9-million-year-old Tiva Canyon Member is offset as much as 10 to 30 m, while only minor offset is documented in the 11.3-million-year-old Rainier Mesa Member (USGS, 1984).

Within each structural block in Yucca Mountain, the faults and the steepness of dip in the tuffs have a consistent pattern (Figure 1-42). In the western part of each block, strata in bedded tuffs and flattened-pumice foliations dip 5 to 30 degrees eastward. Farther east in each block, dips increase from 15 to 55 degrees, in zones of abundant west-dipping normal faults with offsets less than 3 m. If the pattern of tilted strata sandwiched between planar faults, schematically depicted in the imbricate normal fault zones of Figure 1-42, is correct, then individual fault slices must be internally deformed. However in plan view, the bounding faults curve markedly and interweave, probably indicating that the faults are in fact not planar; they probably curve and interweave down dip just as they do along strike. Still farther east, next to major normal faults, chaotic brecciated fault zones as much as 500 m wide occur; some of these zones contain overturned blocks as large as 100 by 500 m. Scott (1984) attributed deformation within the blocks to internal readjustments during movement of brittle hanging-wall rocks over curved normal-fault surfaces.

As currently conceived, the repository would be excavated mainly in the relatively unfaulted western part of one typical structural block. The repository would be bounded on the west by the Solitario Canyon fault, on the northeast by the Drill Hole Wash fault, and on the east and southeast by the western edge of an imbricate normal fault zone (Figures 1-32 and 1-40). Within the perimeter drift (the boundary of the area within which the repository would be excavated), the Tiva Canyon Member caps Yucca Mountain and dips gently (5 to 8 degrees) eastward. Drillhole data indicate that flattened-pumice foliation just north of the repository boundary dips 3 to 8 degrees eastward. South of the proposed repository, the dip increases from 7 degrees eastward near the surface to about 10 degrees southward at a depth of 1,500 m. No sharp discordance in attitudes of foliation or bedding has been recognized at depth.

Within the repository boundary, recognized offset on faults is 5 m or less, except for the Ghost Dance fault, which has 38 m of vertical offset at the southeastern margin of the perimeter drift. Offset decreases northward and is unmeasurable at Drill Hole Wash (Figure 1-40). The fault dips very steeply (80 to 90 degrees) westward and the western side is down dropped. Breccia zones are as much as 20 m wide. The fault offsets the 12.9-million-year-old Tiva Canyon Member; more recent offset has been neither demonstrated nor discounted. North-to north-northwest-striking west-dipping normal faults with small (<5 m) vertical offsets are present, particularly toward the southern and eastern edges of the proposed repository. These small faults are readily identified only where stratigraphic boundaries are distinct and exposures are particularly good. Elsewhere, particularly north and west of Abandoned Wash, the presence of these faults between exposures has been inferred from observed offsets in the projections of recognizable stratigraphic horizons (Scott and Bonk, 1984).

Quaternary history of faulting at Yucca Mountain

Quaternary deposits are offset or fractured by 32 faults in the 1,100-km^2 area shown in Figure 1-34 (Section 1.3.2.2.1) and in Plate 1 of Swadley et al. (1984). Radiometric dating and correlation of stratigraphic units intersected by those faults and fractures suggest that 23 of them moved 1.2 to 2 million years ago, four of them about 1 million years ago, and at least five of them during the past 270,000 yr (Table 1-7). Quaternary dip-slip offset, measured from stratigraphic offset or estimated from well-preserved fault scarps, is typically less than 3 m; however, the occurrence of Q1c fan gravels 10 to 30 m above adjacent Q2c gravels suggests as much as 10 to 30 m of offset on the south segment of the Bare Mountain fault zone 15 km west of Yucca Mountain. Strike-slip offset has been neither demonstrated nor discounted. The maximum length of continuous scarp in Quaternary deposits is 4 km, near the south end of the Solitario Canyon fault zone; the maximum length of fault segments having demonstrable Quaternary offset is 16 km, for the Bare Mountain fault zone.

Quaternary offset has been demonstrated on at least five of the major normal faults at and near Yucca Mountain: the Bare Mountain, Windy Wash, Solitario Canyon, Bow Ridge, and Paintbrush Canyon (Swadley et al., 1984).

Table 1-8. Preliminary fault data for faults showing Quaternary offset

Fault[a]	Aggregate length (km)[b]	Offset (m)	Age of offset unit (my)[c]	Source
Paintbrush Canyon	17-31	200 90 70 45 4.1	12.9 9.6 9.3 7.5 <0.7	Carr (1984); USGS (1984); Dudley (1985)
Bow Ridge	10-19	220 120 Fractures[d]	13.1 12.5 0.27-0.038	USGS (1984); Carr (1984) Swadley et al. (1984)
Solitario Canyon	15-17	500 400 >2	13.1 12.5 1.2	USGS (1984); Carr (1984) Swadley et al. (1984)
Windy Wash	6-19	250-450 60 0.4 0.1	12.9 11.6 0.27 0.003-0.0065	Carr (1984); Whitney et al. (1986)
Bare Mountain	15-22[e]	>2,500 10-30 >1.75	13.5 0.27-0.80 <0.01	Carr (1984); Reheis (1986) Swadley et al. (1984)

[a]Location of faults shown on Figure 1-34.
[b]Maximum lengths scaled from Figure 3 in USGS (1984); minimum lengths scaled from Plate 1 in Swadley et al. (1984). Fault trace has been interpolated between mapped exposures to approximate an aggregate length.
[c]my = million yr.
[d]No discernable offset
[e]Length scaled from maps in Reheis (1986) and Cornwall (1972).

[redacted]

The Bare Mountain range-front fault on the eastern face of Bare Mountain and an adjacent complex of north-northeast-trending faults are about 15 km west of Yucca Mountain; the fault zone probably extends for at least 17 km. [redacted]

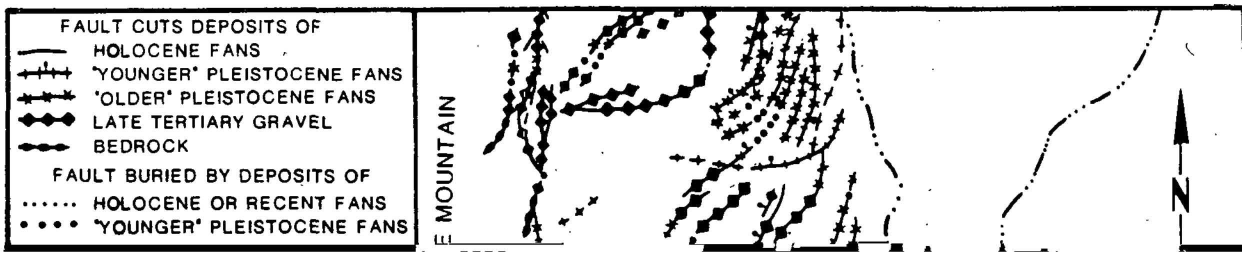
FAULT CUTS DEPOSITS OF
HOLOCENE FANS
'YOUNGER' PLEISTOCENE FANS
'OLDER' PLEISTOCENE FANS
LATE TERTIARY GRAVEL
BEDROCK
FAULT BURIED BY DEPOSITS OF
HOLOCENE OR RECENT FANS
'YOUNGER' PLEISTOCENE FANS
E MOUNTAIN
N

indicated by an underlying unit. A buried soil developed on that unit suggests that it is probably middle Pleistocene in age: calcium carbonate and silica morphology is similar to that in soils formed on late to middle Pleistocene units in Fortymile Wash, and the Harden profile index (Harden, 1982; Harden and Taylor, 1983) for the soil falls in the range of indexes for soils formed on unit Q2b (Taylor, 1986). Fractures are numerous in the buried soil. The fractures are clear and well preserved, so faulting must have fractured the soil after most of the soil properties had formed. All the fractures terminate abruptly at the top of the soil, so the faulting must have occurred before the deposition of the overlying unit.

Two episodes of movement are likely also at site 5. Alluvium of probable late Pleistocene age is in probable fault contact with a Tertiary dike; a soil on the alluvium is similar to soils on unit Q2a (40,000 to 50,000 yr old) in Fortymile Canyon (Taylor, 1986). A second episode of movement is suggested by a near-vertical zone of slickensided calcium carbonate plates parallel to the alluvium-dike contact. Holocene or late Pleistocene offset of bedrock also is likely at site 5; on a splay of the range-front fault, and in a prospect pit, the dike is sheared and brecciated and has slickensides along its contact with a Paleozoic limestone. Near the ground surface, the limestone and the dike are separated by about 1 m of colluvium with vertically oriented clasts. The colluvium may consist of material that fell into an open fracture formed by fault movement. The soil on the colluvium has a thin, sandy A horizon, a weakly oxidized B horizon, and little pedogenic calcium carbonate, which suggests early Holocene age.

The Bare Mountain fault may have a Quaternary displacement rate of 0.1 to 0.01 mm per yr based on a 10 to 30 m offset of Q2c deposits along the fault (Swadley et al., 1984). Using the relationship of Slemmons and Depolo (1986), these rates would indicate a recurrence interval of approximately 4,000 to 40,000 yr for a magnitude 6 1/2 event and 8,000 to 80,000 yr for a magnitude 7 event. Further study of the Bare Mountain fault is planned in Activity 8.3.1.17.4.3.4.

For the four faults at Yucca Mountain (Figure 1-34, Section 1.3.2.2.1), somewhat less information has been published. That information is summarized in the following paragraphs and in Tables 1-7 and 1-8.

The Windy Wash fault (faults M and Q of Swadley et al., 1984) is about 3.5 km west of the proposed repository; the fault zone may be as much as 20 km long. The fault has had at least seven episodes of Quaternary movement, four movement episodes occurred in the past 300,000 yr (Whitney et al., 1986). The fault has demonstrable Holocene offset: it offsets eolian silt, which has been dated by thermoluminescence methods at 3,000 to 6,500 yr. Apparent vertical offset is 40 cm for a 270,000-yr-old gravel and 10 cm for the Holocene silt. Total vertical offset on the Windy Wash fault is estimated as more than 225 m (USGS, 1984). Seismic reflection profiles across the fault suggest strike-slip offset of subsurface structures, but the amount of offset is unknown. For the fault segment at trenches CF2 and CF3 (Figure 1-23), the four episodes of movement during the past 300,000 yr suggest an average recurrence interval of 75,000 yr. If the average offset per event was about 10 cm, each event had a magnitude (M_s) of about 6 to 6.5 (calculated assuming a 30-cm maximum displacement and using the relationships of Bonilla et al. (1984) and Slemmons (1977)). The rate of offset averaged over the past 270,000 yr has been about 0.0015 mm per year which is "extremely low" in the classification scheme of Slemmons and Depolo (1986).

The Solitario Canyon fault adjoins the proposed repository on the west; it may be 15 km or more long. On several fault segments, unit QTa (Section 1.2.2.3) is faulted against Tertiary volcanic rocks along a total distance of 4.5 km (Swadley et al., 1984). The fault shows no evidence of movement during the past 270,000 yr but does show evidence of movement about 1.2 million years ago; a basaltic ash, tentatively correlated with a 1.2-million-year-old basaltic center in Crater Flat, has been reworked into the fracture zone in unit QTa in trench 8. (Figure 1-24b shows these Quaternary units.)

The Bow Ridge fault (fault C of Swadley et al., 1984) is about 1.5 km east of the repository and 0.5 km west of the surface-facilities area and may be nearly 20 km long. At its southern end, it probably abuts the Paintbrush Canyon fault. The fault shows no evidence of movement during the past 38,000 ± 10,000 yr but does show evidence of movement during the past 270,000 ± 90,000 yr; in trench 14, the fault has fractured unit Q2s and the K horizon of the soil developed on it but not the overlying Q2a.

The Paintbrush Canyon fault (at trench 16B, the north end of the Fran Ridge fault of Scott and Bonk, 1984) is about 4 km east of the proposed repository and 0.5 km east of the surface-facilities area; it may be more than 20 km long. The fault shows evidence of movement during the past 700,000 yr. At trenches A1 and 16B, fractures cut unit Q2e (and at trench A1, the fractures cut Q2e soil); at trench A2, fractures cut unit Q2c but not the soil developed on it. The fault shows no evidence of movement during the past 270,000 yr: at trench A2, unit Q2b is unfractured; and at trench 16B, unit Q2s is unfractured. Similarly, at trench A1, the fault shows no evidence of movement during the past 160,000 yr: it does not fracture unit Q2b. At Busted Butte, sand-ramp deposits are displaced 4.1 m by a possible continuation of the Paintbrush Canyon fault. Bishop ash at or near the base of these deposits is faulted, indicating that displacement probably took place within the past 740,000 yr (Dudley, 1985). The rate of offset averaged over the past 740,000 yr has been about 0.005 mm per year, and so the fault would be classified as "inactive or with an extremely low rates of activity" by Slemmons and Depolo (1986). The recurrence interval for an earthquake of magnitude (M_s) about 6.5 would be about 60,000 yr (Slemmons and Depolo, 1986).

The history of movement on the faults in Yucca Mountain has been complex. Data from stratigraphic offsets are not yet available to define the sense of movement on most faults in the Yucca Mountain area. The direction of most recent movement on the faults is indicated by four groups of consistently oriented slickenside striations (Figure 1-44). Groups 1 and 2 occur on both the major and the imbricate normal faults. Large stratigraphic throw and the apparent absence of measurable lateral offset indicate predominantly normal offset, and group 1 slickenside striations confirm dip-slip movement. Similarly, demonstrable offset on faults with group 2 slickenside striations is dip slip, but group 2 slickenside striations plunge less than 20 degrees southwestward on normal faults that strike east of north, which indicates

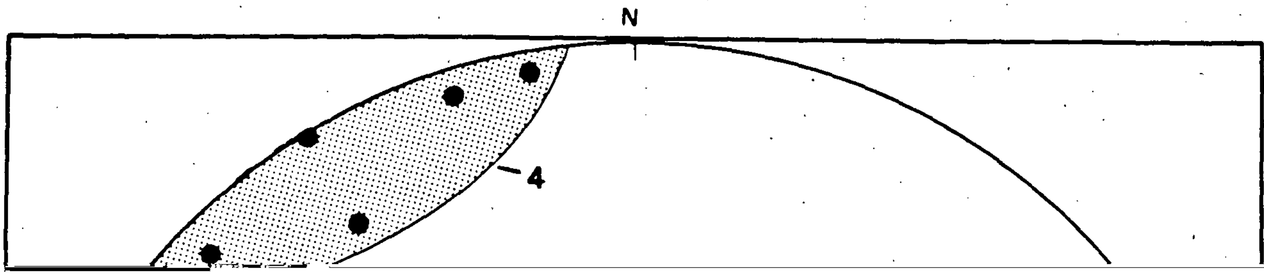
N
4

that the latest movement on these faults was mainly left-lateral strike slip. Group 3 slickenside striations occur on west-dipping normal faults that strike west of north, mainly at the southern end of West Ridge (Figures 1-40 and 1-44); slickenside striations plunge northwestward, indicating dip slip with a small component of right-lateral movement. Group 4 slickenside striations occur on the northwest-striking strike-slip faults; they plunge less than 25 degrees. Further studies of slickenside striations are planned to determine the orientation of the principal stresses that produced the direction and amount of apparent offsets in the different fault groups. However, data from slickensides are not unequivocal in estimating the sense of movement and paleostress orientations, and will need to be supported by other types of data (Section 8.3.1.8).

Fractures at Yucca Mountain

Fractures are common in all the volcanic units at Yucca Mountain. The fractures were produced by cooling, by Basin and Range tectonism, and by unloading due to the removal of overburden. The fractures are commonly stratabound (i.e., their vertical extent is limited to individual units or groups of units); accordingly, pathways through the repository block are by way of complex intersections of fracture networks at strata boundaries as well as by way of some vertically continuous fractures.

Fractures are of particular importance either as barriers or as conduits for the flow of ground water (Section 3.7). Fractures may affect ground-water recharge and movement in the controlled area, and water or vapor transport of radionuclides from the repository to the accessible environment. The hydraulic conductivities of fractured, densely welded ash-flow tuff in the saturated zone are 3 to 8 orders of magnitude greater than the matrix hydraulic conductivities for the same rock (Winograd and Thordarson, 1975; Scott et al., 1983). Fractures might also affect mining conditions and the long-term stability of underground openings.

Detailed studies of fractures in man-made exposures (hydraulically cleaned "pavements") in the welded upper lithophysal unit of the Tiva Canyon Member indicate that the fractures are of three types, formed in at least three different events (Barton, 1984). The first type consists of cooling fractures, which constitute two well-defined sets, striking N.30° to 50°E. and N.35° to 55°W., both dipping perpendicular (±5 degrees) to foliation (pumice flattening); these sets formed simultaneously in 3- to 5-m-wide swarms spaced 150 to 200 m apart. The second fracture type is tectonic, often exhibits small dip-slip displacement, and postdates the cooling fractures. Unlike the cooling fractures, these fractures do not form oriented sets but are apparently due to large-scale regional extensional faulting. The third fracture type also is tectonic, strikes northwest, and exhibits lateral strike-slip displacement. The length of all mapped fracture traces has a log-normal distribution (Barton and Larsen, 1985). This

this measure provides a basis for comparison rather than an absolute count of fractures. For both the surface traverses and the cores, fractures were generally more abundant in densely welded tuff than in moderately welded tuff.

Fracture frequencies were determined for six surface traverses: five in central Yucca Mountain in the Tiva Canyon Member, and one near the northern tip of Yucca Mountain, in the tuffaceous beds of the Calico Hills (Figure 1-45). Fracture frequencies for short traverses in continuous exposures of the densely welded middle part of the Tiva Canyon Member were about six to eight fractures per cubic meter; for long traverses in the Tiva Canyon, two to four fractures per cubic meter. The lower frequencies for the long traverses are probably due to poor exposure in debris-covered gullies and to

as well as the more densely welded middle part.

In cores, fracture frequency generally increased with the degree of welding: frequencies were about 10 times greater in moderately and densely welded tuff than in partially welded or nonwelded tuff; fracture frequency tended to decrease with depth independently of welding (Scott and Castellanos, 1984).

The discussion that follows is based on fracture data from adjacent drillholes USW GU-3 and USW G-3, near the southern end of the proposed repository (Scott and Castellanos, 1984), and from drillhole USW G-4, near the northeastern flank of the repository (Spengler and Chornack, 1984). In drillholes USW GU-3 and USW G-3, the fracture frequency in densely welded tuff ranged from about 15 to 40 fractures per cubic meter and generally varied little over tens of meters of core. In lithophysal zones there were 14 to 20 fractures per cubic meter; nonwelded tuff had as few as little as 1 to 4 fractures per cubic meter. Fracture frequency decreased abruptly below 940 m, independently of welding: moderately welded tuff above 940 m had 8 to

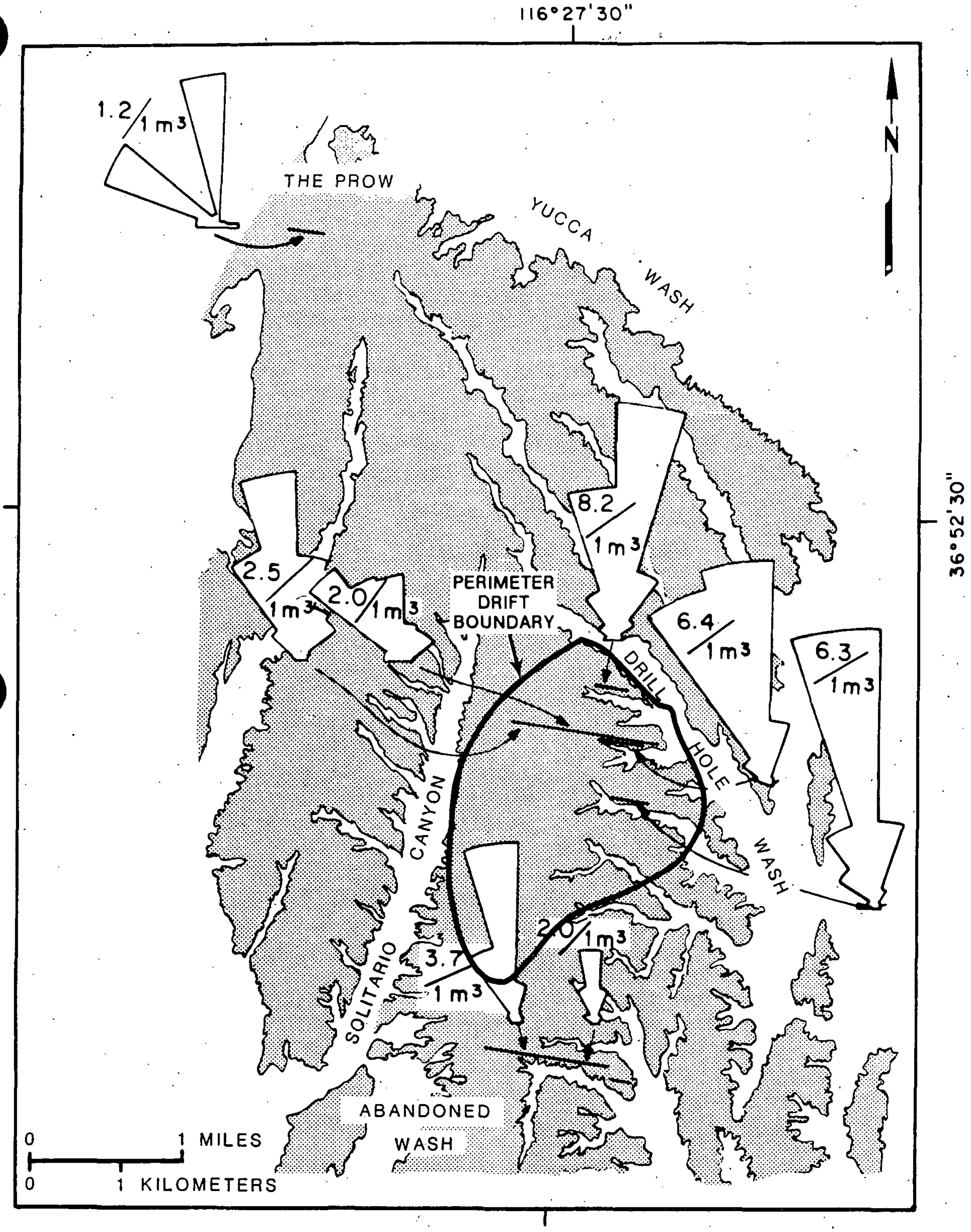

Figure 1-45. Rose diagram of the strikes of high-angle fractures along traverses perpendicular to the average fracture attitude. Five traverses were made in the Tiva Canyon Member. A sixth traverse was made in the Prow in the tuffaceous beds of Calico Hills. The outline of Yucca Mountain is the contact of Tertiary volcanic rocks with Quaternary deposits Some traverses have more than one diagram. Modified from Scott et al. (1983).

On surface pavements in the upper lithophysal unit of the Tiva Canyon Member, the strike of fractures is highly variable; dips are generally greater than 65 degrees and locally are approximately perpendicular to the foliation (Barton and Larsen, 1985).

The attitudes of subsurface fractures were determined from oriented cores (strike and dip), from downhole television camera surveys (strike only), and from conventional cores (inclination only, without correction for drillhole deviation). Fracture attitudes at the south end of the proposed repository (in drillholes USW GU-3 and USW G-3) are similar to those measured at the surface (Scott and Castellanos, 1984). Preliminary analysis also suggests general parallelism between dominant fault attitudes and fracture attitudes in drillholes USW GU-3 and USW G-3; both dip steeply west-southwest. Preliminary results from drillhole USW G-4, in the north-central part of the proposed repository, indicate dominant fracture sets of (1) N.22°E., 65°NW. in the Tiva Canyon Member; (2) N.12°W., 89 to 90°NE. and SW. in the Topopah Spring Member, and (3) N.23°E., 45°NW. and N.50°E., 55°SE. in the Crater Flat Tuff. Drillholes at Yucca Mountain are consistently deflected westward (those in Drill Hole Wash are deflected southwestward), parallel to the dominant dip direction of the fractures.

The data gathered to date, from detailed studies of surface pavements, reconnaissance sampling of traverses, and cores, should be considered preliminary. Because traverses and cores are line samples through three-dimensional fracture networks, they are incomplete and strongly biased and cannot be corrected statistically. Ongoing and planned studies will focus on fractures exposed on surface pavements and in underground shafts and drifts (Section 8.3.1.4) to more accurately determine the extent of subsurface fracturing that may be significant to ground-water flow.

Detailed studies of fault and fracture attitudes at Yucca Mountain may confirm preliminary indications that dominant faults and fractures are parallel and dip steeply or that they flatten and converge with depth. Alternate models for fault block geometry are possible.

Detailed studies of fracture fillings above the static water level in the Topopah Spring Member in drillhole USW-G4 have been completed (Section 4.1.1.3). Detailed investigations of the absolute ages of fracture formation and minerals deposited along fractures have not yet been completed. A preliminary analysis of fracture fillings (14 calcite and 4 opal samples) from 3 zones at depths of about 30 to 140, 170 to 370, and 600 m in drillholes has been completed (Szabo, 1984). Uranium series dates group at about 28,000 ± 5,000, 170,000 ± 30,000, and 280,000 ± 50,000 yr before present. Four of the calcite samples and all of the opal samples were older than 400,000 yr. These preliminary data are suggestive of at least four episodes of recent fracturing (faulting?) at Yucca Mountain. Similarly, 26,000- and 30,000-yr-old calcites filling fractures in cores from drillholes USW GU-3 and USW G-3 have been interpreted as showing the minimum time at which fractures were formed or older fractures reopened (Scott and Castellanos, 1984).

1.3.2.3 Existing stress regime

Yucca Mountain lies in the Basin and Range stress province, a region distinguishable from adjacent regions by singularities in the prevailing stress magnitude and orientation (Zoback and Zoback, 1980a). As pointed out by Zoback and Zoback (1980b), stress provinces correspond in a general way to major physiographic provinces of the United States. The Basin and Range stress province includes the northern and the southern Basin and Range physiographic provinces and the western part of the Colorado Plateau.

This section discusses the stress field in the Basin and Range stress province and at Yucca Mountain. Related discussions of stresses in the southern Great Basin and at Yucca Mountain are given in Section 2.6. Stresses suggested by earthquake focal mechanisms are briefly discussed in Section 1.4.1.1.

Before reviewing the state of stress in the Basin and Range stress province and the Yucca Mountain region, certain terms and concepts are defined. As in the report by Zoback and Zoback (1980a), it is assumed that on a regional scale two of the principal stresses are approximately horizontal and the third is approximately vertical. The larger and smaller components of the principal stresses in the horizontal plane are referred to as SH and Sh, respectively, and the component in the vertical plane as Sv. The conventional view that the style of faulting corresponds to the relative magnitudes of SH, Sh, and Sv is also adopted in the following way:

For normal faulting,
$Sh < SH < Sv$

For strike slip faulting,
$Sh < Sv < SH$

For thrust faulting,
$Sv < Sh < SH$

The chief sources of information on the stress pattern and magnitude are (1) earthquake focal mechanisms, (2) in situ stress measurements, and (3) the orientation and nature of faults. The focal mechanisms of earthquakes in most parts of the province are known, but even for well-constrained solutions, the orientation of the axes of symmetry may vary from that of the corresponding principal stresses by as much as 35 to 40 degrees (Raleigh et al., 1972).

In situ stress in the Basin and Range stress province has been measured only at the NTS. The measurements, discussed more fully below and in Section 2.6.2, show that the orientation of Sh is not substantially different in the stress province therefore is based chiefly on the determination and analysis of focal-plane solutions.

The average direction of Sh within most of the Great Basin is approximately west-northwest, except for southern Nevada, where Sh trends more nearly northwest, and along the eastern border of the province in Utah, where Sh trends east-west (Zoback and Zoback, 1980b). Normal faulting predominates in the central and eastern parts of the province, indicating that Sh < SH < Sv. However, in some areas within the western part of the province, including the central and northern parts of the Walker Lane but excluding the NTS, faulting is dominantly of the strike-slip type at depths of less than 6 km and of the dip-slip type at greater depths (Vetter and Ryall, 1983). This transition implies that through progressive increase in overburden pressure with depth the maximum compressive stress rotates from horizontal near the surface to vertical at depth (Vetter and Ryall, 1983).

In detail, the stress pattern within the immediate region (Figure 1-46) surrounding Yucca Mountain appears to be much more complex than the foregoing remarks imply. This area seems to be a wide zone of transition between the [illegible]

< Sv), and western California, dominated by strike-slip faulting (Sh < Sv < SH). The average trend of Sh swings from east-west at the eastern edge of the stress province (Colorado Plateau) to northwest in eastern Nevada, then to east-west in western California (Figure 1-46), with apparent departures from this pattern of up to 45 degrees in local areas. Focal-mechanism solutions for earthquakes in the vicinity of Yucca Mountain (Figure 1-47) suggest that the average orientation of Sh is about N.60°W., conforming to the pattern within the immediate region, but with local areas of sharply divergent trend. Unlike the in situ stress measurements (discussed below), most of the focal-plane solutions indicate strike-slip faulting, which suggests that Sh < Sv < SH.

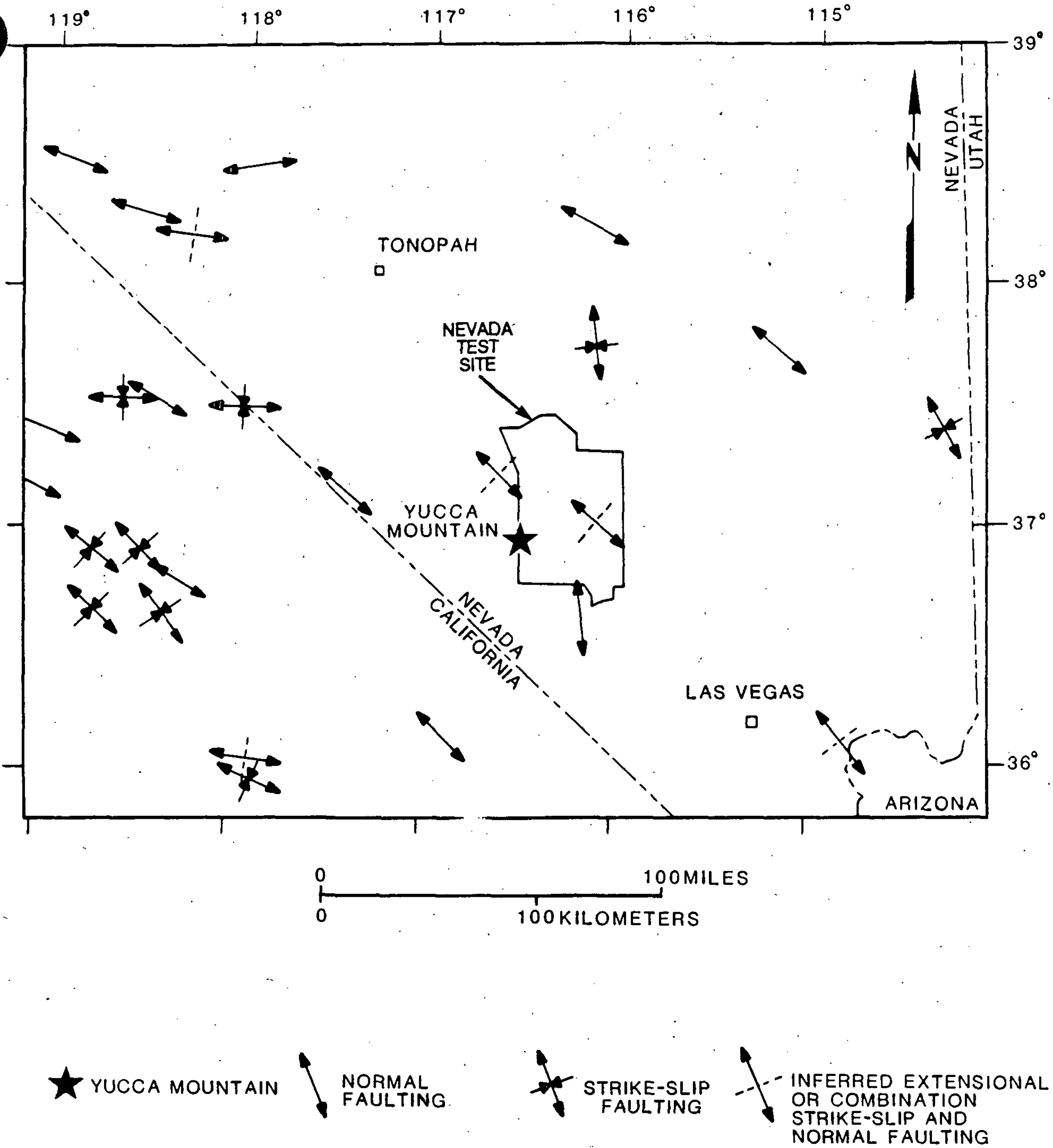

Figure 1-46. State of stress in the Yucca Mountain region, based on focal-plane solutions and geologic indicators. Modified from Zoback and Zoback (1980a).

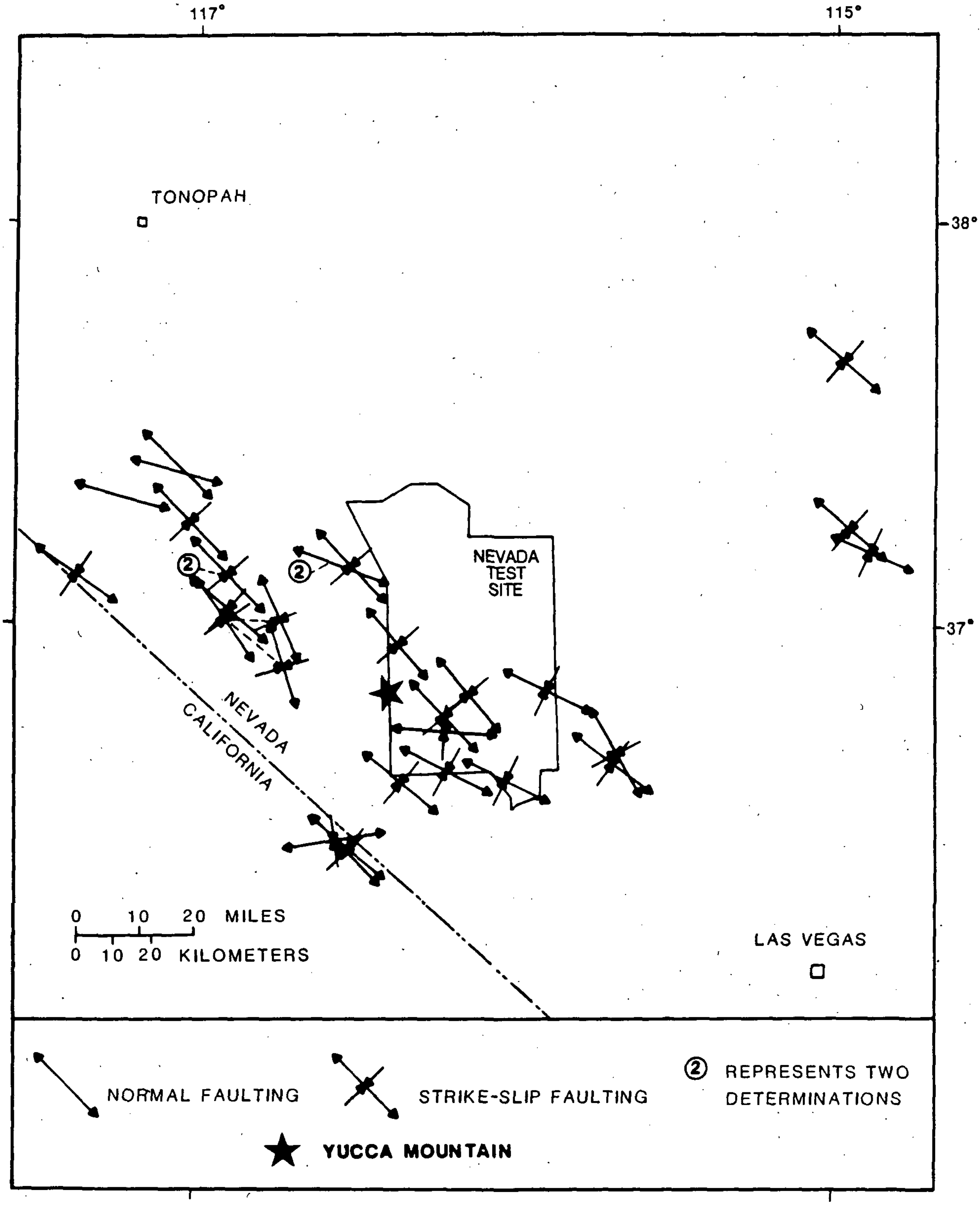

Figure 1-47. State of stress in vicinity of Yucca Mountain, based on focal-mechanism solutions of earthquakes. Modified from Rogers et al. (1987).

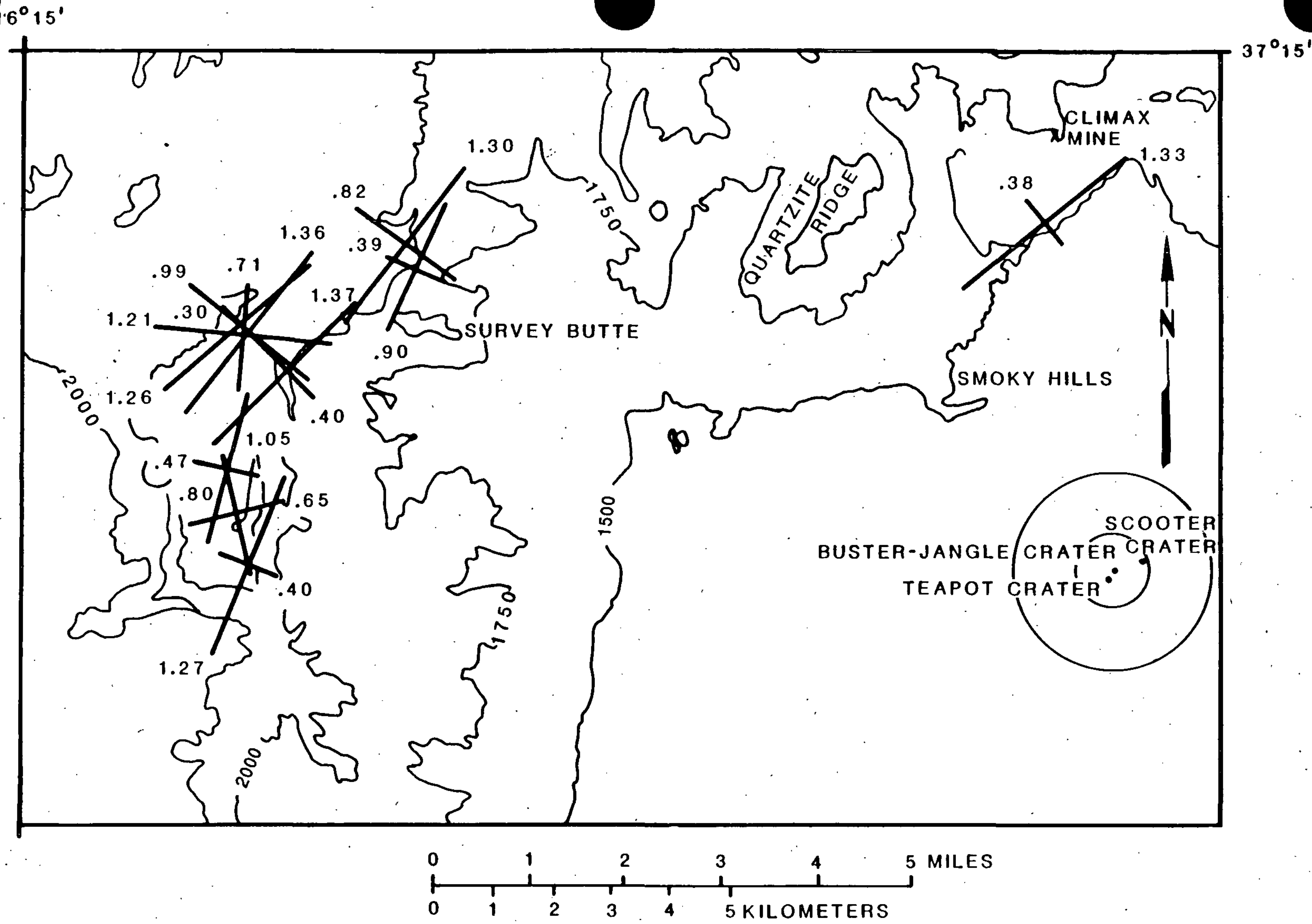
116°15'
37°15'
1.30
.82
1.36
.39
.99
.71
1.37
1.21
.30
.90
SURVEY BUTTE
1.26
.40
1.05
.47
.80
.65
.40
1.27
2000
1750
1500
1750
2000
QUARTZITE RIDGE
CLIMAX MINE
1.33
.38
SMOKY HILLS
N
SCOOTER CRATER
BUSTER-JANGLE CRATER
TEAPOT CRATER
0 1 2 3 4 5 MILES
0 1 2 3 4 5 KILOMETERS

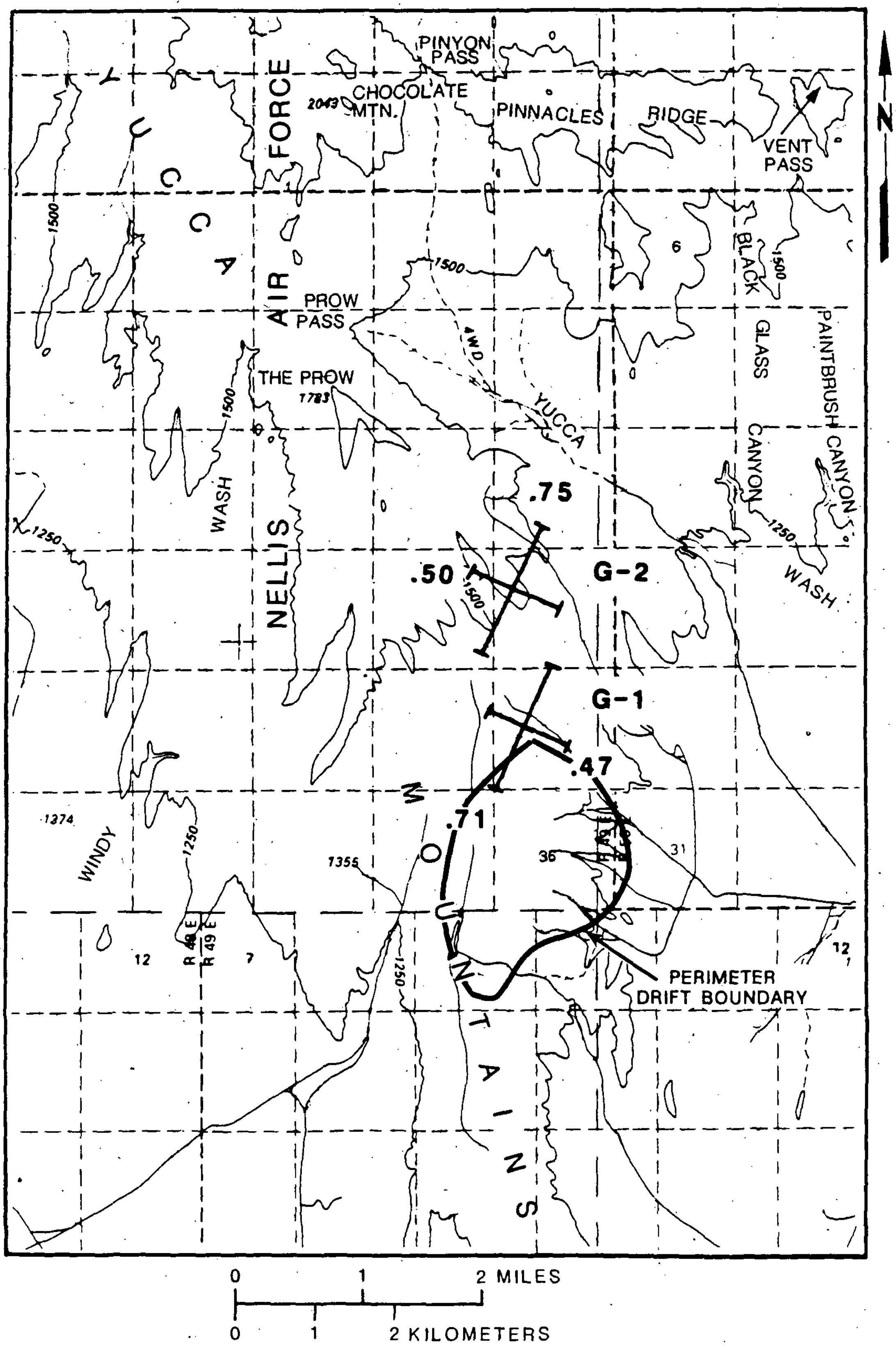

Figure 1-49. In situ stress, drillholes USW G-1 and USW G-2, Yucca Mountain. Length of bars are proportional to the measured horizontal stresses. Numbers adjacent to bars represent the ratio of horizontal to vertical stresses. Modified from Stock et al. (1985).

On the basis of hole ellipticity and the orientation of drilling-induced fractures in USW G-2 and the upper part of drillhole USW G-1, the direction of Sh was determined to be N.60 to 65°W. (Stock et al., 1985). In the lower part of drillhole USW G-1, however, specifically within the 1,113- to 1,202-m depth interval, the average azimuth of hole breakouts was S.80°W. (Stock et al, 1985), which implies a similar orientation for Sh. Taken at face value, the data suggest a 35- to 40-degree rotation in the orientation of Sh and SH between the upper-most and the lower-most parts of drillhole USW G-1.

Carr (1974) has postulated that the general direction of extension for the NTS is N.50°W., based chiefly on the analysis of geologic, seismic, and in situ indicators of stress orientation. Thus, the orientation of the principal stresses in drillhole USW G-2 and the upper part of drillhole USW G-1 at Yucca Mountain is not greatly dissimilar to the general orientation elsewhere at the NTS. However, the relative magnitudes of the principal stresses at Yucca Mountain are compatible with normal faulting, whereas elsewhere they are compatible with strike-slip faulting.

The measured magnitude of Sh at drillhole USW G-1 is quite low--evidently less than the hydrostatic pressure of the fluid column that was present during the drilling of the hole (Ellis and Swolfs, 1983). According to Ellis and Swolfs (1983), return circulation of drilling fluid during the drilling operation was rarely achieved. They state that "even after casing was set to a depth of 310 m, more than 44,000 barrels of drilling fluid were lost to the formations below the casing." The loss of this fluid was attributed to the hydraulic fracturing of the rock and flow into these and other preexisting fractures intersected by the hole.

At Yucca Mountain, the measured magnitudes of Sh are near and perhaps even below the minimum values required to provide the lateral support necessary to prevent extensional failure on moderately dipping faults trending parallel to SH (Stock et al., 1985). Also, as shown by Stock et al. (1985), the magnitude of Sh is less than the fluid pressure that would exist if the water level (in drillholes or fractures) were brought to the surface. Raising the water level to the surface, as was done during the drilling of drillhole USW G-1, causes the fracturing and dilation of existing fractures and hence increases hydraulic conductivity of the fractures. These interpretations seem adequately demonstrated by current information on in situ stress.

Direct measurement of crustal strain at the NTS and in southern Nevada has been attempted through geodetic methods and through the monitoring of strain gauges. An array of six strain meters in south-central Nevada was monitored for an 8-month period in 1970 and 1971 (Smith and Kind, 1972a,b). The array spanned 140 km north to south, and 65 km east to west, with the southernmost station location at Yucca Mountain. The data suggest several distinct episodes of tectonic compression and extension on northeastern and northwestern axes during this period, and somewhat surprisingly, the net deformation was northeastern compression rather than northwestern extension (Smith and Kind, 1972a). The observed strains during this experiment were one to two orders of magnitude greater than those concurrently observed at Mina and Round Mountain, Nevada, 210 km northwest and 200 km north-northwest of Yucca Mountain, respectively (Priestly, 1974). The net strain at Mina showed northwestern extension, whereas that at Round Mountain was northeastern extension. Records at both stations showed reversals indicating that periods of strain accumulation were abruptly followed by strain relaxation (Priestley, 1974).

A seven-station trilateration network was installed in the Pahute Mesa area and surveyed before and after the 1.9-megaton underground nuclear explosion HANDLEY event in 1970 (Dahlman and Israelson, 1977). The network spanned 40 km north to south and 34 km east to west. The southernmost point on the network was Timber Mountain, about 17 km north of Yucca Mountain. Ground zero was in the northern sector of the network, about 40 km north of Yucca Mountain. The line lengths ranged from 11.1 to 31.9 km; changes in line length between surveys ranged from 0 ± 4 to 275 ± 5 mm (unadjusted observations). The estimated standard deviations of changes in line length, adjusted for network geometric constraints, ranged from 5.3 to 10.0 mm (Savage et al., 1974). The network extended in a west-southwest and east-northeast direction in the month between surveys before and after the explosion and subsequently contracted, resulting in a net east-northeast to west-southwest contraction a yr later (Savage et al., 1974). The initial extension was probably caused by tectonic slip on fault planes; the slip was triggered by the transient stress wave of the explosion (Savage et al., 1974) and felt as earthquakes. The processes responsible for the subsequent reversal of strain are less clear. As acknowledged by Savage et al. (1974), focal-plane solutions of post-shot earthquakes (Hamilton et al., 1972) indicate strike-slip faulting in the southern part of Pahute Mesa and normal faulting in the central and northern parts. The preferred fault planes trend north to northeast; thus, post-shot distortion of the trilateration network should have been northwest-southeast extension rather than the observed west-southwest to east-northeast contraction.

The magnitude and the orientation of tectonic stress release triggered by 21 underground nuclear tests including the HANDLEY event, in the Pahute Mesa area was estimated from long-period S-waves by Wallace et al. (1985). Referring to equivalent fault models of the explosions, Wallace et al. (1985) state that "although there is some variation in the tectonic release double-

1.3.2.4 Vertical and lateral crustal movement

Lateral shortening of the crust in the Basin and Range province during the Mesozoic was followed during the Cenozoic by lateral extension. Local patterns of uplift, tilting, and subsidence near Yucca Mountain are typical of shallow crustal response to regional extension and the attendant volcanic activity in the Great Basin. The region is currently undergoing active lateral crustal extension.

Southward or southeastward tilting of the region around Yucca Mountain during the past 8 million years is suggested by Carr (1984). Volcanic units emplaced 8 to 15 million years ago pinch out abruptly southward, which suggests that they were emplaced on a surface that sloped northward or northwestward. By contrast, the present topographic surface slopes generally southward from a regional topographic high in central Nevada. In the Las Vegas Valley, Pahrump Valley, Amargosa Desert Valley, and northern Death Valley, southward or southeastward tilting of 3 to 7 m/km during the past 3 million years is suggested by a southward decrease in the altitude of playa deposits; continued tilting is suggested by the apparent tendency of the centers of deposition in such playas to shift southward with time (Carr, 1984).

Geodetic data sufficient to resolve historical crustal movements are not available, but a geodetic network has been installed. A level line run through the Yucca Mountain area between 1982 and 1983 was resurveyed in 1983 to 1984 and showed no evidence of change. In 1985, the line was upgraded and extended through Mercury, Nevada, to create a level loop and to terminate at a first-order National Geodetic Survey line. Planned geodetic studies (Section 8.3.1.17) will resurvey the existing level lines across Yucca [illegible]

rates of uplift during historical times to establish the locations and rates of uplift. This work is important for determining the potential for tectonic activity after repository closure.

Within what would be the controlled area, there has been no mining or injection or withdrawal of fluids and, consequently, there has been no uplift or subsidence due to such activities.

1.3.2.5.1 In situ temperature in the southern Great Basin

Yucca Mountain is in a region of high heat flow relative to other regions of the United States (Sass et al., 1981). However, the area north of and adjacent to Yucca Mountain has a lower than average heat flow (Figure 1-50) and has been termed the Eureka low by Lachenbruch and Sass (1977) and Sass et al. (1971). The Eureka low has been attributed to complex lateral and vertical interbasin ground-water flow (Sass et al., 1971; 1980; Sass and Lachenbruch, 1982).

The low heat-flow values for the Eureka low are due to low measured temperature gradients, which in turn may be due to lateral regional water flow having a net vertical downward component of a few millimeters per yr. The heat-flow depth relation of drillhole USW G-1 is consistent with the regional vertical flow velocities determined independently by hydrologic techniques (Winograd and Thordarson, 1975), as shown by Sass and Lachenbruch (1982). Other significant factors than can amplify the hydrological circulation effect are discussed in Section 1.7.1.4.

1.3.2.5.2 In situ temperatures at Yucca Mountain

Heat-flow data specific to the NTS (Sass and Lachenbruch, 1982) show that the low heat-flow values of the Eureka low extend southward beneath Yucca Mountain. As in the Eureka low, heat flow appears to be reduced by downward ground-water movement. Even in the unsaturated zone, low heat flow may result from the lower thermal gradients caused by two-phase (vapor and liquid) water flow (Sass and Lachenbruch, 1982). Heat flow is also discussed in the assessment of mineral and hydrocarbon resources in Section 1.7.1.4.

Temperature profiles are provided by Sass and Lachenbruch (1982) for drillholes UE-25a#1, UE-25a#4, UE-25a#5, UE-25a#6, UE-25a#7, USW G-1, USW G-2, USW H-1, USW VH-1, and J-13 from Yucca Mountain. The locations of all these drillholes are shown in Section 1.6. These profiles demonstrate the large variations in thermal gradients with depth near Yucca Mountain. Given the variability of the gradients, the upper and lower bounds (i.e., 37 and 20°C/km (Sass and Lachenbruch, 1982)) are more meaningful than an average.

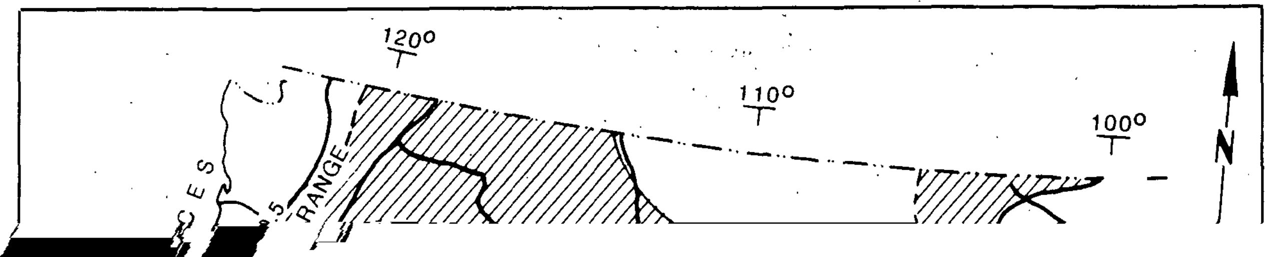
120°
110°
100°
N
RANGE
C E S
5

about gross thermal loading, ventilation requirements, and waste-package design (Chapter 7).

The in situ temperatures before waste emplacement play a very minor role in performance assessment. As an initial condition for calculating the waste-induced temperature field, these temperatures play a role in the analysis of thermally induced water migration and the resulting effects on water flow patterns (Chapter 2). In addition, the in situ temperatures are used to obtain the correct values for the viscosity and density of water for analyzing the present water flow pattern at Yucca Mountain (Chapter 3).

1.3.2.5.4 Relationship to tectonics and energy resource extraction

The high heat flow that is characteristic of the Basin and Range Province, but that may be masked by ground-water flow of the Eureka low and adjoining areas that include Yucca Mountain, is discussed in detail in Section 1.7.1.4.2.

Regional high and low heat flow areas can be generally related to tectonic features or ongoing tectonic activity of the crust. Regional high-heat flow associated with hydrothermal convective systems probably derive their thermal water (1) from very deep-seated near-melting conditions or magmatic sources at the lower crust where thermal water is delivered along faults (Roy et al., 1968, 1972; Renner et al., 1975; Brook et al., 1979) or (2) from the cooling of large high-level silicic magma bodies (Smith and

1.4 SEISMOLOGY OF THE SOUTHERN GREAT BASIN AND YUCCA MOUNTAIN

Section 1.4 discusses the seismicity of the southern Great Basin and Yucca Mountain, the area's seismic history, the relationship of seismicity to geologic structures, and the potential seismic hazard in the vicinity of the repository site. The discussion responds to characterization programs 8.3.1.8 (postclosure tectonics) and 8.3.1.17 (preclosure tectonics).

The discussion considers seismic activity and consequent ground motion (Section 1.4.2.1) that might affect the isolation of radioactive waste or the design, construction, and operation of the repository. The purpose of this section is to provide an understanding of the seismic hazard for the Yucca Mountain site. In particular, for the preclosure period, an understanding is needed regarding potential vibratory ground motion for which structures, systems, and components important to safety must be designed. The potential for vibratory ground motion will depend on the level of seismic activity in the site region and on the earthquake potential of the faults near the site. For the postclosure period, the level and location of seismicity may be used to aid in developing disruptive tectonic scenarios including their probability of occurrence.

This section is divided into two parts, seismology of the southern Great Basin (Section 1.4.1) and seismology of Yucca Mountain (Section 1.4.2). In Section 1.4.1, the objectives are to describe the seismic history and contemporary seismicity of the southern Great Basin including seismic network data obtained through 1983, to identify earthquake-generating potential of geologic structures and seismotectonic zones, to evaluate the effect of seismicity induced by man-made activities, and to assess the earthquake hazard within the southern Great Basin. The objectives are met by using an approach wherein generalized source zones replace traditional maximum earthquakes placed on specific faults. Additionally, plausible alternative hypotheses of earthquake occurrence are described.

Section 1.4.1 provides a regional overview of the seismicity and the potential for earthquake occurrence, and Section 1.4.2 focuses on Yucca Mountain and its immediate vicinity. The objective of Section 1.4.2 is to describe the vibratory ground motion from potential earthquakes that could affect the Yucca Mountain site. Included in the section is a discussion of the potential effect on the site from seismicity induced by man-made sources.

1.4.1 SEISMOLOGY OF THE SOUTHERN GREAT BASIN

This section discusses the seismicity of the region surrounding Yucca Mountain (Figures 1-51 and 1-52) and relates the seismicity to the tectonics of the area of the southern Great Basin shown on Figure 1-53. Although only a small fraction of the earthquakes within 400 km of Yucca Mountain could plausibly affect the proposed facility, events within this radius were considered to provide a regional setting for the seismicity around Yucca Mountain. The pattern of regional seismicity (Figures 1-51 and 1-52), consists of the north-south-trending Nevada-California seismic belt, the southern end of the Intermountain seismic belt in southwestern Utah, and the diffuse East-West seismic belt encompassing the NTS. The following parts of

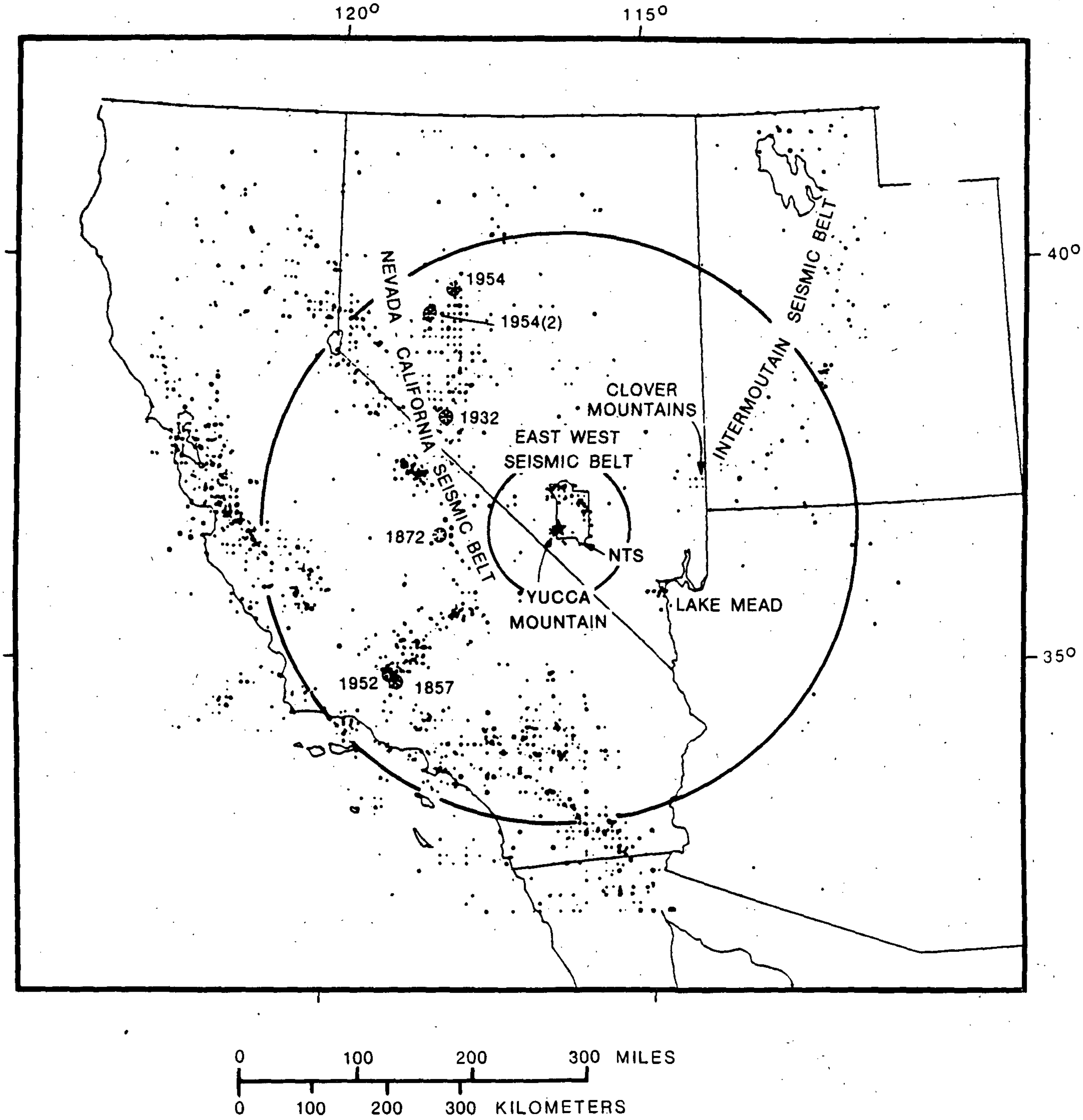

Figure 1-51. Seismicity of southwestern United States, based on historical and instrumental data through 1978, $M \geq 4.0$ or Modified Mercalli intensity $I_o \geq V$, from USGS sources. Circles of radii 100 km and 400 km (similar to circles used by Rogers et al., 1977a) are centered on Yucca Mountain. Stars show locations of major ($M \geq 6.5$) historical earthquakes within 400 km of Yucca Mountain. Many epicenters in the northern NTS and near Lake Mead are presumed to represent induced earthquakes. Compiled from National Earthquake Information Center files, U.S. Geological Survey.

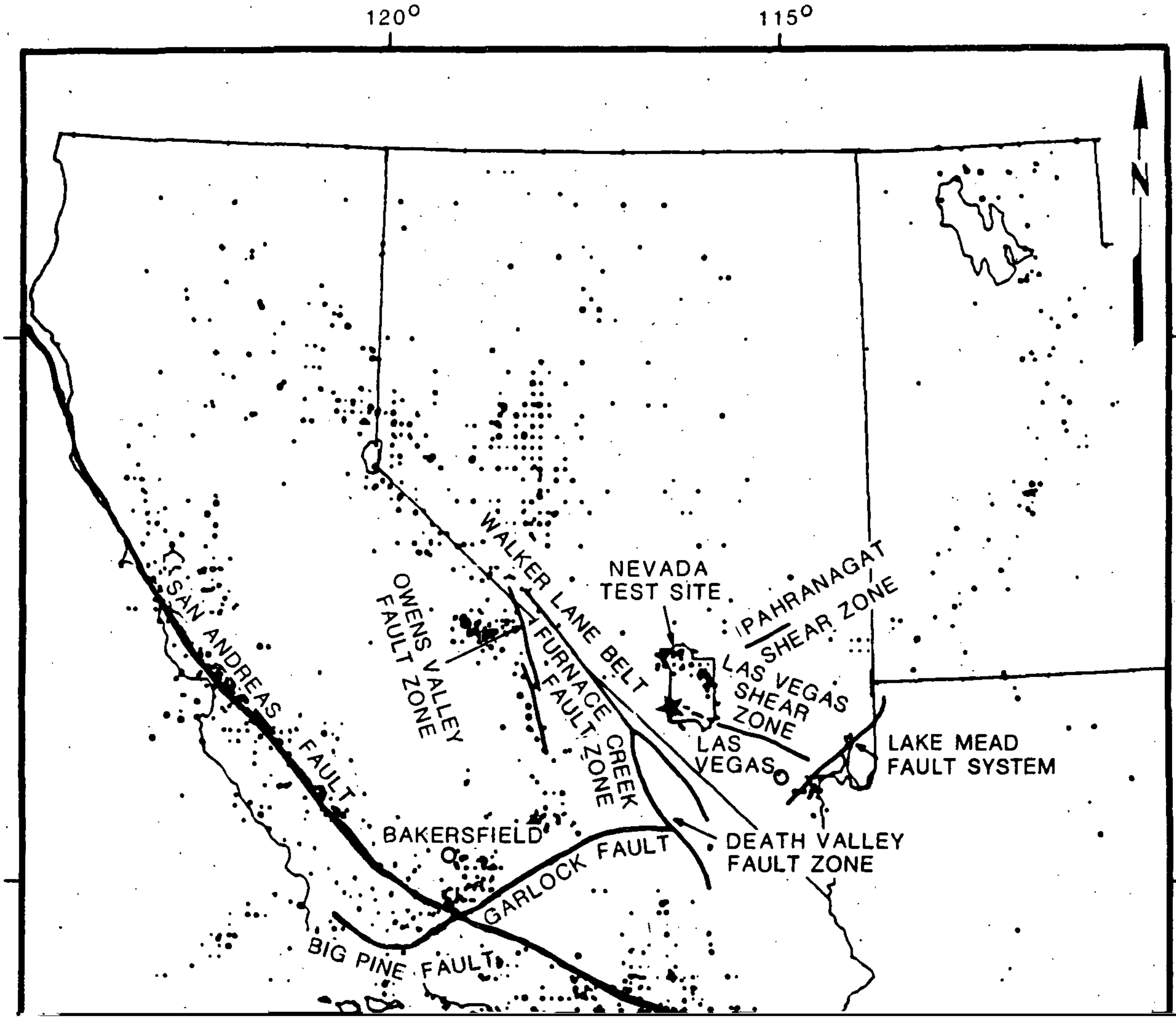
120°
115°
40°
35°
N
NEVADA
TEST SITE
PAHRANAGAT
SHEAR ZONE
WALKER LANE BELT
OWENS VALLEY
FAULT ZONE
FURNACE
FAULT ZONE
CREEK
LAS VEGAS
SHEAR
ZONE
LAS
VEGAS
LAKE MEAD
FAULT SYSTEM
SAN ANDREAS
FAULT
BAKERSFIELD
GARLOCK FAULT
DEATH VALLEY
FAULT ZONE
BIG PINE FAULT

[redacted]

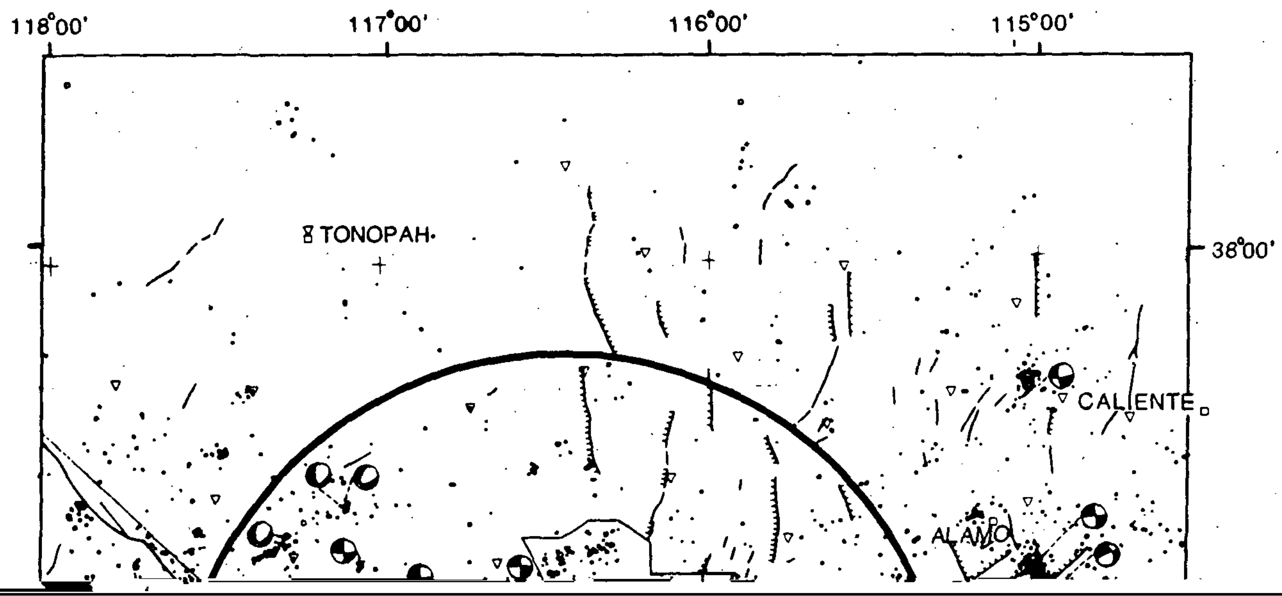
118°00'
117°00'
116°00'
115°00'
38°00'
TONOPAH
CALIENTE
ALAMO

this section discuss the seismic record of the southern Great Basin (Section 1.4.1.1), relate the observed seismicity to the faults and shear zones in the region (Section 1.4.1.2), assess the seismic potential of those faults and shear zones (Section 1.4.1.3), consider earthquake-induced phenomena that could affect the repository (Section 1.4.1.4), and assess the recurrence intervals of maximum earthquakes in the region surrounding the repository (Section 1.4.1.5).

The seismic record of the southern Great Basin is derived almost exclusively from two sources: (1) the catalog of historical earthquakes occurring prior to the installation of the Southern Great Basin Seismic Network (SGBSN) (Meremonte and Rogers, 1987) and (2) the SGBSN earthquake catalog (Rogers et al., 1981, 1983, 1987). Programs for locating hypocenters and determining magnitudes and focal mechanisms, tables of constants, crustal velocity models, and data processing procedures are described in detail by Rogers et al. (1981, 1983, 1987).

The historical catalog (Meremonte and Rogers, 1987) is composed principally of earlier catalogs of regional scope compiled by the National Oceanic and Atmospheric Administration (NOAA), California Division of Mines and Geology, California Institute of Technology, University of Nevada at Reno, and University of California at Berkeley. These catalogs contain locations and origin times derived instrumentally and locations inferred from historical descriptions of large shocks occurring in preinstrumental times; the time period covered is roughly 1868 through 1960. After 1960, the historical catalog contains predominantly instrumental hypocenters and magnitudes extracted from the NOAA catalog and from catalogs compiled as a consequence of weapons testing in southern Nevada (King et al., 1971; Tendall, 1971; Bayer et al., 1972; Fischer et al., 1972; Bayer, 1973a, b, 1974; Rogers et al., 1976) and special studies (Hamilton et al., 1971). The geographic coverage of the historical catalog is shown in Figures 1-54a, 1-54b, and 1-54c for the period 1868-1978. The apparent concentration of seismicity in the northern NTS region represents contamination of the natural data base by weapons testing and associated aftershocks.

Since August 1978, a high-quality seismographic network, the SGBSN, has operated in support of the Yucca Mountain Project (formerly the NNWSI Project). In 1978 and 1979, 47 stations were installed within 160 km of the proposed repository to monitor potential seismic activity of tectonic features thought to be of greatest importance to the seismic assessment of Yucca Mountain (Rogers et al., 1981). In 1981, a mininetwork of an additional six stations was deployed at Yucca Mountain to improve detection thresholds and location accuracy of earthquakes occurring near Yucca Mountain. The installation of the SGBSN meant a significant improvement in the quality of the seismicity data available for the southern Great Basin. The SGBSN catalog used in all discussions in this report (Rogers et al., 1987) covers the period August 1978 through December 1983; hypocenter and magnitude data in earlier bulletins (Rogers et al., 1981, 1983) continue to be revised as a consequence of continuing research. Improved models and procedures are discussed in detail in Rogers et al. (1987). The locations of the seismic stations are shown on Figure 1-53.

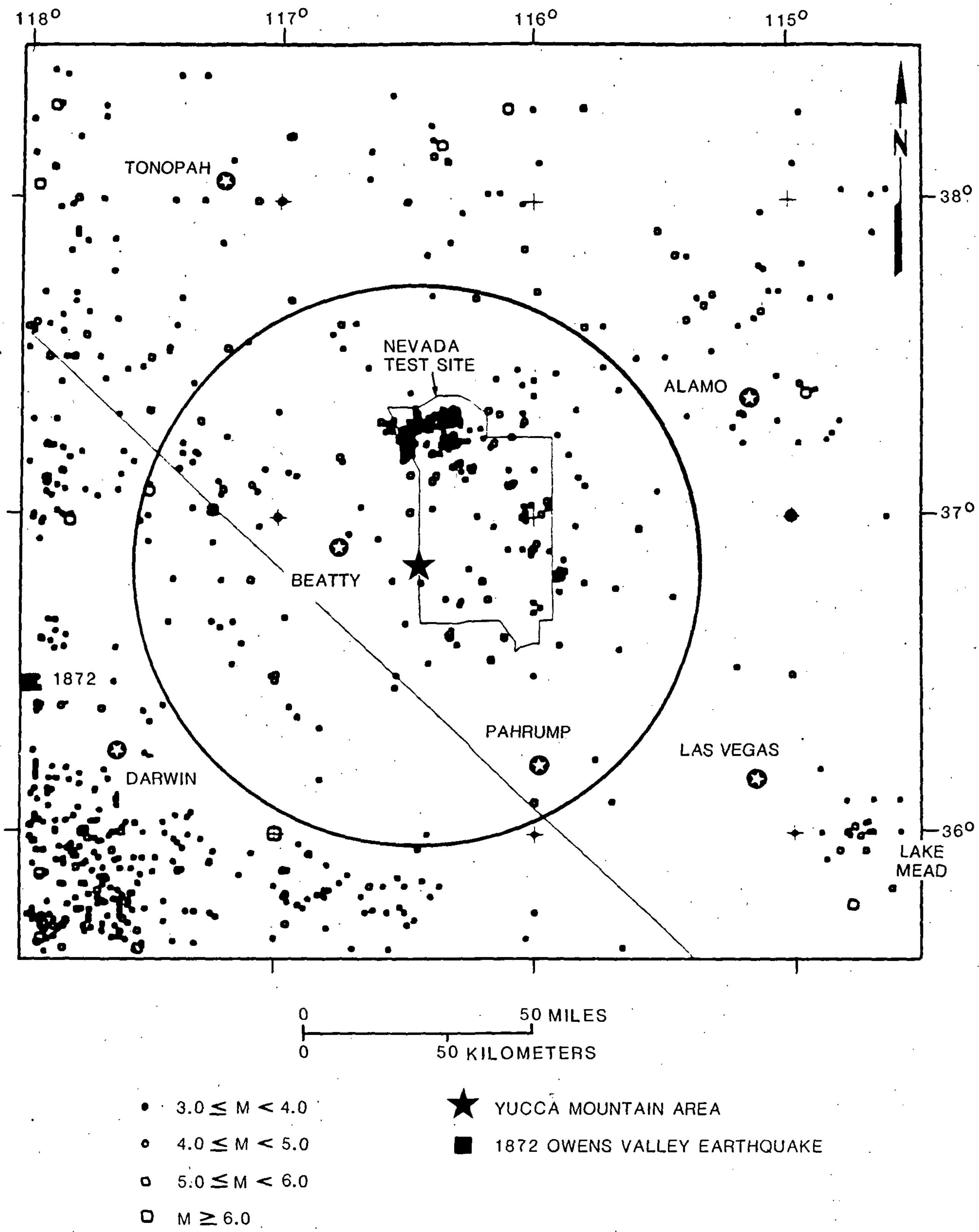

Figure 1-54a. Historical seismicity of the southern Great Basin. 1868 through 1978. for $M \geq 3$; from historical catalog (Meremonte and Rogers. 1987). Circle of radius 100 km is centered on Yucca Mountain. Figures 1-54b and 1-54c clarify locations of seismicity $M \geq 4$ and $M \geq 5$. respectively.

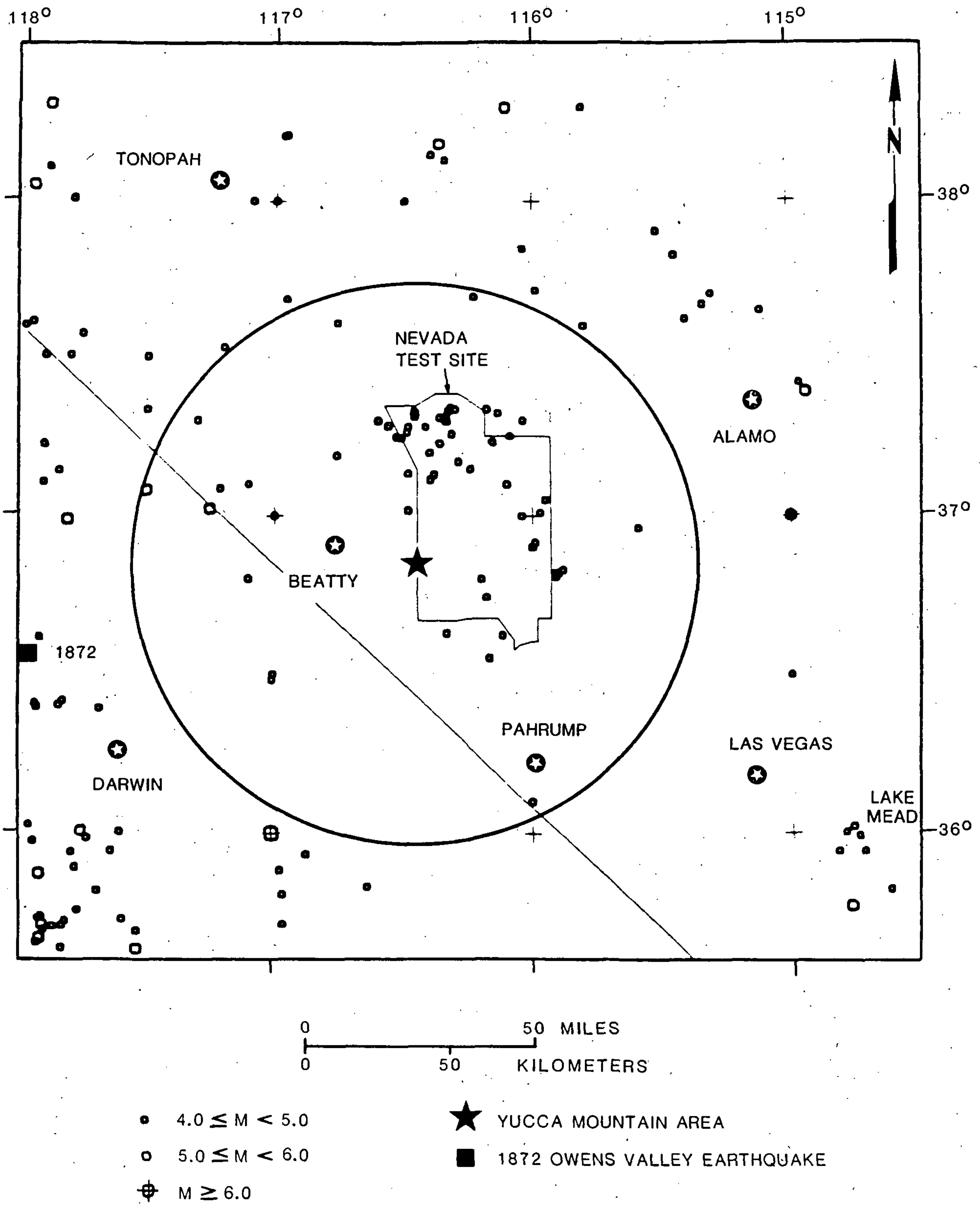

Figure 1-54b. Historical seismicity of the southern Great Basin, 1868 through 1978, for M ≥ 4; from historical catalog (Meremonte and Rogers, 1987). Circle of radius 100 km is centered on Yucca Mountain.

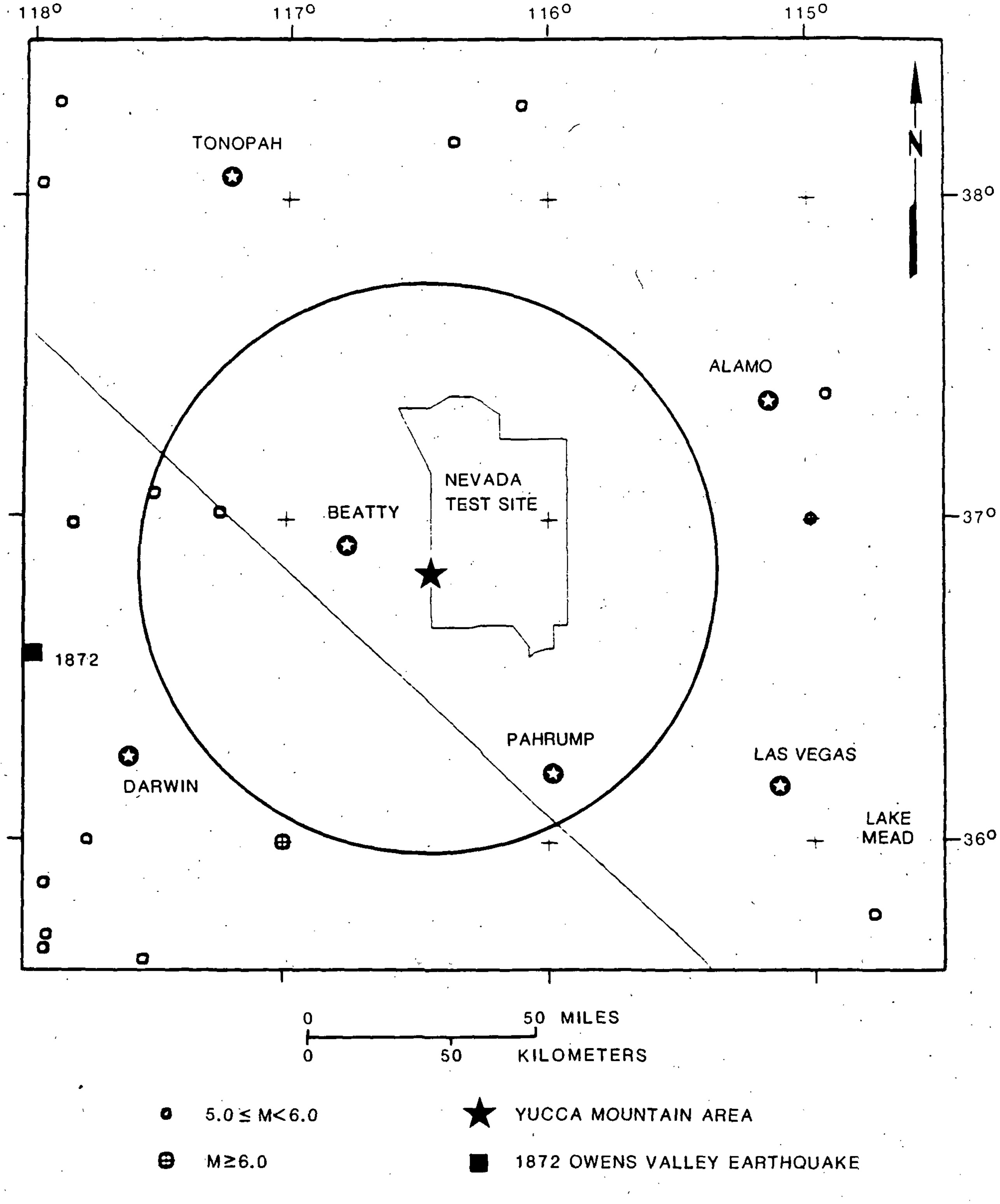

Figure 1-54c. Historical seismicity of the southern Great Basin, 1868 through 1978, for M $\geq$ 5; from historical catalog (Meremonte and Rogers, 1987). Circle of radius 100 km is centered on Yucca Mountain.

In general, the accuracy of hypocenter parameters, magnitude estimates, and completeness of the catalog improves markedly for data acquired after August 1978. The SGBSN locations (Figure 1-53) have estimated modal standard errors of 0.5 km in the horizontal plane and 1.0 km in depth (Rogers et al., 1983). For the historical catalog, Rogers et al. (1977a) estimate errors of 7 km or more for older instrumental locations and errors of 50 km or more for pre-instrumental historical earthquakes, especially those in sparsely populated areas. Fortunately, major historical earthquakes ($M \geq 6.5$) frequently create large fault offsets, which define the general earthquake location; the 1872 Owens Valley shock is a good example of such an earthquake. The depths of most older instrumentally located earthquakes could not be calculated, because of the generally inadequate distribution of seismograph stations in the southern Great Basin before 1970.

Estimates of uncertainty in magnitude determination range from 0.15 magnitude unit for small earthquakes located by the SGBSN to 0.5 magnitude unit for some older noninstrumental earthquakes. In addition, magnitudes reported by the California Institute of Technology for southern Great Basin events may be biased upward by 0.8 magnitude unit (Rogers et al., 1987). Magnitudes in the historical catalog have been converted to Richter magnitude, M, for ease of comparison; earthquake magnitudes in the SGBSN catalog (Rogers et al., 1983, 1987) are local magnitudes M_L computed from coda durations by using calibration constants determined specifically for the southern Great Basin (Rogers et al., 1983, 1987).

Errors in magnitude estimates can arise from errors in measurement of peak amplitude and period or of coda durations and from uncertainties associated with the calibration curve. The need to convert from one magnitude type to another or the need to convert some physical phenomenon (such as fault length or highest intensity) into an equivalent magnitude creates another source of magnitude uncertainty. The two earthquake catalogs used in this report span over eight magnitude units, from the smallest microearthquakes occurring in the vicinity of Yucca Mountain to the Owens Valley earthquake of 1872. Four magnitude scales have been used: coda duration magnitude M_d, local magnitude M_L, body-wave magnitude m_b, and surface-wave magnitude m_s. In the past, all magnitude scales were presumed to be calibrated so as to be compatible with Richter magnitude, M, as used in southern California. However, recent research (Bakun and Joyner, 1984; Hutton and Boore, 1985; Rogerset al., 1987) provides evidence that past techniques for computing magnitude may have systematically overestimated magnitude by 0.8 units. Continuing work on this problem could result in future revision of SGBSN magnitudes (section 8.3.1.17). This work is important in accurately determining earthquake recurrence statistics used to estimate the seismic hazard at the site. In addition, formulas exist that relate fault length and maximum Modified Mercalli (MM) intensity to M. Richter (1958) and Lee et al. (1972) provide a complete discussion of the magnitude scales and the MM scale.

The highest-quality focal mechanisms published in the SGBSN bulletins (Rogers et al., 1983, 1987) have estimated errors in nodal plane orientation of about 10 degrees. Uncertainties in nodal plane orientations arise from several sources, including (1) distribution of first motions and ratios of shear and pressure wave amplitudes on the focal sphere and (2) the extent of departures of the crustal model from the actual velocity structure. Other effects include errors due to depth uncertainty and phase conversions at shallow crustal interfaces (Rogers et al., 1987). Uncertainties in directions of principal stress axes determined from earthquake focal mechanisms are somewhat more difficult to evaluate, because theoretically the axes of minimum and maximum principal stress may be located anywhere within the dihedrals defined by the nodal planes. In the method used by Rogers et al. (1987), the dihedrals from separate focal mechanisms are combined to yield average principal stress axis directions that are within a few degrees of principal stress directions determined by independent methods.

The completeness of the seismicity data for the region including the southern great basin has been evaluated in several studies (Table 1-9).

To estimate the magnitude level at which the catalog fails to completely describe the seismicity of the area covered, it is customary to use an earthquake recurrence model (Richter, 1958) of the form

$$\log N = a - bM, \qquad (1\text{-}1)$$

where N is either an incremental number of events having magnitude M or a cumulative number of events (N_c) having magnitude M or greater and a and b are constants. When the model is fitted to actual data, a and b are constant over a range of magnitude appropriate to the individual catalog (and, therefore, to the region and time interval). When N is large, a straight line generally fits the plotted data quite well down to some magnitude value where the data points consistently fall below the line for smaller magnitudes, which indicates the level at which earthquakes are incompletely reported. Earthquake catalogs are inevitably incomplete; no catalog includes

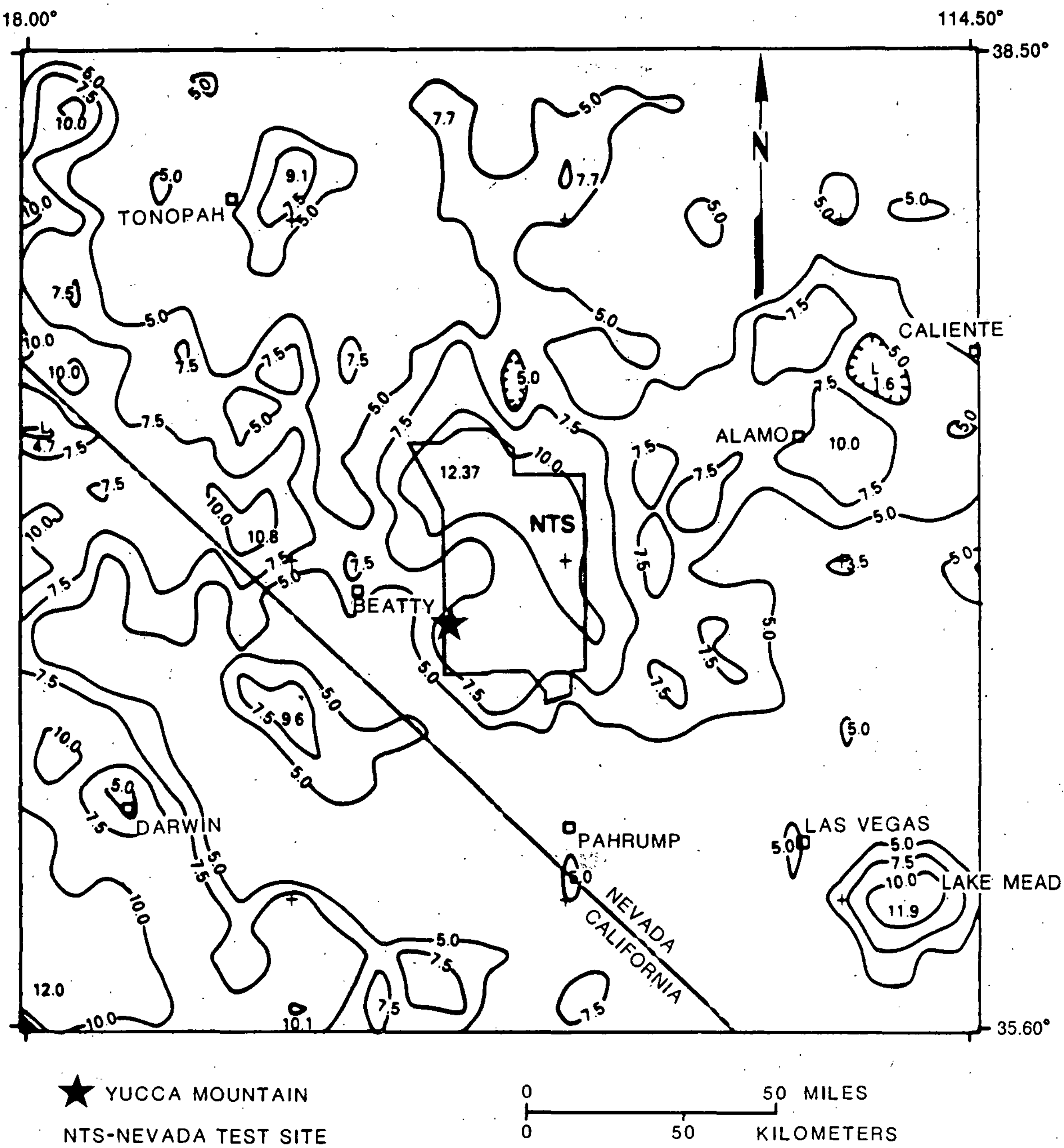

Figure 1-55. Energy release map of southern Great Basin earthquakes, 1868 through 1978, of all magnitudes from historical catalog. Contours represent log E, for E in joules per square kilometer. Highs in the nortnern Nevada Test Site and southeast of Las Vegas are presumed to represent earthquakes induced by nuclear explosions and impounding of Lake Mead, respectively. Modified from Meremonte and Rogers (1987).

DECEMBER 1988

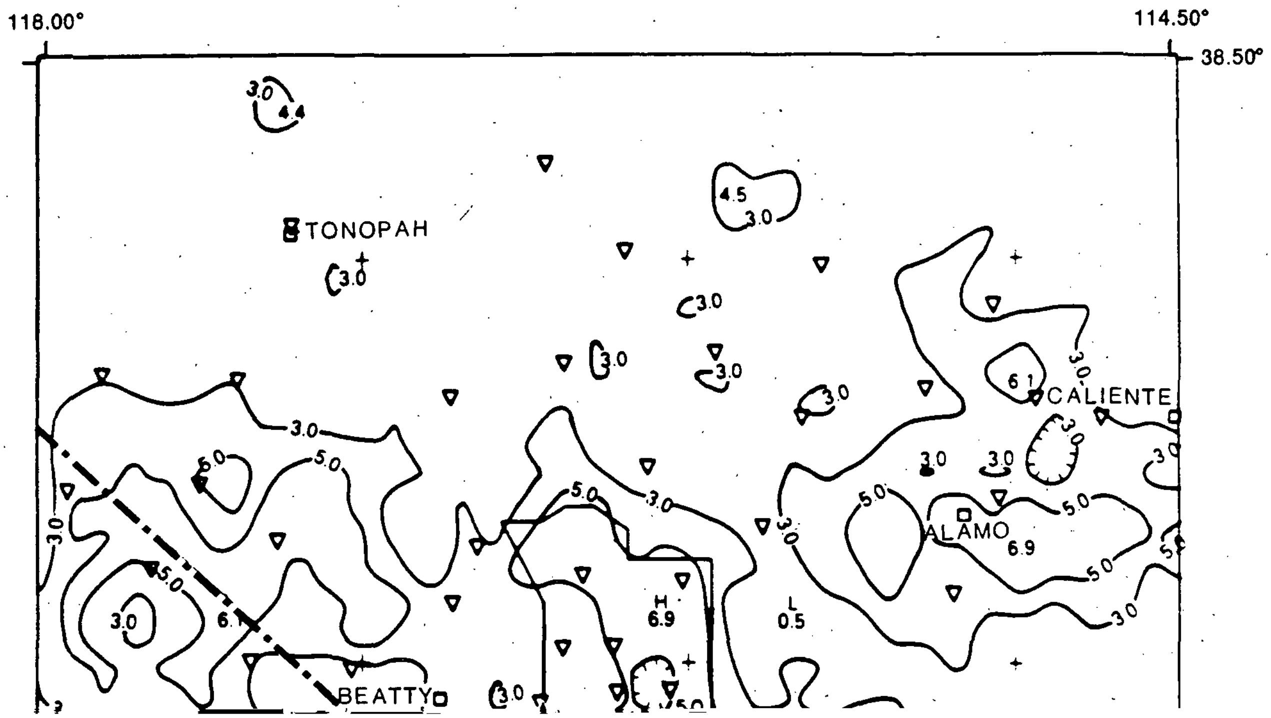

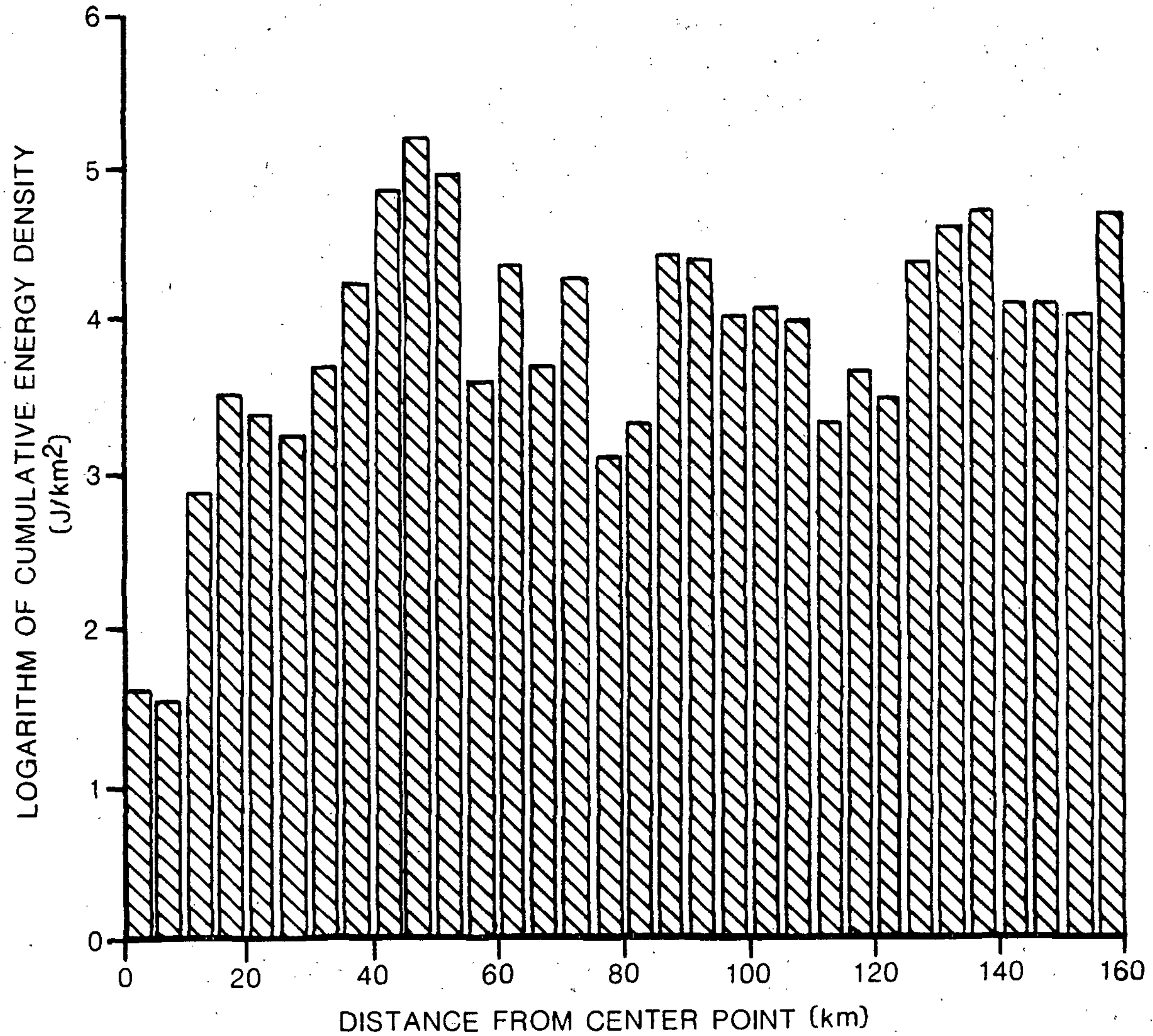

Figure 1-57. Distribution of cumulative energy release per unit surface area as a function of distance from central Yucca Mountain, August 1, 1978 through December 31, 1983. Modified from Rogers et al. (1987).

Table 1-9. Completeness of earthquake record of southern Great Basin

Time interval	Region[a]	M[b]	References
1845-current	SGB	7-8	Rogers et al. (1977a)
1915-current	SGB	6-7	Rogers et al. (1977a)
1925-current	SGB	5-6	Rogers et al. (1977a)
1932-current	SGB	4-5	Greensfelder et al. (1980); Willis et al. (1974)
1935-current	SGB	4-5	Rogers et al. (1977a)
1978-current	SGB	1.0	Rogers et al. (1987)
1981-current	Yucca Mtn.	0.0	Rogers et al. (1987)

[a]SGB = southern Great Basin.

[b]M, magnitude above which earthquake record is complete. Range of magnitude values represents combined effects of variability in location and

(the year of installation of the SGBSN) and includes the description of the seismic geography, estimates of energy release, and recurrence statistics. The second section contains details of the seismicity of the southern Great Basin as revealed by SGBSN seismic data for the period August 1978 through December 1983. This last section includes the results of focal mechanism and stress field determinations which are used in associating seismicity with specific geologic structures (Section 1.4.1.2).

1.4.1.1.1 Prenetwork seismicity (1868 through 1978)

The regional seismicity (Figure 1-51) is dominated by high levels of seismic activity in southern California and western Nevada. The largest historical shocks ($m \geq 6.5$) within 400 km of yucca mountain are labeled on the figure and listed in Table 1-10. Of these large earthquakes, the nearest to Yucca Mountain was the 1872 Owens Valley shock, about 150 km west of the proposed repository. The epicenter density is sparse in the East-West seismic belt except for clusters of aftershocks near weapons testing areas on the NTS (potential catalog contamination), swarms of induced earthquakes at Lake Mead (potential catalog contamination), and a cluster of numerous earthquakes including an M = 6.1 shock (von Hake and Cloud, 1968; Beck, 1970) at Clover Mountain, near the Nevada-Utah border. Large quiescent areas are apparent in the southern Great Basin on the map of the historical catalog (Figure 1-51) and on the regional map (Figure 1-52). Noteworthy areas of quiescence are the southern part of the Death Valley-Furnace Creek fault zone, the Las Vegas shear zone, and most importantly, the vicinity of Yucca Mountain.

Figures 1-54a, 1-54b, and 1-54c show the seismicity of the southern Great Basin from the historical catalog (Meremonte and Rogers, 1987) for $M \geq \geq 3$, $M \geq 4$, and $M \geq 5$, respectively. All earthquakes $M \geq 3$ or $I_o > IV$ are listed in the Meremonte and Rogers (1987) catalog. While Figure 1-54a shows hundreds of earthquakes of $M \geq 3$, it is evident in Figure 1-54c that few historical earthquakes were large enough or near enough to Yucca Mountain to produce strong ground motion. Table 1-10 lists significant historical earthquakes in the southern Great Basin, including major shocks ($M \geq 6.5$) within 400 km of Yucca Mountain, moderate-size shocks ($M \geq 4.0$) within 100 km of Yucca Mountain, and other noteworthy earthquakes of $M \geq 4.0$ more than 100 km from Yucca Mountain. Rogers et al. (1977a) have estimated that mean peak horizontal accelerations from historical earthquakes probably did not exceed 0.1g at a central location at NTS, about 20 km east of Yucca Mountain.

The geographic distribution of seismic activity is shown on a contour map of seismic energy release (Figure 1-55). The Nevada-California seismic belt shows clearly along the western edge of the map and the East-West seismic belt is quite apparent, encompassing the entire NTS. Locally high energy contours emphasize the occurrence of aftershocks at Pahute Mesa and Yucca Flat resulting from weapons testing, and of reservoir-induced activity at Lake Mead (Rogers and Lee, 1976). Other places of historical energy release are the Pahranagat shear zone, at Sarcobatus Flats, and near Tonopah.

Table 1-10. Significant earthquakes in or near the southern Great Basin[a] (page 1 of 2)

Date	Name or region	Location	M[b]	Intensity (MM)[c]	Distance (km)
		EARTHQUAKES OF M ≥ 6.5 WITHIN 400 km OF YUCCA MOUNTAIN SITE			
9 Jan 1857	Fort Tejon	35.0°N 119.0°W[d]	8 1/4	IX[e]	300
26 Mar 1872	Owens Valley	36.5°N 118.0°W[d]	8 1/4[f]	XI[g]	150
21 Dec 1932	Cedar Mountain	38.7°N 117.8°W[g]	7.3[g]	X[g]	202
21 Jul 1952	Kern County	35.0°N 119.0°W[h]	7.7[h]	XI[h]	267
6 Jul 1954	Rainbow Mountain	39.4°N 118.5°W[g]	6.8[i]	IX[k]	331
24 Aug 1954	Rainbow Mountain	39.4°N 118.5°W[g]	6.8[i]	VIII[i]	331
16 Dec 1954	Fairview Peak	39.3°N 118.2°W[g]	7.2[g]	X[h]	276
16 Dec 1954	Dixie Valley	39.8°N 118.1°W[j]	6.9[i]	XI	323
		SELECTED EARTHQUAKES OF M ≥ 4 WITHIN 100 km OF YUCCA MOUNTAIN SITE			
28 Mar 1934	Gold Flat	37.3°N 116.6°W	4.5	V	52
13 Jun 1939	Northern Death Valley	37.02°N 117.25°W	5.0		73
14 Jun 1945	Last Chance Range	37.08°N 117.50°W	5.0	VI	96
30 Aug 1948	Amargosa Desert	36.550°N 116.167°W	4.0	IV	42
13 Jan 1950	Dome Mountain	37.017°N 116.483°W	4.1		19
16 Jun 1951	Eleana Range	37.085°N 117.213°W	4.5	V	72
28 Jan 1959	Skull Mountain	36.8°N 116.2°W	4.0	IV	23
27 Mar 1961	Skull Mountain	36.743°N 116.178°W	4.4	V	28
6 Jan 1969	Pahute Mesa	37.245°N 116.508°W	4.5		44
10 Jan 1969	Pahute Mesa	37.134°N 116.482°W	4.6		32
5 Aug 1971	Massachusetts Mountain	36.916°N 115.990°W	4.5	IV	42
15 Feb 1973	Ranger Mountains	36.810°N 115.910°W	4.0	III	49
12 Jun 1973	Pahute Mesa	37.230°N 116.360°W	4.5		43
28 Oct 1975	Timber Mountain	37.115°N 116.398°W	4.0	V	30
8 Jan 1976	Pahute Mesa	37.310°N 116.360°W	4.6	V	52
7 Feb 1976	Pahute Mesa	37.309°N 116.335°W	4.8	V	52

Table 1-10. Significant earthquakes in or near the southern Great Basin[a] (page 2 of 2)

Date	Name or region	Location	M[b]	Intensity (MM)[c]	Distance (km)
SELECTED EARTHQUAKES OF M ≥ 4 WITHIN 100 km OF YUCCA MOUNTAIN SITE (continued)					
7 Jun 1976	Specter Range	36.630°N 116.330°W	4.1	V	26
7 Jun 1976	Specter Range	36.629°N 116.332°W	4.1	V	26
16 Aug 1977	Ranger Mountains	37.052°N 115.949°W	4.0	V	51
OTHER SELECTED [NOTABLE] EARTHQUAKES OF M < 6.5 WITHIN 400 km OF YUCCA MOUNTAIN SITE					
4 Nov 1908	Death Valley	36.0°N 117.0°W	6-6.5	VII-VIII	106
30 Jan 1934	Excelsior Mountain	38.3°N 118.4°W[k]	6.3[k]	VIII[k]	230
6 Jan 1960	Kawich Peak	38.0°N 116.5°W	4.9	VI	128
1966-1967	Clover Mountain series	37.4°N 114.2°W[k]	3.5-6.1	VI[k]	210
8 Dec 1971	Northern Pahroc Range	37.645°N 115.109°W	4.7	VI	148
9 Feb 1971	San Fernando	34.41°N 118.40°W[k]	6.3[k]	IX[k]	330

[a]Meremonte and Rogers (1987).
[b]M = Richter magnitude.
[c]MM = Modified Mercalli scale.
[d]Coffman and von Hake (1973).
[e]Agnew and Sieh (1978).
[f]Oakeshott et al. (1972).
[g]Slemmons et al. (1965).
[h]Richter (1958).
[i]Ryall and Priestley (1975).
[j]Romney (1957).
[k]Askew and Algermissen (1983).

1.4.1.1.2 Postnetwork seismicity (1978 through 1985)

The seismicity of the southern Great Basin from August 1978 through December 1983 is shown on Figure 1-53. Over 2,800 epicenters derived from data recorded by the SGBSN and 30 focal mechanisms are plotted in the figure. Most features of the seismic geography discerned from the historical catalog appear in Figure 1-53; these include a broad, diffuse seismic belt crossing the area from east to west; substantial activity west of the Death Valley-Furnace Creek fault zone; clusters of activity at Sarcobatus Flats and at the Pahranagat fault zone; and numerous epicenters of induced seismicity near areas of weapons testing at NTS. What distinguishes the SGBSN seismicity map from the historical seismicity map is the amount of detail visible, a consequence of more than an order of magnitude improvement in location capability and reduction in the overall detection threshold by over two magnitude units. Nevertheless, earthquakes are not clearly associated with faults, on Figure 1-53 (Section 1.4.1.2).

The energy release map for the SGBSN catalog (Figure 1-56, Section 1.4.1) is similar to the energy release map for the historical catalog (Figure 1-55, Section 1.4.1) in showing the presence of the East-West seismic belt and part of the Nevada-California seismic belt. The general reduction of energy release toward the edges of the map is a consequence of the reduced capability of the network to detect and accurately locate earthquakes outside the network. Several highs from weapons tests in the northern and northwestern NTS and other highs at Lake Mead, Pahranagat shear zone, and Sarcobatus Flat are noteworthy, matching features seen on the historical energy release map (Figure 1-55). Other highs occur at Indian Springs Valley, Pahroc Valley, and the Coso volcanic field in California.

Focal depths of well-located southern Great Basin earthquakes range from -1 km (1 km above sea level) to 17 km (Rogers et al., 1987). The depth distribution (Figure 1-58) is bimodal, broadly peaking at about zero to 2 km and 5 to 8 km, with a pronounced minimum at about 3.5 to 4 km. The ratio of shallow to deep events is largest for the eastern part of the region. Rogers et al. (1987) have performed an extensive series of computational experiments that show that the peaks in the distribution are not artifacts of data processing, hypocenter location algorithm, velocity model used, or distribution of depth errors, although the peaks and the minimum shift slightly for some velocity models. The underlying cause of the bimodal depth distribution is not yet understood, although it does not appear to be related to nuclear testing (Rogers et al., 1987) because the minimum is evident in the seismicity outside the zone of influence of nuclear testing. Extensive tests, conducted to study the effects of the variation-of-velocity-model on hypocenters in Rogers et al. (1987), were inconclusive and do not rule out the possibility that the bimodal depth distribution is a model-dependent feature. As structural models develop for the southern Great Basin, new velocity models will be developed and evaluated with respect to the depth distribution of earthquakes (Activity 8.3.1.17.4.1.2)

Thirty focal mechanisms are now available from data of the SGBSN (Rogers et al., 1987), extending the set of 11 focal mechanisms determined earlier (Rogers et al., 1983). With only five exceptions, the focal mechanisms demonstrate that strike-slip faulting is predominant in the southern Great

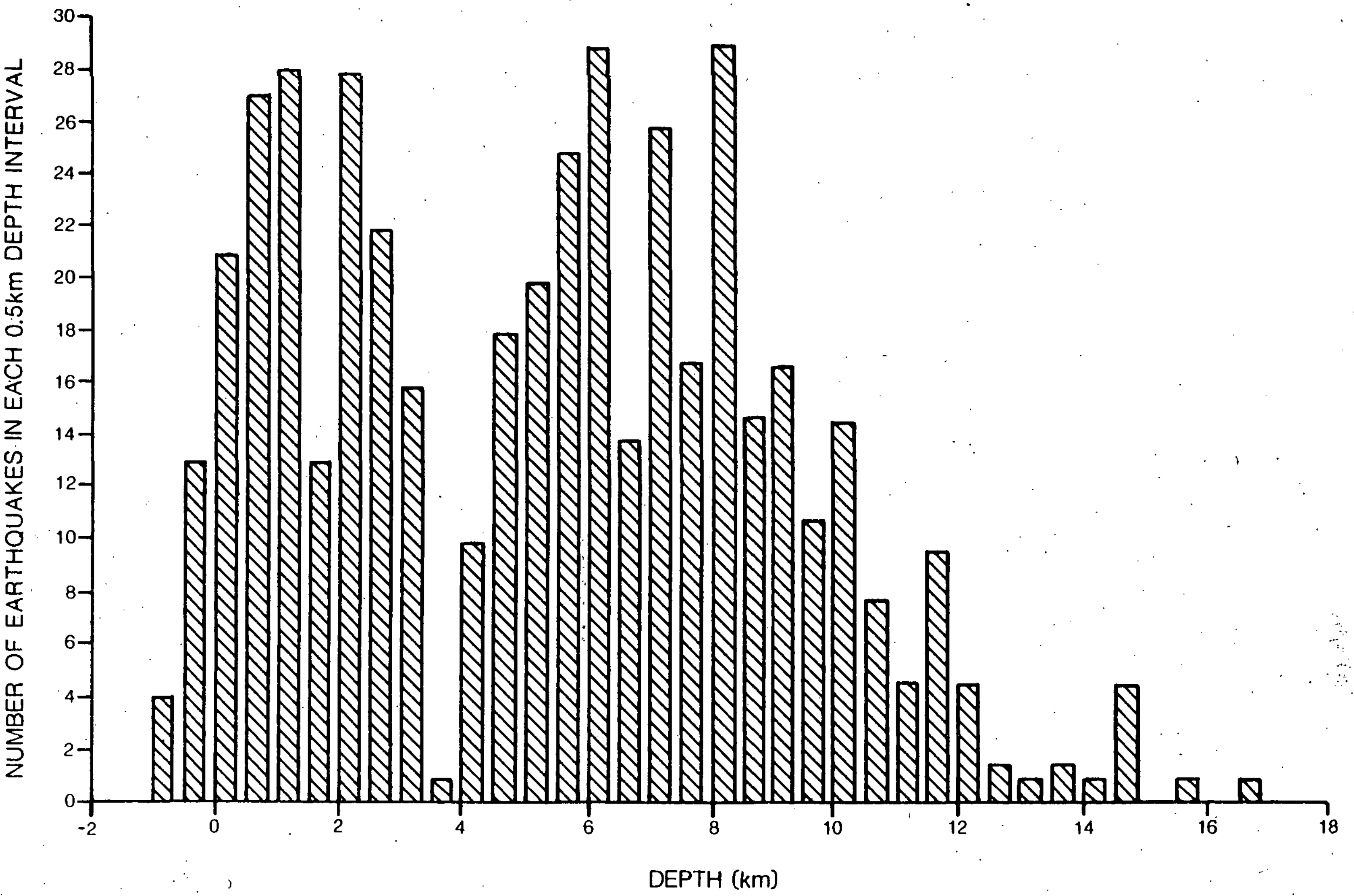

Figure 1-58. Distribution of focal depths of well-located Southern Great Basin Seismic Network (SGBSN) earthquakes, 1982 through 1983. Negative depths represent computed locations above sea level. Modified from Rogers et al. (1987).

Basin; the exceptions are five normal faulting mechanisms at three locations: Mt. Dundee, Scotty's Junction, and Thirsty Canyon near Pahute Mesa. The mechanisms are discussed further in Section 1.4.1.2.

Rogers et al. (1987) have used the focal mechanisms to extract the orientation of principal stresses for the region. The maximum compressive stress axis (s_1) plunges gently N.20°E. to N.35°E. and the minimum compressive stress axis (s_3) plunges gently N.50°W. to N.70°W. This result is consistent with directions of principal stress determined from hydraulic fracturing experiments at Yucca Mountain (Stock et al., 1985). Rogers et al. (1987) have demonstrated that if the shallow and deep focal mechanisms are separated on the basis of depth, the stress orientations are similar.

As the SGBSN continues to monitor the seismicity of the southern Great Basin region the seismicity catalog and the research data base will continue to expand (Section 8.3.1.17). Therefore, it is likely that new patterns of activity (spatial and temporal) will become evident in areas that previously had been quiescent. If a large earthquake were to occur in the region, the SGBSN would be positioned to monitor the aftershock activity, as well as provide potentially useful pre-mainshock information. Additional focal mechanisms and stress axis determinations will add more fault orientation and stress field information and could provide evidence of variations of stress field orientation across the region. The expanding data base of digital seismograms will be a valuable resource for specialized source mechanism studies.

1.4.1.1.3 Summary

The pattern of regional seismicity (Figures 1-51 and 1-52, Section 1.4.1), as defined by historical epicenters within 400 km of Yucca Mountain, consists of the north-south-trending Nevada-California seismic belt, the southern end of the Intermountain seismic belt in southwestern Utah, and the diffuse East-West seismic belt encompassing the NTS. Six major historical earthquakes, magnitude $M \geq 6.5$, have occurred in the Nevada-California seismic belt and two (1857, 1952) have occurred on or near the San Andreas fault. The nearest major earthquake (1872 Owens Valley) was about 150 km west of Yucca Mountain. Yucca Mountain is located in a large, historically quiescent area that includes the southwest quadrant of the NTS and the eastern Mojave Desert.

The pattern of local seismicity (Figure 1-53, Section 1.4.1), as defined by hypocenters within 150 km of Yucca Mountain and determined by a 53-station seismic network, is a widespread but diffuse background corresponding principally to the East-West seismic belt, punctuated by clusters of intense activ-

The direction of minimum principal stress, determined from 29 focal mechanisms, is approximately N.60°W.; intermediate and maximum principal stresses are approximately equal in magnitude. This stress configuration favors right-lateral strike-slip on north-striking faults, normal slip on northeast-striking faults, and left-lateral strike-slip on east-northeast-striking faults.

1.4.1.2 Relationship of seismicity to geologic or tectonic characteristics of the candidate area

This section will summarize available information on the correlation of [redacted]

(1977a) also considered certain faults as active (seismogenic sources) (Table 1-11), primarily based on the presence of known Quaternary offsets. Plans to assess the age, amount, and nature of offset, and the recurrence history of faults that may have Quaternary offset in and near the controlled area (Table 1-8, Section 1.3) are discussed in Section 8.3.1.17.

Greensfelder et al. (1980) also investigated the relationship of seismicity to structure in evaluating the probability of earthquake ground motion in Las Vegas, Nevada. It was observed that the historical seismicity pattern is not an adequate representation of long term seismicity when compared to the distribution of Quaternary faults. The primary reason for this is the short record of instrumentally located seismicity. Some apparently low seismicity regions, such as southern Nevada, manifest late Quaternary faulting, which indicates the occasional occurrence of moderate to large earthquakes over the past 50,000 yr (Greensfelder et al., 1980). These observations indicate the second difficulty in relating seismicity to structure--the brevity of the historic earthquake data as compared with the apparent frequency of occurrence of moderate to large earthquakes. Based on stress kinematics and the intensity of late Quaternary faulting, Greensfelder et al. (1980) defined five tectonic subprovinces within the southern Basin and Range province.

Like Greensfelder et al. (1980), Algermissen et al. (1982) based the seismic source zones primarily on the age of latest fault displacement. Because the purpose of this work was to prepare regional seismic hazard computations, the correlation of specific earthquakes with individual faults was not attempted.

URS/Blume (1986) has also presented seismogenic zonation for the Yucca Mountain site region (Figure 1-59). Zonation was defined based on data using both historical seismicity and Pliocene to Holocene fault patterns. The term seismogenic zonation rather than seismotectonic zonation is used because individual faults were not identified as earthquake sources (URS/Blume, 1986). The two zones closest to the Yucca Mountain site were identified as the Northern Great Basin (NGB), which includes the site, and the southern Nevada seismogenic zone (SNSZ). The SNSZ is characterized by a well-documented concentration of historic seismicity, apparent concentration of late Quaternary normal faults, and an alignment of mapped left-lateral faults (URS/Blume, 1986).

In comparison, the NGB exhibits considerably less seismicity. As described by URS/Blume (1986) the delineation of source zonation boundaries is uncertain. Additional work to more accurately define zone boundaries that may be used to assess vibratory ground motion is identified in Section 8.3.1.17.

Recent work by Rogers et al. (1983), USGS (1984), and Rogers et al. (1987) has attempted to use earthquake locations and focal mechanisms to determine any relation to mapped surface faulting. As discussed by Rogers et al. (1983), and as shown in Figure 1-53, seismicity is widespread throughout the southern Great Basin, although there are areas of near quiescence. The principal pattern is one of widespread diffuse seismicity punctuated by

Table 1-11. Examples of deterministically computed mean peak accelerations at Yucca Mountain for earthquakes on potentially active faults (USGS, 1984) in or near the southern Great Basin[a]

Fault name	Distance from Yucca Mountain (km)	Length (km)	Magnitude	Acceleration (g)
Bare Mountain	14	17	6.8	0.4
Mine Mountain	20	10	6.6	0.3
Wahmonie	23	10	6.6	0.2
Beatty	24	17	6.8	0.2
Rock Valley #1	26	15	6.7	0.2
Rock Valley #2	31	10	6.6	0.2
Amargosa Valley	33	12	6.6	0.2
Carpetbag	38	12	6.6	0.1
Yucca and Boundary	40	38	7.1	0.2
Rock Valley #3	42	10	6.6	0.1
Keane Wonder	43	25	6.9	0.1
Furnace Creek	51	42	7.2	0.1
Death Valley--Fish Lake Valley	51	175	7.9	0.2
South Death Valley				
East side	51	120	7.6	0.2
West side	75	100	7.5	0.1
Kawich Valley	59	33	7.1	0.1
Pahrump	60	38	7.1	0.1
Emigrant Wash	63	20	6.9	0.08
Resting Spring	75	10	6.6	0.05
Ubehebe--Emigrant Wash	80	70	7.4	0.08
Stonewall Mountain	93	10	6.6	0.03
Panamint Valley				
East side	95	100	7.5	0.07
West side	104	40	7.2	0.04
Saline Valley	101	50	7.2	0.05
Sand Spring Valley	103	25	6.9	0.04
Sheep Range	113	35	7.1	0.03
Pahroc	130	32	7.1	0.03

[a]Magnitude and acceleration values determined using one representative attenuation curve (Schnabel and Seed, 1973) and one representative fault-length-magnitude relationship (Mark and Bonilla, 1977).

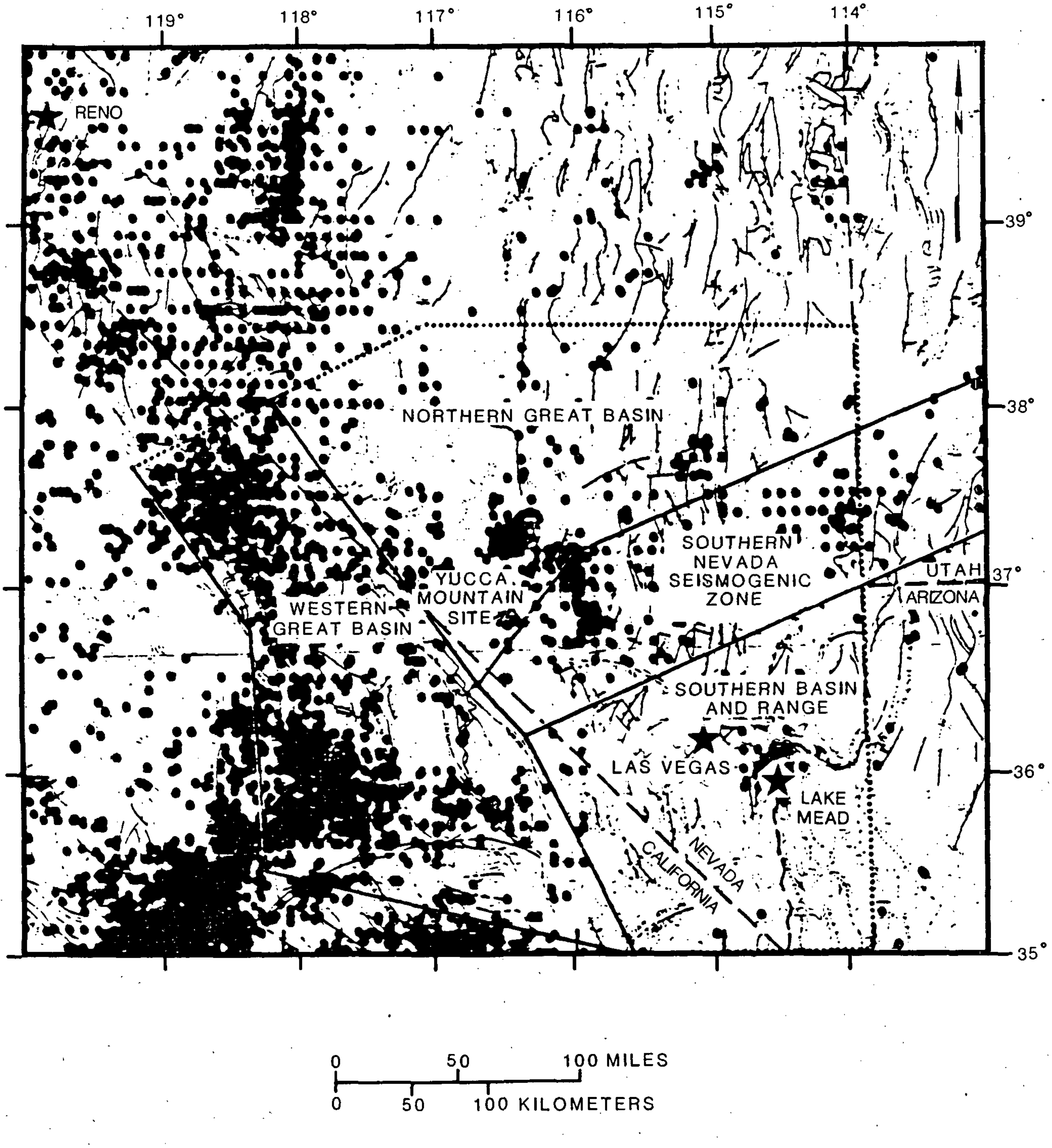

Figure 1-59. Seismogenic zone boundaries are shown by solid lines; limits of seismogenic zones as represented in earthquake hazard calculations are shown by dotted lines; black dots represent epicenters. The concentration of epicenters approximately 50 km north and east of the site represents underground nuclear explosion afterevent activity, rather than natural seismicity. Modified from URS/Blume (1986).

tight clusters of earthquakes. Based on earthquake locations and focal mechanisms, it is suggested that north to northeast-striking faults are more seismically active than faults of other orientations. Several examples are discussed below primarily for events within about 75 km of the site.

Figure 1-57 (Section 1.4.1) is a graph of cumulative energy release density (in J/km^2) as a function of epicentral distance from a center point on Yucca Mountain near the north end of the proposed repository (just south of drillhole USW G-1). Annuli of 5 km width were constructed about this center point. The energy density values were determined by summing the energies released by SGBSN earthquakes within each annulus and dividing by the area of the annulus. Normalized energy density values are listed in Table 1-12. Figure 1-57 shows the striking contrast in energy release across the region. Peaks are at ranges of 40 to 55 km, 85 to 95 km, and 125 to 140 km, while the innermost two annuli (zero to 10 km) display remarkably low energy densities. The circular area of radius 10 km around central Yucca Mountain is fully two to three orders of magnitude less active than the regional level and four orders of magnitude less active than the annuli spanning 40 to 55 km, which include areas of weapons testing. The energy

density results are correlated with the active areas in Table 1-12 and are discussed in the remainder of Section 1.4.1.2. The seismicity, focal mechanisms, Quaternary fault traces, and areas of exposed bedrock and alluvium are plotted on figures accompanying the discussion for each area shown on Figure 1-60. These active areas are discussed in order of increasing distance from the Yucca Mountain center point.

1.4.1.2.1 Vicinity of Yucca Mountain (zero through 10 km)

Yucca Mountain is in a seismically quiet area (Figures 1-51, 1-53 (Section 1.4.1) and 1-61) that has had only a few small scattered earthquakes. Only one earthquake has been detected and located by the SGBSN within 5 km of the Yucca Mountain center point (Rogers et al., 1987) between August 1, 1978, and December 31, 1983; the event, an M = 0.52 earthquake that occurred on April 13, 1981, had a range of 4.7 km. Another four earthquakes were located between 5 km and 10 km during the same time period. Depth of focus and dilatational first-motions at some stations preclude the possibility that the events were dynamite blasts from mining or geophysical experiments. As a result, the energy density within 10 km of the center point is scarcely more than background level, two to three orders of magnitude lower than the overall regional energy density level (Figure 1-56).

1.4.1.2.2 Vicinity of Dome Mountain (15 to 20 km)

Table 1-12. Normalized earthquake densities and energy release densities as a function of epicentral distance from the Yucca Mountain site[a]

Δ[b]	N[c]	n[d]	Log E[e]	Events or features within annular areas[f] discussed in the text
5	1	1.00	1.58	Yucca Mountain event on April 13, 1981
10	4	1.33	1.52	Yucca Mountain, Crater Flat
15	10	2.00	2.84	Dome Mountain, Bare Mountain, Jackass Flats
20	97	13.86	3.49	Skull Mountain, Little Skull Mountain, Jackass Flats
25	90	10.00	3.36	Striped Hills, Lookout Peak, Rock Valley
30	88	8.00	3.23	Rock Valley
35	97	7.46	3.68	Funeral Mountains, Rock Valley
40	154	10.27	4.24	Thirsty Canyon, Funeral Mountains, Mercury Valley, PM, YF
45	152	8.94	4.80	Frenchman Flat, Mercury Valley, Massachusetts Mountain, PM, YF
50	150	7.89	5.14	Sarcobatus Flat C, PM, YF
55	117	5.57	4.91	Sarcobatus Flat B, Ranger Mountains, PM
60	48	2.09	3.56	
65	74	2.96	4.28	Mesquite Flat
70	68	2.52	3.65	Indian Spring Valley
75	79	2.72	4.24	Sarcobatus Flat A (Scotty's Junction)
80	40	1.29	3.06	
85	51	1.55	3.26	
90	123	3.51	4.35	Sarcobatus Flat D, Gold Mountain, Ubehebe Crater
95	145	3.92	4.31	Mount Dunfee
100	59	1.51	3.96	
105	46	1.12	3.99	
110	63	1.47	3.90	
115	50	1.11	3.24	
120	77	1.64	3.58	
125	69	1.40	3.42	
130	76	1.49	4.28	
135	139	2.62	4.49	Pahranagat shear zone
140	118	2.15	4.64	
145	58	1.02	4.02	
150	41	0.69	4.00	
155	62	1.02	3.94	
160	143	2.27	4.57	

[a]Modified from Rogers et al. (1987).
[b]D, outer radius of annulus whose width is 5 km, in km.
[c]N, number of earthquakes located within annulus.
[d]n, earthquake density normalized to 5 km annulus, in number per unit area.
[e]E, cumulative energy release in annulus, in joules per square kilometer.
[f]Nuclear testing areas underlined: PM, Pahute Mesa; YF, Yucca Flat areas.

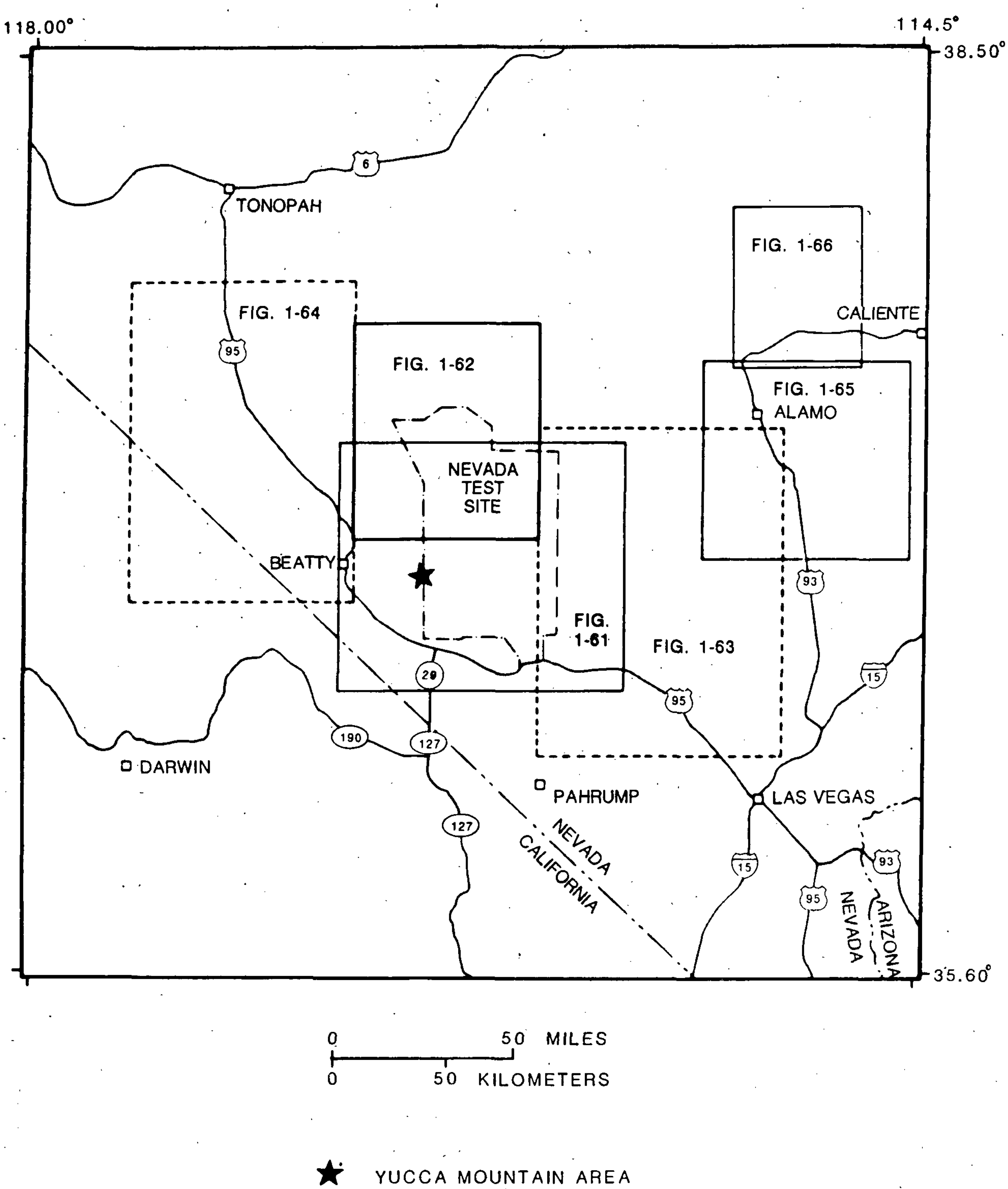

Figure 1-60. Index map of areas shown in Figures 1-61 (southern Nevada Test Site area), 1-62 (northern

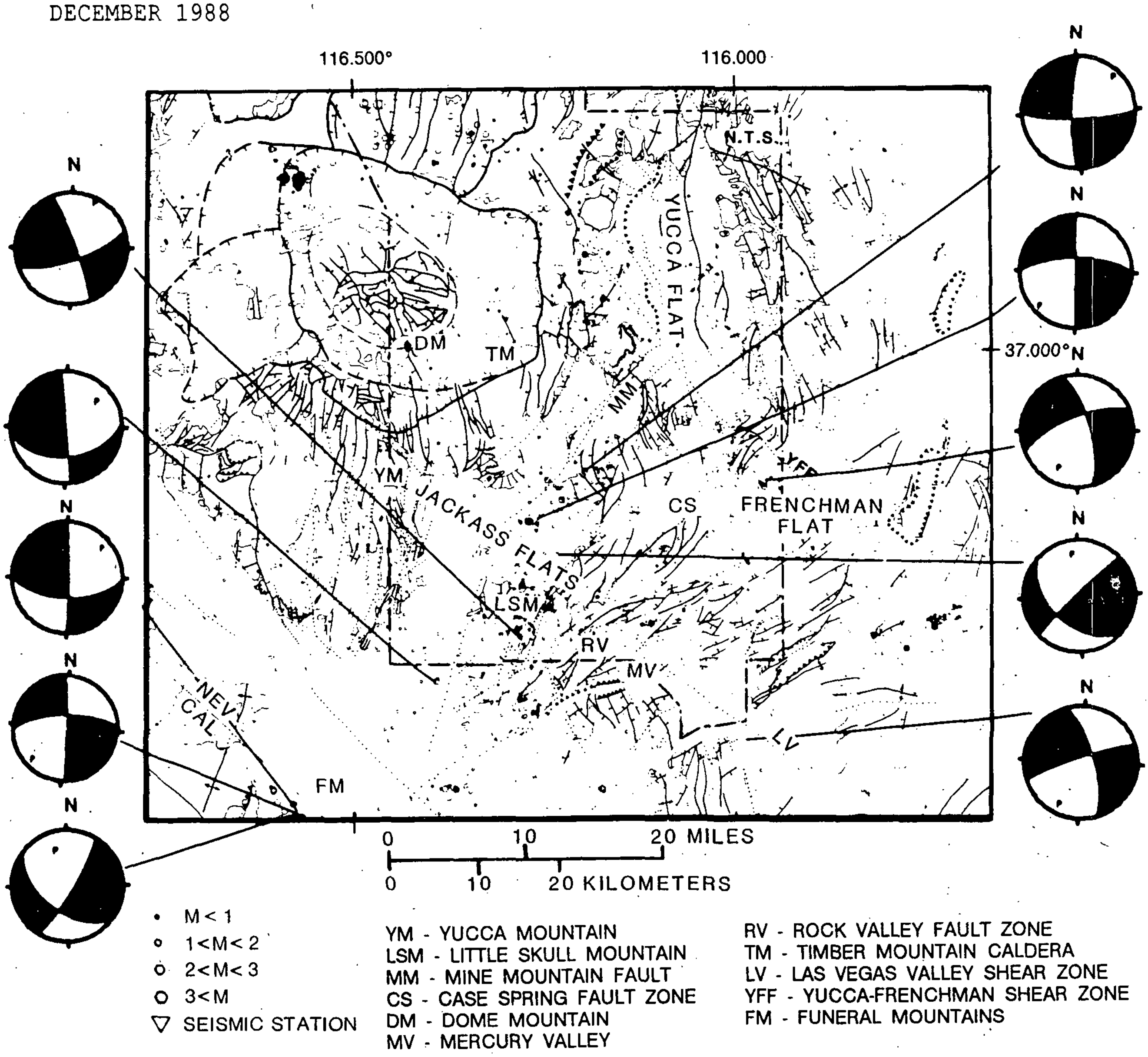

Figure 1-61. Seismicity and focal mechanisms for the southern Nevada Test Site area, August 1, 1978, through December 31, 1983. Modified from Rogers et al. (1987). In this figure, and in Figures 1-62 through 1-66, epicenter symbol size is scaled to magnitude, triangles designate seismograph stations of the Southern Great Basin Seismic Network, and focal-mechanism symbols are lower-hemisphere projections of the focal sphere where shaded and unshaded quadrants represent compressional and dilational first motions, respectively. Heavy solid lines represent mapped faults, dotted where inferred. Some epicenters in the Silent Canyon caldera (Figure 1-62) and Yucca Flat areas are presumed to represent earthquakes induced by nuclear testing.

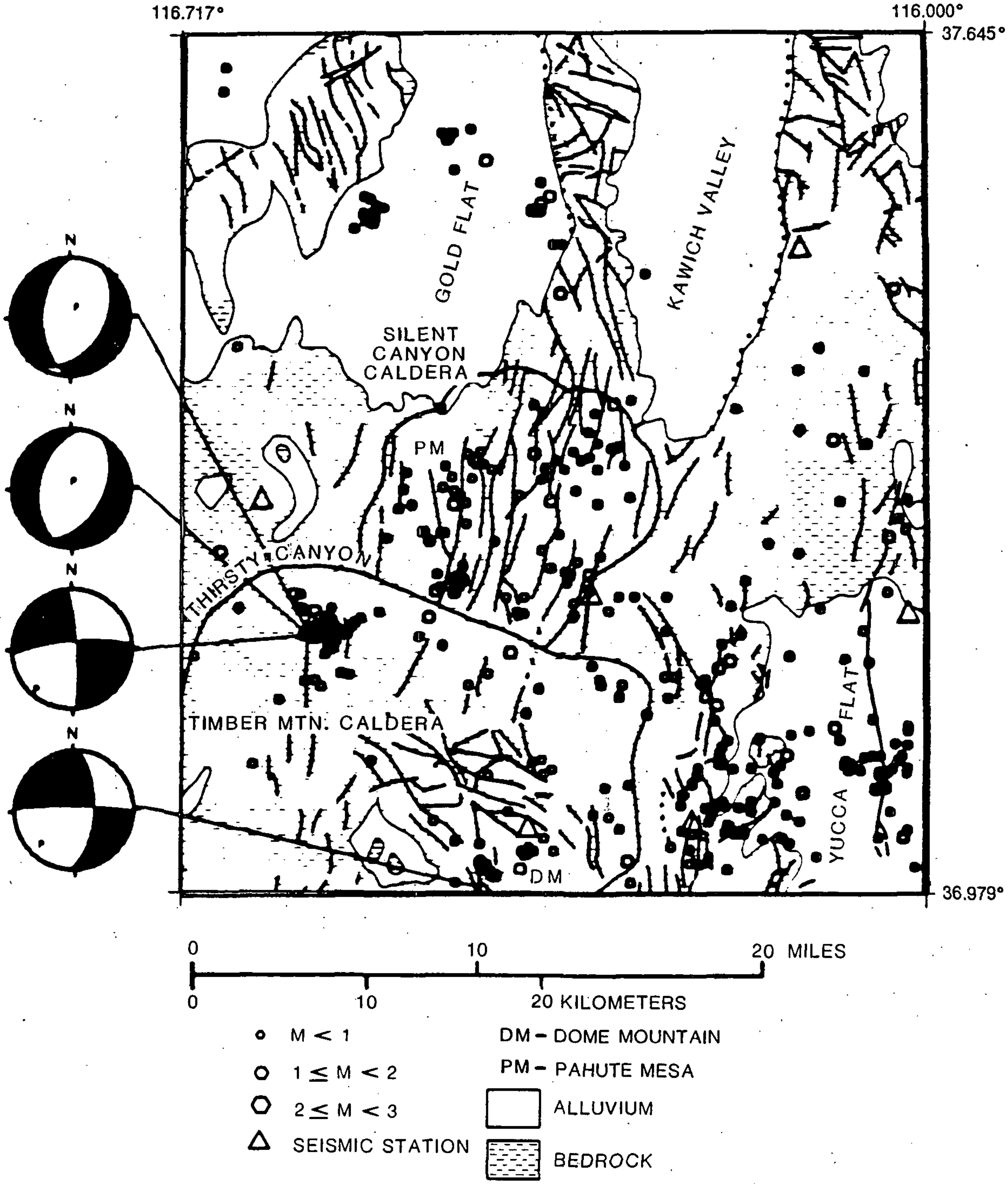

Figure 1-62. Seismicity and focal mechanisms for the northern Nevada Test Site area, August 1, 1978, through December 31, 1983 (Rogers et al., 1987). Figures defined as in Figure 1-61.

the basis of the focal mechanism, depth sections, and geology. The largest event was about 1 km from a mapped east-dipping, north-striking fault (Rogers et al., 1987).

1.4.1.2.3 Vicinity of Jackass Flats (15 to 20 km)

The seismicity of the Jackass Flats area, including Skull Mountain and Lookout Peak, is characterized by many very small earthquakes diffusely distributed over the area, with a few patterns showing weak northeast trends (Figure 1-62); the energy density is consequently low (Figure 1-56). A focal mechanism for an earthquake located near the Mine Mountain fault indicated strike-slip motion (Rogers et al., 1983). However, neither nodal plane was preferred on the basis of depth section plots or strike of the nearby Mine Mountain fault. Another event, located about 3 km west of Skull Mountain, had a northeast-striking nodal plane that agrees both in strike and dip with the majority of mapped Quaternary faults on Skull Mountain (McKay and Williams, 1964). The motion, therefore, would be left-lateral strike-slip on a northeast-striking fault (Rogers et al., 1987). A strike-slip focal mechanism determined for an earthquake located near Lookout Peak has been associated with right-lateral motion on one of several mapped north-striking faults in the area (Rogers et al., 1983).

1.4.1.2.4 Vicinity of Rock Valley and Mercury Valley (25 to 45 km)

Epicenter patterns in the Rock Valley and Mercury Valley area (Figure 1-61) show east-northeast trends, parallel to the Rock Valley fault system (Hinrichs, 1968; Rogers et al., 1987). The focal mechanism for a shallow focus M_L = 1.6 earthquake is consistent with left-lateral strike-slip on the Rock Valley fault; depth sections suggest that the fault planes are steeply dipping (Rogers et al., 1987).

1.4.1.2.5 Vicinity of Funeral Mountains (40 km)

An earthquake series occurred in January 1983 in the vicinity of the Funeral Mountains just west of the California-Nevada border (Figure 1-61). The series occurred as two distinct clusters of activity, a northern group trending approximately north to northwest, and a southern group of five deep events. The range of depths in the northern group is -1 to 12 km. Rogers et al. (1987) conclude that the northwesterly trending lineation is an artifact because none of three composite mechanisms yielded nodal planes that matched the depth profiles. Rogers et al. (1987) prefer north to northeasterly trending nodal planes as the fault planes and concluded that the seismogenic structures in this area are steeply dipping, en echelon, north to N.30°E.

1.4.1.2.6 Vicinity of Thirsty Canyon (40 km)

The Thirsty Canyon area near Pahute Mesa experienced two swarms of activity in 1979 and 1983. The 1979 series showed a north-striking lineation of epicenters that appeared to coincide with a nodal plane from a composite focal mechanism; these data are interpreted as right-lateral strike-slip faulting on a north-trending fault (Rogers et al., 1983). The 1983 hypocenters mapped as a nearly vertical zone of activity. Two composite focal mechanisms indicate normal faulting (Figure 1-62); the geologic evidence of a west dip on a nearby fault (O'Connor et al., 1966) signals a preference for the west-dipping nodal planes (Rogers et al., 1987). All three focal mechanisms are located close to each other, and it is clear that both normal and

strike-slip motions are possible on the same north-striking fault (or set of faults), the slip direction depending only on the dip of the fault. The same pattern of normal and strike-slip mechanisms was observed for aftershocks of the BENHAM nuclear event, located along a north-striking fault just 4 km east of the Thirsty Canyon earthquakes (Hamilton and Healy, 1969).

1.4.1.2.7 Vicinity of Las Vegas Valley (45 to 70 km)

Seismicity of the eastern NTS and the valleys and ranges north of the Las Vegas shear zone are shown on Figure 1-63. The Massachusetts Mountain earthquake of 1971 (Tendall, 1971; Fischer et al., 1972) and the 1973 Ranger Mountain earthquake occurred in this area. Focal mechanisms (Rogers et al., 1983) show strike-slip faulting for events at Frenchman Flat but association with specific faults was not unequivocal. Strike-slip mechanisms were also determined for the Massachusetts Mountain and Ranger Mountain earthquakes. Carr (1974) favored an east-northeast fault plane for the 1971 event but could not choose a preferred plane for the 1973 event. Epicenter alignments and north-striking nodal planes provide evidence that right-lateral strike-slip motion is occurring on north-striking faults in the Indian Springs Valley (Rogers et al., 1983).

1.4.1.2.8 Vicinity of Sarcobatus Flat (50 to 55 km, 75 km, 90 km)

Four earthquake series have been identified at Sarcobatus Flat (northwest of Yucca Mountain) by Rogers et al. (1983, 1987) since 1979 (Figure 1-64). The seismic activity in the clusters has fluctuated in both space and time; one cluster has shown a trend for activity to migrate to shallower depths and another shows migration of activity downdip (Rogers et al., 1987). Depth sections of the southernmost clusters (B and C) indicate very steeply dipping, northerly trending faults extending to about

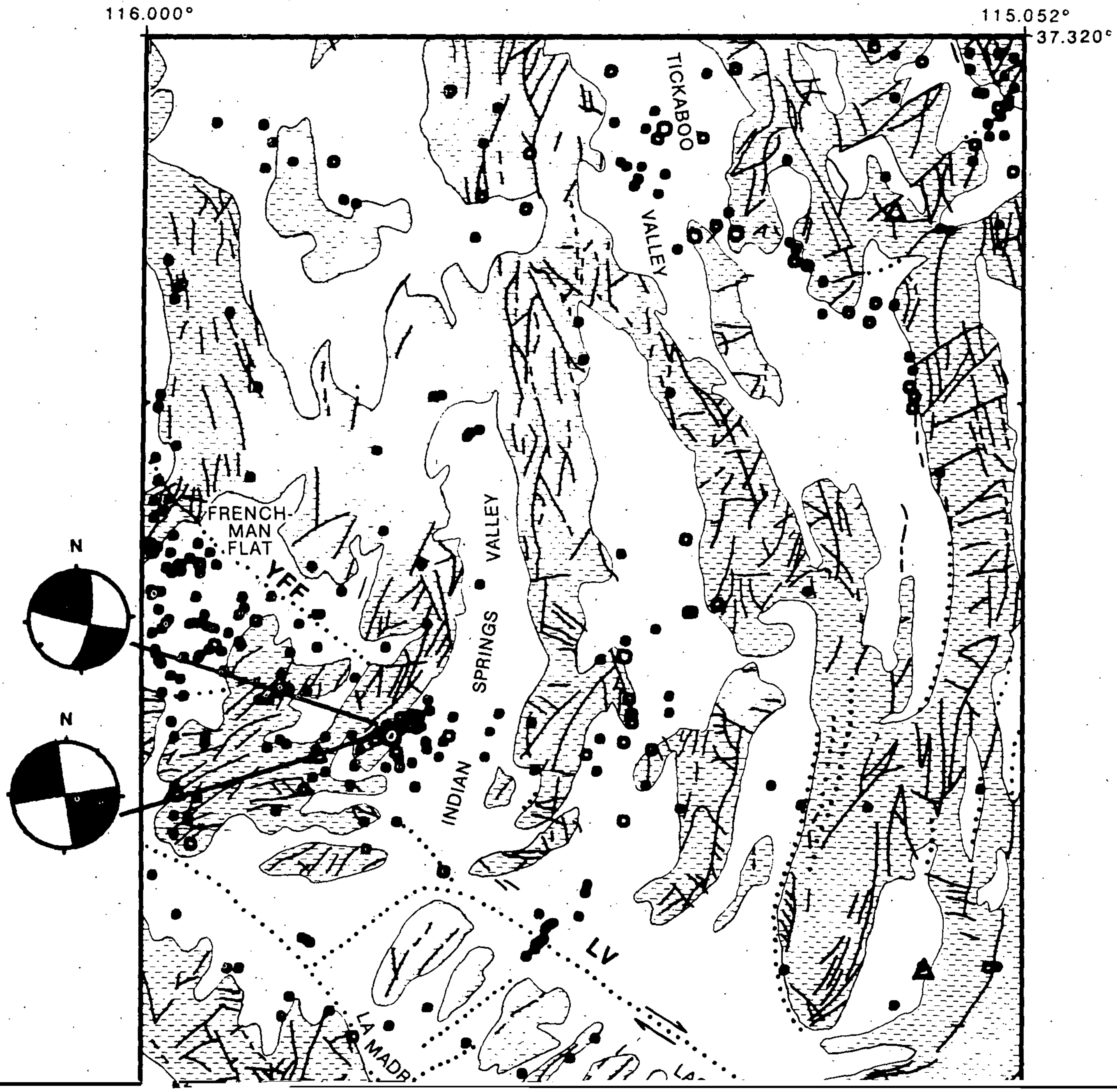
116.000°
115.052°
37.320°
TICKABOO
VALLEY
FRENCH-
MAN
FLAT
YFF
INDIAN
SPRINGS
VALLEY
LV
N
N

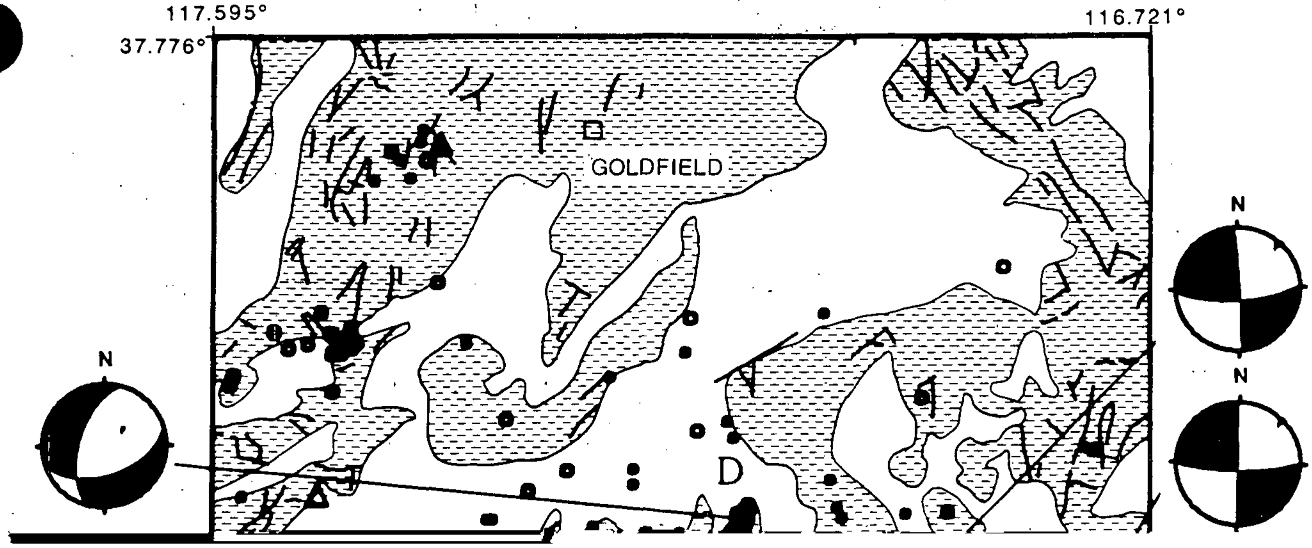
117.595°
116.721°
37.776°
GOLDFIELD
D
N
N
N

right-lateral strike-slip faulting on a north-trending fault (Rogers et al., 1983). However, normal faulting is indicated for two events in a cluster of events (D) 12 km northwest of Scotty's Junction. This cluster occurred on a group of small north-striking, west-dipping faults (Rogers et al., 1987).

1.4.1.2.9 Vicinity of Gold Mountain and Mt. Dunfee (90 to 95 km)

Two extensive earthquake series occurred near Gold Mountain and Mt. Dunfee, about 25 km west of Scotty's Junction and northwest of Yucca Mountain (Figure 1-64). A focal mechanism determined for an M = 4 event at Gold Mountain in January 1981 indicates strike slip with a small normal component. The epicenter lies in an area of east- to northeast-striking faults, which gives preference to left-lateral strike slip on the northeast-striking nodal plane (Rogers et al., 1983). A series of 40 earthquakes occurring in February 1983 forms an east-northeast-striking lineation near Mt. Dunfee (Figure 1-64) that crosses both easterly and northerly trending structural grain. Depth sections indicate that the activity is distributed along a steeply plunging tube of hypocenters and in an isolated cluster. No reliable focal mechanisms have been determined from these events; Rogers et al. (1987) suggest that the activity may result from the intersection of two faults. A composite focal mechanism from four events in the isolated cluster indicates oblique normal faulting; Rogers et al. (1987) prefer a northeast-striking nodal plane as the fault plane.

1.4.1.2.10 Vicinity of Pahranagat shear zone (130 to 135 km)

The Pahranagat shear zone (northeast of Yucca Mountain) is currently one of the most active areas in the southern Great Basin (Figure 1-65). The majority of epicenters appear to be associated with short north-striking fault segments within a major northeast-striking shear zone. The epicenter patterns and two focal mechanisms in the Pahranagat Range suggest that the mode of faulting is right-lateral strike slip on north-striking faults (Rogers et al., 1983).

1.4.1.2.11 Vicinity of Pahroc Valley and North Pahroc Range (150 to 175 km)

An earthquake series that began in July 1982 is the most evident feature of the seismicity of the North Pahroc Range northeast of Yucca Mountain

[redacted]

[redacted]

[redacted]

[redacted]

[redacted]

[redacted]

[redacted]

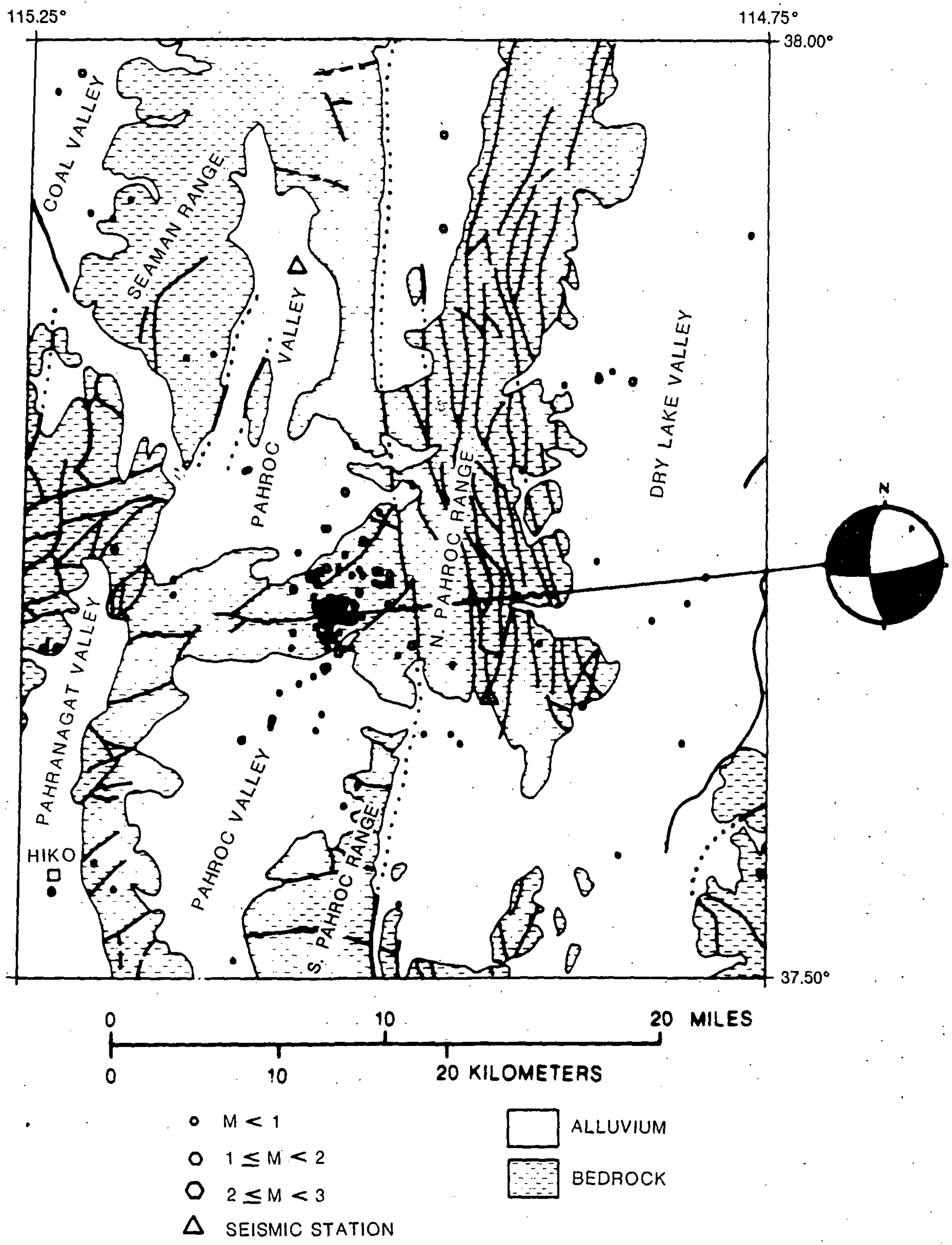

Figure 1-66. Seismicity and focal mechanisms of the Pahroc Valley and North Pahroc Range area, August 1, 1978 through December 31, 1983. Symbols defined as in Figure 1-61. Modified from Rogers et al. (1987).

1.4.1.2.12 Summary of correlation of seismicity, focal mechanisms, and stress axes with recognized geologic structures

The detailed discussion in the previous sections demonstrates the difficulty of showing an unequivocal relationship between seismicity and known faults in the region. For example, it is often difficult to directly associate given earthquakes and specific faults with confidence because of errors in event location and because of the unknown geometry of the faults at the depths of the hypocenters. However, the frequent association of nodal planes with an alignment of earthquakes or with mapped structural grain in the surrounding surficial rocks imparts greater confidence that the faults that define the structural grain at the surface are active and do reflect the general structural pattern at seismogenic depths. On this basis, the data suggest that north- to east-northeast-striking faults should be considered potentially seismogenic. However, this suggestion may not be valid in all cases, when tested against various hypothetical tectonic models proposed for the region. Rogers et al. (1987) concluded, on the basis of examination of a number of wrench and detachment models, that no one tectonic model satisfactorily accounts for all features of the seismic data.

1.4.1.3 <u>Determination of earthquake-generating potential of geologic structures and seismotectonic zones within the southern Great Basin</u>

Currently, there is large uncertainty in the assessment of the earthquake potential of geologic structures and seismotectonic zones in the southern Great Basin. The reasons for this are sparse historical seismicity in the region (Section 1.4.1.1.1), equivocal association of contemporary microseismicity with mapped structures (Section 1.4.1.2.12), large uncertainties associated with critical fault parameters (such as length) of Quaternary faults (Section 1.3.2.2) and the very long earthquake recurrence intervals on local faults relative to the length of the historical earthquake record (Section 1.3.2.2). As a consequence, the shortness of the seismic record means that the magnitude of the largest historical earthquake within any plausible zone defined within 100 km of Yucca Mountain is uncertain. Further, known geologic structures are currently inactive or the dimensions and style of faulting are ambiguous. Accordingly, several investigators (Perkins et al., 1987) have used more generalized sources that replace the more traditional approach of assigning specific earthquakes to specific faults. The general approach is followed in this section. Discussed below are a summary of the methods used by investigators for the southern Great Basin region.

Rogers et al. (1977a) discuss the complex relationship of seismicity and faulting in terms of determining the earthquake potential of individual faults. Based on apparently conservative assumptions, the full length of each evaluated fault was assumed to rupture in an individual earthquake, and the relationship of Bonilla and Buchanan (1970) was used to determine the magnitude. Subsequently, USGS (1984) recalculated the magnitude assuming the full fault length ruptured during an individual earthquake and using the relationship of Mark and Bonilla (1977). The magnitude values are shown in Table 1-11. The closest evaluated fault is the Bare Mountain fault, about 14 km from the site. More recently, Swadley et al. (1984) and Whitney et al. (1986) have discussed evidence of Quaternary faults closer than 14 km.

At present, the length and other physical characteristics of these faults are known only approximately (Table 1-8), and magnitudes and recurrence intervals can be only crudely estimated (Section 1.3.2.2.2); plans to gather additional data are presented in Section 8.3.1.17.

In contrast to determining the earthquake potential of faults, Rogers et al. (1977a), Greensfelder et al. (1980), Algermissen et al. (1982) and URS/Blume (1986), have assigned maximum magnitudes to a variety of assumed seismotectonic zones. In these instances, the choice of maximum magnitude is dependent on a number of assumptions including the maximum historical earthquake and the tectonic character (such as degree of Quaternary faulting) of the zone. In general, it has been assumed that large earthquakes ($M > 6.0$) have the potential of occurring throughout generalized seismotectonic zones (Rogers et al., 1977a; Greensfelder et al., 1980; Algermissen et al., 1982; URS/Blume 1986). As described in Section 1.4.1.5, while large earthquakes have been assumed to be pos~ible, the recurrence intervals for such events appear to be relatively long. As additional work is completed (Section 8.3.1.17) the maximum historical earthquake of each generalized seismotectonic zone will be listed.

In general, large earthquakes could occur in the southern Great Basin if certain conditions were met--namely, if shear stress approached failure over a large area of a fault surface oriented north to east-northeast in the contemporary stress field (or possibly north to northwest in the extreme southwestern Great Basin). The fault surface could extend to depths as great as 10 to 15 km, and the fault surface might be currently quiescent. Consequently, there is potential (although currently unquantified) for movement on north-striking faults near Yucca Mountain, despite the current quiescence of the area. Rogers et al. (1987) note that the lack of contemporary seismic activity could be due either to low stress (because of prehistoric stress relief) or to high stress (because of locked faults); both are factors that could impact the assessment of maximum magnitude. These conclusions are supported by the information given below.

The seismic data indicate that north- to east-northeast-striking faults are more active than faults of other orientations (Rogers et al., 1983; 1987). Although normal faulting occurs on some northeast-striking faults, focal mechanisms indicate that strike-slip faulting is common in the southern Great Basin. All focal mechanisms determined by the SGBSN indicate minimum principal compressive stresses that are consistent with the regional stress field inferred from other data (Carr, 1984; Rogers et al., 1987). The minimum principal stress direction is about N.60°W. (Section 1.4.1.2), thereby favoring seismic slip on faults trending north to east-northeast. However, this stress orientation may be rotated in the southwestern Great Basin: Zoback and Zoback (1980a) indicate the minimum principal compressive stress direction is probably east-west in the Death Valley region as discussed by Rogers et al. (1983). In addition, Walter and Weaver (1980) have suggested a rotation in the stress field orientation on the basis of focal mechanisms of earthquakes in the Coso volcanic field, 80 km west of Death Valley, which showed right-lateral strike-slip faulting on northwest-striking faults and normal faulting on north-striking faults.

Faults on Pahute Mesa having orientation and style similar to those found throughout the southern Great Basin were activated by nearby underground nuclear testing (Hamilton and Healey, 1969; Hamilton et al., 1971, 1972; Wallace et al., 1985). The length of rupture (up to 10 km), the maximum displacement (in excess of 1 m), and the magnitude and depth of aftershocks all indicate that the faults had been previously stressed with the result that the tectonic stress was released by the explosions (Rogers et al., 1977b). Wallace et al. (1985) used SH-wave amplitudes to deduce a double-couple focal mechanism from the tectonic component of stress release from large nuclear explosions at Pahute Mesa. Their stress axis orientations are similar to the maximum compressive stress axis (s_1) and the minimum compressive stress axis (s_3) determined by Rogers et al. (1987).

The potential for the occurrence of large earthquakes on faults with significant vertical dimension is indicated by the full range of focal depths (surface to 10 to 15 km) observed in the seismicity. Strike-slip focal mechanisms (Rogers et al., 1987) for shocks occurring in the deeper active [redacted] shallower depths as in western Nevada (Vetter and Ryall, 1983). Although stress can be relieved aseismically as fault creep, there is little evidence that creep is a significant means of stress relief in the Great Basin (Bucknam et al., 1980; Crone, 1983).

1.4.1.4 Earthquake-induced phenomena within the southern Great Basin that may affect site

Earthquake-induced phenomena, such as liquefaction, landsliding, and lurching of soil masses, are expected to be minimal. The very deep water table, the arid climate, and the lack of bulk thixotropic materials make liquefaction effects highly unlikely. Similarly, landslides and lurching at the site are not expected because of mechanically stable rock types, the lack of rugged topography (at locations proposed for surface facilities), the aridity, and thin soil development. Such phenomena are unlikely and expected to have minor effect on the repository or surface facilities, either before or after closure.

As discussed previously, Rogers et al. (1977a) performed a preliminary analysis of seismic hazard for a location on the NTS about 20 km east of

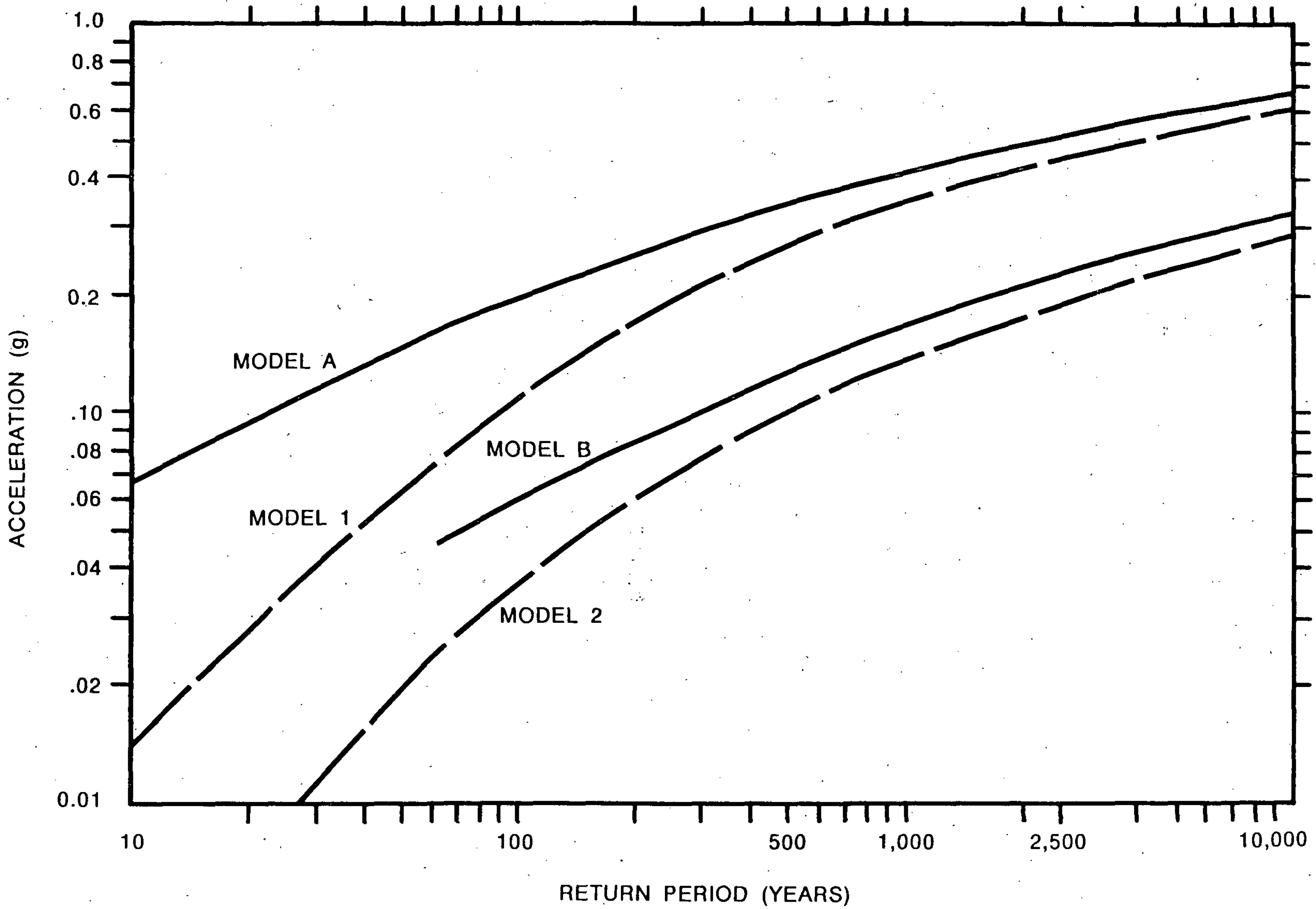

Figure 1-67. Graph of mean peak acceleration versus return period for two hypotheses (Rogers et al., 1977a and Perkins et al., 1987) described in Section 1.4.1.5. Models A and B are from Rogers et al. (1977a); models 1 and 2 are from Perkins et al. (1987).

zones. To avoid the shortcomings of model 1, mapped faults in the region (Rogers et al., 1983; USGS, 1984) were used in model 2 to define source zones, the boundaries being determined on the basis of similarity of fault density and fault orientation. To eliminate induced aftershocks, the seismic rate in each source zone was determined from the historical catalog prior to 1960; geologic considerations helped set the rate for large magnitude shocks. The results of the Perkins et al. (1987) study are discussed in Section 1.4.2.1.

As is apparent from the previous discussion, there is a wide range in estimated recurrence intervals for large (M > 6) earthquakes in the site region, and as a result estimates of seismic hazard are uncertain. Accurate estimates of recurrence intervals are important in evaluating both the preclosure seismic design and the probability of postclosure disruptive events. Additional work will be completed (Sections 8.3.1.8 and 8.3.1.17) to more accurately estimate recurrence intervals, particularly for faults within about 10 km of the site.

1.4.2 SEISMOLOGY OF YUCCA MOUNTAIN

1.4.2.1 Vibratory ground motion at Yucca Mountain resulting from potential earthquakes in the area

Currently, there are two general methods being used to calculate the potential vibratory ground motion for the Yucca Mountain site. These general attenuation curve were chosen to provide examples of mean peak acceleration (Table 1-11). The maximum magnitudes of earthquakes that can occur on the faults listed in Table 1-11 are computed from a formula by Mark and Bonilla (1977). Because the entire mapped fault length is assumed to rupture, the estimate of maximum magnitude is conservative (i.e., almost certainly high). The curves showing attenuation of mean peak acceleration with distance used were from Schnabel and Seed (1973).

The maximum earthquake occurring on the Bare Mountain fault, located about 14 km west of the proposed repository location, has been calculated to be M = 6.8 (Table 1-11) assuming the rupture occurred along the full length of the fault. The maximum mean probable acceleration resulting from this event at Yucca Mountain was estimated to be 0.4g. Although larger shocks are possible elsewhere in the southern Great Basin, the table shows that predicted peak accelerations at Yucca Mountain due to these events are considerably smaller than 0.4g. Faults closer to the repository could give greater accelerations than that calculated for the Bare Mountain fault if they rupture along their full length. However, at this time, the length of Quaternary faults near Yucca Mountain are not known with certainty and are subject to debate. Information such as that contained in Table 1-8 will be used in the future to revise estimates of vibratory ground motion for design analyses. Studies to address the data needed to assess the seismogenic potential for faults and the strategy to assess vibratory ground motion are discussed in Section 8.3.1.17. Data in Table 1-11 will have to be revised as faults nearer than the Bare Mountain fault (e.g., those shown on Table 1-8, Section 1.3.2.2.2) are investigated. Additionally, the attenuation equation and [illegible]

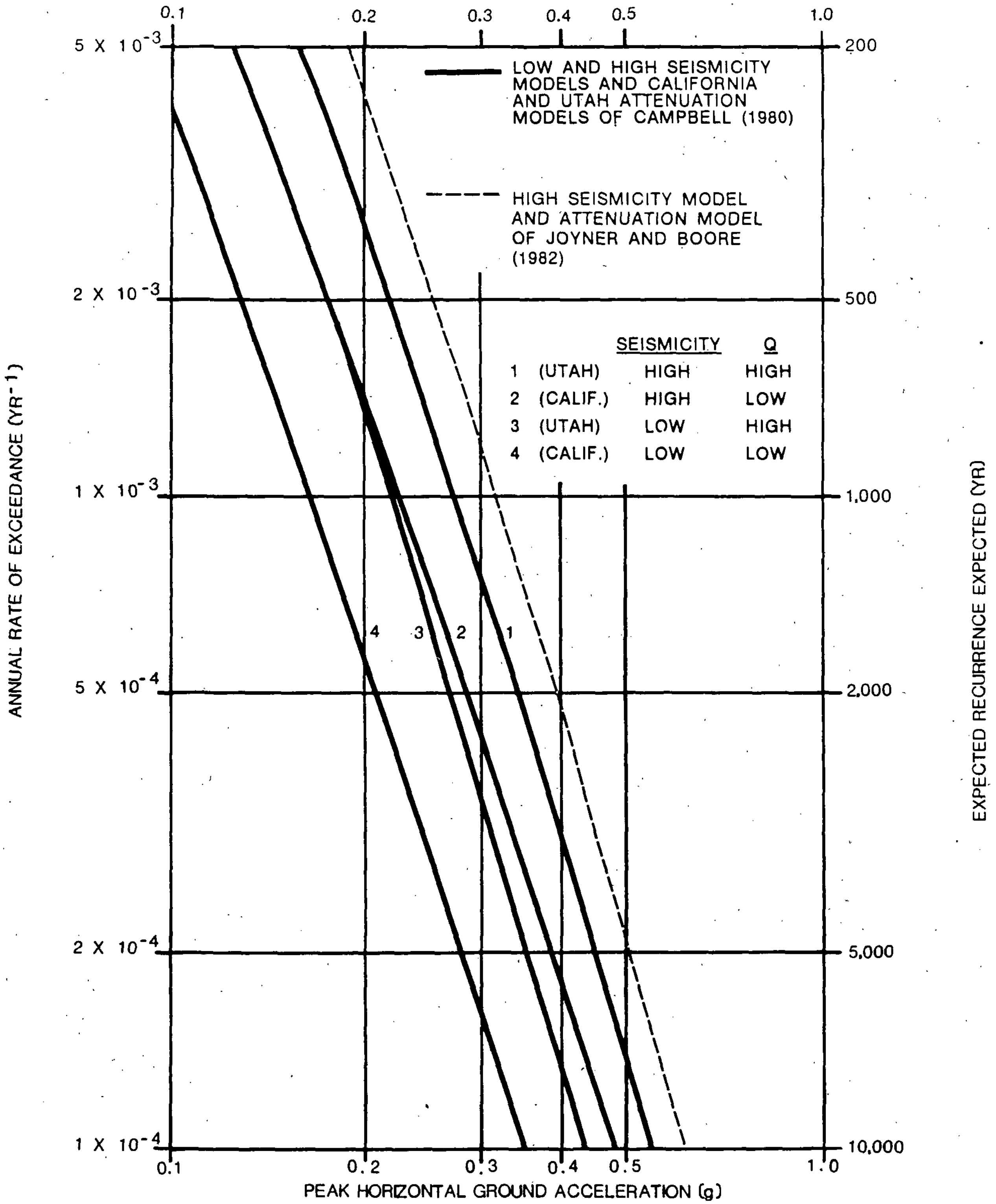

Figure 1-68. Earthquake hazard results for peak horizontal ground acceleration evaluated with a geometric standard deviation of 1.9. Modified from URS/Blume (1986).

Table 1-13. Examples of hazard estimates for mean peak acceleration at Yucca Mountain for two hypotheses[a]

Peak acceleration (g)	Yearly probability of exceedance	Return period (yr)	Time interval (yr)	Hazard
		HYPOTHESIS A		
0.2	0.01	100	1	0.01
			30	0.26
			90	0.59
0.4	0.0017	600	1	0.0017
			30	0.033
			90	0.14
0.7	0.0001	10,000	1	0.0001
			30	0.003
			90	0.009
		HYPOTHESIS B		
0.1	0.0036	280	1	0.0036
			30	0.102
			90	0.275
0.2	0.0007	1,400	1	0.0007
			30	0.021
			90	0.062
0.325	0.0001	10,000	1	0.0001
			30	0.003
			90	0.009

[a]Hypothesis A: All historical earthquakes within 400 km of Yucca Mountain are used to determine recurrence rate. Hypothesis B: same as hypothesis A, except all Nevada-California seismic belt earthquakes are excluded. Hazard (probability that peak acceleration will be exceeded during specified time interval) from Perkins et al. (1987).

Thus, a more accurate probabilistic assessment of the seismic hazard for the Yucca Mountain repository may be somewhere between the extremes of hypotheses A and B, probably closer to curve B (Perkins et al., 1987). Rogers et al. (1977a) and Perkins et al. (1987) have emphasized that additional studies are required to correct for shortcomings in the current method of analysis, and such studies are planned (Section 8.3.1.8). Perkins et al. (1987) propose a list of activities necessary to make future probabilistic assessments more reliable. Three of these activities are purging the catalog of induced aftershocks, revising magnitude estimates of historical shocks, Yucca Mountain. Rogers et al. (1987) have reported results on the second of recordings of earthquakes and nuclear explosions. Research studies that are pertinent to seismic wave transmission at Yucca Mountain (Campbell, 1980; Vortman, 1982, 1986; Vortman and Long, 1982a,b) document scatter in the observed data and uncertainty associated with the method of inferring earthquake response from explosion data.

One difference between earthquake and nuclear explosion sources results from their source spectra and in the energy partition into the several seismic phases. As a result, over comparable distances, earthquake seismograms tend to be relatively rich in low-frequency body-wave (especially S-wave) and surface-wave energy, and explosion seismograms tend to be rich in higher-frequency body-wave (especially P-wave) energy. Another difference results (1) from attenuation of high frequencies, especially over long path distances, at both surface and underground station locations and (2) from attenuation of peak acceleration with distance (Campbell, 1981). The effect of transmission path and site geology on the degree of attenuation on seismic waves from explosion sources appears to be strong (Vortman and Long, 1982a, b; Vortman, 1986). Finally, seismic records at Yucca Mountain are available only for explosion sources at Pahute Mesa and Yucca Flat, thereby restricting the range of azimuths to north to northeast and precluding identification of azimuthal variation in seismic wave transmission.

Transmission of seismic waves from a seismic source to a surface station is a strong function of the geologic conditions under the station as well as the geology along the transmission path. Vortman (1986) has analyzed seismograms of Pahute Mesa nuclear explosions recorded at Yucca Mountain and the Nuclear Rocket Development Station (NRDS) area. He reports accelerations as much as four times higher than the mean acceleration predicted for Yucca Mountain and ten times higher than that predicted at the NRDS site. Vortman (1986) concluded that path effects were dominant at Yucca Mountain, in contrast to the NRDS anomaly which appeared to be site related.

The potential for local site conditions to modify vibratory ground motion has been discussed by URS/Blume (1986). It was estimated that the effect of a low-angle alluvial wedge, present in Midway Valley, would not significantly amplify motions because of the low acoustic impedance contrast between the alluvium and the underlying fractured tuff. Relevant geologic maps, borehole data, and reflection and refraction surveys were reviewed by Neal (1986). Measurements of ultrasonic velocities in Midway Valley rock core, indicates compressional velocities from 2.3 to 3.0 km/s, and shear velocities from 1.4 to 1.9 km/s. Refraction surveys (Pankratz, 1982) have indicated compressional velocities of about 1.0 km/s in alluvium and 1.4 km/s in Tiva Canyon Tuff. These velocities were significantly less than the ultrasonic velocities, and the high state of fracturing in the tuff was suggested as the cause of the extremely low compressional velocity.

The available data do not provide a basis for strongly favoring one surface facility location over another in terms of seismic response. In general, the eastern margins of Midway Valley may experience enhanced amplification due to possible Rayleigh wave motion generated at the alluvium-bedrock interface formed by the Bow Ridge fault. It is possible that multiple reflections of body waves in the alluvial wedges may produce amplification at certain frequencies. Analysis of signals recorded at these stations for other events at Pahute Mesa and Yucca Flat would be informative (Section 8.3.1.17).

1.4.2.2.1 The evaluation of ground motion at depth

At Yucca Mountain, ground motions resulting from both earthquakes and weapons tests are important in the assessment of the stability of the underground repository facilities (SAIC, 1985). Presently, motions at depth have been and continue to be recorded at the NTS for weapons tests (Vortman and Long, 1982b). In contrast, few subsurface recordings of earthquakes have been made.

As discussed in SAIC (1985) Japanese data on earthquakes reported by Kanai and Tamaka (1951) and Kanai et al. (1953; 1966), Iwasaki et al. (1977) and Okamoto (1984), and indicated that motion generally decreases with depth. A velocity attenuation curve developed for a depth of 300 m in rock, predicts velocities less than curves for surface rock velocities at the same focal [illegible] granite, the downhole ratios were relatively small compared to pairs of stations where the surface sites were located on alluvium and the downhole sites were located on rock. In addition, Vortman and Long (1982b) observed topographic effects at Rainier Mesa, factors which may have some significance if surface recordings are made at the top of Yucca Mountain.

Presently, data specific to Yucca Mountain is sparse. Section 8.3.1.17 discusses plans to record weapons tests or natural earthquakes, both at the surface and subsurface at and near Yucca Mountain. These recordings will be used to describe subsurface ground motion as needed for repository design.

1.4.2.3 Potential for induced seismicity affecting Yucca Mountain

Sources of induced seismicity that might affect Yucca Mountain are (1) known areas of induced seismicity such as Lake Mead, Pahute Mesa, and Yucca Flat and (2) possible new areas of induced seismicity such as the Buckboard area discussed by Vortman (1979). The cause of induced seismicity at Lake Mead is believed to be reservoir loading (Carder, 1945) while the seismicity at Pahute Mesa, Yucca Flat, and potentially Buckboard Mesa is the result of weapons testing. Known sources of induced seismicity are sufficiently distant from Yucca Mountain and historically have not had earthquakes large enough to produce peak accelerations at Yucca Mountain greater than 0.1g (Rogers et al., 1977a). Any consideration of the hazard due to naturally occurring earthquakes (as in Section 1.4.2.1) will almost certainly reduce the hazard due to known sources of induced seismicity to a minor role. Table 1-11 shows that 0.2g would be the largest possible acceleration from a single full-length rupture of a fault more than 23 km from Yucca Mountain (the distance to the Buckboard area). This result suggests that an in-depth analysis of the seismic hazard due to new sources of induced seismicity would yield acceptable values of hazard when compared with the seismic hazard due to natural seismicity.

The special case of the seismic hazard due to ground motion from large nuclear tests can be evaluated in a strictly deterministic fashion. The required data are similar to the items discussed above. The location of known and possible new testing areas can be tabulated as source areas, but recurrence rates are unnecessary to the analysis. Vortman (1986) has summarized the method: determine peak ground motion equations from observed seismograms of actual nuclear detonations at a variety of ground conditions and over a wide range of distances, employing standard yield and attenuation models, and adjusting constants in the ground motion equations to match anomalous path effects and local ground conditions.

For man-induced seismicity, the prediction equations for mean peak vector acceleration determined by Vortman (1986) yielded values of 0.04g to 0.07g for a hypothetical 700 kiloton explosion at the Buckboard area, an area about 23 km from Yucca Mountain being considered for future testing. The range in values reflects differing ground conditions at seismic stations and different ways of grouping the data entered into the regression procedure. The prediction equations were determined for a large suite of stations distributed around the region and therefore do not correct for anomalous ground motion enhancement at certain stations. Ground acceleration at Yucca

Mountain stations from nuclear explosions at Pahute Mesa was observed (Vortman, 1986) to be enhanced by as much as four times. As described in Section 8.3.1.17 additional work needs to be completed to quantify the vibratory ground motion from weapons testing as modified by the specific site conditions at the location of the repository surface facilities.

1.5 LONG-TERM REGIONAL STABILITY WITH RESPECT TO TECTONIC AND GEOLOGICAL PROCESSES

This section pertains to postclosure tectonics, which considers the possibility that some form of tectonism or volcanism could occur at or near Yucca Mountain and evaluates the potential effects of such activity. It addresses investigations in the postclosure tectonics program (8.3.1.8).

Section 1.5.1 considers silicic and basaltic volcanism; Section 1.5.2 considers fault rupture of the repository or the controlled area; and Section 1.5.3 considers vertical or lateral crustal movement in response to tectonism. Related discussions elsewhere in Chapter 1 include the potential of seismic shaking (Section 1.4) and erosion and deposition (Section 1.1.3). Other related discussions include those of the regional geologic framework for volcanism (Section 1.3.2.1), for faulting (Section 1.3.2.2), and for crustal movement (Section 1.3.2.4).

Estimates of the potential hazards to a repository from volcanism and tectonism are preliminary. Current estimates are based on past rates of volcanic and tectonic processes in the region surrounding Yucca Mountain. The nature and rates of Miocene volcanism and tectonism are different from those for Pliocene and younger activity (Carr, 1984). The rates of contemporary volcanic and tectonic activity appear to be lower than those in the Miocene, which suggests that fundamental changes in the geologic setting have occurred. Therefore, it may not be valid to use data from the Miocene to predict decelerating rates. The contemporary rates of activity may be constant (albeit lower than in the Miocene) and in equilibrium with new boundary conditions set by the modification of the regional framework. The geologic framework expected to control future activity and the time period during which that framework has controlled past activity must be determined in order to forecast the potential volcanic and tectonic activity. This allows geologic processes no longer active in the region to be excluded from the analysis. Studies of the geologic framework in the southern Great Basin are still in progress, as are studies to assess the effects of potential volcanism and tectonism on the geohydrology, geochemistry, and rock characteristics in the vicinity of Yucca Mountain (Sections 8.3.1.2, 8.3.1.3, 8.3.1.4, and 8.3.1.8).

1.5.1 VOLCANISM

The possibility of future volcanism is suggested by the widespread and voluminous silicic and basaltic volcanism in the southern Great Basin during Tertiary time and the continued basaltic volcanism during the Quaternary.

Deposition of volcanic ash on the repository during the preclosure period could make the facility at least temporarily inaccessible, could make monitoring difficult, and could alter surface drainage. Injection of magma in the vicinity of Yucca Mountain could alter the hydrologic, geochemical, and rock characteristics of the site. If magma were to intersect the repository, there would be the possibility of dispersal of radionuclides by surface eruptions.

The potential effects of future volcanism would depend on the following: (1) magma temperature, chemistry, and viscosity; (2) the distribution of ground water; (3) the geometry and dynamics of magma at its intersection with the environs of the repository; and (4) the timing of the volcanic event with respect to decay time of waste in the repository. These factors have been discussed for volcanism in general by Crowe (1980) and by Link et al. (1982); they are discussed specifically for the Yucca Mountain area by Crowe and Carr (1980) and by Crowe et al. (1983b, 1986). The potential for both silicic and basaltic volcanism has been considered in assessing the volcanic hazard to the Yucca Mountain area.

1.5.1.1 Silicic volcanism

The potential for renewed silicic volcanism is suggested by the youngest (7- to 8-million year old) major silicic volcanic center in the vicinity of Yucca Mountain, the Black Mountain center, 50 km north of Yucca Mountain (Crowe and Sargent, 1979). At Black Mountain, an episode of renewed silicic volcanic activity followed the Timber Mountain-Oasis Valley magmatic cycle. Data pertinent to quantifying this potential is discussed below.

1.5.1.1.1 Silicic volcanism and its effects on the repository

The most likely effect at Yucca Mountain of renewed silicic volcanism in the surrounding region would be deposition of air-fall tuff from eruptions of the silicic centers near the western margin of the Great Basin, as happened at least twice during the Pleistocene (Izett, 1982; Dudley, 1985). Such volcanism could result in the deposition of fine-grained volcanic ash at Yucca Mountain in layers ranging from a few millimeters to tens of centimeters thick. Such deposits could temporarily influence the operation of the surface facilities before closure, but they would pose no recognized hazard to the repository after closure. There is little potential that a silicic eruption near the margins of the Great Basin would affect the hydrology, geochemistry, or rock characteristics at Yucca Mountain because of the great distance separating Yucca Mountain from the potential volcanic centers.

1.5.1.1.2 Likelihood of silicic volcanism

The likelihood of silicic volcanism near Yucca Mountain during the next 10,000 yr was considered unlikely by Crowe et al. (1983b) because

1. No silicic volcanism has occurred in the south-central Great Basin during at least the past 6 million years.

2. Silicic volcanism has decreased throughout the central and southern parts of the Great Basin during the past 10 million years and, in most areas, silicic volcanism appears to have ceased.

3. Silicic volcanism has been restricted entirely to the margins of the Great Basin during the Quaternary (the past 2 million years).

An absence of shallow silicic magma bodies in the region also is suggested by generally low heat flow and by the absence of high-temperature springs, a conclusion reached earlier by Blackwell (1978). Yucca Mountain is in a part of the Great Basin in which heat flow is apparently low when compared with regional values (Lachenbruch and Sass, 1977; Section 1.3.2.5.2). Further studies on the influence of hydrology on heat flow measurements in the Yucca Mountain area are planned (Section 8.3.1.8). There are a few thermal springs and wells (50°C) in the region around Yucca Mountain but no high-temperature springs or wells (Muffler, 1979).

Future silicic eruptions from Crater Flat were considered unlikely by Crowe et al. (1986), who reviewed data relating to the possibility of future bimodal volcanism in the Crater Flat field. They have found no rhyolite associated with basalts erupted there during the past 8 to 9 million years. However, because of uncertainties in estimates of the potential for silicic volcanism, additional studies are in progress to further assess the conclusions that this type of volcanism has no significant potential for initiating a disruptive event after closure (Section 8.3.1.8).

1.5.1.2 <u>Basaltic volcanism</u>

The possibility of future basaltic volcanism near Yucca Mountain is suggested by Quaternary basaltic volcanism, notably that in the Crater Flat basalt field, just west of Yucca Mountain.

1.5.1.2.1 Nature of basaltic volcanism

The main product of future volcanism is likely to be alkalic basalt, the main product during the past 8 million years (Crowe et al., 1983a,b). Hydrovolcanic explosions are considered unlikely, as is the formation of intrusive complexes or sills within the controlled area. The probable nature of basaltic eruptions near Yucca Mountain is further discussed below; the discussion is summarized from Crowe and Carr (1980) and from Crowe et al. (1983a,b; 1986).

Future basaltic eruptions would probably be small and short lived judging from the Quaternary record of basaltic volcanism. Quaternary basalt centers in the south-central Great Basin were formed mainly by Strombolian eruptions. Major products are moderate-size scoria cones and lava flows less than 2 km long. Scoria-fall sheets for typical Strombolian eruptions extend 2 to 10 km from the cones (Crowe et al., 1983a). Magma volumes for eruptions in the vicinity of Yucca Mountain during the past 8 million year were generally less than 0.1 km^3, and the eruptions were of short duration (Crowe et al., 1983a). The small-volume, basalt eruptive cycles in the south-central Great Basin reflect the low rate of magma generation in the region during late Cenozoic time. A decline in the rate of magma production in the region is possible during the past 4 million year (Vaniman and Crowe, 1981). No geologic or geochemical patterns indicate that rates of volcanism in the southern Great Basin are increasing, that such rates might increase in the future, or that basaltic activity could evolve into more voluminous types of basalt fields. However, only three volcanic fields have been compared in the Death Valley-Pancake Range volcanic zone, and temporal and spatial patterns of volcanism in that zone are not well defined (Crowe et al., 1986). Furthermore, volcanism appears to be directly linked to tectonic processes in the region, and tectonic models for the southern Great Basin are both controversial and incomplete.

It appears unlikely that intruding magma will form major intrusive complexes near Yucca Mountain. If basaltic magma were intruded, it would probably move rapidly through narrow dikes. Most exposed basalt centers near Yucca Mountain are fed through narrow linear dikes with aspect ratios on the order of 10^{-2} to 10^{-3} (Crowe et al., 1986). A few dikes commonly are associated with each basalt center based on the eroded cone remnants within the 3.7-million-year-old basalts at Crater Flat and at other localities (Crowe

tens of centimeters per second, and mantle-derived basalt melts are likely to be trapped temporarily and to fractionate at the base of the crust. Magma

Crowe et al. (1986) concluded that explosive hydrovolcanic eruptions sufficient to exhume a repository are unlikely in the event that a basaltic eruption would occur.

1.5.1.2.2 Effects of basaltic volcanism

Waste incorporated into magmas would probably be dispersed in much the same pattern as the extrusive magmatic material. Some of the waste would remain in the flow material and some would be dispersed in the scoria sheet. Lesser amounts of waste would be dispersed in fine-grained (<65 microns) wind-borne particles and in the scoria cone. Previous consequence analyses of radiological release during a basaltic eruption (Link et al., 1982) did not include a scenario of early stage hydrovolcanic activity followed by Strombolian eruption. As discussed by Crowe et al. (1986) current estimates of the probability of a basaltic event that intersects the repository may need to be reevaluated to take into account the potential for hydrovolcanic activity. This work is described in Section 8.3.1.8.

In the event of a Strombolian eruption, potential doses of radiation to maximally exposed individuals, hypothetically living near the eruption or in buildings made from materials generated by the eruption, would be a few millirems for eruptions 100 yr after waste emplacement and less for later eruptions according to Link et al. (1982). These doses would be within the limits currently prescribed by regulation: the most restrictive limits are 25 mrem/yr (10 CFR Part 960).

1.5.1.2.3 Likelihood of basaltic volcanism

The potential for future basaltic volcanism at Yucca Mountain was evaluated by Crowe et al. (1982, 1983b, 1986). They considered the history, geologic setting, and genesis of late Cenozoic basaltic volcanism in the vicinity of Yucca Mountain and attempted some preliminary hazard assessment and probability studies.

Crowe et al. (1982) calculated probabilities for the disruption (i.e., penetration) of a repository at Yucca Mountain by basaltic volcanism. In their probability equation, the probability of disruption is related to a theoretical number of expected eruptions and a probability that disruption would occur during any given eruption. The number of eruptions is determined by a rate of eruptions interpreted from studies of volcanic deposits in the vicinity of Yucca Mountain. Crowe et al. (1982) varied both the length of geologic time over which rates were interpreted and the method for interpreting rates of eruptions to obtain what they considered to be a realistic range of rates. The probability that a repository would be disrupted during a given eruptive event is estimated as the ratio of the area of the repository (or a specific volcanic disruption zone) to a minimal area that encloses all the volcanic deposits used to define the rate of volcanic events. Crowe et al. (1982) varied area configurations for specific volcanic disruption zones in an attempt to accommodate structural control of volcanism in their probability calculations. Probabilities calculated by Crowe et al. (1982) on the basis of the area of a repository used an area larger than that currently being considered for waste emplacement at Yucca Mountain. The correspondence has not been determined between the areas considered by Crowe et al. (1982) and the area within which the magma injection does not intersect the repository but might affect the geohydrologic, geochemical, or rock characteristics of the controlled area. The reason such work is important is because a larger area may imply a higher probability of occurrence for the initiating event. Additional work (Section 8.3.1.8) will determine both the probability of occurrence and the effect of nearby basaltic events on the parameters important to waste isolation.

The annual probability that the repository would be penetrated by magma during basaltic volcanism was estimated as 3.3×10^{-10} to 4.7×10^{-8} by Crowe et al. (1982). The corresponding probability range for 10,000 yr is 3.3×10^{-6} to 4.7×10^{-4}. Based on current knowledge these numbers can be taken as lower and upper bounds, but their accuracy is limited by the validity of the geologic assumptions incorporated into the probability model according to Crowe et al. (1982).

The level of confidence that should be ascribed to probability calculations of future basaltic volcanism for the Yucca Mountain vicinity is difficult to assess. Forecasts of future rates of volcanism are based on projection of past rates (Crowe et al., 1982), but the area surrounding Yucca Mountain has had a sufficiently low rate of basaltic volcanism during Quaternary time that the Quaternary record may be a statistically insufficient guide to future volcanism. The usefulness of data from pre-Quaternary volcanism depends on the degree of preservation and exposure of deposits and on the precision of techniques for age determinations. The validity of using data from older volcanic eruptions depends on the uniformity of the regional geologic and tectonic processes controlling volcanism for the entire period being considered as a data base and on demonstrating probable uniformity of these controlling processes into the near geologic future.

Furthermore, future volcanism may be influenced by regional processes that have not affected past activity, such as changing rates or geometry of crustal plate interaction, changes in the orientation of the regional stress field, or changes in the kinematic behavior of faults that act as conduits for the ascent of magma. Such fundamental changes are unlikely to occur during a time period as short as the next 10,000 yr. Because current estimates for the probability of basaltic volcanism intersecting the repository exceed the cut-off probability (10^{-8} per yr), the level of confidence that should be attached to these probability calculations requires additional characteristics in the vicinity of Yucca Mountain (Section 8.3.1.8) also must progress before risk assessment can be completed.

1.5.2 FAULTING

The potential for future faulting at Yucca Mountain is indicated by the history of Quaternary faulting near Yucca Mountain. Evidence for Quaternary rupture on 32 faults within an 1,100-km^2 area including Yucca Mountain was recognized by Swadley et al. (1984) (Sections 1.3.2.2.1 and 1.3.2.2.2). Recurrent Quaternary movement has been documented on the faults bounding Busted Butte (Dudley, 1985), on the Rock Valley fault system (Yount et al., 1987) and on the Windy Wash fault (Whitney et al., 1986). Evidence for possible Holocene movement on parts of the Bare Mountain eastern range-front fault was described by Reheis (1986). Whitney et al. (1986) indicated that Holocene movement has occurred on the Windy Wash fault. There are other faults in the Yucca Mountain area (Solitario Canyon, Bow Ridge, and Paint-brush Canyon) that have evidence of Quaternary activity (Section 1.3.2.2). In general, additional work is necessary to better document the recurrent nature of faults near the site (Section 8.3.1.17).

1.5.2.1 Effects of faulting

Future faulting in the vicinity of Yucca Mountain could directly affect the repository through ground shaking (Section 1.4.2) or rupture within the repository or controlled area. The hazard from future faulting will depend on facility design, as well as on geologic and hydrologic conditions. Faulting could affect both the preclosure or postclosure phases of the repository. But the potential effects of faulting during the preclosure and postclosure periods would differ, and the hazard from faulting for each period must be evaluated separately.

Study of trenches across the Windy Wash fault and other faults in the Yucca Mountain area indicates that surface rupture is possible along faults in the controlled area (Section 1.3.2). In two of the Windy Wash fault trenches, the apparent vertical displacement of a unit dated at 270,000 to 190,000 yr by the uranium-trend method was 40 cm. A fault recurrence interval of 75,000 yr was suggested on the basis of four episodes of faulting that have occurred during the last 300,000 yr (Whitney et al., 1986). Basalt ash correlated with the Lathrop Wells basalt cone is emplaced within a fault predating the 270,000 to 190,000 yr old deposit (Whitney et al., 1986). This basalt cone currently is considered no older than 300,000 yr on the basis of potassium-argon dating method dates (Crowe and Carr, 1980). Sinnock and Easterling (1983) provide 18 additional potassium-argon dates for this cone (dated by 3 independent laboratories). They report an average age estimate operations. Planned studies to assess the potential of surface rupture from faulting at proposed facility locations are described in Section 8.3.1.17.

Faulting could either directly or indirectly affect the hydrologic system, geochemistry, and (or) rock characteristics at Yucca Mountain. Modification of the hydrologic system might result in changes in the distribution of hydraulic head, localized changes in hydraulic conductivity, and changes in the boundary conditions of the hydrologic system. Such modifications of the hydrology might further affect geochemistry and rock characteristics. Rock characteristics could also be affected directly by faulting.

An outline of our current perception of the effects from faulting is presented in DOE (1986) and summarized here. It appears unlikely that faulting would lead to radionuclide releases to the accessible environment during the first 10,000 yr following closure of the repository. Even if a waste container were breached by fault movement during the postclosure bound the structural blocks at Yucca Mountain (Section 1.3.2.2.2) are preestablished faults with a history of reactivation (Carr, 1984) in the contemporary tectonic framework. It is likely that any future faulting at Yucca Mountain would occur along these preestablished faults.

Slip rates on seismogenic faults in the Great Basin are considered to be nonuniform in both space and time (Wallace, 1985). Segments of faults along determine more accurate estimates of both the type of faulting events, and their probabilities of occurrence (Section 8.3.1.17).

1.5.2.3 Effects of nuclear weapons tests on faulting and the repository

Underground nuclear testing at the NTS can produce ground motion similar to that of natural earthquakes and may also induce surface fault displacement.

The size of nuclear tests is currently limited to a maximum yield of 150 kilotons by the Threshold Test Ban Treaty and the Treaty on Underground Nuclear Explosions for Peaceful Purposes (ERDA, 1977; Vortman, 1979), but the capability to return to larger or former yields is being retained at the NTS. The number of announced nuclear tests has been averaging about 20 per year and is expected to remain at that level for the foreseeable future (DOE/NVO, 1987). At present, tests are conducted at Yucca Flat, Rainier Mesa, and Pahute Mesa (Figure 1-69). The size of tests is also restricted by the [redacted]

Yucca Flat has a yield limit of about 250 kilotons and Pahute Mesa has a 1,100-kiloton limit (Vortman, 1979). Both of these limits are well above the current yield limits specified by treaty. The Buckboard area, a past area of testing that may be used again, has a 700-kiloton yield limit (Vortman, 1979). The yield limit for Mid Valley, a future potential test area, is likely to be similar to that for Yucca Flat.

Vortman (1980) indicated that a given size underground nuclear test in the Buckboard area would produce about the same ground motion as would result from a test of the same size on Pahute Mesa because the rock properties that control ground motion are similar at the two locations. However, the ground motion that would result at Yucca Mountain from Buckboard area tests would be greater than that from tests at Pahute Mesa because the Buckboard area is closer to Yucca Mountain. Mid Valley and Yucca Flat are also likely to produce about the same ground motion from tests of the same size. Similarly,

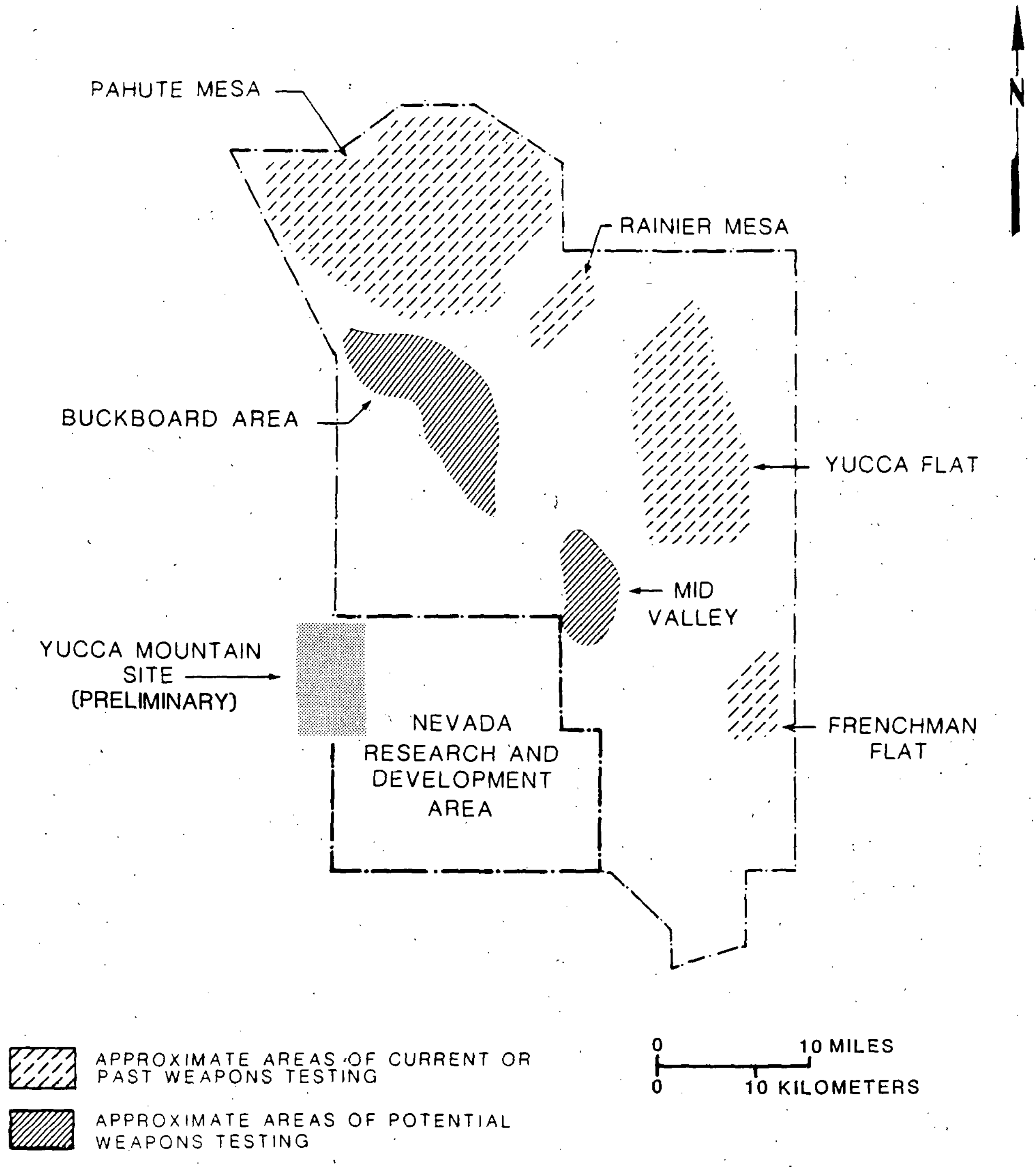

Figure 1-69. Past, current, and potential future weapons-testing areas on the Nevada Test Site. Modified from DOE (1986).

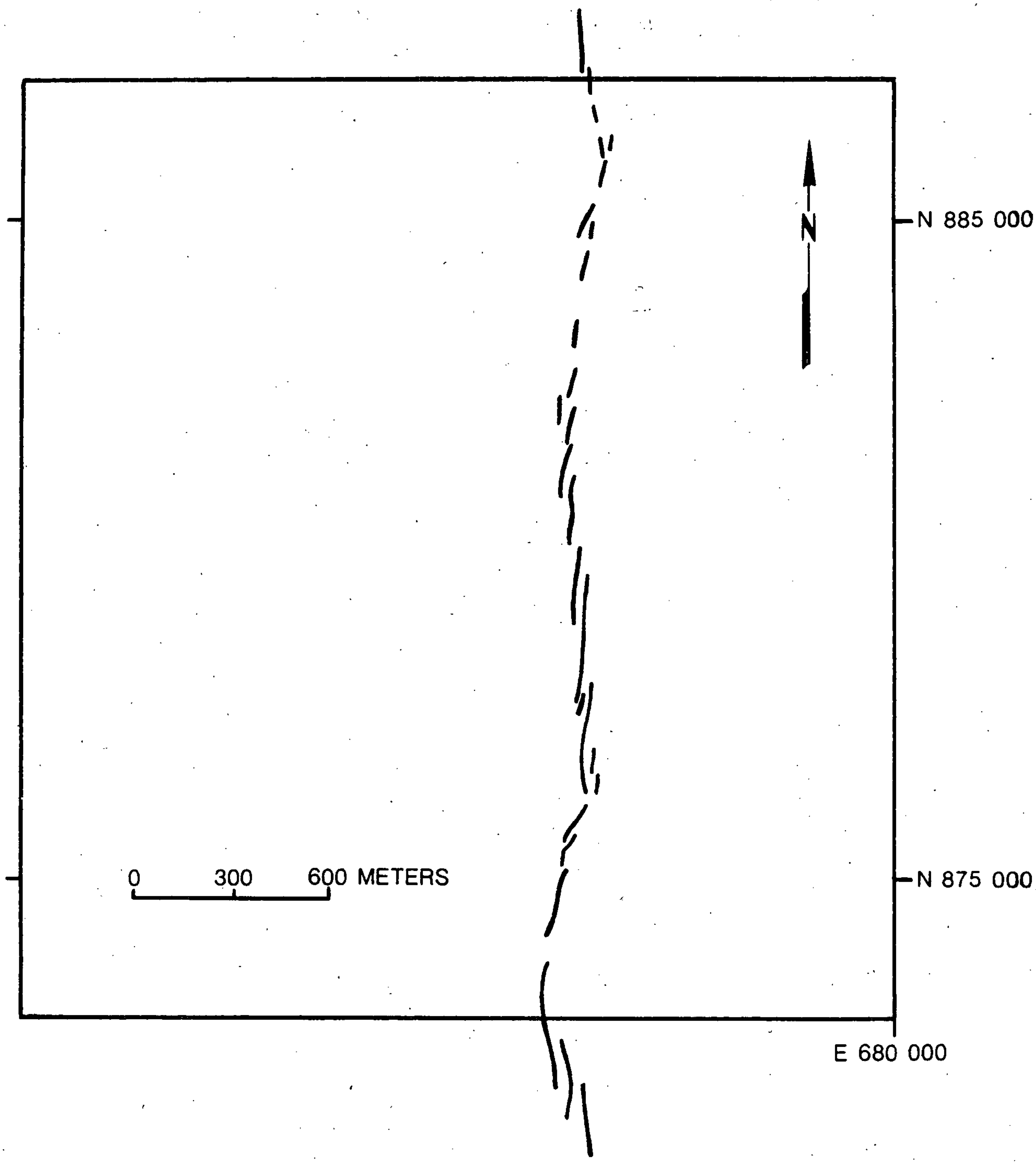

Figure 1-70. Diagram of shot-induced scarplets along part of the Yucca fault. Modified from Carr (1974).

A nuclear test at Rainier Mesa in February 1984 resulted in an unexpected subsidence crater on the surface, causing injuries and one fatality. The nuclear device had been exploded at about 360 m (1,184 ft) below the surface (DOE/NVO, 1984), and the persons injured were involved in post-shot activities only 26 m (85 ft) from the point on the surface that was directly above the explosion. Ninety-five percent of the after-shocks at Pahute Mesa have been found to be within 14 km (8.7 mi) of the explosion site (ERDA, 1977). The Yucca Mountain site is sufficiently distant from present or potential underground test locations that collapse or formation of fractures is highly unlikely.

Using an empirical relationship developed on the basis of ground motion studies from past weapons tests, Vortman (1982) investigated potential conflicts with respect to induced ground motion between the underground weapons-testing program and a geologic repository at Yucca Mountain. His results show that if a repository was designed for 0.75g ground acceleration, then it could be built as close as 6.3 km (3.9 mi) to a 700-kiloton nuclear detonation. The closest location at the NTS with a potential for a 700-kiloton detonation is the Buckboard area, and it is 23 km (14 mi) from the Yucca Mountain site, more than 3 times farther than the 6.3 km (3.9 mi) calculated by Vortman (1980). Ground motion from aftershocks that follow large nuclear tests has also been considered and should not cause additional problems; as noted above, 95 percent of the stimulated earthquake activity is confined to within 14 km (8.7 mi) of the detonation point. Aftershocks fall off to the background level within a period of several weeks, and the strongest aftershock is usually at least 2 magnitude units (on a logarithmic scale) less than the explosion (ERDA, 1977).

Using the empirical equation from Vortman (1979), the predicted mean peak vector ground acceleration at Yucca Mountain from UNEs at the maximum allowable yields, based on offsite damage restrictions, is calculated to be 0.061g. Using a very conservative design criterion of 3 standard deviations, or 99 percent of all probable values, the mean peak vector ground acceleration for Yucca Mountain is calculated to be 0.32g. The yields used for this calculation are well above the 150-kiloton limit currently allowed by the Threshold Test Ban Treaty.

The effects at Yucca Mountain from ground motion from UNEs at the NTS were compared with ground motion from earthquakes in URS/Blume (1986): "The principal conclusion to be drawn from this comparison of earthquake and UNE ground motion hazard is that both must be considered for seismic design. Earthquakes and UNE events produce hazards of distinctly different frequency content, as observed by Vortman (1982)." The probabilistic results in URS/Blume (1986) indicate that at intermediate frequencies, the earthquake and UNE spectra produced by earthquakes and UNEs are very similar.

1.5.3 VERTICAL AND LATERAL CRUSTAL MOVEMENTS

Vertical and lateral crustal movement resulting from tectonism in the southern Great Basin (Section 1.3.2.4) would, by itself, have negligible effect on the proposed repository; hazards would be due mainly to the effects associated with faulting, seismicity, and volcanism. Rates and patterns of crustal movement will be used in assessing such hazards.

Carr (1984) discusses the evidence for the tilting of lake beds in the region to the south or southeast at a rate of 1 to 2.3 m per km (laterally traversed) per million years over the last 3 million years. It is not clear whether this tilting represents regional deformation or represents local tilting related to extension in individual valleys. There is a general southward decrease in elevation from central to southern Nevada, but the timing, causes, and rate of development of the overall southward slope are not established.

Trilateration and leveling networks have proven to be useful for assessing the rates and pattern of strain accumulation in the Great Basin and elsewhere (Savage and Lisowski, 1984; and Savage et al., 1985). These kinds of networks have been installed and are operating in the vicinity of Yucca Mountain. The networks will continue to operate through site characterization and may be continued through the preclosure time frame (Section 8.3.1.17). Data acquired from the networks will be used to measure in situ stress in the vicinity of Yucca Mountain and to relate the in situ stresses to the regional stress pattern. These investigations will be used to better understand the present tectonic framework in the vicinity of Yucca Mountain. The in situ measurements will also be used to evaluate the impact of weapons testing on the Yucca Mountain site.

1.6 DRILLING AND MINING

Section 1.6 discusses the available information on the location and

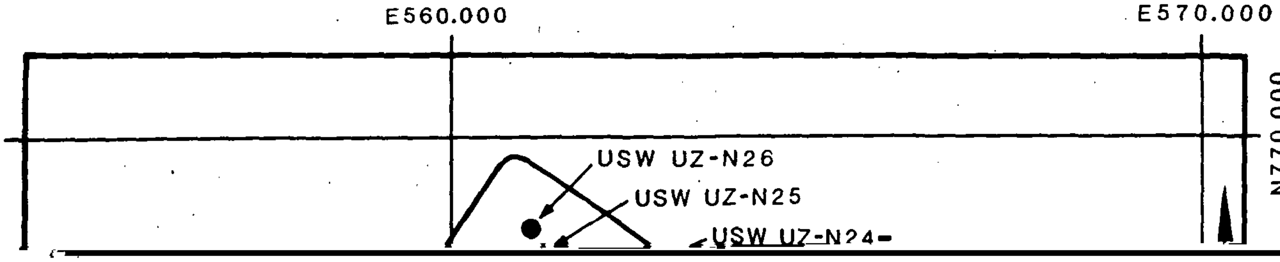
E560.000
E570.000
N770.000
USW UZ-N26
USW UZ-N25
USW UZ-N24

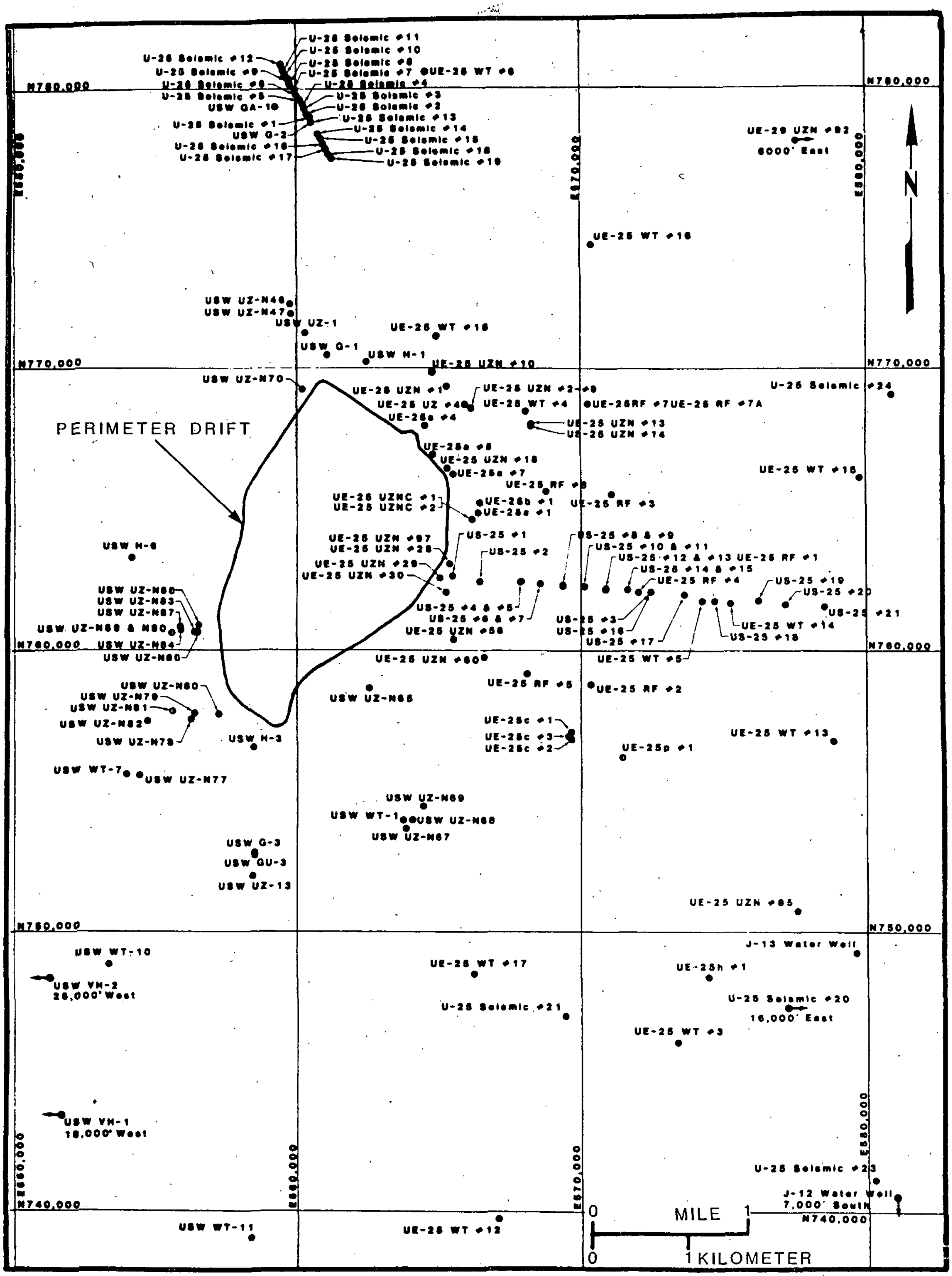

Figure 1-72. Drillholes located outside of the perimeter drift but within 10 km of it.

the NTS controlled by the DOE. A careful examination of existing records (Sections 1.6.1.1.1 and 1.6.4) and the ground surface identified only the evidence of drilling and mining discussed in this report.

1.6.1.1 Summary of drilling activity

A study has been made of the available records, and all of the area

Table 1-14. Drillholes within the outline of the perimeter drift[a] (page 1 of 5)

Hole number and purpose	Location coordinates and ground-level elevation (ft)	Sample type and depth (ft), media, and log type[b]	Casing Depth (ft)	Casing Diameter (in.)	Hole Depth (ft)	Hole Diameter (in.)	Spud date	Completion date
UE-25a#6 Geologic exploratory	N 765,899 E 564,501 4,053	Core (414) Bentonite and water Polymer and water C,D,GR,N,E,V	57 493	8.625 2.375 Tubing	500	6.125	07-17-79	08-08-79
UE-25 UZN#19 Unsaturated zone-neutron	N 763,689 E 564,571 4,025	Cuttings/core (2) Air	40	5.5	40	6.0	11-06-85	11-08-85
UE-25 UZN#20 Unsaturated zone-neutron	N 763,760 E 564,579 4,027	Cuttings Air	41	5.5	41	6.0	05-15-84	05-16-84
UE-25 UZN#21 Unsaturated zone-neutron	N 763,806 E 564,591 4,028	Cuttings/core (4) Air	40	5.5	40 42	6.0 3.937	11-08-85	11-14-85
UE-25 UZN#22 Unsaturated zone-neutron	N 763,880 E 564,605 4,029	Cuttings/core (5) Air	89	5.5	94 95	6.0 3.937	11-14-85	11-18-85
UE-25 UZN#23 Unsaturated zone-neutron	N 763,973 E 564,545 4,043	Cuttings/core (22) Air	35	5.5	35	6.0	11-19-85	11-21-85
USW G-4 Geologic hole	N 765,807 E 563,082 4,165	Cuttings/core (2,962) Air, detergent, and water C,D,GR,N,E,T,V, TR,VT	39 2,017 1,886 2,995	13.375 9.625 1.9 Tubing 1.9 Tubing	3,001 3,003	8.75 8.375	08-23-82	01-13-83

Table 1-14. Drillholes within the outline of the perimeter drift[a] (page 2 of 5)

Hole number	Location coordinates and ground-level ele-	Sample type and depth (ft), media, and	Casing		Hole		Spud	Completion
			Depth	Diameter	Depth	Diameter		
USW H-4 Hydrologic test hole	N 761,644 E 563,911 4,097	Cuttings Air, detergent, and water C,D,GR,N,E,V,T,TR, M,VT	35 311 1,839 3,896 1,725	30.0 16.0 10.75 2.875 Tubing 1.9 Tubing	153 316 1,850 4,000	26.0 20.0 14.75 8.75	03-22-82	06-07-82

Table 1-14. Drillholes within the outline of the perimeter drift[a] (page 3 of 5)

Hole number and purpose	Location coordinates and ground-level elevation (ft)	Sample type and depth (ft), media, and log type[b]	Casing		Hole		Spud date	Completion date
			Depth (ft)	Diameter (in.)	Depth (ft)	Diameter (in.)		
USW UZ-N26 Unsaturated zone-neutron	N 768,757 E 561,023 4,384	Cuttings/core (2) Air	35	5.5	35	6.0	02-10-86	02-11-86
USW UZ-N40 Unsaturated zone-neutron	N 766,176 E 564,221 4,079	Cuttings/core (10) Air	35	5.5	35	6.0	12-19-85	01-07-86
USW UZ-N41 Unsaturated zone-neutron	N 765,867 E 563,521 4,118	Cuttings/core (6) Air	35	5.5	35 37	6.0 4.25	12-12-85	12-16-85
USW UZ-N42 Unsaturated zone-neutron	N 765,729 E 562,859 4,179	Cuttings/core (15) Air	35	5.5	35 40	6.0 4.25	12-16-85	12-17-85
USW UZ-N43 Unsaturated zone-neutron	N 765,997 E 563,264 4,149	Cuttings/core (9) Air	45	5.5	45	6.0	12-05-85	12-09-85
USW UZ-N44 Unsaturated zone-neutron	N 766,193 E 563,140 4,162	Cuttings/core (12) Air	35	5.5	35 36	6.0 4.25	12-18-85	12-19-85
USW UZ-N45 Unsaturated zone-neutron	N 765,977 E 563,429 4,130	Cuttings/core (7) Air	45	5.5	45	6.0	12-09-85	12-12-85
USW UZ-N48 Unsaturated zone-neutron	N 760,835 E 562,414 4,211	Cuttings/core (3) Air	35	5.5	35	6.0	01-07-86	01-08-86
USW UZ-N49 Unsaturated zone-neutron	N 760,860 E 562,322 4,229	Cuttings/core (2) Air	35	5.5	35 36	6.0 4.25	01-09-86	01-10-86

Table 1-14. Drillholes within the outline of the perimeter drift[a] (page 4 of 5)

Hole number and purpose	Location coordinates and ground-level elevation (ft)	Sample type and depth (ft), media, and log type[b]	Casing		Hole		Spud date	Completion date
			Depth (ft)	Diameter (in.)	Depth (ft)	Diameter (in.)		
USW UZ-N50 Unsaturated zone-neutron	N 760,776 E 562,912 4,173	Cuttings Air	20	5.5	20	6.0	08-24-84	08-24-84
USW UZ-N51 Unsaturated zone-neutron	N 760,861 E 562,909 4,169	Cuttings Air	20	5.5	20	6.0	08-24-84	08-24-84
USW UZ-N52 Unsaturated zone-neutron	N 760,894 E 562,909 4,172	Cuttings Air	25	5.5	25	6.0	08-24-84	08-24-84
USW UZ-N71 Unsaturated zone-neutron	N 761,026 E 558,406 4,925	Cuttings Air	52	5.5	52	6.0	05-18-84	05-18-84
USW UZ-N72 Unsaturated zone-neutron	N 761,068 E 558,626 4,889	Cuttings Air	30	5.5	30	6.0	11-20-84	11-20-84
USW UZ-N73 Unsaturated zone-neutron	N 761,049 E 558,926 4,867	Cuttings Air	30	5.5	30	6.0	11-20-84	11-21-84
USW UZ-N74 Unsaturated zone-neutron	N 761,362 E 558,560 4,904	Cuttings/core (6) Air	35	5.5	35 37	6.0 4.25	02-18-86	02-18-86
USW UZ-N75 Unsaturated zone-neutron	N 761,462 E 559,076 4,799	Cuttings/core (10) Air	35	5.5	35 37	6.0 4.25	02-19-86	02-20-86

Table 1-14. Drillholes within the outline of the perimeter drift[a] (page 5 of 5)

Hole number and purpose	Location coordinates and ground-level elevation (ft)	Sample type and depth (ft), media, and log type[b]	Casing Depth (ft)	Casing Diameter (in.)	Hole Depth (ft)	Hole Diameter (in.)	Spud date	Completion date
USW UZ-N76 Unsaturated zone-neutron	N 761,353 E 559,048 4,958	Cuttings Air	35	5.5	40	6.0	11-21-84	11-26-84[c]
USW UZ-N94 Unsaturated zone-neutron	N 759,724 E 558,236 4,926	Cuttings Air	30	5.5	30	6.0	08-15-84	08-15-84
USW UZ-N95 Unsaturated zone-neutron	N 759,899 E 558,172 4,929	Cuttings Air	20	5.5	20	6.0	08-15-84	08-16-84
USW UZ-N96 Unsaturated zone-neutron	N 759,446 E 558,403 4,893	Cuttings Air	35	5.5	35	6.0	08-16-84	08-16-84
USW UZ-N98 Unsaturated zone-neutron	N 767,996 E 562,084 4,223	Cuttings/core (48) Air	31	5.5	75	6.0	02-20-86	02-25-86
USW WT-2 Water table hole	N 760,661 E 561,924 4,270	Cuttings/core (10) Air, detergent and water C,D,GR,N,E,T,V,VT	58 2,040	10.75 2.875 Tubing	58 2,060	14.75 8.75	07-08-83	07-16-83

[a]To convert feet and inches to meters, multiply by 0.3049 and 0.0254, respectively.
[b]Log types are identified as follows: C = caliper; D = density; E = electric; GR = gamma ray; M = magnetometer; N=neutron; T = temperature; TR = tracer; V = velocity; and VT = video tape. Number in parentheses is depth of sample.
[c]Junk in hole USW UZ-N76 at unknown depth.

Table 1-15. Drillholes within 10 km outside of the outline of the perimeter drift (page 1 of 17)

Hole number and purpose	Location coordinates and ground-level elevation (ft)	Sample type and depth (ft), media, and log type[b]	Casing		Hole		Spud date	Completion date
			Depth (ft)	Diameter (in.)	Depth (ft)	Diameter (in.)		
UE-25a#1[c] Geologic exploratory	N 764,900 E 566,350 3,934	Core (2,447) Polymer and water C,D,GR,N,E,T,V	28 2,450	13.375 2.75	1,297 2,501	3.875 2.98	06-25-78	09-02-78
UE-25a#4/ Instrument[d] Geologic exploratory	N 767,972 E 564,472 4,101	Core (369) Bentonite and water C,D,GR,N,E,V,VT	119	8.625	500	6.125	07-02-79	07-03-82
UE-25a#5 Geologic exploratory	N 766,956 E 564,755 4,057	Core (364) Polymer and water Bentonite and water C,D,GR,NE,V,VT	120	8.625	487	6.125	06-26-79	07-12-79
UE-25a#7 Geologic exploratory	N 766,250 E 565,469 4,005	Cuttings/core (420) Bentonite and water Polymer and water C,D,GR,N,E,V	134 956	8.625 2.375 Tubing	501 1,002	5.5 3.875	08-10-79	10-05-80
UE-25b#1 Hydrologic test hole	N 765,243 E 566,416 3,939	Cuttings/core (2,186) Air, detergent, and water C,D,GR,N,E,T,V,TR,VT	292 1,700 3,935	16.0 9.625 2.875 Tubing	1,705 2,131 4,002	12.25 8.75 8.5	04-03-81	09-22-81
UE-25c#1 Hydrologic test hole	N 757,096 E 569,680 3,709	Cuttings/core (150) Air, detergent, and water C,D,GR,N,E,T,V,TR,VT	30 362 1,365	30.0 16.0 10.75	1,515 2,990 3,000	14.75 9.875 8.75	08-13-83	10-17-83
UE-25c#2 Hydrologic test hole	N 756,849 E 569,634 3,714	Cuttings/core (189) Air, detergent, and water C,D,GR,N,E,T,V,TR,VT	40 319 1,365	30.0 16.0 10.75	320 1,520 3,000	24.0 14.75 9.875	01-09-84	03-21-84
UE-25c#3 Hydrologic test hole	N 756,910 E 569,555 3,714	Cuttings/core (80) Air, detergent and water C,D,GR,N,E,T,V,TR,VT	39 313 1,323	30.0 16.0 10.75	315 1,520 3,000	24.0 14.75 9.875	03-20-84	06-11-84

Table 1-15. Drillholes within 10 km outside of the outline of the perimeter drift (page 2 of 17)

Hole number and purpose	Location coordinates and ground-level elevation (ft)	Sample type and depth (ft), media, and log type[b]	Casing Depth (ft)	Casing Diameter (in.)	Hole Depth (ft)	Hole Diameter (in.)	Spud date	Completion date
UE-25h#1[e] Horizontal core hole	N 748,353 E 574,461 3,409	Core (395) Air Air, detergent, and water Air foam C,G	20 240	4.5 3.5	20 240 400	6.25 3.937 3.032	12-10-82	01-30-83
UE-25p#1 Pre-Tertiary test hole	N 756,171 E 571,485 3,655	Cuttings/core (722) Air foam Polymer, bentonite, and water Air foam C,D,GR,N,E,T,V,TR, M,VT	36 325 1,564 1,487-4,256 1,371 1,355	24.0 16.0 10.75 7.625 Liner 1.9 Tubing 1.9 Tubing	341 1,598 4,279 4,322 5,900 5,923	17.5 14.75 9.875 6.875 6.75 6.125	11-13-82	05-24-83
UE-25 RF#1 Repository facility	N 762,190 E 570,890 3,689	Cuttings/core (18) Air, detergent, and water Air and water	99	7.625	98 145	9.875 8.75	01-23-84	02-08-84
UE-25 RF#2 Repository facility	N 758,800 E 570,335 3,657	Cuttings/core (12) Air, detergent, and water	29	7.625	52	8.75	01-18-84	01-23-84
UE-25 RF#3 Repository facility	N 765,575 E 571,100 3,658	Cuttings/core (149) Air foam Polymer and water	138	8.0	151	9.875	03-30-84	04-09-84
UE-25 RF#3B Repository facility	N 765,695 E 571,066 3,661	Cuttings/core (10) Air	106	5.5	106 111	6.0 3.937	07-18-85	07-23-85
UE-25 RF#4 Repository facility	N 762,091 E 572,063 3,637	Cuttings/core (136) Bentonite and water Polymer, bentonite, and water	0	0.0	36 280 306	9.875 6.75 3.9	02-10-84	02-28-84

Table 1-15. Drillholes within 10 km outside of the outline of the perimeter drift (page 3 of 17)

Hole number and purpose	Location coordinates and ground-level elevation (ft)	Sample type and depth (ft), media, and log type[b]	Casing		Hole		Spud date	Completion date
			Depth (ft)	Diameter (in.)	Depth (ft)	Diameter (in.)		
UE-25 RF#5 Repository facility	N 759,199 E 568,098 3,814	Cuttings/core (28) Polymer, bentonite, and water	112	8.0	112 122	9.875 3.937	05-24-84	05-30-84
UE-25 RF#7 Repository facility	N 768,804 E 571,171 3,756	Cuttings/core (25) Polymer, bentonite, and water	100	8.0	140 150	9.875 3.937	05-31-84	06-06-84
UE-25 RF#7A Repository facility	N 768,768 E 570,269 3,756	Cuttings/core (13) Polymer, bentonite, and water	18	8.0	150 153	9.875 3.987	06-29-84	07-06-84
UE-25 RF#8 Repository facility	N 765,631 E 568,790 3,788	Cuttings/core (82) Polymer, bentonite, and water	90	8.0	128	3.937	07-09-84	07-12-84
UE-25 RF#9 Repository facility	N 765,945 E 570,643 3,674	Core (106) Polymer, bentonite, and water	106	6.0	106	9.875	06-27-85	07-09-85
UE-25 RF#10 Repository facility	N 765,308 E 570,230 3,672	Cuttings/core (28) Polymer, bentonite, and water	60	6.0	60	9.875	07-24-85	07-29-85
UE-25 RF#11 Repository facility	N 765,622 E 570,435 3,669	Cuttings/core (44) Polymer, bentonite, and water	78	6.0	78	9.875	07-30-85	08-02-85
UE-25 UZ#4[f] Unsaturated zone	N 768,716 E 566,139 3,939	Cuttings/core (279) Air VT	60	5.5	367	4.25	09-06-84	10-10-84
UE-25 UZ#5[g] Unsaturated zone	N 768,591 E 566,135 3,952	Cuttings/core (270) Air VT	18	5.5	365	6.0	10-11-84	11-19-84
UE-25 UZN#1 Unsaturated zone-neutron	N 769,329 E 565,224 3,995	Cuttings/core (18) Air	50	5.5	50	6.0	10-17-84	10-18-84

Table 1-15. Drillholes within 10 km outside of the outline of the perimeter drift (page 4 of 17)

Hole number and purpose	Location coordinates and ground-level elevation (ft)	Sample type and depth (ft), media, and log type[b]	Casing Depth (ft)	Casing Diameter (in.)	Hole Depth (ft)	Hole Diameter (in.)	Spud date	Completion date
UE-25 UZN#2 Unsaturated zone-neutron	N 768,606 E 566,114 3,948	Cuttings Air	50	5.5	50	6.0	06-11-84	06-14-84
UE-25 UZN#3 Unsaturated zone-neutron	N 768,630 E 566,119 3,943	Cuttings Air	15	5.5	15	6.0	06-15-84	06-15-84
UE-25 UZN#4 Unsaturated zone-neutron	N 768,663 E 566,127 3,944	Cuttings Air	30	5.5	30	6.0	06-15-84	06-15-84
UE-25 UZN#5 Unsaturated zone-neutron	N 768,689 E 566,134 3,943	Cuttings Air	50	5.5	50	6.0	06-18-84	06-21-84
UE-25 UZN#6 Unsaturated zone-neutron	N 768,706 E 566,137 3,938	Cuttings Air	45	5.5	45	6.0	06-21-84	06-22-84
UE-25 UZN#7 Unsaturated zone-neutron	N 768,624 E 566,141 3,939	Cuttings Air	45	5.5	45	6.0	07-13-84	07-16-84
UE-25 UZN#8 Unsaturated zone-neutron	N 768,743 E 566,147 3,939	Cuttings Air	45	5.5	45	6.0	07-16-84	07-17-84
UE-25 UZN#9 Unsaturated zone-neutron	N 768,782 E 566,156 3,941	Cuttings Air	40	5.5	40	6.0	07-17-84	07-18-84
UE-25 UZN#10 Unsaturated zone-neutron	N 769,869 E 564,744 4,038	Cuttings/core (91) Air	94	5.5	94 99	6.0 4.25	12-02-85	12-04-85
UE-25 UZN#12 Unsaturated zone-neutron	N 768,651 E 566,695 3,907	Cuttings Air	50	5.5	50	6.0	07-23-84	07-24-84

Table 1-15. Drillholes within 10 km outside of the outline of the perimeter drift (page 5 of 17)

Hole number and purpose	Location coordinates and ground-level elevation (ft)	Sample type and depth (ft), media, and log type[b]	Casing Depth (ft)	Casing Diameter (in.)	Hole Depth (ft)	Hole Diameter (in.)	Spud date	Completion date
UE-25 UZN#13 Unsaturated zone-neutron	N 768,025 E 568,255 3,821	Cuttings Air	65	5.5	65	6.0	07-18-84	07-19-84
UE-25 UZN#14 Unsaturated zone-neutron	N 767,967 E 568,233 3,824	Cuttings Air	55	5.5	55	6.0	07-20-84	07-23-84
UE-25 UZN#18 Unsaturated zone-neutron	N 766,472 E 565,247 4,086	Cuttings Air	61	5.5	61	6.0	05-16-84	05-18-84
UE-25 UZN#28 Unsaturated zone-neutron	N 763,091 E 565,320 3,958	Cuttings Air	25	5.5	25 26	6.0 4.0	11-21-85	11-21-85
UE-25 UZN#29 Unsaturated zone-neutron	N 762,613 E 565,173 3,973	Cuttings/core (8) Air	35	5.5	35	6.0	11-26-85	11-27-85
UE-25 UZN#30 Unsaturated zone-neutron	N 762,048 E 565,233 3,959	Cuttings/core (4) Air	35	5.5	35	6.0	11-27-85	12-02-85
UE-25 UZN#56 Unsaturated zone-neutron	N 760,394 E 565,480 3,960	Cuttings Air	60	5.5	60	6.0	08-23-84	08-23-84
UE-25 UZN#60 Unsaturated zone-neutron	N 759,757 E 566,567 3,892	Cuttings Air	35	5.5	35	6.0	08-21-84	08-23-84
UE-25 UZN#85 Unsaturated zone-neutron	N 750,716 E 577,567 3,337	Cuttings Air	80	5.5	80	6.0	05-06-85	05-08-85
UE-25 UZN#97 Unsaturated zone-neutron	N 763,094 E 565,321 3,958	Cuttings/core (5) Air	60	5.5	60	6.0	11-25-85	11-26-85

Table 1-15. Drillholes within 10 km outside of the outline of the perimeter drift (page 6 of 17)

Hole number and purpose	Location coordinates and ground-level elevation (ft)	Sample type and depth (ft), media, and log type[b]	Casing Depth (ft)	Casing Diameter (in.)	Hole Depth (ft)	Hole Diameter (in.)	Spud date	Completion date
UE-25 UZNC#1[h] Unsaturated zone-neutron calibration	N 764,671 E 566,159 3,929	Cuttings Air	0	0.0	5	6.0	02-26-86	02-26-86
UE-25 UZNC#2[i] Unsaturated zone-neutron calibration	N 764,668 E 566,158 3,928	Cuttings Air	0	0.0	5	6.0	02-26-86	02-26-86
UE-25 WT#3 Water table hole	N 745,995 E 573,384 3,380	Cuttings/core (4) Air foam C,D,GR,N,E,VT	14 40 1,125	16.0 10.75 2.875 Tubing	14 41 1,142	48.0 14.75 8.75	04-29-83	05-25-83
UE-25 WT#4 Water table hole	N 768,512 E 568,040 3,829	Cuttings/core (10) Air, detergent, and water C,D,GR,N,E,VT	48 1,567	10.75 2.875 Tubing	50 1,580	14.75 8.75	05-28-83	06-06-83
UE-25 WT#5[j]								N
761,826	Cuttings	40	10.75	40	14.75	06-07-83	06-18-83	
Water table hole (abandoned)	E 574,250 3,559	Air foam			1,330	8.75		
UE-25 WT#6 Water table hole	N 780,576 E 564,524 4,307	Cuttings/core (7) Air, detergent, and water C,D,GR,N,E,V,VT	65 251 1,221	10.75 7.625 2.875 Tubing	69 250 1,250 1,257	14.75 9.875 6.75 6.25	06-20-83	06-29-83
UE-25 WT#12 Water table hole	N 739,726 E 567,011 3,527	Cuttings/core (8) Air foam C,D,GR,N,E,V,VT	70 1,276	10.75 2.875 Tubing	70 1,308	15.0 8.75	08-11-83	08-16-83
UE-25 WT#13 Water table hole	N 756,715 E 578,757 3,386	Cuttings/core (4) Air, detergent, and water C,D,GR,N,E,V,VT	222 1,136	10.75 2.875 Tubing	49 224 1,150 1,160	15.0 14.75 8.75 8.062	06-29-83	07-07-83

Table 1-15. Drillholes within 10 km outside of the outline of the perimeter drift (page 7 of 17)

Hole number and purpose	Location coordinates and ground-level elevation (ft)	Sample type and depth (ft), media, and log type[b]	Casing		Hole		Spud date	Completion date
			Depth (ft)	Diameter (in.)	Depth (ft)	Diameter (in.)		
UE-25 WT#14 Water table hole	N 761,651 E 575,210 3,530	Cuttings/core (10) Air foam Air, detergent, and water C,D,GR,N,E,V,VT	120 1,303	10.75 2.875 Tubing	126 1,310	15.0 8.75	08-17-83	09-30-83
UE-25 WT#15 Water table hole	N 766,117 E 579,806 3,553	Cuttings/core (5) Air, detergent, and water C,D,GR,N,E,V,VT	127 1,335	10.75 2.875 Tubing	130 1,360	14.75 8.75	11-12-83	11-22-83
UE-25 WT#16 Water table hole	N 774,420 E 570,395 3,971	Cuttings/core (10) Air, detergent, and water C,D,GR,N,E,V,VT	102 1,686	10.75 2.875 Tubing	108 1,710	14.75 8.75	11-02-83	11-10-83
UE-25 WT#17 Water table hole	N 748,420 E 566,212 3,689	Cuttings Air, detergent, and water C,D,GR,N,E,V,VT	55 1,376	10.75 2.875 Tubing	55 1,453	14.75 8.75	10-20-83	10-30-83
UE-25 WT#18[k] Water table hole	N 771,167 E 564,855 4,383	Cuttings/core (10) Air, detergent, and water C,D,GR,N,E,V,VT	86 1,965	10.75 2.875 Tubing	88 2,043	14.75 8.75	05-09-84	05-23-84
U-25 Seismic #1	N 778,913 E 560,457 not available	Cuttings Air, detergent, and water Air, polymer, detergent, and water	200	4.5 PVC	200	6.25	09-04-81	09-09-81
U-25 Seismic #2	N 779,089 E 560,363 5,107	Cuttings Air, polymer, detergent, and water	200	4.5 PVC	200	6.25	09-10-81	09-12-81
U-25 Seismic #3	N 779,265 E 560,268 5,111	Cuttings Air, detergent, and water Air, polymer, detergent, and water	200	4.5 PVC	200	6.25	09-04-81	09-08-81

Table 1-15. Drillholes within 10 km outside of the outline of the perimeter drift (page 8 of 17)

Hole number	Location coordinates and ground-level ele-	Sample type and depth (ft), media, and	Casing Depth	Casing Diameter	Hole Depth	Hole Diameter	Spud	Completion
U-25 Seismic #4	N 779,441 E 560,174 5,114	Cuttings Air, detergent, and water	200	4.5 PVC	200	6.25	09-03-81	09-04-81
U-25 Seismic #5	N 779,618 E 560,079 5,121	Cuttings Air, detergent, and water	200	4.5 PVC	200	6.25	09-02-81	09-03-81
U-25 Seismic #6	N 779,794 E 559,985 5,085	Cuttings Air, detergent, and water	200	4.5 PVC	200	6.25	09-01-81	09-02-81
U-25 Seismic #7	N 779,970 E 559,891 5,141	Cuttings Air, detergent, and water	200	4.5 PVC	200	6.125	08-30-81	09-12-81
U-25 Seismic #8	E 559,796 5,153	Air, detergent, and water	200	4.5 PVC	200	6.125	08-27-81	09-12-81
U-25 Seismic #9	N 780,323 E 559,702 5,162	Cuttings Air, detergent, and water	200	4.5 PVC	200	6.25	09-18-81	09-20-81
U-25 Seismic #10	N 780,499 E 559,607 5,171	Cuttings Air, polymer, detergent, and water	200	4.5 PVC	200	6.25	09-18-81	09-20-81

Table 1-15. Drillholes within 10 km outside of the outline of the perimeter drift (page 9 of 17)

Hole number and purpose	Location coordinates and ground-level elevation (ft)	Sample type and depth (ft), media, and log type[b]	Casing		Hole		Spud date	Completion date
			Depth (ft)	Diameter (in.)	Depth (ft)	Diameter (in.)		
U-25 Seismic #14	N 778,384 E 560,740 5,076	Cuttings Air, polymer, detergent, and water	200	4.5 PVC	200	6.125	09-17-81	09-17-81
U-25 Seismic #15	N 778,208 E 560,835 5,064	Cuttings Air, polymer, detergent, and water	200	4.5 PVC	200	6.25	09-15-81	09-16-81
U-25 Seismic #16	N 778,031 E 560,929 5,052	Cuttings Air, polymer, detergent, and water	200	4.5 PVC	200	6.25	09-14-81	09-15-81
U-25 Seismic #17	N 777,855 E 561,023 5,040	Cuttings Air, polymer, detergent, and water	200	4.5 PVC	200	6.25	09-13-81	09-13-81
U-25 Seismic #18	N 777,679 E 561,118 5,028	Cuttings Air, polymer, detergent, and water	200	4.5 PVC	200	6.125	09-11-81	09-12-81
U-25 Seismic #19	N 777,503 E 561,212 5,018	Cuttings Air, polymer, detergent, and water	200	4.5 PVC	200	6.25	09-09-81	09-11-81
U-25 Seismic #20	N 747,173 E 593,171 3,357	Cuttings Air, detergent, and water	140	8.0	140	12.25	04-18-84	04-19-84
U-25 Seismic #21	N 746,904 E 569,427 3,526	Cuttings Air, detergent, and water	140	8.0	5 140	15.0 10.625	04-19-84	04-20-84
U-25 Seismic #22	N 718,334 E 581,268 2,949	Cuttings Air, detergent, and water	139	8.0	5 144	15.0 12.25	04-23-84	04-26-84
U-25 Seismic #23	N 741,126 E 580,246 3,215	Cuttings Air, detergent, and water	140	8.0	145	12.25	04-26-84	04-27-84

Table 1-15. Drillholes within 10 km outside of the outline of the perimeter drift (page 10 of 17)

Hole number and purpose	Location coordinates and ground-level elevation (ft)	Sample type and depth (ft), media, and log type[b]	Casing Depth (ft)	Casing Diameter (in.)	Hole Depth (ft)	Hole Diameter (in.)	Spud date	Completion date
U-25 [illegible]	N 769,057 [illegible]	Cuttings [illegible]	140	8.0	5 [illegible]	15.0 [illegible]	05-01-84	05-03-84
US-25 #1 Seismic	N 762,631 E 565,424 4,259	Cuttings Polymer and water	50	6.0 Hose	53	8.75	09-23-83	09-26-83
US-25 #2 Seismic	N 762,403 E 566,427 4,316	Cuttings Polymer and water	50	6.0 Hose	53	8.75	09-21-83	09-23-83
US-25 #3 Seismic	N 762,075 E 572,454 3,620 L/O	Cuttings Polymer and water	50	6.0 Hose	52	8.75	09-20-83	09-21-83
US-25 #4 Seismic	N 762,458 E 567,853 3,800 L/O	Cuttings Polymer and water	50	6.0 Hose	50	8.75	09-19-83	09-19-83
US-25 #5 Seismic	N 762,432 E 567,853	Cuttings Polymer and water	50	6.0 Hose	52	8.75	09-16-83	09-16-83
US-25 #6	N 762,377	Cuttings	50	6.0	52	8.75	09-15-83	09-16-83

Table 1-15. Drillholes within 10 km outside of the outline of the perimeter drift (page 11 of 17)

Hole number and purpose	Location coordinates and ground-level elevation (ft)	Sample type and depth (ft), media, and log type[b]	Casing Depth (ft)	Casing Diameter (in.)	Hole Depth (ft)	Hole Diameter (in.)	Spud date	Completion date
US-25 #10 Seismic	N 762,251 E 570,112 3,724 L/O	Cuttings Polymer and water	50	6.0 Hose	50	8.75	09-08-83	09-08-83
US-25 #11 Seismic	N 762,226 E 570,111 3,724 L/O	Cuttings Polymer and water	50	6.0 Hose	52	8.75	09-07-83	09-07-83
US-25 #12 Seismic	N 762,198 E 570,894 3,688 L/O	Cuttings Polymer and water	50	6.0 Hose	52	8.75	09-06-83	09-07-83
US-25 #13 Seismic	N 762,168 E 570,891 3,688 L/O	Cuttings Polymer and water	50	6.0 Hose	52	8.75	09-02-83	09-06-83
US-25 #14 Seismic	N 762,137 E 571,675 3,653 L/O	Cuttings Polymer and water	50	6.0 Hose	50	8.75	08-31-83	09-02-83
US-25 #15 Seismic	N 762,106 E 571,670 3,654 L/O	Cuttings Polymer and water	50	6.0 Hose	50	8.75	08-30-83	08-31-83
US-25 #16 Seismic	N 762,046 E 572,453 3,620 L/O	Cuttings Polymer and water	50	6.0 Hose	50	8.75	08-30-83	08-30-83
US-25 #17 Seismic	N 761,986 E 573,627 3,576 L/O	Cuttings Polymer and water	50	6.0 Hose	50	8.75	08-29-83	08-29-83
S-25 #18 Seismic	N 761,895 E 574,709 3,545 L/O	Cuttings Polymer and water	50	6.0 Hose	50	8.75	08-26-83	08-29-83
US-25 #19 Seismic	N 761,746 E 576,242 3,499 L/O	Cuttings Polymer and water	50	6.0 Hose	50	8.75	08-25-83	08-26-83

Table 1-15. Drillholes within 10 km outside of the outline of the perimeter drift (page 12 of 17)

Hole number and purpose	Location coordinates and ground-level elevation (ft)	Sample type and depth (ft), media, and log type[b]	Casing Depth (ft)	Casing Diameter (in.)	Hole Depth (ft)	Hole Diameter (in.)	Spud date	Completion date
US-25 #20 Seismic	N 761,613 E 577,175 3,485 L/O	Cuttings Polymer and water	50	6.0 Hose	50	8.75	08-24-83	08-26-83
US-25 #21 Seismic	N 761,628 E 578,543 3,481	Cuttings Polymer and water	49	6.0 Hose	50	8.75	08-23-83	08-26-83
UE-29 UZN#92 Unsaturated zone-neutron	N 778,010 E 583,559 3,669	Cuttings/core (54) Air	105	5.5	105 120	6.0 4.25	01-13-86	01-15-86
J-12 Water well	N 733,509 E 581,011 3,128	Cuttings Cable tool	887	12.75	1,139	11.75	Unknown	1968
J-13 Water well (was USGS HTH #6)	N 749,209 E 579,651 3,218	Cuttings/core Air, detergent, and water	444 1,546 1,484-3,385	18.0 13.375 11.75 5.5 Liner	1,561 2,020 3,488	9.875 9.0 7.625	09-12-62	01-08-83
USW G-1[1] Geologic hole	N 770,500 E 561,000 4,349	Cuttings/core (5,708) Polymer and water Air foam Air, polymer, and water C,D,GR,N,E,V,M	280 290 1,016	13.375 7.625 4.5	6,000	3.875	03-12-80	09-17-80
USW GA-1 Geologic angle hole	N 779,365 E 559,247 5,187	Cuttings/core (403) Polymer and water	6 148	13.375 4.5	148 551	6.25 3.937	03-15-81	03-21-81
USW G-2 Geologic hole	N 778,824 E 560,504 5,098	Cuttings/core (5,716) Air, detergent, and water Air, polymer, detergent, and water Polymer and water C,D,GR,N,E,T,V,TR,VT	278 795	13.375 9.625	2,670 4,115 4,720 6,006	8.75 6.25 6.125 2.98	03-25-81	11-17-82

Table 1-15. Drillholes within 10 km outside of the outline of the perimeter drift (page 13 of 17)

Hole number and purpose	Location coordinates and ground-level elevation (ft)	Sample type and depth (ft), media, and log type[b]	Casing		Hole		Spud date	Completion date
			Depth (ft)	Diameter (in.)	Depth (ft)	Diameter (in.)		
USW G-3[m] Geologic hole	N 752,780 E 558,483 4,857	Cuttings/core (2,422) Air, detergent, and water Polymer and water	36	13.375	1,160 2,364	8.75 6.75	01-08-82	03-21-82
	Sidetrack	C,D,G,N,E,V,M,VT	2,598	5.5	1,144-2,600 2,608 5,031	8.75 4.75 3.937		
USW GU-3[n] Geologic unsaturated hole	N 752,690 E 558,501 4,857	Cuttings/core (2,613) Polymer and water C,D,GR,N,E,V,M,VT	34 1,144	13.375 5.5	1,144 1,768 2,644	6.75 3.937 2.98	01-26-82	06-12-82
USW H-1 /Instrument[o] Hydrologic test hole	N 770,254 E 562,388 4,274	Cuttings/core (764) Air, detergent, and water C,D,GR,N,E,T,V,TR,M	39 334 2,255	30.0 16.0 9.625	384 1,740 2,257 6,000	15.0 13.25 12.25 8.75	09-03-80	07-06-82
USW H-3 Hydrologic test hole	N 756,542 E 558,452 4,866	Cuttings Air, detergent, and water C,D,GR,N,E,T,V,TR,M,VT	29 126 2,600	30.0 16.0 10.75	130 2,650 4,000	26.0 14.75 8.75	01-27-82	03-19-82
USW H-6 Hydrologic test hole	N 763,299 E 554,075 4,272	Cuttings/core (221) Air, detergent, and water C,D,GR,N,E,T,V,TR,M,VT	31 311 1,906 2,468 Tubing 1,752	30.0 16.0 10.75 2.875 1.9 Tubing	1,912 3,990 4,002	14.75 8.75 6.125	08-07-82	10-28-82
USW UZ-1/ Instrument[p] Unsaturated zone test hole	N 771,276 E 560,221 4,426	Cuttings/core (44) Air vacuum C,D,GR,N,E,VT	40	42.0	42 97 101 1,265 1,269 1,270	48.0 36.0 24.0 17.5 15.0 9.25	04-27-83	07-01-83

Table 1-15. Drillholes within 10 km outside of the outline of the perimeter drift (page 14 of 17)

Hole number and purpose	Location coordinates and ground-level elevation (ft)	Sample type and depth (ft), media, and log type[b]	Casing		Hole		Spud date	Completion date
			Depth (ft)	Diameter (in.)	Depth (ft)	Diameter (in.)		
USW UZ-6s Unsaturated zone test	N 759,909 E 558,050 4,949	Cuttings/core (151) Air VT	3	7.625	396 481 519	8.344 4.25 3.99	04-23-85	09-09-85
USW UZ-13 Unsaturated zone test	N 751,953 E 558,489 4,816	Cuttings/core (88) Air VT	330	5.5	410 430	6.0 3.937	01-24-85	04-19-85
USW UZ-N46 Unsaturated zone-neutron	N 772,262 E 559,748 4,501	Cuttings/core (75) Air	99	5.5	99	6.0	01-21-86	01-31-86
USW UZ-N47 Unsaturated zone-neutron	N 771,968 E 559,784 4,480	Cuttings/core (24) Air	85	5.5	85 86	6.0 4.25	01-24-86	01-29-86
USW UZ-N65 Unsaturated zone-neutron	N 758,627 E 562,537 4,372	Cuttings Air	50	5.5	50	6.0	11-27-84	11-27-84
USW UZ-N66 Unsaturated zone-neutron	N 758,434 E 561,881 4,356	Cuttings Air	50	5.5	50	6.0	11-27-84	11-28-84
USW UZ-N67 Unsaturated zone-neutron	N 753,634 E 563,799 3,920	Cuttings Air	25	5.5	25	6.0	07-25-84	07-25-84
USW UZ-N68 Unsaturated zone-neutron	N 753,962 E 564,006 3,925	Cuttings Air	55	5.5	55	6.0	07-25-84	07-25-84
USW UZ-N69 Unsaturated zone-neutron	N 754,461 E 564,402 3,918	Cuttings Air	35	5.5	35	6.0	07-26-84	07-26-84
USW UZ-N70 Unsaturated zone-neutron	N 769,251 E 560,165 4,542	Cuttings/core (3) Air	35	5.5	35	6.0	02-06-86	02-10-86

Table 1-15. Drillholes within 10 km outside of the outline of the perimeter drift (page 15 of 17)

Hole number and purpose	Location coordinates and ground-level elevation (ft)	Sample type and depth (ft), media, and log type[b]	Casing		Hole		Spud date	Completion date
			Depth (ft)	Diameter (in.)	Depth (ft)	Diameter (in.)		
USW UZ-N77 Unsaturated zone-neutron	N 755,526 E 554,397 3,901	Cuttings Air	50	5.5	50	6.0	11-30-84	11-30-84
USW UZ-N78 Unsaturated zone-neutron	N 757,558 E 556,262 4,182	Cuttings Air	30	5.5	30	6.0	12-10-84	12-11-84
USW UZ-N79 Unsaturated zone-neutron	N 757,733 E 556,334 4,155	Cuttings Air	32	5.5	32	6.0	12-07-84	12-10-84
USW UZ-N80 Unsaturated zone-neutron	N 757,634 E 557,201 4,332	Cuttings Air	52	5.5	52	6.0	12-06-84	12-07-84
USW UZ-N81 Unsaturated zone-neutron	N 757,807 E 557,595 4,065	Cuttings Air	70	5.5	70	6.0	12-03-84	12-06-84
USW UZ-N82 Unsaturated zone-neutron	N 757,498 E 554,690 3,975	Cuttings Air	40	5.5	40	6.0	11-30-84	12-03-84
USW UZ-N83 Unsaturated zone-neutron	N 760,624 E 556,349 4,157	Cuttings Air	70	5.5	70	6.0	12-12-84	12-13-84
USW UZ-N84 Unsaturated zone-neutron	N 760,717 E 555,888 4,112	Cuttings Air	45	5.5	45	6.0	12-12-84	12-19-84
USW UZ-N86 Unsaturated zone-neutron	N 760,615 E 556,460 4,172	Cuttings Air	30	5.5	30	6.0	12-18-84	12-18-84
USW UZ-N87 Unsaturated zone-neutron	N 760,714 E 555,887 4,112	Cuttings Air	45	5.5	45	6.0	12-20-84	12-20-84

Table 1-15. Drillholes within 10 km outside of the outline of the perimeter drift (page 16 of 17)

Hole number and purpose	Location coordinates and ground-level elevation (ft)	Sample type and depth (ft), media, and log type[b]	Casing Depth (ft)	Casing Diameter (in.)	Hole Depth (ft)	Hole Diameter (in.)	Spud date	Completion date
USW UZ-N88 Unsaturated zone-neutron	N 760,797 E 556,551 4,202	Cuttings Air	30	5.5	30	6.0	12-17-84	12-17-84
USW UZ-N89 Unsaturated zone-neutron	N 760,610 E 555,589 4,090	Cuttings Air	45	5.5	45	6.0	12-19-84	12-19-84
USW UZ-N90 Unsaturated zone-neutron	N 760,608 E 555,587 4,090	Cuttings Air	45	5.5	45	6.0	12-14-84	12-17-84
USW UZ-N93 Unsaturated zone-neutron	N 759,584 E 558,321 4,924	Cuttings Air	40	5.5	40	6.0	07-27-84	07-27-84
USW VH-1 Volcanic hydrology hole	N 743,356 E 533,626 3,161	Core/cuttings (2,391) Air, detergent, and water C,D,GR,N,E,T,V	48 911	9.625 7.625	912 2,501	8.75 6.25	10-28-80	02-18-81
USW VH-2 Volcanic hydrology hole	N 748,319 E 526,264 3,197	Core/cuttings (3,977) Air, polymer, detergent, and water C,D,GR,N,E,V	19 198 720 3,986	13.375 9.625 5.5 1.9 Tubing	20 197 716 4,000	17.5 12.25 8.75 3.937	02-15-83	04-27-83
USW WT-1 Water table hole	N 753,941 E 563,739 3,942	Cuttings/core (9) Air, detergent, and water C,D,GR,N,E,VT	33 1,665	10.75 2.875 Tubing	34 1,689	26.0 8.75	04-28-83	05-18-83
USW WT-7 Water table hole	N 755,570 E 553,891 3,927	Cuttings/core (10) Air, detergent, and water C,D,GR,N,E,V,VT	52 1,579	10.75 2.875 Tubing	53 1,610	14.75 8.75	07-19-83	07-26-83
USW WT-10 Water-table hole	N 748,771 E 553,302 3,685	Cuttings/core (13) Air, detergent, and water C,D,GR,N,E,V,VT	114 1,321	10.75 2.875 Tubing	116 1,413	14.75 8.75	07-26-83	08-02-83

Table 1-15. Drillholes within 10 km outside of the outline of the perimeter drift (page 17 of 17)

Hole number and purpose	Location coordinates and ground-level elevation (ft)	Sample type and depth (ft), media, and log type[b]	Casing Depth (ft)	Casing Diameter (in.)	Hole Depth (ft)	Hole Diameter (in.)	Spud date	Completion date
USW WT-11 Water-table hole	N 739,070 E 558,377 3,591	Cuttings/core (6) Air, detergent, and water C,D,GR,N,E,V,VT	45 1,365	10.75 2.875 Tubing	45 1,446	14.75 8.75	08-03-83	08-09-83

[a]L/O=surveyed prior to drilling.

[b]Log types are identified as follows: C = caliper, D = density, E = electric, GR = gamma ray, M = magnetometer, N = neutron, T = temperature, TR = tracer, V = velocity, and VT = video tape.

[c]UE-25a#1 has drill rods, core barrel, and bit left in hole from 1,264.5 ft to 1,297 ft and USGS fluid probe at 2,495 ft.

[d]UE-25a#4/Instrument instrumented, stemmed, and grouted from 499 to surface.

[e]UE-25h#1 has core bit pieces left in the hole at unknown depth.

[f]UE-25 UZ-4, 7 ft of casing left in hole below 140 ft.

[g]UE-25 UZ-5, 2-ft casing shoe left in hole at unknown depth.

[h]UE-25 UZNC-1, backfilled to surface. Ditch was dug through hole location.

[i]UE-25 UZNC-2, backfilled to surface. Ditch was dug through hole location.

[j]UE-25 WT#5, 18 ft of fishing equipment left in hole below 1,018 ft.

[k]UE-25 WT#18, geophysical logging (electric) tool left in hole below 200 ft.

[l]USW G-1 has a Sandia instrument in the hole.

[m]USW G-3, the original hole was plugged with cement from 1,362 ft to 1,160 ft; radioactive logging source lost below 1,247 ft.

[n]USW GU-3 has a Sandia instrument in the hole.

[o]USW H-1/Instrument, instrumented and grouted from 5,950 to 2,207 ft.

[p]USW UZ-1/Instrument, drilling equipment left in hole at 1,243 ft. Hole plugged with cement to 1,221 ft. Hole instrumented and grouted from 1,213 to surface.

Rotary drilling rigs were used to drill all drillholes listed with the exception of well J-12, which was drilled with cable tools. The cable tool system uses a hammer type bit on a steel cable to break up the rock.

Cuttings are removed with a bailer on a wire line. Rotary drilling uses a bit or corehead on the bottom of a steel drill pipe string to grind up the rock. It requires a circulating medium to carry drill bit cuttings to the surface while cleaning the bottom of the drillhole. Before June 1985, most drillhole circulating systems for the Yucca Mountain Project used a fluid with direct circulation down through the drill pipe and bit then back to the surface outside the drill pipe. Air was used with a fluid in some drillholes to lower the density. With certain additives this created a stiff foam. Various drilling additives such as bentonite, polymer, and detergent were used to alter viscosity, density, and other characteristics of the circulation medium. Since June 1985, most of the drilling has been limited to the unsaturated zone where air injection or vacuum has been used to remove cuttings to avoid adding fluid to the formation.

Drilling fluid was lost to the formation in varying amounts when fluid was used. Fluid loss was greatest at drillhole USW-G1, located north of the proposed outline of the perimeter drift. It was cored from 292 ft to the total depth of 6,000 ft. Drilling fluid return to the surface was intermittent with the daily losses averaging 488 barrels per day for a total of 44,000 barrels. The fluid loss was greatest below the depth of 3,200 ft after the pump pressure was increased. This loss was in the lower part of the Crater Flat Tuff and in deeper zones. The fluid loss was attributed to high fracture permeability. In a preliminary assessment report of the geomechanical characteristics in drillhole USW G-1, it was concluded that the pressure exerted by the drilling fluid was sufficient to induce hydraulic fracturing and to reopen favorably oriented preexisting fractures, and subsequently to inject drilling fluid into the fractures (Ellis and Swolfs, 1983). Data from hydrofracture tests conducted in this drillhole and vertical fractures detected by the televiewer, that were interpreted as drilling-induced, support these conclusions (Ellis and Swolfs, 1983). The fluid loss in drillhole USW G-1 and other drillholes in the area would be expected to have only localized, temporary, and minor effects on the hydrologic conditions. The five drillholes within the outline of the perimeter drift that were drilled using some fluid lost only a moderate percentage to the formation. Fluid loss ranged from less than 1,000 barrels total for drillhole USW WT-2 up to 16,000 barrels total for drillhole USW H-5. A major part of the fluid used was circulated back out of the drillhole to the reserve pit.

1.6.1.3 Drillhole histories

Detailed drillhole construction histories have been written for all

DECEMBER 1988

Drillhole histories are used as a reference to determine more accurately the status of a drillhole when specific geophysical logs were run or when specific hydrologic tests were made. The availability of such information improves the interpretation of these types of site investigations.

A typical drillhole history reports all activities that took place in a specific drillhole. It includes the data summary and time breakdown sheets, daily activity entries, cementing records, fluid use, coring records, geophysical log index, drillhole deviation surveys, and review of drillhole conditions. The majority of data used to generate a drillhole history have

1.6.2 GEOPHYSICAL LOGGING

1.6.2.1 Summary of logging activities

Geophysical logs have been run in many of the Yucca Mountain drillholes to determine conditions during drillhole construction and to help define formation characteristics. Microfiche copies of the logs from the commercial [illegible]

DEPARTMENT OF THE INTERIOR
UNITED STATES GEOLOGICAL SURVEY

PREPARED ON BEHALF OF
THE U.S. DEPARTMENT OF ENERGY

OPEN-FILE REPORT
84-789 PLATE 1
SHEET 1 OF 2

DECEMBER 1988

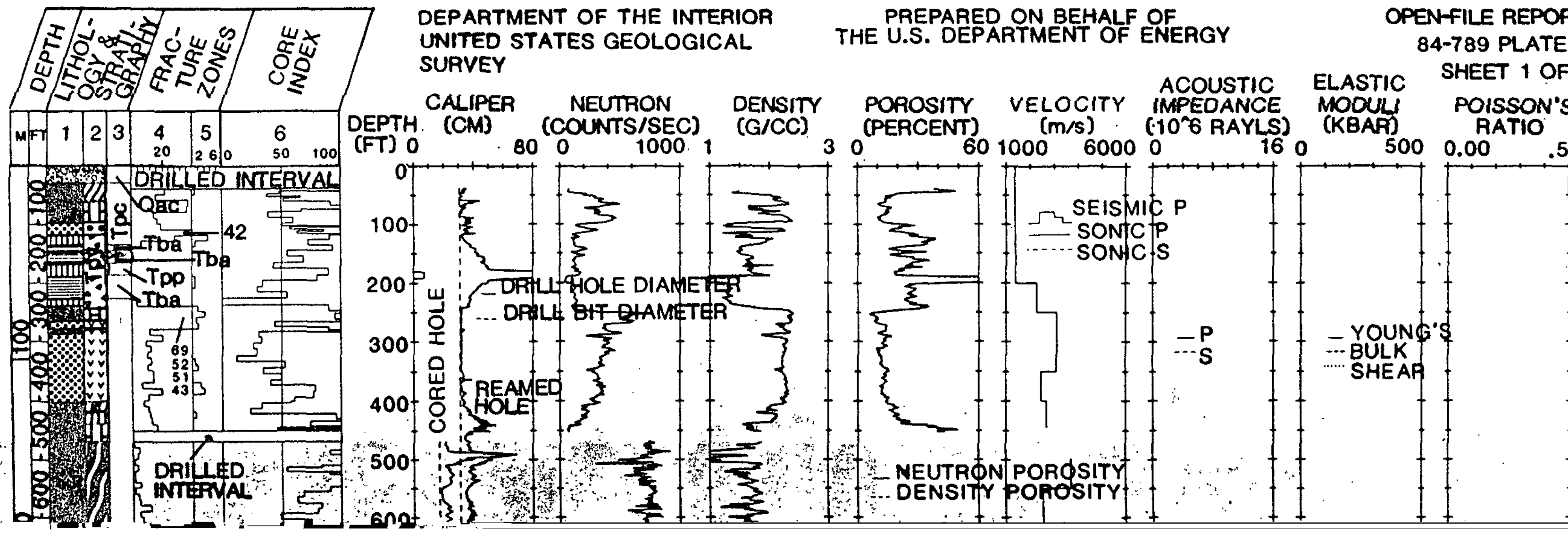

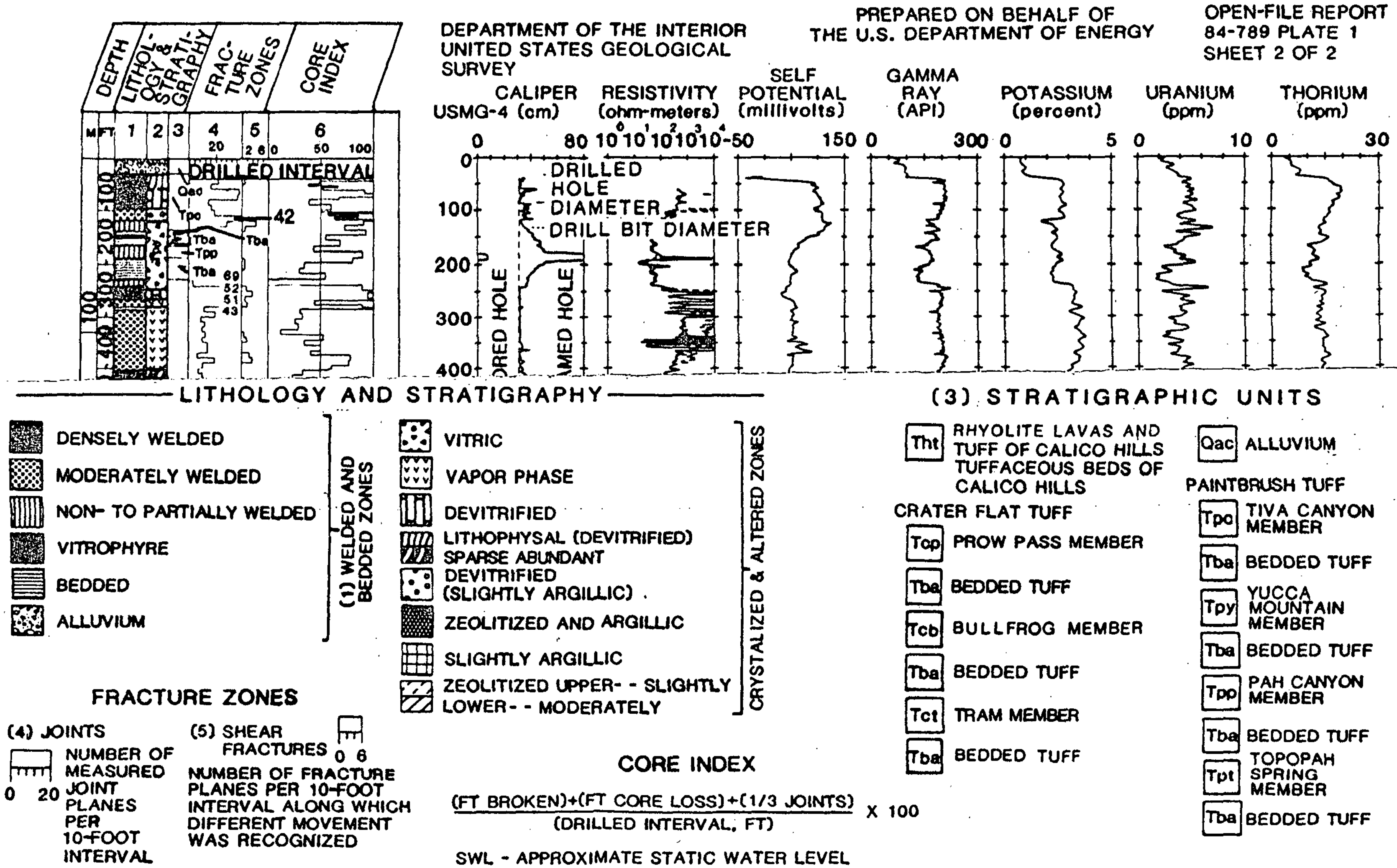

Figure 1-73b. Graphic log showing lithologic, structural, and geophysical features of drillhole USW G-4. Modified from Spengler and Chornack (1984).

DECEMBER 1988

Calibration checks and repeat log sections were recorded on the logs to document quality control and accuracy. Standard logging company procedures

1.6.2.2.2 Neutron logs

Neutron logs include the epithermal neutron porosity (ENP) log, neutron-neutron log (NNL), and neutron borehole compensated (NBC) log. Neutron tools measure the hydrogen index. A plutonium-beryllium source, which emits neutrons, is inserted in the tool. These neutrons are moderated primarily by the hydrogen in the water-filled pore space in the formation matrix. A helium-3 gas discharge or scintillation-type detector counts the thermal neutrons. The ENP tool uses a cadmium shield around the detector, which excludes the lower energy thermal neutrons (Hearst and Nelson, 1985). The NBC tool uses the ratio of count rates from a short and a long detector to determine borehole porosity (Dresser Atlas, 1982).

Muller and Kibler (1985) provide the following discussion of neutron log operation. The primary mechanism for neutron scatter and loss of energy is collision with hydrogen nuclei. For most rocks, essentially all of the hydrogen is bound in water molecules, thus making the neutron log a good indicator of the formation water content. In general, high neutron count rates correspond to low water content and low count rates to high water content.

Below the static water level, where the assumption of total saturation [redacted] reliable porosity for many rock types. Porosity calculated from calibrated, single-detector neutron logs is generally not as reliable as compensated neutron porosity unless core data exist that either confirm the single-detector neutron porosity or can be used to develop corrected calibration curves for the specific rocks encountered in the drillhole.

Above the static water level, in the unsaturated zone, the neutron log count rate can be used as an indicator of relative variations in formation water content. Calibrations exist for many rock types to convert the count variance between runs to be considered accurate enough for quantitative calculations.

Calibration of the NBC log was accomplished by inserting the tool through the hollow center of an aluminum tank filled with water and antifreeze. The data were checked against calibration data traceable to the American Petroleum Institute (API) test pits located at Houston, Texas.

1.6.2.2.3 Gamma ray logs

The tuffs at Yucca Mountain characteristically exhibit high total gamma radiation levels compared with sedimentary rocks. Relatively high uranium radiation levels may mask the radiation from uranium concentrated in cemented and filled fractures so that the individual fracture identification with the uranium trace has not been feasible. However, an overall increase in uranium level through a highly fractured interval may indicate cementing and filling of the fractures. The standard gamma ray log is often run simultaneously with other logs and is used to accurately correlate depths between logs in the same drillhole (Muller and Kibler, 1985). Spectral gamma ray logs (particularly the potassium trace) exhibit similar character between drillholes in some lithostratigraphic units, making spectral gamma logs useful for lithologic identification and stratigraphic correlation.

The basic parameter recorded by the gamma ray (G/R) log is the radiation produced by the decay of radioactive nuclei in the formation. The G/R tool measures the amount of radiation by counting the number of gamma rays that are detected by either a Geiger-Muller tube or a scintillation-type detector. They detect the ionization produced when a gamma ray interacts with matter. The signal produced is counted by surface electronic equipment. A normal gamma ray tool is field calibrated before and checked after a logging run with a 20 microcurie radium source. The gamma ray count was to be used qualitatively (Dresser Atlas, 1982).

The spectral gamma ray (Spectralog) sonde like the standard gamma ray log measures the decay of naturally occurring elements in the formation. This tool counts the emitted gamma rays detected by a sodium iodide crystal. In addition to total gamma ray count, the tool measures the gamma rays emitted specifically by potassium, uranium, and thorium. The curves produced are used to identify minerals and to correlate marker zones (Hearst and Nelson, 1985).

The sonde was calibrated before logging and checked after logging by placing it adjacent to measured concentrations of potassium, uranium, and thorium.

1.6.2.2.4 Temperature logs

A temperature logging tool is used to determine borehole temperatures. The primary sensing element in a temperature log is the thermistor. The thermistor is a semiconductor that decreases in resistance as the temperature increases (Hearst and Nelson, 1985). The thermistor was calibrated before logging by immersion in two containers of water that were at different temperatures and the resulting readings compared to similar checks with a calibrated thermometer. Two maximum-recording thermometers (MRT) were strapped to the logging cable. After logging, the MRT were compared to the maximum temperature reading as shown on the log. The log was required to have no more than a one degree Fahrenheit variance between runs to be considered accurate.

1.6.2.2.5 Tracer logs

Tracer surveys run in the Project drillholes were composed of several logs: a temperature log, a casing collar locator log (CCL), and a gamma ray (G/R) log. The temperature log was used to help determine geothermal gradient, the time elapsed since fluid circulation stopped, thermal conductivity, the flow of fluids from the formation to borehole or vice versa, and the location of cement placed in the drillhole. The temperature tool used for tracer logs was surface calibrated, as described in Section 1.6.2.2.4, and the data were used qualitatively.

The CCL tool was used to provide depth control during tracer surveys. The tool consisted of a wire-wound iron core with magnets mounted on each end of the iron core. When the amount of iron near the tool changes, a current flows through the coil. This current is shown on the log as a deflection pip. Its primary use is to detect casing collars. It can also be used to locate casing perforations and tubing packers. The CCL data were used qualitatively.

A 1.375-in. (3.5-cm) G/R tool was used in the tracer surveys. The gamma count was tailored to the job and the G/R tool was used to count this induced radiation; all data were used qualitatively. A surface electronic check was used to maintain quality.

The ejector was loaded with 50 to 100 millicuries of iodine-131 in 100 to 150 milliliters of water. During the job, small amounts of liquid were ejected into the drillhole and movement was traced (Bird and Dempsey, 1955).

1.6.2.2.6 Electrical resistivity log

Logs run in Project drillholes include the electric survey (ES), the dual induction focused log (DIFL), the induction survey (IS), and the induction electrical survey (IES). The basic parameters measured were the resistivity or the conductivity (the reciprocal of resistivity) of the formation surrounding the borehole. The ES logs require fluid in the drillhole for electrode contact. The IES can be run in a dry or wet drillhole and measures conductivity. The ES and IES are used to correlate stratigraphy, to identify lithology, and help determine water saturation and formation water resistivity.

The ES measures resistivity using three different spacings of downhole electrodes. A constant current flows radially outward from one electrode. Measurement of the voltages at various spacings furnishes data for three resistivity curves. A formation spontaneous or self-potential (SP) curve is also shown on the log. Calibration of the ES was accomplished by calibrating of internal circuits in surface electronic panels. The logs were considered acceptable when the before-logging calibrations and the after-logging checks were within 5 percent.

The IES and DIFL tools use alternating magnetic fields to induce eddy currents in the formation. These eddy currents have their own magnetic fields, which are proportional to the conductivity of the formation. Surface equipment reciprocates conductivity to supply resistivity to the recorder (Dresser Atlas, 1982). In wet drillholes the IES tool also produces standard 16-in. (41 cm) normal resistivity and an SP curve. The calibration procedure used a loop of known resistivity placed around the tool. The DIFL adds 30-in. (76 cm) and 64-in. (162 cm) resistivity curves. Calibration procedures were performed before and checked after the survey. A 5 percent difference was the maximum allowed between before- and after-checks for data to be accepted.

1.6.2.2.7 Sonic velocity logs

Velocity logs include three-dimensional (3-D) velocity, acoustic borehole compensated (ABC), and lock-in geophone records of vibroseis energy. The 3-D log is a film recording of the complete acoustic wave train as it is propagated along the boundary of the fluid-filled borehole. Primary uses include cement bond evaluations, fracture studies, and input for calculations of elastic properties of rocks (Dresser Atlas, 1982). Calibrations for these logs were performed by surface electronic equipment. Checks were made of the wave train by comparing it to velocity of known standards.

The ABC log produces a curve of reciprocal velocity versus depth. Multiple transmitters and receivers are used to minimize borehole effects. A 3-D type presentation from one transmitter receiver pair is also produced (Dresser Atlas, 1982; Nelson and Hearst, 1985).

The basic parameter measured with the lock-in geophone record of vibroseis energy is the travel time of sound waves through the formation in order to obtain a time-depth relationship. The primary uses include calibration of seismic data for estimates of the depth to geologic horizons and the comparison of seismic characteristics with other drillholes. The seismic signal is generated near the borehole on the ground surface with a mechanical vibrator or other source of seismic energy. Seismic frequencies are relatively low, typically lower than 100 Hz (Muller and Kibler, 1985). The resulting plot of velocity versus depth has a square, step-like appearance and indicates the average velocity of the formation through the interval between discrete geophone depths. Seismic velocity determined by this method is a large-volume measurement that includes average effects of fracturing, jointing, lithophysae, inhomogeneities, and in some cases, refraction effects due to stratigraphy and structure (Muller and Kibler, 1985). The log is obtained by lowering a geophone into the borehole and coupling it to the formation. A surface energy source is used to induce sound waves in the formation. The geophone records the time of arrival of [redacted] is repeated. Calibration was done internally by surface electronic equipment.

1.6.2.2.8 Caliper logs

Caliper logs were run with both six-arm and three-arm tools that measured the borehole diameter. The three-arm tool, 1.625-in. (4 cm) outside diameter, was used very sparingly for logging through tubing. The six-arm tool that was most widely used has six independent spring loaded arms located at 60-degree intervals around the circumference of the tool. Each set of opposing arms is linked electronically to display a borehole diameter. The three borehole diameters are also linked electronically to give an average diameter. Uses of the caliper include evaluation of the borehole configuration, identification of caved intervals, calculation of borehole volume to determine cement displacement and liquid fill up, correction of other log data, and location of good formation packer or plug seats. Drillhole volume, obtained from integration of the average borehole curve, was indicated by marks on the log at intervals equivalent to volume units.

Calibration was accomplished by comparing the recorded diameter of each set of arms to the known diameter of two steel rings, one ring that was the closest to borehole diameter, and one that was at least 10 in. larger. The arm diameters were also recorded while opened to their maximum. The three arm positions were recorded on the log before and after logging. A measured accuracy of 0.25 in. (0.6 cm) was required between calibrations before and after logging.

The gravimeter log is created by measuring the gravity within the borehole at stationary levels. Different levels of gravity change the pendulum position. The change in position also affects the amount of light striking the photoelectric cell and thereby affects the voltage. The different energy level is recorded on a strip chart and is used to calculate the exact gravity value.

1.6.2.2.10 Magnetic logs

The magnetometer log is a measure of the magnetic properties of the strata. These properties are a function of the earth's magnetic field strength and polarity at the time of deposition or the time the rock last cooled below the curie point (Hearst and Nelson, 1985) and the amount and size of the magnetic minerals in the rock (Hagstrum et al., 1980a).

The magnetic fields of strata are measured by passing a multiturn coil through the borehole. This causes a current to be induced in the coil. The amount of current is directly proportional to the field strength (Broding et al., 1952).

A slightly modified Scientrex MP-2 portable proton precision magnetometer can be used to create a total magnetic intensity (TMI) log. The TMI log creates a step-like pattern based on the remanent magnetic strength and polarity of the strata. The magnetometer log is of value since the earth's magnetic field affects the whole area of deposition equally. The magnetic signature of a single lithologic formation is, therefore, similar throughout the area of deposition. The TMI log can be of great value in identifying and correlating formations between different boreholes (Douglas and Millett, 1978).

Magnetic susceptibility logs have been run for the USGS using a single coil magnetometer. This log measures the ability of the lithology to induce current in the detector coil. The log can be used in a manner similar to the TMI log in identifying different lithologies. The magnetic susceptibility log, however, appears to be sensitive to mineral size and composition and does not have as repeatable a signature throughout the formation (Hagstrum et al., 1980a).

The induced polarization log is made by measuring the voltage of the formation with a potential electrode 10 cm from an oscillating on-off current electrode during the off period.

Contact between conductive minerals and connate fluids can store electrical energy; conductive minerals include cation-rich clays, zeolites, and most sulfides. A steady current applied to such a mineral water system creates a polarized voltage. This voltage decays through time when the charging current ceases (Hearst and Nelson, 1985). The induced polarization [illegible]

1.6.3 TESTING IN DRILLHOLES

Drillholes drilled at the Yucca Mountain site in support of the Project can be categorized by types of data they were primarily designed to furnish. The drillholes are listed with general information in Tables 1-14 and 1-15 (Section 1.6.1.2). Since 1978 when drillhole UE-25a#1, the first Project drillhole, was completed at Yucca Mountain, the USGS, and various national laboratories have been engaged in an extensive exploratory drilling program to define the geology and the hydrology of the proposed site. Geologic and hydrologic information was obtained from these drillholes. Normally, the drillholes were planned to gather specific types of information, either geologic or hydrologic, but many of the drillholes were interdisciplinary and were designed to furnish both types of data. The reports on hydrologic testing are listed in Appendix C.

The geologic drillholes were cored and drilled to obtain subsurface information about the stratigraphy and structure of the Yucca Mountain site. Core and drill bit cuttings were examined for lithologic data and for detailed fracture data. This information was used to help determine the stratigraphic and structural setting within the repository site. Selected samples of core were preserved for various laboratory tests. Core and cuttings have been stored for future reference in the Project core library. Information was obtained on mechanical properties of the different rock types penetrated by the drillholes. This information was used to design future drillholes and to plan the mining of the repository. Where applicable, water-level measurements were made at the completion of each drillhole. Table 1-16 lists the geologic drillholes with associated published reports.

The hydrologic drillholes were drilled and cored to study hydrologic characteristics in the vicinity of the site. A detailed discussion of hydrologic information on the proposed site is presented in Chapter 3. During the construction of these drillholes, core and drill bit cuttings were examined for stratigraphic and structural information and then stored for future reference. Representative samples were also collected for laboratory analysis. Water level measurements were taken during the drilling and at the completion of the drilling of these drillholes. Hydrologic tests were conducted in these drillholes to help interpret the hydrology of the region (Sections 3.6.1 and 3.9.2). Hydrologic tracejector, surging, swabbing, and pumping tests were employed in this task to identify water-bearing zones, determine composite hydraulic head, and determine composite water producing capacity of the drillhole. Various combinations of these tests were conducted in the hydrologic drillholes. In addition to these tests, packer-injection and shut-in tests were used to isolate stratigraphic and hydrologic intervals for further detailed testing to determine the hydraulic head and permeability of the individual zones. Table 1-16 lists the hydrologic drillholes with associated published reports.

A series of drillholes, designated WT, was drilled to obtain measurements of the static water level in the repository area. The drill bit cuttings and core from these water table drillholes were examined for stratigraphic and structural information. These drillholes are monitored for fluctuations in static water level (Robinson, 1984).

Table 1-16. Drillholes at the Yucca Mountain site and published reports

Drillhole designation	Type of drillhole	Report
UE-25a#1	Geologic	Anderson (1981) Carroll et al. (1981) Spengler et al. (1979) Sykes et al. (1979)
UE-25a#4	Geologic	Spengler and Rosenbaum (1980)
UE-25a#5	Geologic	Spengler and Rosenbaum (1980)
UE-25a#6	Geologic	Spengler and Rosenbaum (1980)
UE-25a#7	Geologic	Spengler and Rosenbaum (1980)
UE-25b#1	Hydrologic	Lahoud et al. (1984)
UE-25h#1	Geologic corehole	Norris et al. (1986)
UE-25p#1	Geologic and hydrologic	Craig and Johnson (1984) Craig and Robison (1984)
USW G-1	Geologic	Bish (1981) Healey et al. (1984) Lappin et al. (1982) Spengler et al.(1981) Waters and Carroll (1981) Zoback et al. (1985)
USW G-2	Geologic	Caporuscio et al. (1982) Maldonado and Koether (1983) Price et al. (1984)
USW G-3/ USW GU-3	Geologic	Scott and Castellanos (1984) Vaniman et al. (1984b)
USW G-4	Geologic	Bentley (1984) Spengler and Chornack (1984) Bish and Vaniman (1985) Byers (1985)
USW VH-1	Volcanic and hydrologic	Carr (1982)
USW H-1	Hydrologic	Rush et al. (1983) Rush etal. (1984) Weeks and Wilson (1984)

Table 1-16. Drillholes at the Yucca Mountain site and published reports (continued)

Drillhole designation	Type of drillhole	Report
USW H-3	Hydrologic	Levy (1984) Thordarson et al. (1984)
USW H-4	Hydrologic	Levy (1984) Whitfield et al. (1984)
USW H-5	Hydrologic	Levy (1984) Bentley et al. (1983)
USW H-6	Hydrologic	Craig et al. (1983)
J-12	Water well	Young (1972)
J-13	Geologic	Byers and Warren (1983)
[illegible]	[illegible]	[illegible]
		Oversby and Knauss (1983) Thordarson (1983) Wolfsburg et al. (1979)
[illegible]	[illegible]	[illegible]

Several hydrologic studies undertaken at the Yucca Mountain site have dealt with the unsaturated (vadose) zone. The unsaturated-zone drillholes, designated UZ, were drilled using only air for drillhole cleaning to eliminate contamination by drilling fluids. The drill bit cuttings and core from these drillholes were logged for stratigraphic and structural information. Samples were preserved for special tests. After completion, these drillholes will be instrumented for in situ unsaturated-zone studies. Section 3.9.2.1 discusses the unsaturated zone.

Two drillholes, USW VH-1 and USW VH-2, were drilled and cored to explore the volcanic stratigraphy and the hydrology of the Crater Flat area. The core from these drillholes was examined to gather lithologic information and to determine the tectonic-structure history of the Crater Flat area (Carr, 1982). Water-level measurements were made during drilling and at the completion of the drillholes. Pumping tests were conducted in these drillholes to obtain information about the hydrology of the Crater Flat area. Water produced from drillhole USW VH-2 has been used for nearby milling ponds for gold ore that was mined at Bare Mountain. The mine is approximately 15 km west of the perimeter drift outline.

Seismic drillholes, U-25 Seismic #1 through #21, and US-25#1 through #21, were drilled for shot holes in the vicinity of the Yucca Mountain site (McGovern, 1983). Stratigraphic and structural information was obtained from the drill bit cuttings.

Three hydrologic test drillholes, designated UE-25c#1, UE-25c#2, and UE-25c#3, were drilled within close proximity to each other to monitor the flow of ground water between them. The stratigraphy and structure of these drillholes were determined using the drill bit cuttings. During drilling and at the completion of the drillholes, water-level measurements were taken. As the drillholes were completed, various hydrologic tests were conducted. When the three drillholes were completed, hole-to-hole hydrologic tests were conducted by isolating the different lithologic and hydrologic zones in all three drillholes using inflatable packers and then pumping water from one drillhole while simultaneously monitoring the drawdown in the other drillholes. Tracers were used to track the flow of ground water between the drillholes. This investigation is still in progress. Section 3.9 contains a discussion of ground-water flow.

The repository-facility drillholes, designated UE-25RF#1 through UE-25RF#8 (UE-25RF#6 has not been drilled), were drilled and cored under the direction of Sandia National Laboratories (SNL) to find a suitable location for the surface support facility for the proposed repository. These drillholes were drilled to study the alluvial material at Yucca Mountain and to determine the depth to competent bedrock. Drill bit cuttings and core were logged and sampled for this purpose. This investigation is still in progress and is discussed in Section 8.3.3.2.

Drillhole UE-25p#1 was drilled through the Tertiary volcanic rocks in the repository area to investigate the Paleozoic rocks beneath the repository site and to study the hydrologic flow characteristics of these rocks (Craig and Johnson, 1984; Craig and Robison, 1984). The drill bit cuttings and core were examined for geologic information. Core samples were taken and preserved for laboratory analysis. During the drilling, water-level measurements were taken. Hydrologic tests were conducted in the volcanic sequence penetrated by the drillhole. Testing was conducted on the Paleozoic rocks encountered in the lower portion of the drillhole. This drillhole was also monitored during pumping tests in drillholes UE-25c#1, UE-25c#2, and UE-25c#3.

A horizontal corehole was drilled into the surface outcrop of Yucca Mountain. This experimental coring was conducted in rock that closely resembles the proposed repository horizon beneath Yucca Mountain. The drillhole was cored using as little fluid as possible and the core was logged for geologic information. The purpose of this drillhole was to study the feasibility of this type of coring in the test facility beneath Yucca Mountain. The drillhole is designated UE-25h#1, horizontal core hole (Norris et al., 1986).

1.6.4 UNDERGROUND MINING ACTIVITIES

This section documents the status of active or inactive mines at and within 10 km of the proposed Yucca Mountain site.

Documents examined included Nevada Bureau of Mines reports and maps, air photos, Nye County, Nevada, record of mining claims, BLM records, and USGS geologic and topographic maps and reports.

At present there are 9 mill sites and 5 lode claims on file for the area within 10 km of the perimeter drift outline. There are also 10 additional lode claims that have been filed for in June 1987 on the crest of Yucca Mountain within the perimeter drift outline. To date, the filing status with the BLM for these claims is unknown. The mill sites described are located approximately 5 km west of the perimeter drift. Mill sites constitute plots of unappropriated public domain land of a nonmineral character, used for the erection of a mill or reduction works. The 5 lode claims are located south of the perimeter drift, right at the 10 km boundary that is being examined. Lode claims include deposits of classic veins or lodes having well-defined boundaries. They also include other rock-bearing valuable minerals and may even include broad zones of mineralization.

A Nevada Bureau of Mines and Geology report reviewed the mining districts and the minerals and metals produced in southern Nevada (Cornwall, 1972). None of the districts are within the proposed Yucca Mountain site. The closest district is Bare Mountain, 15 km west of the site. A variety of minerals were found in the Bare Mountain district; fluorspar accounted for the majority of mining. The only references to Yucca Mountain concerned the Thompson Mine and the Silicon Mine. Both excavations are at the northwest end of Yucca Mountain, more than 10 km from the site. The potential for mining at Yucca Mountain is discussed in Section 1.7.

None of the studies found evidence of underground mining or extensive excavations within 10 km of the proposed site.

1.6.5 GROUND-WATER INJECTION

There are no injection wells located within the candidate area. The only injection of fluid into drillholes at Yucca Mountain occurred during the drilling and hydrologic testing in connection with the Project (Section 1.6.3 and 3.9.2).

1.7 MINERAL AND HYDROCARBON RESOURCES

The resource potential of a repository site could influence the likelihood of future human intrusion and, thus, may impact total system performance. A site with a high potential for resources would be a more likely target for exploration (e.g., drilling, and test pits) and exploitation (e.g., mines) (40 CFR Part 191, Appendix B). Exploitation and exploration activities could have an impact on radionuclide release rates. The existence of little or no resource potential is recognized as a favorable site characteristic (10 CFR Part 60, 10 CFR Part 960, 40 CFR Part 191). The purpose of

Exploration, in common North American parlance, refers to the entire sequence of work ranging from reconnaissance to the evaluation of the prospect. Historically, this was done by the lone prospector. However, present methods of exploration may involve individuals representing several disciplines, and emphasis has changed to large regional efforts that involve the successive identification of favorable areas and targets. The regions are defined by the geologic environment, preconceived ore emplacement models, and techniques that will necessarily vary depending on the commodity type. Targets are defined by the acquisition of a data base of geologic information that may be supplemented by structural interpretation, aerial or satellite imagery, geochemical surveys, geochronological data or geophysical surveys, distribution of known occurrences of mineralization, vegetation type, or other methods. In recent times, exploration successes have been greatly aided by new ore emplacement models, airborne geophysical techniques, and

[redacted]

may be further assessed by exploratory test pits, adits, or drilling to calculate the volume, grade, and tonnage of the commodity. If a potentially economic reserve is outlined, the deposit may be brought into production pending favorable metallurgical or recovery pilot studies. In theory, an evaluation of each step of the exploration procedure is made before a new step is initiated; and the decision to bring a commodity on line is ultimately based on expected life and projected marketability.

Exploration and production techniques that could affect a repository include drilling and the extraction of subsurface materials to produce the commodity being sought. Thus, a desirable quality of a repository site is large reserves of high-grade ore elsewhere). Other commodities, for which prices are currently low or have never been economic, will undoubtedly become more attractive prospects as prices escalate due to overall global population growth, and by the historical human tendency to translate economic growth into increased material consumption. It is the abundance of these commodities (relative to crustal averages) that must be combined with other factors, such as current exploration models and ore-forming concepts, in order to judge whether Yucca Mountain might be identified as a potential target.

The general geology, rock types, and tectonics of Yucca Mountain and the surrounding area are summarized in the introduction of this chapter and Sections 1.1 to 1.4. Yucca Mountain includes Cenozoic and underlying Paleozoic rocks. Mesozoic rocks are not known to occur below Yucca Mountain (Section 1.2). Cenozoic rocks include tuffaceous rocks locally covered by varying thicknesses of surficial deposits. The Paleozoic rocks lie 1,200 to several thousand meters below the surface (Section 1.2) based on drillhole data (Craig and Johnson, 1984; W. J. Carr et al., 1986) and structural projections of the Paleozoic strata beneath Yucca Mountain (Robinson, 1985). Resources contained in the deep Paleozoic rocks, except potentially oil, gas, coal, oil shale, or tar deposits, would not be economically recoverable now or in the future unless they were of extremely large tonnage or high grade deposits. There are no precedents for defining resource potential, or assessing costs of mine development at great depths except in cases where existing shallow ore bodies can be projected to depth. It is standard practice to exclude evaluation of mineral resources below 1 km, for example Erickson (1973). Due to these constraints, hypothetical resources in the Paleozoic rocks can not be evaluated, except in the most general, qualitative sense.

Definition of mineral resources and reserves

A definition of mineral or energy resources has been established by the U.S. Geological Survey (USGS) and the U.S. Bureau of Mines (USBM) in Circular 831 (USBM/USGS, 1980) and is adapted for use in this assessment. This definition would include as a mineral or energy resource, "a concentration of naturally occurring solid, liquid, or gaseous material in or on the Earth's crust in such form and amount that economic extraction of a commodity from the concentration is currently or potentially feasible" (USBM/USGS, 1980). Prediction in the minerals industry is difficult (Cook, 1986) and thus, this classification system is only intended to be used as a present day classification approach.

A distinction is drawn between identified resources and undiscovered resources. The following terms have been defined by the USGS and the USBM

AREA (MINE, DISTRICT, FIELD, STATE, ETC.) UNITS (TONS, BARRELS, OUNCES, ETC.)

CUMULATIVE PRODUCTION	IDENTIFIED RESOURCES			UNDISCOVERED RESOURCES	
	DEMONSTRATED		INFERRED	PROBABILITY RANGE (or)	
	MEASURED	INDICATED		HYPOTHETICAL	SPECULATIVE
ECONOMIC	RESERVES		INFERRED RESERVES		
MARGINALLY ECONOMIC	MARGINAL RESERVES		INFERRED MARGINAL RESERVES		
SUB-ECONOMIC	DEMONSTRATED SUBECONOMIC RESOURCES		INFERRED SUBECONOMIC RESOURCES		

OTHER OCCURRENCES	INCLUDES NONCONVENTIONAL AND LOW-GRADE MATERIAL

Figure 1-74. Major elements of mineral-resource classification. Modified from USBM/USGS (1980).

2. Undiscovered resources: Resources, the existence of which are only postulated, comprising deposits that are separate from identified resources. Undiscovered resources may be postulated in deposits of such grade and physical location as to render them economic, marginally economic, or subeconomic. To reflect varying degrees of geologic certainty, undiscovered resources may be divided into two parts:

   a. Hypothetical resources: Undiscovered resources that are similar to known mineral bodies and that may be reasonably expected to exist in the same producing district or region under analogous geologic conditions. If exploration confirms their existence and reveals enough information about their quality, grade, and quantity, they will be reclassified as identified resources.

   b. Speculative resources: Undiscovered resources that may occur either in known types of deposits in favorable geologic settings where mineral discoveries have not been made, or in types of deposits as yet unrecognized for their economic potential. If exploration confirms their existence and reveals enough information about their quantity, grade, and quality, they will be reclassified as identified resources.

USBM/USGS (1980) further states that "materials that are too low grade or for other reasons not considered to be economic may be recognized and their magnitude estimated, but they are not classified as resources." A separate category, labeled "other occurrences," is included in Figure 1-74 for materials of this nature. Further details on this classification system are given in USBM/USGS (1980).

A mineral or energy reserve is that part of the total resource that can be economically extracted or produced at the present time, or at the time the resource evaluation is conducted (USBM/USGS, 1980). Current economic conditions define the difference between a resource and a reserve. As economic conditions change, production of a mineral reserve could become subeconomic and the mineral would be reclassified as a resource. A commodity classified as a resource could be reclassified as a reserve as the value of the commodity increases.

Methods of mineral-energy-resource assessment

Mineral-energy-resource assessments are conducted for a variety of reasons, such as establishing a national policy, location of a company's future exploration target, or projecting future availability of a commodity. Methods used in resource assessments vary widely (Singer and Mosier, 1981) due to several factors, including varied goals, scale or size of the area considered, time available, the acceptable level of uncertainty, and the particular user of an assessment.

The methods of resource assessment used in this section are varied and depend upon a number of factors, including (1) the abundance of the resource at Yucca Mountain, in the vicinity of Yucca Mountain, and in the surrounding region; (2) the present technological procedures of resource assessment for a particular resource; (3) the type of resource involved (the resource assessment for gold has many characteristics different from an assessment of geothermal energy); and (4) the type and amount of data available to perform the assessment. For instances in which the amount of data or information are insufficient to perform the assessment, the need for additional studies will be specified.

Resource assessments make wide use of two broad overlapping categories of methods: extrapolation and analogy (Singer and Mosier, 1981). These two methods will be used to a large extent in this section, although specific details of the two methods may vary. A quantitative approach to resource assessment is very desirable, but the immense and varied data base required for statistical treatment or other quantitative and analytical methods is rarely available (Taylor and Stevens, 1983). Many resource assessment methods and approaches are available (Harris and Agterberg, 1981; Singer and Mosier, 1981; Zwartendyk, 1981; Taylor and Stevens, 1983), but existing quantitative assessments often only apply in situations where a potential ore body has already been discovered and to resource assessments of large scale.

At the present time, the concept of zones, belts, and knots of mineralization is only empirically supported, for instance, on the scale of the western United States (Kutina, 1969). Generally, these types of analyses consider only the largest deposits. A statistical analysis of mineral deposits on an area that covered greater than 50 percent of Nevada was attempted by Horton (1966). Horton found that silver and lead fell into statistically significant mineralized belts, whereas other elements considered, including other precious metals and other base metals, did not. Recently, attempts have been made to relate ore deposit types to tectonic settings and to determine the spatial and temporal distribution of these tectonic settings. For example, Guilbert and Park (1986) presented a plate tectonic-lithotectonic classification of ore deposits in which a major category of ores associated with consuming, subducting plate margins has been subdivided into several types. The Nevada setting most appropriately falls within the ocean/continent-extension type. This setting includes the (1) porphyry copper (soda-alkalic affinity); (2) Climax-type molybdenum; and (3) epithermal-ignimbrite association, which include the Tonopah, the McDermitt, the Round Mountain, the so-called "invisible gold" deposits of the Carlin-Cortez, and the "bulk low-grade silver-gold" deposits or Candelaria and Rochester type (Berger and Eimon, 1983; Guilbert and Park, 1986). These models will be considered in the economic evaluation of Yucca Mountain, in terms of which commodities should be considered to have a potential for economic occurrence. Detailed geologic knowledge of a particular site (e.g., Yucca Mountain) or regional geologic information on a particular site is probably more important than the large scale characteristics and localization of ore deposits discussed previously.

Factors such as location, grade, and tonnage have a profound influence of 100 or 1,000 (Brooks and Andrews, 1974). Therefore, elements or materials below or equal to average crustal abundances may never be considered reserves. For example, copper occurs in the Topopah Spring Member at concentrations greatly below average crustal abundance (Schuraytz et al., 1986); thus, copper will never be considered a resource at Yucca Mountain. This will remain true even with large increases in the value of copper or great improvements in extraction technology, because significant resources will always occur elsewhere with a higher grade. Thus, only those commodities that (1) are known to occur in significant abundance (e.g., zeolites); (2) are known to occur in comparable areas or settings; or (3) are presently, or historically have been, mined in the vicinity of Yucca Mountain will be assessed.

The resource assessment of the area in and around Yucca Mountain is presented in three parts: (1) mineral resources (Section 1.7.1), (2) nonhydrocarbon energy resources (i.e., uranium and geothermal) (Section 1.7.1.5), and (3) hydrocarbon resources (Section 1.7.2).

1.7.1 MINERAL RESOURCES

Nevada ranks approximately 12th in value of nonfuel mineral production in the United States (Carrillo and Schilling, 1985). Nevada leads the nation in the production of barite, magnesite, and mercury, but gold is the State's leading commodity in terms of value (Carrillo and Schilling, 1985). Table 1-17 lists the nonfuel mineral production in Nevada for 1982, 1983, and 1984. Clays, gemstones, gypsum, iron ore, lead, sand, gravel, and crushed stone are also important commodities in Nevada. The mineral industry in Nevada will likely remain highly ranked in comparison to other states far into the future.

In this section, mineral resources are discussed within the framework of the regional and site-specific characteristics and associations of gold, silver, and base metal resources (Section 1.7.1.2), mercury resources

Table 1-17. Nonfuel mineral production in Nevada[a]

	1982		1983		1984	
	Quantity	Value (thousands)	Quantity	Value (thousands)	Quantity	Value (thousands)
Barite (thousand short tons)	1,575	$ 52,727	663	$ 21,736	615	$ 14,924
Clays (thousand short tons)	103	2,640	58	2,348	20[b]	1,191[b]
Gem stones	NA[c]	1,200	NA	1,200	NA	1,300
Gold (recoverable content of ores, etc.) (troy ounces)	757,099	284,601	914,531[d]	387,761[d]	997,508	359,759
Gypsum (thousand short tons)	656	4,523	998	7,896	1,192	8,860
Iron ore (thousand long tons)	77	1,119	W[e]	W	W	W
Lead (recoverable contents of ores, etc.) (metric tons)	W	W	14	7	W	W
Mercury (76-pound flasks)	25,760	W	25,070	W	19,048	W
Sand and gravel						
Construction (thousand short tons)	6,027	11,724	7,500[f]	16,200[f]	8,202	20,505
Industrial (thousand short tons)	W	W	W	W	489	W
Silver (recoverable content of ores, etc.) (thousand troy ounces)	3,142	24,981	5,164	59,073	6,477	52,727
Stone, crushed (thousand short tons)	1,300[f]	4,500[f]	1,269	5,358	1,100[f]	4,700[f]
Combined value of cement (portland), clays (Fuller's earth and kaolin, 1984), copper, diatomite, fluorspar lime, lithium, magnesite, molybdenum, perlite, salt, tungsten ore and concentrate (1982 and 1984), and values indicated by symbol W	--[g]	$ 144,448	--	$ 111,178[d]	--	$ 151,787
TOTAL	--	$ 532,463	--	$ 612,757[d]	--	$ 615,753

[a]Modified from Ballard (1985).
[b]Excludes certain clays; value included in "combined value" figure.
[c]NA = not available.
[d]Revised.
[e]W = information withheld by producer.
[f]Estimated.
[g]-- indicates not applicable.

gravity low (Carr, 1984) corresponding to the thick Cenozoic volcanic cover and the presence of several caldera complexes (Snyder and Carr, 1982; USGS, 1984; Robinson, 1985). The presence of caldera complexes in the region of Yucca Mountain is further discussed in Section 1.7.1.2. However, local gravity and magnetic highs have been interpreted to include the existence of a deep pluton that may extend from northern Bare Mountain, to northern Yucca Mountain, to the Calico Hills area (Snyder and Oliver, 1981; Hoover et al., 1982; Carr, 1984; USGS, 1984) and/or to reflect a northeast-trending buried ridge of Paleozoic rocks extending from the gravity high of Bare Mountain to Calico Hills (Snyder and Carr, 1984). The inferred pluton is believed to be responsible for some of the metamorphism observed at Calico Hills and Bare Mountain (Carr, 1984). Based on gravity interpretations and magnetotelluric data, the inferred pluton is greater than 7,200 ft (2,200 m) below Calico Hills (Hoover et al., 1982; Snyder and Carr, 1982), and probably much deeper below Yucca Mountain, if it exists (Robinson, 1985). The age of the inferred pluton is thought to be Mesozoic by Carr (1984). Additional evaluation of the available gravity and magnetic data is planned (Section 8.3.1.9).

Other geologic models, in part based on geophysical data, have been suggested for Yucca Mountain and include the possible presence of detachment faults below Yucca Mountain (Scott, 1986; Scott and Rosenbaum, 1986), the possible presence of a metamorphic core complex beneath Yucca Mountain (Robinson, 1985), and a postulated caldera complex next to Yucca Mountain in Crater Flat (Carr, 1984; Maldonado, 1985a) (Figure 1-75). As these and further models are refined, their significance to the resource potential of the Yucca Mountain area will be evaluated (Section 8.3.1.9).

Where geophysical data are available for areas of mineralization (e.g., Wahmonie and Calico Hills), the geophysical signatures are markedly different from that of the site. Additional geologic comparisons are made in Sections 1.7.1.2.2 and 1.7.1.2.3 and further detailed comparisons are planned (Section 8.3.1.9).

A shallow pluton is thought to exist below the Wahmonie area, 20 km to the east of the site, based on the presence of (1) a large aeromagnetic high, (2) a gravity high, (3) a zone of alteration coincident with the geophysical anomalies, and (4) two small outcrops of granodiorite (Smith et al., 1981; Hoover et al., 1982). These factors, in conjunction with the lithologic variation observed (Sections 1.7.1.2.2 and 1.7.1.2.3) and the geophysical interpretation of vertical electrical soundings (VES), induced polarization (IP) measurements, and magnetotelluric (MT) surveys, support the significant potential for disseminated mineralization at Wahmonie (Smith et al., 1981; Hoover et al., 1982; Quade and Tingley, 1983), particularly precious and base metals.

The observed magnetic high at Calico Hills is, in part, believed to be associated with the magnetite-rich Paleozoic Eleana Formation and the gravity high due to a contrast between the density of the Paleozoic rocks and the overlying volcanics (Hoover et al., 1982). However, a pluton is postulated

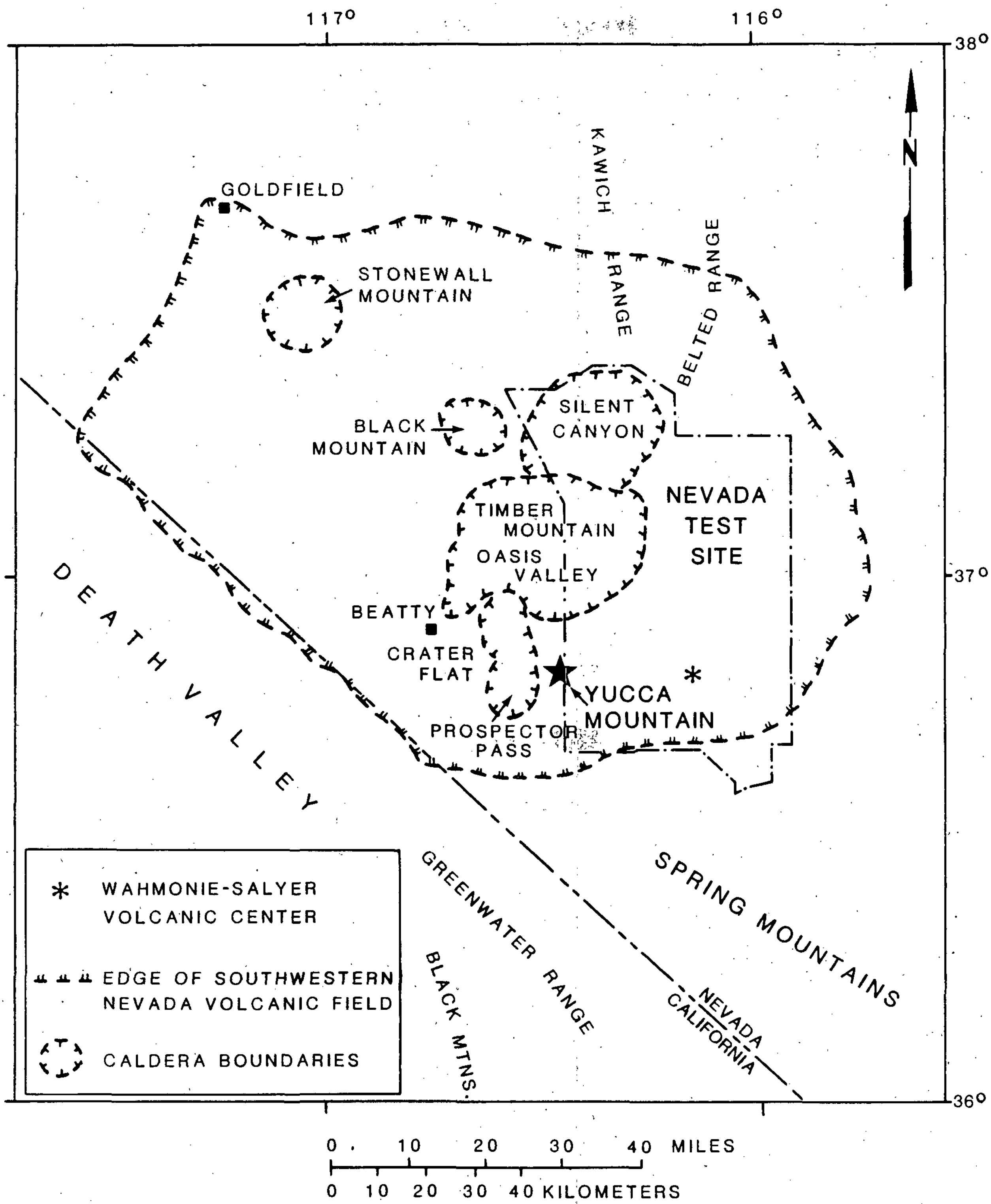

Figure 1-75. Calderas within the southwestern Nevada volcanic field. Modified from Carr (1984).

alteration, and a probable intrusive body at depth (Hoover et al., 1982). The IP data have outlined an area of increased polarizability that may indicate mineralization (Hoover et al., 1982). Based on the above evidence and that contained in Sections 1.7.1.2.2 and 1.7.1.2.3, explorationists would likely deem these areas as favorable targets.

In contrast to the previously mentioned areas, the Yucca Mountain site does not have similar magnetic highs, gravity highs, and alteration characteristic of mineralization at the surface or at depth (Section 1.7.1.2.3). In addition, anomalously low resistive bodies located by IP surveys on the east flank of Yucca Mountain are interpreted to indicate the presence of zeolitization or clay alteration along fractured zones. Furthermore, uniformly high resistivities are reported for a large block located at the site and thought to represent the presence of densely welded tuff (Smith and Ross, 1982). No potential for mineralization was reported from analysis of these surveys. In general, this geophysical interpretation is supported by petrologic, surficial mapping, and downhole studies (e.g., Bish et al., 1982; Scott and Bonk, 1984; Scott and Castellanos, 1984; Vaniman et al., 1984b;

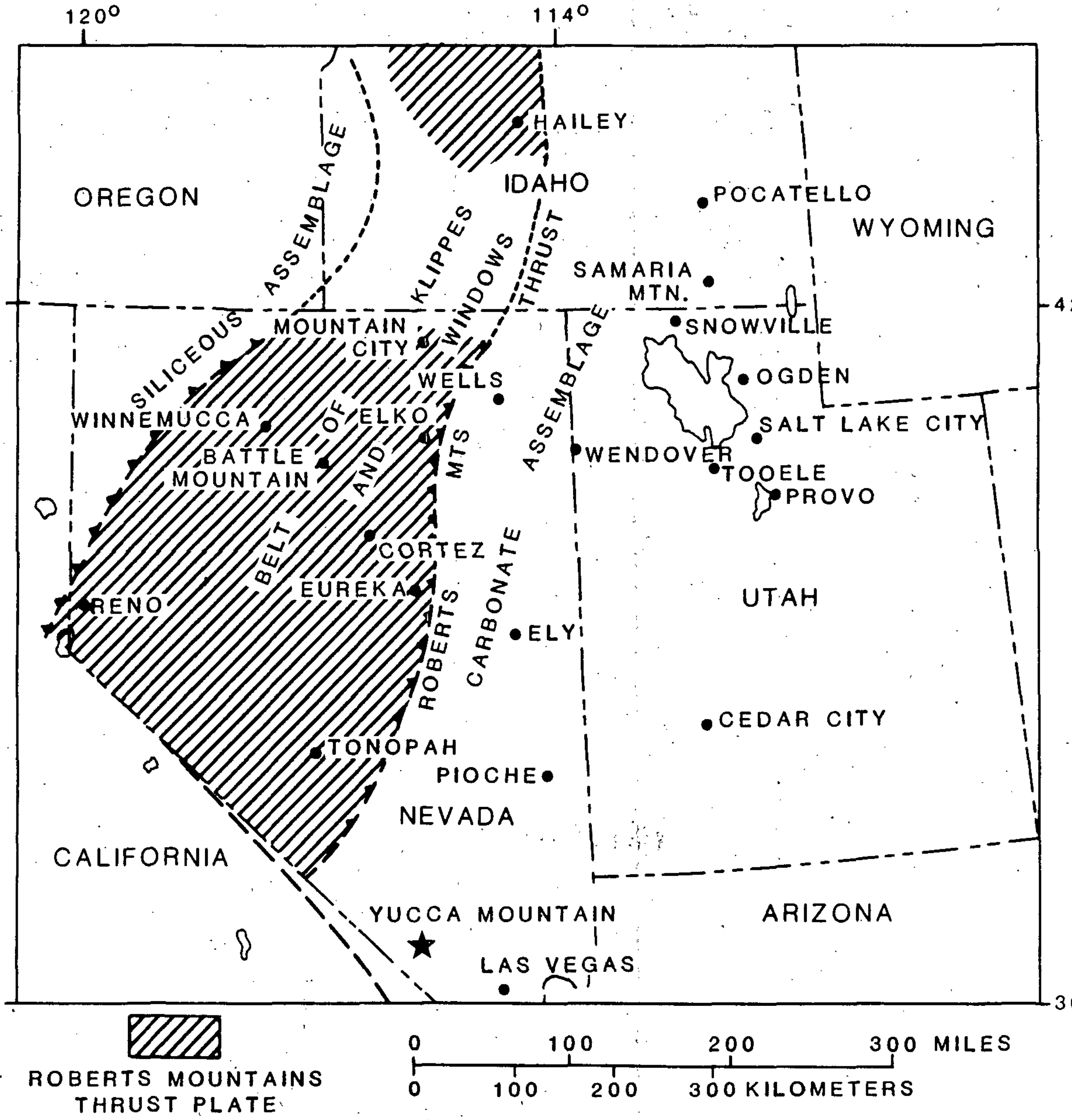

Figure 1-76. Map showing distribution of Paleozoic rocks in Roberts Mountains thrust plate after Mississippian thrusting. Modified from Roberts et al. (1971).

trending structural trend called the Walker Lane (Figure 1-36) (Billingsley and Locke, 1941; Silberman, 1985). Many of the Nevada mineral belts proposed by Roberts (1966) parallel the Walker Lane (Horton, 1966).

Within the last two decades, economic trends and new geologic discoveries have expanded the precious-metal reserves in Nevada. Increases in the value of gold and silver have provided an impetus for renewal of mining operations and exploration. In turn, new exploration models have proven successful in revealing a diversity of geologic occurrences of silver and gold that was greater than previously perceived. For example, during this renewed exploration activity the entirely new concept of mobilization and reprecipitation of gold along thrust faults or detachment structures was introduced. These models are revealing new, potentially important environments of precious metals. In addition, bulk low-grade and disseminated silver-gold deposits (e.g., Carlin, Candelaria, and Goldfield) have been discovered in a variety of rock types, including hydrothermally altered tuff (e.g., Round Mountain) (Sander and Einaudi, 1987).

Tertiary ash-flow tuff constitutes greater than half of the total surface outcrops in Nevada. However, 93 percent of all major metal-mining districts in Nevada are in lithologies other than silicic tuff (McKee, 1979). Much of Nevada, Nye County, and all Yucca Mountain at the surface consists predominantly of Tertiary ash-flow tuffs. The tuffs are the products of eruption from magma chambers that vented through numerous volcanos, now recognized as calderas, throughout the State. The age of the calderas and their associated tuffs partially overlap in space and time (Section 1.3; Christiansen et al., 1977). The general relationship between calderas, ash-flow sheets, and mineralization has been summarized and evaluated by McKee (1979).

Areas within calderas are typically barren of economically important base and precious metals while strongly metamorphosed and altered rocks located on the margins of calderas are more economically important. Only 2 of Nevada's 31 recognized calderas (6 percent) have produced 1 million dollars or more of gold, silver, copper, lead, zinc, mercury, antimony, and iron (McKee, 1979). The two mineralized districts found within calderas in Nevada are the Goldfield district (largely a gold producer) and the Opalite district (a mercury district) (McKee, 1979). Mineralization is often associated with the margins of calderas (e.g., the Jefferson Caldera) (Shawe, 1987) and often associated with thick plies of silicic ash-flow tuffs within and around their calderas elsewhere in the western United States (Bethke and Lipman, 1987).

Ash-flow tuffs have also proved to be relatively barren of precious- and base-metal deposits in Nevada, with only 5 mineral districts located in metamorphosed tuffaceous rocks subjected to secondary processes after deposition are the most likely tuff environments for mineralization.

1.7.1.2.1 Gold, silver, and base-metal genesis

Gold, silver, and base-metal deposits will be discussed together because they are often closely associated and occur together in veins, disseminations, and replacement type ore bodies in Nevada (Hewitt, 1968; Roberts et al., 1971; Stewart et al., 1977; Bonham, 1985). Hewitt (1968) tabulated that within the Great Basin 68 percent of all gold production has been as a byproduct of base-metal operations, 25 percent has been produced from only gold producing operations, and 7 percent from only gold and silver producing operations. Exploration and production of precious metals has recently centered around bulk-mineable and disseminated deposits that are not produced for base-metals.

Of the elements listed in Table 1-18, vanadium, chromium, cobalt, nickel, lead, zinc, copper, thorium, and uranium all exhibit values near average crustal abundances or near average abundances for silicic tuff and thus are not indicative of any resource potential. Furthermore, the distribution of these elements does not exhibit any anomalous values that might indicate secondary processes (e.g., weathering) that could concentrate these elements (Section 1.7.1.5.1). Concentrations of lead and zinc are generally low and their average abundances are near crustal abundances (Table 1-18). A few anomalous values (compared with crustal abundance) have been identified but probably do not represent a wider variation in these elements than that expected in a silicic tuff. Further elemental abundances including lead and zinc, will be collected and evaluated during site characterization (Section 8.3.1.9).

The data listed in Table 1-18 were collected to evaluate petrogenetic models of magma evolution. Where the present data base is determined to be insufficient for evaluating resource potential, more detailed chemical data will be collected (Section 8.3.1.9). A composite average of elemental abundances in silicic tuffs will also be generated for comparison with the silicic tuffs of Yucca Mountain Section 8.3.1.9.

At present in Nevada, disseminated and bulk low-grade deposits are the most likely targets of exploration, exploitation, and extraction. Disseminated deposits of gold, silver, and/or base metals, with notable exceptions, such as Round Mountain, are typically not reported in Tertiary volcanic rocks, but occur in Paleozoic carbonate rocks. These include the Carlin, Gold Quarry, Cortez, and Jerritt Canyon deposits (Hewitt, 1968; Berger and Eimon, 1983; Sawkins, 1984). High-grade (bonanza) gold deposits, including Florida Canyon, Paradise Peak, and the Sleeper Deposit, are also hosted in silicic ash flow tuffs (Schafer and Vikre, 1988; Bonham, 1986; Dayton, 1987). Because Yucca Mountain is composed of tuff, the gold and silver resource potential in volcanic-hosted deposits will be the main focus of this section rather than deposits in Paleozoic sedimentary rocks.

In the period between 1859 and 1962, the recorded gold production in Nevada was approximately 27 million ounces (Bonham and Tingley, 1984).

Table 1-18. Elemental abundance data for tuffs at and in the vicinity of the Yucca Mountain site in comparison to average crustal abundance and preliminary average silicic tuff[a] (page 1 of 2)

	Average[b] crustal abundances	Average[c] values found in high silica tuff	Range of Yucca Mountain data	Average	Number of samples	Data source	Member of Paintbrush Tuff Formation
Vanadium	135	X=16 N=1 R=N/A	0.5-17.0	5.0	70	d	Topopah Spring
Chromium	100	X=3.35 N=15 R=(0.9-6.3)	1.0-41.0	4.4	40	d	Topopah Spring
Cobalt	25	X=0.34 N=34 R=(0.05-2.35)	0.1-1.10 0.30-0.50 0.06-0.43 0.08-2.20	0.51 0.40 0.14 0.46	72 24 25 46	d,e f f f	Topopah Spring Pah Canyon Yucca Mountain Tiva Canyon
Nickel	75	X=11.6 N=8 R=(1-35)	4.0-157	10.8	71	d	Topopah Spring
Copper	55	X=10.2 N=11 R=(2-37)	1.0-40.0	9.3	72	d	Topopah Spring
Zinc	70	X=72.3 N=24 R=(20-225)	19-390 56.5-79.9 29.1-96.1 39.1-145.1	63.5 64.4 72.7 81.7	91 25 25 46	d,e f f f	Topopah Spring Pah Canyon Yucca Mountain Tiva Canyon

Table 1-18. Elemental abundance data for tuffs at and in the vicinity of the Yucca Mountain site in comparison to average crustal abundance and preliminary average silicic tuff[a] (page 2 of 2)

	Average[b] crustal abundances	Average[c] values found in high silica tuff	Range of Yucca Mountain data	Average	Number of samples	Data source	Member of Paintbrush Tuff Formation
Lead	12.5	N/A	5-575	34.5	72	d	Topopah Spring
Thorium	10	X=23.8	18.4-54.0	21.4	166	d,e	Topopah Spring
		N=102	17.3-20.7	19.4	23	f	Pah Canyon
		R=(1.4-191)	23.0-25.1	24.1	25	f	Yucca Mountain
			12.6-25.4	21.6	46	f	Tiva Canyon
Uranium	2.7	X=4.82	1.2-8.7	3.7	166	d,e	Topopah Spring
		N=56	4.0-10.9	5.2	25	f	Yucca Mountain
		R=(0.6-15.9)	1.4-5.9	4.4	44	f	Tiva Canyon

[a]Table modified from Mattson (1988); all data reported in parts per million.
[b]Levinson (1974).
[c]Preliminary compilation of average high silica tuff found in localities other than Yucca Mountain. X = average, N = number of samples, R = range, N/A = not applicable.
[d]Schuraytz et al. (1986), pumice and whole-rock analyses.
[e]Broxton et al. (1986), whole-rock analyses.
[f]Flood (1987), pumice analyses.

Increases in the market value of gold and the discovery of previously unsuspected gold reserves (i.e., Carlin-type disseminated gold deposits) have stimulated exploration. Deposits located in the period from 1962 to 1982 contain 34 million ounces; this total includes gold which has been mined or exists as reserves (Bonham and Tingley, 1984). The new gold discoveries in Nevada have been subdivided into two main groups: sediment-hosted or volcanic-hosted deposits. Two-thirds of the total reserves occurs in the sediment-hosted deposits (Bonham and Tingley, 1984).

Approximately 60 percent of the world's Tertiary epithermal precious- and base-metal vein districts associated with volcanic rocks have been analyzed and tabulated by Mosier et al. (1986) in terms of their geology, grade-tonnage information, and ore associations. Of these deposits, 46 percent have a clear association with rhyolite or rhyodacite tuffs. Although the ages differ, the volcanic rock associations discussed previously for the rhyolite and rhyodacite tuffs are similar and directly comparable to the associations found in volcanic rocks of the Great Basin (Figure 1-77). In the Great Basin, most of the gold production has been from vein deposits in andesites associated with calc-alkalic volcanic suites that formed between 22 to 6 million years ago and in two other major suites of rocks which consist of (1) both intermediate and silicic ash-flow tuffs formed from 43 to 17 million years ago and (2) bimodal assemblages of both basalt and rhyolite that range in age from 17 million years old to the present (Silberman et al., 1976). The compositional range of rock types associated with most vein type deposits generally do not occur at Yucca Mountain. The volcanic rocks at Yucca Mountain have affinities with silicic volcanic systems (Lipman et al., 1966; W. J. Carr et al., 1986; Flood and Schuraytz, 1986). Thus, the compositional range of the erupted tuffs are different than the volcanic suites associated with vein deposits in the Great Basin.

Based upon experimental and empirical techniques, precious-metal and base-metal vein deposits form at temperatures between 50 and 300°C and at depths less than 1,000 m from the surface (Sillitoe, 1977; Berger and Eimon, 1983; Nelson and Giles, 1985; White, 1985; Guilbert and Park, 1986). These deposits are postulated to exhibit an ore zonation with depth (Berger and Eimon, 1983; Sawkins, 1984), with gold and silver ore mineralization nearer to the surface than sulfide mineralization (Figure 1-78). Both high-volume, low-grade (bulk-mineable) and low-volume, high-grade (bonanza) precious-metal deposits are known to be of the epithermal disseminated and vein style of origin. Gangue mineralogy also exhibits a zonation with depth (Figure 1-78) and occurs as three-dimensional alteration halos around the epithermal deposits (Berger and Eimon 1983; Bird et al., 1984; Cole and Ravinsky, 1984; Sawkins, 1984; Mosier et al., 1986). Alterations and ore zonations have been

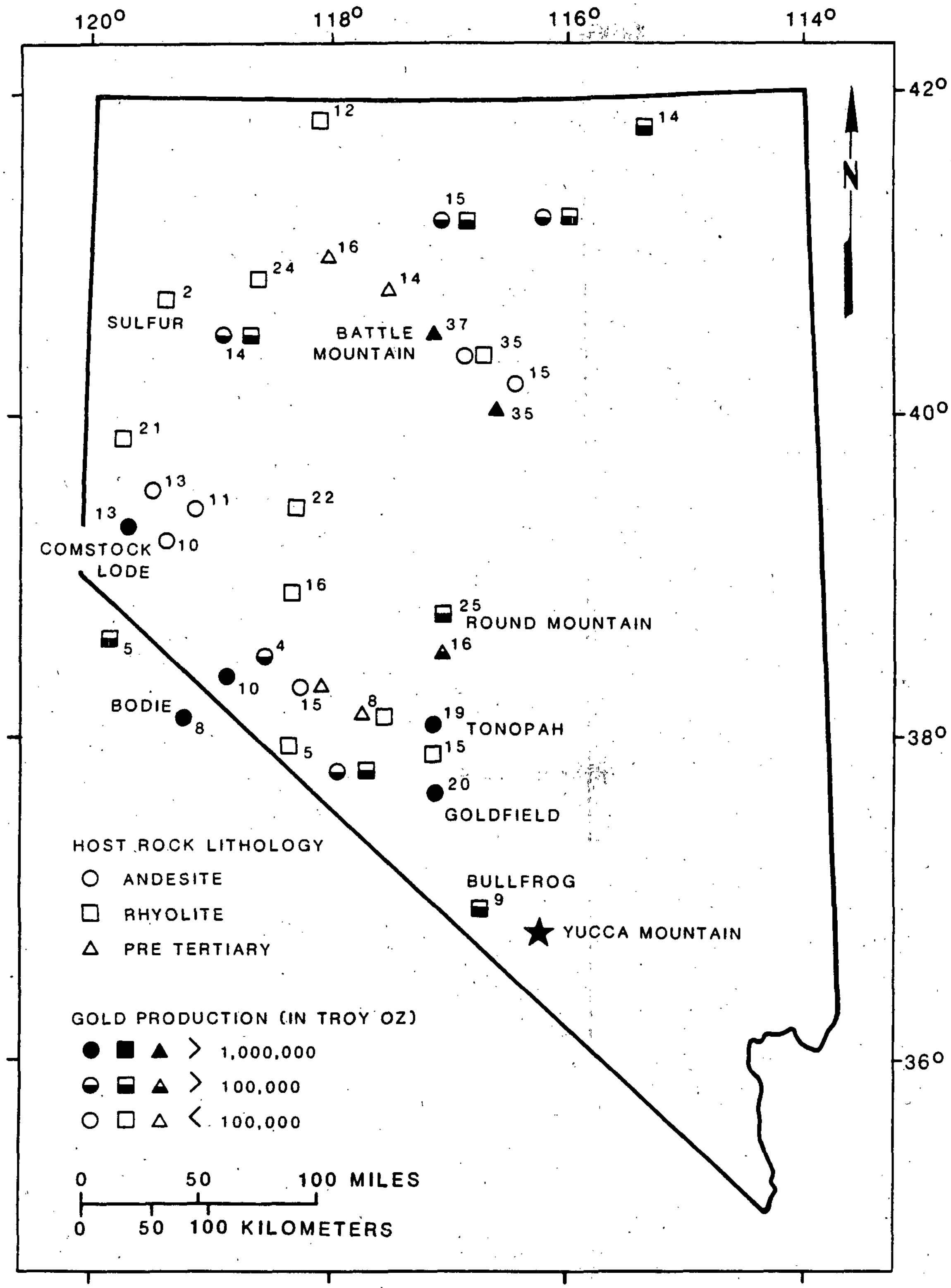

Figure 1-77. Map showing the distribution of ore deposits dated by potassium-argon dating methods, lithologies of the host rock, and approximate production of gold. Potassium-argon dates are mineralization ages and are represented by numbers (million years) next to symbols. Modified from Silberman et al. (1976) and Silberman (1985). Further information on the location of gold deposits and prospects in Nevada can be found in Bonham (1986).

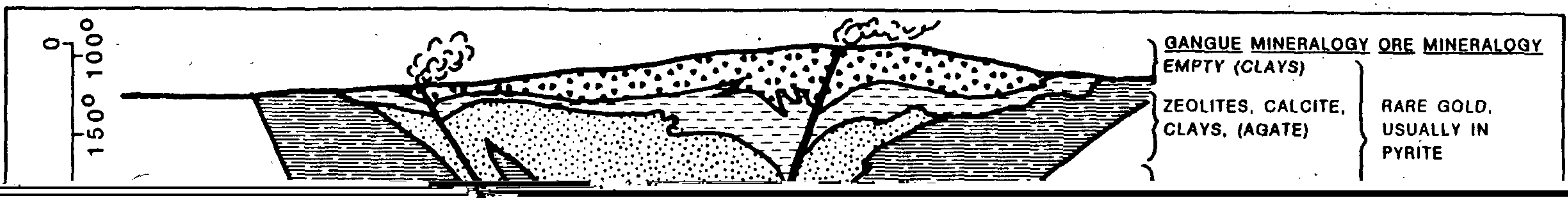

0
100°
150°
GANGUE MINERALOGY
ORE MINERALOGY
EMPTY (CLAYS)
ZEOLITES, CALCITE, CLAYS, (AGATE)
RARE GOLD, USUALLY IN PYRITE

Table 1-19. Generalized mineralogy with increasing depth in an epithermal precious-metal deposit and mineralogy in some Nevada deposits[a]

	Gangue mineralogy	Ore mineralogy	Comment
TYPICAL MINERALOGY IN EPITHERMAL PRECIOUS METAL DEPOSITS			
Increasing depth	Siliceous minerals, zeolites, calcite, clays, kaolinite	Rare gold in pyrite	
Increasing	Calcite, zeolites	Gold in pyrite	Alteration is
[illegible]	[illegible]	[illegible]	[illegible]
	alunite, jarosite, dickite	sulfosalts	ore zones
Increasing depth	Quartz, calcite, pyrite, barite, fluorite, illite, dickite	Pyrargyrite, proustite, argentite, electrum	
Increasing depth	Quartz, adularia,		
	Sericite, pyrite, dickite, calcite, chlorite, fluorite, illite	Argentite, electrum	
Increasing	Quartz, fluorite,		

Table 1-20. Major and minor alteration phases observed at Yucca Mountain[a]

Major alteration phases	Minor alteration phases

1.7.1.2.2 Epithermal volcanic associated gold, silver, and base-metal deposits and occurrences in the vicinity of Yucca Mountain

A comparison of known mineralized districts and possible ore genesis models within the Yucca Mountain area is important in evaluating the economic potential of a repository site. A brief discussion of the most important gold-silver districts that are hosted in volcanic rocks, in comparison to Yucca Mountain, is presented below. Also presented is a discussion of deposits located near Yucca Mountain, regardless of their host rock lithologies. Silberman (1985) has subdivided precious-metal deposits related to volcanic centers into (1) caldera-connected (e.g., Round Mountain) and (2) hot spring types (e.g., Steamboat Springs, Colorado). Within Nevada, caldera-connected deposits of the bulk mineable type are genetically complex. At Round Mountain, for example, mineralization is in intracaldera tuff on the margins of the caldera and is apparently genetically related to the eruptive phase of the caldera cycle (Silberman et al., 1976). At Goldfield, however, potentially bulk-mineable gold mineralization, within hydrothermal breccia on the margin of a small caldera, clearly postdates the eruptive phase of the caldera cycle (Silberman, 1985).

Many descriptions of the occurrences, location, and history of Nevada's gold, silver, and base-metal deposits exist in the current literature. A few of these summary articles concerning southern Nevada include Ball (1907), Ransome (1907), Lincoln (1923), Kral (1951), Cornwall and Kleinhampl (1964), USGS/NBM (1964), Albers and Stewart (1972), Cornwall (1972), Bell and Larson (1982), Quade and Tingley (1983), Smith et al. (1983), Kleinhampl and Ziony (1984), Tooker (1985), Mosier et al. (1986), Johnson and Abbott (1987), and Garside et al. (1987). Some of the most important mineralized districts in the vicinity of Yucca Mountain are the Tonopah, Goldfield, and Bullfrog Hills (Rhyolite) districts (Figure 1-77, Section 1.7.1.2.1). These deposits were actively mined beginning around the turn of the century and now are being reassessed or produced as bulk low-grade gold deposits. The deposits are associated with Tertiary volcanic rocks which are related to andesitic volcanic rocks (Cornwall and Kleinhampl, 1964; Cornwall, 1972; Stewart et al., 1977; Ashley, 1979; Sawkins, 1984). These deposits exhibit a range in mineralization ages from 9 to 23 million years (Silberman, 1985; White, 1985).

The Goldfield deposits produced 4.2 million ounces of gold, 1.5 million ounces of silver, and 7.7 million pounds of copper and they occur as linear features in volcanic rocks associated with andesite (Albers and Stewart, 1972; Smith et al., 1983). The Tonopah district produced 150 million dollars worth of silver with lesser amounts of gold. The deposits of this district occur as veins in faults and joints that are located in andesitic and rhyolitic volcanics (Kleinhampl and Ziony, 1984). The Bullfrog district produced more than 2.7 million dollars worth of gold and silver between 1905 and 1921. The ore deposits of this district occur as veins along faults and joints in rhyolitic welded tuffs associated with basalt and quartz latite flows and tuffs (Cornwall, 1972; Smith et al., 1983; Mosier et al., 1986). The Bullfrog district has no current production, but does have active claims (Smith et al., 1983). The associated bimodal and intermediate composition volcanic rocks of the previously discussed deposits and their associated extensive hydrothermal alteration (Table 1-19, Section 1.7.1.2.1) are not typical of the volcanic rocks at Yucca Mountain.

The Round Mountain gold and silver district (Figure 1-77) was discovered in 1906 (Ferguson, 1921; Shawe et al., 1986) and by 1959 had produced approximately 0.5 million ounces of gold from placer and lode deposits (Shawe et al., 1986). The lode deposits were found in fractured and altered rhyolitic welded ash-flow tuffs that are associated with quartz veining located along both steep and flat lying faults that often contain strongly brecciated rocks (Kleinhampl and Ziony, 1984; Shawe et al., 1986). Low-grade disseminated and bulk-mineable gold deposits are the focus of the present day mining operations from which greater than one-half million ounces of gold have been obtained (Shawe et al., 1986). Two types of alteration are recognized: Type I alteration is characterized by the replacement of sanidine by K-Feldspar and plagioclase by albite; Type II alteration is characterized by strong potassium metasomatism, where the tuff is densely welded. The Round Mountain deposit contains quartz-adularia veins that may contain gold (Sander and Einaudi, 1987). The district is associated with uranium, mercury, tungsten, and copper mineralization and gangue mineralogy consisting of veins of quartz, adularia, limonite (oxidized from pyrite), manganese oxide, and subordinate alunite, fluorite, and realgar (Kleinhampl and Ziony, 1984; Shawe et al., 1986). Similar gangue mineralogy, a similar high-degree of alteration or mineral assemblage, and shallow plutonism or gold-silver mineralization associated with the Round Mountain deposits (Kleinhampl and Ziony, 1984; Shawe et al., 1986) have not been found at Yucca Mountain. Further compari-

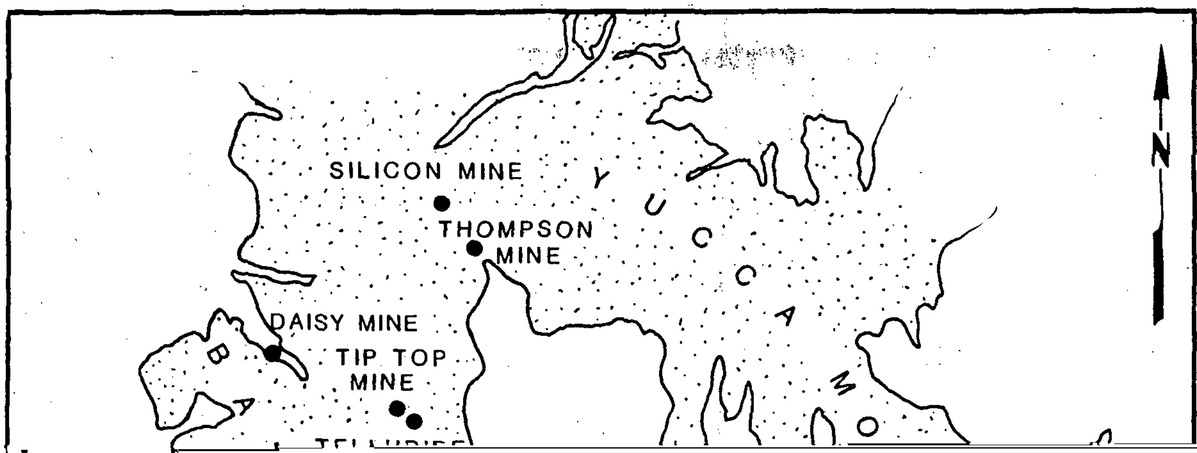
SILICON MINE
THOMPSON MINE
DAISY MINE
TIP TOP MINE
N

DECEMBER 1988

UE-25p#1, hand-specimen and microscopic studies of the limited core available have not revealed any significant mineralization. Exploration for precious metals in a deeply buried Paleozoic terrain, such as at Yucca Mountain, cannot be dismissed.

Other gold, silver, and base-metal prospects, test pits, exploratory

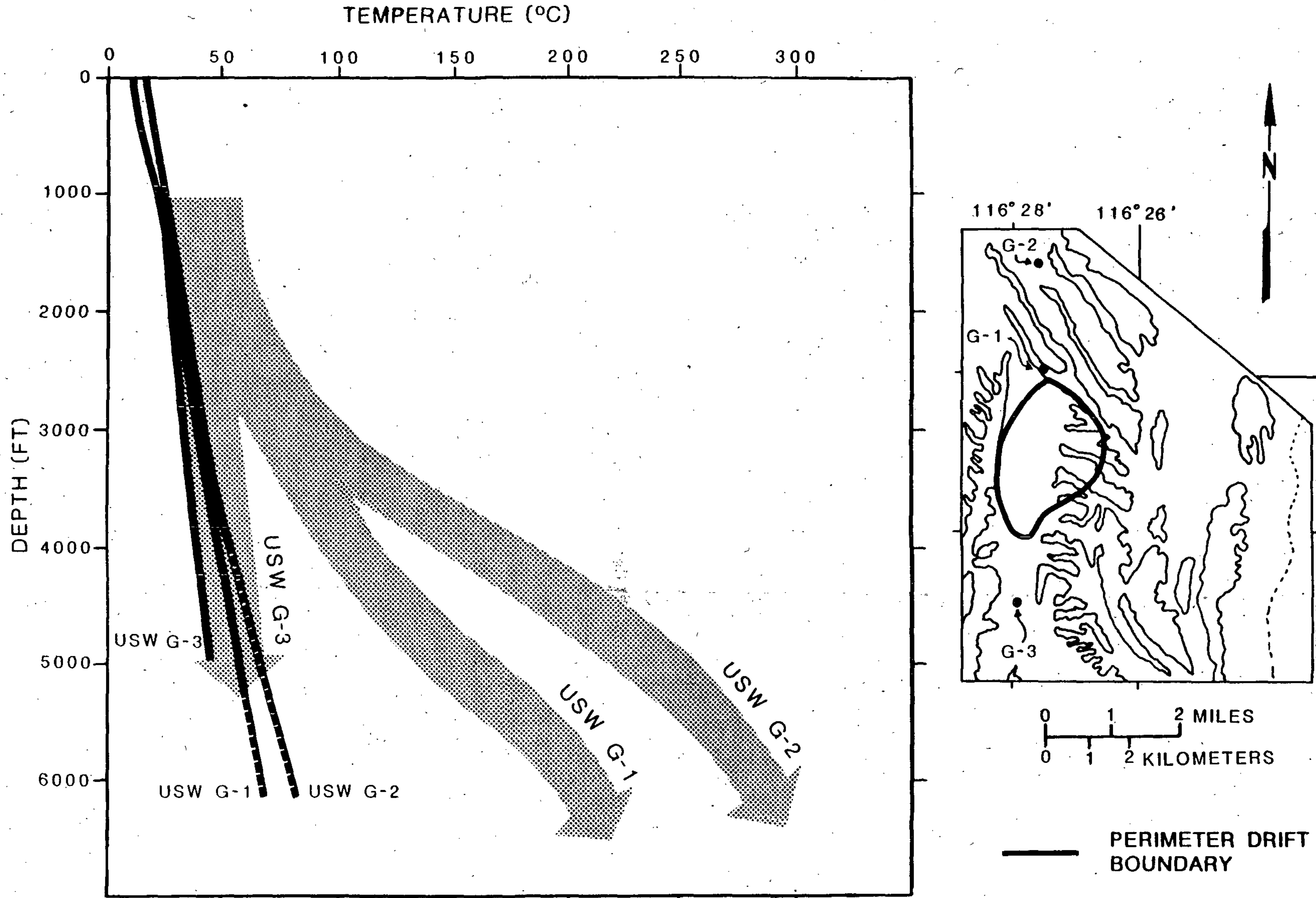

Figure 1-80. Schematic paleotemperatures for USW G-1, USW G-2, and USW G-3 estimated from clay mineral reactions and fluid inclusion data (broad, arrowed lines) with the present-day measured temperature profiles from Sass et al. (1983) (solid and dashed narrow lines). Modified from Bish (1987). Map insert shows location of drillholes.

paleotemperatures from the Silurian at depths between 1,250 and 1,500 m were never greater than 140 to 180°C (CAI-3).

At depth under Yucca Mountain, higher temperatures of hydrothermal alteration are found at progressively shallower depths from south to north. An abrupt increase in the intensity of alteration, below approximately 3,000 ft (914 m), is reported for drillhole USW G-2 (Spengler et al., 1981). The alteration is confined to the Tram Member of the Crater Flat Tuff and lithologic units below the Tram Member in drillhole USW G-2 (Spengler et al., 1981). Similar alteration is confined to units below and including the Bullfrog Member of the Crater Flat Tuff in drillhole USW G-1 below 1,067 m (Caporuscio et al., 1982). The hydrothermal alteration may be interpreted as being regional in extent because similar alteration is observed, albeit at different depths, in drillholes USW G-1 and USW G-2, which are greater than 2 km apart (Bish 1987). Potassium-argon ages determined on illite/smectite clays from drillholes USW G-1 and USW G-2 are greater than ten million years old and equivalent to the timing of the Timber Mountain Tuff (Bish, 1987).

The hydrothermal alteration minerals include albite, calcite, potassium feldspar, chlorite, smectite-kaolinite clays, and rare finely disseminated pyrite (Spengler et al., 1981; Caporuscio et al., 1982; Bish, 1987). No significant alteration is believed to have occurred since 10 million years ago (Bish, 1987). Important alteration phases found in many epithermal deposits, in contrast to Yucca Mountain, include adularia, pyrrhotite, arsenopyrite, alunite, jarosite, and pervasive secondary silica phases, such as chalcedony, opal, or quartz (Table 1-19 and 1-20, Section 1.7.1.2.1). Deposits of calcite and opaline silica are found locally along fault zones near Yucca Mountain (Section 1.2.2.2.10) and will be further assessed for any resource potential (Section 8.3.1.9).

Deposits consisting of calcite and opaline silica occur along fault zones near Yucca Mountain (Voegele, 1986a, 1986b; Vaniman et al., 1988). An assessment of fault-related deposits will be performed (Section 8.3.1.9) because some similar appearing silica cemented breccias are known to be mineralized and occur in Nevada (Nelson and Giles, 1985). Large tonnage volcanic-hosted deposits are known to occur in association with fault-related deposits and pervasive alteration of the host rock, for example the Sleeper deposit (Wood, 1988). There is some possibility that fault-related deposits of this type could exist at shallow depth, buried by alluvium, near Yucca Mountain. Geochemical surveys of bedrock and alluvium are being planned and additional work along with geophysical work or drilling will be evaluated as a part of mineral assessment process (Section 8.3.1.9).

Ninety-three gold analyses are available that were obtained from drill core and surface samples. An atomic absorption analysis obtained from drillhole USW G-1 at a depth of 3,515 ft (1,071.4 m) located within the Tram Member of the Crater Flat Tuff was reported to be below the analytical detection limits (less than 20 parts per million silver and 0.05 parts per million gold) (Spengler et al., 1981; Spengler, 1986). Ninety-two analyses for gold were determined by a variety of analytical methods (Broxton et al., 1986) for purposes of modeling magma genesis. The samples were obtained from drillholes USW G-1, USW G-2, USW GU-3, and surface outcrops, and are reported to be below analytical detection limits with the exception of two samples. Sixty-nine samples are below analytical detection limits of 0.12 parts per million, 14 samples below the analytical detection limits of 0.36 parts per million, and 7 samples below the analytical detection limits of 0.02 parts per million (Broxton et al., 1986). Laboratory methods with the lowest analytical detection limits detected the presence of gold in two samples: from drillhole USW G-1 at a depth of 3,659 ft (1,115 m) of 0.003 parts per million ± 90 percent and in drillhole USW G-2 at a depth of 1,691 ft (515 m) 0.06 parts per million ± 15 percent. The first analysis is close to the average crustal abundance of 0.004 parts per million (Levison, 1974) and the second is slightly anomalous, but does not represent any economic potential [redacted] information becomes available these new occurrences and deposits will be evaluated for their influence on the assessment at Yucca Mountain. Planned work and resource assessment at Yucca Mountain includes (1) comparisons of the mineralization that occurs in association with caldera complexes to the mineralization found in the region of Yucca Mountain (2) the evaluation of hypothetical ore deposits located along faults, and (3) geochemical analysis of surface and subsurface samples (Section 8.3.1.9).

1.7.1.3 Mercury resources

Mercury occurs as cinnabar (HgS) and rarely as native mercury or salt calomel (Hg_2Cl_2). Most of the worldwide reserve occurs as cinnabar (Bateman, 1950).

Nevada has been the only producer of mercury in the United States since 1982. There are at least 100 mines in Nevada from which some mercury production has been recorded (Bailey, 1964). As of 1984, however, there were only four mercury-producing mines in operation in Nevada: (1) the McDermitt, (2) the Carlin, (3) the Pinson, and (4) the Borealis. The McDermitt Mine is the principal producer of domestic mercury. The Carlin, Pinson, and Borealis mines produce mercury as a coproduct of their gold mining operations. The total production from all four mines was 16,530 flasks in 1985 with producers operating at 47 percent of capacity. This figure represents slightly more than eight percent of the total world production, making the United States the fifth largest producer of mercury in the world.

In Nevada, mercury-bearing deposits are distributed throughout the central one-third of the state in a north-south trending belt (Figure 1-81) that extends into Oregon. The larger and richer deposits are located in the northernmost portion of the belt along the Oregon border, with the richest deposits located in southern Oregon (Bailey and Phoenix, 1944; Fisk, 1968). Within the central portion of the belt, mercury is produced as a coproduct of

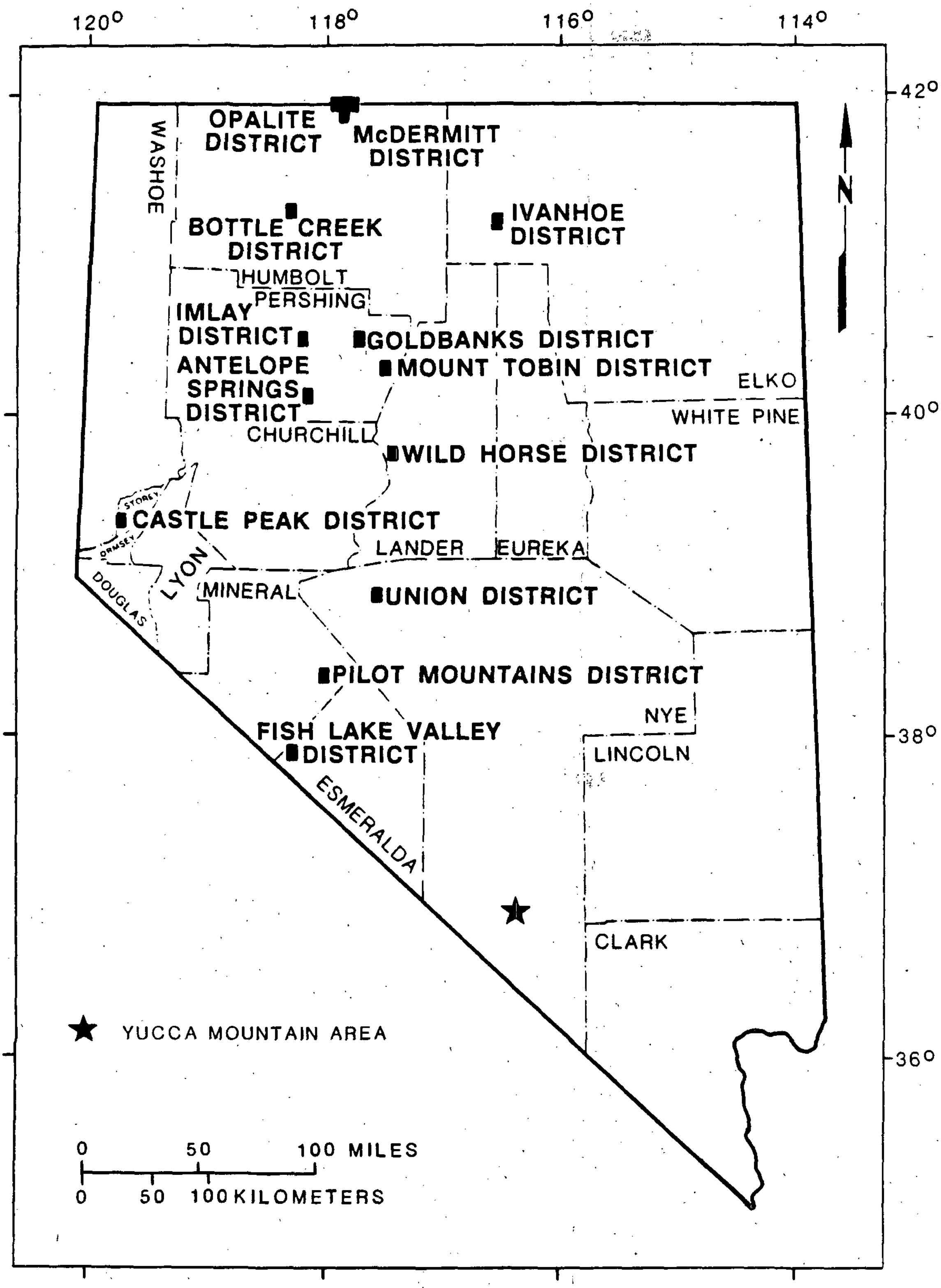

Figure 1-81. Nevada mining districts that have reported more than 100 flasks of mercury production since 1908. The deposits lie within the central one-third of Nevada, along a north-south trending belt which extends into Oregon. Modified from Bailey and Phoenix (1944) and Jones and Papke (1984).

DECEMBER 1988

Field and laboratory studies indicate that mercury deposits form from ascending hydrothermal alkaline solutions that range in temperature from 100

Small amounts of mercury have been produced from highly silicified volcanic rock at the Thompson Mine at the northwest end of Yucca Mountain (Figure 1-79, Section 1.7.1.2.2), Cornwall and Kleinhampl, 1961). No production figures have been reported, but it is assumed production was less than 100 flasks. The mercury in this area occurs as sparsely disseminated grains of cinnabar in a highly silicified and opalized tuff. The tuffs, which have been heavily altered, are probably of middle Miocene age (Carr, 1984). Additional occurrences of cinnabar have been reported from the Silicon Mine located in altered tuff to the northwest of the Thompson Mine (Figure 1-79) and at the Telluride Mercury Mine area located at Northern Bare Mountain (Cornwall and Kleinhampl, 1961; Tingley, 1984).

No indications of highly silicified, opalized, and mercury-bearing minerals have been recognized from north-central or southern Yucca Mountain during the surface geologic mapping (Lipman and McKay, 1965; Maldonado, 1985a) or in any of the drillholes (Bish, 1981; Bish et al., 1981; Carroll et al., 1981; Scott and Castellanos, 1984; Vaniman et al., 1984a). Minor occurrences of pyrite have been encountered, but only at depths (Caporuscio et al., 1982) that were likely too great to be favorable for the deposition of mercury-bearing ores. The alteration observed in the middle Miocene volcanic rocks formed under sufficient temperature, but are too deep (3,600 ft (1,097.3 m)) according to Bish and Semarge (1982), and Bish (1987) for mercury mineralization. The tuffs shallower than 1,000 m never reached

sufficient temperatures for mercury mineralization, having undergone alteration temperatures no greater than 100°C (Bish, 1987). Temperatures of 100 to 200°C are necessary for the deposition of mercury from solution.

Data gathered to date support the conclusion that there is very little potential for economic deposits of mercury at Yucca Mountain. This is supported by the following: (1) the lack of alteration typically associated with mercury deposits in north-central and southern Yucca Mountain, (2) the low alteration temperatures found in tuffs shallower than 1,148 m, (3) the shallow depth of occurrence of mercury deposits (less than 1,200 ft (366 m)), and (4) the lack of mercury mineralization in drillholes and at the surface in north-central and southern Yucca Mountain, which has approximately 1,100 ft (335 m) of relief (near the site of the perimeter drift). Primarily because of the lack of surface alteration characteristic of mercury deposits, [illegible]

1.7.1.4.1 Barite resources

Economic deposits of barite occur in igneous, metamorphic, and sedimentary rocks in many geologic environments. Deposits are classified by their mode of occurrence as (1) bedded deposits, (2) vein and cavity-filling deposits, or (3) residual deposits. Most high-grade ore is found in bedded deposits where the barite content is from 50 to 95 percent (Brobst, 1975).

Bedded deposits are widely distributed geographically and generally found in rocks of mid-Paleozoic age that are frequently associated with stratiform sulfides (Stanton, 1972). These deposits vary from a few inches to more than 100 ft (30 m) in thickness, and are believed to be of marine sedimentary origin (Shawe et al., 1969; Papke, 1984).

The vein and cavity-filling barite deposits occur with associated minerals along faults, gashes, joints, bedding planes, breccia zones, and solution channels and sink structures. The host rocks are of Precambrian to Tertiary age in the United States, and in the western states many deposits occur in association with igneous rocks of Tertiary age. The grade of barite ore in vein and cavity-fillings varies greatly between districts, as well as within districts. Although this type of deposit has yielded rich ore (e.g., collapse and sink structures in Missouri), the individual ore bodies tend to be small (Brobst, 1975). The barite and other minerals found in epithermal vein and cavity-filling deposits are believed to precipitate from low-temperature hydrothermal solutions, although there is evidence that some vein deposits may result from circulating connate and ground waters (Sawkins, 1966).

Residual deposits of barite are formed by weathering of preexisting materials, frequently Cambrian and Ordovician dolomites and limestones, and occur in unconsolidated materials. The grade of ore in these deposits is highly variable, as is the size, shape, and depth of the ore body. Some larger deposits in Georgia, Tennessee, and Missouri span several hundred acres. The shape of the deposits tends to reflect that of the original deposit (e.g., those derived from veins and channels are elongate, while those derived from sink structures are circular). In the United States, residual deposits of economic value occur primarily in the eastern and midwestern regions. Deposits of this type as well as the vein and cavity-filling types are becoming less economically attractive as more bedded barites are discovered (Brobst, 1975; Papke, 1984).

Nevada is the nation's leading producer of barite. Most of Nevada's barite reserve occurs as bedded deposits (Papke, 1984) within the central Nevada barite province (Figure 1-82; Shawe et al., 1969; Papke, 1984). Papke (1984) estimates that Nevada's barite reserves currently total 90 million short tons. All of the barite produced is from open-pit mines in near-surface, bedded deposits.

In Nevada, the most productive areas are located in the Shoshone and Toquima ranges, 390 and 215 km north of Yucca Mountain, respectively. Barite production in these areas is from bedded sedimentary deposits in the Devonian Slaven Chert Formation (Brobst, 1975), a black chert and carbonaceous shale and siltstone with minor amounts of intercalated dark limestone and brown,

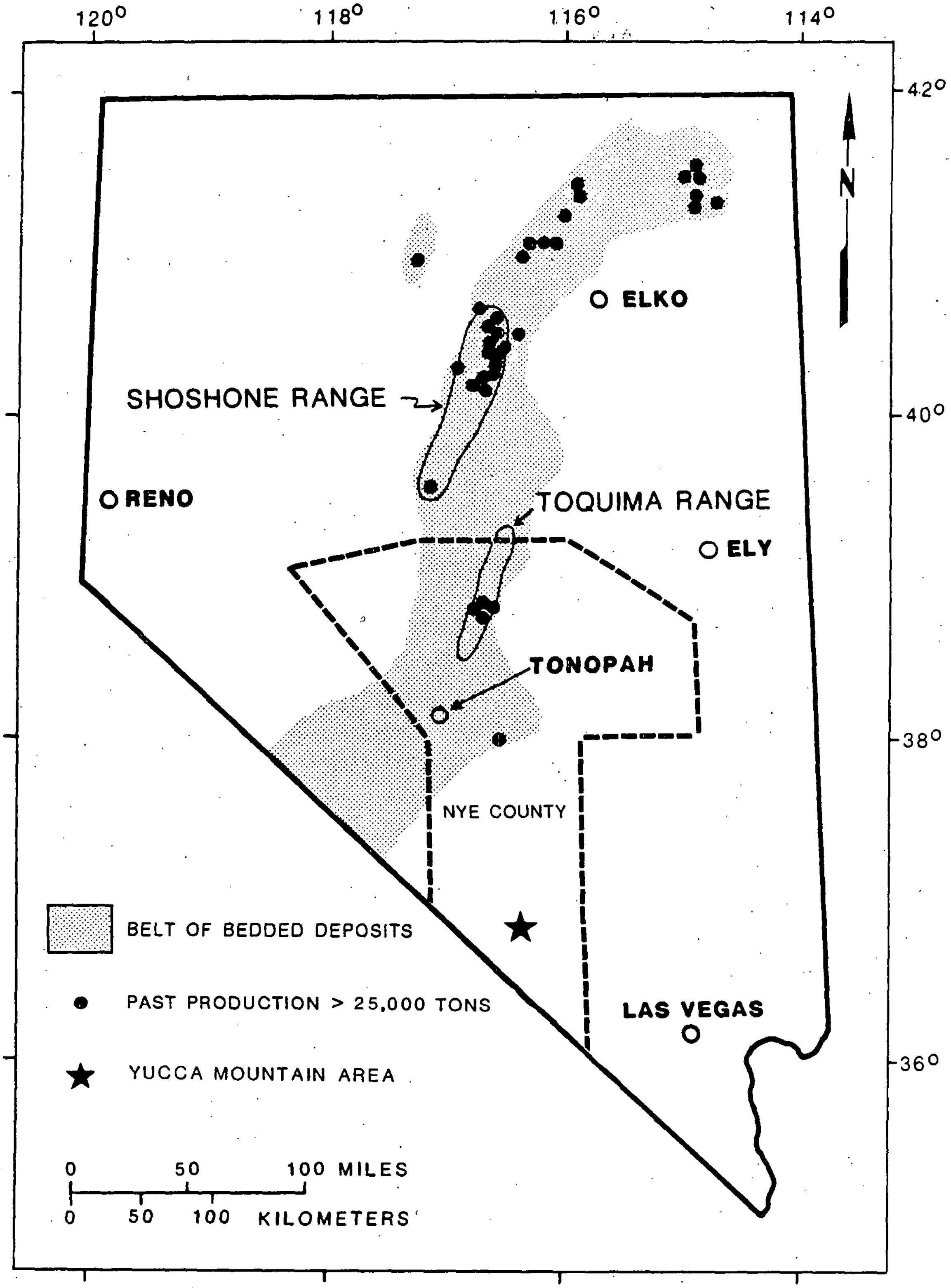

Figure 1-82. Map of Nevada showing locations of bedded barite deposits and past production within the central Nevada barite province. Modified from Shawe et al. (1969) and Papke (1985).

limey sandstone. Within other districts, bedded barites occur in similar rocks of Ordovician age (Brobst, 1975).

A barite vein was identified at Mine Mountain approximately 32 km east-northeast of Yucca Mountain, in fault breccias associated with the Devonian Devils Gate Limestone and the Mississippian Eleana Formation (Quade and Tingley, 1983). The vein, approximately 1.5 m thick, is traceable for 100 m along strike. The ore is high-grade and is associated with various sulfide minerals and minor amounts of silver (Quade and Tingley, 1983). The area was mined for mercury in the late 1920s; no barite production was ever recorded.

Barite occurrences also have been noted in the central and southeastern portion of the Calico Hills at the Nevada Test Site, approximately 18 km east of Yucca Mountain (Quade and Tingley, 1983). The barite occurs as a gangue mineral along contact zones between argillites of the Eleana Formation and the unconformably overlying dolomites of the Devils Gate Limestone. The minute quantity and the low grade of the ore in this location (Quade and Tingley, 1983) precludes it from consideration as an economic deposit. Non-economic occurrences of barite associated with calcite and fine-grained silica veins occur at Bare Mountain (Smith et al., 1983) in Paleozoic rocks.

The geologic setting at Yucca Mountain is not favorable for the occurrence of bedded barite deposits. As discussed in Section 1.2, Yucca Mountain is composed entirely of welded and nonwelded volcanic tuffs. On the basis of Silurian dolomites encountered in drillhole UE-25P#1, at least part of Yucca Mountain is underlain by Silurian rocks. Bedded barite deposits may therefore be located under Yucca Mountain at greater depth. To date, only minor occurrences of barite have been reported; one was identified in a 1-cm-thick vein at a depth of 1,736 m (dacite lava and flow breccia) in drillhole USW G-2 in association with calcite and quartz (Caporuscio et al., 1982; Maldonado and Koether, 1983). Other veins may be present, but deposits of this type are not currently economic, nor has an increase in their value been projected.

In summary, based on the current knowledge of the geologic setting at Yucca Mountain, the reported minor occurrences of barite in veins at great depth, and the absence of bedded barites in local Paleozoic rocks, the future ore are defined: acid, ceramic, and metallurgical. Acid-grade fluorspar is required to contain at least 97 percent CaF_2; ceramic-grade fluorspar at least 95 percent CaF_2, and metallurgical-grade fluorspar greater than 60 effective percent CaF_2 (Papke, 1979). The classification is additionally based upon chemical composition where unwanted silica, for example, would reduce the effective CaF_2 content of the product. Economic deposits of fluorspar are associated with igneous related hydrothermal environments and occur as replacement bodies, veins, stockworks, breccia pipes, and disseminations in a variety of rock types. The deposits commonly occur along faults, breccia zones, and fractures (Bateman, 1950; Grogan and Montgomery, 1975; Papke, 1979). Gangue minerals are commonly quartz, pyrite, and calcite (Papke, 1979). Major fluorite districts are associated with continental rifts and lineaments (Van Alstine, 1976) and are typically found in carbonate, clastic sedimentary, and volcanic rocks (Bateman, 1950; Papke, 1979). Limestones and dolomites are statistically the most important host rocks in Nevada, with clastic sedimentary rocks and silicic-intermediate volcanic rocks following in importance (Papke, 1979). Tungsten, copper, gold, mercury, zinc, molybdenum, berryllium, antimony, and lead can occur in association with fluorite (e.g., Bateman, 1950; Van Alstine, 1976; Papke, 1979).

[redacted]

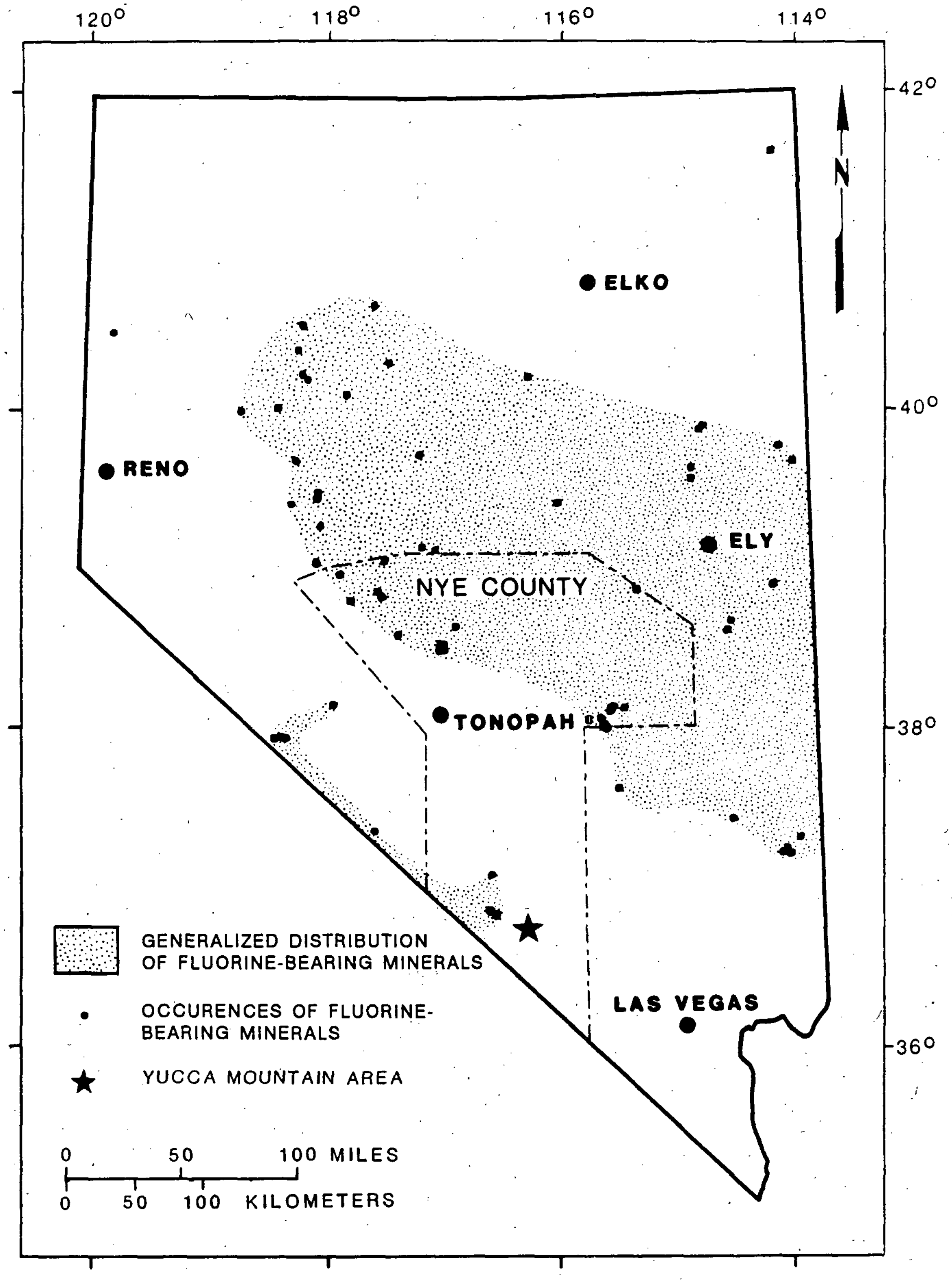

Figure 1-83. Deposits and occurrences of fluorine-bearing minerals in Nevada. Compiled from Horton (1964a). Sainsbury and Kleinhampl (1969). and Sherlock and Tingley (1985).

The single active area of production (Bare Mountain) in Nevada is located near Yucca Mountain (Carrillo and Schilling, 1985; Papke, 1985). The Daisy Mine at Bare Mountain (Figure 1-79, Section 1.7.1.2.7) has produced nearly half of the total production of fluorspar in Nevada (Papke, 1979) and is the largest deposit in Nevada (Smith et al., 1983). The Bare Mountain deposits are replacement type deposits or breccia pipes in dolomite (Papke, 1979; Smith et al., 1983). The deposits are structurally controlled by thrust and normal faults (Smith et al., 1983). The Bare Mountain fluorspar deposits include gangue minerals of montmorillonite, sericite, calcite, quartz, and kaolinite with localized minor occurrences of cinnabar, gold, stibiconite, and traces of uranium in fluorite (Cornwall and Kleinhampl, 1964; Papke, 1979; Smith et al., 1983). Fluorspar deposits could occur under Yucca Mountain in the deeply covered Paleozoic rocks, but would generate little or no future exploration interest because of (1) the great depth, (2) the typically small size of deposits in Nevada, and (3) the vast abundance of known worldwide reserves and probable resources that occur

No occurrences or deposits of fluorspar are reported on the Nevada Test Site or the Nellis Bombing and Gunnery Range (Quade and Tingley, 1983). Rare occurrences of fluorite in small veinlets and fracture fillings within tuff have been reported at Yucca Mountain; these were located during drilling in the tuffs and are of limited extent, of very low grade, or both; likely contaminated by silica; and typically occur at great depth (drillhole USW GU-3: samples 1027.0 at 313 m and 4803.2 at 1,464 m and drillhole UE-25b#1H: sample 3185 at 970 m and sample 3602 at 1,097 m) (Caporuscio et al., 1982; Vaniman et al., 1984a). In drillhole USW G-2, fluorite was observed in thin-section filling vesicles and replacing plagioclase phenocrysts at a depth of 1,595 m (Maldonado and Koether, 1983). These occurrences of fluorite indicate some hydrothermal activity within the tuff. Because these occurrences are rare, of very low grade, and occur at great depth, they are not thought to be indicative of any potential for deposits of fluorite within Yucca Mountain.

Yucca Mountain has a low potential for future economic deposits or future exploration for fluorite because (1) known occurrences are rare and of low grade; (2) deposits in ash-flow tuffs are typically low-grade; (3) numerous, but poorly described reserves exist elsewhere in Nevada; (4) worldwide reserves are vast and indicate that much more readily extractable fluorspar probably exists worldwide and in the United States at the surface; and (5) known occurrences at Yucca Mountain are minor replacements of limited extent and size. The site is not considered to be a resource with respect to fluorite, and fluorite is classified as an other occurrence (Figure 1-74).

1.7.1.4.3 Zeolite resources

Zeolite minerals are hydrated aluminosilicates containing alkali and alkali earth cations, principally sodium, potassium, and calcium. Zeolite minerals are the most common authigenic phase in sedimentary rocks (Sheppard, 1975). Only small tonnages are mined today, approximately 300,000 tons per

In comparison, the large proportion of reserves known to exist is measured in trillions of tons (Sheppard, 1975). Higher quality synthetic zeolites have been commercially produced since the 1950s (Sheppard, 1975). Zeolites have many industrial and agricultural uses, including uses as an ion exchange material with radioactive materials (Mumpton, 1975, 1977b). The use of zeolites is expected to greatly increase in the future (Sheppard, 1975; Mumpton, 1975, 1977b). Zeolite minerals are also discussed in Section 1.2.2 and Section 4.1.1.

Large tonnages are known to exist in the United States, particularly in Cenozoic deposits in the gulf coast and the western half of the United States (Olson, 1975; Sheppard, 1975). Exploration and sampling of deposits have occurred in Arizona, Wyoming, Texas, and Nevada and have been mined in Bowie, Arizona; Hector, California; and Jersey Valley, Nevada (Sheppard, 1975). In addition, it is estimated that 120 million tons of zeolites, which occur as pure and readily extractable surface deposits, are available in the Basin and Range province (Sheppard, 1975). Large reserves at or near the surface are also available in Nevada (Papke, 1972).

Papke (1972) has described four major deposits in Nevada: the Eastgate deposit located in Churchill County, the Jersey Valley deposit located in Pershing County, the Pine Valley deposit located in Eureka County, and the Reese River deposit located in Lander County. these major zeolite deposits are derived from silicic ash falls that were deposited in saline or alkaline lakes that are Pliocene to Pleistocene in age (Papke, 1972). The deposits are described as being extensive, but no volume estimates are given.

Zeolites form during diagenesis and most commonly result from the reaction of meteoric or connate waters with volcanic glass in sediments (Sheppard, 1975; Hay, 1978). Of the 30 or more known zeolites, the most common are analcime, clinoptilolite, heulandite, laumontite, phillipsite, and mordenite (Sheppard, 1975; Hay, 1978), with clinoptilolite, mordenite, and analcime being the most common on the NTS (Hoover, 1968) and at Yucca Mountain (Bish and Vaniman, 1985). Zeolites form in a variety of geologic environments where volcaniclastic rocks are available: (1) saline and alkaline lake and soil environments, (2) sea-floor sediment piles, (3) hydrothermal environments, (4) environments resulting from burial diagenesis, and (5) percolating water in an open system (Sheppard, 1975; Hay, 1978). Very high tonnages of monomineralic deposits are found in saline and alkaline desert lakes that contain airfall tuffs (Sheppard, 1975; Mumpton, 1975; Hay, 1978) and in sea-floor sediments were zeolites may comprise 80 percent of the sediment (Boles, 1977). The lower-grade zeolite occurrences on the NTS and at Yucca Mountain are formed by the percolation of water down through the unsaturated zone in an open system environment (Hoover, 1968). In some locations on the NTS, the locus of zeolitization is controlled by impermeable horizons in the silicic tuffs (Gibbons et al., 1960). In contrast, closed system deposits are common in the sediment filled basins of the Basin and Range Province (Surdam, 1977, 1979).

The variety of zeolite minerals formed in an open system environment changes with or is zoned with depth, and these zonations crosscut stratigraphic boundaries (Hay and Sheppard, 1977). With increasing depth, zones rich in clinoptilolite, mordenite, and analcime, respectively, are observed on the NTS and at Yucca Mountain (Hoover, 1968; Bish and Vaniman, 1985).

These zonations are thought to have formed predominantly, at temperatures between 25 and 65°C (Hay and Sheppard, 1977) and, thus, are not the result of hydrothermal or burial metamorphic conditions (Hoover, 1968).

Four zeolite zones, which can be mapped, have been identified at Yucca Mountain (Section 1.2.2) from drillhole data (Bish et al., 1984; Vaniman [redacted]

ash flows that remain glassy during the cooling of the sheet and (2) correlated with the nondevitrified and nonwelded tops, bottoms, and distal edges of the ash-flow sheets (Bish and Vaniman, 1985). Exceptions do occur; for instance, zeolites are found in the fractures of the tuff units (Carlos, 1985). The zeolitized zones are commonly discontinuous, highly variable in the amount of zeolites present, and laterally vary in thickness (Bish and Vaniman, 1985). All of the significant occurrences in Yucca Mountain are in bedrock and occur at depths greater than 500 m (Bish and Vaniman, 1985).

To evaluate or compare any potential resources or reserves, an estimate of the tonnages of zeolites available at Yucca Mountain was calculated. A summed thickness of zeolites was obtained from drillhole data presented in Bish and Vaniman (1985). The maximum thickness (summed total) of zeolites observed was found in drillhole USW G-2 with 300.9 m of zeolitized tuff, having greater than 50 percent zeolites. From one drillhole to another, the thickness of zeolites can be highly variable. This is considered to be a conservative analysis because this maximum thickness obtained from drillhole USW G-2 is used to calculate the total tonnage of zeolites available at Yucca Mountain. As described previously, this zeolite thickness is not continuous, of constant grade, or laterally of the same thickness. An area of 5 by 9 km was used to estimate the tonnage over southern Yucca Mountain (the approximate area where drillhole coverage is available). The density of zeolite minerals range between 2.0 and 2.3 g/cm^3 (Deer et al., 1963). A density of 2.3 g/cm^3 was used in the calculations. Approximately 30 trillion long tons of zeolites are available using the conservative estimates described previously.

The tonnages, for the general alluvial valley fill of the NTS, were also calculated using a conservative 13 by 17 km area and the same thickness of zeolitization used for Yucca Mountain. This thickness is considered to be a conservatively low estimate for making comparisons to Yucca Mountain because much thicker deposits of volcaniclastic material containing zeolites are

Nevada has never been estimated because the present day economic incentives are low. However, vast reserves exist in Nevada and large reserves exist near Yucca Mountain. For example, there are plans to mine zeolites near Eastgate, Nevada (Eyde, 1987) and zeolitic ash-fall tuff of Miocene Age is being mined near Ash Meadows (Pexton, 1984), but estimates of reserves are not available. New production at Ash Meadows is expected to have an initial production capacity of 45 kilotons per annum of clinoptilolite (Eyde, 1986; Schilling, 1987). In comparison within the easily extractable zeolite resources available, the zeolite tonnages available at Yucca Mountain are analogous to the elemental content of the average continental rock, where the element is present, but in such low concentrations that it will not likely ever be an economic resource (see "methods of mineral-energy-resource assessment" in Section 1.7, introduction). The definition of a resource specifies that it is or may be economically extractable, now or in the future (see discussion in introduction to Section 1.7 under "definition of mineral resources and reserves").

In summary, zeolites at Yucca Mountain are not classified as resources or reserves because of the following: (1) zeolites are common in sedimentary volcaniclastic rocks that are widely distributed over the region; (2) small tonnages will probably be mined in the future compared with the large volume

Table 1-21. Construction materials found in the vicinity of Yucca Mountain[a] (page 1 of 4)

Number	Location	District	Commodity	Status	Description	Operation	Production	Owner or claimant
(1)	Sec 19 T11S R48E Bare Mountain	Silicon (Monarch)	Ceramic silica	White Lode: 7 claims	Hydrothermal alteration and silicification of rhyolitic tuff. Ore runs 99.7% SiO_2 and 0.04% Fe	Surface pit 150" wide	Produced from 1918-1929	B. London
(2)	NW/4 Sec 19 T11S R48E	Bare Mountain	Bentonite	Future Grp. claims	Alteration of rhyolitic tuff	1 shaft, 1 adit, 1 prospect, pit	ND[b]	Spicer Mining, Beatty
(3)	Secs 20, 25 T11S R48E	Bare Mountain	Bentonite?		Alteration of rhyolitic tuff	5 prospect pits, 1 shaft	ND	
(4)	NW/4 Sec 29 T11S R48E	Shepard Bare Mountain	Kaolin clay	Inactive White Lode: 7 claims	700 by 125 ft NW-trending outcrop. Is alteration product of quartz porphyry of tuff. First opened as cinnabar deposit but contains little Hg.	3 pits	1 carload shipped in 1918	B. London
(5)	Sec 32 T11S R48E	Elizalde Bare Moun-	Halloysite clay	Inactive	ND	ND	ND	
(6)	NW/4 Sec 8 T12S R48E	Bare Mountain	Bentonite and zeolite		ND	ND	ND	
(7)	SW/4 Sec 18 T12S R48E	Kiernan Bare Mountain	Clays		Occurs in area of limestone and quartzite. Contains too much hematite for pottery.	Surface	Past producer: 1 carload shipped in 1917	
(8)	Sec 18, 23 T12S R48E	Bond & Marks Bare Mountain	Clays		Halloysite and alunite in carbonaceous argillaceous bed. Contains too much hematite for pottery. Some rutile present.	Pit	Past producer: 4 cars, 1918	

Table 1-21. Construction materials found in the vicinity of Yucca Mountain[a] (page 2 of 4)

Number	Location	District	Commodity	Status	Description	Operation	Production	Owner or claimant
(9)	SW/4 Sec 25 T11S R47E	Beatty Wash Bare Mountain	Perlite	B.J. Grp. claims	Glassy facies of rhyolitic flows		None	W. G. Ohm
(10)[c]	NE/4 Sec 10 T12S R17E	Bare Mountain	Perlite		Glassy facies of rhyolitic flows		None	
(11)[d]	Sec 15 T13S R48E	Black Cone Crater Flat	Pumice	Hg 1 + 2 claims	Pumiceous basalt		Some	J. Spicer
(12)	SE/4 Sec 28 T11S R47E	Oasis Valley	Pumice	ND	Pumiceous basalt		Some	
(13)	Sec 28, 29 T13N R48E	Red Cone Crater Flat	Cinder	RE-Hg 4 claims	Volcanic cinder cone			J. Spicer
(14)	Sec 36 T14S R48E, Sec 31 T14S R49E, Sec 6 T15S R49E	Cind-R-lite 8 claims: Lost, Found, Red Cone, Nevada-Genesis, Revelation, Red Cone Ext., Red Bird, Right Spot-Overnight	Pumice, volcanic cinders	Active Pat. pending on Lost, Found, Red Cone Ext. claims	Mining of edges of volcanic cinder cones	Pit mining with multiple benches	ND	Cind-R-Lite Block Co., Las Vegas
(15)	SW/4 Sec 13 T14S R47E		Gravel			1 pit		
(16)	W/2 Sec 34 T14S R48E	Yucca Mountain	Gravel			2 pits		
(17)	T10S R52E, T11S R53E	Yucca Lake	Gravel	ND		10 pits	Some	
(18)	Secs 8, 18 T13S R51E	Jackass Flat	Gravel			6 pits	Some	
(19)	Sec 14, 15, 31, 32 T14S R52E		Gravel			5 pits	Some	
(20)	SW/4 Sec 9 T14S R49E	Lathrop Wells	Gravel			1 pit	Some	

(21)	SW/4 Sec 10 T15S R49E	NV-03-2 Pit Lathrop Wells	Gravel	Int. active	1 pit, crusher and screens. Single bench	Some	L.A. Young, Lathrop Wells
(22)	Secs 18, 19 T15S R50E	Lathrop Wells	Gravel		2 pits	Some	
(23)	NW/4 Sec 30 T15S R51E	Lathrop Wells	Gravel		1 pit	Some	
(24)	Secs 22, 25, 26	Amargosa	Gravel		4 pits, 3 prospect	Some	

Table 1-21. Construction materials found in the vicinity of Yucca Mountain[a] (page 4 of 4)

Number	Location	District	Commodity	Status	Description	Operation	Production	Owner or claimant
(33)	Sec 29 T16S R50E	K-B Amargosa	Montmorillonite	Interm. active Ewing claims	Horizontal, bedded, playa lake deposits 2 to 6 ft thick overlain by calcerous siltstone and underlain by gypsiferous clay. Deposits probably Plio-Pleistocene.	Surface trench and pit, 4 shafts, 27 prospect pits	?	Ind. Min. Ventures
(34)	Secs 31, 33, 34, 35, 36 T16S R50E	Amargosa	Clay?	Cat claims		25 prospect pits		Ind. Min. Ventures

[a]Data from Bell and Larson (1982) except as noted otherwise. Question marks indicate data uncertainty.
[b]ND = no data.
[c]From Cornwall and Kleinhampl (1964).
[d]From Cornwall and Kleinhampl (1961).

(7) the amount of production, and (8) the owner of the claim or mine (if applicable).

The clay deposits listed in Table 1-21 were formed in two different types of geologic environments. Those in the Amargosa District (numbers 26 to 34 in Table 1-21) probably formed by the alteration of glassy, air-fall volcanic ash that was deposited in the alkaline playa lakes that existed during the Plio-Pleistocene time (Bell and Larson, 1982). Production of this clay is continuing (Jones, 1987) and new reserves are being defined. This geologic setting is absent at Yucca Mountain.

The second type of clay deposits is located in the Bare Mountain district, and includes bentonite, kaolin, and halloysite (numbers 2 to 8 in Table 1-21); these were formed by the alteration of rhyolitic tuffs. These deposits have had minimal production (Lincoln, 1923) and are not considered to be of economic importance (Bell and Larson, 1982). Deposits located in the densely welded and nonwelded tuff that occur 1.5 mi (2.4 km) south of Beatty have had historical production (Cornwall and Kleinhampl, 1964). No deposits of this type are known to occur at Yucca Mountain.

Travertine, a massive layered calcium carbonate deposit formed by deposition from springs (especially hot springs), is known to occur in the Amargosa Desert (Table 1-21). No spring deposits are known to occur in close proximity to Yucca Mountain. Calcite, opaline-silica, and sepiolite deposits are known to occur in association with faults in proximity to Yucca Mountain (Section 1.2.2.2.10), but the origin of these deposits is not known (further work is planned and is presented in Section 8.3.1.9). Regardless of the origin of these deposits, because they (1) are of such limited extent, (2) contain abundant and variable amounts of opaline silica, and (3) contain abundant and variable amounts of sepiolite, they would likely never be considered to be of economic importance.

Perlite, a glassy volcanic rock that is used as a lightweight aggregate, occurs in Quaternary to Tertiary andesite and rhyolite tuffs (Chesterman, 1975). Specifications for industrial use include that the perlite contain no more than two percent mineral grains or lithic fragments, and that the weight percent of bound water is between two and five percent. Two occurrences of perlite (9 and 10 in Table 1-21) have been identified in the vicinity of Yucca Mountain: one in Beatty Wash at Bare Mountain in a glassy facies of rhyolitic ash flows, and another located in the NE 1/4, Section 10, T. 12 S., R. 47 E. (Cornwall and Kleinhampl, 1964). There has been no production from these deposits (Bell and Larson, 1982) and no occurrences of perlite have been identified at Yucca Mountain. Petrographic and mineralogic studies of the tuffs present at Yucca Mountain revealed abundant lithic fragments (highly variable from 0 to 40 percent) in most units (Warren et al., 1984), and bound water to be less than one percent by weight (Cornwall, 1972). Thus, if perlite is present at Yucca Mountain, it would probably not be suitable for industrial uses.

Volcanic cinders and pumice (numbers 11 to 14 in Table 1-21) have been mined from the basaltic cones at Crater Flat, 5 to 10 km to the west and southwest of the proposed controlled area boundary. The Lathrop Wells basaltic cinder cone is currently being mined. Basaltic cones are shown in

Figure 1-79. Yucca Mountain, which is composed of welded and nonwelded silicic tuffs, has no potential for cinders and pumice that are derived from basaltic eruptions.

A single deposit of silica was mined at the Silicon Mine for ceramic silica (number 1 in Table 1-21). The Silicon Mine is located in the silicified and altered rhyolite tuffs northeast of Bare Mountain on the northwestern end of Yucca Mountain, more than 10 mi (16 km) from central and southern Yucca Mountain (Figure 1-79, Section 1.7.1.2). The mine (a shallow pit) had a moderate, but unknown, amount of production from 1918 to 1929 (Bell and

1.7.1.5.1 Uranium resources

Refined uranium ore is principally used to make weapons and generate electric power (Butler, 1964; Garside, 1973). Uranium minerals and oxides are found in a variety of different geologic environments and temporal spacings. Ninety percent of readily accessible reserves are found in Precambrian age rocks or in Phanerozoic rocks immediately and unconformably overlying Precambrian rocks (Bowie, 1974). Sandstones of various ages contain nearly a third of the world's resources and in excess of 95 percent of the United States' reserves (Adler, 1974). Less important deposits in the United States occur in limestone and carbonaceous organic-rich deposits, and in young and distinctly subordinate vein and fracture related deposits (Garside, 1973; Proffett, 1979).

In Nevada, 28 mines have produced 137,792 pounds (62,633 kg) of uranium oxide (U_3O_8), 80 percent of which was from the Apex Mine in Lander County (Garside, 1973). No production has occurred in Nevada since 1968 (Garside, 1973). Deposits and occurrences of uranium in Nevada are concentrated in central and northern Nevada along the State's western boundary (Sherlock and Tingley, 1985). Almost all of the production in Nevada has been from the vein-type deposits. These vein deposits are irregularly distributed, small in size (Butler, 1964), and occur in rocks altered by hydrothermal activity (Butler, 1964; Schrader, 1977).

Disseminated occurrences of uranium are known to occur in silicic tuffs, such as the McDermitt Caldera Complex deposits, which are also well known as areas of mercury mineralization (Figure 1-81, and Section 1.7.1.3). The uranium mineralization and occurrences are associated with hydrothermal activity (Rytuba et al., 1979; Rytuba and Conrad, 1981; Rytuba and McKee, 1984). The Apex Mine is another Tertiary-age vein and disseminated uranium deposit that is localized in highly fractured and faulted metasediments where the uranium mineralization is believed to have resulted from the chemical interactions at an ancient ground-water table boundary (Garside, 1973; Plut, 1979).

Garside (1973) has reviewed all known occurrences of uranium in Nevada. The type of host rock and kind of uranium occurrences are highly varied. The nearest occurrences of uranium to Yucca Mountain are located at Bare Mountain in Paleozoic carbonate rocks associated with fluorite. These occurrences at Bare Mountain are described by Garside (1973), Tingley (1984), and discussed in Section 1.7.1.4.2 (fluorspar resources). Uranium deposits that occur in silicic tuffs are more appropriately compared to Yucca Mountain. Uranium occurrences in Tertiary volcanic rocks are divided into two lithologic subtypes by Garside (1973), those that occur in (1) plugs and lava flows and (2) ash-flow tuffs. Fifty-five occurrences of uranium are known in ash-flow tuffs, mostly in Elko County and Washoe County, Nevada (Garside, 1973). Generally, these occurrences are associated with ground-water interactions or hot thermal waters that interact with the tuff rock and deposit uranium. The Bullfrog and Tonopah districts (Section 1.7.1.2.2, Table 1-19, Figure 1-77) have occurrences of uranium that may be associated with hot thermal waters or leaching of tuff by ground water (Garside, 1973).

Tuffaceous rocks, such as those at Yucca Mountain, are thought to be possible sources for uranium deposits by weathering, ground-water, and near-surface processes that leach uranium and concentrate it elsewhere (Rosholt et al., 1971; McKee, 1979; Kizis and Runnels, 1984). Results of experimental leaching of glassy volcanic rocks are interpreted to indicate that the most important environmental parameter is the prolonged contact of glass with circulating thermal waters and thus intra-caldera areas are most favorable for economic deposits (where uranium traps are available) (Zielinski, 1981). Volatilization has also been shown to be a major factor in the location of uranium in silicic volcanic rocks (Gabelman, 1981). Tuffaceous rocks may be the source of many of the deposits in Nevada, even though tuffs typically contain only small amounts of uranium. For example, the Bishop Tuff contains only 2 to 8 parts per million of uranium (Hildreth, 1979). The 166 samples obtained from the surface and subsurface at Yucca Mountain and from the Topopah Spring Member of the Paintbrush Tuff contain from 1.2 to 8.7 parts per million uranium (Table 1-18) with an average concentration of 3.7 parts per million (Broxton et al. 1986; Schraytz et al., 1986). Thorium contents are also low in these same rocks with an average concentration of 21.4 parts per million for 166 samples (Table 1-18). The thorium to uranium ratio is 5.7 which suggests that little if any uranium has been leached from these rocks. This in turn argues against possible uranium accumulations nearby due to leaching of uranium from the tuffs.

Uranium deposits may result from the interaction of hot solutions. Deposits of this type in tuffaceous rocks are commonly small vein deposits, often occurring with fluorite or base metals, gold, and silver, in altered rock that is often silicified, opalized, and bleached (Butler, 1964; Garside, 1973; McKee, 1979; Cunningham et al., 1982). Uranium concentrates along faults, permeable zones, localities that contain charcoal or carbonized wood (Butler, 1964; Garside, 1973), or potentially in rocks that underlie the tuffaceous rocks.

The potential at Yucca Mountain for uranium deposits is considered to be low. Most reserves and resources are contained in sedimentary rocks in the western United States (Guilbert and Park, 1986). The abundance of uranium mined and counted as reserves and resources in Nevada is low (Garside, 1973) in comparison with other known deposits in the United States. For example, the sandstone-roll-front deposit at the Yellow Chief Mine in Utah produced greater than 40 million pounds (18 million kilograms) of U_3O_8 (Lindsey, 1978) in comparison with the State of Nevada's total production of 137,792 pounds (62,633 kg) of uranium oxide (Garside, 1973).

Vein deposits are considered only to be a small source of uranium in the United States (Butler, 1964). In addition, exploration costs for vein deposits are exceedingly high because exploration techniques other than close spaced drilling cannot be recommended (Garside, 1973). Thus, future production of uranium in Nevada will probably be as a byproduct of mining other resources.

Because of the lack of any known uranium mineralization at Yucca Mountain, the site is considered to have a low potential for uranium, given the typical content of uranium in ash-flow tuffs of up to 30 parts per million (Garside,1973). Available data (Table 1-18) on the variation of the uranium content found in the Topopah Spring Member and other tuff units present at

Yucca Mountain (Broxton et al., 1986; Schuraytz et al., 1986) suggest that little remobilization of uranium has occurred and that the processes responsible for vein or disseminated deposits have not been active. Based on the existing data base, uranium is considered to be a speculative, undiscovered resource of subeconomic grade (Figure 1-74). Further evaluation is planned in the form of geochemical analysis of surface and subsurface samples (Section 8.3.1.9). No other evaluation of uranium resources at Yucca Mountain will be necessary unless silicified bleached rock, extensive fluorite veins, charcoal carbonized wood, indications of significant uranium mobilization, or other associations indicative of uranium are discovered during the course of sampling, drilling, or mining.

1.7.1.5.2 Geothermal resources

The short exploitation history of hydrothermal resources (White et al., 1971) leads to the difficult problem of assessing the future potential of hydrothermal resources and reserves. Problems arise from the new technologies, evaluation procedures, and often conflicting use of new terminology being developed for hydrothermal resources and reserves. Nonetheless, the definition of differing thermal regimes for hydrothermal resources has been based on an engineering and a geologic rationale for their potential.

Various schemes have been developed for classifying thermal reservoirs. One of the most widely used classifications divides thermal reservoirs into three regimes (Muffler and Guffanty, 1979): (1) high-temperature systems, greater than 150°C; (2) intermediate-temperature systems, 90 to 150°C; and (3) low-temperature systems, less than 90°C. These thermal regimes correspond to potential uses of the thermal waters; for example, (1) high-temperature systems provide the steam used in the generation of electrical power, (2) intermediate-temperature systems provide the heat used in various industrial processes (Brook et al., 1979), and (3) low-temperature systems are potentially available for use in space heating and agriculture (Samuel, 1979). This classification is for evaluation of geothermal reservoirs and not necessarily applicable to spring or near-surface drillhole temperatures. Other factors that play a role in determining the potential for a geothermal resource or the value of a reserve include (1) that the depth of thermal water be less than 3 km (White, 1973) or in low-temperature geothermal systems at depths less than 1 km (Sammel, 1979), (2) that the volume of available fluid be large enough to sustain its use or greater than 5 km^3 (White, 1973), (3) that the rock has an adequate permeability to sustain its water flow (White, 1973), and (4) that the thermal fluid does not contain a high proportion of corrosive dissolved solids (White et al., 1971; Trexler et al., 1979).

The ultimate source of geothermal water is discussed in terms of two models in which thermal waters are generated from (1) areas of deep-seated regional high heat flow that form hydrothermal conductive system which may be aided by convection (Renner et al., 1975; Brook et al., 1979) and (2) igneous related hydrothermal systems where cooling high-level silicic or mafic magma bodies provide the energy for high heat flow (Smith and Shaw, 1975, 1979).

the high temperatures found in most regional geothermal systems for extended periods of time (Renner et al., 1975). Low-temperature systems may occur as a result of either model but typically are dominated by conduction-related

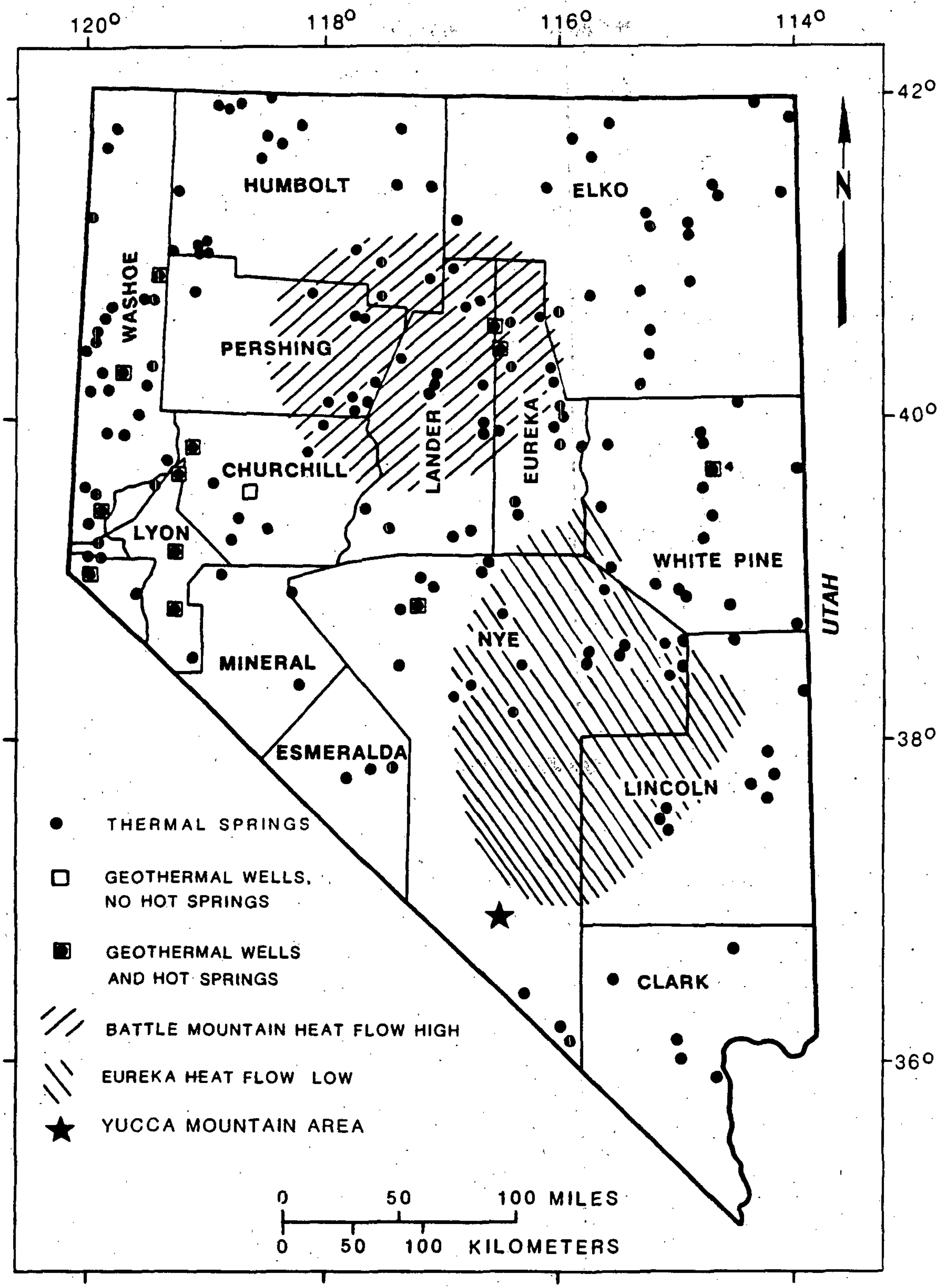

Figure 1-84. Hot springs and geothermal wells and low-temperature thermal resources in Nevada. The Battle Mountain high and the Eureka low heat-flow regions are also shown. Modified from Garside (1974).

accurately reflect the amount of energy available than do simple down-hole temperatures. Simple down-hole temperature measurements can be affected by a variety of hydraulic flow conditions and the changing thermal conductivities of the rock along the flow path.

Heat flow and the thermal gradient

Generally, heat flow and thermal gradient are considered in assessing geothermal reservoirs because heat flow, thermal gradient, and thermal conductivity of the rocks are simply related by Fourier's Law, such that

$$r = q/K \qquad (1\text{-}2)$$

where

r = the thermal gradient expressed in °C/km
q = heat flow in 10^{-6} cal/cm^{2}s
K = thermal conductivity in µcal/((cm)(s)(°C)).

Thermal gradient is directly proportional to heat flow, but inversely proportional to thermal conductivity (White, 1973).

Average continental geothermal gradients typically range from 20 to 30 Celsius degrees per kilometer (Press and Siever, 1982). In Nevada, thermal gradients generally range from 30 to 60°C per kilometer (Garside and Schilling, 1979). Thus, by comparison, Nevada has a higher than average thermal gradient. The average heat flow in Nevada is 2×10^{-6} cal/cm^{2}s (2 heat flow units (HFU)) (Garside and Schilling, 1979). The average continental heat flow is 1.5×10^{-6} cal/cm^{2}s (1.5 HFU) (Sass et al., 1971). In general, Nevada would be expected to have a high potential for geothermal energy based on the heat flow data.

Regional heat flow maps can be useful in delineating areas of above average potential for geothermal resources. Regional heat flow maps are available from several sources, including Lachenbruch and Sass (1977) (Figure 1-85), Sass et al. (1978), Blackwell et al. (1981), Nathenson et al. (1983), and Nathenson and Guffanti (1988). Within Nevada, several regions of abnormally high or low heat flow are present. The Battle Mountain high in northern Nevada (Figure 1-85) has an average heat flow of 3×10^{-6} cal/cm^{2}s (3 HFU) (Garside and Schilling, 1979) and the Eureka low (Figure 1-85) has an average heat flow of less than 0.7 to 1.5×10^{-6} cal/cm^{2}s, or less than 0.7 to 1.5 HFU (Sass et al., 1971; Lachenbruch and Sass, 1977). The Battle Mountain high is interpreted as having a very high heat flow region due to the transient effect of recent crustal intrusion by silicic magma (Sass et al., 1971), whereas, nearly the whole of the Basin and Range has high heat flow because of near-melting conditions in the lower crust and upper mantle (Roy et al., 1968, 1972; Lachenbruch, 1970). The Eureka low is interpreted in two ways by Sass et al. (1971). It could be a crustal region where temperatures in the lower crust and upper mantle have been below the solidus for some time, or more likely, it could be the result of complex interbasin water flow. The complex interbasin water flow would be regionally systematic with appreciable downward flow of relatively cool waters to a depth of approximately 3 km (Sass et al., 1971). Sass and Lachenbruch (1982) indicated that this latter model would require that (1) ground water is

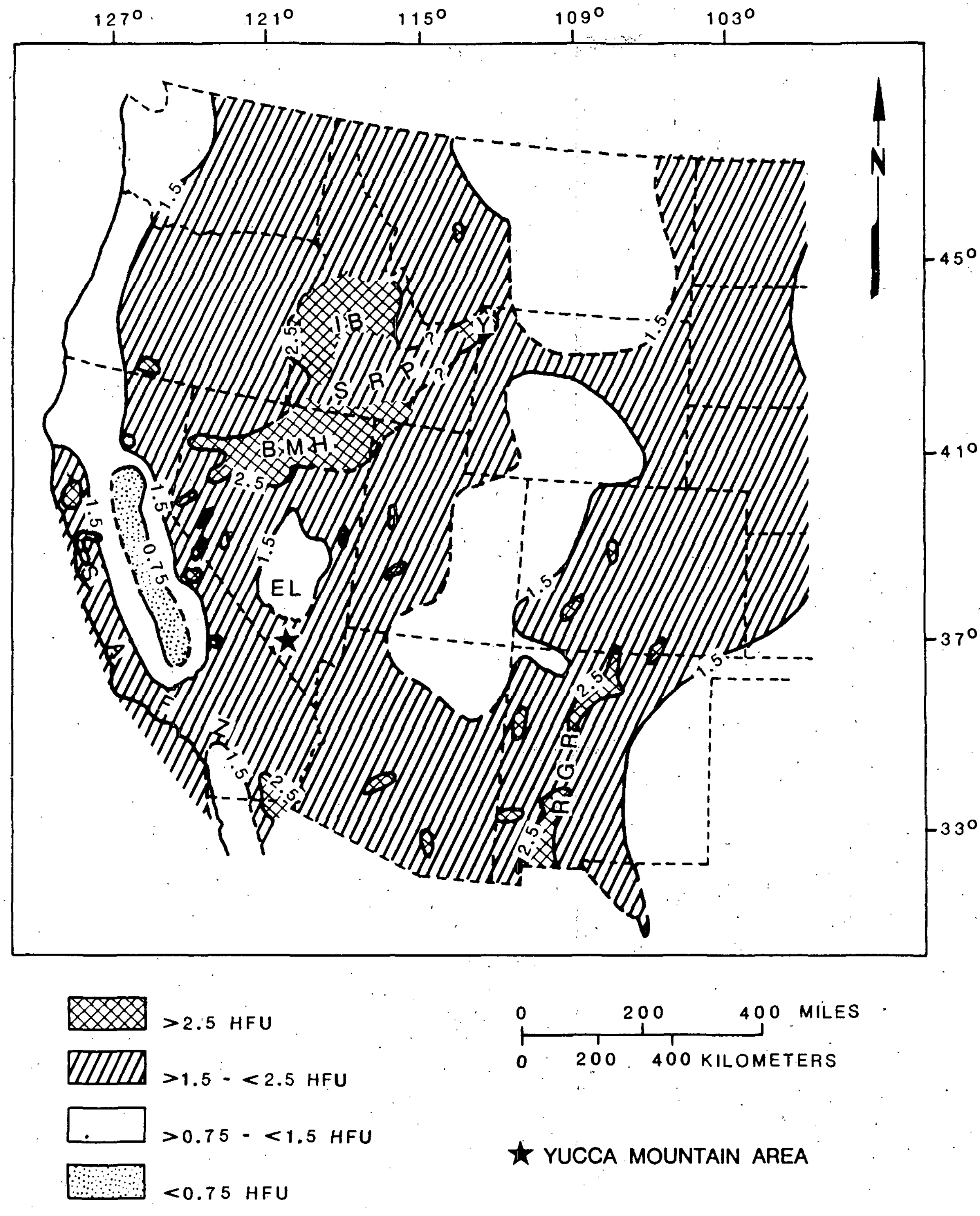

Figure 1-85. Regional heat flow and distribution of hydrothermal systems. Abbreviations are BMH for Battle Mountain high, EL for Eureka low, IB for Idaho batholith, SRP for eastern and central Snake River Plain, Y for Yellowstone thermal area, RGR for Rio Grande Rift, and SAFZ for San Andreas fault zone. Modified from Lachenbruch and Sass (1977).

carrying off much of the earth's heat in the upper 3 km and delivering it elsewhere and that (2) the heat flow at depth, beneath the Eureka low, could be the same as that characteristic of the Great Basin (2 HFU) or may be as high as 2.3 HFU. Blackwell (1978) related the Eureka low to a crustal region where older volcanism has occurred, in comparison to the Battle Mountain high where more recent volcanism has occurred. Finally, Lachenbruch and Sass (1978) related the heat flow in the Basin and Range to areas of rapid active crustal extension, such as the Battle Mountain high. Sites near the Battle Mountain high would have a higher potential for geothermal resources and sites near the Eureka low may have a lower potential for exploitation of geothermal resources. Yucca Mountain is located just outside the southern fringe of the Eureka low (Figure 1-85).

Interpretation of silica geothermometry data (used to predict heat flow) may suggest that the heat flow under the Eureka low is near the average for Nevada (2.0 to 2.5 HFU). Swanberg and Morgan (1979, 1981) have produced heat flow contour maps of the western United States based upon regional silica geothermometry data and these maps indicate that most of Nevada, including the Eureka low and Yucca Mountain, would fall in a zone of greater than 2.5 HFU. Caution must be employed in the interpretation of this silica geothermometry data because (1) the geothermometer has only been calibrated in a few areas in carbonate aquifers (i.e., much of Nevada is covered by silica-rich volcanics which could influence the abundance of silica), (2) the data base has been applied on the scale of the continental United States so care should be taken in applying interpretation to a localized area, and (3) the silica geothermometer is based on an empirical relationship that, in turn, is related to heat flow by another empirical relationship. Further assessment of the Eureka low, site-specific silica geothermometry, and other heat flow and temperature gradient data are planned (Section 8.3.1.9).

Potential for hydrothermal resources at and near Yucca Mountain

The assessment of the potential for economic hydrothermal resources at or near Yucca Mountain considers the temperatures of local ground waters, local heat flow estimates, local geothermal gradients, and local chemistry of the ground waters in comparison to the statewide and regional geothermal areas of the Basin and Range Province discussed under the previous two subheadings of this section.

Regional spring and down-hole temperatures range from 21 to 65°C (Sass et al., 1980; Bell and Larson, 1982; Sass and Lachenbruch, 1982) with one exception reported for drillhole UE-20f of 125°C at approximately 3,700 m depth. Reported down-hole temperature for drillholes near Yucca Mountain range from 22 to 56°C (Benson et al., 1983; Benson and McKinley, 1985).

1982) with the exception of the deepest drillhole (UE-20f). Evidence from drillhole UE-20f demonstrates (1) a temperature gradient of 26 Celsius degrees per kilometer for the first 1.5 km, (2) a zone from 1.5 km to nearly 3 km that is probably disturbed by a complex combination of lateral and vertical water flow, and (3) a linear thermal gradient of 37 Celsius degrees per kilometer below approximately 3 km. Thus, the thermal gradient in drillhole UE-20f is similar to that observed over large regions of Nevada and within the Basin and Range province and is only slightly elevated in comparison with gradients observed near Yucca Mountain. The down-hole temperature data will be reviewed because down-hole temperatures should be taken 3 to 6 months after drilling to allow thermal equilibration (Section 8.3.1.9).

Local heat-flow measurements at and around the NTS range from 1.0 x 10^{-6} to 3.1 x 10^{-6} cal/cm^2s (1.0 to 3.1 HFU) (Sass et al., 1980; Sass and Lachenbruch, 1982). This regional variation in heat flow is quite large with respect to distances between drillholes (Sass and Lachenbruch, 1982). For example, Yucca Mountain has a low heat flow of approximately 1.3 HFU in drillhole UE-25a#1 and about 20 km away a high heat flow of approximately 3.1 HFU is found in drillhole UE-25a#3 southeast of Calico Hills (Sass et al., 1980). However, only one of the sixty boreholes studied by Sass and Lachenbruch (1982) was completed in the manner required for confident analysis of the thermal effects of natural ground-water flow. This borehole (Ue-17e) is located in the Syncline Ridge area and had a measured heat flow of 1.58 HFU. The nearly threefold variation in conductive heat flow over greater than 11 km has been interpreted as resulting from a deep-seated convective system with a net upward flow near Calico Hills and a net downward flow beneath Yucca Mountain (Sass et al., 1980; Sass and Lachenbruch, 1982).

In addition to the complexity of hydrologic circulation, a thermal blanket effect due to low thermal conductivities of sedimentary cover (Diment et al., 1975; Brook et al., 1979) may also contribute to the variation. The thermal pulse could also be impacted by changes in thermal conductivities (White, 1973) between the Eureka low and rock immediately to the south. A complex pattern of faulting provides conduits for deep circulation of water in the Basin and Range province (Brook et al., 1979; Garside and Schilling, 1979). Small localized heat-flow highs are probably indicative of deep circulation along faults in areas of generally high heat flow (Brook et al., 1979). Heat flow and ground-water flow paths are further discussed in Section 3.7.2. The low average heat flow at Yucca Mountain and the regional, complex heat-flow pattern are likely typical of deep-seated large scale conductive flow and do not indicate a strong potential for significant geothermal resources at Yucca Mountain. Further evaluation and work on existing heat flow, temperature gradient data, and the timing of the measurement taken in comparison to drilling are planned, and the need for new data will be considered (Sections 8.3.1.2, 8.3.1.8, and 8.3.1.9). These activities and data collected will be used to assess various models for geothermal areas proposed for the Basin and Range (e.g., Blackwell and Chapman, 1977) in comparison to Yucca Mountain.

Water chemistries and the isotopic character of waters from springs (Section 3.5) and drillholes can be used in some instances to quantitatively and qualitatively estimate the temperatures at depth with which the thermal water equilibrated. These data can be used to predict water temperatures that might be encountered by deep drilling. These chemical parameters include the sodium-potassium-calcium geothermometer of Fournier and Truesdell (1973) and the silica (SiO_2) geothermometer of Fournier and Rowe (1966). Criteria for the appropriate use of these geothermometers can be found in Fournier and Rowe (1966), Fournier and Truesdell (1973), Renner et al. (1975), and Fournier et al. (1979). Silica concentrations in well waters from within approximately 10 km of Yucca Mountain range from 40 to 57 mg/L (Benson and McKinley, 1985). These concentrations indicate temperatures of equilibration of less than 60°C and average temperatures of approximately 35°C, using the methods of Fournier and Rowe (1966). These low temperatures are in general agreement with measured down-hole temperatures. However, caution is advised by Renner et al. (1975) when temperatures below 125°C are encountered. A comparison between different methods will provide a better calibration of temperatures of equilibration. These various geothermometers will be used in detail with all published well-water data and new data that are collected during site characterization (Sections 8.3.1.2, 8.3.1.8, and 8.3.1.9).

Isotopic data of deuterium and oxygen-18 can be used qualitatively to assess whether waters have equilibrated with meteoric water, hot thermal waters, or result from a mixture of the two (Craig, 1963; Mariner and Willey, 1976). Deuterium and oxygen-18 are calculated ratios reported in parts per thousand relative to Standard Mean Ocean Water (SMOW). Thus, reported values of deuterium (δD) and oxygen-18 ($\delta^{18}O$) are reported as differences between the values of the measured samples and seawater. Deuterium and oxygen-18 isotopic data range from -93 to -108 for δD (mean = -101, number of measurements = 15) and 12.8 to 14.2 for $\delta^{18}O$ (mean = 13.4, number of measurements = 15), respectively, for well-water data within approximately 10 km of Yucca Mountain (Benson et al., 1983). Using a deuterium value of -101, the curve of Mariner and Willey (1976) would predict an oxygen-18 value of approximately -14 for meteoric water. Much lower values (approximately less than -9) would likely indicate a high thermal source and intermediate values a possible mixed source. The oxygen-18 values above, represent a meteoric to slightly mixed source. In general, thermal waters react with reservoir rocks, resulting in moderate-to-large shifts in oxygen-18 content of the water. Analysis of the shifts provides information on the reservoir and its equilibration. As new isotopic data are made available, a reassessment of the above analysis will be made (Sections 8.3.1.2, 8.3.1.8 and 8.3.1.9).

Several other qualitative chemical indicators of thermal reservoir temperatures are also available and have been summarized, for example, by Wollenberg (1982) and Henley and Ellis (1983). These include calcium-

[redacted]

2. The area surrounding Yucca Mountain has a low potential for [redacted]

1.7.2.1 Deposits of coal, tar sands, and oil shales occurrences of hydrocarbons within the northern part of the Basin and Range province. Most notable of these, with regard to similarity to tar sands, is the well-known Bruffey oil seep located in Pine Valley, southeast of Elko in Eureka County, Nevada (Foster et al., 1979). Of further interest is the Blackburn oil field that was discovered in 1982 by Amoco Oil Company in Eureka County located only a few kilometers west of this seep, where Quaternary conglomerate is partially impregnated by black, tar-like hydrocarbons (Bortz, 1983).

Horton (1964c), Cornwall (1972), and Bell and Larson (1982) do not report any occurrences of tar sands or similar deposits in either southern Nye County or near the NTS. In addition, no evidence of such deposits appears in any of the subsurface data from drilling at or near Yucca Mountain. Thus, it is concluded that Yucca Mountain has no known potential for tar sands now or in the future.

1.7.2.1.3 Oil shale resources

Shales and related rocks can be associated with hydrocarbon resources in four possible relationships:

1. As oil shales, or rocks enriched in solid organic matter or kerogen, that can yield synthetic crude oil through the destructive distillation of the mined rock.

2. As reservoirs in which hydrocarbons accumulate within fractures.

3. As impermeable confining layers above many petroleum traps.

4. As a source rock whose organic matter is converted into hydrocarbons by natural thermal maturation and expelled to migrate into petroleum traps elsewhere.

It is not unusual for certain shales, as discrete stratigraphic units, to perform in the capacity of more than one of these roles. Oil shales are discussed in this section, whereas the oil and gas generating capacities of oil shales are discussed in Section 1.7.2.2.

The United States possesses the largest deposits of oil shales in the world within the well-known Eocene Green River Formation (Smith, 1980). These kerogen-rich, dolomite shales (marlstones) are found mainly within the Piceance and Unita Basins of Colorado and Utah, and the Green River and Washakie Basins of Wyoming. Economic development has been repeatedly plagued by economic restrictions relative to extraction costs versus the price of conventional crude oil. The reserves of oil in these western United States deposits are measured as 1500×10^9 barrels, while additional resources as lower grade oil shale (less than 15 gallons per ton of rock) amount to an estimated 300×10^9 barrels (Smith, 1980).

As early as 1917, synthetic crude oil was produced from Nevada oil shales at Elko in Elko County (Knutson and Dana, 1983). A single processing plant produced approximately 12,000 barrels, over a 7-yr period, from oil

DECEMBER 1988

fields were discovered. In addition to the Eagle Springs field, four of these more recent fields (Trap Spring, Currant, Bacon Flat, and Grant Canyon) are located in the Railroad Valley area of northeastern Nye County. The Blackburn field is situated in the Pine Valley area of Eureka County, whereas the single-well Jiggs field is in south westernmost Elko County. Both the Jiggs and Currant fields are shut in and the former field may ultimately be considered noncommercial. Characteristics and production data of these fields are summarized in Table 1-22. Additional information and discussion can be found in Garside et al. (1977), Bortz and Murray (1979), French (1983), Jones and Papke (1984), Bortz (1985), Chamberlain (1986), and Fritz (1987).

Even though Nevada does not rank among the leading petroleum-producing states, its cumulative production has passed 16.9 million barrels (Garside and Weimer, 1986; 1987). Nearly 80 percent of that production has been achieved during the last decade. Sizeable, quantities of oil have been produced from the Grant Canyon field (Railroad Valley, Nye County) where cumulative production through August 1987 has risen to 4.7 million barrels (Veal et al., 1988a). In a state with less than 30 active producing oil wells, it is somewhat ironic that the Grant Canyon No. 3 well, with an average, controlled production rate of 4,000 barrels per day, is currently the most productive single onshore well in the United States (Fritz, 1987). Chamberlain (1986) has also shown a dramatic increase in the barrels of oil produced versus feet of exploratory drilling conducted since the mid-1970s.

For nearly six decades, ranches in the Fallon area of Churchill County have produced natural gas (mainly methane) from very shallow (less than 50 m) wells drilled into the organic-rich sediments of the Quaternary Wyermaha Formation (Brady, 1984b; McDaniel, 1985). In addition, shows of natural gas have been reported from several seeps (located at Bruffey, Pine Valley, Eureka County and Diana's Punch Bowl, Monitor Valley of northern Nye County) and from various exploratory wells. Except for the Fallon area no production of gas is known in Nevada.

In comparison with many western states in which major petroliferous basins have been developed, the level of oil and gas exploration has been decidedly less within the Basin and Range province of California, Utah, Oregon, Arizona, and within Nevada in particular. There are indications, despite the current downturn in the U.S. petroleum industry, that eastern Nevada is likely to become the focus of increased exploration interest. Southeastern Nevada is now recognized as part of the so-called Western overthrust belt (equivalent to the Cordilleran thrust belt, or Cordilleran fold and thrust belt of other authors, Section 1.3). This structural province is now known to extend from Alberta, Canada south through the states of Montana, Idaho, Wyoming, Utah, and eastern Nevada, and western Arizona (Hayes, 1976). This province has proven to be a major petroliferous trend in western Wyoming and northeastern Utah (Dixon, 1982).

Additional interest in east-central Nevada has been created by the recent production from the Grant Canyon and Blackburn fields (Chamberlain, 1986; Fritz, 1987). These two fields lie northwest of the Cordilleran overthrust belt, as currently defined, but within the zone of regional thrust faulting termed the Sevier-Laramide thrust belt (Chamberlain, 1986). Another

Table 1-22. Location, date of discovery, producing formation, depth of production, and cumulative production for Nevada oil and gas fields[a]

Field	Location	Discovery date and company	Producing formations	Production depth (ft)	Cumulative 30 Sept 1984 (barrels)	Remarks
Fallon Area	T17-18N, R28-30E	1920s-?	Quaternary	160 ±	Unknown	97-98% CH_4 Tr $C_2H_6^{+4}$
Eagle Springs	T9N-R57E	1954-Shell	Oligocene volcanics, Eocene Sheep Pass, Paleozoics	5,780-7,256	3,569,943	26-29° API[b] 65-80°F Pour point
Trap Spring	T9N-R56E	1976-NW Expl.	Oligocene volcanics	3,330-4,865	5,551,841	21-25° API 0-5°F Pour point
Currant	T10N-R57E	1979-NW Expl.	Eocene Sheep Pass	6,856-7,080	635-SI[c]	15°F API 95°

promising indication of the presence of oil in east-central Nevada is the presence of source rocks (shales, Section 1.7.2.1.3) that have been interpreted as having favorable thermal-maturation characteristics (Sandberg, 1983; Sandberg and Gutschick, 1984; Poole and Claypool, 1984; Chamberlain, 1986). The source rocks include the Mississippian Chainman and Pilot shales, the Woodman Formation, the Devonian Woodruff Formation, and the Ordovician Vinini Formation (Section 1.7.2.1.3). The fields in Nevada produce principally from Paleozoic (Devonian) carbonate reservoirs with some production from highly fractured and porous Tertiary ash-flow tuffs (Garside et

The paleogeothermal history of the Yucca Mountain area may be significant in the preservation of any hydrocarbons that might have been generated from source beds within the deeper Paleozoic sequences. The presence of several large calderas (the Oasis Valley and Timber Mountain calderas) and nearby plutonic rock masses suggests that the paleogeothermal gradient could have been greater during the Tertiary when these igneous-volcanic processes took place. Alteration studies of the deeper tuffs (greater than 1,300 m) under Yucca Mountain (drillhole USW G-2) indicate paleogeothermal temperatures as high as 230°C (Caporuscio et al., 1982; Bish, 1987). This hydrothermal alteration has been dated at over 10 million years ago (Bish, 1987).

Source rocks for oil and gas are sedimentary rocks containing organic matter; with age and burial, the organic matter eventually breaks down to form oil and gas. Igneous rocks and most metamorphic rocks do not contain organic matter necessary for the generation of oil and gas and, thus, the vast abundance of volcanic and subordinate plutonic and metamorphic rocks found in the vicinity of the NTS are not potential source rocks for hydrocarbons. However, porous igneous rocks (e.g., tuffs and basalts) can become potential reservoir rocks for oil, as is the case in Railroad Valley where oil is being produced, in some cases, from porous and fractured Tertiary ash-flow tuffs (Garside et al., 1977). Although, the silicic tuffs at Yucca Mountain are potentially suitable as reservoir rocks, the source rocks, if present, would have to be located in the underlying Paleozoic strata. No potential source rocks are known to exist in the vicinity of Yucca Mountain based upon Paleozoic outcroppings at Bare Mountain on the west, the Skull Mountains on the east, and Paleozoic rocks on the Nevada Test Site to the north.

Thermal maturity (conodont color alteration index maps) of Ordovician through Triassic age rocks has been mapped, where available, by Harris et al. (1980). These maps generally indicate that the Paleozoic rocks that lie to the north and south of Yucca Mountain have thermal maturation indexes of greater than 4 (beyond significant gas or oil production). A mixture of areas to the southeast and east exhibit thermal maturation indexes of greater [illegible]

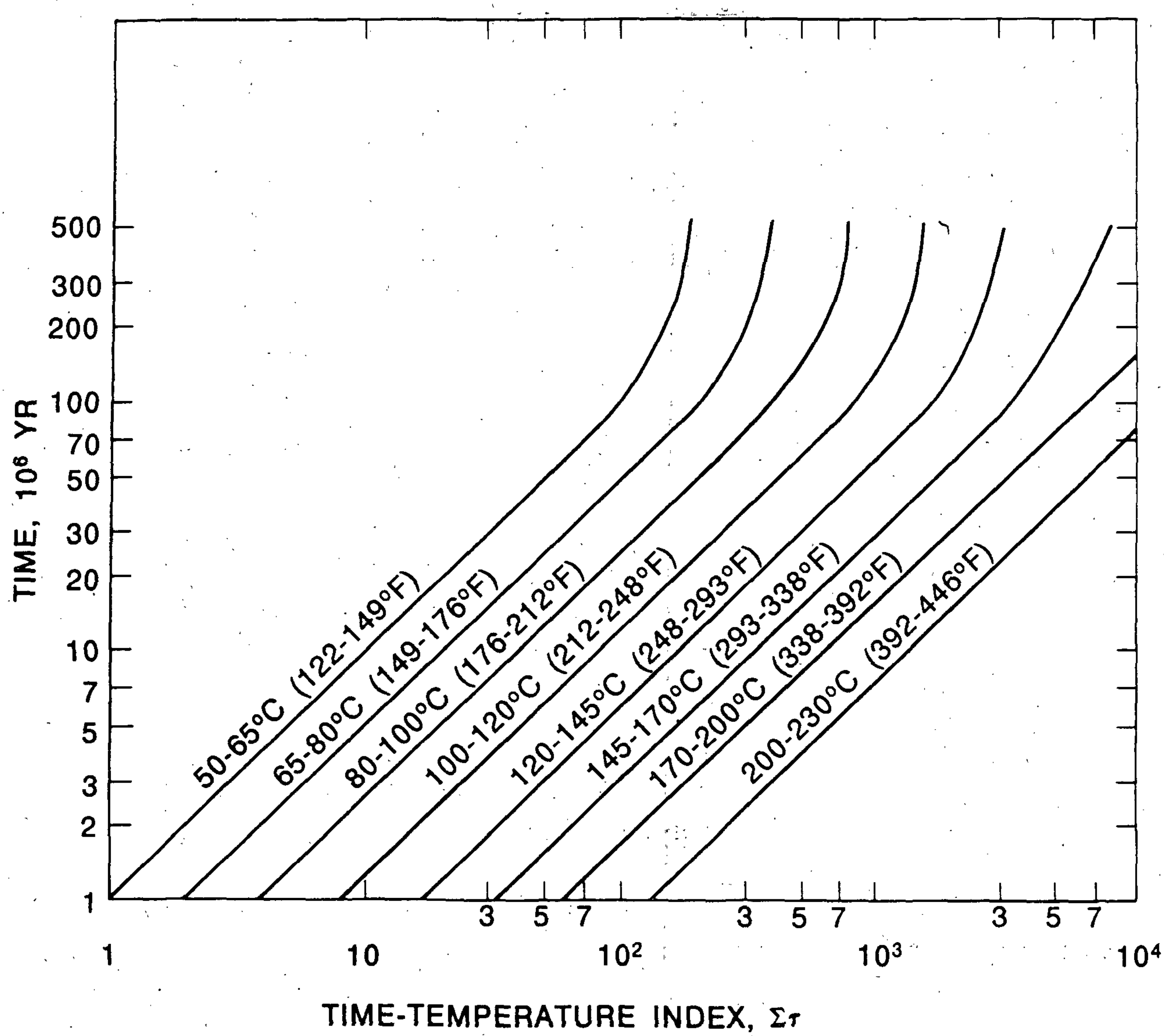

Figure 1-86. Lopatin's time-temperature index for estimating the maturation of potential hydrocarbons. Modified from Hunt (1979).

Mountain are as follows: (1) a slightly raised geothermal gradient for the last 10 million years, such that the ambient temperature of any potential reservoir rocks was 100 to 120°C for τ_1; (2) a period of raised geothermal gradient for 7 million years corresponding to the major period of volcanism (10 to 17 million years before present) at a temperature of 200 to 230°C for τ_2; and (3) a long period of time under a more average geothermal gradient since the end of the Paleozoic, approximately 208 million years (17 to 225 million years before present) at 80 to 100°C for τ_3. This analysis is likely conservative for northern Yucca Mountain because any potential Paleozoic source strata (1) have been through at least one regional deformation-metamorphic tectonic event (Section 1.3), (2) were subjected to a raised geothermal gradient for a longer period of time than assumed for τ_3, and (3) the calculation does not account for depth of burial. The estimates that follow are for shallowly buried strata and any increase in depth of burial would increase τ_1. The nomograph in Figure 1-86 and the previously discussed information yields

$$\Sigma\tau = \tau_1 + \tau_2 + \tau_3 \qquad (1\text{-}3)$$

$$\Sigma\tau = 80 + 800 + 320 = 1,200$$

The value for τ_1 can be found by locating 10 million years on the ordinate and finding the intersection with the 100 to 120°C curve on the graph; the τ value is to be read from the abscissa directly below the point of intersection (i.e., approximately 80 in this case). Table 1-23 lists the corresponding interpretations for values of τ as given in Hunt (1979). Using this preliminary evaluation, the Paleozoic rocks would be at the end of any oil generating phase and nearly at the end of any gas generating phase. The potential for oil in this analysis is very conservative because it does not fully take into account (1) the regional deformation and metamorphism (Section 1.3.2.2) of the Paleozoic strata, (2) the likely possibility of pervasive cretaceous or Tertiary plutonism at depth, or (3) account for older Paleozoic rocks known to occur at depth (e.g., Silurian and older rocks; drillhole UE-25p#1). In addition, the analysis assumed shallowly buried rock units. These geologic events would increase the value of τ to even higher values and would further decrease the potential for oil and gas reserves being present at Yucca Mountain.

In summary, no Paleozoic rocks in the area or from drill core (UE-25p#1; drilled to a depth of 1,807 m (5,923 ft) (Chipera and Bish, 1988))

Table 1-23. Time-temperature index ($\Sigma\tau$) values from Hunt (1979)

Value	Phases of oil and gas generation
70-85	Beginning of principal phase of oil generation
160-190	Maximum phase of oil generation
170-210	Zone of maximum oil migration into reservoir rock
380-400	End of principal oil-generation phase
550-650	Maximum gas generation
1,500-2,000	End of gas generation

of the Lopatin time-temperature index (particularly for southern Yucca Mountain), (2) examination of Paleozoic rocks in the area and available drillcore for the presence of organic matter and its thermal maturation state, if present, (3) an evaluation of other methods of determining thermal maturation, if applicable, and (4) further comparisons of the source and reservoir rock found in Nevada's oil fields with the rocks found at Yucca Mountain, and (5) evaluation of the potential for structural and stratigraphic maps.

1.8 SUMMARY

This section summarizes the information from preceding sections within this chapter. Combined with input from performance assessments and design needs, this information provides a basis for the studies planned for site characterization (Section 8.3.1). Section 1.8.1 summarizes significant geologic information about Yucca Mountain and its vicinity from the current geologic literature; Section 1.8.2 discusses the needs for geologic information in the design of the repository and the waste container; Section 1.8.3 identifies information needs pertinent to geology and relates significant geologic results to the studies of the site characterization program; and Section 1.8.4 briefly shows that the data required by NRC Regulatory Guide 4.17 have been included in Chapter 1.

1.8.1 SUMMARY OF SIGNIFICANT RESULTS

This section summarizes the geologic information presented in the preceding sections and discusses its significance in terms of the following:

1. Performance objectives.
2. Conceptual models and boundary conditions.
3. Need for further data from site characterization.
4. Quality of data, including uncertainties.

The following subsections are arranged in the same order as the major sections to which they apply in Chapter 1. Each subsection comprises a summary and a discussion.

1.8.1.1 Geomorphology

1.8.1.1.1 Significant results

Current geomorphic data suggest that the region including Yucca Mountain is relatively stable geomorphically and that general downwasting on the mountain will probably not exceed 1 to 2 m during the next 10,000 yr.

The rate of erosion in the Yucca Mountain area will probably not change

1.8.1.1.2 Discussion of significant results

Geomorphic data bear on the postclosure performance objectives for the repository. After closure, erosion must not degrade the geologic or hydrologic setting of the repository such that radionuclides will be released to the accessible environment in concentrations above U.S. Environmental Protection Agency mandated standards within 10,000 yr. Also, the estimated effects of erosion must be incorporated into the design of the monuments that designate the controlled area.

Erosion in the Yucca Mountain area will probably not prevent either the repository or its geologic setting from meeting the performance objectives. This conclusion is based on estimated average rates of upland and piedmont erosion for the southwestern Basin and Range province for the late Tertiary and Quaternary. These rates suggest that present erosion rates will probably not be exceeded by an appreciable amount over the next 10,000 yr, assuming that the climate continues to be dry and that faulting and volcanism remain relatively quiescent, as they have through the Quaternary.

Geomorphic processes were considered over a wide geographic range, from the northern Mojave Desert to the central Great Basin, to ensure that all processes that might affect Yucca Mountain were recognized. These studies were then applied to Yucca Mountain and its immediate surroundings, and integrated with site-specific findings.

The present geomorphic data base for Yucca Mountain is sufficient to define average rates of erosion during the Quaternary but does not adequately characterize the likelihood and effects of short-lived episodes of local erosion in drainages such as Fortymile Wash. Further study of past episodes of short-lived and localized but rapid erosion near Yucca Mountain will refine predictions of the likelihood of such episodes and their probable effects both before and after closure (Section 8.3.1.6).

1.8.1.2 <u>Stratigraphy and lithology</u>

1.8.1.2.1 Significant results

Yucca Mountain is underlain by a sequence of Miocene silicic volcanic rocks 1,000 to 3,000 m thick, dipping 5 to 10 degrees eastward, at the proposed repository location. These rocks were erupted from nearby calderas and volcanoes about 14 to 11 million years ago and consist mainly of welded and nonwelded ash-flow and ash-fall tuffs. Lavas and volcanic breccias are area. It is 287 to 369 m thick, and crops out extensively on the west side of Yucca Mountain.

The Topopah Spring Member is a multiple-flow compound cooling unit that has seven zones: caprock, upper lithophysal, middle nonlithophysal, lower lithophysal, lower nonlithophysal, basal vitrophyre, and lower non- to moderately welded. The repository is currently expected to be in the lower nonlithophysal zone, which is 27 to 56 m thick in the Yucca Mountain area and has 0 to 2 percent lithophysal cavities. The host rock is a devitrified, moderately to densely welded ash-flow tuff and is rhyolitic, with less than 2 percent plagioclase and alkali feldspar phenocrysts.

Overlying the volcanic rocks on the flanks of Yucca Mountain are Pleistocene to Holocene fluvial deposits, eolian dunes and sand sheets, local debris flows, and pedogenic deposits. The surface facilities would be built on such deposits east of Yucca Mountain.

The rocks beneath the volcanic sequence of Yucca Mountain are known from only one of the drillholes in the Yucca Mountain area. This hole has penetrated Silurian carbonate rocks of the lower carbonate aquifer below 1,220 m on the eastern flank of the mountain. Gravity data suggest that the contact between Tertiary and pre-Cenozoic rocks may be at least 3,000 m below the ground surface under much of Yucca Mountain. In the northern part of Yucca Mountain, the Mississippian Eleana Formation may occur at a depth of 2,200 to 2,400 m. A deep-seated granitic body has been postulated in the subvolcanic basement of the northern part of the mountain.

1.8.1.2.2 Discussion of significant results

The stratigraphy and lithology in the controlled area bear on both preclosure and postclosure objectives. The design of the repository will be based in part on the stratigraphy at Yucca Mountain, particularly the thickness, lateral extent, and vertical and lateral variations of physical properties of the host rock (Chapters 2 and 6). Before closure, the host ability, facies changes, petrography (e.g., degree of welding, presence of lithophysae), petrology and mineralogy, alteration (e.g., zeolitization), and mechanical properties.

The rocks beneath the volcanic sequence are known only from geophysical surveys and from a single drillhole. Planned studies will identify and characterize the subvolcanic rocks and delineate their contact with the overlying volcanic rocks (Section 8.3.1.17) to allow for refinement of hydrologic and tectonic models.

1.8.1.3 Structural geology and tectonics

1.8.1.3.1 Significant results

Significant information on structural geology and tectonics is summarized in the following categories: volcanic history, structure, existing stress regime, vertical and lateral crustal movement, and geothermal regime.

Volcanic history

Most of the volcanic rocks at and near Yucca Mountain were emplaced during middle Tertiary time. No Paleocene or Eocene volcanics are known in the area.

Middle Tertiary silicic and intermediate rocks in Nevada and western Utah erupted in east-trending belts. Volcanism began 43 to 34 million years ago about 250 km north of Yucca Mountain, and the belts migrated southward. By 28 to 20 million years ago volcanic centers were far enough south to

deposit silicic ash flows and tuffs near Yucca Mountain. By 16 million years basalt centers of this zone became distinct from the silicic southwestern Nevada volcanic field about 8 million years ago, and some are as young as 0.13 million years.

Some of the basalt fields in the zone are large in volume, vary in their component basalt types, and were active for several million years. Other fields are small in volume and consist of one or a cluster of scoria cones and associated basaltic lavas. The fields occur in zones of extension between strike-slip faults, near ring fracture zones, and in association with normal faults. The oldest basaltic centers occur near the earlier silicic centers; the younger basalts show no known relation to these features.

The youngest basalts were formed in isolated Strombolian eruptions of small volume and short duration. Rates of basaltic volcanic activity during the last 8 million years have been consistently low. The youngest basaltic centers near Yucca Mountain are in southern and northern Death Valley, near

Miocene rocks of the NTS, forming the southeastern part of the Walker Lane. Displacement along the Walker Lane is by strike slip and bending, and may be as great as 130 to 190 km. Displacement there may have begun as early as the Jurassic, and has been active into the Quaternary. Northeast-trending, left-lateral faulting is also significant in the area around Yucca Mountain. These faults have also been active in the Quaternary.

Recent conceptual models on the style of middle and late Tertiary faulting emphasize the role of detachment faults in producing significant amounts of regional extension. In the models of Davis et al. (1980), Wernicke (1981), and Wernicke and Burchfiel (1982), upper plate blocks are translated for considerable distances along gently dipping, undulating or domiform extensional faults that form major crustal penetrating features. High-angle listric or planar faults may be shallow features that are confined to the upper plate of the detachment. Strike-slip faults, such as the Furnace Creek fault zone and the southeastern part of the Walker Lane, [redacted] upper plate blocks and are also relatively shallow features.

Other conceptual models have been proposed that are consistent with the geological constraints in various parts of the Great Basin. These alternate conceptual models include

1. Extensional faulting occurs on high-angle faults that are progressively rotated to shallow dips as they are cut by multiple generations of younger high-angle faults (Proffett, 1977).

2. Extensional faulting occurs on high-angle planar or listric faults that extend to a zone of decoupling at the base of the brittle crust (about 15 km). Extension below the depth of faulting is accommodated by ductile stretching, thinning, and/or intrusion. This model results in a series of tilted blocks that form basin-and-range topography. Metamorphic core complexes represent exposed elements of older zones of decoupling that have been subsequently uplifted (Smith, 1978; Eaton, 1979, 1982; Miller et al., 1983; Smith and Bruhn, 1984; Gans et al., 1985).

3. Significant strike-slip faults are present at depth in parts of the Great Basin and movement on these faults produces transtension, which is accommodated at shallow depths by low-angle detachment

Not all the above models are necessarily mutually exclusive, and it is possible that various combinations of these models may exist or that different models may be operating in different parts of the Great Basin at the same time (Anderson et al., 1983; Smith and Bruhn, 1984; Allmendinger et al., 1987). It is also possible that episodic changes in the stress field may cause changes through time in the faulting style that is active at any given location (e.g., alternating changes between and extension mode and a strike-slip mode) (Stewart, 1986).

The various models related to faulting styles may be significant because of their possible impact on predictions of future surface faulting and ground motion that might affect the repository system. Therefore, the emphasis is on defining Quaternary faulting models that can be projected to predict behavior over the next 10,000 yr. Historic and contemporary seismicity studies can provide data on faulting styles that are currently significant in the Great Basin region. Historical earthquakes in the Basin and Range province have been produced by either dominantly normal or strike-slip faulting. Studies of significant earthquake (M > 6.8) in the region with a dominantly normal component of movement, such as the 1954 Dixie Valley-Fairview Peak earthquakes, the 1959 Hebgen Lake earthquake, and the 1983 Borah Peak earthquake, show that these events occurred on relatively planar faults extending from focal depths of 12 to 16 km to the surface with dips of 45 to 60 degrees (Doser, 1985b, 1986; Okaya and Thompson, 1985; Stein and Barrientos, 1985; Richens et al., 1985). Studies of earthquakes in the region with a dominantly strike-slip component of movement and surface rupture, such as the 1932 Cedar Mountain earthquake (M 7.3) and the 1986 Chalfant Valley earthquake (M 6.3), show that these events occurred on faults with dips of 60 to 80 degrees and had focal depths of 11.2 to 12.2 km (Doser, 1987; Cockerham and Corbett, 1987). The data from large historical earthquakes therefore do not seem to be consistent with a detachment model.

The data from contemporary seismic monitoring of the southern Great Basin that are discussed in Section 1.4 indicate that strike-slip faulting is predominant in the southern Great Basin. Roger et al. (1987) concluded, on the basis of an examination of a number of wrench and detachment models, that no one tectonic model satisfactorily accounts for all features of the contemporary seismic data. The poor correlation between currently popular geologic models that favor detachment faulting and the historical and contemporary seismicity data leads to several alternatives that should be considered in evaluating the potential for future faulting and seismicity:

There is enough uncertainty in the data that it is premature to categorize particular structures in the region surrounding the site with one or another model of faulting style as the primary tectonic mechanism producing these structures.

Structures in the Yucca Mountain area. Gravity data suggest the geometry of the pre-Tertiary surface near Yucca Mountain. A gravity high between Busted Butte and the Calico Hills may be either a buried structural high or an eroded escarpment. Beneath the southern part of Yucca Mountain, structural relief in the subvolcanic rocks is at least 2,000 m. A structural depression beneath Crater Flat has been interpreted both as a buried caldera complex and as a Cenozoic basin overlying Miocene(?) detachment faults.

Quaternary offset has been observed on many faults in the region surrounding Yucca Mountain, and late Pleistocene and Holocene movement has been documented on several. On or near Yucca Mountain, Quaternary movement is known on 32 faults. Radiometric ages and stratigraphic evidence suggest that 23 of the faults were active 1.2 to 2 million years ago, and the rest were active during the past 1 million years. Measured dip-slip offset in Quaternary deposits is typically less than 4 m, but 10 to 30 m of offset is postulated on the south segment of the Bare Mountain fault zone (15 km west of Yucca Mountain). Strike-slip offset has been neither demonstrated nor discounted on most of these faults. On the Windy Wash fault, on the west flank of Yucca Mountain, there have been at least seven episodes of Quaternary movement. Four of them have been in the past 300,000 yr, and one of these has a Holocene date of 3,000 to 6,500 yr. Total vertical offset since the Miocene on this fault is estimated at more than 225 m. Holocene movement has also been suggested for the eastern range-front fault at Bare Mountain.

Yucca Mountain is the erosional remnant of a volcanic plateau. It consists of a series of north-trending structural blocks that have been tilted eastward along major west-dipping, high-angle normal faults.

Alternative models for the geometry of these faults are

1. The faults extend to great depth into the upper crust as planar or listric faults.

2. The faults flatten and merge with detachment faults either at the Tertiary-Paleozoic boundary or deeper.

3. The faults abut against a detachment at depth forming stranded blocks of upper crustal rock between them.

4. The faults are oblique-slip faults related to significant strike-slip faulting in the Walker Lane.

Several activities in Section 8.3.1.17.4 are directed at determining the history and nature of movement on these faults and their subsurface geometry.

East and west of Yucca Mountain, the detachment appears to be between Tertiary and older rocks, suggesting that the uppermost detachment beneath Yucca Mountain is at the base of the Tertiary rocks. The normal faults bounding the structural blocks generally strike north to north-northeast and dip steeply west; they are widely spaced with vertical offsets generally greater than 100 m. Within each block are numerous steep, west-dipping normal faults of a second type; these are closely spaced imbricate faults with small (usually less than 3 m) offsets. Northwest-striking strike-slip faults appear to be superposed on the structural blocks; they have less than 100 m of right-lateral offset and breccia zones less than 20 m wide. Several of these faults have been mapped in upper Drill Hole Wash, and they are postulated to underlie its lower reaches.

In the western part of each structural block, foliations dip 5 to 30 degrees eastward; farther east in each block, dips increase to 15 to 55 degrees in zones of abundant anastomosing west-dipping normal faults. Still farther east, next to major bounding normal faults, are chaotic brecciated zones as much as 500 m wide.

The proposed repository would be excavated in the relatively unfaulted part of one typical structural block. It would be bounded on the west by the Solitario Canyon fault, on the northeast by the Drill Hole Wash fault, and on the east and southeast by the western edge of an imbricate normal fault zone. Dips within the proposed repository envelope range from about 5 to 10 degrees eastward. Recognized vertical offsets on faults within the proposed repository are 5 m or less, except for the Ghost Dance fault, which is offset 38 m at the southeast end of the proposed repository. This fault dips 80 to 90 degrees westward and is downdropped to the west; its offset decreases to the north and is unmeasurable at Drill Hole Wash. Breccia zones in the Ghost Dance fault are as wide as 20 m. North- to north-northwest-striking, west-dipping normal faults with small (less than 5 m) vertical offsets bound the proposed repository envelope on its southern and eastern edges.

On the major normal faults at Yucca Mountain, most offset occurred between 12.5 and 8 million years ago, but offset has continued into the Pliocene and Quaternary on many of them. Notable examples are the Bow Ridge, Paintbrush Canyon, Solitario Canyon, and Windy Wash faults. On the northwest-striking right-lateral faults, cross-cutting relationships suggest that most offset occurred 12.9 to 11.6 million years ago (Carr, 1984; USGS, 1984). Normal offset dominated latest movement on the major and imbricate normal faults, but the latest movement on faults striking east of north was mainly left-lateral strike slip. West-dipping normal faults striking west of north had dominantly normal offset with a small right-lateral component. Lineations on northwest-striking strike-slip faults plunge less than 25 degrees.

The fractures common in all the Yucca Mountain volcanic rocks can be either open (apertures or breccia zones) or healed (by secondary mineralization or fault gouge). Three recognized fracture types were formed in separate events. The first type consists of cooling fractures perpendicular to foliation, forming two sets striking N.30° to 50°E. and N.35° to 55°W.; they occur in swarms 3 to 5 m wide and spaced 150 to 200 m apart. The second type is tectonic, often has small dip-slip offset, and postdates the cooling fractures; these tectonic fractures are apparently due to regional extensional faulting, and do not form oriented sets. The third set consists of tectonic northwest-striking fractures having lateral strike-slip offsets. Subsurface fracture frequency in moderately to densely welded tuff (1 to 40 per cubic meter) is much greater than in partially welded tuff, nonwelded tuff, and bedded tuff, and has been observed to decrease abruptly with depth, independently of welding in drillholes USW GU-3, USW G-3, AND USW G-4. Subsurface fracture attitudes at the south end of the repository envelope are similar to orientations at the surface, and to dominant fault attitudes.

Existing stress regime

Tectonic and seismic data and a few stress and strain measurements suggest that the least principal stress orientation for the southern Great Basin is not substantially different from the general N.50°W. direction of least principal stress at the NTS (Carr, 1974). Subsurface studies suggest a range of N.65° to 70°W. The present orientation probably originated about 4 to 10 million years ago.

Experimental hydraulic fracturing in Yucca Mountain drillholes has shown that magnitudes for least principal horizontal stress (Sh) are low relative to vertical principal stress (Sv). This difference in magnitude could affect the design and construction of the repository, and may have an important bearing for the possibilities of incipient normal faulting. At two drillholes, Sh values may be close to those at which frictional sliding might be expected on faults striking N.25° to 30°E.

Vertical and lateral crustal movement

Cenozoic lateral crustal extension has occurred throughout the Basin and Range Province. Patterns of uplift, tilting, and subsidence near Yucca Mountain are typical of shallow crustal response to extension and volcanism in the Great Basin. The region is currently undergoing active lateral crustal extension.

Geothermal regime

The southern Great Basin is a region of high heat flow relative to the rest of the United States. However, the region north of and adjacent to Yucca Mountain (the Eureka low) has lower than average heat flow for the southern Great Basin. Low temperatures in the Eureka low have been attributed to the complex local interbasin ground-water regime, in which low temperature gradients result from lateral regional ground-water flow with a very low rate of downward flow.

Heat-flow values at the NTS show that the values of the Eureka low extend southward beneath Yucca Mountain and appear to be reduced by downward ground-water flow at that location. Temperature profiles from drillholes at Yucca Mountain display high variations of thermal gradient with depth. Assuming its depth to be about 300 m, expected ambient preemplacement temperfavorable for geothermal development of low-temperature water, but develop-

1.8.1.4 Seismology and seismicity

1.8.1.4.1 Significant results

Yucca Mountain is in a region of diffuse seismicity, no closer than 90 km to the Nevada-California seismic belt to the west, and no closer than 170 km to the Intermountain seismic belt to the northeast. Eight major earthquakes ($M \geq 6.5$) have occurred within 400 km of Yucca Mountain, six of them in the Nevada-California seismic belt and two on or near the San Andreas fault. The nearest recorded major earthquake was the 1872 Owens Valley event ($M = 8.25$), about 150 km west of Yucca Mountain. However, the area surrounding Yucca Mountain (including the eastern Mojave Desert and the southwest quadrant of the NTS) has been relatively seismically quiescent in historic time. In a radius of about 10 km centered on the proposed repository, seismic energy release since 1978 has been two or three orders of magnitude lower than in the surrounding region.

In general, in the vicinity of Yucca Mountain, it has not been possible to correlate earthquakes with specific faults or tectonic structure. In some instances epicenters in the southern Great Basin apparently cluster on north- to northeast-trending mapped faults and structural grain. Most of them cluster in zones of major Tertiary northeast-trending left-lateral shear (notably, the Rock Valley, Pahranagat, and Gold Mountain shear zones); others cluster on north-trending fault zones (e.g., at Yucca Flat, Thirsty Canyon, and Pahute Mesa). Focal depths range from 1 km above sea level to 17 km below sea level, with two broad peaks at 0 to 2 km and 5 to 8 km and a distinct low at 3.5 to 4 km.

The direction of minimum principal stress determined from 29 focal mechanisms in the Yucca Mountain area is about N.60°W.; intermediate and maximum principal stresses are about equal in magnitude. This stress configuration favors right-lateral strike slip on north-striking faults, normal slip on northeast-striking faults, and left-lateral slip on east-northeast-striking faults.

1.8.1.4.2 Discussion of significant results

Seismic information bears mainly on preclosure performance objectives. Structures, systems, and components that are important to safety must be designed to withstand anticipated seismic vibrations, to provide protection against radiation exposures and releases of radioactive materials and to allow for retrieval of the waste.

The seismologic data used for studies described in Section 1.4 are principally in two data sets: historical seismicity data and Southern Great Basin Seismic Network (SGBSN) seismic data. The SGBSN data are of high quality and are completely adequate for their intended application: the determination of hypocenters, magnitudes, and focal mechanisms. The completeness of the SGBSN seismicity catalog (August 1978 to the present) is over three magnitude units better than the historical catalog (1868 to 1978), and SGBSN hypocenters are over an order of magnitude more accurate than historical epicenters. Although the historical data are fewer and less precise, they are important for estimating recurrence rates of larger earthquakes because they cover a long time period.

As described in Section 8.3.1.17, future work will involve continued seismologic data compilations, evaluations of seismotectonic sources and earthquake recurrence intervals, evaluations of vibratory ground motion, and assessments of ground motion that are needed for design. Three of the more important unresolved problems in the seismic data base are as follows: (1) contamination of earthquake catalogs with man-induced seismic activity, (2) the lack of good regional and local attenuation curves, and (3) the need to identify the most likely seismogenic faults in the Yucca Mountain area for use in hazard analysis.

Contamination of earthquake catalogs by aftershocks induced by nuclear tests can distort or obscure interpretations such as seismicity maps, energy

The small but finite possibility of silicic volcanism affecting Yucca Mountain is suggested by an episode of renewed silicic volcanism about 8 to 7 million years ago, after the Timber Mountain-Oasis Valley magmatic cycle, at the Black Mountain center, about 50 km north of Yucca Mountain. However, renewed silicic volcanism is considered highly unlikely because (1) there has been no silicic volcanism within the southern Great Basin for at least the past 6 million years, (2) silicic volcanism has decreased throughout the southern Great Basin and ceased in most parts of the basin over the past 10 million years, and (3) silicic volcanism during the past 2 million years has been restricted entirely to the margins of the Great Basin. Local studies of possible future bimodal volcanism at the Crater Flat basalt field indicate that new silicic eruptions there are unlikely. No major magma chambers have been detected by velocity structure studies. Heat-flow measurements and the lack of high-temperature hot springs also suggest the absence of shallow magma bodies in the region. The most likely effect of silicic volcanism from silicic centers near the western margin of the Great Basin would be the deposition of ash at Yucca Mountain. Before closure, this could make the facility temporarily inaccessible, could make monitoring difficult, and could alter surface drainage depending on the depth of ash. It would pose no recognized hazard after closure.

The possibility of new basaltic volcanism at Yucca Mountain is considered higher than for silicic; basalt has been the predominant product of volcanism in the southern Great Basin over the past 8 to 9 million years, and is likely to be the future product. Basaltic eruptions were mostly Strombolian, producing moderate-sized scoria cones and short lava flows. Shallow sill-like intrusions were emplaced at some basaltic centers in the region, but these are considered unlikely to occur at Yucca Mountain. Centers of hydrovolcanic activity associated with Strombolian eruptions occur throughout the southern Great Basin; hydrovolcanic explosions are considered possible but unlikely at Yucca Mountain.

Basaltic eruptions have been localized and of short duration and low volume; the rate of magma generation in the region has been low during the late Cenozoic and may have declined over the past 4 million years. There is no geologic or geochemical evidence to suggest that the rate of southern Great Basin volcanism is increasing or may increase in the future, or that more voluminous basalt fields may evolve.

A principal hazard from basaltic volcanism would be the intersection of ascending magma with the repository, the incorporation of radioactive waste into the magma, and the dispersal of waste during a subsequent eruption. The greatest amount of dispersed waste from a Strombolian eruption would be in the scoria sheet, with lesser quantities dispersed with fine-grained wind-blown particles and in the scoria cone. Potential radiation doses to those living in the area or in houses built of materials from such eruptions would be a few millirems, for an eruption occurring within 100 yr of emplacement and less for a later eruption.

Injection of magma within the controlled area could alter the hydrologic setting and change transport paths of the waste elements.

The annual probability for the disruption of the repository by basaltic volcanism falls between 4.7×10^{-8} and 3.3×10^{-10}; the corresponding range for 10,000 yr is 4.7×10^{-4} to 3.3×10^{-6}. These numbers can be considered as best- and worst-case probability bounds. This low conditional probability along with the low estimated level for radiological release suggest that the risk associated with basaltic volcanism at Yucca Mountain is low.

Faulting and vertical movements

Although the Yucca Mountain area has been seismically quiescent during the monitoring period of the SGBSN, recurrent Pleistocene and Holocene movement has been demonstrated on significant faults in the vicinity. Some of the major faults in the Yucca Mountain area have moved repeatedly in the present tectonic regime. Additional faulting may be possible at Yucca Mountain because major faults are favorably oriented for movement in the present stress field.

Slip rates along seismogenic faults in the Great Basin are considered to be nonuniform in both space and time. During a given period, the rate of movement for an individual fault segment may be above or below its long-term average rate. The Yucca Mountain area is seismically quiet compared to adjacent parts of the Great Basin, although the area has a higher density of Quaternary faults. However, its faults could experience periods of above-average slip rates within the next 10,000 yr. This possibility is based on observed variations in fault-slip patterns in the Great Basin and on a history of recurrent faulting in the Crater Flat-Yucca Mountain structural depression.

Regional rates of faulting events (those estimated to have been accompanied by earthquakes of $M \geq 7$) for the Yucca Mountain area are estimated to range from 5×10^{-5} to 5×10^{-6} events per year per 1,000 km^2. In the Yucca Mountain area, the average regional rate of vertical offset during the Quaternary is estimated to range from <0.01 to 0.001 mm/yr. However, Yucca Mountain is considered to lie within a belt of contemporary right-lateral shear, and it is possible that strike-slip exceeds dip-slip offset on local faults (such as at Windy Wash). Measurements of Quaternary strike-slip offsets have not yet been made for faults in the vicinity of Yucca Mountain and the discovery of larger offsets than presently known would raise estimates of Quaternary offset rates.

Vertical and lateral crustal movement

Vertical and lateral crustal movement would pose only an indirect hazard to the prospective repository, insomuch as it is associated with faulting, seismicity, and volcanism. Study of the rates and patterns of crustal movement bears upon assessing the hazard from these sources.

The southern Great Basin volcanic field forms a well-defined oval province (Christiansen et al., 1977) with Yucca Mountain on a southern digitation of the field. The circularity of the Timber Mountain and Black Mountain calderas to the north indicates a minimum amount of either vertical or lateral disruption for the past 11 million years at those locations. The southern end of Yucca Mountain has apparently undergone somewhat more extension that these calderas as suggested by the paleomagnetic results of Scott and Rosenbaum (1986) and the decrease in the number of faults and amount of fault displacement to the north along Yucca Mountain.

1.8.1.5.2 Discussion of significant results

This section discusses the tectonic and geologic processes of volcanism, faulting, and crustal movement in the context of long-term regional stabil- [illegible]

Section 1.8.1.3.2.

Tectonic and geologic processes in the region surrounding Yucca Mountain bear on both preclosure and postclosure performance objectives. Before closure, the potential for movement on faults at and near the prospective repository must be recognized to ensure that radionuclides would be isolated and that the waste would be retrievable. After closure, faulting and volcanism in the Yucca Mountain area bear on the ability of the geologic setting to limit releases of radionuclides. Fault rupture at or near the repository might allow radionuclides to reach the environment at higher than mandated concentrations before 10,000 yr.

Chapter 1 has emphasized volcanism in the southern Great Basin during Tertiary and Quaternary time. For silicic volcanism, emphasis has been on Tertiary volcanic centers of the southwest Nevada volcanic field; for basaltic volcanism, on late Tertiary and Quaternary basaltic centers in the Death Valley-Pancake Range volcanic zone.

The Cenozoic history of silicic volcanism in the the southern Great Basin is well documented through geologic and geophysical studies. The existing data appear adequate to support the interpretation that the hazard from silicic volcanism is negligible.

The Cenozoic history of basaltic volcanism describes localized low-volume eruptions of short duration, with the rate of basaltic magma production declining over the past 4 million years, and with no occurrences in the Yucca Mountain area for at least the past 100,000 yr. The model will probably undergo some changes resulting from site investigations, particularly in the ages of more recent events.

DECEMBER 1988

In the data base for assessing hazard from fault rupture, information on the rates and magnitudes of younger fault movements in the Yucca Mountain area is sparse, but studies are ongoing. The present tectonic model is a environment during preclosure and to keep such releases below mandated concentration limits over the next 10,000 yr.

The data base for the drilling and mining history is of high quality but will require careful updating during site characterization and repository construction.

1.8.1.7 Mineral and hydrocarbon resources

1.8.1.7.1 Significant results

Section 1.7 discussed and described the mineral and hydrocarbon resource potential of the site and compared several areas of similar geology. The section also referred to future work that will be necessary to complete the assessment of mineral and hydrocarbon resources at the site located at Yucca Mountain. Commodities that were classified "other occurrences" (Figure 1-74) and not considered as resources using the definitions contained in USBM/USGS (1980), and which will not receive further attention, include the industrial minerals and rocks (i.e., barite, fluorite, zeolites, and other industrial commodities). Many other commodities or minerals were not addressed in Section 1.7 because (1) they are not known to occur in, or are not associated with, silicic tuffs or (2) because the known abundances of a particular commodity or mineral in tuff are known to be near crustal abundance and thus, could never become resources. However, a literature search is planned to evaluate if any other mineral or commodity should be addressed in this assessment (Section 8.3.1.9).

Commodities or minerals that can occur in silicic tuffs, but occur in quantities close to crustal abundances and, thus, are not considered to be resources include diamonds, chromium-bearing minerals, iron-bearing minerals, gypsum, titanium or titanium-bearing minerals, and lithium raw materials. The Yucca Mountain site will not be assessed directly for the above commodities as their presence would have or will be detected during the course of many other site characterization activities.

The site represents an unattractive locality for exploration because the surface rocks do not exhibit evidence of mineralization, past mining or exploration activities, any geophysical anomalies that would suggest mineralization, or alteration characteristic of economic deposits of gold, silver, and base metals. In comparison, Bare Mountain, north-northwestern Yucca Mountain, Calico Hills, and the Wahmonie District exhibit most of the features described above and would be considered likely prospects if future exploration efforts were conducted. On the basis of present knowledge, gold, silver, mercury, uranium, and base metals are considered to be speculative, undiscovered resources at the site.

The geothermal resources (Section 1.7.1.5.2) at the site are classified as low-temperature (<90°C) resources located at depths greater than 1 km. The site's potential for exploitation is considered to be very low because shallow resources of this type are widely available throughout Nevada. Moderate- and high-temperature resources are more likely to be exploited

The potential for geothermal resources will be further assessed through the interpretation of chemical indicators (Section 8.3.1.9).

The hydrocarbon resource potential at Yucca Mountain is considered to be low for the following reasons:

1. Primary hydrocarbons do not form in volcanic rocks, nor have petroliferous interbeds been encountered in drill core.

2. Paleozoic accumulations may have been destroyed by the regional heat flow fluxes through time.

3. Of the more than 60 reported oil and gas exploration holes drilled in the Death Valley region, all were dry.

Additional work includes (1) refinement of the regional heat-flow history; (2) determination of the presence or absence of organic matter in the Paleozoic rocks in the area and available from drill core samples, and its thermal maturation state; (3) further analysis of thermal maturity for the Paleozoic rocks located near and beneath Yucca Mountain; and (4) a comparison of potential source and reservoir rocks at Yucca Mountain with known producing fields in Nevada (Section 8.3.1.9).

1.8.1.7.2 Discussion of significant results

Consideration of mineral and hydrocarbon resources at Yucca Mountain bears upon postclosure performance objectives for the repository. The possible future exploitation of these resources must not allow the release of radionuclides to the accessible environment above mandated concentration limits before 10,000 yr.

The favorability assessments for different mineral and hydrocarbon resources depended in part on comparing the geologic settings of occurrences in nearby areas, and elsewhere in the Basin and Range Province, to the geology of Yucca Mountain. The assessments also included consideration of mineral occurrences in drill core from Yucca Mountain.

Although the potential for mineral resources and future exploration is considered to be low for the site, more detailed, site-specific work will be done to characterize possible resources. Some commodities or minerals will be evaluated further. For example, precious metals will be evaluated more fully by comparison with additional analog environments and geochemical data even though the potential for precious-metal resources is likely to be low (Section 1.7.1.2). Future work includes comparisons of the mineralization that occurs adjacent to caldera complexes with the mineralization found in the region of Yucca Mountain. Also, detailed geochemical data will be obtained from surface and down-hole samples with particular emphasis on gold, silver, and base metals (Section 8.3.1.9). Undoubtedly, many parameters beyond the scope of this chapter cannot be addressed until further work is completed on other aspects of site characterization. These concerns include the work planned on calcite and silica deposits located along faults

(Section 8.3.1.3) and the possible presence of detachment faults at the site (Section 8.3.1.17).

1.8.2 RELATION TO DESIGN

This section briefly discusses how geologic information bears on the design of the repository and the waste package. Much of the following discussion is drawn from Chapters 6 (Sections 6.1.2.2 and 6.1.2.3) and 7. Understanding the geologic framework of the area is essential for the assembly of the geotechnical and hydrologic data bases, both of which are important to the placement and design of the repository and to the design of the waste package. Integrating geoengineering and hydrology with the geologic framework will yield an overall physical model of Yucca Mountain to be used in the various engineering aspects of repository design.

1.8.2.1 Relation of geology to repository design

Detailed topographic maps will be used in the design of the surface facilities and in assessing the flood potential at the surface facilities.

The physical and mechanical characteristics of surficial deposits and soils will be considered in locating and designing the surface facilities. The geologic description of these units provides a basis for gathering geo-technical data essential for foundation design. Present geomorphic processes may also bear upon site selection for surface facilities (e.g., avoiding areas of possible future flooding).

The stratigraphy and lithologies of Yucca Mountain provide a framework for defining the thermal and mechanical properties of the rock used for waste storage. The vertical and lateral variations in the physical and geochemical properties of the host rock and enclosing units (e.g., thickness, mineralogy and alteration, degree of welding, and presence of lithophysae) are a basis for calculating the thermomechanical response of the host rock to waste storage, and for subdividing the Yucca Mountain volcanic strata into thermal-

mechanical units. Variations in thickness and physical properties of the repository horizon must be known for the layout of the underground facility spatial distribution of these units are defined, in part, by stratigraphic contacts and by the positions, attitudes, and offsets of faults.

The existing in situ stress regime at Yucca Mountain (magnitude and direction of the three principal stresses) bears upon repository design because mechanical (from mining) and thermal (from the waste package) stresses will be imposed upon ambient stress conditions. The maximum stress is vertical and depends on weight of overburden. The minor and intermediate stress directions are nearly in the horizontal plane; their orientations and magnitudes will be derived from direct measurement and from interpretation of faulting and fracture patterns.

The geothermal regime at Yucca Mountain bears upon repository design because it is the framework for analysis of host-rock thermomechanical response to waste storage. Important geothermal aspects of the repository horizon are temperature, thermal conductivity, and heat flux.

Important seismic considerations at Yucca Mountain are ground motion and surface rupture. The design earthquake for the repository must allow it to meet preclosure objectives.

Exploratory drilling of Yucca Mountain during site investigations has a peripheral effect on repository design, in that all drillholes must be properly sealed to ensure compliance with postclosure performance objectives.

1.8.2.2 Relation of geology to waste package design

Geologic information affects waste package design through geoengineering, hydrology, and geochemistry.

The geothermal regime provides a basis for analyzing thermomechanical response of the host rock to the heat generated by the waste packages (e.g., possibility for creep under the postemplacement thermal regime). The host rock thermomechanical properties will be used to calculate the maximum heat loading that can be sustained by each waste package. The mechanical properties of the host rock will be used to assess the stability of the borehole openings for the waste canisters.

With regard to hydrology, the choice of a repository horizon in the unsaturated zone simplifies the design of the waste packages and limits the adverse conditions to which they will be subjected.

1.8.3 IDENTIFICATION OF INVESTIGATIONS

This section identifies the investigations that draw on geologic information about Yucca Mountain and the surrounding region; the section considers required data still to be gathered by ongoing studies (some yet unpublished) and by the planned site investigations (Section 8.3.1). In the following subsections, topics are discussed in the same order as in major sections to which they apply in Chapter 1.

1.8.3.1 Investigations bearing on geomorphology

Investigations in the following characterization programs have a bearing on geomorphology: 8.3.1.6 (erosion), 8.3.1.9 (human interference), and 8.3.1.14 (surface characteristics).

Planned site investigations in geomorphology (Section 8.3.1.6) will address the likelihood of short-lived episodes of rapid erosion in the Yucca Mountain area and the probable effects of such episodes within the next 10,000 yr. The effort will consider probable future climatic and tectonic conditions.

Recent and current investigations have been directed toward understanding locations and rates of erosion at Yucca Mountain and vicinity. Isotopic and rock varnish dating are now being used to determine the ages of surficial deposits, to ascertain hillslope erosion rates and downcutting rates of streams and to clarify the paleoclimatic history of the region surrounding Yucca Mountain. The surficial deposits are also being studied sedimentologically to estimate past processes of erosion. These studies also bear on the understanding of Quaternary faulting. Ongoing studies in contrasts between modern and ancient alluvial and eolian processes will assist in assessing future erosion. Plans for mapping surficial deposits are being formulated (Section 8.3.1).

Ongoing studies are aimed at correlation of age results among standardized and new dating techniques. The methods involved include thermoluminescence, cation-ratio, uranium-series, uranium-trend, potassium-argon dating, and radiocarbon dating.

Soil studies are in progress to clarify paleoenvironmental conditions, and to assist with establishing the chronology and correlation of the different types of surficial deposits.

In the planned site investigations, the assessment of present locations and rates of erosion (Section 8.3.1.6) will consider both present and past rates of erosion due to movement along range-front faults and evaluating the future impact of tectonic movement on Yucca Mountain and vicinity.

The potential effects of erosion on hydrologic, geochemical, and rock characteristics (Section 8.3.1.6) will entail predicting future erosion rates using data from completed studies described in the previous paragraphs. Existing data are judged sufficient to evaluate these characteristics.

The topographic characteristics of potential locations of surface facilities are defined by topographic maps for the Yucca Mountain area. Geomorphic studies will also provide data for the evaluation of potential locations of surface facilities.

Some of the geomorphology activities undertaken to complete site investigations bearing on erosion will apply to ranges and recurrence intervals of future climatic conditions (Section 8.3.1.5). Examples are soils investigations, surficial deposits mapping, evaluation of eolian history at Yucca Mountain, and the analysis of alluvial fan sequences.

1.8.3.2 Investigations bearing on stratigraphy and lithology

Investigations in the following characterization programs bear on stratigraphy and lithology: 8.3.1.4 (rock characteristics) and 8.3.1.14 (surface characteristics).

The site investigations for stratigraphy and lithology of Yucca Mountain and the surrounding area will be oriented toward refining the existing geologic model to the point at which it will be a reliable guide for engineering design (e.g., final vertical and lateral placement of the repository in the Topopah Spring Member) and for assessing the geologic framework for the ground-water regime and related radionuclide transport characteristics. In the Tertiary volcanics, the vertical and lateral variations in the geometric and physical characteristics of the rock units will be of particular concern, especially in the Topopah Spring Member and the bedded tuffs. For the pre-Cenozoic rocks, the investigations will address the identities of the units, their distribution and lithologies, and the nature of the Tertiary and pre-Cenozoic contact. Pre-Cenozoic stratigraphy may bear upon the hydrologic regime and the tectonic setting.

Work is currently under way to answer some of these data requirements. Geologic data from the water-table, unsaturated zone, and tracer-study drill-holes are being incorporated with the existing stratigraphic model; this work includes correlation, petrographic, mineralogic, and geophysical studies. Outcrop studies are under way in areas surrounding Yucca Mountain to gather additional stratigraphic data on the Paintbrush Tuff (including the Topopah Spring Member) and the rhyolite of Calico Hills. There is ongoing investigation of the vertical and lateral variations in thickness and lithology in the zones or subunits of the Topopah Spring Member, and in the bedded tuff units. Correlation of downhole geophysical data with physical properties of rock units and their lateral variation is part of the contribution of downhole geophysics to current subsurface studies. Zeolites in the volcanic rocks are being studied because of their sorptive characteristics. Seismic refraction surveys are under way in the northernmost and southernmost parts of Yucca Mountain to aid in defining the distribution of the pre-Cenozoic units.

The planned site investigations in stratigraphy and lithology include (Section 8.3.1.4) the characterization of the vertical and lateral stratigraphy of Yucca Mountain, and consists of several activities. Outcrop studies of subunits of the Topopah Spring Member are oriented toward correlating them with their subsurface occurrences within the proposed repository. Subsurface investigation of the Topopah Spring Member will complete the ongoing correlation of its subunits in all of the drillholes that penetrate it, and better define their distribution, lithology, and history. Subsurface studies will also include other members of the Paintbrush Tuff, rhyolite of Calico Hills, Crater Flat Tuff, and older tuffs beneath the repository. Petrographic study of the bedded tuffs will continue, in order to further define their continuity and physical properties. Investigation of the distribution and genesis of mordenite in the volcanic rocks will also be continued, using light and electron microscopy and x-ray diffraction. The paleomagnetism of the volcanic rocks will be used to improve stratigraphic correlation, through the study of mappable paleomagnetic anomalies between lithostratigraphic units. The walls of the exploratory shaft and underground drifts will be mapped; this effort will include both the geologic mapping of variations in lithology and the detailed mapping of fractures.

These geologic studies will be complemented by geophysical and rock properties testing (Section 8.3.1.15.1), including paleomagnetic, borehole geophysical, and petrophysics studies.

Finally, the results of the geologic investigations in Section 8.3.1.4 will be integrated with structural conclusions (Section 8.3.1.4) to develop a synthesis of the repository stratigraphy and structure, a three-dimensional model of its geology (Section 8.3.1.4).

1.8.3.3 Investigations bearing on structural geology and tectonics

Investigations in the following characterization programs bear on structural geology and tectonics: 8.3.1.4 (rock characteristics), 8.3.1.8 (postclosure tectonics), 8.3.1.14 (surface characteristics), 8.3.1.15 (thermal and mechanical properties), and 8.3.1.17 (preclosure tectonics).

The discussion in this section is presented according to the order of subjects in Section 1.8.1.3: volcanism, structure, existing stress regime, vertical and lateral crustal movement, and geothermal regime.

1.8.3.3.1 Volcanism

Ongoing work in volcanism includes the correlation and dating of volcanic ashes in and adjacent to the NTS; minor element and isotope geochemistry of basalts in the Death Valley-Pancake Range belt; age studies of late Neogene volcanics in the NTS and vicinity; and drilling and study of core recovered from aeromagnetic anomalies near Yucca Mountain, to delineate buried volcanic centers.

Site investigations of the SCP include the potassium-argon dating of known basalt flows and scoria cones and volcanic flows discovered through drilling, and a review of the potential impacts of hydrovolcanic eruptive phases. This data will be used in revised probability calculations on the probability of volcanic events disrupting the proposed repository. Geophysical studies will be carried out to determine whether magmas or partial melts are present in the upper crust below Crater Flat.

Section 8.3.1.8 describes the studies that will assess the potential effect of tectonic activity on hydrology, rock geochemical properties, and rock characteristics. The potential surface volcanic and subsurface igneous processes at Yucca Mountain and vicinity will be integrated with the topographic, structural, and climatic framework to estimate potential impacts on hydrologic, geochemical, and rock characteristics.

1.8.3.3.2 Structure

The site investigations for structure are chiefly focused on studies of specific structural features at Yucca Mountain and include regional studies of faulting and other structural features of the southern Great Basin that are relevant to waste isolation at the site. The site-specific studies are oriented toward refining current understanding of faulting and fracturing at the proposed repository site, and will be used in engineering design, in assessing the potential for future fault movement (and attendant seismicity), and in assessing the impact of fault rupture on the hydrologic regime and thus on waste isolation.

There are various ongoing regional and site-specific investigations pertaining to structure. Geologic activities include the geologic mapping of Bare Mountain, focusing on (1) the possible detachment faulting in the Paleozoic section; (2) the geologic synthesis at 1:100,000 of the NTS area; (3) the geologic synthesis and fault mapping of the Beatty 1:100,000 quadrangle; (4) the mapping of the Bullfrog NW and NE quarter quadrangles, focusing on detachment faults between the Miocene volcanics and the pre-Cenozoic basement; (5) the study of the distribution of Paleozoic units to aid in correlating their subsurface locations with seismic reflection profiles; (6) a basin analysis of Oligocene/Miocene continental and lacustrine formations at the NTS and their correlatives in the Sheep Range; and (7) a fracture density and orientation analysis using satellite imagery.

Ongoing age studies of faulting include Quaternary mapping of the Beatty quadrangle, focusing on its western and eastern quarters; mapping of the Bare and geomorphic development of Yucca Wash; and study of erosion rates at the NTS and vicinity.

Geophysical studies underway include (1) seismic refraction profiles in Crater Flat and Jackass Flats; (2) shallow reflection seismology near Beatty, at Crater Flat, on the northeast flank of Bare Mountain, and in the Rock Valley area; (3) gravity synthesis of the Beatty quadrangle; and (4) gravity, magnetic, and magneto-telluric surveys of the NTS and surroundings.

Regional studies for site characterization

The planned regional site investigations that deal with the different styles of faulting in the southern Great Basin are (1) wrench faulting along geologic province boundary (Walker Lane), (2) left-lateral strike-slip faulting on northeast-trending systems, (3) detachment faults in and adjacent to Yucca Mountain, and (4) normal and strike-slip faulting on north- to northwest-trending systems.

The various regional structural studies will be integrated with results from seismologic, stress regime, and vertical and lateral crustal movement studies (Sections 1.8.3.3.3, 1.8.3.3.4, and 1.8.3.4) to yield a tectonic model synthesis of the regional geology, geophysics, and structure (mainly styles of faulting) for the southern Great Basin and Yucca Mountain. This synthesis will make possible the generation of probable tectonic scenarios for the Yucca Mountain area.

Site-specific studies

The site-specific investigation of faulting and fracturing at Yucca Mountain (Sections 8.3.1.4, 8.3.1.8, and 8.3.1.17) includes both geologic and geophysical activities. Fracture studies will encompass (1) development of surface fracture networks, (2) vertical seismic profiling studies of the subsurface fracture network, (3) seismic property studies of fractured rock, (4) mineralogic studies of fracture-lining minerals in core samples, and (5) the characterization of fractures in boreholes and the exploratory shaft. Structural studies will include characterization of faults in boreholes and the exploratory shaft and drift walls; and the geologic mapping of zonal features in the Tiva Canyon and Topopah Spring members, aimed at identifying fault offsets on the order of a few meters. Structural interpretation will be aided by data from paleomagnetic, borehole geophysics, and petrophysics studies. Site characterization faulting studies will concentrate on gathering data on the location, displacement, length, Quaternary slip rate and the width and distribution of zones of Quaternary rupture. This data will be collected by detailed geologic mapping, structure contouring, and trenching in and around the controlled area. Data on faulting and fault geometry will also be provided from boreholes, the exploratory shaft facility, and geophysical surveys. Site-specific structural data will be integrated with the stratigraphy to synthesize a three-dimensional model of Yucca Mountain geology.

Integration of regional and site-specific studies

The first important object of the tectonic studies is to describe the location, nature, amount, and probability of potential fault movement at the proposed Yucca Mountain repository (Section 8.3.1.17). Accomplishing this requires integrating results from regional and site-specific studies. Among the required data will be (1) slip rates and recurrence rates of movements on Quaternary faults, (2) probability of future faulting on different styles of faults, (3) character of the regional stress field, and (4) probabilities from the tectonic scenarios.

The second important object of the tectonic studies is to assess the impact of future faulting (rupture) and other potential tectonic activity on the hydrologic regime at Yucca Mountain (Section 8.3.1.8). This effort will require integrating the results of the faulting studies with the climatic and hydrologic framework to analyze the effect of rupture on ground-water flow in the saturated and unsaturated zones. A secondary consideration will be the effect on hydrology of vertical and lateral crustal movement.

1.8.3.3.3 Existing stress regime

Ongoing work consists of a synthesis of in situ stress conditions at the repository.

In the site investigations, studies of the existing regional stress regime must address its relation to the orientations and styles of fault movement in the southern Great Basin and Yucca Mountain (Section 8.3.1.17). Activities will include (1) in situ stress tests in shallow and deep boreholes, (2) evaluating paleostress as it applies to regional and local stress stability, (3) modeling the present stress field at Yucca Mountain and vicinity, and (4) analyzing stress field changes in the Pahute Mesa-Yucca Flat area due to detonation of nuclear devices. Results from the above study will bear upon formulating the tectonic model synthesis.

The characterization of the site ambient stress (Section 8.3.1.15) must provide initial and boundary conditions for geomechanical models used in repository performance assessment. This will require overcore stress tests in the exploratory shaft to observe in situ stress conditions above, below, and within the proposed repository horizon, and in the part of the unsaturated zone penetrated by the shaft.

1.8.3.3.4 Vertical and lateral crustal movement

Ongoing work consists of gathering measurements from the existing geodetic network.

In the planned site investigations, geodetic leveling (Section 8.3.1.17) will have the object of measuring the historic rate of uplift and subsidence. Activities will include (1) the resurvey of the geodetic leveling network; (2) analyzing the existing geodetic data base on the historical uplift rate; and (3) the geodetic profiling of any identified active uplift areas.

Characterization of regional lateral crustal movement will aim at defining historic rates and orientation of this movement. Activities include inferring movement from historic faulting and seismicity, and geodesy analysis.

1.8.3.3.5 Geothermal regime

Ongoing work includes the construction of cross sections based on existing drillholes at Yucca Mountain, showing temperature distribution using isothermal lines; and heat-flow calculations for the drillholes, including the WT (water table) series.

Site investigations for the geothermal regime must address refining the

Seismic Network (SGBSN) with data processing and earthquake location, (2) acceleration attenuation studies, (3) evaluation of crustal velocity structure, (4) evaluation of the tectonic significance of the east-west seismic zone, (5) evaluation of the stress regime at Yucca Mountain relative to other areas, (6) study of nuclear-induced seismicity, and (7) investigation of earthquake source characteristics in an extensional regime.

In the planned site investigations, regional studies of seismicity (Section 8.3.1.17) consist of several activities aimed at refining the seismicity model for the southern Great Basin and Yucca Mountain. Continued operation of the SGBSN will record and locate all detectable earthquakes in the region; these data will be integrated with the historical seismic record and with existing SGBSN data. Interpretations of seismic data (e.g., epicenter maps, recurrence rates, and focal mechanisms) will be used together with the structural and geologic data (e.g., fault maps and cross sections) to produce a ground motion analysis for use in design. Investigation of regional ground motion characteristics will entail characterizing ground motions at the Yucca Mountain site from locally severe earthquakes. The approach is to assign exceptional earthquake sources to those active faults and potentially active fracture zones at depth that could account for extreme motions at the site. The exceptional earthquake sources are at or near the maximum magnitude for the individual source zones with an average return period of at least several thousand years. From these exceptional sources, controlling sources are identified as those that produce the most severe motions at the site. The ground motions from locally severe earthquakes will then be characterized by a suite of accelerograms scaled to the magnitudes and distances of the controlling sources and modified, as needed, to account for the effects of the local site geology. The effects of the NTS nuclear tests on earthquake occurrence rates in the region will be evaluated to determine if seismic rates have been significantly increased by nuclear testing.

1.8.3.5 Investigations bearing on long-term regional stability

Investigations in the following characterization programs have a bearing on long-term regional stability: 8.3.1.8 (postclosure tectonics) and 8.3.1.17 (preclosure tectonics).

The evaluation of long-term regional stability at Yucca Mountain and its surroundings mainly involves estimating probabilities for volcanic disruption and fault rupture affecting the prospective repository. As discussed in Section 1.8.1.5.2, dependable estimates will require additional data on the Quaternary volcanic and tectonic history of Yucca Mountain and the surrounding area. The site investigations of the SCP (along with ongoing work) that will address these goals are discussed in Section 1.8.3.3. The approach to be used to identify and resolve licensing issues associated with significant tectonic events is discussed in Sections 8.3.1.8 and 8.3.1.17.

1.8.3.6 Investigations bearing on drilling and mining

There are no investigations addressing drilling and mining because [illegible]

previous studies have shown that there is no evidence of mining activity at Yucca Mountain and because all drilling there has been associated with the proposed repository. There are no specific plans in the SCP to further address these subjects.

1.8.3.7 Investigations bearing on mineral and hydrocarbon resources

Investigations in human interference program 8.3.1.9 bear on mineral and hydrocarbon resources.

Future work on the assessment of mineral (including precious metals) and hydrocarbon resources located at the site includes probabilistic approaches to resource distributions in a regional framework, the application of geochemical techniques to exploration and assessment of mineral and energy resources, and further comparisons of locations comparable to the site in terms of geology and any present or future potential for mineralization or energy resources. Additional work is also planned using the data collected under other activities. This includes an analysis of the available geophysical data in relation to new geophysical data to be collected, the evaluation of ground-water chemical data and heat flow data in relation to the potential for geothermal resources in the region of the site, and the evaluation of petrologic data and geochemical data collected on rocks of the site and nearby localities. Section 8.3.1.9 describes the activities planned and references the activities planned under other studies that may be used in assessing potential mineral and hydrocarbon resources at the site.

1.8.4 RELATION TO REGULATORY GUIDE 4.17

This section considers information that is required by NRC Regulatory Guide 4.17 (NRC, 1987) but may not be included in Chapter 1. A comparison of the regulatory guide with the prescribed contents of Chapter 1 shows that none of the information required by the guide is missing from Chapter 1. The only differences between the two are minor matters of organization and terminology, such as the following:

1. Information on surface geology prescribed by the regulatory guide (Section 1.2.1) is incorporated into Sections 1.1 (geomorphology) and 1.2 (stratigraphy and lithology) of Chapter 1.

2. "Active stress field" (Section 1.3.2.6) in the regulatory guide has been changed to "existing stress regime" (Section 1.3.2.3) in

DOE/RW-0199

Nuclear Waste Policy Act
(Section 113)

Site Characterization Plan

Yucca Mountain Site, Nevada Research and Development Area, Nevada

Volume I, Part A

Chapter 1 References

December 1988

U. S. Department of Energy
Office of Civilian Radioactive Waste Management

REFERENCES FOR CHAPTER 1

Adler, H. H., 1974. Concepts of Uranium-Ore Formation in Reducing Environments in Sandstones and Other Sediments, IAEA-SM-183/43, International Atomic Energy Agency, Vienna, Austria, pp. 141-168.

Agnew, D. C., and K. E. Sieh, 1978. "A Documentary Study of the Felt Effects of the Great California Earthquake of 1857," Bulletin of the Seismological Society of America, Vol. 68, No. 6, pp. 1717-1729.

Albers, J. P., 1967. "Belt of Sigmoidal Bending and Right-Lateral Faulting in the Western Great Basin," Geological Society of America Bulletin, Vol. 78, pp. 143-156.

Albers, J. P., and J. H. Stewart, 1972. Geology and Mineral Deposits of Esmeralda County, Nevada, Nevada Bureau of Mines & Geology Bulletin 78, University of Nevada, Reno.

Algermissen, S. T., D. M. Perkins, P. C. Thenhaus, S. L. Hanson and B. L. Bender, 1982. Probabilistic Estimates of Maximum Acceleration and Velocity in Rock in the Contiguous United States, USGS-OFR-82-1033, Open-File Report, U.S. Geological Survey.

Allmendinger et al, 1987.

Anderson, L. A., 1981. Rock Property Analysis of Core Samples from the Yucca Mountain UE25a-1 Borehole, Nevada Test Site, Nevada, USGS-OFR-81-1338, Open-File Report, U.S. Geological Survey.

Anderson, L. A., 1984. Rock Property Measurements on Large-Volume Core Samples from Yucca Mountain USW GU-3/G-3 and USW G-4 Boreholes, Nevada Test Site, Nevada, USGS-OFR-84-552, Open-File Report, U.S. Geological Survey, 39 p.

Anderson, L. W., and F. F. Hawkins, 1984. "Recurrent Holocene Strike-Slip Faulting, Pyramid Lake Fault Zone, Western Nevada," Geology, Vol. 12, pp. 681-684.

Anderson, R. E., 1971. "Thin-Skin Distension in Tertiary Rocks of Southeastern Nevada," Geological Society of America Bulletin, Vol. 82, pp. 43-58.

Anderson, R. E., 1973. Large Magnitude Late Tertiary Strike-Slip Faulting North of Lake Mead, Nevada, Geological Survey Professional Paper 794, U.S. Government Printing Office, Washington, D.C.

Anderson, R. E., M. L. Zoback, and G. A. Thompson, 1983. "Implications of Selected Subsurface Data on the Structural Form and Evolution of Some Basins in the Northern Basin and Range Province, Nevada and Utah," Geological Society of America Bulletin, Vol. 94, pp. 1055-1072.

Arabasz, W. J., 1986. "Seismotectonics of the Basin and Range - Colorado Plateau Transition in Utah," Geological Society of America, Abstracts with Programs 1986, Rocky Mountain Section, Flagstaff, Arizona, April 30-May 2, 1986, Vol. 18, No. 5, p. 338.

Armstrong, R. L., 1968. "Sevier Orogenic Belt in Nevada and Utah," Geological Society of America Bulletin, Vol. 79, pp. 429-458.

Armstrong, R. L., 1974. "Magmatism, Orogenic Timing, and Orogenic Diachronism in the Cordillera from Mexico to Canada," Nature, Vol. 247, No. 5440, pp. 348-351.

Armstrong, R. L., and J. Suppe, 1973. "Potassium-Argon Geochronometry of Mesozoic Igneous Rocks in Nevada, Utah, and Southern California," Geological Society of America Bulletin, Vol. 84, pp. 1375-1392.

Ashley, R. P., 1979. "Relation Between Volcanism and Ore Deposition at Goldfield, Nevada," papers on Mineral Deposits of Western North America, J. D. Ridge (ed.), Nevada Bureau of Mines Geology Report 33, University of Nevada, Reno, pp. 77-86.

Askew, B., and S. T. Algermissen, 1983. An Earthquake Catalog for the Basin and Range Province 1803-1977, USGS-OFR-83-86, Open-File Report, U.S. Geological Survey, 40 p.

Atwater, T., 1970. "Implications of Plate Tectonics for the Cenozoic Tectonic Evolution of Western North America," Geological Society of America Bulletin, Vol. 81, No. 12, pp. 3513-3535.

Averitt, P., 1975. Coal Resources of the United States, January 1, 1974, Geological Survey Bulletin 1412, U.S. Government Printing Office, Washington, D.C., 131 p.

Babcock, J. W., 1984. "Introduction to Geologic Ore Deposit Modeling," Mining Engineering, Vol. 36, No. 12, pp. 1631-1636.

Bailey, E. H., 1964. "Mercury," Mineral and Water Resources of Nevada, U.S. Geological Survey and Nevada Bureau of Mines 88th Congress, 2nd Session, Document No. 87, U.S. Government Printing Office, Washington, D.C.

Bailey, E. H., and M. C. Blake, 1969. "Late Mesozoic Tectonic Development of Western California," Geotectonics, pp. 148-154.

Bailey, E. H., and D. A. Phoenix, 1944. Quicksilver Deposits in Nevada, University of Nevada Bulletin, Geology & Mining Series 41, Vol. 38, No. 5, Reno, Nev.

Bakun, W. H., and W. B. Joyner, 1984. "The ML Scale in Central California," Bulletin Seismological Society of America, Vol. 74, No. 5, pp. 1827-1843.

Ball, S. H., 1907. A Geologic Reconnaissance in Southwestern Nevada and Eastern California, U.S. Geological Survey Bulletin 308, Reprinted as Ball, S. H., 1983. "Mines of Silver Peak Range, Kawich Range and Other Southern Nevada Districts," Stanley Paher, Nevada Publications, Las Vegas, Nev., 218 p.

Ballard, R. L., 1985. "Statistical Summary," 1984 Bureau of Mines Minerals Yearbook, U.S. Department of the Interior, Bureau of Mines, Washington, D.C.

Barnes, H., and F. G. Poole, 1968. "Regional Thrust Fault System in Nevada Test Site and Vicinity," Nevada Test Site, E. B. Eckel (ed.), Geological Society of America Memoir 110, pp. 233-238.

Bartley, J. M., and B. P. Wernicke, 1984. "The Snake Range Decollement Interpreted as a Major Extensional Shear Zone," Tectonics, Vol. 3, No. 6, pp. 647-657.

Barton, C. C., 1984. "Tectonic Significance of Fractures in Welded Tuff, Yucca Mountain, Southwest Nevada," Geological Society of America, Abstracts with Programs, Vol. 16, No. 6, p. 438.

Barton, C. C., and E. Larsen, 1985. "Fractal Geometry of Two-Dimensional Fracture Networks at Yucca Mountain, Southwestern Nevada," in Proceedings of the International Symposium on Fundamentals of Rock Joints, Bjorkliden, Sweden, September 15-20, 1985, O. Stephansson (ed.), pp. 77-84.

Bateman, A. M., 1950. Economic Mineral Deposits, Second Edition, John Wiley & Sons, Inc., New York.

Bates, R. L., 1975. "Introduction," Industrial Minerals and Rocks, S. J. Lefond (ed.), 4th Edition, American Institute of Mining, Metallurgical & Petroleum Engineers, Inc., New York, pp. 3-7.

Bath, G. D., and C. E. Jahren, 1984. Interpretations of Magnetic Anomalies at a Potential Repository Site Located in the Yucca Mountain Area, Nevada Test Site, USGS-OFR-84-120, Open-File Report, U.S. Geological Survey.

Bath, G. D., C. E. Jahren, J. G. Rosenbaum, and M. J. Baldwin, 1983. "Magnetic Investigations," Geologic and Geophysical Investigations of Climax Stock Intrusive, Nevada, USGS-OFR-83-377, Open-File Report, U.S. Geological Survey, pp. 40-77.

Bayer, K. C., 1973a. Seismic Data Report Southern Nevada Region December 22.

Bish, D. L., 1981. Detailed Mineralogical Characterization of the Bullfrog and Tram Members in USW-G1, with Emphasis on Clay Mineralogy, LA-9021-MS, Los Alamos National Laboratory, Los Alamos, N. Mex.

Bish, D. L., 1987. Evaluation of Past and Future Alterations in Tuff at Yucca Mountain, Nevada Based on the Clay Mineralogy of Drill Cores USW G-1, G-2, and G-3, LA-10667-MS, draft, Los Alamos National Laboratory, Los Alamos, N. Mex.

Bish, D. L., and R. E. Semarge, 1982. "Mineralogic Variations in a Silicic Tuff Sequence: Evidence for Diagenetic and Hydrothermal Reactions," [abs.] The 19th Annual Clay Minerals Society Meeting, Hilo, Hawaii, August 8-14, 1982.

Bish, D. L., and D. T. Vaniman, 1985. Mineralogic Summary of Yucca Mountain, Nevada, LA-10543-MS, Los Alamos National Laboratory, Los Alamos, N. Mex.

Bish, D. L., F. A. Caporuscio, J. F. Copp, B. M. Crowe, J. D. Purson, J. R. Smyth, and R. G. Warren, 1981. Preliminary Stratigraphic and Petrologic Characterization of Core Samples from USW-G1, Yucca Mountain, Nevada, A. C. Waters and P. R. Carroll (eds.), LA-8840-MS, Los Alamos National Laboratory, Los Alamos, N. Mex.

Bish, D. L., D. T. Vaniman, F. M. Byers, Jr., and D. E. Broxton, 1982. Summary of the Mineralogy-Petrology of Tuffs of Yucca Mountain and the Secondary Phase Thermal Stability in Tuffs, LA-9321-MS, Los Alamos National Laboratory, Los Alamos, N. Mex.

Bish, D. L., A. E. Ogard, D. T. Vaniman, and L. Benson, 1984. "Minerology-Petrology and Groundwater Geochemistry of Yucca Mountain Tuffs," in Scientific Basis for Nuclear Waste Management VII, Materials Research Society Symposia Proceedings, Boston, Massachusetts, November 1983, G. L. McVay (ed.), Vol. 26, North-Holland, Elsevier Science Publishing Co., Inc., New York, pp. 283-291.

Blackwell, D. D., 1978. "Heat Flow and Energy Loss in the Western United States," Cenozoic Tectonics and Regional Geophysics of the Western Cordillera, R. B. Smith and G. P. Eaton (eds.), Geological Society of America Memoir 152, pp. 175-208.

Blackwell, D. D. and D. S. Chapman, 1977. "Interpretation of Geothermal Gradient and Heat Flow Data for Basin and Range Geothermal Systems," Geothermal Resource Council, TRANSACTIONS, Vol. 1, pp. 19-20.

Blackwell et al, 1981.

Bohannon, R. G., 1979. "Strike-Slip Faults of the Lake Mead Region of Southern Nevada," Cenozoic Paleogeography Symposium 3, J. M. Armentrout, M. Cole, and H. TerBest (eds.), Pacific Section, Society of Economic Paleontologists & Mineralogists, Los Angeles, Calif., pp. 129-139.

Bohannon, R. G., 1983. "Mesozoic and Cenozoic Tectonic Development of the Muddy, North Muddy, and Northern Black Mountains, Clark County, Nevada," Tectonic and Stratigraphic Studies in the Eastern Great Basin, Geological Society of America Memoir 157, pp. 125-148.

Bohannon, R. G., 1984. Nonmarine Sedimentary Rocks of Tertiary Age in the Lake Mead Region, Southeastern Nevada and Northwestern Arizona, Geological Survey Professional Paper 1259, U.S. Government Printing Office, Washington, D.C.

Boles, J. R., 1977. "Zeolites in Deep-Sea Sediments," Mineralogy and Geology

Bortz, L. C., and D. K. Murray, 1979. "Eagle Springs Oil Field, Nye County, Nevada," Basin and Range Symposium and Great Basin Field Conference, G. W. Newman and H. D. Goode (eds.), Rocky Mountain Association of Geologists and Utah Geological Association, Denver, Colo., pp. 441-454.

Bowie, S. H. U., 1974. "Where to Prospect for Uranium," in Proceedings of [illegible]

IAEA-TC-25/12, pp. 151-163.

Brady, B. T., 1984a. "Mineral and Energy Resources," Studies of Geology and Hydrology in the Basin and Range Province, Southwestern United States, for Isolation of High-Level Radioactive Waste, M. S. Bedinger, K. A. Sargent, and W. H. Langer (eds.), USGS-OFR-84-743, Open-File Report, U.S. Geological Survey, pp. 118-173.

Brady, B. T., 1984b. Selected Geologic and Hydrologic Characteristics of the Basin and Range Province, Western United States: Coal, Oil and Gas Wells, Seeps and Tar Sandstone Occurrences, Miscellaneous Investigations Series Map I-1522-E, Scale 1:2,500,000, U.S. Geological Survey.

Brobst, D. A., 1975. "Barium Minerals," Industrial Minerals and Rocks, S. J.

Bull, W. B., 1984. "Tectonic Geomorphology," Journal of Geological Education, Vol. 32, pp. 310-324.

Bull, W. B., and L. D. McFadden, 1977. "Tectonic Geomorphology North and South of the Garlock Fault, California," in Geomorphology in Arid Regions, Proceedings of the 8th Annual Geomorphology Symposium Held at the State University of New York at Binghamton, September 23-24, 1977, D. O. Doehring (ed.), pp. 115-138.

Burchfiel, B. C., 1965. "Structural Geology of the Specter Range Quadrangle, Nevada, and Its Regional Significance," Geological Society of America Bulletin, Vol. 76, pp. 175-192.

Burchfiel, B. C., and G. A. Davis, 1975. "Nature and Controls of Cordilleran Orogenesis, Western United States: Extensions of an Earlier Synthesis," American Journal of Science, Vol. 275-A, pp. 363-369.

Burchfiel, B. C., and J. H. Stewart, 1966. "Pull-Apart Origin of the Central Segment of Death Valley, California," Geological Society of America Bulletin, Vol. 77, pp. 439-442.

Burchfiel, B. C., R. J. Fleck, D. T. Secor, R. R. Vincelette, and G. A. Davis, 1974. "Geology of the Spring Mountains, Nevada," Geological Society of America Bulletin, Vol. 85, pp. 1013-1022.

Butler, A. P., Jr., 1964. "Uranium," Mineral and Water Resources of Nevada, Nevada Bureau of Mines Bulletin 65, University of Nevada, Reno, pp. 161-165.

Byers, F. M., Jr., 1985. Petrochemical Variation of Topopah Spring Tuff Matrix with Depth (Stratigraphic Level), Drill Hole USW G-4 Yucca Mountain, Nevada, LA-10561-MS, Los Alamos National Laboratory, Los Alamos, N. Mex.

Byers, F. M., Jr., and H. Barnes, 1967. Geologic Map of the Paiute Ridge Quadrangle, Nye and Lincoln Counties, Nevada, Geological Quadrangle Map GQ-577, Scale 1:24,000, U.S. Geological Survey.

Byers, F. M., Jr., and R. G. Warren, 1983. Revised Volcanic Stratigraphy of Drill Hole J-13, Fortymile Wash, Nevada, Based on Petrographic Modes and Chemistry of Phenocrysts, LA-9652-MS, Los Alamos National Laboratory, Los

Campbell, K. W., 1980. Seismic Hazard Analysis for the NTS Spent Reactor Fuel Test Site, UCRL-15260, report prepared by TERA Corporation for Lawrence Livermore National Laboratory, Livermore, Calif.

Campbell, K. W., 1981. "Near-Source Attenuation of Peak Horizontal Acceleration," Bulletin of the Seismological Society of America, Vol. 71, No. 6, pp. 2039-2070.

Caporuscio, F. A., D. Vaniman, D. Bish, D. Broxton, D. Arney, G. Heiken, F. Byers, R. Gooley, and E. Semarge, 1982. Petrologic Studies of Drill Cores USW-G2 and UE25b-1H, Yucca Mountain, Nevada, LA-9255-MS, Los Alamos National Laboratory, Los Alamos, N. Mex.

Carder, D. S., 1945. "Seismic Investigations in the Boulder Dam Area, 1940-1944, and the Influence of Reservoir Loading on Earthquake Activity", Bulletin of the Seismological Society of America, Vol. 35, pp. 175-192.

Carlos, B. A., 1985. Minerals in Fractures of the Unsaturated Zone from Drill Core USW G-4, Yucca Mountain, Nye County, Nevada, LA-10415-MS, Los Alamos National Laboratory, Los Alamos, N. Mex.

Carpenter, D. W., and D. H. Chung, 1985. Effects of Earthquakes on Underground Facilities: Literature Review and Discussion, UCID-20505, Lawrence Livermore National Laboratory, Livermore, Calif.

Carr, M. D., S. J. Waddell, G. S. Vick, J. M. Stock, S. A. Monsen, A. G. Harris, B. W. Cork, and F. M. Byers, Jr., 1986. Geology of Drill Hole UE25p#1: A Test Hole into Pre-Tertiary Rocks near Yucca Mountain, Southern Nevada, USGS-OFR-86-175, Open-File Report, U.S. Geological Survey.

Carr, W. J., 1974. Summary of Tectonic and Structural Evidence for Stress Orientation at the Nevada Test Site, USGS-OFR-74-176, Open-File Report, U.S. Geological Survey.

Carr, W. J., 1982. Volcano-Tectonic History of Crater Flat, Southwestern Nevada, as Suggested by New Evidence from Drill Hole USW-VH-1 and Vicinity, USGS-OFR-82-457, Open-File Report, U.S. Geological Survey.

Carr, W. J., 1984. Regional Structural Setting of Yucca Mountain, Southwestern Nevada, and Late Cenozoic Rates of Tectonic Activity in Part of the Southwestern Basin, Nevada and California, USGS-OFR-84-854, Open-File Report, U.S. Geological Survey.

Carr, W. J., and L. D. Parrish, 1985. Geology of Drill Hole USW VH-2, and Structure of Crater Flat, Southwestern Nevada, USGS-OFR-85-475, Open-File Report, U.S. Geological Survey, 41 p.

Carr, W. J., F. M. Byers, Jr., and P. P. Orkild, 1984. Stratigraphic and Volcano-Tectonic Relations of Crater Flat Tuff and Some Older Volcanic Units, Nye County, Nevada, USGS-OFR-84-114, Open-File Report, U.S. Geological Survey.

DECEMBER 1988

Carr, W. J., F. M. Byers, Jr., and P. P. Orkild, 1986. Stratigraphic and Volcano-Tectonic Relations of Crater Flat Tuff and Some Older Volcanic

Compton, R. R., V. R. Todd, R. E. Zartman, and C. W. Naeser, 1977. "Oligocene and Miocene Metamorphism, Folding, and Low-Angle Faulting in Northwestern Utah," Geological Society of America Bulletin, Vol. 88, No. 9, pp. 1237-1250.

Coney, P. J., 1972. "Cordilleran Tectonics and North American Plate Motion," American Journal of Science, Vol. 272, No. 7, pp. 603-628.

Coney, P. J., 1978. "Mesozoic-Cenozoic Cordilleran Plate Tectonics," Cenozoic Tectonics and Regional Geophysics of the Western Cordillera, R. B. Smith and G. P. Eaton (eds.), Geological Society of America Memoir 152, pp. 33-50.

Cook, D. R., 1986. "Analysis of Significant Mineral Discoveries in the Last 40 Years and Future Trends," Mining Engineering, Vol. 38, No. 2, pp. 87-94.

Cornwall, H. R., 1972. Geology and Mineral Deposits of Southern Nye County, Nevada, Nevada Bureau of Mines & Geology Bulletin 77, University of Nevada, Reno.

Cornwall, H. R., and F. J. Kleinhampl, 1961. "Geology of the Bare Mountain Quadrangle, Nevada," U.S. Geological Survey Quadrangle Map GQ-157, Scale 1:62,500, U.S. Geological Survey.

Cornwall, H. R., and F. J. Kleinhampl, 1964. Geology of the Bullfrog Quadrangle and Ore Deposits Related to the Bullfrog Hills Caldera, Nye County, Nevada and Inyo County, California, Geological Survey Professional Paper 454-J, U.S. Government Printing Office, Washington, D.C.

Craig, H., 1963. "The Isotopic Geochemistry of Water and Carbon in Geothermal Areas," Nuclear Geology on Geothermal Areas--Spoleto 1963, E. Tongiorgi (ed.), Consiglio Nazionale Delle Ricerche, Laboratorio di Geologia Nucleare, Pisa, pp. 17-53.

Craig, R. W., and K. A. Johnson, 1984. Geohydrologic Data for Test Well UE-25p#1, Yucca Mountain Area, Nye County, Nevada, USGS-OFR-84-450, Open-File Report, U.S. Geological Survey.

Craig, R. W., and J. H. Robison, 1984. Geohydrology of Rocks Penetrated by Test Well UE-25p#1, Yucca Mountain Area, Nye County, Nevada, USGS-WRI-84-4248, Water-Resources Investigations Report, U.S. Geological Survey.

Craig, R. W., R. L. Reed, and R. W. Spengler, 1983. Geohydrologic Data for Test Well USW H-6, Yucca Mountain Area, Nye County, Nevada, USGS-OFR-83-856, Open-File Report, U.S. Geological Survey, 35 p.

Crone, A. J., 1983. "Amount of Displacement and Estimated Age of a Holocene Surface Faulting Event, Eastern Great Basin, Millard County, Utah," Geologic Excursions in Neotectonics and Engineering Geology in Utah, K. D. Gurgel (ed.), Utah Geological & Mineralogical Survey Special Studies 62, pp. 49-55.

Cross, T. A., and R. H. Pilger, Jr., 1978. "Constraints on Absolute Motion and Plate Interaction Inferred from Cenozoic Igneous Activity in the Western United States," American Journal of Science, Vol. 278, No. 7, pp. 865-902.

Crowder, D. F., E. H. McKee, D. C. Ross, and K. B. Krauskopf, 1973. "Granitic Rocks of the White Mountain Area, California-Nevada--Age and Regional Significance," Geological Society of America Bulletin, Vol. 84, pp. 285-296.

Crowe, B. M., 1978. "Cenozoic Volcanic Geology and Probable Age of Inception of Basin-Range Faulting in the Southeasternmost Chocolate Mountains, California," Geological Society of America Bulletin, Vol. 89, pp. 251-264.

Crowe, B. M., 1980. Disruptive Event Analysis: Volcanism and Igneous Intrusion, PNL-2882, Pacific Northwest Laboratories, Richland, Wash., 28 p.

Crowe, B. M., and W. J. Carr, 1980. Preliminary Assessment of the Risk of Volcanism at a Proposed Nuclear Waste Repository in the Southern Great Basin, USGS-OFR-80-357, Open-File Report, U.S. Geological Survey.

Crowe, B. M., and K. A. Sargent, 1979. Major-Element Geochemistry of the Silent Canyon-Black Mountain Peralkaline Volcanic Centers, Northwestern Nevada Test Site: Applications to an Assessment of Renewed Volcanism, USGS-OFR-79-926, Open-File Report, U.S. Geological Survey.

Crowe, B. M., and D. T. Vaniman, (comps.), 1985. Research and Development Related to the Nevada Nuclear Waste Storage Investigations, January 1 - March 31, 1984, LA-10154-PR, Los Alamos National Laboratory, Los Alamos, N. Mex.

Crowe, B. M., M. E. Johnson, and R. J. Beckman, 1982. "Calculation of the Probability of Volcanic Disruption of a High-Level Radioactive Waste Repository within Southern Nevada, USA," Radioactive Waste Management and the Nuclear Fuel Cycle, Vol. 3, No. 2, pp. 167-190.

Crowe, B. M., S. Self, D. Vaniman, R. Amos, and F. Perry, 1983a. "Aspects of Potential Magmatic Disruption of a High-Level Radioactive Waste Repository in Southern Nevada," Journal of Geology, Vol. 91, pp. 259-276.

Crowe, B. M., D. T. Vaniman, and W. J. Carr, 1983b. Status of Volcanic Hazard Studies for the Nevada Nuclear Waste Storage Investigations, LA-9325-MS, Los Alamos National Laboratory, Los Alamos, N. Mex.

Crowe, B. M., K. H. Wohletz, D. T. Vaniman, E. Gladney, and N. Bower, 1986. Status of Volcanic Hazard Studies for the Nevada Nuclear Waste Storage Investigations, LA-9325-MS, Vol. II, Los Alamos National Laboratory, Los Alamos, N. Mex.

Crowe, B. M., F. V. Perry, B. D. Turrin, S. G. Wells, and L. D. MacFadden, 1988. "Volcanic Hazard Assessment for Storage of High-Level Radioactive Waste at Yucca Mountain, Nevada," Geological Society of America, Cordilleran Section, Vol. 20, No. 3, p. 153.

Crowell, J. C., 1973. "Problems Concerning the San Andreas Fault System in Southern California," Stanford University Publications in Geological Sciences, Vol. 13, pp. 125-135.

Crowell, J. C., 1975. The San Andreas Fault in Southern California, J. C. Crowell (ed.), California Division of Mines & Geology Special Report 118, pp. 7-27.

Cunningham, C. G., K. R. Ludwig, C. W. Naeser, E. K. Weiland, H. H. Mehnert, T. A. Steven, and J. D. Rasmussen, 1982. "Geochronology of Hydrothermal Uranium Deposits and Associated Igneous Rocks in the Eastern Source Area of the Mount Belknap Volcanics, Marysvale, Utah," Economic Geology, Vol. 77, pp. 453-463.

DOE (U.S. Department of Energy), 1986. Final Environmental Assessment: Yucca

DOE/NVO (U.S. Department of Energy/Nevada Operations Office), 1984. Report of the Investigation of the Accident at the Midas Myth/Milagro Trailer Park on Rainier Mesa at Nevada Test Site on February 15, 1984, NVO-280, Nevada Operations Office, Las Vegas, Nev.

DOE/NVO (U.S. Department of Energy/Nevada Operations Office), 1987. Announced

Dickey, D. D., W. J. Carr, and W. B. Bull, 1980. "Geologic Map of the Parker NW, Parker, and Parts of the Whipple Mountains SW and Whipple Wash Quadrangles, California and Arizona," U.S. Geological Survey Miscellaneous Investigations Series Map I-1124, Scale 1:24,000, U.S. Geological Survey.

Dickinson, W. R., 1970. "Relations of Andesites, Granites, and Derivative Sandstones to Arc-Trench Tectonics," Reviews of Geophysics and Space Physics, Vol. 8, No. 4, pp. 813-860.

Dickinson, W. R., 1977. "Paleozoic Plate Tectonics and the Evolution of the Cordilleran Continental Margin," Paleozoic Paleogeography of the Western United States, C. H. Stewart and A. Fritsche (eds.), Society of Economic Paleontologists & Mineralogists, Pacific Coast Paleogeography Symposium 1, pp. 137-155.

Dickinson, W. R., and W. S. Snyder, 1979. "Geometry of Triple Junctions Related to the San Andreas Transform," Journal of Geophysical Research, Vol. 84, No. B2, pp. 561-572.

Diment, W. H., T. C. Urban, J. H. Sass, B. V. Marshall, R. J. Munroe, and A. H. Lachenbruch, 1975. "Temperatures and Heat Contents Based on Conductive Transport of Heat," Assessment of Geothermal Resources of the United States--1975, D. E. White and D. L. Williams (eds.), Geological Survey Circular 726, U.S. Geological Survey, pp. 84-103.

Dixon, J. S., 1982. "Regional Structure Synthesis, Wyoming Salient of Western Overthrust Belt," American Association of Petroleum Geologists Bulletin, Vol. 66, No. 10, pp. 1560-1580.

Dohrenwend, J. C., 1982. Surficial Geology, Walker Lake 1 deg. by 2 deg. Quadrangle, Nevada-California, U.S. Geological Survey Miscellaneous Field Studies Map MF-1382-C, Scale 1:250,000, U.S. Geological Survey.

Dohrenwend, J. C., 1984. "Nivation Landforms in the Western Great Basin and Their Paleoclimatic Significance," Quaternary Research, Vol. 22, pp. 275-288.

Dohrenwend, J. C., 1985. "Patterns and Processes of Middle and Late Quaternary Dissection in the Tecopa Basin, California," Quaternary Lakes of the Eastern Mojave Desert, California, G. R. Hale (ed.), Friends of the Pleistocene, Pacific Cell 1985 Annual Meeting Guidebook, pp. 113-144.

Dohrenwend, J. C., 1987. Morphometric Comparison of Tectonically Defined Areas within the West-Central Basin and Range, USGS-OFR-87-83, Open-File Report, U.S. Geological Survey.

Dohrenwend, J. C., 1987. "Basin and Range," Geomorphic Systems of North America W. L. Graf (ed.), The Geological Society of America, Boulder, Colo. p. 331.

Dohrenwend, J. C., S. G. Wells, B. D. Turrin, and L. D. McFadden, 1984. "Rates and Trends of Late Cenozoic Landscape Degradation in the Area of the Cima Volcanic Field, Mojave Desert, California," Surficial Geology of the Eastern Mojave Desert, California, J. D. Dohrenwend (ed.), Geological Society of America 97th Annual Meeting Guidebook, pp. 101-115.

Dohrenwend, J. C., B. D. Turrin, and M. F. Diggles, 1985. "Topographic Distribution of Dated Basaltic Lava Flows in the Reveille Range, Nye County, Nevada: Implications for Late Cenozoic Erosion of Upland Areas in the Great Basin (abs.)," Geological Society of America, Abstracts with Programs, Vol. 17, p. 351.

Doser, D. I., 1985a. "The 1983 Borah Peak, Idaho and 1959 Hebgan Lake, Montana Earthquakes: Models for Normal Fault Earthquakes in the Intermountain Seismic Belt," in Proceedings of Workshop XXVIII On Borah Peak, Idaho, Earthquake, Volume A, National Earthquake Prediction and Hazards Programs, October 3-6, 1984, R. S. Stein and R. C. Bucknam (eds.), USGS-OFR-85-290-A, Open-File Report, U.S. Geological Survey, pp. 368-384.

Doser, D. I., 1985b. "Source Parameters and Faulting Processes of the 1959 Hebgen Lake, Montana, Earthquake Sequence," Journal of Geophysical Research, Vol. 90, No. B6, pp. 4537-4555.

Doser, D. I., 1986. "Earthquake Processes in the Rainbow Mountain-Fairview Peak-Dixie Valley, Nevada, Region 1954-1959," Journal of Geophysical Research, Vol. 91, No. B12, pp. 11,572-12,586.

Doser, D. I., 1987. "Source Parameters of the December 20, 1932 Cedar Mountain, Nevada , Earthquake," Seismological Research Letters, Vol. 58, No. 1, p. 19.

Douglas, A. C., and M. R. Millett, 1978. Total Intensity Magnetometer Logging as a Stratigraphic Tool in Tertiary Volcanic Rock, UCRL-52617, Lawrence Livermore National Laboratory, Livermore, Calif.

Dresser Atlas, 1982. Well Logging and Interpretation Techniques, The Course for Home Study, Second Edition, Dresser Industries, Houston, Tex.

Dudley, W. W., Jr., 1985. Letter from W. W. Dudley Jr. (USGS) to D. L. Vieth (WMPO), October 31, 1985; regarding status of on-going neotectonic studies.

Duffield, W. A., C. R. Bacon, and G. B. Dalrymple, 1980. "Late Cenozoic Volcanism, Geochronology, and Structure of the Coso Range, Inyo County, California," Journal of Geophysical Research, Vol. 85, No. B5, pp. 2381-2404.

ERDA (U.S. Energy Research and Development Administration), 1977. Nevada Test Site, Nye County, Nevada, Final Environmental Impact Statement, ERDA-1551, Washington, D.C.

Eaton, G. P., 1979. "A Plate-Tectonic Model For Late Cenozoic Crustal Spreading in the Western United States," Rio Grande Rift: Tectonics and Magmatism, R. E. Riecker (ed.), American Geophysical Union, Washington, D.C., pp. 7-32.

Eaton, G. P., 1982. "The Basin and Range Province: Origin and Tectonic Significance," Annual Review of Earth and Planetary Science, Vol. 10, pp. 409-440.

Eckel, E. B. (ed.), 1968. Nevada Test Site, Geological Society of America Memoir 110, The Geological Society of America, Inc., Boulder, Colo.

Ekren, E. B., 1968. "Geologic Setting of Nevada Test Site and Nellis Air Force Range," Nevada Test Site, E. B. Eckel (ed.), Geological Society of America Memoir 110, pp. 11-19.

Ekren, E. B., and F. M. Byers, Jr., 1986. "Geologic Map of the Murphys Well, Pilot Cone, Copper Mountain, and Poinsettia Spring Quadrangles, Mineral County, Nevada," U.S. Geological Survey Miscellaneous Invetigations Series Map I-1576, Scale 1:48,000, U.G. Geological Survey.

Ekren, E. B., and K. A. Sargent, 1965. Geologic Map of the Skull Mountain Quadrangle, Nye County, Nevada, Geologic Quadrangle Map GQ-387, U.S. Geological Survey.

Ekren, E. B., C. L. Rogers, R. E. Anderson, and P. P. Orkild, 1968. "Age of Basin and Range Normal Faults in Nevada Test Site and Nellis Air Force Range, Nevada," Nevada Test Site, E. B. Eckel (ed.), Geological Society of America Memoir 110, pp. 247-250.

Ekren, E. B., R. E. Anderson, C. L. Rogers, and D. C. Noble, 1971. Geology of Northern Nellis Air Force Base Bombing and Gunnery Range, Nye County, Nevada, Professional Paper 651, U.S. Geological Survey.

Ekren, E. B., E. N. Hinrichs, W. D. Quinlivan, and D. L. Hoover, 1973. Geologic Map of the Moores Station Quadrangle, Nye County, Nevada, U.S. Geological Survey Miscellaneous Investigations Series Map I-756, U.S. Geological Survey.

Ekren, E. B., G. D. Bath, G. L. Dixon, D. L. Healey, and W. D. Quinlivan, 1974a. "Tertiary History of Little Fish Lake Valley, Nye County, Nevada, and Implications as to the Origin of the Great Basin," U.S. Geological Survey Journal of Research, Vol. 2, No. 1, pp. 105-118.

Ekren, E. B., W. D. Quinlivan, R. P. Snyder, and F. J. Kleinhampl, 1974b. "Stratigraphy, Structure, and Geologic History of the Lunar Lake Caldera of Northern Nye County, Nevada," U.S. Geological Survey Journal of Research, Vol. 2, No. 5, pp. 599-608.

Ekren, E. B., P. P. Orkild, K. A. Sargent, and G. L. Dixon, 1977. Geologic Map of Tertiary Rocks, Lincoln County, Nevada, Miscellaneous Investigations Series Map I-1041, Scale 1:14,000, U.S. Geological Survey.

Ellis, W. L., and J. E. Magner, 1980. Compilation of Results of Three-Dimensional Stress Determinations Made in Rainier and Aqueduct Mesas, Nevada Test Site, Nevada, USGS-OFR-80-1098, Open-File Report, U.S. Geological Survey.

Ellis, W. L., and J. E. Magner, 1982. Determination of the In Situ State of Stress at the Spent Fuel Test--Climax Site, Climax Stock, Nevada Test Site, USGS-OFR-82-458, Open-File Report, U.S. Geological Survey.

Ellis, W. L., and H. S. Swolfs, 1983. Preliminary Assessment of In Situ Geomechanical Characteristics in Drill Hole USW G-1, Yucca Mountain, Nevada, USGS-OFR-83-401, Open-File Report, U.S. Geological Survey.

Engebretson, D. C., A. Cox, and R. G. Gordon, 1985. Relative Motions between Oceanic and Continental Plates in the Pacific Basin, Geological Society of America Special Paper 206, Geological Society of America, Boulder, Colo., 59 p.

Erickson, R. L., 1973. "Crustal Abundance of Elements, and Mineral Reserves and Resources," United States Mineral Resources, D. A. Probst and W. A. Pratt (eds.), Geological Survey Professional Paper 820, U.S. Government Printing Office, Washington, D.C., pp. 21-25.

Eyde, T. H., 1986. "Zeolites," Mining Engineering, Vol. 38, No. 5, pp. 369-370.

Eyde, T. H., 1987. "Zeolites," Mining Engineering, Vol. 39, No. 6, pp. 422-423.

F & S (Fenix & Scisson, Inc.), 1982. Procedure for the Surveillance of Logging Operations, Quality Assurance Procedure QAP-9.16, Las Vegas, Nev.

F & S (Fenix & Scisson, Inc.), 1986. NNWSI Hole Histories, DOE/NV/10322-9 thru 21 & 24. Mercury, Nev.

Fenneman, N. M., 1931. "Sierra Cascade Province," Physiography of Western United States, Chapter IX, McGraw-Hill Book Co., Inc., New York, pp. 396-441.

Ferguson, H. G., 1921. The Round Mountain District, Nevada, U.S. Geological Survey Bulletin 725-I, U.S. Government Printing Office, Washington, D.C., pp. 383-406.

Fiero, B., 1986. Geology of the Great Basin, University of Nevada Press, Reno, Nev., pp. 67-96.

Fischer, F. G., P. J. Papanek, and R. M. Hamilton, 1972. The Massachusetts Mountain Earthquake of 5 August 1971 and Its Aftershocks, Nevada Test Site, USGS-474-149, U.S. Geological Survey, 20 p.

Fisk, E. L., 1968. "Cordero Mine, Opalite Mining District," Ore Deposits of the United States, 1933-1967, J. D. Ridge (ed.), The American Institute of Mining, Metallurgical & Petroleum Engineers, Inc., New York, pp. 1573-1591.

Fleck, R. J., 1970. "Age and Possible Origin of the Las Vegas Valley Shear Zone, Clark and Nye Counties, Nevada," Abstracts with Programs of the Geological Society of America, Rocky Mountain Section, 23rd Annual Meeting, May 6-9, 1970, Rapid City South Dakota Vol. 2, No. 5, p. 333.

Flood, 1987.

Flood, T. P., and B. C. Schuraytz, 1986. "Evolution of a Magmatic System, Geochemistry and Mineralogy of Glassy Pumices from the Pah Canyon, Yucca Mountain, and Tiva Canyon Members of the Members of the Paintbrush Tuff, Southern Nevada," EOS, Vol. 67, No. 44, p. 1261.

Forester, R. M., 1985. "Limnocythere Bradburyi N. Sp.: A Modern Ostracode from Central Mexico and a Possible Quaternary Paleoclimatic Indicator," Journal of Paleontology, Vol. 59, No. 1, pp. 8-20.

Forester, R. M., 1985. Letter from R. M. Forester (USGS) to J. Downey (USGS), WR-85-1D, October 1985; regarding fossil samples from a Quaternary Spring deposit at Nevada Test Site.

Foster, N. H., E. L. Howard, F. F. Meissner, and H. K. Veal, 1979. "The Bruffey Oil and Gas Seeps, Pine Valley, Eureka County, Nevada," Basin and Range Symposium and Great Basin Field Conference, G. W. Newman and H. D. Goode (eds.), Rocky Mountain Association of Geologists and Utah Geological Association, Denver, Colo., pp. 531-540.

Fournier, R. O., and J. J. Rowe, 1966. "Estimation of Underground Temperatures from Silica Content of Water from Hot Springs and Wet-Stream Well," American Journal of Science, Vol. 264, pp. 685-697.

Fournier, R. O., and A. H. Truesdell, 1973. "An Empirical Na-K-Ca Geothermometer for Natural Waters," Geochimica et Cosmochimica Acta, Vol. 37, pp. 1255-1275.

Fournier, R. O., M. L. Sorey, R. H. Mariner and A. H. Truesdell, 1979. "Chemical and Isotopic Prediction of Aquifer Temperatures in the Geothermal System at Long Valley, California," Journal of Volcanology and Geothermal Research, Vol. 5, Elsevier Scientific Publishing Co., Amsterdam, pp. 17-34.

Fouty, S. C., 1984. Index to Published Geologic Maps in the Region Around the Potential Yucca Mountain Nuclear Waste Repository Site, Southern Nye County, Nevada, USGS-OFR-84-524, Open-File Report, U.S. Geological Survey.

Fox, K. F., Jr., R. J. Fleck, G. H. Garniss, and C. E. Meyer, 1985. "Implications of the Northwestwardly Younger Age of the Volcanic Rocks of West-Central California," Geological Society of America Bulletin, Vol. 96, pp. 647-654.

French, D. E., 1983. "Origin of Oil in Railroad Valley, Nye County, Nevada," Earth Science Bulletin, Vol. 16, Wyoming Geological Association, pp. 9-21.

Friedman, S. A., R. W. Jones, and M. L. W. Jackson, 1985. "Developments in Coal in 1984," The American Association Petroleum Geologists Bulletin, Vol. 69, No. 10, pp. 1898-1902.

Fritz, F., 1987. "Good Fortune Found in Nevada," AAPG Explorer, January, American Association of Petroleum Geologists, Tulsa, Okla., pp. 14-15.

Gabelman, J. W., 1981. "Microscopic Distribution of Thorium and Uranium in Volcanic Rock Textures," Uranium in Volcanic and Volcanoclastic Rocks, P. C. Goodell, and A. C. Waters (eds.), Vol. 13, American Association of Petroleum Geologists Studies in Geology, pp. 23-36.

Gans, P. B., E. L. Miller, J. McCarthy, and M. L. Ouldcott, 1985. "Tertiary Extensional Faulting and Evolving Ductile-Brittle Transition Zones in the Northern Snake Range and Vicinity: New Insights from Seismic Data," Geology, Vol. 13, pp. 189-193.

Garside, L. J., 1973. Radioactive Mineral Occurrences in Nevada, Nevada Bureau of Mines & Geology Bulletin 81, University of Nevada, Reno, 121 p.

Garside, L. J., 1974. Geothermal Exploration and Development in Nevada Through 1973, Nevada Bureau of Mines & Geology Report 21, University of Nevada, Reno.

Garside, L. J., 1983a. Nevada Oil Shale, Nevada Bureau of Mining & Geology [illegible]

Garside, L. J., 1983b. "Geothermal Energy," The Nevada Mineral Industry - 1983, Nevada Bureau of Mines & Geology Special Publication MI-1983, University of Nevada, Reno, pp. 23-25.

Garside, L. J., 1987. "Geothermal Energy," The Nevada Mineral Industry 1986, Nevada Bureau of Mines & Geology Special Publication MI-1986, University of Nevada, Reno, pp. 21-24.

Garside, L. J., and J. H. Schilling, 1979. Thermal Waters of Nevada, Nevada Bureau of Mines & Geology Bulletin 91, University of Nevada, Reno.

Garside, L. J., and Weimer, B. S., 1986. "Oil and Gas," The Nevada Mineral Industry, 1985, Nevada Bureau of Mines & Geology Special Publication MI-1985, University of Nevada, Reno, pp. 19-24.

Garside, L. J., and B. S. Weimer, 1987. "Oil and Gas," Nevada Mineral Industry 1986, Nevada Bureau of Mines & Geology Special Publication MI-1986, University of Nevada, Reno, pp. 25-30.

Garside, L. J., B. S. Weimer, and I. A. Lutsey, 1977. Oil and Gas [illegible]

Glanzman, V. M., 1981. Bibliography of Reports by U.S. Geological Survey Personnel Pertaining to Underground Nuclear Testing and Radioactive Waste Disposal at the Nevada Test Site, and Radioactive Waste Disposal at the Waste Isolation Pilot Plant Site, New Mexico, January 1, 1980, to December 31, 1980, USGS-OFR-81-892, Open-File Report, U.S. Geological Survey.

Glanzman, V. M., 1983. Bibliography of Reports by U.S. Geological Survey Personnel on Studies of Underground Nuclear Test Sites and on Waste Management Studies at the Nevada Test Site and the Waste Isolation Pilot Plant Site, New Mexico, January 1 to December 31, 1981, USGS-OFR-83-478, Open-File Report, U.S. Geological Survey.

Glanzman, V. M., 1984. Bibliography of Reports by U.S. Geological Survey Personnel on Studies of Underground Nuclear Test Sites and on Waste Management Studies at the Nevada Test Site and the Waste Isolation Pilot Plant Site, New Mexico, January 1 to December 31, 1982, USGS-OFR-84-23, Open-File Report, U.S. Geological Survey.

Glanzman, V. M., 1985. Bibliography of Reports by U.S. Geological Survey Personnel on Studies of Underground Nuclear Test Sites and on Waste Management Studies at the Nevada Test Site and the Waste Isolation Pilot Plant Site, New Mexico, January 1, 1983, to December 31, 1984, USGS-OFR-85-363, Open-File Report, U.S. Geological Survey.

Grant, T. A., 1986. Memo from T. A. Grant (SAIC) to J. L. Younker (SAIC), M86-RTB-TAG-015, November 11, 1986; regarding trip report on field trip to Yucca Mountain.

Greensfelder, R. W., F. C. Kintzer, and M. R. Somerville, 1980. "Seismotectonic Regionalization of the Great Basin and Comparison of Moment Rates Computed from Holocene Strain and Historic Seismicity," Geological Society of America Bulletin Part II, Vol. 91, pp. 2039-2111.

Grogan, R. M., and G. Montgomery, 1975. "Fluorspar and Cryolite," Industrial

Hagstrum, J. T., J. J. Daniels, and J. H. Scott, 1980a. Analysis of the Magnetic Susceptibility Well Log in Drill Hole UE25a-5, Yucca Mountain, Nevada Test Site, USGS-OFR-80-1263, Open-File Report, U.S. Geological Survey.

Hagstrum, J. T., J. J. Daniels, and J. H. Scott, 1980b. Interpretation of Geophysical Well Log Measurements in Drill Hole UE25a-1, Nevada Test Site, USGS-OFR-80-941, Open-File Report, Radioactive Waste Program, U.S. Geological Survey.

Hamilton, R. M., and J. H. Healy, 1969. "Aftershocks of the Benham Nuclear Explosion," Bulletin of the Seismological Society of America, Vol. 59, No. 6, pp. 2271-2281.

Hamilton, R. M., B. E. Smith, F. G. Fisher, and P. J. Papanek, 1971. Seismicity of the Pahute Mesa Area, Nevada Test Site, 8 December 1968 through 31 December 1970, USGS-474-138, U.S. Geological Survey.

Hamilton, R. M., B. E. Smith, F. G. Fisher, and P. J. Papanek, 1972. "Earthquakes Caused by Underground Nuclear Explosions on Pahute Mesa, Nevada Test Site," Seismological Society of America Bulletin, Vol. 62, No. 5, pp. 1319-1341.

Hamilton, W., 1978. "Mesozoic Tectonics of the Western United States,"

Mesozoic Paleogeography of the Western United States, Pacific Coast Paleogeography Symposium 2, D. G. Howell and K. A. McDougall (eds.), Pacific Section, Society of Economic Paleontologists & Mineralogists, pp. 33-70.

Hamilton, W., 1982. "Structural Evolution of the Big Maria Mountains, Northeastern Riverside County, Southeastern California," Mesozoic-Cenozoic Tectonic Evolution of the Colorado River Region, California, Arizona, and Nevada, E. G. Frost and D. L. Martin (eds.), Cordilleran Publishers, San Diego, Calif., pp. 1-27.

Hamilton, W., 1987. Detachment Faulting in the Death Valley Region, California and Nevada, USGS-OFR, Open-File Report, U.S. Geological Survey.

Hamilton, W., and W. B. Myers, 1966. "Cenozoic Tectonics of the Western

Hardyman, 1984. "Strike-slip, Normal, and Detachment Faults in the Northern Gillis Range, Walker Lane of West-Central Nevada, Western Geological Excursions, J. Lintz, Jr. (ed.), Vol. 4, Geological Society of America Guidebook, Annual Meeting, Reno, Nev., pp. 184-199.

Hardyman, R. F. E. B. Ekren, and F. M. Byers, Jr., 1975. "Cenozoic Strike-Slip, Normal, and Detachment Faults in Northern Part of the Walker Lane, West-Central Nevada," Geological Society of America Abstracts with Programs, Vol. 7 p. 1100.

Harris, A. G., B. R. Warlow, C. C. Rust and G. K. Merrill, 1980. Maps for Assessing Thermal Maturity (Conodont Color Alteration Index Maps) in Ordovician Through Triassic Rocks in Nevada and Utah and Adjacent Parts of Idaho and California, Miscellaneous Investigations Series Map I-1249, U.S. Geological Survey.

Harris, D. P., and F. P. Agterberg, 1981. "The Appraisal of Mineral Resources," Economic Geology, B. J. Skinner (ed.), Seventy-Fifth Anniversary Volume, 1905-1980, The Economic Geology Publishing Co., New Haven, Conn., pp. 897-938.

Hay, R. L., 1978. "Geologic Occurrence of Zeolites," Natural Zeolites: Occurrence, Properties, Use, L. B. Sand and F. A. Mompton (eds.), Pergamon Press, New York, pp. 135-143.

Hay, R. L., and R. A. Sheppard, 1977. "Zeolites in Open Hydrologic Systems," Mineralogy and Geology of Natural Zeolites, F. A. Mumpton (ed.), Mineralogical Society of America Short Course Notes, Vol. 4, pp. 93-102.

Hay, R. L., R. E. Pexton, T. T. Teague, and T. K. Kyser, 1986. "Spring-Related Carbonate Rocks, Mg Clays, and Associated Minerals in

Site, December 13-22, 1981, USGS-OFR-84-15, Open-File Report, U.S. Geological Survey.

Hearst, J. R., and P. H. Nelson, 1985. Well Logging for Physical Properties, McGraw-Hill Book Co., New York, pp. 70, 94-102, 155, 191, 234, 251, 324, 339.

Henley, R. W., and A. J. Ellis, 1983. "Geothermal Systems Ancient and Modern: A Geochemical Review," Earth Science Reviews, Vol. 19, Elsevier Scientific Publishing Co., Amsterdam, pp. 1-50.

Horton, R. C., 1964a. "Fluorspar," Mineral and Water Resources of Nevada, Nevada Bureau of Mines & Geology Bulletin 65, University of Nevada, Reno, pp. 198-202.

Horton, R. C., 1964b. "Mineral Fuels - Coal," Mineral and Water Resources of Nevada, Nevada Bureau of Mines & Geology Bulletin 65, University of Nevada, Reno, pp. 49-53.

Horton, R. C., 1964c. "Mineral Fuels - Petroleum," Mineral and Water Resources of Nevada, Nevada Bureau Mines & Geology Bulletin 65, University of Nevada, Reno, pp. 54-57.

Horton, R. C., 1966. "Statistical Studies of the Distribution of Mining Districts in Nevada," papers presented at the AIME Pacific Southwest Mineral Industry Conference, Sparks, Nevada, May 5-7, 1965, Nevada Bureau of Mines Report 13, University of Nevada, Reno, pp. 109-123.

Hulen, J. B., and D. L. Nielson, 1988. "Hydrothermal Brecciation in the Jemez Fault Zone, Valles Caldera, New Mexico: Results From Continental Scientific Drilling Program Core Hole VC-1," Journal of Geophysical Research, Vol. 93, No. B6, pp. 6077-6089.

Hunt, C. B., 1974. Natural Regions of the United States and Canada, W. H. Freeman & Co., San Francisco, Calif.

Hunt, C. B., and D. R. Mabey, 1966. Stratigraphy and Structure, Death Valley, California, General Geology of Death Valley, California, U.S. Geological Survey Professional Paper 494-A, U.S. Goverment Printing Office, Washington, D.C.

Hunt, J. M., 1979. Petroleum Geochemistry and Geology, W. H. Freeman & Co., San Francisco, Calif.

Hutton, L. K., and D. M. Boore, 1985. "The ML Scale in Southern California," Earthquakes Notes, Seismological Society of America, Eastern Section 57th Meeting, Program and Abstracts, Knoxville, Tenn., October 16-19, 1985, Vol. 56, No. 3, p. 78.

Iwasaki, T., S. Wakabayashi, and F. Tatsuoka, 1977. "Characteristics of Underground Seismic Motions at Four Sites Around Tokyo Bay," Wind and Seismic Effects, H. S. Lew (ed.), U.S. Department of Commerce, Washington, D.C., pp. III-41 to III-56.

Izett, G. A., 1982. The Bishop Ash Bed and Some Older Compositionally Similar Ash Beds in California, Nevada, and Utah, USGS-OFR-82-582, Open-File Report, U.S. Geological Survey, 44 p.

Jefferson, G. T., 1985. "Stratigraphy and Geologic History of the Pleistocene Manix Formation, Central Mojave Desert, California," Geologic Investigations along Interstate 15, Cajon Pass to Manix Lake, California, San Bernardino County Museum, Redlands, Calif., pp. 157-170.

Jennings, C. W., 1977. Geologic Map of California, Geologic Data Map No. 2, California Geologic Data Map Series, Scale 1:750,000, California Division of Mines & Geology, Sacramento, Calif.

Johnson, J. L., and E. Abbott, 1987. A Symposium Bulk Mineable Precious Metal Deposits of the Western United States, April 6-8, 1987, Sparks, Nevada, Geological Society of Nevada, Reno.

Johnstone, J. K., R. R. Peters, and P. F. Gnirk, 1984. Unit Evaluation at Yucca Mountain, Nevada Test Site: Summary Report and Recommendation, SAND83-0372, Sandia National Laboratories, Albuquerque, N. Mex.

Jones, R. B., 1987. "Directory of Nevada Mine Operations Active During 1985 (Excluding Sand and Gravel) Active During 1985," Nevada Mineral Industry 1986, Nevada Bureau of Mines & Geology Special Publication MI-1986, University of Nevada, Reno, pp. 31-44.

Jones, R. B., and K. G. Papke, 1984. Active Mines and Oil Fields in Nevada--1983, Nevada Bureau of Mines & Geology Map 84, University of Nevada, Reno.

Joyner, W. B., and D. M. Boore, 1982. Prediction of Earthquake Response Spectra, USGS-OFR-82-977, Open-File Report, U.S. Geological Survey, 14 p.

Kanai, K., and T. Tanaka, 1951. "Observations of the Earthquake-motion at the Different Depths of the Earth," Bulletin of the Earthquake Research Institute, Vol. 29, pp. 107-113.

Kanai, K., K. Osada, and S. Yoshizawa, 1953. "Observational Study of Earthquake Motion in the Depth of the Ground, IV. (Relation between the Amplitude at Ground Surface and the Period)," Bulletin of the Earthquake Research Institute, Vol. 31, pp. 227-234.

Kanai, K., T. Tanaka, S. Yoshizawa, T. Morishita, K. Osada, T. Suzuki, 1966. "Comparative Studies of Earthquake Motions on the Ground and Underground, II.," Bulletin of the Earthquake Research Institute, Vol. 44, pp. 609-643.

Kane, M. F., and R. E. Bracken, 1983. Aeromagnetic Map of Yucca Mountain and Surrounding Regions, Southwest Nevada, USGS-OFR-83-616, Open-File Report, U.S. Geological Survey.

Keller, G. R., L. W. Braile, and P. Morgan, 1979. "Crustal Structure, Geophysical Models and Contemporary Tectonism of the Colorado Plateau," Tectonophysics, Vol. 61, Elsevier Scientific Publishing Co., Amsterdam. pp. 131-147.

Kerns, R., 1984. "Utah Tar Sands," Survey Notes, Vol. 17, No. 4, Utah Geological and Mineral Survey, pp. 4-9.

Kimball, J. K., and L. Reiter, 1985. "Current Estimates of Seismic Hazard in the Eastern United States," in Proceedings: EPRI/NRC Workshop on Nuclear Power Plant Reevaluation to Quality Seismic Margins, EPRI NP-4101-SR, Electric Power Research Institute, Palo Alto, Calif., pp. 1-1 to 1-15.

King, K. W., 1982. A Study of Surface and Subsurface Ground Motions at Calico Hills, Nevada Test Site, USGS-OFR-82-1044, Open-File Report, U.S. Geological Survey.

King, K. W., K. C. Bayer, and S. R. Brockman, 1971. Earthquakes on and around the Nevada Test Site, 1950-1971, CGS-746-12, U.S. Department of Commerce, NOAA Earth Sciences Laboratories, 32 p.

King, P. B., 1977. The Evolution of North America, revised edition, Princeton University Press, Princeton, New Jersey, pp. 136-137.

Kistler, R. W., and Z. E. Peterman, 1978. Reconstruction of Crustal Blocks of California on the Basis of Initial Strontium Isotopic Compositions of Mesozoic Granitic Rocks, Professional Paper 1071, U.S. Geological Survey, 17 p.

Kizis, J. A., Jr., and D. D. Runnells, 1984. "The Mobility of Uranium and Associated Trace Elements in the Bates Mountian Tuff, Central Nevada," Economic Geology, Vol. 79, pp. 558-564.

Kleinhampl, F. J., and J. I. Ziony, 1984. Mineral Reseources of Northern Nye County, Nevada, Nevada Bureau of Mines & Geology Bulletin 99B, University of Nevada, Reno.

Klemperer, S. L., T. A. Hauge, E. C. Hauser, J. E. Oliver, and C. J. Potter, 1986. "The Moho in the Northern Basin and Range Province, Nevada, along the COCORP 40 deg. N. Seismic-Reflection Transect," Geological Society of America Bulletin, Vol. 97, No. 5, pp. 603-618.

Knutson, C. F., and G. F. Dana, 1983. "Developments in Oil Shale in 1982," American Association of Petroleum Geologists Bulletin, Vol. 67, No. 10, pp. 2009-2030.

Kral, V. E., 1951. Mineral Resources of Nye County, Nevada, University of Nevada Bulletin, Geology and Mining Series No. 50, Vol. 45, No. 3, Nevada State Bureau of Mines and the Mackay School of Mines, Reno, Nev.

Kutina, J., 1969. "Hydrothermal Ore Deposits in the Western United States: A New Concept of Structural Control of Distribution," Science, Vol. 165, pp. 1113-1119.

Kuuskraa, V. A., and E. C. Hammershaimb, 1984. Major Tar Sand and Heavy Oil Deposits of the United States, Vol. XXV, No. 1, Interstate Oil Compact Commission, pp. 1-7.

Lachenbruch, A. H., 1970. "Crustal Temperature and Heat Production: Implications of the Linear Heat-Flow Relation," Journal of Geophysical Research, Vol. 75, No. 17, pp. 3291-3300.

Lachenbruch, A. H., and J. H. Sass, 1977. "Heat Flow in the United States and the Thermal Regime of the Crust," The Earth's Crust, Its Nature and Physical Properties, J. G. Heacock (ed.), American Geophysical Union Monograph 20, Washington, D.C., pp. 626-675.

LaCoste, L. J. B., and A. Romberg, 1942. Force Measuring Device, U.S. Patent 2,293,437. United States Patent Office, Washington, D.C.

Lahoud, R. G., D. H. Lobmeyer, and M. S. Whitfield, Jr., 1984. Geohydrology of Volcanic Tuff Penetrated by Test Well UE-25b#1, Yucca Mountain, Nye County, Nevada, USGS-WRI-84-4253, Water-Resources Investigations Report, U.S. Geological Survey.

Langenheim, R. L., Jr., and E. R. Larson, 1973. Correlation of Great Basin Stratigraphic Units, Nevada Bureau of Mines & Geology Bulletin 72, University of Nevada, Reno, 36 p.

Langkopf, B. S., and P. R. Gnirk, 1986. Rock-Mass Classification of Candidate Repository Units at Yucca Mountain, Nye County, Nevada, SAND82-2034, Sandia National Laboratories, Albuquerque, N. Mex.

Lanphere, M. A., and B. L. Reed, 1973. "Timing of Mesozoic and Cenozoic Plutonic Events in Circum Pacific North America," Geological Society of America Bulletin, Vol. 84, pp. 3773-3782.

Lappin, A. R., R. G. VanBuskirk, D. O. Enniss, S. W. Butters, F. M. Prater, C. B. Muller, and J. L. Bergosh, 1982. Thermal Conductivity, Bulk Properties, and Thermal Stratigraphy of Silicic Tuffs from the Upper Portion of Hole USW-G1, Yucca Mountain, Nye County, Nevada, SAND81-1873, Sandia National Laboratories, Albuquerque, N. Mex.

Lee, W. H. K., R. E. Bennett, and K. L. Meagher, 1972. A Method of Estimating Magnitude of Local Earthquakes from Signal Duration, Open-File Report, U.S. Geological Survey.

Levinson, A. A., 1974. Introduction to Exploration Geochemistry, 2nd edition, Applied Publishing Ltd., Wilmette, Ill., pp. 43-44.

Levy, S. S., 1984. Petrology of Samples from Drill Holes USW H-3, H-4 and H-5, Yucca Mountain, Nevada, LA-9706-MS, Los Alamos National Laboratory, Los Alamos, N. Mex.

Lincoln, F. C., 1923. Mining Districts and Mineral Resources of Nevada, reprinted in 1982, Nevada Publications, Reno.

Lindsey, D. A., 1978. Geology of the Yellow Chief Mine, Thomas Range, Juab County, Utah, D. R. Shawe (ed.), Nevada Bureau of Mines Report No. 32, U.S. Geological Survey, pp. 65-68.

Link, R. L., S. E. Logan, H. S. Ng, F. A. Rockenbach, and K. J. Hong, 1982. Parametric Studies of Radiological Consequences of Basaltic Volcanism, SAND81-2375, Sandia National Laboratories, Albuquerque, N. Mex., pp. 4-347.

Lipman, P. W., and R. L. Christiansen, 1964. "Zonal Features of an Ash-Flow Sheet in the Piapi Canyon Formation, Southern Nevada," Geological Survey Research 1964, Chapter B, Professional Paper 501, U.S. Geological Survey, pp. B74-B78.

Lipman, P. W., and E. J. McKay, 1965. "Geologic Map of the Topopah Spring SW Quadrangle, Nye County, Nevada," U.S. Geological Survey Quadrangle Map GQ-439, Scale 1:24,000, U.S. Geological Survey.

Lipman, P. W., and D. R. Mullineaux (eds.), 1981. The 1980 Eruptions of Mount St. Helens, Washington, Geological Survey Professional Paper 1250, U.S. Government Printing Office, Washington, D.C.

Lipman, P. W., R. L. Christiansen, and J. T. O'Connor, 1966. A Compositionally Zoned Ash-Flow Sheet in Southern Nevada, Geological Survey Professional Paper 525-F, U.S. Geological Survey.

Lipman, P. W., H. J. Prostka, and R. L. Christiansen, 1972. "Cenozoic Volcanism and Plate-Tectonic Evolution of the Western United States; I. Early and Middle Cenozoic," Philosophical Transactions Royal Society of London, Series A, Vol. 271, pp. 217-248.

Locke, A., P. Billingsley, and E. B. Mayo, 1940. "Sierra Nevada Tectonic Patterns," Bulletin of the Geological Society of America, Vol. 51, pp. 513-540.

Longwell, C. R., 1949. "Structure of the Northern Muddy Mountain Area, Nevada," Bulletin of the Geological Society of America, Vol. 60, pp. 923-968.

Longwell, C. R., 1960. "Possible Explanation of Diverse Structural Patterns in Southern Nevada," American Journal of Science, Bradley Volume, Vol. 258-A, pp. 192-203.

Longwell, C. R., E. H. Pampeyan, B. Bowyer, and R. J. Roberts, 1965. Geology and Mineral Deposits of Clark County, Nevada, Nevada Bureau of Mines Bulletin 62, University of Nevada, Reno.

Lubetkin, L., and M. M. Clark, 1985. "Late Quaternary Activity along the Lone Pine Fault, Eastern California," in Proceedings of Workshop XXVIII on the Borah Peak Idaho Earthquake, R. S. Stein and R. C. Bucknam (eds.), USGS-OFR-85-290-A, Open-File Report, Vol. A, U.S. Geological Survey, pp. 118-140.

Lucchitta, I., 1979. "Late Cenozoic Uplift of the Southwestern Colorado Plateau and Adjacent Lower Colorado River Region," Tectonophysics, Vol. 61, pp. 63-95.

Mahon, W. A. J., 1970. "Chemistry in the Exploration and Exploitation of Hydrothermal Systems," in Proceedings of the United Nations Symposium on the Development and Utilization of Geothermal Resources, Pisa, Italy, September 22-October, 1970, Geothermics, Special Issue 2, Vol. 2, Part 2, pp. 1310-1322.

Maldonado, F. (comp.), 1985a. Geologic Map of the Jackass Flats Area, Nye County, Nevada, Miscellaneous Investigations Series Map I-1519, U.S. Geological Survey.

Maldonado, F., 1985b. "Late Tertiary Detachment Faults in the Bullfrog Hills, Southwestern Nevada [abs.]," Geological Society of America, Abstracts with Programs, Vol. 17, No. 7, p. 651.

Maldonado, F., and S. L. Koether, 1983. Stratigraphy, Structure, and Some Petrographic Features of Tertiary Volcanic Rocks at the USW G-2 Drill Hole, Yucca Mountain, Nye County, Nevada, USGS-OFR-83-732, Open-File Report, U.S. Geological Survey.

Maldonado, F., D. C. Muller, and J. N. Morrison, 1979. Preliminary Geologic and Geophysical Data of the UE25a-3 Exploratory Drill Hole, Nevada Test Site, Nevada, USGS-1543-6, U.S. Geological Survey.

Marchand, D. E., 1971. "Rates and Modes of Denudation, White Mountains, Eastern California," American Journal of Science, Vol. 270, pp. 109-135.

Mariner, R. H., and L. M. Willey, 1976. "Geochemistry of Thermal Waters in Long Valley, Mono County, California," Journal of Geophysical Research, Vol. 81, No. 5, pp. 792-800.

Mariner, R. H., C. A. Brook, M. J. Reed, J. D. Bliss, A. L. Rapport, and R. J. Lieb, 1983. "Low-Temperature Geothermal Resources of the United States," Assessment of Low-Temperature Geothermal Resources of the United States-1982, M. J. Reed (ed.), Geological Survey Circular 892, U.S. Department of the Interior, pp. 31-40.

Mark, R. K., and M. G. Bonilla, 1977. Regression Analysis of Earthquake Magnitude and Surface Fault Length Using the 1970 Data of Bonilla and Buchanan, USGS-OFR-77-614, Open-File Report, U.S. Geological Survey.

Marvin, R. F., F. M. Byers, Jr., H. H. Mehnert, P. P. Orkild, and T. W. Stern, 1970. "Radiometric Ages and Stratigraphic Sequence of Volcanic and Plutonic Rocks, Southern Nye and Western Lincoln Counties, Nevada," Geological Society of America Bulletin, Vol. 81, No. 9, pp. 2657-2676.

Marvin, R. F., H. H. Mehnert, and E. H. McKee, 1973. "A Summary of Radiometric Ages of Tertiary Volcanic Rocks in Nevada and Eastern California, Part III - Southeastern Nevada," Isochron/West, Vol. No. 6, pp. 1-30.

Mattson, S. R., 1988. "Mineral Resource Evaluation: Implications of Human Intrusion and Interference on a High Level Nuclear Waste Repository," Waste Management Eighty Eight, Vol. 2, pp. 915-924.

McDaniel, S., 1985. "Small Methane Pockets Found in Nevada," Western Oil World, Vol. 42, No. 5, p. 15.

McDonald, R. E., 1976. "Tertiary Tectonics and Sedimentary Rocks along the Transition: Basin and Range Province to Plateau and Thrust Belt Province, Utah," Geology of the Cordilleran Hingeline, Rocky Mountain Association of Geologists - 1976 Symposium, J. G. Hill (ed.), Rocky Mountain Association of Geologists, Denver, Colo., pp. 281-317.

McFadden, L. D., S. G. Wells, and J. C. Dohrenwend, 1985. "The Influence of Eolian Flux Rates and Climatic Change on the Development of Stone Pavements and Associated Soils in the Cima Volcanic Field, Mojave Desert, California [abs.]," Geological Society of America, Abstracts and Programs, Vol. 17, 368 p.

McGovern, T. F., 1983. An Evaluation of Seismic Reflection Studies in the Yucca Mountain Area, Nevada Test Site, with an introduction by L. W. Pankratz and H. D. Ackermann, USGS-OFR-83-912, Open-File Report, U.S. Geological Survey.

McKay, E. J., and W. P. Williams, 1964. Geology of the Jackass Flats Quadrangle, Nye County, Nevada, Geological Quadrangle Map GQ-368, Scale 1:24,000, U.S. Geological Survey.

McKee, E. H., 1979. "Ash-Flow Sheets and Calderas: Their Genetic Relationship to Ore Deposits in Nevada," Geological Society of America Special Paper 180, pp. 205-211.

McKenzie, D., 1978. "Some Remarks on the Development of Sedimentary Basins," Earth and Planetary Science Letters, Vol. 40, pp. 25-32.

McKenzie, D. P., and W. J. Morgan, 1969. "Evolution of Triple Junctions," Nature, Vol. 224, pp. 125-133.

Meremonte, M. E., and A. M. Rogers, 1987. Historical Catalog of Southern Great Basin Earthquakes 1868-1978, USGS-OFR-87-80, Open-File Report, U.S. Geological Survey.

Mifflin, M. D., and M. M. Wheat, 1979. Pluvial Lakes and Estimated Pluvial Climates of Nevada, Nevada Bureau of Mines & Geology Bulletin 94, University of Nevada, Reno.

Miller, C. D., 1985. "Holocene Eruptions at the Inyo Volcanic Chain, California: Implications for Possible Eruptions in Long Valley Caldera," Geology, Vol. 13, No. 1, pp. 14-17.

Miller, E. L., P. B. Gans, and J. Garing, 1983. "The Snake Range

Muffler, L. J. P. (ed.), 1979. Assessment of Geothermal Resources of the United States--1978, Circular 790, U.S. Geological Survey, 163 p.

Muffler, L. J. P., and M. Guffanti, 1979. "Introduction," Assessment of Geothermal Resources of the United States--1978, L. J. P. Muffler (ed.), Geological Survey Circular 790, U.S. Geological Survey, pp. 1-7.

Mulhern, M. E., 1982. "Lacustrine, Fluvial, and Fan Sedimentation: A Record of Quaternary Climate Change and Tectonics," Zeitschrift fur Geomorphologie, Vol. 42, pp. 117-133.

Muller, D. C., and J. E. Kibler, 1983. Commercial Geophysical Well Logs from the USW G-1 Drill Hole, Nevada Test Site, Nevada, USGS-OFR-83-321,

Open-File Report, U.S. Geological Survey, 7 p.

Muller, D. C., and J. E. Kibler, 1984. Preliminary Analysis of Geophysical Logs from Drill Hole UE-25p#1, Yucca Mountain, Nye County, Nevada, USGS-OFR-84-649, Open-File Report, U.S. Geological Survey, 14 p.

Muller, D. C., and J. E. Kibler, 1985. Preliminary Analysis of Geophysical Logs from the WT Series of Drill Holes, Yucca Mountain, Nye County, Nevada, USGS-OFR-86-46, Open-File Report, U.S. Geological Survey.

Mumpton, F. A., 1975. "Commercial Utilization of Natural Zeolites," Industrial Minerals and Rocks, S. J. Lefond (ed.), 4th Edition, American Institute of Mining, Metallurgical & Petroleum Engineers, Inc., New York, pp. 1262-1274.

Mumpton, F. A., 1977a. "Natural Zeolites," Mineralogy and Geology of Natural Zeolites, Mineralogical Society of America Short Course Notes, Vol. 4, pp. 1-17.

Mumpton, F. A., 1977b. "Utilization of Natural Zeolites," Mineralogy and Geology of Natural Zeolites, Mineralogical Society of America Short Course Notes, Vol. 4, pp. 177-204.

Murphy, T. D., 1975. "Silica and Silicon," Industrial Minerals and Rocks, S. J. Lefond (ed.), 4th Edition, American Institute of Mining, Metallurgical & Petroleum Engineers, Inc., New York, pp. 1043-1060.

NRC (U.S. Nuclear Regulatory Commission), 1987. Standard Format and Content of Site Characterization Plans for High-Level-Waste Geological Repositories, Regulatory Guide 4.17, Washington, D.C.

Nathenson, M., and M. Guffanti, 1988. "Geothermal Gradients in the Conterminous United States," Journal of Geophysical Research, Vol. 93, No. B6, pp. 6437-6450.

Nelson, C. E., and D. L. Giles, 1985. "Hydrothermal Eruption Mechanisms and Hot Spring Gold Deposits," Economic Geology, Vol. 80, pp. 1633-1639.

Norris, A. E., F. M. Byers, Jr., and T. J. Merson, 1986. Fran Ridge Horizontal Coring Summary Report Hole UE-25h#1, Yucca Mountain Area, Nye County, Nevada, LA-10859-MS, Los Alamos National Laboratory, Los Alamos, N. Mex.

Nur, A., H. Ron, and O. Scott, 1986. "Fault Mechanics and the Kinematics of Block Rotations", EOS, Vol. 67, No. 16, p. 358.

Oakeshott, G. B., R. W. Greensfelder, and J. E. Kahle, 1972. "One Hundred Years Later," California Geology, Vol. 25, No. 3, California Division of Mines & Geology, pp. 55-61.

O'Conner, J. T., R. E. Anderson, and P. W. Lipman, 1966. Geologic Map of the Thirsty Canyon Quadrangle, Nye County, Nevada, Geological Survey Geological Quadrangle GQ-524, U.S. Geological Survey.

Odt, D. A., 1983. Geology and Geochemistry of the Sterling Gold Deposit, Nye County, Nevada, unpublished M.S. Thesis, University of Nevada, Reno, 100 p.

Okamoto, S., 1984. Introduction of Earthquake Engineering, Second Edition, University of Tokyo Press, pp. 11-14.

Okaya, D. A., and G. A. Thompson, 1985. "Geometry of Cenozoic Extensional Faulting: Dixie Valley, Nevada," Tectonics, Vol. 4, No. 1, pp. 107-125.

Oldow, J. S., 1978. "Triassic Pamlico Formation: An Allochthonous Sequence of Volcanogenic-Carbonate Rocks in West-Central Nevada," Mesozoic Paleogeography of Western United States, Pacific Coast Paleogeography Symposium 2, D. G. Howell and K. A. McDougall (ed.), Society of Economic Paleontologists & Mineralogists, pp. 223-235.

Olson, R. H., 1975. "Zeolites," Industrial Minerals and Rocks, S. J. Lefond (ed.), 4th Edition, American Institute of Mining, Metallurgical & Petroleum Engineers, Inc., New York, pp. 1235-1242.

O'Neil, J. R., 1984. Letter Report from J. R. O'Neil (USGS) to D. Vaniman (LANL), December 19, 1984; regarding stable isotope analyses of three samples from Yucca Mountain.

O'Neil, J. R., 1985. Letter Report from J. R. O'Neil (USGS) to S. Levy (LANL), April 29, 1985; regarding stable isotype analysis and oxygen isotype temperatures of samples.

Orkild, P. P., 1965. "Paintbrush Tuff and Timber Mountain Tuff of Nye County, Nevada," Changes in Stratigraphic Nomenclature by the U.S. Geological Survey 1964, G. V. Cohee and W. S. West (eds.), U.S. Geological Survey Bulletin 1224-A, U.S. Geological Survey, pp. A44-A51.

Orkild, P. P., and J. T. O'Connor, 1970. Geologic Map of the Topapah Spring Quadrangle, Nye County, Nevada, Geologic Quadrangle Map GQ-849, Scale 1:24,000, U.S. Geological Survey.

Osmond, J. C., 1962. "Stratigraphy of Devonian Sevy Dolomite in Utah and

[redacted]

Oversby, V. M., 1984a. Reaction of the Topopah Spring Tuff with J-13 Well Water at 90 deg. C and 150 deg. C, UCRL-53552, Lawrence Livermore National Laboratory, Livermore, Calif.

Oversby, V. M., 1984b. Reaction of the Topopah Spring Tuff with J-13 Well Water at 120 deg. C, UCRL-53574, Lawrence Livermore National Laboratory, Livermore, Calif.

Oversby, V. M., and K. G. Knauss, 1983. Reaction of Bullfrog Tuff with J-13 Well Water at 90 deg. C and 150 deg. C, UCRL-53442, Lawrence Livermore National Laboratory, Livermore, Calif.

Peterson, F. F., 1981. Landforms of the Basin and Range Province Defined for Soil Survey, Technical Bulletin 28, Nevada Agricultural Experiment Station, University of Nevada, Reno, 52 p.

Pexton, R. E., 1984. Geology and Paleohydrology of a Part of the Amargosa Desert, Nevada, unpublished Master's thesis, University of California, Berkeley.

Plut, F. W., 1979. "Geology of the Apex Uranium Mine Near Austin, Nevada," Basin and Range Symposium and Great Basin Field Conference, G. W. Newman and H. D. Goode (eds.), Rocky Mountain Association of Geologists and Utah Geological Association, pp. 413-420.

Poole, F. G., 1974. "Flysch Deposits of Antler Foreland Basin, Western United States," Tectonics and Sedimentation, W. R. Dickinson (ed.), Society of Economic Paleontologists & Mineralogists Special Publications No. 22, pp. 58-82.

Poole, F. G., and G. E. Claypool, 1984. "Petroleum Source-Rock Potential and Crude-Oil Correlation in the Great Basin," Hydrocarbon Source Rocks of the Greater Rocky Mountain Region, J. Woodward, F. F. Meissner, and J. L. Clayton (eds.), Rocky Mountain Association of Geologists, Denver, Colo., pp. 179-229.

Poole, F. G., D. L. Baars, H. Drewes, P. T. Hayes, K. B. Ketner, E. D. McKee, C. Teichert, and J. S. Williams, 1967. "Devonian of the Southwestern United States," International Symposium on the Devonian System, D. H. Oswald (ed.), Alberta Society of Petroleum Geologists, Calgary, Alberta, pp. 879-912.

Porter, S. C., and K. L. Pierce, and T. D. Hamilton, 1983. "Late-Wisconsin Mountain Glaciation in the Western United States," Late-Quaternary Environments of the United States, Volume I, The Late Pleistocene, S. C. Porter, Jr. (ed.), University of Minnesota Press, Minneapolis, pp. 71-114.

Pratt, H. R., W. A. Hustrulid, and D. E. Stephenson, 1978. Earthquake Damage to Underground Facilities, DP-1513, E. I. du Pont de Nemours & Co., Aiken, S.C.

Press, F., and R. Siever, 1982. Earth, Third Edition, W. H. Freeman & Co., San Francisco, Calif., p. 326.

Price, R. H., S. J. Spence, and A. K. Jones, 1984. Uniaxial Compression Test Series on Topopah Spring Tuff from USW GU-3, Yucca Mountain, Southern Nevada, SAND83-1646, Sandia National Laboratories, Albuquerque, N. Mex.

Priestley, K., 1974. "Crustal Strain Measurements in Nevada," Bulletin of the Seismological Society of America, Vol. 64, No. 4, pp. 1319-1328.

Proffett, Jr. J. M., 1977. "Cenozoic Geology of the Yerington District, Nevada, and Implications for the Nature and Origin of Basin and Range Faulting," Geological Society of America Bulletin, Vol. 88, No. 2, pp. 247-266.

Proffett, J. M., Jr., 1979. "Ore Deposits of the Western United States: A Summary," Papers on Mineral Deposits of Western North America, J. D. Ridge [redacted] Reno, pp. 13-32.

Quade, J., and J. V. Tingley, 1983. A Mineral Inventory of the Nevada Test Site, and Portions of Nellis Bombing and Gunnery Range, Southern Nye County, Nevada, DOE/NV/10295-1, U.S. Department of Energy, Nevada Operations Office, Las Vegas, Nev.

Raleigh, C. B., J. H. Healy, and J. D. Bredehoeft, 1972. "Faulting and Crustal Stress at Rangely, Colorado," Flow and Fracture of Rocks, H. C. Heard (ed.), Vol. 16, Geophysics Monograph Series, American Geophysical Union, Washington, D.C., pp. 275-284.

Ransome, F. L., 1907. Preliminary Account of Goldfield, Bullfrog, and Other Mining Districts in Southern Nevada, U.S. Geological Survey Bulletin 303, Reprinted as F. L. Ransome, 1983. "Mines of Goldfield, Bullfrog and Other Southern Nevada Districts," Nevada Publications, Reno.

Rautman, C. A., B. C. Whittet, and D. L. South, 1987. Definitions of Reference Boundaries for the Proposed Geologic Repository at the Yucca Mountain, Nevada, SAND86-2157, Sandia National Laboratories, Albuquerque, N. Mex.

Reheis, M., 1986. Preliminary Study of Quaternary Faulting on the East Side of Bare Mountain, Nye County, Nevada, USGS-OFR-86-576, Open-File Report, U.S. Geological Survey, 14 p.

Reiter, L., 1984. "Uses of Probabilistic Estimates of Seismic Hazard and Nuclear Power Plants in the U.S.," in Proceedings of the Second CSNI Specialist Meeting on Probabilistic Methods in Seismic Risk Assessment for Nuclear Power Plants, Livermore, California, May 16-18, 1983, CSNI Report No. 76, pp. 105-113.

Reiter, L., and R. E. Jackson, 1983. Seismic Hazard Review for the Systematic Evaluation Program--A Use of Probability in Decision Making, NUREG-0967, U.S. Nuclear Regulatory Commission, Washington, D.C.

Renner, J. L., D. E. White, and D. L. Williams, 1975. "Hydrothermal Convection Systems," Assessment of Geothermal Resources of the United States--1975, D. E. White and D. L. Williams (eds.), Geological Survey [redacted]

Reynolds, M. W., 1974b. "Recurrent Middle and Late Cenozoic Deformation, Northeastern Death Valley, California-Nevada," Geological Society of America Abstracts with Programs, Cordilleran Section, Vol. 6, No. 3, pp. 241-242.

Richins, W. D., R. B. Smith, C. J. Langer, J. E. Zollweg, J. J. King, and J. C. Pechman, 1985. "The 1983 Borah Peak, Idaho Earthquake: Relationship of Aftershocks to the Main Shock, Surface Faulting, and Regional Tectonics", in Proceedings of Workshop XXVIII on the Borah Peak, Idaho, Earthquake, Vol. A, R. S. Stein and R. C. Bucknam (eds.), USGS-OFR-85-290-A, Open-File Report, U.S. Geological Survey, pp. 285-310.

Richter, C. F., 1958. Elementary Seismology, W. H. Freeman & Co., San Francisco, Calif., 768 p.

Robbins, S. L., J. W. Schmoker, and T. C. Hester, 1982. Principal Facts and Density Estimates for Borehole Gravity Stations in Exploratory Wells Ue4ah, Ue7j, Uelh, Uelq, Ue2co, and USW-H1 at the Nevada Test Site, Nye County, Nevada, USGS-OFR-82-277, Open-File Report, U.S. Geological Survey.

Roberts, R. J., 1966. "Metallogenic Provinces and Mineral Belts in Nevada," papers presented at the AIME Pacific Southwest Mineral Industry

Rogers, A. M., S. C. Harmsen, and W. J. Carr, 1981. Southern Great Basin Seismological Data Report for 1980 and Preliminary Data Analysis, USGS-OFR-81-1086, Open-File Report, U.S. Geological Survey.

Rogers, A. M., S. C. Harmsen, W. J. Carr, and W. Spence, 1983. Southern Great Basin Seismological Data Report for 1981 and Preliminary Data Analysis, USGS-OFR-83-669, Open-File Report, U.S. Geological Survey.

Rogers, A. M., S. C. Harmsen, and M. E. Meremonte, 1987. Evaluation of the Seismicity of the Southern Great Basin and Its Relationship to the Tectonic Framework of the Region, USGS-OFR-87-408, Open-File Report, U.S. Geological Survey.

Romney, C., 1957. "Seismic Waves from the Dixie Valley-Fairview Peak Earthquakes," Bulletin of the Seismological Society of America Bulletin, Vol. 47, pp. 301-319.

Ron, H., R. Freund, and Z. Garfunkel, 1984. "Block Rotation by Strike-Slip Faulting: Structural and Paleomagnetic Evidence," Journal of Geophysical Research, Vol. 89, No. B7, pp. 6256-6270.

Ron, H., A. Aydin, and A. Nur, 1986. "The Role of Strike-Slip Faulting in the Deformation of Basin and Range Provinces", EOS, Vol. 67, No. 16, p. 358.

Roquemore, G. R., and J. T. Zellmer, 1986. "Neotectonic Development of the Coso Range, California [abs.]," Geological Society of America, Abstracts with Programs, Vol. 18, No. 2, p. 178.

Rosenbaum, J. G., and D. B. Snyder, 1985. Preliminary Interpretation of Paleomagnetic and Magnetic Property Data from Drill Holes USW G-1, G-2, GU-3, G-3, and VH-1 and Surface Localities in the Vicinity of Yucca Mountain, Nye County, Nevada, USGS-OFR-85-49, Open-File Report, U.S. Geological Survey.

Rosholt, J. N., Prijana, and D. C. Noble, 1971. "Mobility of Uranium and Thorium in Glassy and Crystallized Silicic Volcanic Rocks," Economic Geology, Vol. 66, pp. 1061-1069.

Rosholt, J. N., C. A. Bush, W. J. Carr, D. L. Hoover, W C Swadley, and J. R. Dooley, Jr., 1985. Uranium-Trend Dating of Quaternary Deposits in the Nevada Test Site Area, Nevada and California, USGS-OFR-85-540, Open-File Report, U.S. Geological Survey.

Ross, R. J., Jr., and C. R. Longwell, 1964. "Paleotectonic Significance of Ordovician Sections South of the Las Vegas Shear Zone," Middle and Lower Ordovician Formations in Southernmost Nevada and Adjacent California, R. J. Ross, Jr. (ed.), U.S. Geological Survey Bulletin 1180-C, pp. C88-C95.

Roy, R. F., D. D. Blackwell, and F. Birch, 1968. "Heat Generation of Plutonic Rocks and Continental Heat-Flow Provinces," Earth and Planetary Science Letters, Vol. 5, North-Holland Publishing Co., Amsterdam, pp. 1-12.

Roy, R. F., D. D. Blackwell, and E. R. Decker, 1972. "Continental Heat Flow," The Nature of the Solid Earth, E. C. Robertson (ed.), McGraw-Hill Book Co., New York, pp. 506-543.

Rush, F. E., W. Thordarson, and L. Bruckheimer, 1983. Geohydrologic and Drill-Hole Data for Test Well USW H-1, Adjacent to Nevada Test Site, Nye County, Nevada, USGS-OFR-83-141, Open-File Report, U.S. Geological Survey.

Rush, F. E., W. Thordarson, and D. G. Pyles, 1984. Geohydrology of Test Well USW H-1, Yucca Mountain, Nye County, Nevada, USGS-WRI-84-4032, Water-Resources Investigations Report, U.S. Geological Survey.

Ryall, A., and K. Priestly, 1975. "Seismicity, Secular Strain, and Maximum Magnitude in the Excelsior Mountains Area, Western Nevada and Eastern California," Geological Society of America Bulletin, Vol. 86, pp. 1585-1592.

Rytuba, J. J. and W. K. Conrad, 1981. "Petrochemical Characteristics of Volcanic Rocks Associated with Uranium Deposits in the McDermitt Caldera Complex," Uranium in Volcanic and Volcanoclastic Rocks, P. C. Goodell and A. C. Waters (eds.), Vol. 13, American Association of Petroleum Geologists Studies in Geology, pp. 63-72.

Rytuba, J. J., and E. H. McKee, 1984. "Peralkaline Ash Flow Tuffs and Calderas of the McDermitt Volcanic Field, Southeast Oregon and North Central Nevada," Journal of Geophysical Research, Vol. 89, No. B10, pp. 8616-8628.

Rytuba, J. J., R. K. Glanzman, and W. K. Conrad, 1979. "Uranium, Thorium and Mercury Distribution through the Evolution of the McDermitt Caldera Complex," Basin and Range Symposium and Great Basin Field Conference, G. W. Newman and H. D. Goode (eds.), Rocky Mountain Association of Geologists and Utah Geological Association, pp. 405-412.

SAIC (Science Application International Corporation), 1985. Tectonic Stability and Expected Ground Motion at Yucca Mountain, Report of a Workshop at SAIC - La Jolla August 7-8, 1984 and January 25-26, 1985, DOE/NV/10270-2 (Rev. 1), National Technical Information Service, U.S. Department of Commerce, Springfield, Va., pp. 3-5.

Sainsbury, C. L., and F. J. Kleinkampl, 1969. Fluorite Deposits of the Quinn Canyon Range, Nevada, Geological Survey Bulletin 1272-C, U.S. Government Printing Office, Washington, D.C.

Sammel, E. A., 1979. "Occurrence of Low-Temperature Geothermal Waters in the United States," Assessment of Geothermal Resources in the United States--1978, L. J. P. Muffler (ed.), Geological Survey Circular 790, U.S. Geological Survey, pp. 86-131.

Sandberg, C. A., 1983. "Petroleum Potential of Wilderness Lands in Nevada," Petroleum Potential of Wilderness Lands in the United States, U.S. Geological Survey Circular 902-H, U.S. Geological Survey, pp. H1-H11.

Sandberg, C. A., and R. C. Gutschick, 1984. "Distribution, Microfauna, and Source-Rock Potential of Mississippian Delle Phosphatic Member of Woodman Formation and Equivilents, Utah and Adjacent States," Hydrocarbon Source Rocks of the Greater Rocky Mountain Region, J. Woodward, F. F. Meissner, and J. L. Clayton (eds.), Rocky Mountain Association of Geologists, Denver, Colo., pp. 135-178.

Sander, M. V., and M. T. Einaudi, 1987. "The Round Mountain Gold-Silver Mine, Nye County, Nevada," Bulk Mineable Precious Metal Deposits of the Western

Nevada 1987 Symposium, Guidebook for Field Trips, Reno, Nev., pp. 130-135.

Sass, J. H., and A. H. Lachenbruch, 1982. Preliminary Interpretation of Thermal Data from the Nevada Test Site, USGS-OFR-82-973, Open-File Report, U.S. Geological Survey.

Sass, J. H., A. H. Lachenbruch, R. J. Munroe, G. W. Greene, and T. H. Moses, Jr., 1971. "Heat Flow in the Western United States," Journal of Geophysical Research, Vol. 76, No. 26, pp. 6376-6413.

Sass, J. H., W. H. Diment, A. H. Lachenbruch, B. V. Marshall, R. J. Monroe, T. H. Moses, Jr., and T. C. Urban, 1976. A New Heat-Flow Contour Map of the Conterminous United States, USGS-OFR-76-756, Open-File Report, U.S. Geological Survey.

Sass, J. H., A. H. Lachenbruch, and C. W. Mase, 1980. Analysis of Thermal Data from Drill Holes UE24a-3 and UE25a-1, Calico Hills and Yucca Mountain, Nevada Test Site, USGS-OFR-80-826, Open-File Report, U.S. Geological Survey.

Sass, J. H., D. D. Blackwell, D. S. Chapman, J. K. Costain, E. R. Decker, L. A. Lawver, and C. A. Swanberg, 1981. "Heat Flow from the Crust of the United States," Physical Properties of Rocks and Minerals, Y. S. Touloukin, W. R. Judd, and R. F. Roy (eds.), Vol. II, Chapter 13, McGraw-Hill, New York, pp. 503-540.

Sass, J., A. Lachenbruch, F. Grubb, and T. Moses, 1983. Status of Thermal Observations at Yucca Mountain, Nevada, USGS Letter Report, 10 p.

Savage, J. C., and M. Lisowski, 1984. "Deformation in the White Mountain Seismic Gap, California-Nevada, 1972-1982," Journal of Geophysical Research, Vol. 89, No. B9, pp. 7671-7687.

Savage, J. C., W. T. Kinoshita, and W. H. Prescott, 1974. "Geodetic

Schilling, J., 1987. "Minerals," The Nevada Mineral Industry 1986, Nevada Bureau of Mines & Geology Special Publication MI-1986, University of Nevada, Reno, pp. 3-14.

Schnabel, P. B., and H. B. Seed, 1973. "Accelerations in Rock for Earthquakes in the Western United States," Bulletin of the Seismological Society of America, Vol. 63, No. 2, pp. 501-516.

Schrader, E., 1977. "Relationships Between Uranium and Trace Metal Concentrations in Volcanic Rocks from Nevada," Economic Geology, Vol. 72, No. 1, pp. 104-107.

Schuraytz, B. C., T. A. Vogel, and L. W. Younker, 1986. Geochemical Gradients in the Topopah Spring Member of the Paintbrush Tuff: Evidence for Eruption across a Magmatic Interface, UCRL-53698, Lawrence Livermore National Laboratory, Livermore, Calif.

Schweig, E. S., III, 1986. "The Inception of Basin and Range Tectonics in the Region Between Death Valley and the Sierra Nevada, California [abs.]," Geological Society of America, Abstracts with Programs, Vol. 18, No. 2, pp. 181-182.

Scott, C., and A. K. Chamberlain, 1987. "Blackburn Field, Nevada: A Case History," Oil and Gas Journal, August 17, 1987, 4 p.

Scott, R. B., 1984. "Internal Deformation of Blocks Bounded by Basin-and-Range Style Faults," Geological Society of America, Abstracts with Programs, Vol. 16, No. 6, p. 649.

Scott, R. B., 1986. "Extensional Tectonics at Yucca Mountian, Southern Nevada," Geological Society of America, Abstracts with Programs, 1986, Rocky Mountain Section, Flagstaff, Ariz., April 30-May 2, 1986, Vol. 18, No. 5, p. 411.

Scott, R. B., and J. Bonk, 1984. Preliminary Geologic Map of Yucca Mountain, Nye County, Nevada, with Geologic Sections, USGS-OFR-84-494, Open-File Report, U.S. Geological Survey.

Scott, R. B. and M. Castellanos, 1984. Stratigraphic and Structural Relations of Volcanic Rocks in Drill Holes USW GU-3 and USW G-3, Yucca Mountain, Nye County, Nevada, USGS-OFR-84-491, Open-File Report, U.S. Geological Survey.

Scott, R. B., and J. G. Rosenbaum, 1986. "Evidence of Rotation About a

Scott, R. B., G. D. Bath, V. J. Flanigan, D. B. Hoover, J. G. Rosenbaum, and R. W. Spengler, 1984a. Geological and Geophysical Evidence of Structures in Northwest-Trending Washes, Yucca Mountain, Southern Nevada, and Their Possible Significance to a Nuclear Waste Repository in the Unsaturated Zone, USGS-OFR-84-567, Open-File Report, U.S. Geological Survey.

Scott, R. B., F. M. Byers, and R. G. Warren, 1984b. "Evolution of Magma below Clustered Calderas, Southwestern Nevada Volcanic Field," Transactions, American Geophysical Union, EOS, Vol. 65, No. 45, pp. 1126-1127.

Shawe, D. F., 1987. "Complex History of Precious-Metal Deposits, Southern Toquima Range, Nevada," A Symposium Bulk Mineable Precious Metal Deposits of the Western United States, April 6-8, 1987, Programs with Abstracts, Geological Society of Nevada, Reno, p. 47.

Shawe, D. R., F. G. Poole, and D. A. Brobst, 1969. "Newly Discovered Bedded Barite Deposits in East Northumberland Canyon, Nye County, Nevada," Economic Geology, Vol. 64, No. 3, pp. 245-254.

Shawe, D. R., R. F. Marvin, P. A. M. Andriessen, H. H. Mehnert, and V. M. Merritt, 1986. "Ages of Igneous and Hydrothermal Events in the Round Mountain and Manhattan Gold Districts, Nye County, Nevada," Economic Geology, Vol. 81, pp. 385-407.

Sheppard, R. A., 1975. "Zeolites in Sedimentary Rocks," Industrial Minerals and Rocks, S. J. Lefond (ed.), 4th Edition, American Institute of Mining, Metallurgical & Petroleum Engineers, Inc., New York, pp. 1257-1262.

Sherlock, M. G., and J. V. Tingley, 1985. Nevada Mineral-Resource Data: Information Available Through the U.S. Geological Survey Mineral Resource Data System, U.S. Geological Survey Circular 966, U.S. Geological Survey.

Silberman, M. L., 1985. "Geochronology of Hydrothermal Alteration and Mineralization: Tertiary Epithermal Precious-Metal Deposits in the Great Basin," Geologic Characteristics of Sediment- and Volcanic-Hosted Disseminated Gold Deposits--Search for and Occurrence Model, E. W. Tooker (ed.), U.S. Geological Survey Bulletin 1646, U.S. Government Printing Office, Washington, D.C., pp. 55-70.

Silberman, M. L., J. H. Stewart, and E. H. McKee, 1976. "Igneous Activity, Tectonics, and Hydrothermal Precious-Metal Mineralization in the Great Basin during Cenozoic Time," Society of Mining Engineers, Vol. 260, American Institute of Mining Engineers, pp. 253-263.

Sillitoe, R. H., 1977. "Metallic Mineralization Affiliated to Subaerial Volcanism--A Review," Volcanic Processes in Ore Genesis, Special Publication No. 7, The Institute of Mining & Metallurgy, and The Geological Society of London, pp. 99-116.

Singer, D. A., and D. L. Mosier, 1981. "A Review of Regional Mineral Resource Assessment Methods," Economic Geology, Vol. 76, pp. 1006-1015.

Sinnock, S., 1982. Geology of the Nevada Test Site and Nearby Areas, Southern Nevada, SAND82-2207, Sandia National Laboratories, Albuquerque, N. Mex.

Sinnock, S., and R. G. Easterling, 1983. Empirically Determined Uncertainty in Potassium-Argon Ages for Plio-Pleistocene Basalts from Crater Flat, Nye County, Nevada, SAND82-2441, Sandia National Laboratories, Albuquerque, N. Mex.

Sinnock, S., Y. T. Lin, and J. P. Brannen, 1984. Preliminary Bounds on the Expected Postclosure Performance of the Yucca Mountain Repository Site, Southern Nevada, SAND84-1492, Sandia National Laboratories, Albuquerque, N. Mex.

Slemmons, D. B., 1977. State-of-the-Art for Assessing Earthquake Hazards in

Smith, P., J. V. Tingley, J. L. Bentz, L. J. Garside, K. G. Papke, and J. Quade, 1983. A Mineral Inventory of the Esmeralda-Stateline Resource Area, Las Vegas District, Nevada, Nevada Bureau of Mines & Geology Open-File Report 83-11, University of Nevada, Reno.

Smith, R. B., 1978. "Seismicity, Crustal Structure, and Intraplate Tectonics of the Interior of the Western Cordillera," Cenozoic Tectonics and Regional Geophysics of the Western Cordillera, R. B. Smith and G. P. Eaton (eds.), Geological Society of America Memoir 152, pp. 111-144.

Smith, R. B., and R. L. Bruhn, 1984. "Intraplate Extensional Tectonics of the Eastern Basin-Range: Inferences on Structural Style from Seismic Reflection Data, Regional Tectonics, and Thermal-Mechanical Models of Brittle-Ductile Deformation," Journal of Geophysical Research, Vol. 89 No. B7, pp. 5733-5762.

Smith, R. L., 1960. Zones and Zonal Variations in Welded Ash Flows, Geological Survey Professional Paper 354, U.S. Geological Survey, pp. 149-159.

Smith, R. L., and R. G. Luedke, 1984. "Potentially Active Volcanic Lineaments and Loci in Western Conterminous United States," Explosive Volcanism: Inception, Evolution and Hazards, National Academy Press, Washington, D.C., pp. 47-66.

Smith, R. L., and H. R. Shaw, 1975. "Igneous-Related Geothermal Systems," Assessment of Geothermal Reseources of the United States--1975, D. E. White and D. L. Williams (eds.), Geological Survey Circular 726, U.S. Geological Survey, pp. 58-83.

Smith, R. L., and H. R. Shaw, 1979. "Igneous-Related Geothermal Systems," Assessment of Geothermal Resources of the United States--1978, L. J. P. Muffler (ed.), Geological Survey Circular 790, U.S. Geological Survey, pp. 12-17.

Smith, R. S. U., 1979. "Holocene Offset and Seismicity along the Panamint

Snyder, D. B., and W. J. Carr, 1984. "Interpretation of Gravity Data in a Complex Volcano-Tectonic Setting, Southwestern Nevada," Journal of Geophysical Research, Vol. 89, No. B12, pp. 10,193-10,206.

Snyder, D. B., and H. W. Oliver, 1981. Preliminary Results of Gravity Investigations of the Calico Hills, Nevada Test Site, Nye County, Nevada, USGS-OFR-81-101, Open-File Report, U.S. Geological Survey.

Sorey, M. L., M. Nathenson, and C. Smith, 1983. Methods for Assessing Low-Temperature Geothermal Resources, Assessment of Low-Temperature Geothermal Resources of the United States-1982, M. J. Reed (ed.), Geological Survey Circular 892, U.S. Department of the Interior, pp. 17-30.

Spaulding, W. G., 1985. Vegetation and Climates of the Last 45,000 Years in the Nevada Test Site and Vicinity, U.S. Geological Survey Professional Paper 1329, U.S. Government Printing Office, Washington, D.C.

Spaulding, W. G., E. B. Leopold, and T. R. Van Devender, 1983. "The Late Wisconsin Paleoecology of the American Southwest," Late-Quaternary Environments of the United States, Volume I, The Late Pleistocene, S. C. Porter (ed.), University of Minnesota Press, Minneapolis, pp. 259-293.

Speed, R. C., 1977. "Island-Arc and Other Paleogeographic Terranes of Late Paleozoic Age in the Western Great Basin," Paleozoic Paleogeography of the Western United States, Pacific Coast Paleogeography Symposium 1, J. H. Stewart, C. Stevens, and A. Fritsche (eds.), Society of Economic Paleontologists & Mineralogists, Pacific Section, Pacific Coast Paleogeography Symposium 1, pp. 349-362.

Speed, R. C., 1978. "Paleogeographic and Plate Tectonic Evolution of the Early Mesozoic Marine Province of the Western Great Basin," Mesozoic Paleogeography of the Western United States, D. G. Howell and K. A. McDougall (eds.), Society of Economic Paleontologists & Mineralogists, Pacific Section, Pacific Coast Paleogeography Symposium 2, pp. 253-270.

Spengler, R. W., 1986. Letter from R. W. Spengler (USGS) to S. R. Mattson (SAIC), November 3, 1986; regarding USGS laboratory report (job no. QU02).

Spengler, R. W., and M. P. Chornack, 1984. Stratigraphic and Structural Characteristics of Volcanic Rocks in Core Hole USW G-4, Yucca Mountain, Nye County, Nevada, with a section on geophysical logs by D. C. Muller and J. E. Kibler, USGS-OFR-84-789, Open-File Report, U.S. Geological Survey.

Spengler, R. W., and J. G. Rosenbaum, 1980. Preliminary Interpretations of Geologic Results Obtained from Boreholes UE25a-4, -5, -6, and -7, Yucca Mountain, Nevada Test Site, USGS-OFR-80-929, Open-File Report, U.S. Geological Survey.

Spengler, R. W., D. C. Muller, and R. B. Livermore, 1979. Preliminary Report on the Geology and Geophysics of Drill Hole UE25a-1, Yucca Mountain, Nevada Test Site, USGS-OFR-79-1244, Open-File Report, U.S. Geological Survey.

Spengler, R. W., F. M. Byers, Jr., and J. B. Warner, 1981. Stratigraphy and Structure of Volcanic Rocks in Drill Hole USW G-1, Yucca Mountain, Nye County, Nevada, USGS-OFR-81-1349, Open-File Report, U.S. Geological Survey.

Stanton, R. L., 1972. Ore Petrology, McGraw-Hill Book Co., New York, pp. 305-351, 522.

Stein, R. S., and S. E. Barrientos, 1985. "Planar High-Angle Faulting in the Basin and Range: Geodetic Analysis of the 1983 Borah Peak, Idaho, Earthquake," Journal of Geophysical Research, Vol. 90, No. B13, pp. 11,355-11,366.

Stewart, J. H., 1967. "Possible Large Right-Lateral Displacement along Fault and Shear Zones in the Death Valley-Las Vegas Area, California and Nevada," Geological Society of America Bulletin, Vol. 78, pp. 131-142.

Stewart, J. H., 1971. "Basin and Range Structure: A System of Horsts and

Stewart, J. H., and J. E. Carlson, 1978. Geologic Map of Nevada, MF-930, Scale 1:500,000, U.S. Geological Survey.

Stewart, J. H., and F. G. Poole, 1974. "Lower Paleozoic and Uppermost Precambrian Cordilleran Miogeocline, Great Basin, Western United States," Tectonics and Sedimentation, W. R. Dickinson (ed.), Society of Economic Paleontologists & Mineralogists Special Publication 22, pp. 28-57.

Stewart, J. H., J. P. Albers, and F. G. Poole, 1968. "Summary of Regional Evidence for Right-Lateral Displacement in the Western Great Basin," Geological Society of America Bulletin, Vol. 79, No. 10, pp. 1407-1414.

Stewart, J. H., W. J. Moore, and I. Zietz, 1977. "East-West Patterns of Cenozoic Igneous Rocks, Aeromagnetic Anomalies, and Mineral Deposits, Nevada and Utah," Geological Society of America Bulletin, Vol. 88, pp. 67-77.

Stock, J. M., J. H. Healy, S. H. Hickman, and M. D. Zoback, 1985. "Hydraulic Fracturing Stress Measurements at Yucca Mountain, Nevada, and Relationship

Sykes, M. L., G. H. Heiken, and J. R. Smyth, 1979. Mineralogy and Petrology of Tuff Units from the UE25a-1 Drill Site, Yucca Mountain, Nevada, LA-8139-MS, Los Alamos National Laboratory, Los Alamos, N. Mex.

Szabo, B. J., 1984. "Uranium-Series Dating of Fault-Related Fracture- and Cavity-Filling Calcite and Opal in Drill Cores from Yucca Mountain, Southern Nevada," Geological Society of America, Abstracts with Programs, Annual Meeting, Reno, Nev., November 5-8, 1984, Vol. 16, No. 6, pp. 672-673.

Szabo, B. J., and T. K. Kyser, 1985. Uranium, Thorium Isotopic Analyses and Uranium-Series Ages of Calcite and Opal, and Stable Isotopic Compositions of Calcite from Drill Cores UE25a#1, USW G-2, and USW G-3/GU-3, Yucca Mountain, Nevada, USGS-OFR-85-224, Open-File Report, U.S. Geological Survey.

Szabo, B. J., and P. A. O'Malley, 1985. Uranium-Series Dating of Secondary Carbonate and Silica Precipitates Relating to Fault Movements in the Nevada Test Site Region and of Caliche and Travertine Samples from the Amargosa Desert, USGS-OFR-85-47, Open-File Report, U.S. Geological Survey.

Szabo, B. J., W. J. Carr, and W. C. Gottschall, 1981. Uranium-Thorium Dating of Quaternary Carbonate Accumulations in the Nevada Test Site Region, Southern Nevada, USGS-OFR-81-119, Open-File Report, U.S. Geological Survey.

Taylor, E. M., 1986. Impact of Time and Climate on Quaternary Soils in the Yucca Mountain Area of the Nevada Test Site, unpublished M.S. thesis, University of Colorado, Boulder.

Taylor, E. M., and H. E. Huckins, 1986. "Carbonate and Opaline Silica Fault-Filling on the Bow Ridge Fault, Yucca Mountain, Nevada--Deposition from Pedogenic Processes or Upwelling Ground Water?," Geological Society of America, Abstracts with Programs, Vol. 18, No. 5, p. 418.

Taylor, E. M., and R. R. Shroba, 1986. "Morphology of Secondary Carbonate and Opaline Silica in Soils of Different Ages at the Nevada Test Site, Nye County, Nevada," Geological Society of America, Abstracts with Programs, Vol. 18, No. 6, p. 769.

Taylor, R. B., and T. A. Steven, 1983. "Definition of Mineral Resource Potential," Economic Geology, Vol. 78, pp. 1268-1270.

Tendall, D. M., 1971. Epicenter Location of NTS Earthquake on August 5, 1971, Technical Memorandum SC-TM-710593, Sandia National Laboratories, Albuquerque, N. Mex., 18 p.

Theobald, P. K., 1987. "Exploration in Desert Environments," Geoexpo/86; Exploration in the North American Cordillera, May 12-14, 1986, Vancouver, British Columbia, I. L. Elliot and B. W. Smee (eds.), The Association of Exploration Geochemists, pp. 213-214.

Thompson, G. A., 1985. "Perspective from the Fairview Peak-Dixie Valley Earthquakes of 1954," in Proceedings of Workshop XXVIII on the Borah Peak, Idaho, Earthquake, Vol. A, R. S. Stein and R. C. Bucknam (eds.), USGS-OFR-85-290-A, Open-File Report, U.S. Geological Survey, pp. 27-42.

Thomson, I., 1986. "Getting It Right," Exploration Geochemistry: Design and Interpretation of Soil Surveys, J. M. Robertson (ed.), Vol. 3, Society of Economic Geologists, pp. 1-18.

Thordarson, W., 1983. Geohydrologic Data and Test Results from Well J-13

USBM/USGS (U.S. Bureau of Mines/U.S. Geological Survey), 1980. Principles of a Resource/Reserve Classification for Minerals, Geological Survey Circular 831, U.S. Geological Survey.

USGS (U.S. Geological Survey), 1952a. Big Dune Quadrangle, Nevada-California, U.S. Geological Survey 15 Minute Series (Topographic), Scale 1:62,500, U.S. Geological Survey.

USGS (U.S. Geological Survey), 1952b. Topopah Spring Quadrangle Map, Nevada-Nye County, U.S. Geological Survey 15 Minute Series (Topographic), Scale 1:62,500, U.S. Geological Survey.

USGS (U.S. Geological Survey), 1954. Bare Mountain Quadrangle, Nevada, U.S. Geological Survey 15 Minute Series (Topographic), 1:62,500, U.S. Geological Survey.

USGS (U.S. Geological Survey), 1961a. Lathrop Wells Quadrangle, Nevada-Nye County, U.S. Geological Survey 7.5 Minute Series (Topographic), Scale 1:24,000, U.S. Geological Survey.

USGS (U.S. Geological Survey), 1961b. Lathrop Wells Quadrangle, Nevada-Nye County, Nevada, U.S. Geological Survey 15 Minute Series (Topographic), Scale 1:62,500, U.S. Geological Survey.

USGS (U.S. Geological Survey), 1961c. Topopah Spring Quadrangle, Nevada-Nye County, U.S. Geologic Survey 7.5 Minute Series (Topographic), Scale 1:24,000, U.S. Geological Survey.

USGS (U.S. Geological Survey), 1983. Busted Butte Quadrangle, Nevada-Nye County, U.S. Geological Survey 7.5 Minute Series (Topographic), Scale 1:24,000, U.S. Geological Survey.

USGS (U.S. Geological Survey) (comp.), 1984. A Summary of Geologic Studies through January 1, 1983, of a Potential High-Level Radioactive Waste Repository Site at Yucca Mountain, Southern Nye County, Nevada, USGS-OFR-84-792, Open-File Report, U.S. Geological Survey.

USGS/NBM (U.S. Geological Survey/Nevada Bureau of Mines), 1964. Mineral and Water Resources of Nevada, Nevada Bureau of Mines Bulletin 65, University of Nevada, Reno.

Van Alstine, R. E., 1976. "Continental Rifts and Lineaments Associated with Major Fluorspar Districts," Economic Geology, Vol. 71, No. 6, pp. 977-987.

Vaniman, D., and B. Crowe, 1981. Geology and Petrology of the Basalts of Crater Flat: Applications to Volcanic Risk Assessment for the Nevada Nuclear Waste Storage Investigations, LA-8845-MS, Los Alamos National Laboratory, Los Alamos, N. Mex., 67 p.

Vaniman, D. T., B. M. Crowe, and E. S. Gladney, 1982. "Petrology and Geochemistry of Hawaiite Lavas from Crater Flat, Nevada," Contributions to Mineralogy and Petrology, Vol. 80, Springer-Verlag, pp. 341-357.

Vaniman, D. T., D. Bish, D. Broxton, F. Byers, G. Heiken, B. Carlos, E. Semarge, F. Caporuscio, and R. Gooley, 1984a. Variations in Authigenic Mineralogy and Sorptive Zeolite Abundance at Yucca Mountain, Nevada, Based on Studies of Drill Cores USW GU-3 and G-3, LA-9707-MS, Los Alamos National Laboratory, Los Alamos, N. Mex.

Vaniman, D., D. Bish, and S. Levy, 1984b. Progress Report: Studies on the Origin of Soil and Fault-Related Mineralogy in the Vicinity of Yucca Mountain, TWS-ESS-1-11/84-22. Los Alamos National Laboratory, Los Alamos, N. Mex.

Vaniman et al, 1988.

Veal, H. K., H. D. Duey, L. C. Bortz, and N. H. Foster, 1988a. "Grant Canyon and Bacon Flat Oil Fields, Railroad Valley, Nye County, Nevada," Oil and Gas Journal, Vol. 86, No. 13, pp. 67-70.

Veal, H. K., H. D. Duey, L. C. Bortz, and N. H. Foster, 1988b. "Basin and Range May Hold More Big Fields," Oil and Gas Journal, Vol. 86, No. 13, pp. 56-59.

Vetter, U. R., and A. S. Ryall, 1983. "Systematic Change of Focal Mechanism with Depth in the Western Great Basin," Journal of Geophysical Research, Vol. 88, No. B10, pp. 8237-8250.

Voegele, M. D., 1986a. Letter from M. D. Voegele (SAIC) to M. B. Blanchard (DOE/NVO), L86-TPD-SM-81; regarding final summary of workshop on calcite-silica deposits near Yucca Mountain held on February 28, 1986.

Voegele, M. D., 1986b. Letter from M. D. Voegele (SAIC) to M. B. Blanchard (DOE/NVO), L86-TPO-SRM-93; regarding summary of workshop on calcite-silica deposits near Yucca Mountain held on April 28, 1986.

von Hake, C. A, and W. K. Cloud, 1968. United States Earthquakes - 1966, COM 74 10712; NOAA-74030414, Environmental Science Services Administration, Coast & Geodetic Survey, National Earthquake Information Center, Washington, D.C., 110 p.

Vortman, L. J., 1979. Prediction of Ground Motion from Nuclear Weapons Tests at NTS, SAND79-1002, Sandia National Laboratories, Albuquerque, N. Mex.

Vortman, L. J., 1980. Prediction of Ground Motion from Underground Nuclear Weapons Tests as It Relates to Siting of a Nuclear Waste Storage Facility at NTS and Compatibility with the Weapons Test Program, SAND80-1020/1, Sandia National Laboratories, Albuquerque, N. Mex.

Vortman, L. J., 1982. Ground Motion from Earthquakes and Underground Nuclear Weapons Tests: A Comparison as It Relates to Siting a Nuclear Waste Storage Facility at NTS, SAND81-2214, Sandia National Laboratories, Albuquerque, N. Mex.

Vortman, L. J., 1986. Ground Motion Produced at Yucca Mountain from Pahute Mesa Underground Nuclear Explosions, SAND85-1605, Sandia National Laboratories, Albuquerque, N. Mex.

Vortman, L. J., and J. W. Long, 1982a. Effects of Repository Depth on Ground Motion-The Pahute Mesa Data, SAND82-0174, Sandia National Laboratories, Albuquerque, N. Mex.

Vortman, L. J., and J. W. Long, 1982b. Effects of Ground Motion on Repository Depth, The Yucca Flat Data, SAND82-1647, Sandia National Laboratories, Albuquerque, N. Mex.

Walker, G. P. L., 1973. "Lengths of Lava Flows," Philosophical Transactions of the Royal Society of London, Series A, Vol. 274, Royal Society, London, pp. 107-118.

Wallace, R. E., 1979. "Earthquakes and the Prefractured State of the Western Part of the North American Continent," in Proceedings of the International Research Conference on Intra-Continental Earthquakes, September 17-21, 1979, Ohrid, Yugoslavia, pp. 69-81.

Wallace, R. E., 1981. "Active Faults, Paleoseismology and Earthquake Hazards in the Western United States," Earthquake Prediction--An International Review, D. W. Simpson and P. G. Richards (eds.), America Geophysical Union, Maurice Ewing Series 4, Washington, D.C., pp. 209-216.

Wallace, R. E., 1984. "Patterns and Timing of Late Quaternary Faulting in the Great Basin Province and Relation to Some Regional Tectonic Features," Journal of Geophysical Research, Vol. 89, No. B7, pp. 5763-5769.

Wallace, R. E., 1985. "Variations in Slip Rates, Migration, and Grouping of Slip Events on Faults in the Great Basin Province," in Proceedings of Workshop XXVIII on the Borah Peak, Idaho, Earthquake, R. S. Stein and R. C. Bucknam (eds.), USGS-OFR-85-290-A, Open-File Report, U.S. Geological Survey, pp. 17-26.

Wallace, T. C., D. V. Helmberger, and G. R. Engen, 1983. "Evidence for Tectonic Release from Underground Nuclear Explosions in Long-Period P Waves," Bulletin of the Seismological Society of America, Vol. 73, No. 2, pp. 593-613.

Wallace, T. C., D. V. Helmberger, and G. R. Engen, 1985. "Evidence of Tectonic Release from Underground Nuclear Explosions in Long-Period S Waves," Bulletin of the Seismological Society of America, Vol. 75, No. 1, pp. 157-174.

Walter, A. W., and C. S. Weaver, 1980. "Seismicity of the Coso Range, California," Journal of Geophysical Research, Vol. 85, No. B5, pp. 2441-2458.

Waples, D. W., 1984. "Modern Approaches in Source-Rock Evaluation," Hydrocarbon Source Rocks of the Greater Rocky Mountain Region, J. Woodward, F. F. Meissner, and J. L. Clayton (eds.), Rocky Mountain Association of Geologists, Denver, Colo., pp. 35-49.

Warren, R. G., and F. M. Byers, Jr., 1986. Letter from R. G. Warren and F. M. Byers, Jr. (LLNL) to J. T. Neal (SNL), October 21, 1986; regarding post-Tpc stratigraphic sequence.

Warren, R. G., F. M. Byers, and F. A. Caporuscio, 1984. Petrography and Mineral Chemistry of Units of the Topopah Spring, Calico Hills and Crater Flat Tuffs, and Older Volcanic Units, with Emphasis on Samples from Drill Hole USW G-1, Yucca Mountain, Nevada Test Site, LA-10003-MS, Los Alamos National Laboratory, Los Alamos, N. Mex.

Wasserburg, G. J., G. W. Wetherill, and L. A. Wright, 1959. "Ages in the Precambrian Terrane of Death Valley, California," Journal of Geology, Vol. 67, pp. 702-708.

Waters, A. C., and P. R. Carroll (eds.) 1981. Preliminary Stratigraphic and Petrologic Characterization of Core Samples from USW-G1, Yucca Mountain, Nevada, LA-8840-MS, Los Alamos National Laboratory, Los Alamos, N. Mex.

Weeks, E. P., and W. E. Wilson, 1984. Preliminary Evaluation of Hydrologic Properties of Cores of Unsaturated Tuff, Test Well USW H-1, Yucca Mountain, Nevada, USGS-WRI-84-4193, Water-Resources Investigations Report, U.S. Geological Survey.

Wells, S. G., J. C. Dohrenwend, L. D. McFadden, B. D. Turrin, and K. D. Mahrer, 1985a. "Late Cenozoic Landscape Evolution on Lava Flow Surfaces of the Cima Volcanic Field, Mojave Desert, California," Geological Society of America Bulletin, Vol. 96, No. 12, pp. 1518-1529.

Wells, S. G., L. D. McFadden, J. C. Dohrenwend, T. F. Bullard, B. F. Feilberg, R. L. Ford, J. P. Grimm, J. R. Miller, S. M. Orbock, and J. D. Pickle, 1985b. "Late Quaternary Geomorphic History of the Silver Lake Area, Eastern Mojave Desert, California: An Example of the Influence of Climatic Change on Desert Piedmonts," Quaternary Lakes of the Eastern Mojave Desert, California, Friends of the Pleistocene, Pacific Cell, 1985 Annual Meeting, Field Trip Guidebook, G. R. Hale (ed.), pp. 82-100.

Wells, S. G., L. D. McFadden, C. Renault, and B. M. Crowe, 1988. "A Geomorphic Assessment of Quaternary Volcanism in the Yucca Mountain Area, Nevada Test Site, Southern Nevada," Geological Society of America, Cordilleran Section, Vol. 20, No. 3 p. 242.

Wernicke, B., 1981. "Low-Angle Normal Faults in the Basin and Range Province: Nappe Tectonics in an Extending Orogen," Nature, Vol. 291, pp. 645-648.

Wernicke, B., and B. C. Burchfiel, 1982. "Modes of Extensional Tectonics," Journal of Structural Geology, Vol. 4, No. 2, pp. 105-115.

Wernicke, B., J. E. Spencer, B. C. Burchfiel, and P. L. Guth, 1982. "Magnitude of Crustal Extension in the Southern Great Basin," Geology, Vol. 10, pp. 499-502.

White, D. E., 1970. "Geochemistry Applied to the Discovery, Evaluation, and Exploitation of Geothermal Energy Resources," in Proceedings of the United Nations Symposium on the Development and Utilization of Geothermal Resources, Pisa, Italy, Septmber 22-October 1, 1970, Geothermics, Special Issue 2, E. Barbier (ed.), Vol. 1, pp. 58-80.

White, D. E., 1973. "Characteristics of Geothermal Resources," Geothermal Energy, Resources, Production, Stimulation, P. Kruger and C. Otte (eds.), Stanford University Press, Stanford, Calif.

White, D. E., 1985. "Vein and Disseminated Gold-Silver Deposits of the Great Basin through Space and Time," Geologic Characteristics of Sediment- and [illegible]

Model, E. W. Tooker (ed.), U.S. Geological Survey Bulletin 1646, U.S. Government Printing Office, Washington, D.C., pp. 5-14.

White, D. E., L. J. P. Muffler, and A. H. Truesdell, 1971. "Vapor-Dominated Hydrothermal Systems Compared with Hot-Water Systems," Economic Geology, Vol. 66, pp. 75-97.

Whitfield, M. S., W. Thordarson, and E. P. Eshom, 1984. Geohydrologic and Drill-Hole Data for Test Well USW H-4, Yucca Mountain, Nye County, Nevada, USGS-OFR-84-449, Open-File Report, U.S. Geological Survey.

Whitney, J. W., W C Swadley, and R. R. Shroba, 1985. "Middle Quaternary Sand Ramps in the Southern Great Basin, California and Nevada [abs.]," Geological Society of America, Abstracts with Programs, Vol. 17, No. 7, p. 750.

Whitney, J. W., R. R. Shroba, F. W. Simonds, and S. T. Harding, 1986. "Recurrent Quaternary Movement on the Windy Wash Fault, Nye County, Nevada [abs.]," Geological Society of America, Abstracts with Programs, Vol. 18, No. 6, p. 787.

Willis, D. E., R. W. Taylor, R. D. Torfin, P. T. Tater, K. L. Revock, R. G. Poetzl, G. D. George, and C. G. Bufe, 1974. Explosion-Induced Ground Motion, Tidal and Tectonic Forces and Their Relationship to Natural Seismicity, COO-2138-13, Department of Geological Sciences, University of Wisconsin, Milwaukee.

Wilson, W. E., 1985. Letter from W. E. Wilson (USGS) to D. L. Vieth (DOE/NVO), December 24, 1985; regarding unsaturated zone flux.

Winchester, D. E., 1923. Oil Shale of the Rocky Mountain Region, U.S. Geological Survey Bulletin 729, U.S. Government Printing Office, [illegible]

Wise, D. U., 1963. "An Outrageous Hypothesis for the Tectonic Pattern of the North American Cordillera," Geological Society of America Bulletin, Vol. 74, pp. 357-362.

Wolfsberg, K., B. P. Bayhurst, B. M. Crowe, W. R. Daniels, B. R. Erdal, F. O. Lawrence, A. E. Norris, and J. R. Smyth, 1979. Sorption-Desorption Studies on Tuff; I. Initial Studies with Samples from the J-13 Drill Site, Jackass Flats, Nevada, LA-7480-MS, Los Alamos National Laboratory, Los Alamos, N. Mex.

Wollenberg, H. A., 1982. "Geothermal Resource Exploration," Recent Trends in Hydrogeology, Geological Society of America Special Paper 189, Geological Society of America, Boulder, Colo., pp. 375-386.

Wood, C. A., 1980. "Morphometric Evolution of Cinder Cones," Journal of Volcanology and Geothermal Research, Vol. 7, Elsevier Scientific Publishing Co., Amsterdam, pp. 387-413.

Wood, J. D., 1988. "Geology of the Sleeper Gold Deposit, Humbolt County, Nevada," in Bulk-Mineable Precious-Metal Deposits of the Western United States, Symposium Proceedings, R. W. Schafer, J. J. Cooper, and P. G. Vikre (eds.), The Geological Society of Nevada, Reno, pp. 293-302.

Young, R. A., 1972. Water Supply for the Nuclear Rocket Development Station

Zoback, M. L., and M. D. Zoback, 1980a. "Faulting Patterns in North-Central Nevada and Strength of the Crust," Journal of Geophysical Resources, Vol. 85, No. B1, pp. 275-284.

Zoback, M. L., and M. D. Zoback, 1980b. "State of Stress in the Conterminous United States," Journal of Geophysical Research, Vol. 85, No. B11, pp. 6113-6156.

Zoback, M. L., R. E. Anderson, and G. A. Thompson, 1981. "Cainozoic Evolution of the State of Stress and Style of Tectonism of the Basin and Range

Province of the Western United States," Philosophical Transactions of the Royal Society of London, Ser. A, Vol. 300, pp. 407-434.

Zohdy, A. A. R., and R. J. Bisdorf, 1979. Schlumberger Soundings and Geoelectric Cross Sections in Yucca Lake, Nevada Test Site, Nevada, USGS-OFR-79-220, Open-File Report, U.S. Geological Survey.

Zwartendyk, J., 1981. "Economic Issues in Mineral Resource Adequacy and in the Long-Term Supply of Minerals," Economic Geology, Vol. 76, No. 5, pp. 999-1005.

CODES AND REGULATIONS

10 CFR Part 60 (Code of Federal Regulations), 1987. Title 10, "Energy," Part 60, "Disposal of High-Level Radioactive Wastes in Geologic Repositories," U.S. Government Printing Office, Washington, D.C., pp. 627-658.

10 CFR Part 960 (Code of Federal Regulations), 1987. Title 10, "Energy," Part 960, "General Guidelines for the Recommendation of Sites for Nuclear Waste Repositories," U.S. Government Printing Office, Washington, D.C., pp. 518-551.

40 CFR Part 191 (Code of Federal Regulations), 1986. Title 40, "Protection of Environment," Part 191, "Environmental Radiation Protection Standards for Management and Disposal of Spent Nuclear Fuel, High-Level and Transuranic Radioactive Wastes," U.S. Government Printing Office, Washington, D.C., pp. 7-16.

DOE/RW-0199

Nuclear Waste Policy Act
(Section 113)

Site Characterization Plan

Yucca Mountain Site, Nevada Research and Development Area, Nevada

Volume I, Part A

Chapter 2, Geoengineering

U. S. Department of Energy
Office of Civilian Radioactive Waste Management

Chapter 2

GEOENGINEERING

INTRODUCTION

Chapter 2 summarizes the available information on the geoengineering properties that contribute to the demonstration that performance objectives and design criteria will be met. The performance objectives and design criteria for the geologic operations area are described in 10 CFR Part 60.

The Yucca Mountain Project (formerly called Nevada Nuclear Waste Storage Investigations Project) has assembled an issues hierarchy, as defined in Sections 8.1 and 8.2, which provides a structured approach to defining information that must be obtained to demonstrate that the performance objectives will be met. The reader is referred to those sections for details about the issues hierarchy structure and content. The issues, and subsidiary information needs; and characterization programs and subsidiary investigations that contribute to individual issues, are described in detail in Section 8.3.

The list of specific issues that use geoengineering data as input is extensive. The relationship between the issues and specific geoengineering parameters is elucidated in Section 2.9.3. These parameters form the basis for discussion for most of the remainder of Chapter 2.

The behavior of tuff as an engineering material must be understood to design, license, construct, operate, and decommission a repository at Yucca Mountain. The uniqueness of a repository design (when compared with mines or tunnels) results from the addition of heat and radiation to the rock mass and from the need for long-time stability. The heat produces changes in the preexisting temperature field, which in turn changes the state of stress and possibly the distribution and flow of ground water within the rock mass. Two important tasks must be completed to understand the behavior of tuff:

1. Identify and understand the geotechnical phenomena, properties, and parameters important to the design and evaluation of a repository system.

2. Develop the data base for these required geotechnical phenomena, properties, and parameters to form the basis for technical decisions to be made in site evaluation, repository and waste package design, and performance assessment.

The remainder of this introduction is devoted to the following:

1. Delineating the quantities that must be known to evaluate thermal, mechanical, and hydrothermal phenomena.

2. Identifying the specific properties or measured values that are needed to make or to evaluate the required predictions.

3. Delineating the strategy being used for developing the data base of geotechnical properties.

4. Summarizing the philosophy of sample selection for laboratory testing.

5. Summarizing the status of the geotechnical measurement activities.

6. Identifying conceptual models for which the data provide input.

REPOSITORY CONDITIONS TO BE EVALUATED

Demonstration that a repository will be in compliance with regulatory criteria must rely on analyses of the behavior of the repository system as a whole and its subsystems (e.g., the waste package). Such analyses must treat thermal, mechanical, hydrologic, and geochemical effects, and coupled effects in relation to the emplacement, retrieval, long-term isolation, and containment of the radioactive waste. The relationship between the regulatory criteria and repository design and the resulting definition of data needs are discussed in Section 6.1.1.

Input data necessary for performing the analyses will vary with the approach selected to resolve an issue (see Section 8.2 for a general discussion of the issue resolution strategy), the conceptual model used to represent the process being analyzed (see Section 8.3.1.15 for a discussion of alternative conceptual models), the type of behavior being addressed (e.g., thermal or mechanical), the amount of detail or complexity in each analysis, and the scale of the problem both in space and in time. As the understanding of the system improves, data needs and analysis techniques may change or be refocused to increase the quality and relevance of analyses of system behavior.

The demonstration of compliance will require, among other things, a minimum ground-water travel time over some designated distance from the repository. Calculation of this travel time requires input data on the distribution and characterization of fractures (Chapter 1) and porosity (Sections 2.4.2.4 and 2.4.3) and the distribution and movement of water within the fractures and pores (Chapter 3). Knowledge of ground-water movement is also implicit in the determination of radionuclides release rates. The effects of variations in temperature and pressure on these data must then be estimated to calculate the effect that a waste repository will have on water movement and thus on radionuclide movement and release rates.

The stability of waste emplacement holes will play a role in the estimation of radionuclide releases through estimates of waste container integrity and containment capability. Thus, the potential for movement of rock surrounding the waste canister or for coupled hydrologic and thermal effects on waste container corrosion (Chapter 7) must be assessed; the data needs in this area are discussed in Section 8.3.4.2.

Demonstration of compliance with the retrievability requirement of a repository involves the retrievability of the waste, which in turn requires demonstration that mined openings and waste emplacement holes remain usable during construction, operation, caretaker period, and possibly waste retrieval. This time period currently is estimated to be 84 yr (Flores, 1986). Such a demonstration requires selection and application of appropriate mechanical constitutive models (see Section 8.3.1.15 for a description of alternative conceptual models for mechanical constitutive behavior) to develop a knowledge of how the rock will respond to the presence of a combination of mined openings and waste-generated heat over long periods of time.

To quantify the effects of the heat generated by the waste, a model for the process of heat transfer must be selected (see Section 8.3.1.15 for a description of alternative conceptual models for the heat transfer process) and temperatures must be calculated. The resulting stresses and displacements in the rock must be calculated to assess the opening stability, waste container integrity, and the nature of fracture and porosity distribution as a function of time and location. This last consideration will also affect the development of a zone of material around the repository that has different fracture characteristics than those of the remainder of the rock mass. This is a consideration in the evaluation of the extent of the disturbed zone. The interaction between the repository, including the zone of material with different fracture characteristics, and the hydrologic system must be assessed to obtain realistic estimates of radionuclide releases.

The application of individual data needs are summarized in the following lists. No attempt has been made to set priorities for the various applications.

Analyses of rock temperature are needed to

1. Establish the acceptable gross thermal loading within the repository horizon, accounting for constraints on repository and waste container design (Section 8.3.4.2).

2. Evaluate the stability of pillars, waste emplacement holes, and mined openings (Section 8.3.1.15).

3. Determine the waste container environment (Chapter 7).

4. Establish the ventilation requirements (Chapter 6).

5. Evaluate the relative importance of different physical mechanisms of mechanical deformation (Sections 2.1.2.3.1.3 and 2.1.2.3.1.4).

6. Conduct tradeoff studies for such alternatives as horizontal versus vertical waste emplacement, ramp versus shaft as a means of underground access, age of the waste to be emplaced, the size of the waste package, the spacing of the canisters, and the spacing of the drifts (Section 8.3.4.2).

7. Evaluate the potential for thermally induced water movement (Section 2.7.2).

Stress and displacement analyses are needed to

1. Perform detailed analyses of room size, shape, spacing, and support requirements (Section 8.3.1.15).

2. Evaluate emplacement hole stability (including liner requirements, if any, for stability) (Section 8.3.4.2).

3. Determine the repository horizon spatial extent acceptable for waste emplacement (particularly with regard to lithophysae content and gross thermal loading) (Sections 8.3.1.4 and 8.3.1.15).

4. Evaluate shaft designs with respect to opening stability and liner loading (Section 8.3.1.15).

5. Evaluate the amounts and consequences of far-field displacements (Section 8.3.2.2).

6. Evaluate potential coupling between induced stresses and displacements and the movement of ground water (Section 8.3.2.1).

Analyses of the quantities and mechanisms of thermally induced water migration are needed to

1. Accurately calculate rock temperatures (Section 8.3.1.15).

2. Establish ventilation requirements (Chapter 6).

3. Define the waste container environment (Chapter 7).

4. Assess the impact of the thermal pulse on ground-water travel time and thus on radionuclide releases (Section 8.3.5.12).

Details of the relationships between the analyses mentioned previously and the design process are provided in Chapters 6 and 7.

PROPERTIES AND INITIAL CONDITIONS TO BE MEASURED

This section discusses the properties and initial conditions that must be measured to predict temperatures, stresses, displacements, and thermally induced water movement and specifies the sections of this document that present relevant data. Although the discussion is divided into three categories (temperature, stress and displacement, and water migration), these categories are not totally independent. Coupled processes such as temperature effects on mechanical properties or the effects of water migration on temperature will be an integral part of the response of the rock mass to a repository.

The initial condition required for the calculation of temperature fields is the distribution of temperatures before waste emplacement. Such data are presented in Section 1.3.2.5. This preexisting temperature field will be altered by the construction and operation of the repository including the emplacement of heat-producing waste. The rock properties necessary to calculate the conduction of heat away from the waste are the thermal conductivity (Sections 2.4.2.1, 2.5.2, and 2.5.3), the heat capacity (Sections 2.4.2.2, 2.5.2, and 2.5.3), and the density (Sections 2.4.2.4, 2.5.2, and 2.5.3). Heat transfer also could occur by the convection of water in the pores and fractures, as discussed in Section 2.7.2. Alternative conceptual models for the process of heat transfer are discussed in Section 8.3.1.15.

The prediction of stresses and displacements around a repository first requires a knowledge of the mechanical behavior of the rock mass. Different mechanical constitutive models for rock deformation require different

on the elastic properties (e.g., Young's modulus and Poisson's ratio; Sections 2.1.2.2, 2.3.2, and 2.3.3) for the prediction of displacements. At elevated temperatures or over long times, the rock may exhibit inelastic deformation rather than the elastic behavior expected to predominate over short time intervals (Section 2.1.2.3.1.4). In addition, the strength of the rock (Section 2.1.2.3) may be exceeded in some locations, which would result in stresses and displacements different from those resulting from prefailure

DATA BASE DEVELOPMENT--HISTORY AND STRATEGY

A strategy for the development of the geoengineering properties data base needed for technical decisions has been developed and implemented in the Yucca Mountain Project. The strategy relies primarily on data determined in laboratory tests that are then evaluated and later confirmed in field tests in G-Tunnel and in the exploratory shaft facility.

The laboratory data presently available consist of test results on core samples from the following locations (Figure 2-1):

1. Coreholes at Yucca Mountain (UE-25a#1, UE-25b#1, USW G-1, USW G-2, USW GU-3, and USW G-4).

2. An underground test facility (G-Tunnel) located in Rainier Mesa.

3. Topopah Spring Member outcrops at Busted Butte.

When the Yucca Mountain Project began, no suitable site-specific samples were available for studying the effects of parameters like temperature and pressure on the mechanical properties of tuff. Both welded and nonwelded tuffs are exposed in G-Tunnel at Rainier Mesa and were used in early studies of parameter effects. Laboratory testing on samples from G-Tunnel also has been performed to support in situ testing in the tunnel. These data have been included in the existing geoengineering properties data base because the tuffs at G-Tunnel are similar (Section 2.8.2) to those found at Yucca Mountain. Data on the properties of tuffs in G-Tunnel will be replaced by data specific to Yucca Mountain tuffs as such data become available.

Since the Topopah Spring Member was recommended as the repository horizon (Johnstone et al., 1984), testing has been performed on samples from outcrops of the Topopah Spring Member at Busted Butte. Large samples (about 0.5 m^3) have been cored (up to 30 cm in diameter) for use primarily in measuring the effects of lithophysae on thermal and mechanical properties and for establishing the effect of sample size on the measured strength of the Topopah Spring Member. Examination of the properties of the lithophysae-rich material contributes to decisions regarding the volume of the Topopah Spring Member that is suitable for a repository, whereas the determination of sample-size effects enhances the ability to extrapolate laboratory test results to the rock mass in situ. Samples from Busted Butte also have been examined to determine whether surface weathering has changed the mineralogy, texture, or porosity from that found in underground samples to determine whether data from Busted Butte samples are representative of the upper litho-

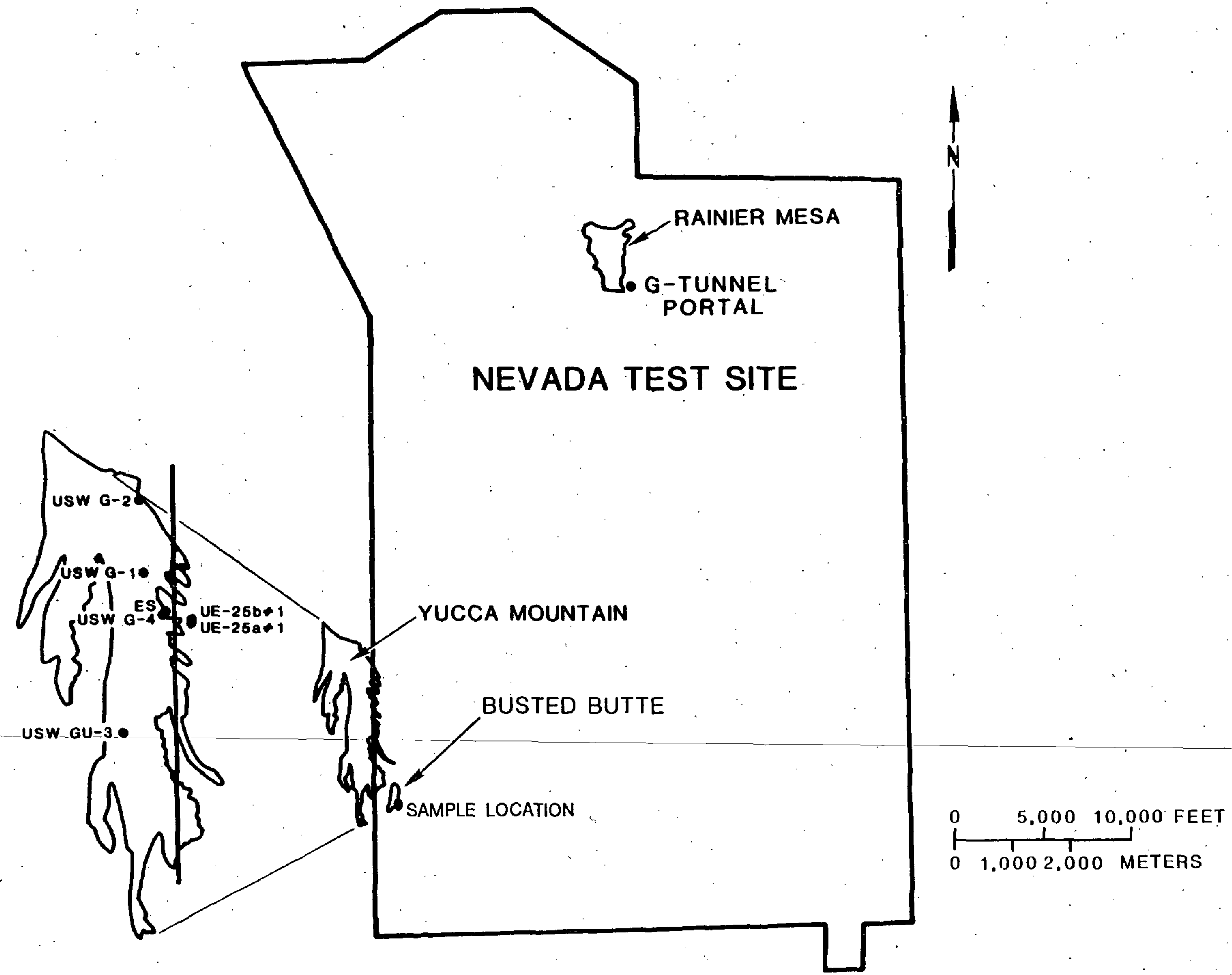

Figure 2-1. Locations of corehole samplings for the Yucca Mountain Project.

Table 2-1. Applicable test procedures from the American Society of Testing and Materials (ASTM) and the International Society for Rock Mechanics (ISRM)

Measurement	Test procedures[a]
Uniaxial compressive strength	ASTM D 2938-79 (ASTM, 1979b), ISRM (1979a)
Triaxial compressive strength	ASTM D 2664-80 (ASTM, 1980a), ISRM (Kovari et al., 1983)
Tensile strength (Brazilian test)	ASTM D 3967-81 (ASTM, 1981b), ISRM (1978)
Elastic properties (static)	ASTM D 3148-80 (ASTM, 1980b), ISRM (1979a)
Elastic properties (dynamic)	ASTM D 2845-83 (ASTM, 1983b),
Thermal conductivity	ASTM C 202-84 (ASTM, 1984),
Thermal expansion	ASTM E 228-71 (ASTM, 1971), (reapp. 1979)
Bulk density (paraffin coated)	ASTM C 97-83 (ASTM, 1983a), ASTM C 1188-83 (ASTM, 1983c), ISRM (1979b)
Grain density	ASTM C 135-66 (ASTM, 1966), (reapp. 1976), ASTM C 604-79 (ASTM, 1979a), ISRM (1979b)
Soil density	ASTM D 1556-82 (ASTM, 1982), ASTM D 1557-78 (ASTM, 1978), ASTM D 2922-81 (ASTM, 1981a)

[a]Complete citations are provided in references at the end of Chapter 2.

procedures. In developmental tests, such as those for the measurement of either time-dependent thermal expansion coefficients or joint slip, detailed documentation of the test procedures is provided in the technical procedure relevant to each type of test.

A second part of the data base development has been the field testing program currently under way in welded and nonwelded tuff in G-Tunnel. The extent of the underground openings in the G-Tunnel rock mechanics facility, which was developed as part of the Yucca Mountain Project rock mechanics program, is shown in Figures 2-2 and 2-3. The data from the experiments and observations in the welded Grouse Canyon Member of the Belted Range Tuff in G-Tunnel are especially valuable to the current design evaluation of the Topopah Spring Member emplacement horizon for the following reasons:

1. The bulk, thermal, and mechanical properties of both formations are similar (Zimmerman et al., 1984b). (Lithophysae are, however, not present in the Grouse Canyon Member welded tuff in G-Tunnel. A detailed comparison of properties is presented in Section 2.8.)

2. The overburden loadings and opening dimensions (up to 5-m span) are similar (Tillerson and Nimick, 1984).

3. The degrees of saturation are similar for geoengineering purposes (0.65 ± 0.19 in the Topopah Spring Member (Montazer and Wilson, 1984) versus 0.6 to 0.9 in the Grouse Canyon Member (Zimmerman et al., 1984b)); however, for hydrologic purposes these differences may be significant.

4. The degree and nature of fracturing are similar (Langkopf and Gnirk, 1986).

Field data and observations (thermal conductivity, elastic moduli, strength, support requirements, room and borehole stability, motion on fractures, and water migration) obtained in G-Tunnel will be used as supporting data for site evaluations and repository conceptual design for Yucca Mountain.

The G-Tunnel tests also will allow development of measurement techniques and instrumentation evaluations before testing in the exploratory shaft facility. As data are obtained from tests in the exploratory shaft facility, these newer data will supplement, and will eventually replace, G-Tunnel data as input to the design and site evaluation processes.

The data gathered to date, as described in this chapter, have been used in preliminary selection of conceptual models for heat transfer processes and mechanical constitutive models, and performance assessment and design analyses. The testing in which the data originated may be classified as exploratory in the sense that an initial examination has been made of many of the geoengineering properties important to determination of compliance with regulatory criteria.

Future data gathering will be guided by issue resolution strategies and will focus on properties for which insufficient data are available or on properties that have been identified as potentially important by analysis but which have not yet been considered in the experimental program. Such interactions among the issue resolution strategies, experiments, and calculations will occur throughout the future of the repository program as the understanding of the system and the relevant physical processes becomes increasingly sophisticated.

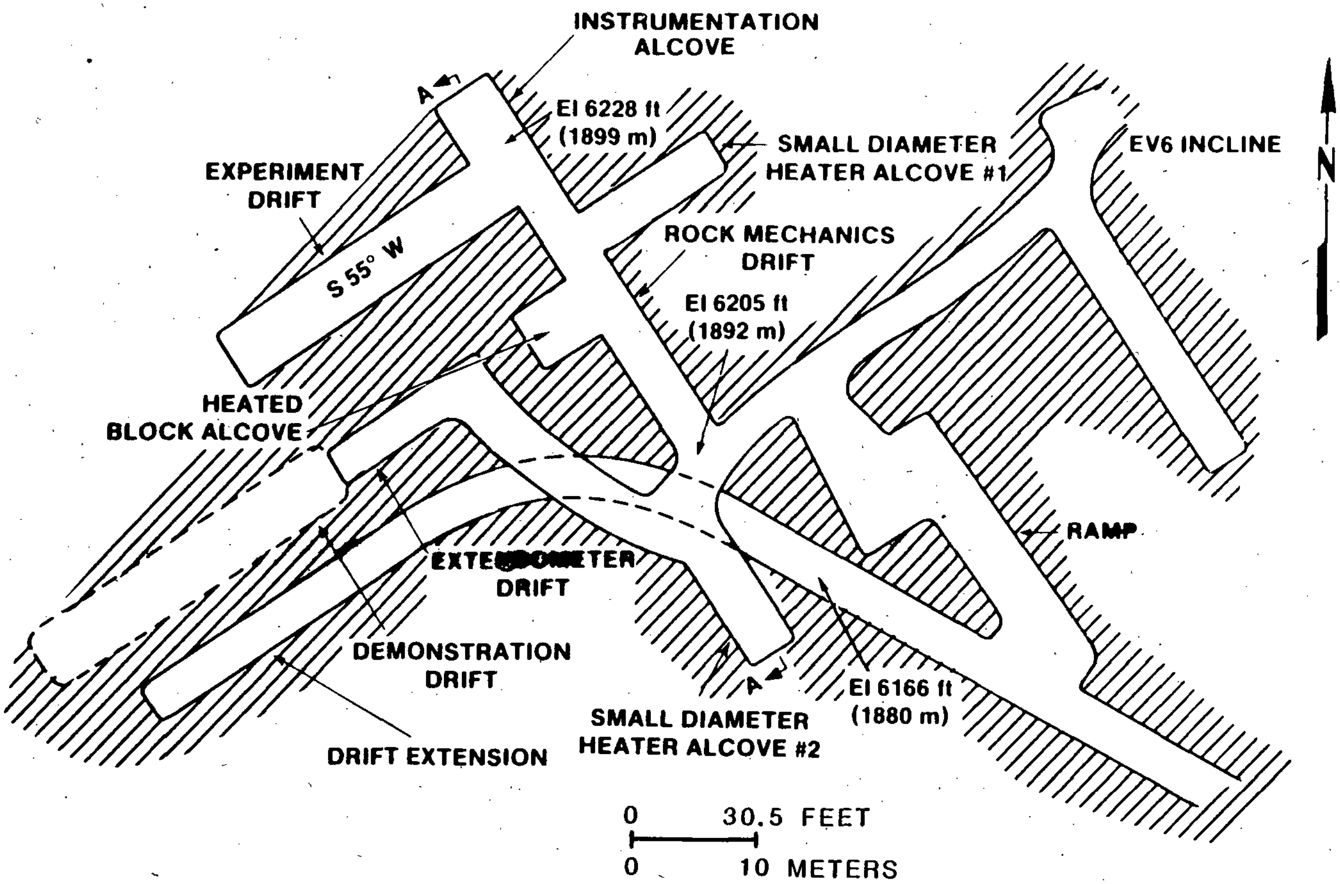

Figure 2-2. Plan view of G-Tunnel underground rock mechanics facility.

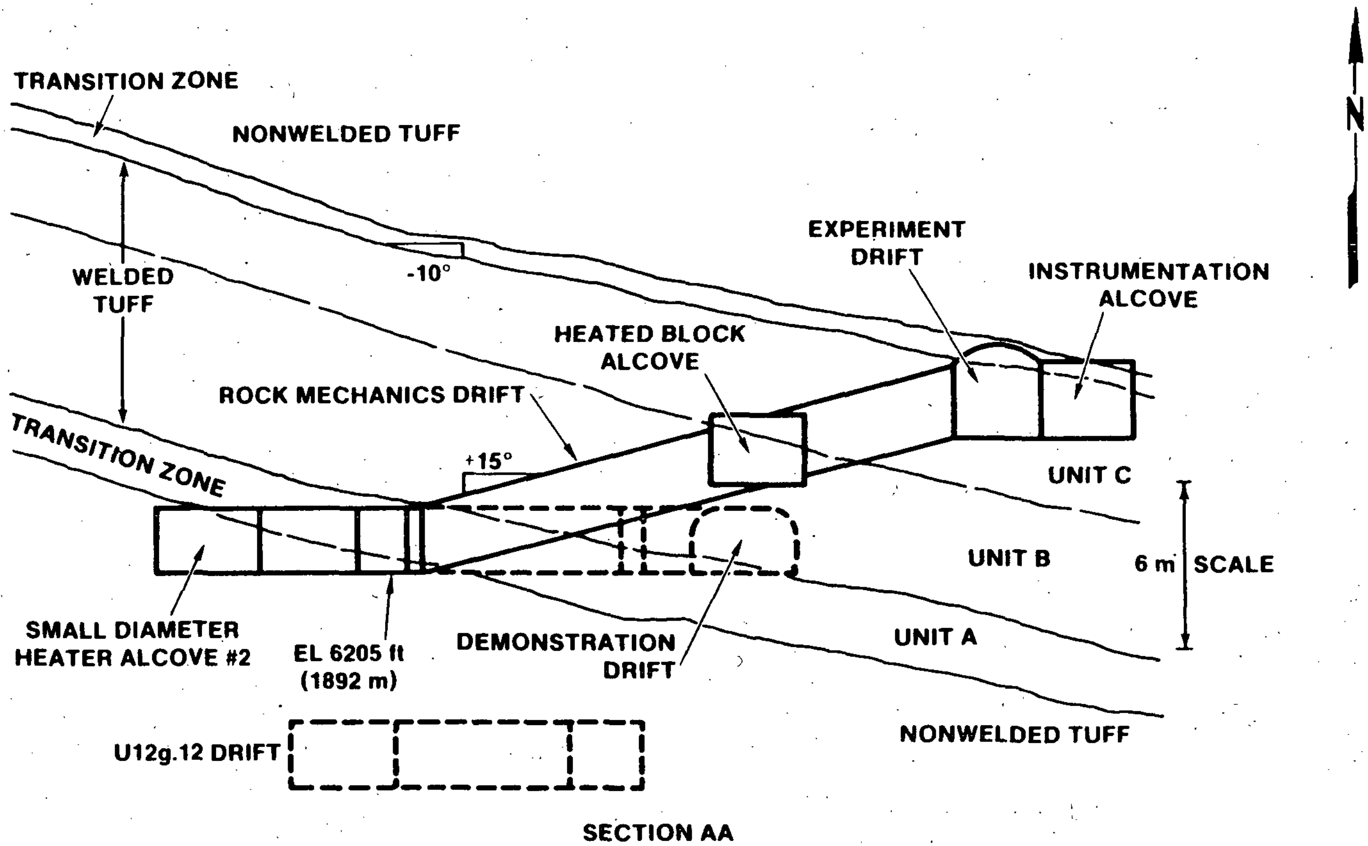

Figure 2-3. Elevation view of G-Tunnel underground facility.

DECEMBER 1988

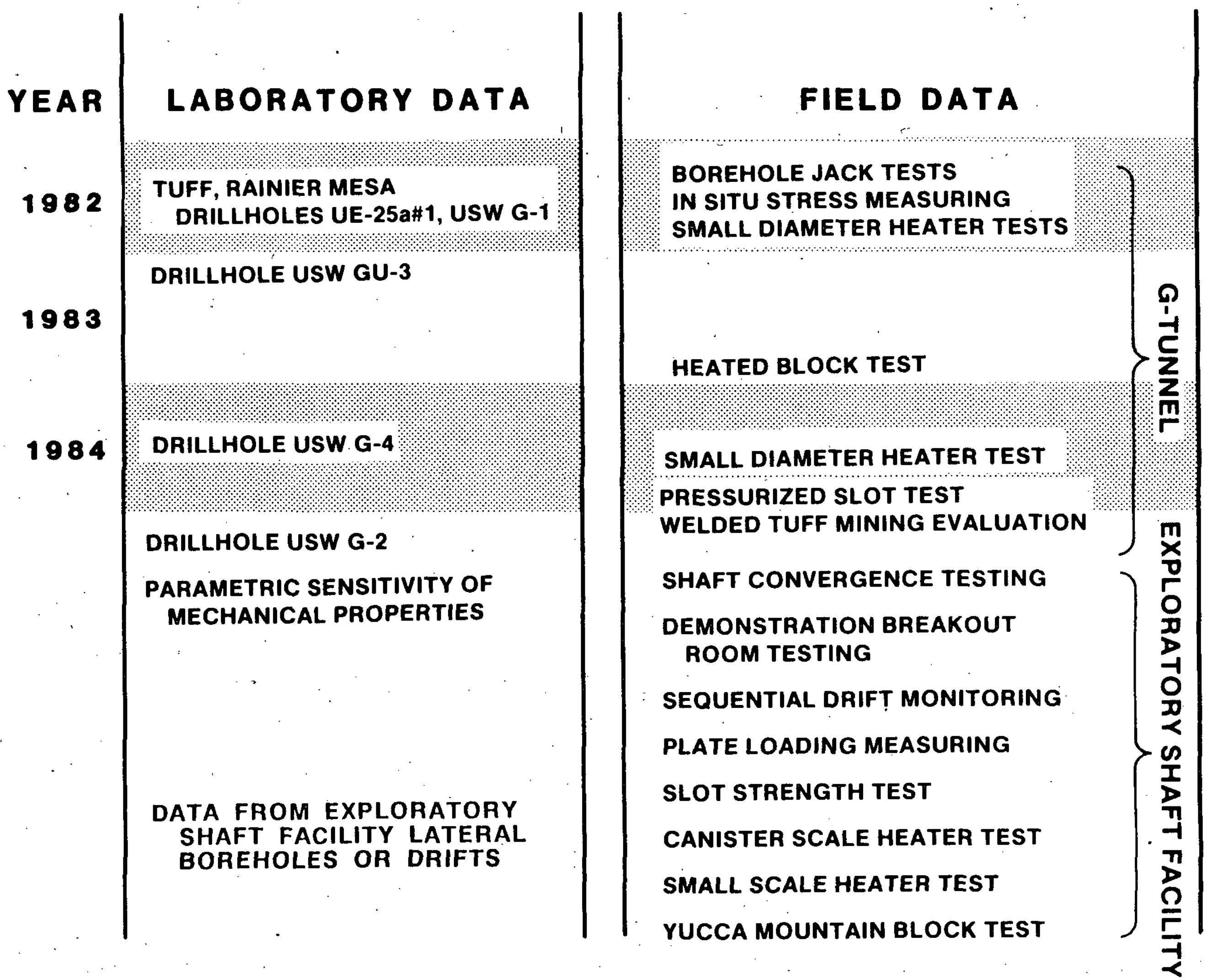

Figure 2-4. Data base development for host rock geoengineering properties.

SAMPLE SELECTION LOGIC

The procedures and philosophy used in sample selection for laboratory testing of cores from Yucca Mountain are important in assessing how representative the data base is of the in situ material. Within the Yucca Mountain Project, this philosophy has evolved with time. Both the inherent sampling limitations (both procedural and lithological) and the progression of the philosophy are described in the following discussion.

In general core from drillholes at Yucca Mountain is logged at the drill site, then transported to the core library at Mercury, Nevada, for storage. Some percentage of the core is wrapped and waxed at the drill site to preserve, as nearly as possible, the original moisture content of the rock as the core was removed from the ground. (The exact value of this original moisture content is not important in the determination of the properties discussed in Chapter 2 because the saturation state of the sample usually is changed before the measurement of thermal or mechanical properties.)

Several limitations to obtaining geoengineering property data have resulted from past coring procedures. Because the primary objective for every cored hole at Yucca Mountain has been the determination of the stratigraphic relationships in the cored interval, sections of core containing stratigraphic contacts had to be preserved in the Yucca Mountain Project core library. Thus, these sections were unavailable for thermal and mechanical testing. This procedural limitation has little impact on the testing of relatively thick units, such as the lower devitrified portion of the Topopah Spring Member, but it could hinder representative sampling in thinner layers.

A more important limitation has been that of sample size. Compressive mechanical tests have required samples at least 2.5 cm in diameter and 5.1 cm in length, and samples for confined thermal tests have had to be approximately 5 cm in diameter and 10 cm long. The core obtained from drillholes at Yucca Mountain typically is 6 cm in diameter. In addition, core from welded tuffs such as the Topopah Spring Member is often fractured (Section 1.3.2.3), which limits the number and size of samples available for testing. Larger core samples have been obtained from outcrop material (Section 2.1.2.3.1.7); tests on these samples and in situ tests will provide additional information about the properties of the material.

Another problem related to sample size occurs when zones containing lithophysae are considered. Many lithophysae are larger than the typical core diameter of 5.7 cm and even in locations in which smaller lithophysae are present, the cavities are often too large in relation to core (and thus to test sample) diameter for meaningful test results to be obtained. This latter sampling problem has been addressed by the collection of samples of lithophysal tuff from Busted Butte (Price et al., 1985) and by plans to test large samples of lithophysal tuff collected from the exploratory shaft.

The laboratory testing program was initiated in 1979. At that time, the program focus was to investigate generally several tuff formations located below the water table. Rather than obtaining samples from evenly spaced vertical intervals, emphasis was placed on testing core samples from below the water table in drillhole UE-25a#1 (particularly from the Bullfrog Member) and on a limited number of samples from other units.

During the testing of samples from drillhole USW G-1 (mid-1981 through mid-1982) and the initial tests made using core from drillholes USW G-2, USW G-3, and USW GU-3 core, two important events took place:

1. The concept of a functional engineering-properties stratigraphy was implemented (see next section). A functional stratigraphy categorizes units according to some set of characteristic properties; in this instance, mechanical and thermal properties.

2. The tuffs in the zone above the water table began to receive serious consideration for waste disposal.

The sampling process at this stage was designed to provide regularly spaced bulk-property data and thermal and mechanical measurements. Such sampling allows the thermal and mechanical properties of layered-tuff stratigraphies to be estimated with an accuracy that is adequate for input data for the needed analyses and computer codes. As a result of the revised sampling process, the uniformity of the coverage, especially with respect to bulk properties, is much better in these later drillholes. In addition, more samples were obtained in the Topopah Spring Member than were collected from drillhole UE-25a#1. Sample depths and frequencies at which bulk-property samples were to be taken from the continuous core were requested in drilling criteria before the initiation of each drillhole. The emphasis has been toward maintaining an even spacing of samples rather than toward selecting the best material in each interval.

Two additional considerations are being incorporated in the planning of future sample selection. In instances in which properties have not been reliably determined because of sample-size limitations, larger samples have been obtained from outcrop material and also will be obtained from the exploratory shaft.

Increasing attention is being paid to the number of measurements necessary to provide statistical confidence that a true measure of a property has been obtained. To date, replicate tests have been made sporadically to explore what statistical variation in properties is present in the tuff units. Ideally, the first step in a statistical determination of the number of replicate tests that will be necessary is to conduct parametric sensitivity studies to determine how well a property must be known. Such sensitivity studies have not been made but are planned (Section 8.3.5). As results from these studies become available, existing plans for sample selection (e.g., those for the laboratory tests described throughout Section 8.3) will be modified to optimize the number of tests for each geoengineering property.

STRATIGRAPHIC FRAMEWORK FOR TESTING

The increasing number of data on laboratory properties has provided increasing evidence that the formal stratigraphic units at Yucca Mountain, described in Section 1.2, could be subdivided into a different stratigraphy. In this functional stratigraphy, each unit has values of the bulk, thermal, and mechanical properties that are characteristic of that unit and at least one of which differs from the corresponding property for adjacent units. The functional division is better suited to the presentation of geoengineering properties than are the formal stratigraphic units, which may encompass large variations in mineralogic composition, porosity, and fracturing. Nevertheless, the formal stratigraphy provides a useful framework for defining functional stratigraphies. (Other functional stratigraphies are defined for hydrogeology and geochemistry.)

The first functional stratigraphy for Yucca Mountain, proposed by Lappin et al. (1982), was based on the bulk and thermal properties measured on tuff samples from drillhole USW G-1. Refinement of this initial stratigraphy to a system applicable to all Yucca Mountain (Ortiz et al., 1985) has resulted in the set of thermal/mechanical units shown in Figure 2-5, which also lists the lithologic equivalents of these units. The majority of the thermal/mechanical units are identifiable in all the drillholes at Yucca Mountain and, therefore, serve as a useful framework for examining the spatial variation of geoengineering properties. The proposed horizon for repository development is a nonlithophysal portion of the Topopah Spring Member. The Topopah Spring Member is composed of a number of distinct ash flows, some of which contain more lithophysae than others. Further, the lithophysae content varies laterally within individual flows. Therefore, although the major flows can be correlated reliably, they can be categorized only as nonlithophysal, moderately lithophysal, or heavily lithophysal. The actual lithopysae content can be predicted reliably only in these broad classes. The thermal/mechanical stratigraphy is used as such a framework for summarizing data on geoengineering properties in the remainder of Chapter 2, as well as in Section 6.1.2.

The thermal/mechanical stratigraphy as presently defined is based on the properties of intact rock. As more information on rock mass properties is obtained, the thermal/mechanical stratigraphy may need to be revised to better reflect the large-scale property variation.

To increase efficiency in performance assessment and design analyses, the Yucca Mountain Project is in the process of defining the parameters for which reference data are to be assigned for each of the thermal/mechanical units, and a reference data set is being collated. This data set will be updated periodically as new data become available. Thus, at any given time,

DEPTH (m)	DEPTH (ft)	THERMAL/ MECHANICAL UNIT	LITHOLOGIC EQUIVALENT
		UO	ALLUVIUM
		TCw	WELDED, DEVITRIFIED TIVA CANYON
		PTn	VITRIC, NONWELDED TIVA CANYON, YUCCA MOUNTAIN, PAH CANYON, TOPOPAH SPRING
200	500	TSw1	LITHOPHYSAL TOPOPAH SPRING; ALTERNATING LAYERS OF LITHOPHYSAE-RICH AND LITHOPHYSAE-POOR WELDED, DEVITRIFIED TUFF
	1,000	TSw2	NONLITHOPHYSAL TOPOPAH SPRING <u>POTENTIAL REPOSITORY HORIZON</u> (CONTAINS SPARSE LITHOPHYSAE)
400		TSw3	VITROPHYRE, TOPOPAH SPRING
	1,500	CHn1	ASH FLOWS AND BEDDED UNITS, TUFFACEOUS BEDS OF CALICO HILLS; MAY BE VITRIC (v) OR ZEOLITIZED (z)
		CHn2	BASAL BEDDED UNIT OF CALICO HILLS
		CHn3	UPPER PROW PASS
600	2,000	PPw	WELDED, DEVITRIFIED PROW PASS
		CFUn	ZEOLITIZED LOWER PROW PASS AND UPPER BULLFROG
800	2,500	BFw	WELDED, DEVITRIFIED BULLFROG
		CFMn1	ZEOLITIZED LOWER BULLFROG
		CFMn2	ZEOLITIZED BASAL BEDDED UNIT OF BULLFROG
		CFMn3	UPPER ZEOLITIZED TRAM
	3,000	TRw	WELDED, DEVITRIFIED TRAM

Figure 2-5. Thermal/mechanical stratigraphy at Yucca Mountain. (Depths and thicknesses plotted are averages from drillholes UE-25a#1, USW G-1, USW G-2, USW GU-3, and USW G-4.)

sources will be added as it becomes available. Interpretations of the thermal and mechanical properties and their statistical variations have relied heavily upon the use of the bulk-property data and mineralogic analyses to establish correlation. The properties for the thermal/mechanical units (including statistical variations) are described in Sections 2.1.3, 2.3.3, and 2.4.3.

Data gathering efforts are now directed at evaluating the mechanical behavior of the densely welded portion of the Topopah Spring Member, with emphasis on lateral variability; lithophysal effects; temperature, pressure, strain rate, and sample size effects on the mechanical properties of the matrix material; and the mechanical properties of the fractures.

CONCEPTUAL ROCK MECHANICS MODELS

The analysis of the response of the rock at Yucca Mountain to applied loads requires the definition of initial conditions, boundary conditions, material properties, process of heat transfer, and descriptions of the mechanical constitutive models that describe the rheologic behavior of the material. These requirements together contribute to the definition of the conceptual rock mechanics models being applied in the design process to understand the material response of Yucca Mountain.

The initial conditions for such a model are the geometry of the unit (see previous section on stratigraphic framework for testing), the pre-existing state of stress (Sections 1.3, 2.3 and 2.6), the in situ temperature

Section 8.3.1.15, where (1) Table 8.3.1.15-2 summarizes the current mechanical constitutive model representing the rheological behavior and material properties of the tuff units at Yucca Mountain, (2) performance measures and design parameters associated with the hypothesis are tabulated along with [illegible]

the sensitivity of the performance measures and design parameters to the hypothesis is described, and (4) testing activities designed to reduce the uncertainty in the selection of the current hypothesis are referenced.

The empirical approaches used in analyses of the mechanical behavior of the welded Topopah Spring Member, by definition, are not founded in system or theory. In contrast, state-of-the-art numerical methods are founded on constitutive laws that mathematically describe or define the physical nature of deformation of fractured tuff. The constitutive laws that have been selected to describe mechanical deformation of tuff are elastic, elastic-plastic, and compliant-joint. A description of each of these constitutive laws and the justification for their applications to tuff follows.

Almost all engineering materials possess to a certain extent the property of elasticity. The term "elastic" describes a material for which, if the external forces producing deformation do not exceed a certain limit, the deformation disappears with the removal of the forces. Chapter 2 discusses mechanical properties of both the intact rock and the rock mass that indicate that for certain stress and strain states tuff behaves as an elastic solid (Section 2.1.2.2). For example, like many other crustal rocks, the stress-strain response for intact tuff is approximately linear through approximately two-thirds of the short-term breaking strength.

The tuff rock mass at Yucca Mountain contains fractures, as described in Chapter 1. For large stress changes, the normal and shear behavior of fractures has been observed to be inelastic and nonlinear (Goodman, 1980). For small stress changes, such as those predicted in the vicinity of underground openings for the proposed tuff repository, linear elastic material behavior has been considered appropriate. This same material response has been considered appropriate in many mining applications. Field experiments in densely welded tuff performed over small (10 MPa) stress ranges intended to measure the rock-mass material response have thus far indicated that an elastic constitutive model can be used to adequately represent deformation of the yield surface (the boundary separating elastic and elastic-plastic behavior) changes during the deformation.

Elastic-plastic analyses have been used in some instances to assess the state of stress resulting from excavation and thermally induced loads. This type of constitutive description is considered applicable to a fractured rock mass because both slip on fractures and intact rock failure are mechanisms through which irrecoverable strain must be accounted for, given sufficient deviatoric stress. Two general types of plasticity models have been used by the Yucca Mountain Project. In the first model, a general yield condition may be satisfied by consideration of the deviatoric stress resulting from the general applied stress state. This type of analysis has been used extensively in assessments of stability of underground tunnels in other rock types (see summary and review by Goodman, 1980). In the second model, the yield condition may be satisfied by consideration of the deviatoric stress and a prescribed direction of fracturing. This second plasticity model has been called the ubiquitous joint model and carries with it the assumption that there is one predominant direction of fractures in the rock along which slip may be accommodated. Thus far, field studies at Yucca Mountain have indicated that the preponderance of fractures are near vertical (Spengler and Chornack, 1984), so that use of this type of model is considered to be justified.

Compliant-joint constitutive models (Thomas, 1982; Chen, 1987) are an extension and improvement upon the models just described. Extensive field and drillhole data at Yucca Mountain (Chapter 1) suggest that a constitutive model should incorporate the mechanical response of both the intact rock (matrix) and fractures. In general these models are composed of two parts: (1) a continuum-based technique to average the discontinuous displacements across fracture planes within a representative elementary volume and (2) a constitutive description based on the linear elastic behavior of the matrix material and the nonlinear behavior of the fractures. The constitutive model takes the continuum approach in the sense that every material point in the model behaves as would a representative elementary volume composed of a matrix material and a suitably large number of fractures. The total strains are decomposed into contributions from the matrix and fractures so that load sharing takes place. Normal and shearing motions of fractures are related to the conjugate stresses through the stiffness matrix.

Material property constants are required for both the rock matrix and the fractures. The matrix is assumed to be isotropic and linearly elastic, requiring specifications of only Young's modulus and Poisson's ratio. The assumed shear behavior of the fractures was deduced from laboratory experiments on fractures (Teufel, 1981; Olsson, 1987) to be elastic-perfectly plastic. The elastic part is described by a joint shear stiffness, and the plastic part is described by a linear slip criterion with a friction coefficient and cohesion. The normal stiffness is nonlinear elastic in accord with observed laboratory results (Goodman, 1980; Olsson, 1987). It is described by a hyperbolic function that contains two material constants: the half-closure stress and the unstressed aperture.

The compliant-joint model as described then contains the primary components that can contribute to mechanical deformation in a rock mass. Models of this type have been used to analyze field experiments in densely welded tuff (Zimmerman et al., 1986). In this experiment the stress changes imposed were small, so that the experiment cannot be used as a means to discriminate between this modeling approach and an elastic analysis.

The conceptual rock mechanics models, and especially the detailed treatment of the rheologic behavior of tuff, will continue to evolve as more data are obtained and as the understanding of the system matures. Such changes will be made as either test data or observed in situ behavior indicate the need for changes in the mathematical representations of the mechanical behavior of tuff.

The data described in Chapter 2 are necessary, but are not yet sufficient, for the complete implementation of the available rheologic models. Where the measured data required by a model are not available, values have been assumed based either on experimental data from similar rock types or on theoretical calculations, and tests to obtain the data are either underway or planned. Table 8.3.1.15-2 summarizes the need to reduce uncertainty in the existing data, and Section 8.3.1.15 describes tests planned to acquire additional data.

DATA UNCERTAINTY FOR GEOENGINEERING PROPERTIES

Evaluation of uncertainty associated with measured parameters has been addressed, where possible, by testing and sampling programs that are structured so that experimental uncertainty and sampling uncertainty are independently or jointly characterized.

Experimental uncertainty is attributed to variations in sample handling and preparation, instrument response, and human factors, which affect experimental outcome. Standard practice typically calls for evaluation of experimental uncertainty by repeated testing, replicate testing, or testing of special materials with known properties. Investigations of this type were [illegible]

Throughout the functional stratigraphy there are strong associations between index properties, such as porosity, and parameters for which data coverage is relatively sparse, such as strength and deformability. The most common reason for scarcity of mechanical properties test data is limited availability of samples, especially core samples of a minimum size. Correlations have been developed using data originating from wherever samples were available in the tuff sequence at Yucca Mountain and also from lithologically similar tuffs at G-tunnel. Generally there is some conceptual basis for using correlation with index properties. These correlations were used in compiling Table 2-7 (2.1.3) and are discussed in later sections as follows:

Compressive strength versus porosity	2.1.2.3.1.8
Tensile strength versus porosity	2.1.2.3.2
Coulomb failure criteria versus porosity	2.1.2.3.1.2
Young's modulus versus porosity	2.1.2.2

It is important to note that the data uncertainty for parameter values that are based on correlation with index properties is compounded by the uncertainty of index property determination and the uncertainty implicit in correlation. Parameter values based on correlation are presented for comparison purposes only and will eventually be replaced, if possible, with values based directly on test results. Accordingly, the relatively large standard deviations for values based on correlation are not included in Tables 2-7 (Section 2.1.3) or 2-14 (Section 2.4.3).

The properties of tuffs from locations other than Yucca Mountain, which have not been investigated by the Yucca Mountain Project, are presented in Chapter 2 for comparison purposes. Mechanical properties, large-scale mechanical properties, and thermal and thermomechanical properties for other rocks are tabulated in Tables 2-2 (Section 2.1.1), 2-8 (Section 2.3.1), and 2-10 (Section 2.4.1), respectively. These comparison data are typically from published studies for which uncertainty information is available in some form, but is not included in the tables because it is not applicable to site characterization. Another application of data from other rocks is the analysis of excavation characteristics and rock mass classification in Section 2.8.2.2 and 2.8.2.3. Rating systems for rock classification will be used in site characterization to evaluate conformity with design criteria. Uncertainty information is provided for these empirically derived ratings and support specifications in the form of a range of values that may apply to the site.

2.1 MECHANICAL PROPERTIES OF ROCK UNITS--INTACT ROCK

Predicting the mechanical response of the rock surrounding the repository requires knowledge of the properties of the intact (matrix) rock and the discontinuities that are present (joints, faults, fractures, and bedding planes). This section summarizes current information and data on the intact rock properties of tuff, including elastic constants and strength parameters. These and subsequent data will be used as input to the calculational models of the underground structures to evaluate the design and compliance with performance objectives. An extensive data base is required to understand the spatial distribution and variability of these properties, so that conservatism in the calculations is ensured.

The properties of intact rock samples represent upper limit values of the strength and deformability of the in situ rock mass, which includes discontinuities and other defects not reflected in the intact rock alone. The reduction of strength and stiffness typically observed in the field is a function of the frequency and nature of existing discontinuities (Section 2.2).

Detailed results of laboratory mechanical tests on samples from drillholes in Yucca Mountain are contained in numerous reports (Olsson and Jones, 1980; Blacic et al., 1982; Olsson, 1982; Price and Jones, 1982; Price and Nimick, 1982; Price et al., 1982a, b; Price, 1983; Price et al., 1984; Nimick et al., 1985). Data from these reports are discussed in Section 2.1.2.

These reports also include detailed discussions of sample treatment, equipment, experimental procedures, and calibrations. Most of the samples tested in compression have been right-circular cylinders with a diameter of 2.54 cm and a length-to-diameter ratio of approximately 2:1, which is in accord with the recommended American Society for Testing and Materials (ASTM) procedures (ASTM D 2664-80 (ASTM, 1980a), ASTM D 2938-79 (ASTM, 1979b)), but is less than the minimum ratio of 2.5:1 suggested by the International Society for Rock Mechanics (ISRM) (1979a). Because of this disagreement between the specifications, comparative tests on samples with a ratio of 2.5:1 or greater will be undertaken as discussed in Section 8.3.1.15.2. For the present purposes, however, the 2:1 ratio is advantageous because it allows more test samples to be obtained. Because the amount of core material is limited, the smaller sample size maximizes the statistical data base of individual measurements.

The effect of sample size on the mechanical properties of intact tuff is addressed further in Section 2.1.2.3.1.7. For most of the samples tested, the grain and flaw (pore) sizes were less than one-tenth of the specimen diameter. Thus, the effects of such individual features on the bulk mechanical properties are minimal.

Calibrations of force and displacement gages using materials with well-established properties before each experimental series have shown that the accuracy and the precision of these measurements are better than ±3 percent in all instances. The inference is that these accuracies and precisions are representative of those to be expected on tuff samples. Any major differences in mechanical properties for adjacent tuff samples, therefore, result from sample variability (mineralogic composition, porosity, grain density, crack frequency, etc.) or test conditions.

Tensile tests were performed on right-circular cylinders with nominal dimensions of 2.54 cm (diameter) and 1.25 cm (thickness) (Blacic et al., 1982). The Brazilian indirect strength test was the technique used because of the relative ease with which the test can be performed and because more samples could be tested than in other methods that require larger samples. The limitations of the Brazilian test are recognized (McWilliams, 1966); future testing will examine the applicability of existing data. No estimates of measurement errors have been made.

2.1.1 MECHANICAL PROPERTIES OF OTHER ROCKS

To provide a basis for understanding the mechanical behavior of the tuff at Yucca Mountain, it is appropriate to present a brief summary of mechanical properties of other tuffaceous rocks. A survey of the mechanical properties of tuff is provided by Guzowski et al. (1983). The data collected by these investigators on the mechanical properties of tuffs other than those discussed later in this section are summarized in Table 2-2. The table is intended to provide perspective on the ranges of the mechanical properties of tuff. Data for the welded, devitrified portion of the Topopah Spring Member (Section 2.1.2, especially Table 2-7, Section 2.1.3) indicates that the potential repository horizon (TSw2) has a high unconfined compressive strength and Young's modulus compared with other tuffs.

2.1.2 MECHANICAL PROPERTIES OF ROCKS AT THE SITE

2.1.2.1 Existing mechanical properties data

Detailed results of laboratory mechanical property tests on samples from drillholes at Yucca Mountain and from G-Tunnel at Rainier Mesa are contained in numerous reports (Olsson and Jones, 1980; Blacic et al., 1982; Price and Jones, 1982; Price and Nimick, 1982; Price et al., 1982a, b; Price et al., 1984; Nimick et al., 1985). These references cover approximately 280 unconfined compression tests, 100 indirect tensile tests, and 30 triaxial compression tests; the extent of the compressive tests is shown in Table 2-3. In addition, the results of all compression experiments performed on samples from drillholes UE-25a#1 and USW G-1 have been compiled (Price, 1983). Where possible, statistical evaluations of the data have been made. These evaluations have culminated in the data presented in Section 2.1.3 as the mechanical properties stratigraphy for the Yucca Mountain tuffs.

Test results for the elastic properties and the compressive and tensile strengths of Yucca Mountain tuffs are summarized in the next two sections. The discussion includes the current status of evaluations of the effects of water saturation, confining and fluid pressure, elevated temperature, time-dependent behavior, lithophysae, mechanical anisotropy, and sample size.

2.1.2.2 Elastic properties

Data on Young's modulus and Poisson's ratio have been collected for Yucca Mountain tuffs for use in modeling the elastic response of repository rooms, waste emplacement holes, and shafts. All the data are from compression experiments run on nominally fully saturated samples at atmospheric pressure (unconfined), a nominal strain rate of 10^{-5} s^{-1}, and room temperature (23°C). The test conditions were chosen as baseline conditions because the majority of compressive tests on Yucca Mountain tuff samples to date have been performed under these conditions. The applicability of the data to other temperatures, pressures, or strain rates is being evaluated in an ongoing test program, as discussed in Section 8.3.1.15.

Table 2-2. Summary of mechanical properties of tuffs not studied by the Yucca Mountain Project[a]

Location or tuff unit	Unconfined compressive strength (psi)[b]	Young's modulus (10^6 psi)[b]	Poisson's ratio	Lithology[c]
Ohya tuff, Japan	0.804	--[d]	--	Nonwelded
Rainier Mesa tuff units	1,350-5,125	0.45-2.26	0.09-0.38	Nonwelded
Tuff, E-Tunnel, NTS[e]	3,500	--	--	Nonwelded
Tuff, NTS	5,282-9,512	--	--	--
Oak Springs Formation, NTS	3,400-8,700	0.40-1.60	0.02-0.04	Bedded
Oak Springs Formation, NTS	6,800-29,100	0.86-1.75	0.05-0.15	Welded
Tuff, Oregon	3,141-4,999	0.85	--	--
Tuff, Red Hot Deep Well Experiment, NTS	1,560-4,910	0.33-0.95	0.13-0.49	--
Tuff and tuff breccia, USSR	--	3.23	0.13	--
Tuff, Japan	--	1.32-3.47	--	--
Tuff breccia, India	--	0.20-3.62	--	--
Tuff, locality unknown	--	0.99-2.92	--	--

[a]Source: Guzowski et al. (1983).
[b]To convert from psi to Pa, multiply the entries by 6,895.
[c]Lithologies have been assessed on the basis of original references when available.
[d]-- = data not available.
[e]NTS = Nevada Test Site.

Table 2-3. Summary of compressive mechanical testing for the Yucca Mountain Project. Numbers of compressive mechanical tests performed at baseline test conditions[a] and with variations in one or more test parameters.

		Thermal/ mechanical	Number of tests						
Reference	Drillhole or location	unit or formation[b]	Confining pressure	Saturation	Temperature	Sample size	Strain rate	Standard tests	Total[c]
Olsson and Jones (1980)	UE-25a#1	TCw	3	--[d]	1	--	--	1	4
		PTn	3	--	--	--	--	1	1
		TSw1	1	--	1	--	--	1	2
		TSw2	2	--	--	--	--	1	3
		CHnlz	3	--	--	--	--	2	5
		PPw	3	--	--	--	--	0	3
		CFUn	--	--	--	--	--	2	2
		BFw	3	--	--	--	--	1	4
	G-Tunnel	Grouse Canyon	--	9	--	--	20	0	20
Blacic et al. (1982)	UE-25a#1	TSw1	--	--	--	7[e]	--	0	7[e]
		TSw2	--	--	--	20[e]	--	0	20[e]
		[illegible]	[illegible]	[illegible]	[illegible]	[illegible]	[illegible]	[illegible]	[illegible]

Figure 2-6 is a representative plot of axial stress versus axial strain measured on a sample of welded, devitrified tuff from the Topopah Spring Member. The figure demonstrates the strong linearity of the deformation response to a stress on the order of 95 percent of the failure stress. This behavior is typical for intact samples of this material, suggesting that the rock matrix of the Topopah Spring Member is an elastic material, at least for the baseline test conditions.

A preliminary study of the effects of differences in confining pressure and strain rate on the mechanical properties of the Topopah Spring Member from drillhole USW G-4 has been completed (Nimick et al., 1985). No definitive trend in Young's modulus was found as a function of either effective confining pressure or strain rate for the ranges tested (0 to 10 MPa; 10^{-3} to 10^{-7} s^{-1}). Additional studies of the effect of differences in test parameters on the mechanical properties of the Topopah Spring Member are ongoing using outcrop material, and a test series will be conducted on material from the exploratory shaft facility (Section 8.3.1.15.1). Both of these test series include variations in temperature and saturation as well as in confining pressure and strain rate.

An early study (Olsson and Jones, 1980) suggested that the elastic moduli of the Grouse Canyon Member are anisotropic. The results of this study indicated a correlation between the degree of welding (i.e., the amount of porosity) and the degree of anisotropy. Whereas welded tuff is stiffest perpendicular to bedding (i.e., approximately vertical), the nonwelded tuff is stiffest parallel to bedding (i.e., approximately horizontal). The dynamic elastic moduli for samples of the densely welded Topopah Spring Member from drillhole USW GU-3 showed that anisotropy of elastic properties for orientations parallel and perpendicular to the rock fabric is insignificant (Price et al., 1984). On the basis of these results, the matrix of the Topopah Spring Member is assumed to be isotropic. The tests planned to investigate the possibility of anisotropic elastic response and strength anisotropy in samples from the Topopah Spring Member are discussed in Section 2.1.2.3.1.6.

Values have been obtained for dynamic elastic moduli for 10 samples of the Topopah Spring Member from drillhole USW GU-3 (Price et al., 1984). In general, dynamic Young's moduli were higher than static values measured on the same samples, whereas Poisson's ratios were approximately the same for both methods. The ratio of the average dynamic to the average static Young's modulus for the samples is 1.30, well within the range of ratios described by Lama and Vutukuri (1978).

Analyses to determine the correlation between the elastic properties and porosity, grain density, and mineralogic composition were performed to assess the possibility of extending such a relationship to other tuffs on which mechanical testing has not been performed (Price, 1983; Price and Bauer, 1985). Data for the analyses reported by Price (1983) were taken from compressive tests conducted at the baseline conditions on samples from the Bullfrog Member, the Tram Member, and the tuffaceous beds of Calico Hills. The analysis of the data set, which includes results from the Topopah Spring Member, is summarized by Price and Bauer (1985) and in the paragraphs that follow:

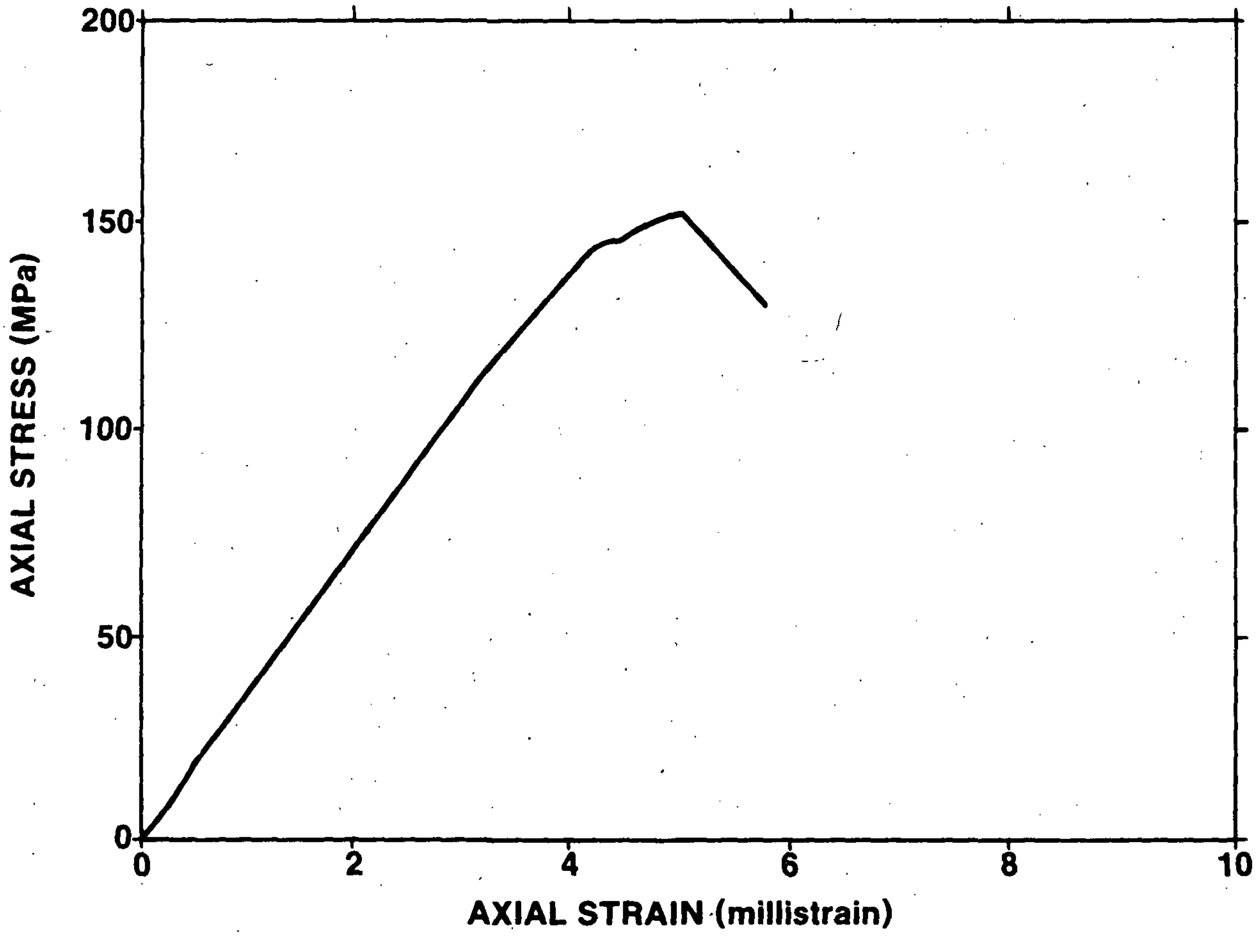

Figure 2-6. Representative axial stress-axial strain plot for the welded, devitrified Topopah Spring Member (test sample GU-3 1050.4/3; test conditions ambient temperature and pressure, saturated, $10^{-5}/_{s}$) Modified from Price et al. (1984).

Price (1983) determined that there is a correlation between the porosity of tuff and the Young's modulus. Test data for 111 samples of Yucca Mountain tuffs have been fit by linear least squares (Price and Bauer, 1985) to provide the following equation relating the two parameters:

$$E = 85.5e^{-6.96n} \qquad (2\text{-}1)$$

where E is Young's modulus (GPa) and n is the functional porosity (volume fraction), defined as the sum of the volume fraction of void space and the volume fraction of clay in the sample.

The correlation coefficient (r) for this fit is 0.93. The range in n for which the equation is thought to be valid is approximately 0.10 to 0.65. However, the equation does not apply to welded vitric tuff (vitrophyre). The grain structure and bonding in a vitrophyre are sufficiently different from those in all other types of tuff at Yucca Mountain so that the physical processes leading to successful application of the correlation in equation 2-1 do not occur in the vitrophyre.

For the analysis of data on Poisson's ratio, Price (1983) reports using a multivariate fit. This fit has not been revised to include the data from the Topopah Spring Member. The equation relating Poisson's ratio to porosity and grain density as given by Price (1983) has an r value of 0.48. The correlation is not considered useful for estimating Poisson's ratio from these other measured properties.

Additional analyses will be performed as more data become available. The results should increase the confidence in estimates of the Young's modulus of tuff with a given porosity and grain density.

2.1.2.3 Matrix compressive and tensile strengths

2.1.2.3.1 Compressive strength

Compressive strength values have been documented (Olsson and Jones, 1980; Olsson, 1982; Price and Jones, 1982; Price and Nimick, 1982; Price et al., 1982a,b; Price, 1983; Price et al., 1984; Nimick et al., 1985) for a wide range of tuff samples from Yucca Mountain. Additional data are being gathered and will be available before the start of exploratory shaft activities.

2.1.2.3.1.1 Effect of water saturation on compressive strength

A series of drained uniaxial compression tests were run to quantify the effect of water saturation on the compressive strength of tuff (Olsson and Jones, 1980). Closely spaced samples were obtained from the Grouse Canyon

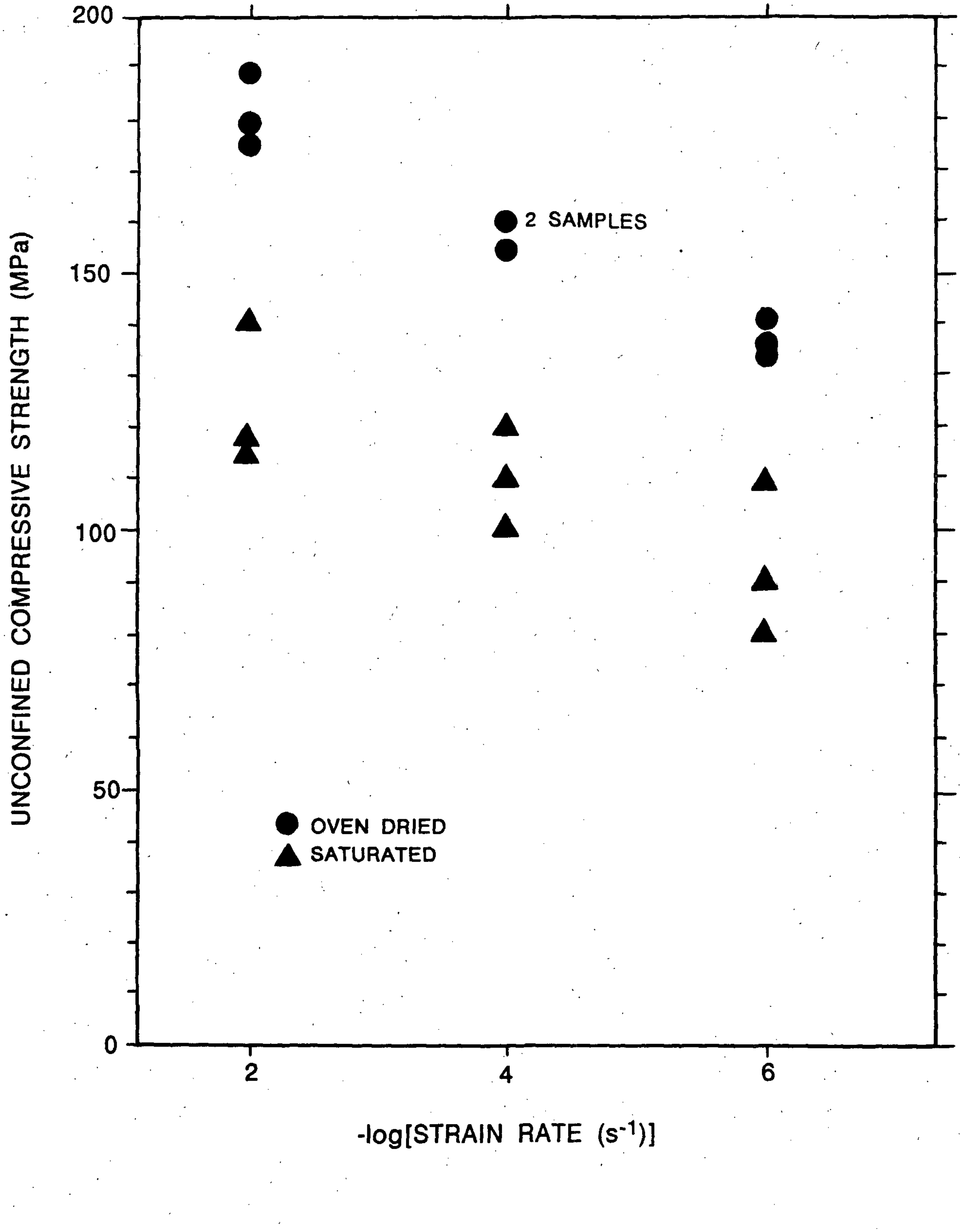

Figure 2-7. Compressive strength as a function of strain rate for dry and saturated samples of Grouse Canyon Member. Modified from Olsson and Jones (1980).

Table 2-4. Effects of saturation and strain rate on the compressive strength of tuff samples from the Grouse Canyon Member[a]

Strain rate (s^{-1})	Compressive strength (MPa)	Young's modulus (GPa)
	UNSATURATED SAMPLES	
10^{-2}	175	25.9
10^{-2}	189	28.7
10^{-2}	177	28.4
10^{-4}	160	26.2
10^{-4}	155	28.5
10^{-4}	160	27.4
10^{-6}	135	27.4
10^{-6}	141	28.3
10^{-6}	134	29.5
	FULLY SATURATED SAMPLES	
10^{-2}	142	26.1
10^{-2}	114	22.8
10^{-2}	118	23.8
10^{-4}	112	24.8
10^{-4}	122	25.3
10^{-4}	102	24.0
10^{-6}	81.1	25.9
10^{-6}	110	25.4
10^{-6}	91.8	26.8

[a]Source: Olsson and Jones (1980). These data were obtained on tuff samples from the Grouse Canyon Member in unconfined, ambient temperature, uniaxial compression tests allowed to drain during testing. The porosity of all samples was estimated to be 13 to 18 percent.

each strain rate, the average strengths of nominally saturated specimens are approximately 30 percent lower than the average strengths of the corresponding dry samples. Data from another seven samples of the Grouse Canyon Member (Board et al., 1987) showed that the mean strengths of vacuum-saturated samples were approximately 15 percent lower than the mean strengths for corresponding dry samples. Similar results were obtained in four experiments on samples of the tuffaceous beds of Calico Hills (Price and Jones, 1982). These tests were conducted at approximately the same conditions (unconfined pressure, a constant strain rate of 10^{-5} s^{-1}, room temperature) with two fully saturated specimens and two room-dry specimens (unknown degree of saturation). The average strength of the saturated specimens was approximately 23 percent lower than the average strength of the air-dried samples.

The data just summarized indicate that water-saturated tuff is expected to have a lower compressive strength than tuff in which the saturation is less than 100 percent. Use of the strengths measured on saturated samples as input to calculations in support of the design process thus will add a degree of conservatism to the process. A quantitative estimate of this conservatism is not possible because the saturation state will vary during the history of a repository. Tests of samples from the exploratory shaft facility and surface outcrops will be conducted to investigate the effects of variations in temperature, saturation, confining pressure, and strain rate on the mechanical properties (including deformation modulus and compressive strength of the Topopah Spring Member).

2.1.2.3.1.2 Effects of confining and fluid pressure on compressive strength

Numerical analyses of the structural stability of mined openings, boreholes, and shafts require the use of a strength criterion for the rock. The commonly used criterion is the coulomb criterion, which defines the limiting state of stress for static equilibrium within the material at which inelastic deformation begins (Jaeger and Cook, 1979). The criterion itself is expressed as follows:

$$\tau = \tau_o + \sigma \tan \phi \qquad (2\text{-}2)$$

where

τ = shear stress on the failure plane at the onset of failure

σ = normal stress on the failure plane at the onset of failure

τ_o = cohesion

ϕ = angle of internal friction

Uniaxial and triaxial compression tests are used to determine these parameters.

Twenty sets of triaxial compression tests on 90 tuff samples have been run (Olsson and Jones, 1980; Olsson, 1982; Price and Jones, 1982; Price et al., 1982b; Morrow and Byerlee, 1984; Nimick et al., 1985). The experimental results for the test series in which all samples were obtained from a single location or depth were fit by using linear least squares to obtain the Coulomb parameters (cohesion and angle of internal friction) as listed in Table 2-5. The correlation coefficients for the fit also are

Table 2-5. Summary of coulomb failure criteria parameters[a]

Thermal/ mechanical unit[b]	Depth (m) USW G-4	Depth (m) USW G-1	Depth (m) UE-25a#1	Effective pressure (MPa)	Temp- erature (°C)	Strain rate (s^{-1})	Satu- ration (S,R)[c]	Drained condition (Y,N)[d]	Cohe- sion (MPa)	Angle of internal friction (°)	Correlation coefficient
TCw	--[e]	--	26.7	0,10,20	23	10^{-4}	R	N	28.1	68.0	0.89
TSw2	--	--	381.0	0,10,20	23	10^{-4}	R	N	17.5	66.7	0.999
TS[c]	--	--	--	10,20,30,50	23	10^{-4}	S	N	92.0	29.1	0.47
TS[c]	--	--	--	10,20,30,40	23	10^{-6}	S	N	48.9	45.6	0.70
TSw2	209.3	--	--	0,5,10	23	10^{-5}	S	Y	37.1	51.8	0.31
TSw2	294.2	--	--	0,10	23	10^{-5}	S	Y	47.4	27.2	0.16
CHn1z	426.9	--	--	0,5,10	23	10^{-5}	S	Y	6.6	15.9	0.45
CHn1z	--	453.4	--	0,10,20	23	10^{-5}	S	Y	10.2	11.1	0.04
CHn1z	--	453.4	--	0,10,20	23	10^{-5}	S	N	10.6	7.8	0.62
CHn1z	--	507.6	--	0,10	23	10^{-5}	R	N	10.2	32.2	0.96
CHn1z	--	507.6	--	0,10,20	23	10^{-5}	S	N	13.2	6.8	0.55
CHn1z	--	508.4	--	0,10	23	10^{-5}	S	N	9.7	4.8	0.21
BFw	--	759	--	5,12.5,20.7	200	10^{-4}	S	Y	23.6	19.6	0.93
BFw	--	759	--	5,10,20.7	200	10^{-4}	R	Y	16.5	37.7	0.89
BF[f]	--	--	--	10,30,40,50	23	10^{-4}	S	N	22.7	42.1	0.93
BF[f]	--	--	--	10,20,30,40,50	23	10^{-6}	S	N	15.2	44.3	0.98

[a]Olsson and Jones (1980); Olsson (1982); Price and Jones (1982); Price (1983); Morrow and Byerlee (1984); Nimick et al. (1985).

[b]Unit identifications, thicknesses, and relation to the formal stratigraphy are shown in Figure 2-5.

[c]Saturation: R = room dried (unknown degree of saturation) and S = fully saturated.

[d]Drained condition: N = undrained and Y = drained .

[e]Data not available.

Four of the test series were conducted on room-dry samples. Three of these four series were at ambient temperature, two were on welded tuffs and one was on nonwelded tuff (tuffaceous beds of Calico Hills). The friction angles in the two welded tuffs are similar (68.0 and 66.7 degrees), whereas the cohesion of tuff from the Topopah Spring Member is lower than that of the Tiva Canyon Member. Both the cohesion and the friction angle are lower for the nonwelded tuff than for the welded tuffs. The one test series conducted on room-dry samples at 200°C used moderately welded tuff from the Bullfrog Member; the test results cannot be directly compared with those for ambient-temperature tests because of differences in both porosity and temperature.

Two test series were run on outcrop samples from the Bullfrog Member at two different strain rates. The results suggest that the friction angle is not sensitive to the strain rate. Cohesion, on the other hand, decreases with the strain rate. This behavior follows that of unconfined compressive strength (Section 2.1.2.3.1.4).

The seventh test series for which a relatively high correlation coefficient was obtained was conducted at 200°C. Comparison with the results from ambient temperature tests on similar material (Bullfrog Member) suggests that the friction angle decreases with increasing temperature but that cohesion is unaffected.

The observations in the preceding paragraphs are inconclusive because they are based on limited data. Mechanical tests on tuff samples have shown large variability at any single set of test conditions, especially for compressive strength. Thus, the trends inferred from the limited available data may be either spurious or real. More definitive conclusions cannot be made until more data become available. Additional scoping tests on the welded portion of the Topopah Spring Member are being conducted, and a test program with a better statistical basis has been designed for the Topopah Spring Member (Section 8.3.1.15).

In general both the cohesion and the friction angle are inversely confining pressures of 5, 10, and 20 MPa. Three samples were saturated and tested at effective pressures (confining pressure minus pore-fluid pressure) of 5, 12.5, and 20 MPa. The test results are provided in Figure 2-8. Although data are limited to these seven tests, the results indicate that the concept of effective stress developed for other porous rocks (Hubbert and Willis, 1957; Handin et al., 1963) may hold for tuff as well. Additional testing to examine pore pressure and confining pressure effects on the mechanical properties of the Topopah Spring Member is discussed in Section 8.3.1.15.

2.1.2.3.1.3 Effects of elevated temperature on compressive strength

The strength of most engineering materials (metals, plastics, concretes, rocks) decreases with increasing temperature. The experimental data on tuff at elevated temperatures are limited (Olsson and Jones, 1980; Olsson, 1982; Price, 1983), and the data from the 15 tests completed to date are inconclusive in quantifying strength changes. The tests differed not only in temperature but also in other test conditions (pressure, strain rate, and confining pressure) and intrinsic rock properties (density and porosity). A test series on cores of the Topopah Spring Member has been initiated to evaluate the strength and deformability of samples at elevated temperatures, and additional tests are planned for the exploratory shaft activities (Section 8.3.1.15.).

2.1.2.3.1.4 Rate-dependent behavior and effect on compressive strength

The strength of rock depends on of the rate of loading or strain. The possibility that the compressive strength of the Topopah Spring Member is rate-dependent must be assessed to help establish a conservative lower bound on this parameter.

The data from 5 series of experiments on site-specific tuffs (Price and Jones, 1982; Price et al., 1982b; Nimick et al., 1985; Nimick and Schwartz, 1987) are listed in Table 2-6, while the results from 2 series on Rainier Mesa tuffs (Olsson and Jones, 1980) are listed in Table 2-4. The test series show average strength decreases of 3 to 14 percent per order-of-magnitude decrease in the strain rate. The sequence of experiments on the Topopah Spring Member reported by Price et al., (1982b) showed virtually no strain rate effect on strength, but the 3 other test series on this material showed decreases of 5 to 14 percent per order-of-magnitude decrease in the strain rate (Nimick and Schwartz, 1987). No effect of strain rate was observed for the Topopah Spring and Bullfrog members when tested at elevated confining pressures (Morrow and Byerlee, 1984). These results showing no rate dependence may reflect the physical and mineralogical variability of the samples tested. Because of a lack of adjacent samples, the core used by Price et al., (1982b) was from an interval ranging from 371.3 to 390.0 m in depth (drillhole USW G-1) and, therefore, probably had a range of physical and mineralogical characteristics. The effects of variations in strain rate on the compressive strength of the Topopah Spring Member are being examined, and additional tests are planned as part of the exploratory shaft program (Section 8.3.1.15).

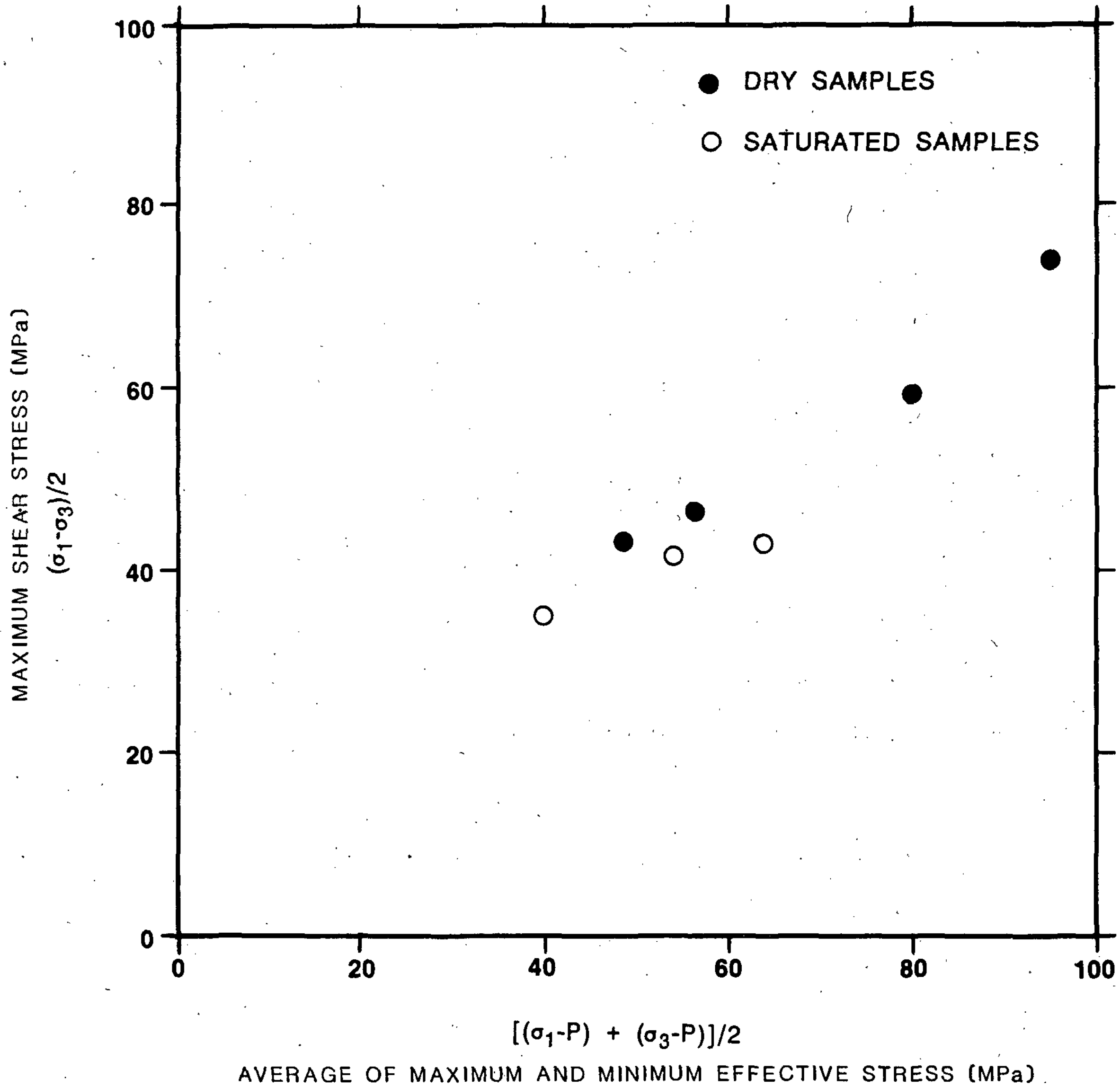

Figure 2-8. Maximum shear stress at failure for the Bullfrog Member, as a function of the average of maximum and minimum effective stresses (Mohr diagram for triaxial tests). Key: σ_1 = maximum normal stress, σ_3 = minimum normal stress, and P = pore pressure.

Table 2-6. Effects of changes in strain rate on rock strength for Yucca Mountain tuffs[a]

Unit[b]	USW G-1 depth (m)	USW G-4 depth (m)	Strain rate (s^{-1})	Strength (MPa)	Axial strain to failure (%)	Young's modulus (GPa)	Poisson's ratio	Reference[c]
TSw2	372.5	--[d]	10^{-2}	157.2	0.48	29.2	0.31	P
TSw2	384.8	--	10^{-2}	149.7	0.49	36.6	--[d]	P
TSw2	372.5	--	10^{-4}	133.8	0.57	27.7	--	P
TSw2	373.0	--	10^{-4}	157.2	0.46	37.5	0.25	P
TSw2	371.3	--	10^{-6}	176.6	0.51	40.8	0.25	P
TSw2	373.0	--	10^{-6}	156.6	0.47	35.3	0.21	P
TSw2	390.0	--	10^{-6}	44.9	0.41	22.9	0.27	P
TSw2	--[d]	226.4	10^{-3}	319	0.95	37.4	0.29	N1
TSw2	--	226.4	10^{-3}	283	0.94	34.0	0.28	N1
TSw2	--	226.4	10^{-3}	280	0.89	38.4	0.25	N1
TSw2	--	226.4	10^{-5}	235	0.72	35.6	0.21	N1
TSw2	--	226.4	10^{-5}	256	0.83	36.8	0.21	N1
TSw2	--	226.4	10^{-5}	279	0.93	34.6	0.21	N1
TSw2	--	226.4	10^{-7}	243	0.69	37.5	0.20	N1
TSw2	--	226.4	10^{-7}	230	0.75	33.6	0.11	N1
TSw2	--	305.5	10^{-5}	179	0.56	33.6	0.32	N1
TSw2	--	305.5	10^{-5}	137	0.45	31.1	--[e]	N1
TSw2	--	305.5	10^{-7}	123	0.44	22.0	0.11	N1
TSw2	--	305.5	10^{-7}	138	0.45	32.8	0.20	N1
TSw2[f]	--	--	10^{-5}	167	0.46	42.0	0.30	N2
TSw2[f]	--	--	10^{-5}	157	0.33	49.0	0.26	N2
TSw2[f]	--	--	10^{-7}	115	0.30	41.9	0.26	N2
TSw2[f]	--	--	10^{-7}	117	0.32	42.1	0.26	N2
CHnlz	508.4	--	10^{-3}	24.7	0.61	5.41	0.33	PJ
CHnlz	508.4	--	10^{-3}	23.4	0.58	5.45	--[e]	PJ
CHnlz	508.4	--	10^{-5}	25.4	0.57	6.15	0.36	PJ
CHnlz	508.4	--	10^{-5}	16.7	0.43	4.92	0.18	PJ
CHnlz	508.4	--	10^{-7}	21.5	0.55	7.86	0.21	PJ
CHnlz	508.4	--	10^{-7}	19.9	0.51	7.03	0.22	PJ

[a]Data from unconfined, ambient temperature, constant-strain-rate tests on saturated samples allowed to drain during testing.

[b]Unit identifications, thicknesses, and relation to formal stratigraphy are shown in Figure 2-5.

[c]References: P = Price et al. (1982b); PJ = Price and Jones (1982); N1 = Nimick et al. (1985); N2 = Nimick and Schwartz (1987).

[d]The symbol "--" in this column indicates that the column is not relevant to the row in which the dashes appear.

[e]Data not available.

[f]Samples from drillhole USW G-2, 289.1 m depth.

To predict rock behavior that is nonlinearly rate-dependent, Costin (1983) has developed a preliminary model that uses the assumption that rate- and stress-dependent microcrack growth is responsible for the deformation observed in mechanical tests on low-porosity (<15 percent) materials. The evolution of microcrack density is specified by extrapolating the experimentally determined behavior of single cracks to that of a random ensemble of microcracks. In the Costin (1983) model, stress corrosion is assumed to be the dominant mechanism of rate-dependent crack growth. Therefore, the model assumes an initial population of microcracks that is modified by the stress history.

As a test of the model's capability, simulations of uniaxial compression tests were performed at various strain rates over the range 10^{-1} to 10^{-10} s^{-1}. The material parameters of the model were chosen to match those of the previously tested Grouse Canyon Member (Olsson and Jones, 1980). The results of the simulation are compared with the mechanical data in Figure 2-9 (data are the same as those shown in Figure 2-7 for saturated samples).

For strain rates between 10^{-2} and 10^{-6} s^{-1}, the model predictions show a reasonable agreement with the limited experimental data that are available. The model predicts that at lower strain rates, the strength decrease with strain rate is less than that indicated by a linear extrapolation from the experimental data. Because in situ strain rates are expected to be lower than the limit of 10^{-10} s^{-1} for which the model has been applied (on the order of 10^{-12} to 10^{-13} s^{-1} before the permanent closure of the repository)

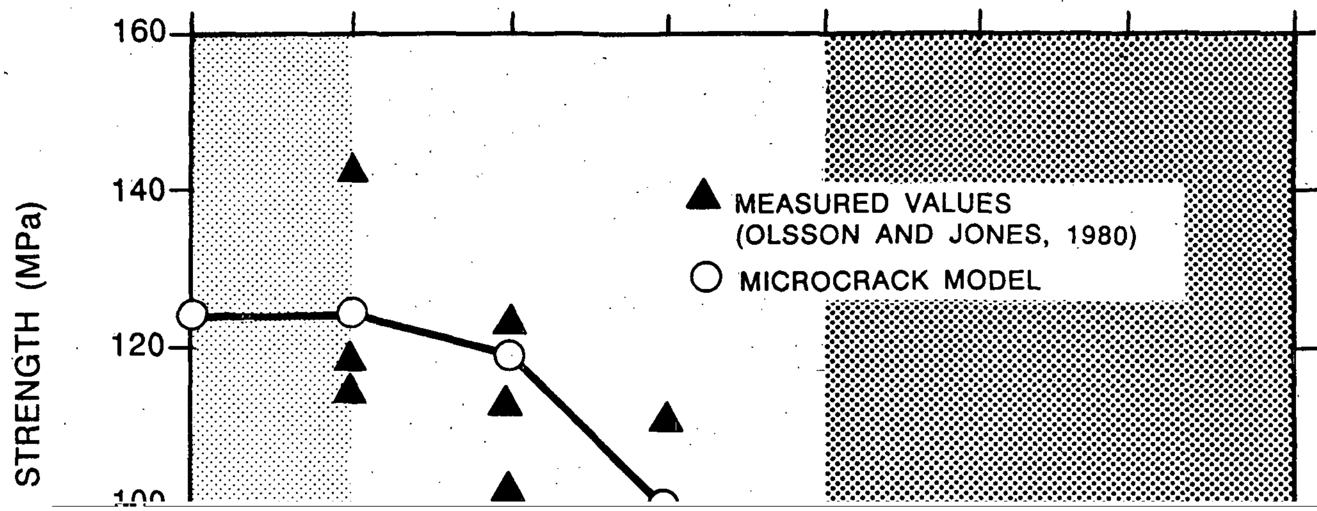
160
140
120
STRENGTH (MPa)
MEASURED VALUES
(OLSSON AND JONES, 1980)
MICROCRACK MODEL

Mountain Project, only portions of the Topopah Spring Member have been observed to contain abundant lithophysal cavities. Ten samples of lithophysae-rich Topopah Spring Member collected from an outcrop at Busted Butte (Figure 2-1) have been deformed in mechanical tests (Price et al., 1985). Samples were right-circular cylinders with diameters of 26.7 cm and lengths of 53.3 cm and contained lithophysal cavities up to several centimeters in diameter. The tests were conducted at room temperature, atmospheric pressure, and a strain rate of 10^{-5} s^{-1}. In addition, to obtain a lower bounding value for strength, the samples were water saturated. The resulting unconfined compressive strengths ranged from 10.3 to 27.8 MPa, somewhat lower than those predicted by the model presented in Section 2.1.2.3.1.8 for the porosities (31 to 40 percent) measured for the samples (Price et al., 1985). The lower strengths probably are due to the large cavity sizes in relation to the sample diameter. Tests on larger samples from the exploratory shaft facility are planned to confirm these results (Section 8.3.1.15).

2.1.2.3.1.6 Anisotropy of compressive strength

To date, all mechanical experiments, except those on five samples of the Topopah Spring Member from drillhole USW GU-3, have been performed on samples with their loading axes parallel with the original coring direction; i.e., approximately vertical and, therefore, approximately perpendicular to bedding (Price et al., 1984). (For orientation of units, see Section 1.2.2.) Tests on samples of the Topopah Spring Member taken from the outcrop at Busted Butte will be conducted to quantify the degree of anisotropy in the elastic properties and in the unconfined compressive strength. The test series, discussed in Section 8.3.1.15, will include measurements on adjacent samples with at least three different orientations to the dominant rock fabric.

2.1.2.3.1.7 Sample size effects on compressive strength

Most tests completed to date have been performed on samples that have a diameter of 2.5 cm and a length of 5 cm. Because of defects (inhomogeneities and fractures) inherent in the rock samples, size effects are expected in both the strength and the deformation behavior of the tuff. Sample size effects are expected to result in lower rock strengths and moduli for the larger samples (Bieniawski and Van Heerden, 1975). A series of unconfined compression tests on samples with diameters of 2.5, 5, 8.3, 12.7 and 22.8 cm has been completed (Price, 1986). A power-law fit to the test results gives the following equation:

$$\sigma_c = 1944D^{-0.846} + 69.5 \quad (2\text{-}4)$$

where σ_c is unconfined compressive strength in MPa and D is sample diameter in mm.

Additional tests will be performed on samples from the exploratory shaft facility, as discussed in Section 8.3.1.15.1.

2.1.2.3.1.8 Statistical correlation of compressive strength and functional porosity

Approximately the same sets of tests (unconfined compression, constant strain rate, room temperature on saturated samples) analyzed for elastic properties were also studied to determine whether the uniaxial strength could be related to functional porosity or grain density (Price, 1983; Price and Bauer, 1985). The results showed that changes in compressive strength between samples can be correlated with changes in functional porosity (except for the vitrophyre of the Topopah Spring Member, as discussed in Section 2.1.2.2).

With the availability of data from the Topopah Spring Member, the analysis of data from 113 samples has provided the following empirical relationship (Price and Bauer, 1985):

$$\sigma_c = 4.04n^{-1.85} \quad (2\text{-}5)$$

where σ^c is the unconfined compressive strength (MPa) and n is expressed as a volume fraction.

The correlation coefficient r for this fit is 0.93. The approximate range of n for which this correlation is valid is 0.10 to 0.60.

Analysis of existing data by Nimick and Schwartz (1987) suggests that the equation given above will provide a reliable estimate of the unconfined compressive strength of unit TSw2 (see Figure 2-5 for definitions of units). The equation estimates strengths that are lower than experimental values for the nonlithophysal portion of unit TSw1. Additional analysis is under way to refine the equation.

2.1.2.3.2 Tensile strength

Data on the tensile strength of Yucca Mountain tuffs can be used in the interpretation of in situ stress data obtained by hydraulic fracturing or in the definition of a failure criterion for intact rock. Tensile strengths of Yucca Mountain tuff were calculated from Brazilian (indirect tensile) tests on 20 samples from 4 lithologic units (Blacic et al., 1982). The relationship between these calculated tensile strengths and the corresponding porosities is approximately linear, as determined by Price (1983) and shown in Figure 2-10. This linear relationship may be used for a first-order approximation of the tensile strength of any tuff from Yucca Mountain for which physical properties have been determined; however, a linear extrapolation to lower porosities than those already tested may not be reasonable. As described in Section 8.3.1.15, additional tests on outcrop material are planned to measure the tensile strength of the Topopah Spring Member. The measurements will include both direct tensile tests and Brazilian tests on adjacent material in order to assess the applicability of existing data obtained by the latter test method. In addition, some tensile strength data will be obtained from samples of the Topopah Spring Member from the exploratory shaft facility.

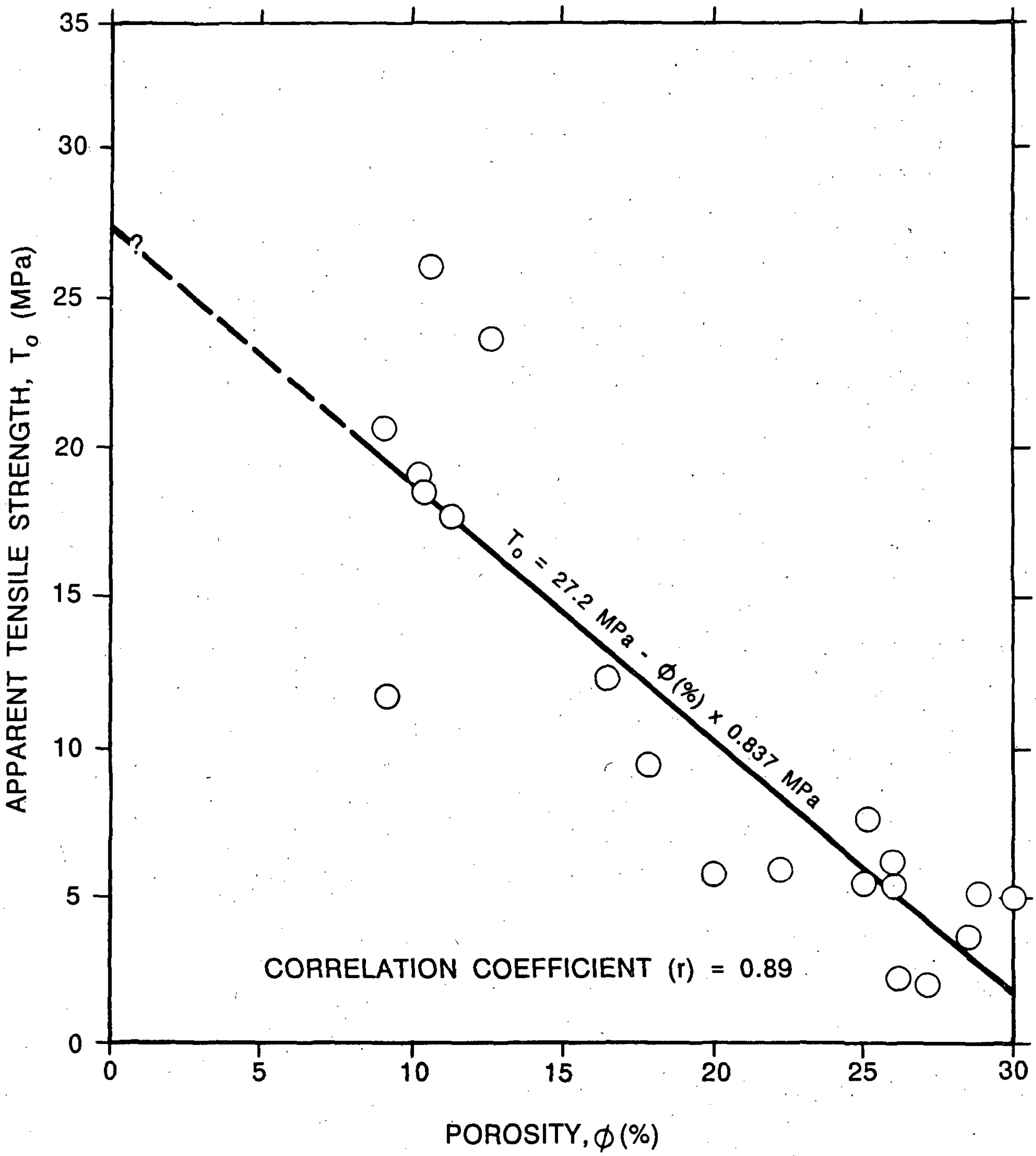

Figure 2-10. Apparent tensile strength of saturated Yucca Mountain tuff as a function of porosity. Modified from Price (1983)

2.1.3 STRATIGRAPHIC VARIATIONS OF THE MECHANICAL PROPERTIES OF TUFF

To reduce the large volume of data referenced in the preceding sections to a comprehensible basis for analyses of the repository conceptual design, a mechanical-property stratigraphy has been defined (Figure 2-5 and Table 2-7). Each zone in the thermal/mechanical stratigraphy represents an interval for which mean matrix mechanical properties (and, in some instances, standard deviations) have been determined. Zone boundaries were defined to reflect changes in mineralogical and bulk properties (hence, significant changes in the mechanical properties) and are not always the same as the formal (geologic) stratigraphic divisions described in Section 1.2. The properties presented in Table 2-7 for each zone are the results of experiments where data are available. For other zones, the values of properties have been calculated from the empirical equations presented in Sections 2.1.2.2 and 2.1.2.3 relating mechanical properties to functional porosity, using mean porosity values given in Section 2.4.3. As discussed in Sections 2.1.2.2 and 2.1.2.3, the correlations cannot be used for the vitrophyre of the Topopah Spring Member (unit TSw3).

The bulk properties used to calculate mechanical properties are discussed in Section 2.4.2.4. The properties predicted with the correlation equations in Section 2.1 inevitably will differ somewhat from experimental data, primarily because of the natural variability of the various tuff units.

2.2 MECHANICAL PROPERTIES OF ROCK UNITS--DISCONTINUITIES

Discontinuities (e.g., joints, faults, bedding planes) and inhomogeneities (e.g., lithophysae and inclusions of pumice or lithic fragments) cause the mechanical response of the rock mass to be different from that of the unfractured intact rock. In general, the strength and deformation modulus of the rock mass will be lower than that of the matrix material. The approach taken in the Yucca Mountain Project has been to include the effects of lithophysae and inclusions in studies of intact rock properties (Section 2.1). Thus, this section addresses only the mechanical properties of joints, faults, and bedding planes. Data concerning the geologic and mineralogic characteristics of these features at Yucca Mountain are provided in Chapter 1.

In conventional mine design approaches, the effects of fractures are approximated by assuming that the effective rock mass strength is some percentage of the strength measured for intact material, as shown by experience in similar rocks. More detailed stress analyses use the frictional properties (cohesion and coefficient of friction), orientation, and spacing of joints to determine whether slip can occur along the discontinuities and to evaluate the impact of the slip on support requirements or the usability of the opening. The unique aspect of repository analyses and testing is that the changes in the joint properties with temperature need to be bounded to evaluate opening stability at the temperature expected in the rock before permanent closure. Analyses to bound the effects of possible underground conditions in the tuff will be made to determine whether there are likely to

Table 2-7. Mechanical properties for intact rock in the Yucca Mountain tuff zones

Zone[a]	Young's modulus (GPa)	Poisson's ratio	Unconfined compressive strength (MPa)	Tensile strength (MPa)	Angle of internal friction (°)	Cohesion (MPa)
TCw	40.0	0.24 (TSw2)[b]	240	17.9	44.7	51
PTn	3.8	0.16 (CHnlz)[b]	19	1.0	8.5	8
TSw1	31.7±17.9[c,d]	0.25±0.07[c,d]	127±16[c,d]	21.1±4.6[c]	34.9[c]	36[c]
	15.5±3.2[d,e]	0.16±0.03[d,e]	16±5[d,e]	1.0[e]	12.5[e]	11[e]
TSw2	30.4±6.3[d]	0.24±0.06[d]	166±65[d]	15.2	23.5[d]	34.5[d]
TSw3	NA[g]	NA	NA	NA	NA	NA
CHnlv	7.1	0.16 (CHnlz)[b]	27	1.0	12.0	11
CHnlz[f]	7.1±2.1[d]	0.16±0.08[d]	27±9[d]	1.0	7.6±2.6[d]	10.9±1.6[d]
CHn2	11.5	0.16 (CHnlz)[b]	40	2.6	16.4	15
CHn3	7.1	0.16 (CHnlz)[b]	27	1.0	12.0	11
PPw	16.3	0.13 (BFw)[b]	57	6.9	21.0	20
CFUn	7.6±3.8[d]	0.16 (CHnlz)[b]	31±11[d]	1.8	15.6	14
BFw[f]	10.8±4.7[d]	0.13±0.02[d]	42±14[d]	6.9	21.0	20
CFMn1	15.2	0.16 (CHnlz)[b]	52	6.0	19.9	19
CFMn2	16.3	0.16 (CHnlz)[b]	57	6.9	21.0	20
CFMn3	13.2	0.16 (CHnlz)[b]	45	4.3	18.0	17
TRw[f]	17.6±3.8[d]	0.13 (BFw)[b]	72±23[d]	11.1	27.6	27

[a]Zone identifications, thicknesses, and relation to formal stratigraphy are shown in Figure 2-5.
[b]Value assumed to be the same as mean value of thermal/mechanical unit listed in parentheses.
[c]Representative of nonlithophysal zones within unit TSw1.
[d]Experimental results for mechanical properties at baseline test conditions (see text); standard deviations are 1σ. All other mechanical data entries are calculated using porosity with empirical equations; no standard deviations are available for these entries.
[e]Representative of lithophysal zones within unit TSw1.
[f]Zones previously considered for waste emplacement horizon.
[g]NA = not available.

be regions where significant support is required to maintain a stable opening. The data from laboratory tests on jointed tuff that form the basis of current detailed stress analyses are discussed below.

Laboratory-derived mechanical properties of joints are believed to provide data applicable to the mechanical properties of faults and bedding planes (Barton, 1973; Byerlee, 1978). Therefore, current investigations have concentrated on the laboratory properties of joints. Initial tests used simulated joints (precut) in about 60 samples of both welded and nonwelded tuffs to determine the coefficient of friction for the joints and to compare the results with those for other rock types. The use of relatively smooth simulated joints is a reasonable means of estimating lower-bound properties for natural fractures, especially for exploratory tests; however, inferences about the behavior of natural fractures that can be drawn from test results may be limited. Additional tests are being conducted on samples of the Topopah Spring Member with both simulated and natural joints, as discussed in Section 8.3.1.15. The applicability of these data ultimately will be determined by comparison with larger-scale in situ tests.

The data discussed below constitute an initial data base for conceptual design and performance assessment modeling studies. Such studies are required to ensure compliance of a repository with regulatory criteria. Specifically, to estimate stability of openings, the retrievability of the emplaced waste, and the effect of potential changes in joint apertures on ground-water movement and radionuclide releases, the response of joints to the presence of a repository must be understood.

In the laboratory tests performed on joints, specimens in the form of right-circular cylinders with sawcuts at 35 degrees to the cylinder axis were deformed in triaxial compression at room temperature, confining pressures to 40 MPa, and axial displacement rates from 10^{-2} to 10^{-6} cm/s with various saturation states (Olsson and Jones, 1980; Teufel, 1981). Because neither the American Society for Testing and Materials nor the International Society for Rock Mechanics has published standard procedures for jointed-rock testing, these reports include detailed discussions of the test apparatus, instrumentation, sample preparation techniques, and test procedures.

2.2.1 MECHANICAL PROPERTIES OF DISCONTINUITIES IN OTHER ROCKS

The magnitude of shear stress that can be transmitted across a joint depends on the cohesion and the frictional properties of the joint, or joint infilling, or both. Shear-strength parameters for discontinuities in similar rock types have been reviewed and are summarized here to allow comparison with the tuff properties presented in the remainder of Section 2.2.

higher value is probably not a true friction angle at low normal stresses, because multiple surfaces are involved in sliding (Patton, 1966). At higher normal stresses, surface roughness becomes less significant because asperities are sheared off and incorporated into gouge along the sliding surface. Quasi-static measurements of coefficients of friction for joints of differing surface roughness in a wide variety of rock types have been compiled (Byerlee, 1978). They show that the coefficient of friction ranges from 0.4 to 1.0 at normal stresses greater than 10 MPa. The results of an experimental study (Teufel, 1981) on simulated joints in welded tuff are consistent with Byerlee's compilation. Normal stresses across the joints in the experi-

2.2.2.1 Simulated fractures

Teufel (1981) determined the shear strength in triaxial compression of a simulated joint in the welded Grouse Canyon Member as a function of normal stress, time of stationary contact, displacement rate, and saturation. Joints were simulated by using a right-circular cylinder with a precut inclined at 35 degrees to the cylinder (load) axis. Room temperature tests were conducted at confining pressures from 5 to 40 MPa, at axial displacement rates from 10^{-2} to 10^{-6} cm/s, and with both dry and fully saturated samples.

The shear strength of a simulated joint in welded tuff fits the linear relation

$$\tau = \tau_o + \sigma \tan \phi \quad (2\text{-}6)$$

where

τ = shear strength
τ_o = cohesion
σ = applied normal stress
ϕ = friction angle
$\tan \phi$ = coefficient of friction.

The coefficient of friction at the initiation of slip was found to be independent of the normal stress for air-dried samples, with a value of 0.64 at a displacement rate of 1.2×10^{-4} cm/s (Figure 2-11). Similar results ($\tan \phi = 0.59$) were obtained for air-dried samples of partially welded tuff (Prow Pass Member) at a displacement rate of 10^{-3} cm/s (Olsson and Jones, 1980) (Figure 2-12). Data provided by Morrow and Byerlee (1984, Figure 2) can be used to derive a coefficient of friction of 0.59 for the initiation of slip in saturated samples of the Topopah Spring Member at a strain rate of 10^{-4} s^{-1} (equal to a displacement rate on the fracture surface of approximately 7×10^{-4} cm/s). The independence of the coefficient of friction with respect to the confining pressure and the corresponding normal stress across the sliding surface is consistent with rock-friction literature as reviewed by Byerlee (1978). However, at low normal stresses the coefficient for friction of rough natural joints may have some dependence on normal stress. This possibility will be examined in future testing (Section 8.3.1.15).

Data presented by Morrow and Byerlee (1984, Figures 2 and 6) suggest that the coefficient of friction increases with progressive-shear displacement across a joint. For saturated samples of the Topopah Spring Member at a strain rate of 10^{-4} s^{-1}, the increase would be from 0.59 to 0.76.

2.2.2.2 Natural joints

The mechanical properties of natural and artificial joints in the Topopah Spring Member are being investigated. The natural joints present at Yucca Mountain can be categorized into three groups: (1) healed joints with mineralized surfaces, (2) unhealed joints with no infilling, and (3) unhealed joints with infilling. Frictional behavior will depend on the composition of the infilling. From a mechanical effects standpoint, the behavior of the

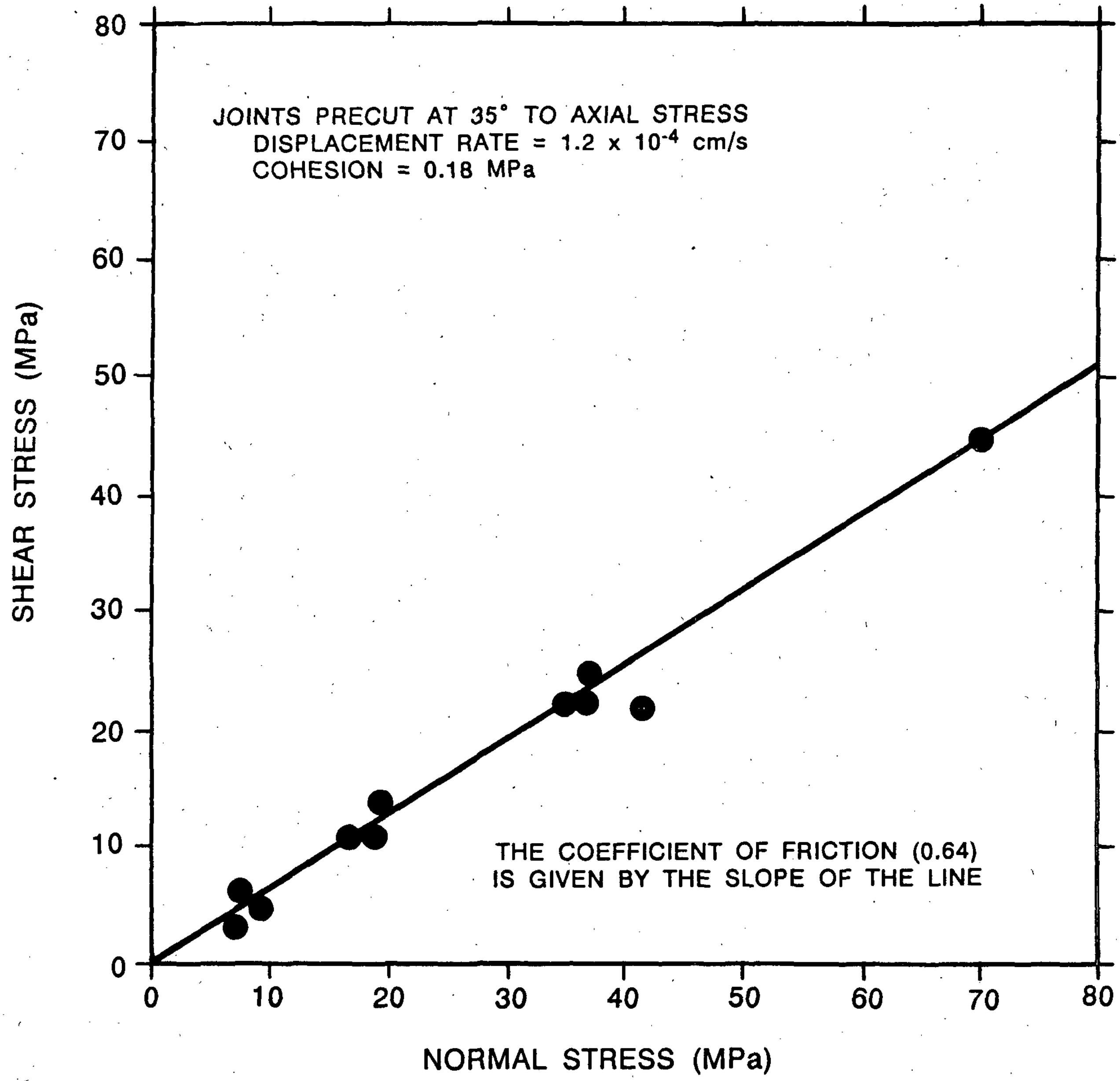

Figure 2-11. Shear stress-to-normal stress relation at slip initiation for air-dried, precut joints in Grouse Canyon Member welded tuff. Modified from Teufel (1981).

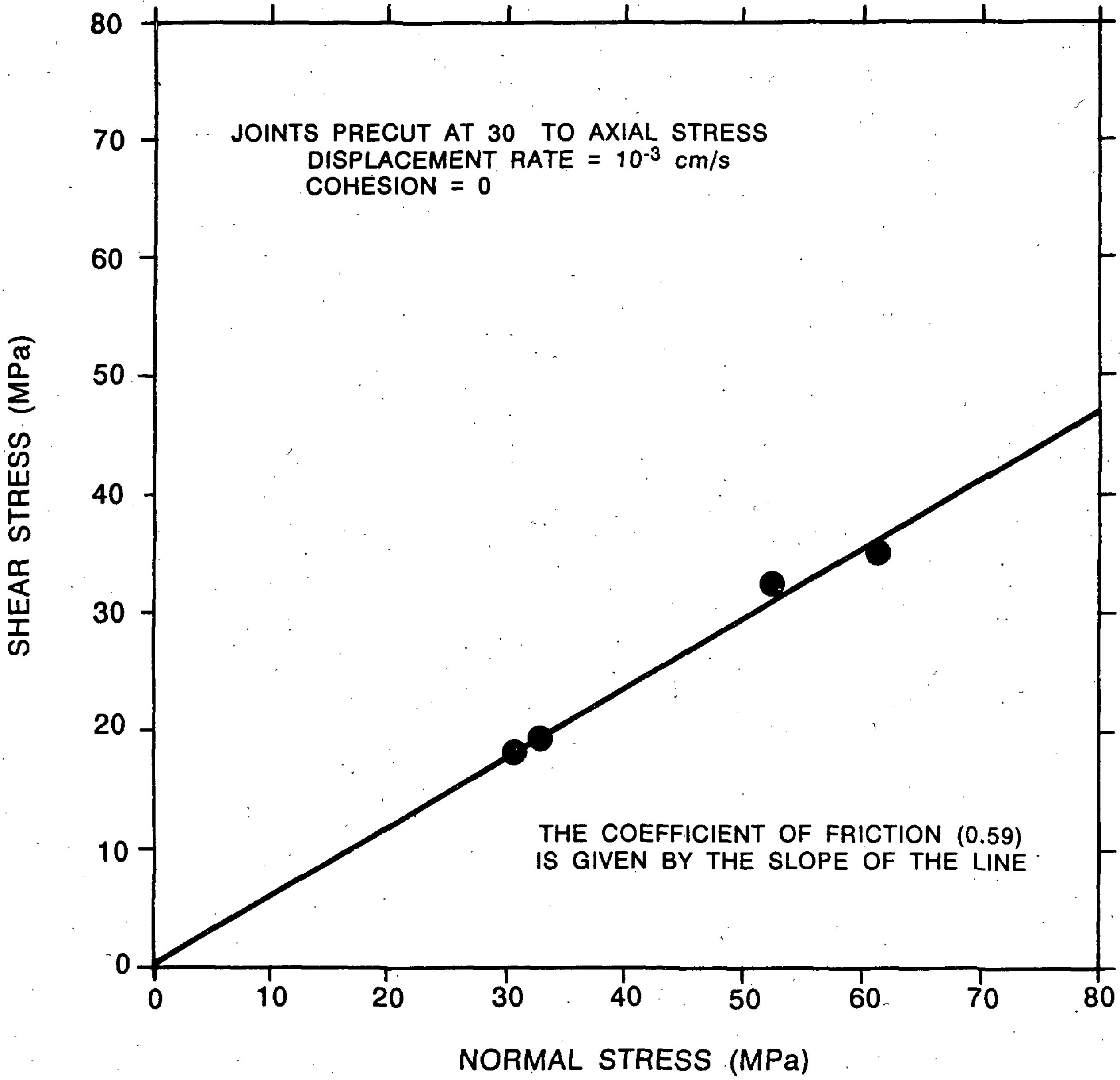

Figure 2-12. Shear stress-to-normal stress relation at slip initiation for air-dried, precut joints on Prow Pass Member partially welded tuff. Modified from Olsson and Jones (1980).

unhealed joints is expected to be more significant to rock mass response. The condition of core from Yucca Mountain with unhealed joints has been inadequate for representative laboratory mechanical tests. It is expected that joints or faults containing gouge or other infilling may have a lower coefficient of friction than clean, unfilled joints (Byerlee, 1978). The coefficient of friction for typical saturated gouges generally ranges from 0.2 to 0.6 (Morrow et al., 1982), whereas the coefficient of friction for dry clay gouges has a range of 0.2 to 0.7 (Shimamoto and Logan, 1981). Lower values for the coefficient of friction will result in lower shear strengths for the joints, at constant values of cohesion τ_o and applied normal stress σ (Section 2.2.2.1).

2.2.2.3 Effects of water saturation

Even though the Topopah Spring Member is above the water table, Montazer and Wilson (1984) suggest that very limited amounts of water may flow through some fractures. The effects of water saturation on the mechanical properties

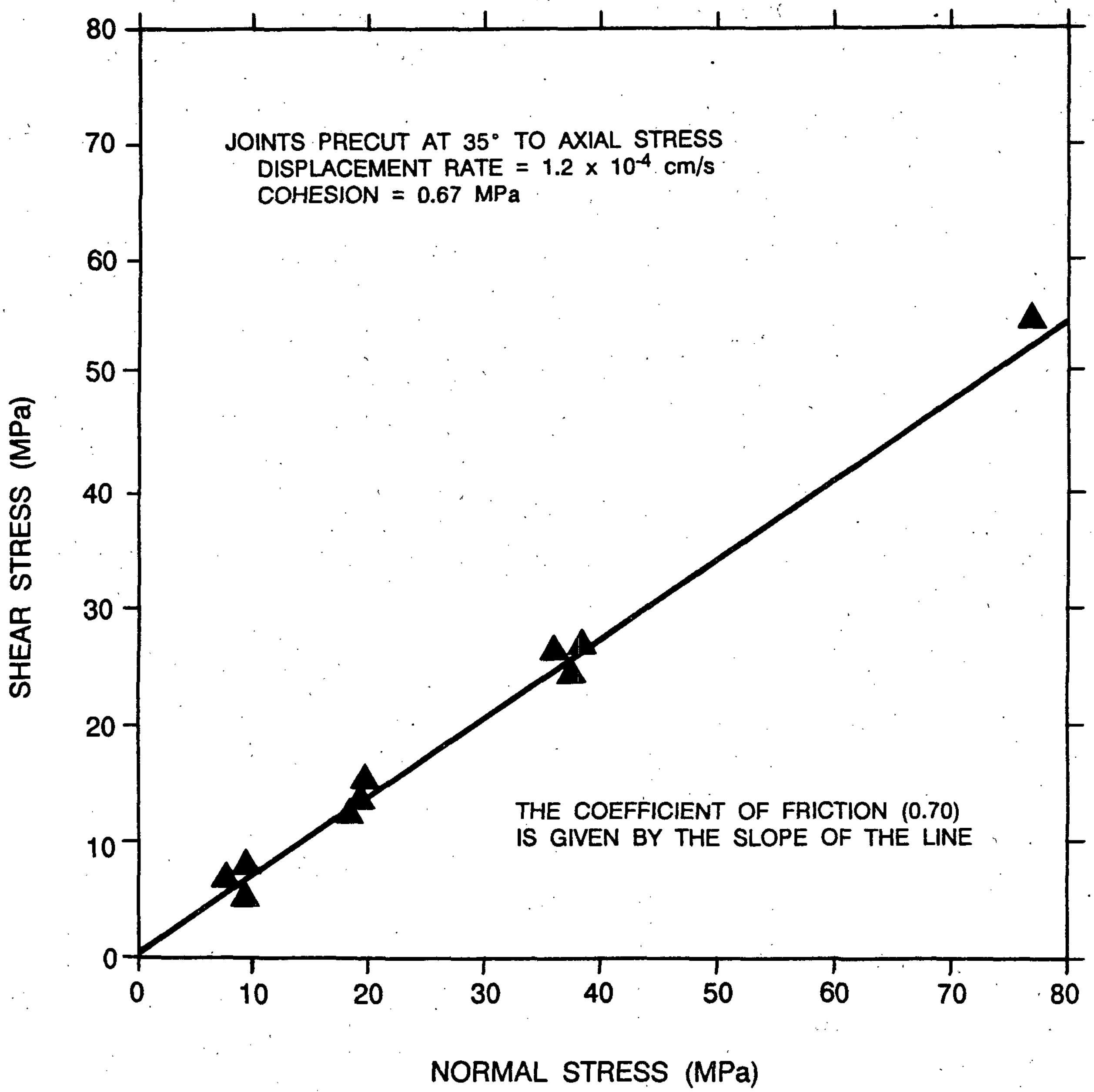

Figure 2-13. Shear stress-to-normal stress relation at slip initiation for water-saturated precut joints in Grouse Canyon Member welded tuff. Modified from Teufel (1981).

10^{-6} cm/s (Teufel, 1981). As shown in Figure 2-14, the coefficient of friction for oven-dry samples increased from 0.62 at 10^{-2} cm/s to 0.66 at 10^{-6} cm/s, a 6 percent increase in the coefficient of friction over four orders of magnitude decrease in displacement rate. These results are consistent with the work of Dieterich (1978) and Teufel and Logan (1978) for granites and sandstones, respectively. For water-saturated joints, the displacement rate effects are slightly greater, but again, the effect is small; only a 9 percent increase in the coefficient of friction over 4 orders of magnitude decrease in displacement rate (Figure 2-14). As noted in the previous section, over the observed range of displacement rates the coefficient of friction for water-saturated precuts is slightly greater than for dry precuts.

To evaluate time-dependent joint strength increases, the time dependence of the frictional shear strength of oven-dried and water-saturated Grouse Canyon Member welded tuff was investigated in triaxial compression by examining the response of 35 degree precuts (Teufel, 1981). A confining pressure of 10 MPa was used. The test procedure was slightly different from that used in the previous quasi-static tests. In the tests of time-dependent behavior, axial load was increased until slip occurred along the precut at a constant sliding velocity of 1.2×10^{-3} cm/s. The test was stopped for a given time

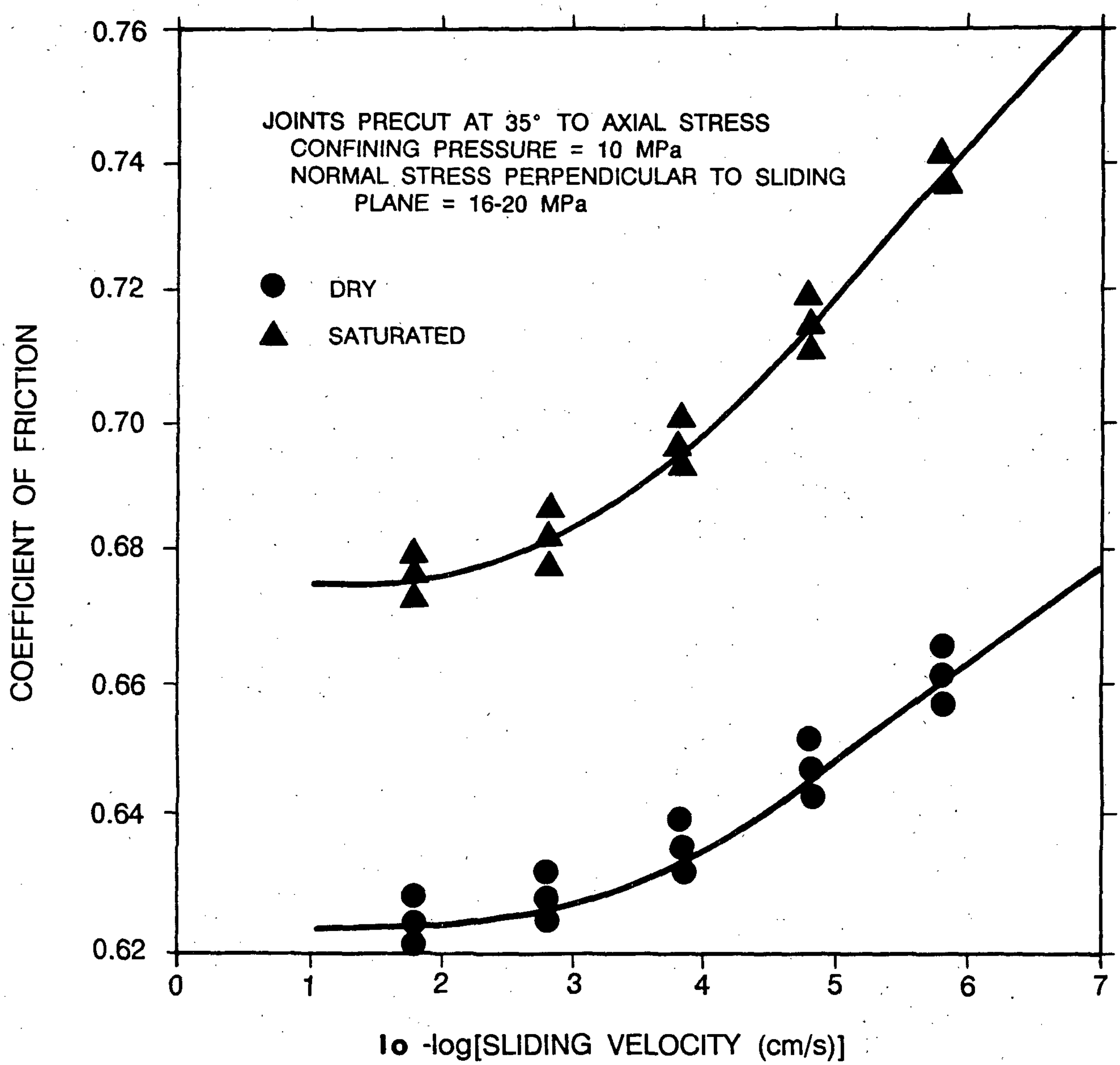

Figure 2-14. Plot of the coefficient of friction against log sliding velocity for oven-dried and water-saturated joints for Grouse Canyon Member welded tuff. Modified from Teufel (1981).

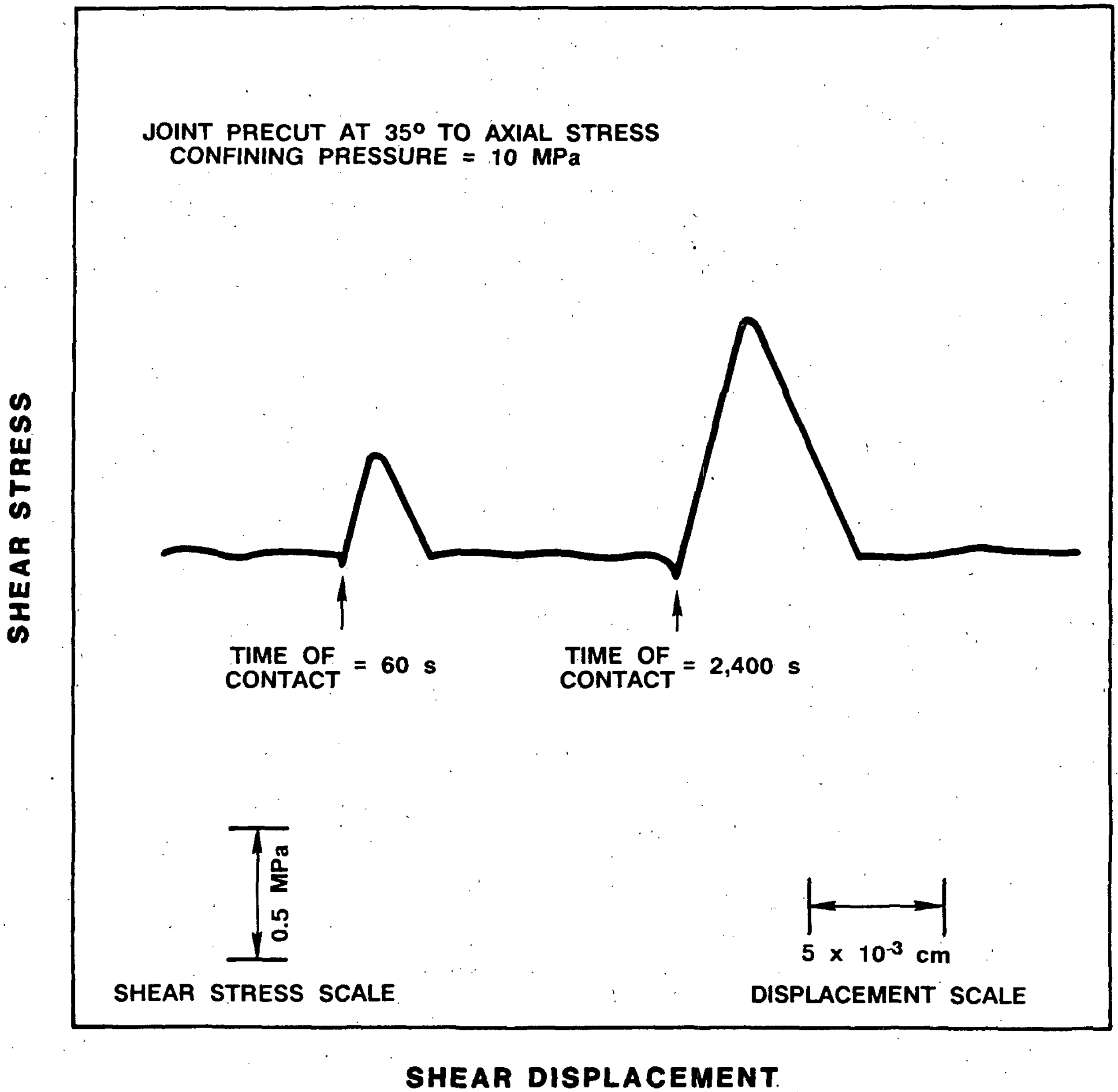

Figure 2-15. Shear stress versus shear displacement for oven-dried Grouse Canyon Member welded tuff sample for 60 and 2,400 s. periods of static contact. Modified from Teufel (1981)

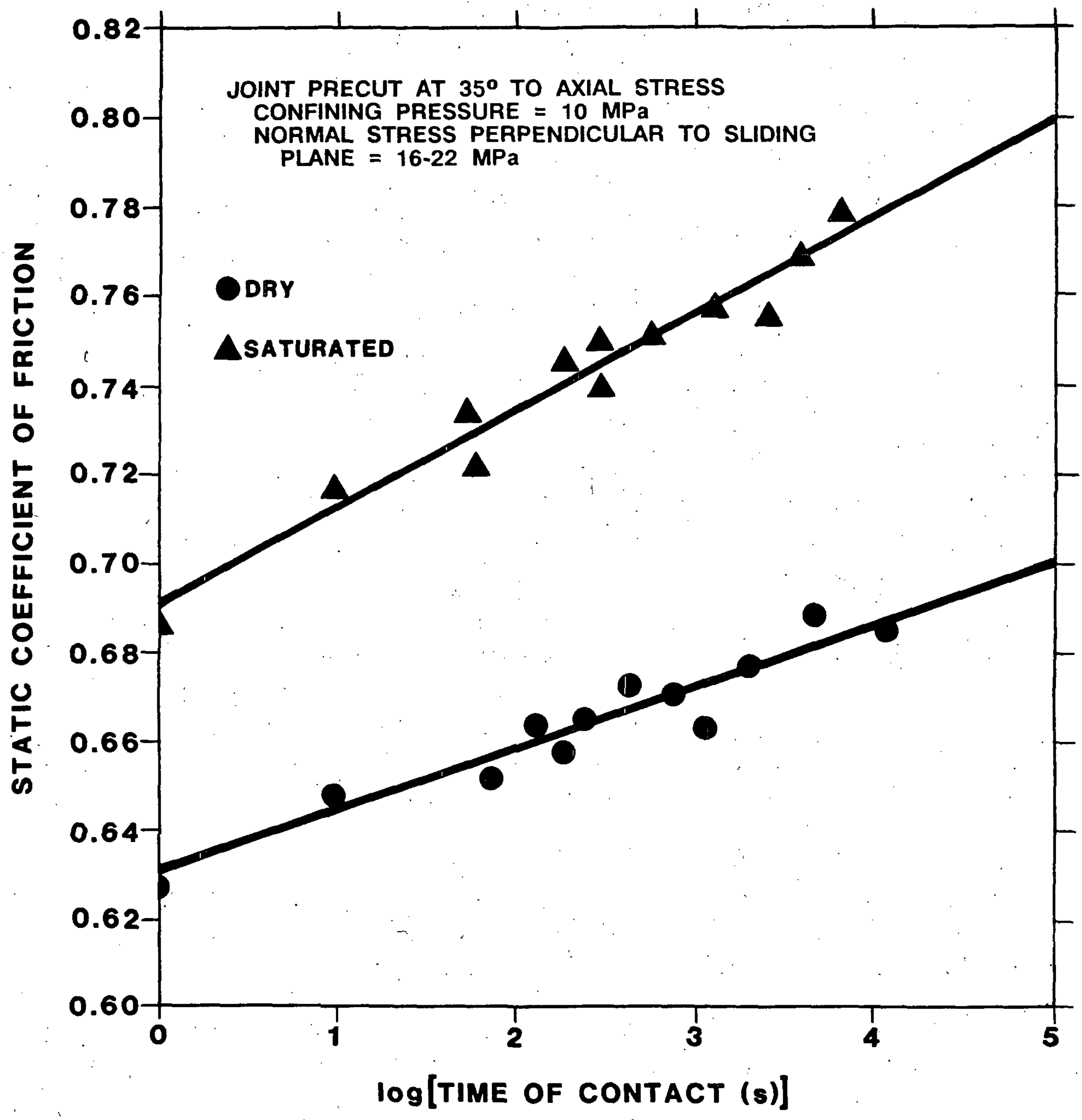

Figure 2-16. Plot of static coefficient of friction against the log time of contact for oven-dried and water-saturated joints in Grouse Canyon Member welded tuff. Modified from Teufel (1981)

will be conducted to investigate the time dependence of joint properties as a function of temperature (Section 8.3.1.15).

2.2.2.5 Scale effects

Experimental and theoretical examinations of joints in other rock types suggest that the shear behavior of joints is scale-dependent (see, for examopenings is the change in the stress state of the rock resulting from excavation of the openings. A field parameter that is useful in describing this process is the ratio of stress change to the total strain change (elastic and inelastic). This parameter is termed the "modulus of deformation." In contrast, the modulus of elasticity is based only on the ratio of the stress change to the elastic strain change (the linear portion of the stress-strain curve, as shown in Figure 2-17). If no inelastic behavior occurs, the moduli will be identical. Both the modulus of deformation and the modulus of elasticity are used to predict how the rock surrounding the repository opening deforms after excavation.

The amount of eventual stress change that occurs in the rock around an underground opening in response to excavation is a strong function of the distance from the opening. As discussed in the preceding paragraph, the modulus may change with a change in stress, but other properties (e.g., fracture permeability, thermal conductivity, and strength) may also be affected. Thus, to perform relevant analyses of the repository and the surrounding rock, it is important to incorporate the effects of the zone around a repository wherein property changes have occurred. Tests to provide the required data are described in Section 8.3.1.15.1.

Before 1984, field measurements on G-Tunnel tuffs were limited to borehole jacking tests (Zimmerman and Vollendorf, 1982) to determine rock deformability. The parameter derived from such testing is the modulus of deformation. The original data have been updated by Nimick (1987) to reflect recent changes in the theoretical basis for reduction of the test data (Hustrulid, 1976; Heuze and Salem, 1977; Heuze and Amadei, 1985).

Large-scale studies performed or under way in G-Tunnel include a heated-block test and three pressurized-slot experiments. Standardized test procedures for these tests are unavailable, although a suggested American Society for Testing and Materials procedure for heated-block tests has been published (Hardin et al., 1985). A thorough evaluation of the limitations of the instrumentation and data will be made to define in detail the procedures for testing in the exploratory shaft facility.

2.3.1 MECHANICAL PROPERTIES OF OTHER ROCKS

Available data on large-scale mechanical properties of other rocks have been reviewed to assess the relative magnitude of typical in situ and laboratory-scale moduli values and to compare tuff properties. These data are presented in Table 2-8. Seventy percent of the ratios of field-to-laboratory moduli fall between 0.2 and 0.62 with an average ratio for this group of 0.43. If all the ratios in the table are included, the average ratio is 0.53. Comparison with the data for the Grouse Canyon Member (Section 2.3.3) shows the ratio to be slightly higher than for the average of other rocks.

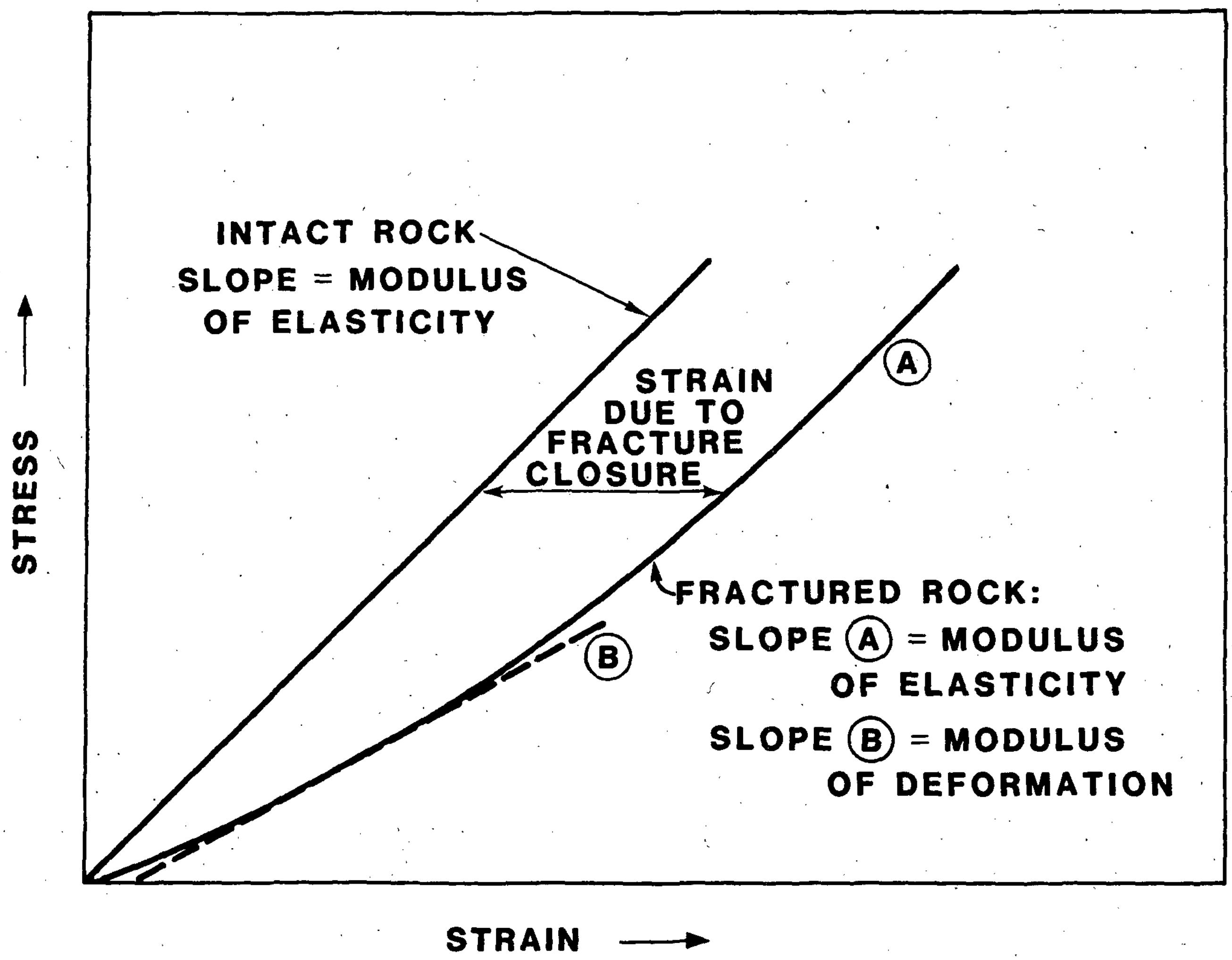

Figure 2-17. Schematic comparison of stress-strain relationship for intact rock and fractured rock mass. Modified from Tillerson and Nimick (1984).

Table 2-8. Large-scale mechanical properties of other rock[a]

Rock type	Field test method	Average field modulus of deformation (GPa)	Corresponding laboratory modulus of elasticity (GPa)	Ratio of field to laboratory value
Massive amphibolite	Flatjacks	51.8	89.0	0.58
Gneiss/granite	Flatjacks	57.5	59.1	0.97
Mudstone	Flatjacks	20.6	34.5	0.60
Massive granite gneiss	Goodman jack	23.6	51.7	0.45
Fractured diorite gneiss	Goodman jack	5.8	77.9	0.07
Blocky marble	Flatjacks	12.4	47.5	0.26
	Goodman jack	14.0	47.5	0.30
Granite	Large flatjacks	29.2	15.0	1.95
Quartzite	Flatjacks	58.0	67.0	0.87
Quartzite gneiss	Flatjacks	28.8	27.0	1.07
	Goodman jack	16.6	27.0	0.61
Greywacke	Small flatjacks	45.5	73.4	0.62
	Large flatjacks	42.2	73.4	0.57
	Goodman jack	28.4	73.4	0.39
Phyllite	Small flatjacks	33.7	56.0	0.60
	Goodman jack	12.0	56.0	0.21
Copper Ore	Flatjacks	13.3	94.5	0.14
		19.0	94.5	0.20
Quartzite	Borehole jack	27.9	56.5	0.49
Granite[b]	Borehole jack	26	70	0.37
Basalt[c]	Flatjacks	40	87	0.46
	Borehole jack	20	87	0.23
Quartz diorite[d]	Block Test	3.0	3.7-4.5	0.67-0.81
Granodiorited	Block Test	22.8	37.2-57.9	0.39-0.60
Basalt[e]	Block Test	35.1-42.7	89	0.39-0.48
Gneiss[f]	Block Test	10.7-13.0	63.0	0.17-0.21
Basalt[g]	Modified borehole deformation gage	28.4	75-85	0.33-0.38

[a]Data from Heuze (1980) except as noted.
[b]Hueze et al. (1981).
[c]Lanigan et al. (1983).
[d]Pratt et al. (1972).
[e]Hart et al. (1985).
[f]Richardson et al. (1985).
[g]Dischler and Kim (1985).

2.3.2 MECHANICAL PROPERTIES OF ROCKS AT THE SITE

Using a borehole jack the modulus of deformation has been measured in two boreholes in G-Tunnel. The uncorrected average modulus of deformation obtained from the 20 measurements is 12.1 GPa with a standard deviation of 5.0 GPa (Zimmerman and Vollendorf, 1982). Nimick (1987) reports a corrected mean value between 14.7 and 17.6 GPa. This modulus of deformation represents a relatively small volume of material around a borehole; heated-block and pressurized-slot tests should provide modulus values for larger volumes. Ambient temperature testing of the G-Tunnel heated block has been conducted, and field values for the modulus of deformation are available (Zimmerman et al., 1984a). Figure 2-18 shows a schematic diagram of the test. Flat-jacks grouted in slots around the block are used to create uniaxial or biaxial stress fields in the block. The heaters (located outside the block) have been positioned so that relatively uniform temperatures can be obtained in the block (Blanford, 1982). Hence, independent thermal and mechanical loads can be applied to a 2-m block of jointed tuff. Ambient temperature testing is used to determine the mechanical properties, and thermal cycle testing is used to measure the coefficient of thermal expansion and changes in the modulus of deformation at elevated temperatures.

A range in deformation moduli of 9.7 to 17.0 GPa was determined during the ambient temperature testing, with stresses ranging from 3.1 to 10.6 MPa (Zimmerman et al., 1984a). Figure 2-19 is a typical load-deformation curve. The lower end of the stress range from Figure 2-19 is considered representative of the in situ preexcavation stress conditions at the test facility. No anisotropy was observed, which is not surprising because of the orientation of the joints (45 degrees to block edges) and the equal spacing (approximately 0.4 m) for the two orthogonal joint sets. In addition, no change in the modulus with temperature was observed (Zimmerman et al., 1986). The modulus of deformation would be expected to be lower near excavated surfaces because of the joint relaxation and fracturing related to excavation.

Values for the elastic moduli of the G-Tunnel welded tuff were obtained during unconfined compressive strength tests in the laboratory. An average value of 24.7 GPa was obtained at a strain rate of 10^{-4} s^{-1} and a value of 26.0 GPa at 10^{-6} s^{-1} (Olsson and Jones, 1980). Comparison of the laboratory moduli with the field value suggests a preliminary value for the average field modulus of deformation of between 51 and 56 percent of the intact rock modulus.

Ellis and Swolfs (1983) have published data on the in situ dynamic elastic moduli of tuff units in drillhole USW G-1 that were below the fluid level in the drillhole at the time geophysical logging was performed. The dynamic Young's moduli for units like the tuffaceous beds of Calico Hills and the Bullfrog and Tram members are much higher than values estimated for the in situ static Young's modulus from laboratory data. As discussed in Section 2.1.2.2, dynamic moduli typically are higher than correlative static values (Lama and Vutukuri, 1978).

A pressurized slot (modified Rocha slot) technique (Rocha, 1970) is being developed to measure the modulus of deformation and to evaluate the effect of joint proximity and orientation on the modulus. In this test (Figure 2-20), a flatjack is inserted in a relatively narrow slot and

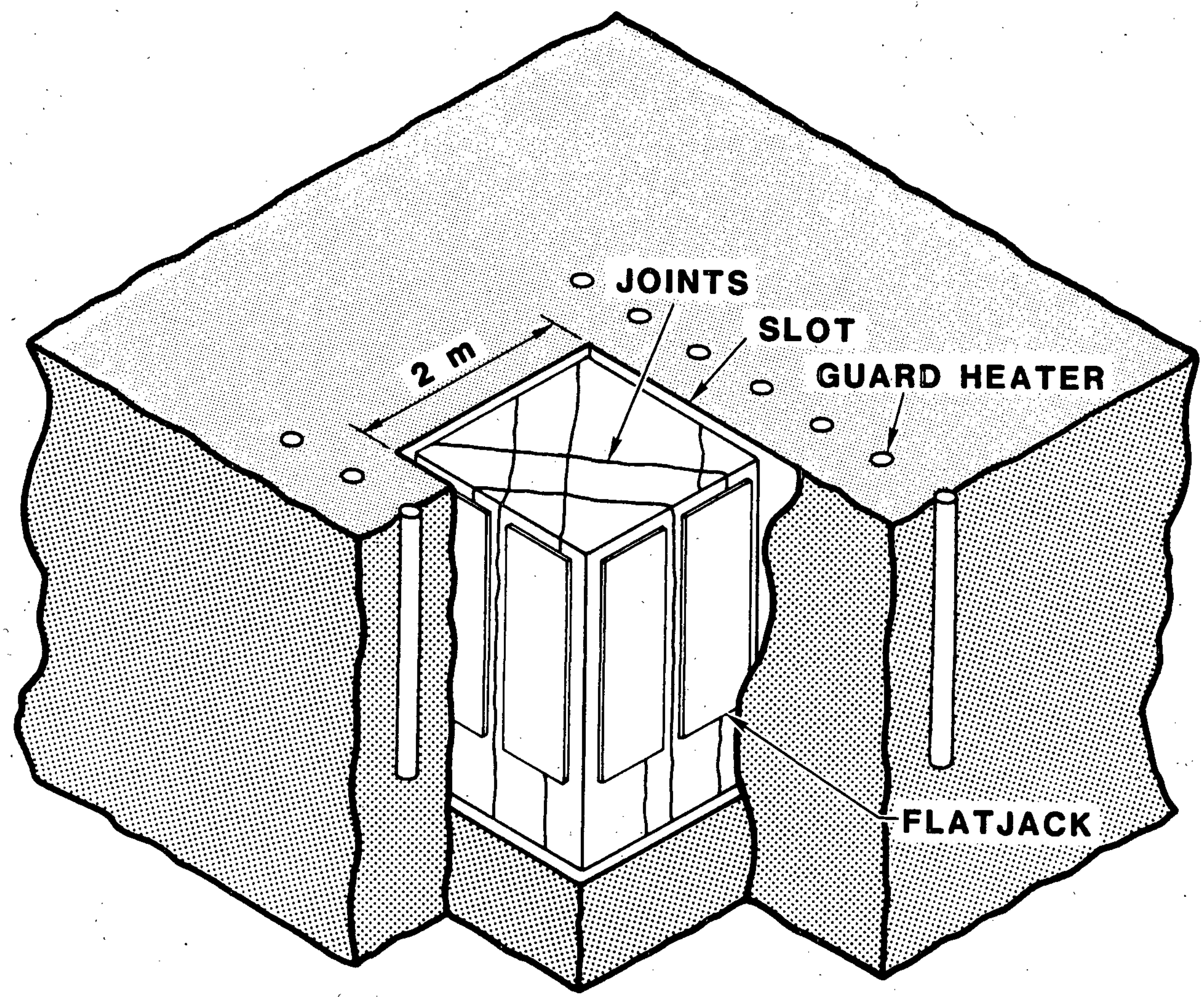

Figure 2-18. Schematic diagram of the heated-block experiment in G-Tunnel underground facility.

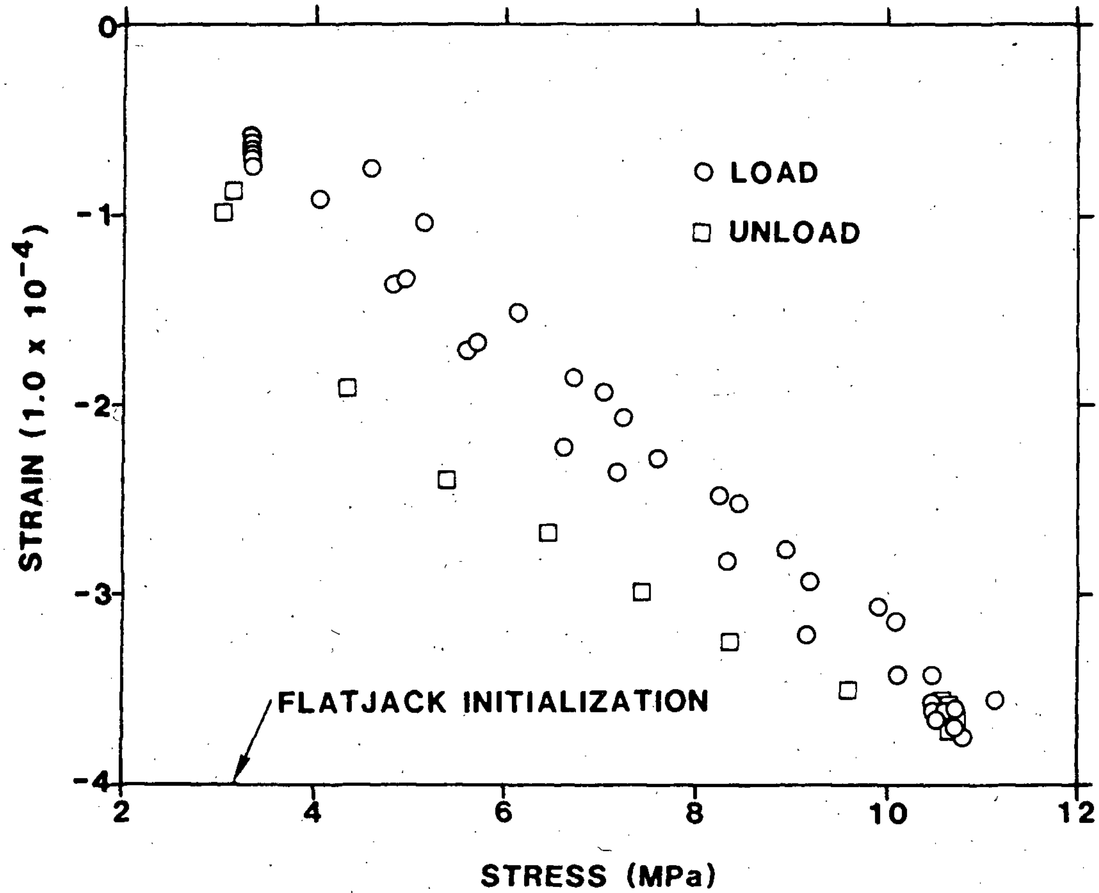

Figure 2-19. Representative plot of horizontal strain versus flatjack pressure (stress) for G-Tunnel heated-block test. Modified from Zimmerman et al. (1984a).

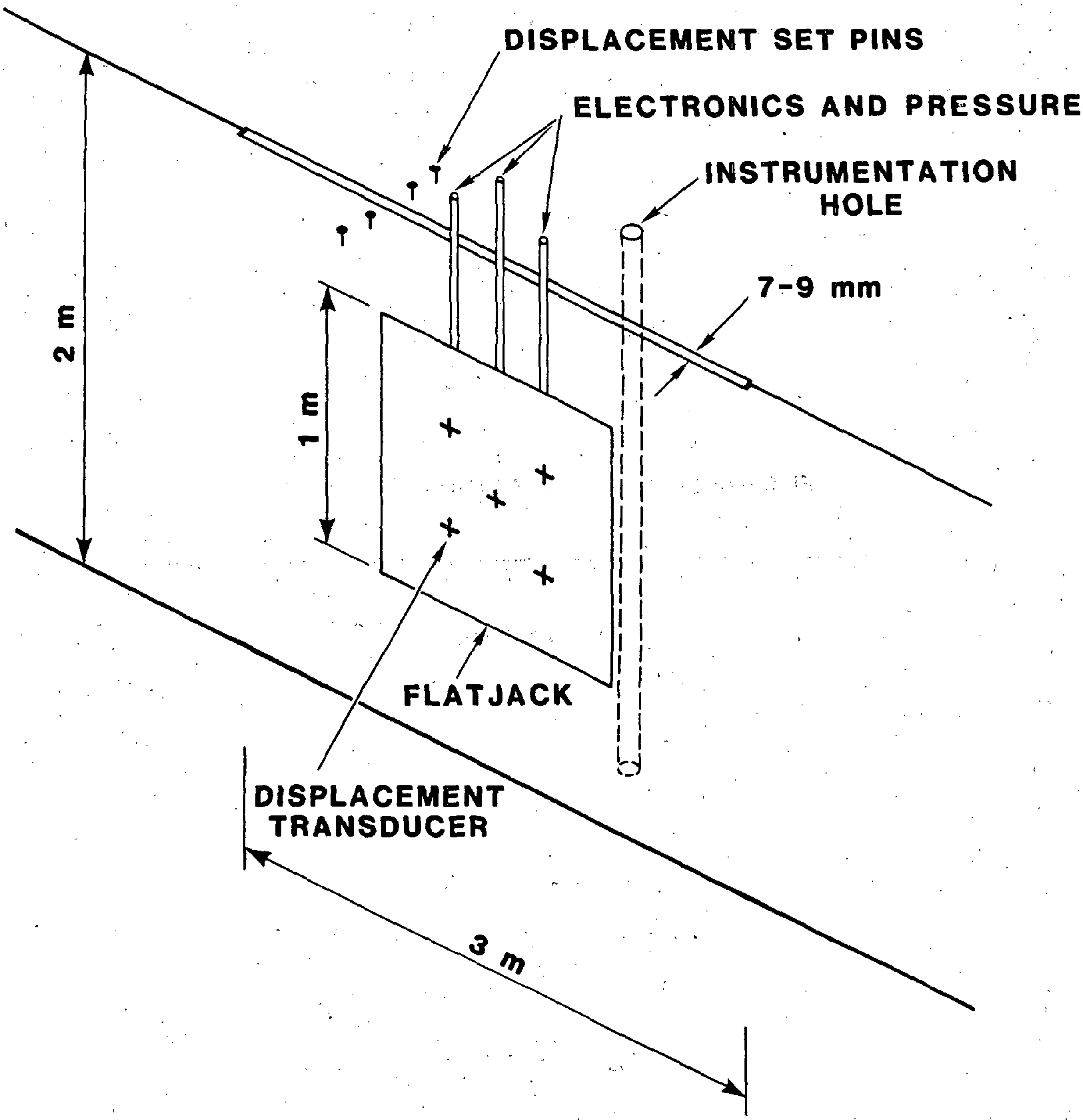

RLN-08/85a

Figure 2-20. Schematic diagram of the pressurized slot test in G-Tunnel underground facility.

pressurized. As in the borehole-jacking test, the displacement of the flatjack is monitored during loading and unloading for use in determining the deformation modulus of the rock mass. In this test, the modulus measured is representative of a larger volume of rock than in the borehole measurements. Slot-cutting techniques being developed for these tests were evaluated in field trials in 1984, and the slot tests were fielded in 1985 and 1986.

Measurements of large-scale rock-mass properties will be made in several of the tests planned for the exploratory shaft facility (Section 8.3.1.15). Plate-loading tests and the Yucca Mountain heated-block test are planned to provide direct measurements of the modulus of deformation. If the rock-mass properties are known, then planned shaft-convergence measurements, excavation-monitoring data (stress, permeability, roof-bolt loads, displacements), and the motion observed in the canister-scale heater test will evaluate the degree to which complicated rock mass response can be modeled with the aid of numerical analysis codes. The use of data from field tests for the validation of these codes is discussed in Chapter 8. The feasibility of in situ evaluation of rock-mass strength is being examined in terms of geometry, loading techniques, fracture spacing, and mining requirements. An in situ strength test will be performed in the exploratory shaft facility, and evaluation is ongoing to determine the appropriate test method.

2.3.3 RELATIONSHIP BETWEEN INTACT ROCK, DISCONTINUITIES, AND LARGE-SCALE ROCK PROPERTIES

The preceding section describes efforts to measure the in situ mechanical properties of the tuff, which generally involves a rock volume greater than can be accommodated in the laboratory. However, calculations for design and performance assessment may require rock mass properties before such properties have been measured in field tests. In addition, the number of in situ tests that can reasonably be performed is probably not sufficient to provide direct measurements of rock-mass properties under every unique set of geologic conditions that may be encountered in the rock mass. Therefore, as discussed in Section 8.3.1.15.1, predictive models are necessary to estimate these properties from widely available information. Various methods can be used to estimate these rock mass properties from laboratory data; Table 2-9 provides data pertinent to these methods, and a brief discussion is provided

Table 2-9. Reference values for intact rock and rock-mass mechanical properties and fracture properties for use in analysis of rock-mass mechanical behavior

Unit[b]	Intact rock properties[a]: Unconfined compressive strength (MPa)	Young's modulus (GPa)	Poisson's ratio	Tensile strength (MPa)	Angle of internal friction (°)	Cohesion (MPa)	Rock-mass deformation modulus (GPa)[c]	Fracture properties: Cohesion (MPa)	Coefficient of friction
TCw	240	40.0	0.24	17.9	44.7	51	20.0	0.2	0.54
PTn	19	3.8	0.16	1.0	8.5	8	1.9	0.2	0.59
TSw1	127±16	31.7±17.9	0.25±0.07[d]	12±4.6[d]	34.9[d]	36[d]	15.9[d]	0.2[d]	0.54[d]
	16±5[e]	15.5±3.2[e]	0.16±0.03[e]	1.0[e]	12.5[e]	11[e]	7.8[e]	0.2[e]	0.54[e]
TSw2	166±65	30.4±6.3	0.24±0.06	15.2	23.5	34.5	15.2	0.2	0.54
TSw3	NA[f]	NA	NA	NA	NA	NA	NA	0.2	0.54
CHnlv	27	7.1	0.16	1.0	12.0	11	3.6	0.2	0.59
CHnlz	27±9	7.1±2.1	0.16±0.08	1.0	7.6±2.6	10.9±1.6	3.6	0.2	0.59
CHn2	40	11.5	0.16	2.6	16.4	15	5.8	0.2	0.59
CHn3	27	7.1	0.16	1.0	12.0	11	3.6	0.2	0.59
PPw	57	16.3	0.13	6.9	21.0	20	8.2	0.7	0.59
CFUn	31±11	7.6±3.8	0.16	1.8	15.6	14	3.8	0.7	0.64
BFw	42±14	10.8±4.7	0.13±0.02	6.9	21.0	20	5.4	0.7	0.59
CFMn1	52	15.2	0.16	6.0	19.9	19	7.6	0.7	0.64
CFMn2	57	16.3	0.16	6.9	21.0	20	8.2	0.7	0.64
CFMn3	45	13.2	0.16	4.3	18.0	17	6.6	0.7	0.64
TRw	72±23	17.6±3.8	0.13	11.1	27.6	27	8.8	0.7	0.59

[a]Data from Table 2-7.
[b]See Figure 2-5 for definition of thermal/mechanical units.
[c]Taken as 50 percent of values in Table 2-7, as discussed in text.
[d]Nonlithophysal layers within unit TSw1.
[e]Lithophysal layers within unit TSw1.
[f]NA = not available.

these parameters in Table 2-9 are identical to the intact rock values in Table 2-7. The use of these parameters in estimating corresponding rock mass values for use in design analysis is discussed in detail in Section 6.1.2.

The fracture properties given in Table 2-9 are preliminary because of a given thermal loading, repository geometry, and rock mass thermal capacitance, higher thermal conductivity means more rapid heat diffusion and lower temperatures in the rock surrounding the waste container. Lower thermal conductivity results in slower heat dispersal and higher temperatures in the waste container and in the rock surrounding the container.

Heat capacity is a measure of the amount of energy required to raise the about 8 percent lower than those measured with the transient line source (Lappin et al., 1982; Moss et al., 1982a).

Experimental equipment and analytical procedures for unconfined thermal expansion measurements have been described (Lappin, 1980a). Sample sizes are 6 by 6 by 25 mm for these measurements, whereas representative sizes of components are 0.1 to 2.0 mm (phenocrysts), <0.05 mm (matrix), and <3 mm (lithic fragments) (Broxton et al., 1982). Some pumice fragments may be 10 mm in diameter (Broxton et al., 1982); these constituents have been avoided or accounted for during expansion measurements. The uncertainty in the measured expansion coefficients is $1 \times 10^{-6} K^{-1}$ for welded, devitrified samples analyzed to date, the same as that for a fused silica standard (Lappin, 1980a). This uncertainty corresponds to an accuracy of 3 to 9 percent for welded tuff.

The thermal expansion of welded, devitrified tuffs is independent of heating rate between 0.5 and 10°C/min (Lappin, 1980a). Unconfined thermal expansion measurements on zeolitized tuffs are sensitive to additional variables (Lappin, 1980a). These tuffs, like tuffs containing appreciable amounts of hydrated glass, expandable clays, or both, contract when dewatered. Thus, their behavior is sensitive to the locally effective fluid pressure, which in laboratory tests depends on sample size, heating rate, and permeability. Unconfined measurements on this type of tuff indicate only minimum contractions at a given temperature. Even this interpretation must be based on tests run at a slow rate. Such tuffs may continue to contract slowly for more than 24 h when held at constant temperature. The times required to reach stable length in situ at a given temperature might be much longer if the fracture spacing is large.

Because of concern about the possible effects of both microcracking and variable fluid pressures, a method has been developed to measure thermal expansion under controlled confining and fluid pressures. Test and calibration procedures suggested by the American Society for Testing and Materials are detailed by Van Buskirk et al. (1985). Multiple measurements on fused silica indicate that the precision and accuracy of the confined testing apparatus at a confining pressure of 10 MPa and a pore pressure of 0.1 to 1.5 MPa are on the order of $\pm 1.5 \times 10^{-6} K^{-1}$ (Lappin and Nimick, 1985b).

Bulk properties--including grain density, dry bulk density, natural-state bulk density, saturated bulk density, and porosity--are also required for thermal and thermomechanical analyses. These properties can be measured on small samples taken either from core or from outcrop material. The minimum sample size should be 20 g, although data have been obtained directly from mechanical test samples with diameters of up to 26.7 cm (Price et al., 1985). Smaller samples are the usual starting material. In general, the dry bulk density and the grain density of a sample are measured, and the other bulk properties are calculated as follows:

$$\rho_b = (1 - \phi)\rho_g + s \qquad (2\text{-}7)$$

where

ρ_b = dry, natural-state, or saturated bulk density
ϕ = porosity (volume fraction)

ρ_g = grain density
s = saturation (volume fraction)

(The density of water was assumed to be 1.0 g/cm^3).

On the basis of replicate measurements on tuff samples, dry bulk density values have a precision of ±0.1 g/cm^3, whereas grain-density measurements on welded tuff are precise to ±0.04 g/cm^3 and grain densities of zeolitic tuffs have a precision of ±0.06 g/cm^3 (Lappin et al., 1982). The accuracies for these measurements are assumed to be similar to the precisions (Lappin et al., 1982).

The existing information consists almost exclusively of data from laboratory measurements on core samples. The laboratory studies reported here have been conducted for the following two purposes:

1. To develop a data base that defines the spatial variations in the thermal properties of the tuffs encountered at Yucca Mountain.

2. To correlate the measured thermal properties with measured physical properties like porosity, grain density, and bulk density to develop a functional thermal-conductivity and thermal-expansion stratigraphy for use in heat-transfer and thermomechanical stress analyses. These correlations allow the extrapolation of the measured thermal properties to regions of the boreholes for which only geophysical logs and bulk-property data are available.

2.4.1 THERMAL AND THERMOMECHANICAL PROPERTIES OF OTHER ROCKS

Ranges of the published values of the thermal conductivity, heat capacity, coefficient of thermal expansion, and bulk properties of tuffs other

Table 2-10. Thermal and thermomechanical properties of tuffs not studied by the Yucca Mountain Project[a]

Lithology or tuff unit	Thermal conductivity (W/mK)	Heat capacity (J/gK)	Coefficient of thermal expansion (10^{-6} K^{-1})	Grain density (g/cm^3)	Porosity (%)
Mt. Helen tuff	--[b]	--	--	2.45	37
Diamond Dust tuff	--	--	--	2.43	35
Schooner tuff	--	--	--	2.64	40.5
Schooner tuff	--	--	--	2.60	--
Zeolitized tuff, Survey Butte	--	--	--	2.44-2.47	--
Diamond Mine tuff	--	--	--	2.38	--
Mt. St. Helens tuff	--	--	--	2.32	35-39
Oak Springs Formation,					
Bedded tuff	--	--	--	2.44 ± 0.11	38.8 ± 7.0
Friable tuff	--	--	--	2.33 ± 0.24	35.5 ± 13.8
Welded tuff	--	--	--	2.55 ± 0.09	14.1 ± 8.9
Tuff	--	--	--	2.38-2.57	31-42
Oak Springs Formation	--	--	--	2.6 ± 0.16	30.6 ± 3.2
Ohya tuff	--	--	--	2.38	34.8
Tuff, Ontario	--	--	--	2.78	--
Tuff	--	--	--	--	34.7-43.1
Tuff, Yucca Flat	1.12-1.36	--	--	--	16
Tuff, Red Hot Deep Well Experiment	--	--	--	--	15.9-23.3
Ash-fall tuff	--	--	--	--	30-40
Tuff and tuff breccia, USSR	--	--	--	--	8.3
Ignimbrite, Italy	--	--	--	--	≈20
Tuff, Japan	--	--	--	--	10.2-21.6
Obsidian	--	--	--	--	1.2-11.5
Tuff, Oregon	--	--	--	--	44.4
Tuff, Rhine Valley	--	--	--	--	24.7-45.1
Tuff, southern Italy	--	--	--	--	6-58.4
Ignimbrite, New Zealand	--	--	--	--	9.0-28.7
Andestic to dacitic tuff	0.60-1.03	0.38-1.24	--	--	--
Oak Springs Formation	0.44-1.05	--	--	--	--
Tuff, drillhole U12b07	0.64-2.14	--	--	--	--
Welded tuff, locality unknown	--	--	4.2-12.9	--	--
Tuff, locality unknown	--	--	-22.2-6.0	--	--
Bandelier tuff, New Mexico	--	--	13.1-17.1	--	--

[a]Source: Guzowski et al. (1983).
[b]-- = data not available.

Table 2-11. Average values and standard deviations for measured thermal conductivities (K^{avg}) and calculated zero-porosity conductivities (K_o) for various tuff units and rock types[a]

Rock type	Unit	K_{sat}^{avg} (W/mK)[d]	K_{dry}^{avg} (W/mK)[d]	K_o^{sat}[b] (W/mK)	K_o^{dry}[c] (W/mK)
Nonzeolitized/ welded	Topopah Spring	2.16 ± 0.19	1.93 ± 0.17	2.43	3.45
	Bullfrog	2.00 ± 0.27	1.35 ± 0.30	2.71	NA[e]
	Tram	2.09 ± 0.18	1.78 ± 0.36	2.77	NA
Vitric	Topopah Spring	1.35 ± 0.08	1.37 ± 0.12	1.31	1.98
Zeolitized/non-welded to partially welded	Topopah Spring	1.33 ± 0.05	1.04 ± 0.12	1.88	4.77
	Calico Hills	1.51 ± 0.16	1.03 ± 0.15	2.36	4.24
	Prow Pass	1.40 ± 0.03	1.04 ± 0.08	1.79	NA
	Bullfrog	1.44 ± 0.01	1.07 ± 0.06	1.94	NA
	Tram	1.46	1.11	NA	NA

[a]Source: Nimick and Lappin (1985).

[b]K_o^{sat} calculated at 25°C.

[c]K_o^{dry} calculated at 200°C.

[d]Estimated accuracy in thermal conductivity measurements is 10 percent of reported value (Lappin et al., 1982).

[e]NA = not available.

Values for the zero-porosity (matrix) conductivity for each sample, calculated by the geometric means approach (Lappin, 1980b), are also given. The

matrix thermal conductivities can be used, together with values for porosity and saturation, to calculate thermal conductivity for any saturation state.

2.4.2.1.1 Measured thermal conductivities

The thermal conductivities of saturated and dehydrated tuff are variable, depending on variations in porosity and grain density (mineralogic composition). The average saturated conductivities of nonzeolitized, welded, devitrified material from the Bullfrog and Tram members of the Crater Flat

The conductivities of dehydrated samples of these same tuffs appear to be different, with the Topopah Spring and Tram members losing relatively little conductivity when dried. The matrix porosities and grain densities of the Bullfrog and Tram members are nominally the same, whereas both the porosity and the grain density of the nonlithophysal Topopah Spring Member are significantly lower. The lower grain density in the Topopah Spring Member results from the presence of cristobalite (the Topopah Spring Member has been found to contain 0 to 30 volume percent cristobalite, as discussed in Section 4.1.1.3).

The conductivities of saturated and dehydrated samples, porosities, and grain densities of all nonwelded to partially welded zeolitized ash flows examined to date appear to be consistent and independent of stratigraphic unit, depth, and drillhole location (Nimick and Lappin, 1985). The conductivities and grain densities are lower than those for corresponding nonzeolitized material, while porosities are generally higher. Zeolitized bedded intervals have higher grain densities and conductivities than do the zeolitized ash flows (Nimick and Lappin, 1985).

2.4.2.1.2 Calculated zero-porosity conductivities

The zero-porosity or matrix conductivities given in Table 2-11 are the calculated conductivity of the matrix in the absence of porosity and contained pore water. The matrix conductivities were calculated from experimental data by the geometric means approach outlined by Lappin (1980b); alternatives to the geometric means approach are being examined. The matrix conductivities are different below and above the dehydration temperature because any hydrous phases present lose some of the water within their structures during dehydration. The extent of the discontinuity in matrix conductivity at the dehydration temperature depends on the type of hydrous phases in a given sample.

The matrix conductivity of tuffs depends weakly on temperature except for the behavior at the dehydration temperature discussed earlier. The matrix conductivities given in Table 2-11 for saturated and dry samples were calculated at 25 and 200°C, respectively, and are representative of the temperature interval over which the relevant saturation state applies.

The matrix conductivity, which depends primarily on mineralogic composition is generally related to the measured grain density (i.e., the density at zero porosity) for tuff samples from Yucca Mountain. The calculated zero-porosity conductivity for a mineralogically homogeneous tuff layer can be used to estimate the in situ conductivity of that tuff for any given porosity and saturation (Lappin, 1980b; Lappin et al., 1982).

2.4.2.1.3 Influence of textural anisotropy and lithophysae on conductivity

2.4.2.1.3.1 Textural anisotropy

Thermal-comparator measurements on welded tuff from the Grouse Canyon Member of the Belted Range Tuff were collected to examine potential effects of layering anisotropy in welded tuffs (Moss et al., 1982b). The results indicate that there is no statistically significant anisotropic effect of layering on the matrix thermal conductivity of welded tuffs, even in the fully dehydrated state. The difference in thermal conductivities for different orientations relative to bedding is less than 5 percent as compared with variations of more than 20 percent between samples (Moss et al., 1982b; Nimick and Lappin, 1985). Because welded ash-flow tuffs have the strongest fabric anisotropy, it is concluded that the matrix thermal anisotropy is also negligible for nonwelded ash flows.

2.4.2.1.3.2 Lithophysae

Lithophysae are found in varying abundance in portions of the Topopah Spring Member of the Paintbrush Tuff outside of the proposed repository horizon. In addition, the thermal effects of these cavities on conductivity are difficult to measure because the void spaces, which are up to 5 cm or more in diameter, are large in relation to usual laboratory specimens. Tests on six samples of lithophysal Topopah Spring Member from Busted Butte are under way to provide thermal conductivity data for this rock type.

2.4.2.2 Heat capacity

No measurements of the specific heat or heat capacity of tuffs have yet been made for the Yucca Mountain Project. Instead, the product of heat capacity and density (volumetric heat capacity) has been calculated assuming a constant heat capacity (C_p) of 0.84 J/gK for the silicate mineral assemblage, 4.18 J/gK for water, and 1.0 J/gK for air as shown in Equation 2-8.

$$(\rho C_p)\text{bulk} = \rho_g\ (1-\rho) C_p(\text{silicates}) + \rho_{(H_2O)} \phi s C_p(\text{water}), \qquad (2\text{-}8)$$

where

C_p = heat capacity (J/gK)

ρ_{bulk} = bulk density (g/cm^3) = $\rho_g\ (1-\phi) + \rho_{(H_2O)}\ (\phi s)$

ρ_g = grain density (g/cm^3)

$\rho_{(H_2O)}$ = density of water = 1 g/cm^3

s = saturation (volume fraction)

ϕ = porosity (volume fraction).

The calculated values of the volumetric heat capacity (Table 2-12) indicate a broad range that is strongly dependent on both porosity and the degree of saturation. A series of measurements of the heat capacity of tuffs from Yucca Mountain is planned to examine the validity of the assumed value of heat capacity of the silicate mineral assemblage (Section 8.3.1.15). Preliminary analysis suggests that the constant value of 0.84 J/gK is incorrect;the heat capacity of the mineral assemblage is in fact a function of temperature (Nimick and Schwartz, 1987).

Table 2-12. Calculated volumetric heat capacity as a function of porosity and saturation[a]

	Volumetric heat capacity (J/cm^3K)			
	Grain density = 2.65 g/c^3		Grain density = 2.38 g/cm^3	
Porosity	Saturated	Dry	Saturated	Dry
0.0	2.22	2.22	2.01	2.01
0.1	2.43	2.01	2.22	1.80
0.2	2.59	1.76	2.43	1.59
0.3	2.80	1.55	2.64	1.38

[a]Source: Tillerson and Nimick (1984).

The water present in the pores of tuffs from Yucca Mountain gives rise to a large endothermic reaction associated with volatilization of contained pore fluids at temperatures near the in situ boiling point of water. Variability in the in situ temperatures and pressures expected near a repository will cause variability in the importance of this volatilization to heat transfer calculations.

2.4.2.3 Thermal expansion

This section summarizes the results of earlier studies of unconfined thermal expansion (Lappin, 1980a), as well as with the results of more-recent confined measurements. The newer data are consistent with previous results and describe both the predehydration behavior of zeolitic tuffs and the effects of increased fluid pressures on the dehydration temperatures of expandable clays (neither of which can be assessed adequately in unconfined tests). Current calculations suggest that temperatures in the Bullfrog and Tram members and in most of the tuffaceous beds of the Calico Hills will not be high enough to cause dehydration (Johnstone et al., 1984). Comparison of the measured and calculated thermal expansion of zeolitic tuffs is difficult because of the lack of data for pure phases. Data for pure zeolite minerals are being collected to allow calculation of the thermal expansion of zeolitic tuffs.

Summarized in Table 2-13 are average linear thermal-expansion coefficients for material from the welded devitrified Tram and Bullfrog members of the Crater Flat Tuff, the densely welded Topopah Spring Member of the Paintbrush Tuff, and the highly zeolitized nonwelded to partially welded ash flows in the tuffaceous beds of Calico Hills and lower units. Because of the presence of variable amounts of hydrous phases, such as clays, zeolites, glass, and opaline silica, three temperature ranges must be defined for the thermal expansion behavior of the tuffs from Yucca Mountain: pretransition, transition, and post-transition. Transition behavior for samples containing significant amounts of the various hydrous phases (e.g., zeolitized tuffs) is likely to vary with the amount of expansion or contraction on heating and the temperature range over which dehydration takes place.

The Bullfrog and Tram members of the Crater Flat Tuff are devitrified welded tuffs, generally found below the water table. Because of the relatively uniform mineral composition, the expansion behavior of devitrified welded tuffs from below the water table is quite uniform, except for the effects of small fractions (generally less than 5 percent) of expandable clays (Bish, 1981; Waters and Carroll, 1981). The results of confined and unconfined tests are consistent and agree well with calculated behavior.

The Topopah Spring Member of the Paintbrush Tuff contains devitrified densely welded tuffs, generally found above the water table. The mineralogic composition of devitrified welded tuffs above the water table locally reflects past vapor-phase activity. This has resulted in the deposition of variable amounts of secondary feldspar and cristobalite, with locally important amounts of quartz, tridymite, and possibly expandable clay (Section 4.1.1.3). The thermal expansion of vapor-phase-altered tuffs changes above about 200°C because of the variable content of cristobalite, tridymite, and/or expandable clays. Even at high waste emplacement densities, temperatures approaching 200°C would occur only very close to waste canisters.

Thermal expansion data for zeolitized nonwelded to partially welded tuff layers were collected before the Topopah Spring Member was recommended as the repository horizon. The data are summarized here because of the possibility that these tuffs may be located within the region of elevated temperature around a repository. Under unconfined conditions, thermal expansion behavior is more complex and variable than that of devitrified tuffs. Three distinct types of behavior have been noted (Lappin and Nimick, 1985a):

1. A linear contraction of 0.2 to 0.3 percent upon dehydration, to temperatures as high as 300°C, with a contraction of 0.2 percent generally occurring by about 150°C. This behavior is dominant in quartz- and feldspar-poor, heavily zeolitized tuffs.

2. A maximum linear contraction of 0.2 percent at temperatures near 150°C (unconfined), followed by expansion to nearly initial length on additional heating. This type of behavior appears to be most prominent in nonwelded or partially welded zeolitized tuffs from below the water table, which are richer in quartz and feldspar than analogous tuffs higher in the section.

3. A very small amount of contraction at temperatures near dehydration, followed by expansion to more than the initial length. This type of

Table 2-13. Summary of average thermal expansion coefficients for silicic tuffs from Yucca Mountain

Rock type	Units	Linear expansion coefficient ($10^{-6}K^{-1}$)[a] Pre-transition	Transition	Post-transition
Nonzeolitized/ welded, devitrified	Bullfrog and Tram members	8.3 ± 1.4[b] (25 to 100°C)	-12 ± 4[b] (100 to 125°C)	10.9 ± 0.8 (125 to 300°C)
Nonzeolitized/ densely welded, devitrified	Topopah Spring Member	TSw1[c] 9.5 TSw2 8.9 ± 0.9 (25 to 200°C)	27.4(+27.1,-13.6)[c,d] 28.7 ± 11.4[d] (200 to 300°C)	NA[e]
Zeolitized, nonwelded to partially welded	Calico Hills (also portions of Topopah Spring, Prow Pass, Bullfrog, Tram)	6.7 ± 3.7[b] (25 to 100°C)	Variable -29 to -56[f] depending on mineralogy and degree of welding (100 to 150°C)	Variable -4.5 to +4.4 depending on mineralogy and degree of welding (150 to 300°C)
Vitric, welded	Topopah Spring Member	5.2 ± 1.1 (25 to 150°C)	3.5 ± 4.9 (150 to 250°C)	NA NA

[a]Data for TSw1, TSw2, and vitric welded material adapted from Nimick and Schwartz (1987).

[b]Confined expansion measurements (10 MPa confining pressure), all other measurements made under unconfined conditions. Accuracy of unconfined measurements $\pm 1.0 \times 10^{-6}K^{-1}$ (Lappin, 1980a); accuracy of confined measurements $\pm 1.5 \times 10^{-6}K^{-1}$ (Lappin and Nimick, 1985b).

[c]Nonlithophysal layers; transitional behavior measured only for 200 to 250°C. Nonsymmetrical standard deviation for data in transitional interval result from log-normal distribution of data. No standard deviation is available for 25 to 200°C because of change in statistical distribution of data between low-temperature intervals (25 to 50°C, 50 to 100°C) and high-temperature intervals (100 to 150°C, 150 to 200°C).

[d]Nonlinear transitional behavior of the Topopah Spring Member (200 to 350°C) results from the α to β transformations of cristobalite and tridymite.

[e]NA = not applicable. These materials do not show post-transition behavior.

[f]Calculated coefficient based on measured unconfined expansion through 100°C and the measured, confined, predehydration expansion coefficient.

behavior is prominent in the few relatively thin, bedded, or reworked intervals identified in the stratigraphic section at Yucca Mountain.

In confined tests (confining pressure of 10 MPa, pore fluid pressure of 0.1 to 1.5 MPa) all zeolitized tuffs expand continuously, until the onset of dehydration, at rates ranging from 3 to 13 x 10^{-6} K^{-1} (Lappin and Nimick, 1985a). Detailed correlation of predehydration expansion with mineralogic composition is under way.

Comparison of replicate unconfined expansion runs made parallel and perpendicular to bedding in a devitrified, densely welded sample from the Grouse Canyon Member of the Belted Range Tuff indicates that there is no

Table 2-14. Recommended values for thermal and physical properties of thermal/mechanical units

	Grain density (g/cm^3)		Porosity		Thermal conductivity (W/mK)				Coefficient of thermal expansion (10^{-6} K^{-1})						Volumetric heat capacity (J/cm^3K)	
					Saturated[a]		Dry		Pretransition		Transition		Posttransition			
Unit[b]	Mean	St. dev.	Mean	St. dev.	Mean	St. dev.	Mean	St. dev.	Mean	T(°)	Mean	T(°C)	Mean	T(°C)	Saturated[k]	Dry
TCw	2.51	0.04	0.11	0.04	2.03[c]	0.20[c]	1.76[c]	0.29[c]	8.8[d]	25-200[d]	NA[e]	NA	NA	NA	2.18	1.88
PTn	2.37	0.15	0.45	0.15	1.35	0.06	1.02	0.19	5.3[f]	25-150[f]	3.5[f]	150-250[f]	NA	NA	2.24	1.09
TSw1[g]	2.54	0.04	0.14	0.04	2.03	0.20	1.76	0.29	11.8	25-200	51.8	200-250	NA	NA	2.09	1.98
TSw1[h]	2.53	0.02	0.35[i]	0.03	1.96	0.41	1.21	0.14	NA	NA	NA	NA	NA	NA	1.87[i]	1.38[i]
TSw2	2.55	0.03	0.12	0.03	2.29	0.17	1.88	0.24	8.8	25-200	24.0	200-300	NA	NA	2.16	2.17
TSw3	2.39	0.02	0.04	0.03	1.34	0.10	1.40	0.16	5.3	25-150	3.5	150-250	NA	NA	2.06	2.45
CHn1v	2.34	0.06	0.36	0.09	1.35	0.06	1.02	0.19	5.3[f]	25-150[f]	3.5[f]	150-150[f]	NA	NA	2.61	1.26
CHn1z	2.41	0.06	0.33	0.04	1.48	0.17	1.01	0.14	6.7	25-T_b[j]	-56.0	T_b-150	-4.5	150-300	2.61	1.36
CHn2	2.54	0.12	0.29	0.06	1.61	0.04	1.21	0.04	6.7k	25-T_b[k]	-56.0[k]	T_b-150[k]	-4.5[k]	150-300[k]	2.62	1.51
CHn3	2.41	0.04	0.36	0.08	1.43[l]	0.03[l]	1.04[l]	0.05[l]	6.7[k]	25-T_b[k]	-56.0[k]	T_b-150[k]	-4.5[k]	150-300[k]	2.66	1.30
PPw	2.58	0.04	0.24	0.07	2.00[m]	0.27[m]	1.35[m]	0.30[m]	8.3[m]	25-T_b[m]	-12.0[m]	T_b-125[m]	10.9[m]	>125[m]	2.65	1.65
CFUn	2.43	0.07	0.30	0.08	1.43	0.03	1.04	0.06	6.7[k]	25-T_b[k]	-56.0[k]	T_b-150[k]	-4.5[k]	150-300[k]	2.68	1.43
BFw	2.60	0.04	0.24	0.08	2.00	0.27	1.35	0.30	8.3	25-T_b	-12.0	T_b-125	10.9	>125	2.66	1.66
CFMn1	2.41	0.06	0.25	0.06	1.43	0.00	1.11	0.07	6.7[k]	25-T_b[k]	-56.0[k]	T_b-150[k]	-4.5[k]	150-300[k]	2.56	1.52
CFMn2	2.52	0.06	0.24	0.03	1.61	0.04[n]	1.21[n]	0.04[n]	6.7[k]	25-T_b[k]	-56.0[k]	T_b-150[k]	-4.5[k]	150-300[k]	2.61	1.61
CFMn3	2.44	0.07	0.27	0.03	1.46	NA	1.11	NA	6.7[k]	25-T_b[k]	-56.0[k]	T_b-150[k]	-4.5[k]	150-300[k]	2.62	1.50
TRw	2.63	0.04	0.19	0.06	2.09	0.18	1.79	0.37	8.3[m]	25-T_b[m]	-12.0[m]	T_b-125[m]	10.9[m]	>125[m]	2.58	1.79

[a]Thermal conductivity data for all units except TSw1 (nonlithophysal), TSw2, TSw3, and volumetric heat capacity data for PPw and underlying units are for a nominal saturation of 1.0, whereas volumetric heat capacity data are calculated using saturations from Montazer and Wilson (1984) for CHn3 and overlying units.

[b]See Figure 2-5 for definition of thermal/mechanical units.

[c]Assumed to be the same as correlative property for TSw1 (nonlithophysal).

[d]Assumed to be the same as correlative property for TSw2.

[e]NA = not applicable or no data.

[f]Assumed to be the same as correlative property for TSw3.

[g]Nonlithophysal layers within unit TSw1.

[h]Lithophysal layers within unit TSw1.

[i]Note that, for lithophysal layers, the total porosity is $\phi_M M + \phi_A A + \phi_L$, where ϕ_M is matrix porosity, ϕ_A is porosity of vapor-phase-altered material, ϕ_L is the volume percent lithophysal cavities, and M and A are volume fractions of matrix and vapor-phase-altered material, respectively. In order to calculate volumetric heat capacity, M = 0.55, A = 0.29, ϕ_M = 0.08 and ϕ_A = 0.49 (Price et al., 1985).

[j]T_b = boiling point of water.

[k]Assumed to be the same as correlative property for CHn1z.

[l]Assumed to be the same as correlative property for CFUn.

[m]Assumed to be the same as correlative property for BFw.

[n]Assumed to be the same as correlative property for CHn2.

TSw3, the heat capacities of the silicate mineral assemblages were assumed to be those given by Nimick and Schwartz (1987). For the lithophysal zones, lithophysal cavities (17 volume percent as determined by Price et al., 1985) are assumed to be dry. For units above the water table (assumed to be CHn3 and above) the saturation is assumed to be as given by Montazer and Wilson (1984) for temperatures below the boiling temperature.

2.5 THERMAL AND THERMOMECHANICAL PROPERTIES--LARGE SCALE

This section provides an overview of the field tests in tuff that have provided information on the in situ values of thermal conductivity, heat capacity, and thermal expansion. To date, these field tests have been performed with the objective of observing thermal and hydrothermal phenomena in simulated nuclear waste repository environments. As such, the measurements of thermal properties generally have not been a direct goal of a test.

All field tests to date have been performed in tuffs in G-Tunnel. Four small-diameter heater tests have been completed, although the data from the most recently completed test have yet to be reduced and analyzed. In addition, the testing of the heated block (Section 2.3.2) included thermal-cycle testing from which thermal expansion behavior has been quantified.

Of the tests mentioned in the preceding paragraph, information on in situ thermal conductivity can be extracted from three of the heater tests. Small-scale cylindrical heaters were emplaced in drillholes in the Grouse Canyon Member and in tunnel bed 5 in G-Tunnel (Zimmerman, 1983; Johnstone et al., 1985). By comparing the temperatures and temperature gradients predicted by thermal modeling of these tests with the actual temperatures and gradients measured in situ, an assessment can be made of whether in situ thermal conductivity can be accurately predicted from laboratory values. Specific limitations or uncertainties inherent in such tests follow:

1. Variable and uncontrolled degrees of saturation may have existed in the rock mass containing the heater. Such variations would have affected thermal conductivity, amounts of fluid released, and fluid movements during heating.

2. Thermocouples spring-mounted on the heater could not be fully shielded from thermal radiation between the heater and the drillhole wall. As a result, these thermocouples can register a temperature as much as 20 Celsius degrees too high (Johnstone et al., 1985).

Direct measurement of the in situ thermal expansion of the rock mass has been accomplished in other rock types by means of standard extensometers (wire, rod, or both) (Lappin et al., 1981). Laser strain interferometry has been attempted in G-Tunnel (Johnstone et al., 1985), but the lack of a suitably stable platform from which to make the measurement made the resulting data difficult to interpret. Deformations related to the thermal expansion of the heated block were measured with horizontal surface extensometers and multiple-point borehole extensometers (Zimmerman et al., 1985). Both types of instrumentation provided reliable data for the duration of the test.

DECEMBER 1988

Indirect observations of the thermal expansion behavior of the Grouse from field measurements on biotite gneiss are consistent with laboratory-determined coefficients for other granitic rocks (Stripa and Climax granites). In contrast, Cook et al. (1983) found that the ratio of field-to-laboratory values for the thermal expansion coefficient of Stripa granite was approximately 0.68. This latter observation appears to conflict with the data from other rocks, but no error bands or experimental ranges are provided with which to analyze the discrepancy.

2.5.2 THERMAL AND THERMOMECHANICAL PROPERTIES OF ROCK AT THE SITE

2.5.2.1 Thermal conductivity

The in situ thermal conductivity of tuff has been determined during the G-Tunnel heated-block experiment. Measured values ranged from 1.53 to 1.63 W/mK over a temperature range of 18 to 80°C (Zimmerman et al., 1986). These values are consistent with data obtained in the laboratory.

In addition to the in situ values, an approach slightly different from that used in analyzing the in situ tests in Section 2.5.1 was used. Laboratory data for thermal conductivity and heat capacity were used in the calculation of the temperature fields to be expected in the tuff surrounding the heaters. A comparison of these predicted temperatures with those actually observed indicated that when laboratory data for the thermal properties were used in the calculations, the measured temperatures were within 6 percent of the predicted values in 2 tests (Zimmerman, 1983), whereas measured temperatures were 12 percent less than predicted values for a third heater test during the heating phase (Johnstone et al., 1985). The discrepancies in the last test were attributed to the modeling of the heat source and the water transport, because predicted and measured temperatures were almost identical during cooldown (Johnstone et al., 1985).

The results obtained to date in tuff suggest that little additional in situ testing of thermal conductivity is required for welded tuffs above the water table to determine the rock mass thermal conductivity for use in far-field or room-scale calculations. Additional evaluations will be made in tests conducted in the exploratory shaft to increase confidence in the values of thermal conductivity used in the heat transfer analyses for repository design (Section 8.3.1.15).

The effects of joints or fracture porosity on the in situ thermal conductivity of devitrified welded tuffs have been estimated, assuming a fracture porosity of 3 percent (Lappin et al., 1982). This assumption ignores the possibility of joint closure resulting from overburden pressures or from the thermal expansion of the rock and, therefore, is assumed to provide an

The thermal conductivity of the rock mass of the Topopah Spring Member will be examined in tests in the exploratory shaft facility (Section 8.3.1.15).

2.5.2.2 Thermal expansion

The attempt to measure directly the thermal expansion of welded tuff in situ during the earliest heater test (Johnstone et al., 1985) was unsuccessful. However, the measurement of thermally induced stresses was at least partially successful. In this test, measured thermally induced stresses were approximately 40 percent of expectations on the basis of thermomechanical modeling using laboratory-derived expansion values.

Data taken during the thermal-cycle testing of the heated-block test yielded in situ values for the thermal expansion coefficients ranging from 5.0 to 8.7 x $10^{-6}K^{-1}$ (Zimmerman et al., 1985). This range compares favorably with the range in mean values from laboratory tests, 6.4 to 8.0 x $10^{-6}K^{-1}$ (Lappin and Nimick, 1985b).

The approximate equivalence of laboratory and rock mass thermal expansion coefficients determined for the Grouse Canyon Member of the Belted Range Tuff suggests that the discrepancy between predicted and measured thermal stresses observed by Johnstone et al. (1985) is attributable to differences between laboratory and in situ elastic moduli.

2.5.3 RELATIONSHIP BETWEEN INTACT ROCK AND LARGE-SCALE PROPERTIES

The results of the in situ heater tests in G-Tunnel described above indicate that the laboratory measured thermal conductivity can be used in successfully modeling temperatures observed in field tests. Thus, as a good approximation, the values of rock mass thermal conductivity are assumed to be the same as those for intact rock. The same approximation is made concerning heat capacity and the coefficient of linear expansion. The latter will be measured in situ in the exploratory shaft facility to examine the validity of extrapolating laboratory values to the rock mass.

2.6 EXISTING STRESS REGIME

Designing the Yucca Mountain repository will require knowledge of the magnitude, direction, and variability of the preconstruction in situ state of stress, excavation-induced stresses, and thermally induced stresses. The preconstruction state of stress is particularly vital to the determination of site suitability. Design parameters (such as room dimensions and pillar widths) can be varied to change the magnitude and direction of excavation-induced stresses. Similarly, parameters such as gross thermal loading, waste package dimensions, and emplacement orientations can be adjusted to modify thermally induced stresses. Because the preconstruction in situ stress field cannot be modified, the design analyses will treat the in situ stresses as an initialized stress state on which the excavation and thermal stresses must be superposed. The magnitude, direction, and variability of principal stresses are of importance in the analysis and design of stable underground openings as well as in the prediction of rock mass deformation for both long and short times and the resulting applications to performance assessment calculations. Subsurface openings must be designed to provide stability from construction through permanent closure.

This section reviews the current understanding of the state of stress at Yucca Mountain and its vicinity. Regional geologic studies, field measurements at Yucca Mountain and nearby Rainier Mesa, and finite-element calculations of the overburden-induced component of in situ stress are presented to summarize the state of knowledge.

Detailed results of in situ stress measurements in tuffs at Yucca Mountain or at Rainier Mesa are contained in several references (Hooker et al., 1971; Haimson et al., 1974; Tyler and Vollendorf, 1975; Ellis and Ege, 1976; Ellis and Magner, 1980; Warpinski et al., 1981; Zimmerman and Vollendorf, 1982; Stock et al., 1984). These references also discuss details of testing techniques and potential limitations and errors. Additional discussion of some of the results is provided in Chapter 1, along with information on regional geologic studies relevant to the stress state.

Two methods were used by most of the workers cited in the previous paragraph for measuring in situ stress: overcoring and hydraulic fracturing. With the overcoring technique (Hooker and Bickel, 1974), changes in strain are measured in a small borehole before, during, and after overcoring with a larger core barrel. As such, the rock around the overcored region is strain relieved. The complete state of stress can be calculated from such strain relief measurements in three nonparallel drillholes by using the appropriate equations (Jaeger and Cook, 1979). Triaxial cells have been developed that (see for example, Leeman, 1964; Doe et al., 1981) allow the measurement of principal stresses by overcoring in a single hole. The advantage of the overcoring technique is that it allows for an estimation of the full stress tensor. A limitation of the method is that the deformation modulus of the rock must be known to obtain the stresses from the measurements.

For the hydraulic fracturing technique, the borehole is assumed to be parallel to a principal stress. First, a selected section of a borehole is sealed off with packers. Then, fluid pressure is increased within the sealed section until the rock at the borehole wall fractures. Theory predicts that at a high enough borehole pressure, the rock will fail in tension. For a borehole that parallels a principal stress direction, the fracture that forms at the borewall is generally perpendicular to the minimum horizontal stress, and the pressure required to hold the fracture open provides a reasonable estimate of the minimum horizontal stress (Stock et al., 1984). (If the borehole axis does not coincide with a principal stress, the testing will provide a measure of the stresses normal to the borehole rather than the principal stresses.) The maximum horizontal stress can be calculated if other properties can be acquired (Stock et al., 1984). Borehole televiewer or impression packers are required to determine the orientation of hydraulic fractures at the borehole wall and, hence, the orientation of the minimum stress acting normal to the borehole. It is possible, with the hydraulic fracturing technique, to make stress measurements anywhere that a borehole exists. A limitation to the technique is that the results may be difficult to interpret in heavily fractured or otherwise permeable rock.

It is apparent that both measurement techniques could be used at a particular site to minimize the limitations and to maximize the advantages of each technique. Overcoring can provide an indication of the validity of assuming that a borehole used for hydraulic fracturing is parallel to a principal stress. Hydraulic fracturing measures the in situ stress state on a larger scale than does overcoring. Satisfactory correlation has been observed between the measurement techniques when used together in the past (Miller, 1976; Doe et al., 1981; Haimson, 1981; Doe et al., 1983). However, Dischler and Kim (1985) point out that overcoring results from experiments on closely jointed rocks show great variability, making the stress measurements difficult to compare with those from other techniques. Both techniques generally assume an isotropic, elastic material. As discussed in Section 2.1, these two assumptions are probably reasonable for the intact tuffs at Yucca Mountain.

Numerical modeling (finite elements) has been used to estimate the overburden-induced component of in situ stress at Rainier Mesa. Using linear elastic behavior and isotropic material properties within each tuff layer, plane-strain approximations of the gravity-induced component (including surface topography) of the in situ stress agree rather well with in situ measurements (Holland and Bauer, 1984). Used in combination with in situ most movement is strike-slip along steeply dipping planes that strike north to northeast.

Fractures, interpreted to be tensile, in a playa at the NTS have strikes of approximately N.50°E., suggesting relative extension in a N.40°W., direction (Carr, 1974). Dimensional changes of vertical boreholes in the alluvium of the playa, determined by borehole caliper, indicate an average direction

of drillhole elongation of N.60°W., consistent with the relative extension in

2.6.1.2 Overcoring measurements

Vertical hydraulic fracture studies in Rainier Mesa (Warpinski et al., 1981) document the vertical variation in minimum stress, which has been correlated to the vertical variation in material properties. Minimum horizontal stresses tend to be lower in the welded tuffs, which have high values of Young's modulus and low values of Poisson's ratio, and higher in the nonwelded tuffs, which have lower Young's moduli and higher Poisson's ratios.

2.6.1.4 Finite-element calculations

Using a two-dimensional finite-element model of Rainier Mesa, the stresses resulting from gravity loading and elasticity of the rocks have been calculated (Holland and Bauer, 1984; Bauer et al., 1985). The calculations assumed plane strain conditions and linear elastic material response. The material properties were assumed to be different for welded and nonwelded units. The ground surface was assumed to be a free surface, whereas the remaining boundaries were sufficiently far from the region of interest as to have no effect on the calculational results. These analyses, which incorporated topographical and stratigraphic effects but neglected tectonic and residual stresses, appear to account for the vertical variation in stresses reported by Warpinski et al. (1981).

2.6.2 STRESS REGIME AT THE SITE

2.6.2.1 Field observations

The preceding discussions have focused on observations and measurements of stress fields at the NTS as a whole and under Rainier Mesa. The evidence, which is discussed in greater detail in Chapter 1, suggests a dominating regional stress field in which the minimum principal stress is oriented approximately along the axis N.65°W. to N.70°W. (USGS, 1984). The maximum principal stress in the region is generally also horizontal indicating a strike-slip regime, whereas at Yucca Mountain the maximum stress axis is vertical as is discussed below. The mean value for the magnitude of the vertical stress, determined by the product of overburden, density, and gravitational acceleration is 7 MPa at 300 m depth. A discussion of ranges in this value is given in Section 6.1.2.2.2.

Hydraulic stress measurements and borehole televiewer observations in drillhole USW G-2 (Stock et al., 1985) indicate an orientation of N.60 to 65°W. for the direction of least horizontal stress and a minimum horizontal stress (S_h) to vertical stress (S_v) ratio of ≤ 0.84 at a depth of 295 m decreasing to 0.47 at 1,209 m (Figure 2-21). The inequality on the first ratio listed is based on discussion by Stock et al. (1984, 1985), which suggests that the values calculated for the minimum horizontal stress from the measurements may be greater than the actual values for this stress in the unsaturated zone.

In situ stress data from drillhole USW G-1 are also shown in Figure 2-21; in this drillhole, all data are from tests in the saturated

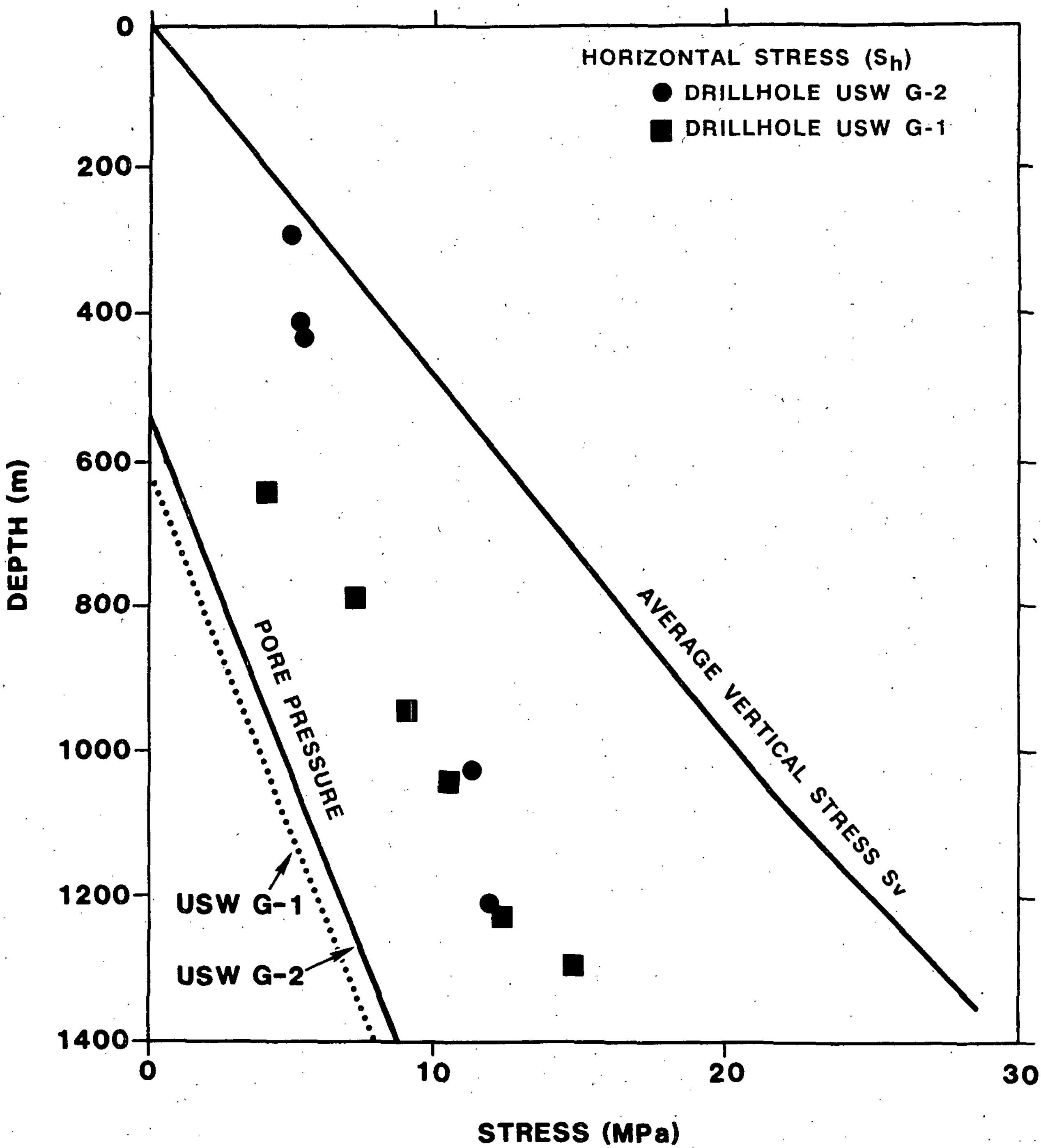

Figure 2-21. Least horizontal and vertical principal stress values and pore pressure plotted against depth. Modified from Stock et al. (1984).

zone. Ratios of S_h to S_v in drillhole USW G-1 are approximately 0.3 to 0.5, and are consistent with ratios for tests in the saturated zone in drillhole USW G-2. Televiewer observation of drillholes has indicated the presence of drilling-induced hydraulic fractures in the shallow parts of drillholes USW G-1 and USW G-2 (Stock et al., 1985). These fractures have orientations consistent with the orientations measured by hydraulic fracturing tests.

The magnitude of the maximum horizontal stress (S_H) was estimated by Stock et al. (1985) to be approximately halfway between S_h and S_v. This conclusion was based on calculations from hydraulic fracturing data combined with observations of well bore spalling in drillholes USW G-1 and USW G-2. The relative magnitudes of the three principal stresses are consistent with a normal faulting regime (Stock et al., 1985), and differs from the strike-slip regime that is typical of the NTS region.

The possibility that movement on favorably oriented fault planes may occur under the existing stress regime has been mentioned by the USGS (1984) and Stock et al. (1985). Further discussion of this topic is presented in Section 1.3.2.3.

The in situ stress at Yucca Mountain has also been measured in drillholes UE-25p#1, USW GU-3, and USW G-3. Data from these tests are being reduced and analyzed. In addition, some data will be obtained during exploratory shaft activities (Section 8.3.1.15).

2.6.2.2 Finite-element calculations

Finite-element calculations similar to those described in Section 2.6.1.4 for Rainier Mesa have been performed to estimate the gravity-induced component of in situ stress at Yucca Mountain (Bauer et al., 1985). At the 300-m depth range, gravity loading alone produced a ratio of S_h to S_v of approximately 0.3. Since the maximum value measure in drillhole USW G-2 for this ratio was 0.8, the gravity load can account for at least 38 percent of the minimum horizontal stress and may account for more if the ratio from field data is actually less than 0.8. The remainder of the minimum horizontal stress comes from tectonic stresses, residual stresses, or both.

Another analytic calculation of the stress state at Yucca Mountain has been described by Swolfs and Savage (1985) who also conclude that gravity plays a major role in determining the in situ stresses. In addition, they suggest that the distribution of near-vertical fractures and faults causes transverse anisotropy in rock mass elastic properties, which in turn affects the relative stress magnitudes.

The two studies mentioned in the preceding paragraphs have attempted to provide a general understanding of stress distribution with depth at Yucca Mountain. Although the two studies took somewhat different approaches, both explained the limited available measurements. Neither modeling effort considered all the possible relevant parameters. Bauer et al. (1985) assumed that each tuff unit was isotropic, in contrast to the transverse anisotropy examined by Swolfs and Savage (1985). Swolfs and Savage (1985) did not consider the variation in elastic properties between differing lithologies.

Bauer et al. (1985) found a model that incorporated variable elastic properties to be more successful at reproducing measured data at Rainier Mesa than a model using homogeneous properties. In addition, both studies assumed instantaneous gravity loading rather than the sequential loading imposed by normal depositional processes. This last deficiency may lead to results that differ from the theoretically correct calculated stresses (Goodman and Brown, 1963).

Nevertheless, finite-element calculations have the potential to be a useful tool in estimating the two- or three-dimensional distribution of in situ stresses for use in repository design or performance-assessment calculations. Care must be taken to understand the limitations of such an estimate and to incorporate measured data into the calculation to the degree possible.

2.7 SPECIAL GEOENGINEERING PROPERTIES

Two special geoengineering considerations are recognized to be of potential importance for evaluating the effects of waste emplacement in Yucca Mountain tuffs: thermally induced degradation of the rock mass and thermally induced dewatering (water migration). Both of these phenomena were hypothesized because of the varying porosity, permeability, and degree of saturation, coupled with the geologically instantaneous thermal loading. Additional phenomena or processes requiring study may be identified during site characterization. Performance assessment work will determine the sensitivity of repository performance to all identified processes.

Thermally induced degradation was considered because of its potential impact on the mechanical and transport properties of the rock mass. Conse-

2.7.1.1 Near-field decrepitation

Emplacing hot nuclear waste in relatively cold (25°C), partially saturated tuff produces a geologically instantaneous load on the rock-water system. Both the temperature and the temperature gradient change (in rock these temperature changes are interdependent (Johnson and Gangi, 1980)) with resulting development of thermal strains, stresses, or both. A number of phenomena, including mineral phase changes, dehydration, and mineral and water expansion, contribute to the reaction of the rock mass to the changes in the temperature field. The total effect has been quantified by numerous [illegible]

Topopah Spring Member from ambient temperature to 225°C was quantified by measuring the relative changes of the moisture content between pre- and post-thermal treatment measurements (Nimick, 1987). No measurable changes in the moisture content were observed. It was concluded that (1) if new void spaces (cracks) were induced in the rock, they were of insufficient magnitude to be measured and (2) if new cracks were induced, they did not act to enhance interconnectivity to previously isolated void space. From these conclusions it was further speculated that, when the saturated rock was heated, no anomalously high pore pressures from water trapped in voids (on the order of the tensile strength of grain boundaries as a maximum) were generated. This means that either all pore spaces were initially well interconnected or high temperatures facilitated fluid flow (by decreasing water viscosity and opening preexisting cracks), or both. This experiment and analysis together imply that changes in microstructure resulting from realistic thermal loading do not occur, and thus alteration of mechanical and transport properties (thermal degradation) in the very-near-field is not predicted. The effects of elevated temperature on the mechanical properties of intact Topopah Spring Member will be measured, as mentioned in Sections 2.1.2.2 and 2.1.2.3.1.3, and discussed in more detail in Section 8.3.1.15.1.

Expected stratigraphic variations in the potential for rock mass degradation can be qualitatively assessed and extended on the basis of the results of work performed to date. Increases in thermal conductivity should decrease the potential for degradation at any given thermal loading because very-near-field temperatures and thermal gradients decrease when thermal conductivity increases. Partial saturation of the rock mass should decrease the degradation potential because it would provide additional free volume for fluid expansion. Increasing fracture frequency should decrease the degradation potential because the path lengths to be traversed by the fluid to achieve pressure release would be shorter. Finally, decreasing the thermal loading of a repository should decrease the degradation potential because the volume of rock that experiences sufficiently rapid heating will be smaller.

Because of these considerations, the degradation of tuffs in general is considered improbable. Degradation of the Topopah Spring Member is considered extremely improbable because of the high fracture frequency (Section 1.3.2.2) and partial saturation (65 percent) (Montazer and Wilson, 1984). In addition, no evidence of degradation has been observed in the walls of heater holes in three heater tests conducted in G-Tunnel in both welded (two tests) and nonwelded tuff. No additional tests are planned specifically for obtaining data on thermal degradation, but the response of the Topopah Spring Member to elevated temperatures will be observed during exploratory shaft facility testing.

2.7.2 THERMALLY INDUCED WATER MIGRATION

Formation of convection cells of liquid water is not expected to occur in a partially saturated host rock above the water table because of the lack of global continuity of the liquid phase. The thermal gradients produced by the emplaced waste allow the possibility of vapor convective cells to be produced. Fractures in partially saturated systems are considered to be generally unsaturated because water they might contain is drawn into the rock matrix by capillarity (Montazer and Wilson, 1984). The fractures therefore have relatively high vapor conductivity and exert a strong effect on both moisture movement and convective heat transfer. The discussion in the following two paragraphs pertains to a conceptual model for thermally induced moisture movement in a continuum.

Water movement is generally recognized to occur because of a vaporization-condensation mechanism (Gurr et al., 1952; Somerton, 1982). As the boiling point is reached in the partially saturated rock matrix, liquid water vaporizes and tends to move down the temperature gradient away from the emplaced waste. The phase change produces a gas pressure that drives vapor away from the location of boiling. Vapor moves in the direction of a potential gradient that is a function of static pressure and temperature. Gas pressure might also drive the movement of liquid water away from the emplaced waste although it is anticipated to be a smaller flux than the vapor transport (Gurr et al., 1952). Vapor will condense at the leading edge of the dewatered region around the borehole, causing a locally increased level of saturation.

The gas pressure equilibrates rapidly with the flow of displaced liquid water. A dewatered region around the emplacement borehole develops that expands with time, and produces a gradient in the liquid saturation. The liquid potential is a function of saturation as well as temperature and static pressure. The saturation gradient tends to drive liquid water toward the emplaced waste. Even in the simplest form of this conceptual model, the magnitudes and directions of the liquid and vapor fluxes depend on many parameters including the permeability of the medium, in situ saturation, the hydraulic characteristics of the unsaturated matrix, and the specific heat source.

Pruess et al. (1984) formulated numerical models of the thermal migration problem in fractured tuff, using both an explicit representation of idealized discrete fractures, and an equivalent continuum approach that

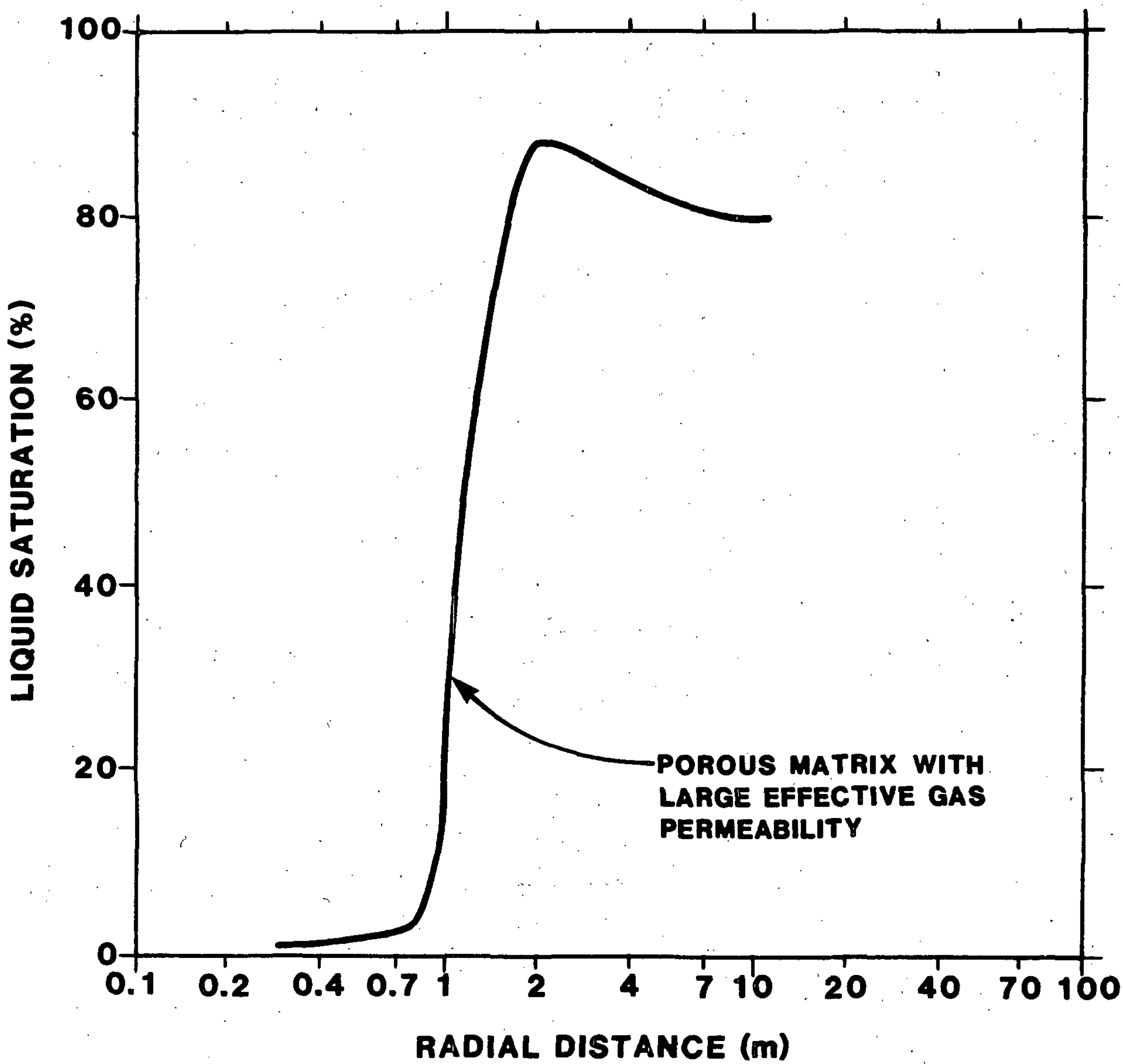

Figure 2-22. Simulated liquid saturation profile near a container in tuff (t = 160 days, initial saturation = 80 percent). Modified from Pruess et al. (1984).

mobilized from the boiling region, and conduct it outward to a region of condensation. The liquid condensate is then drawn into the matrix by capillary action, and tends to flow down the saturation gradient back toward the boiling region. The vapor flux exceeds the liquid return flux, so the dewatered region expands around the borehole. If the fracture characteristics are adjusted to permit liquid movement in the fractures, then the saturation gradient drives liquid back toward the boiling region along the fractures. A vapor-liquid counterflow develops, which accounts for much of the heat flow away from the borehole. Movement of the boiling front in the matrix is accordingly reduced.

Preliminary design specifications associated with the work of Pruess et al. (1984) indicate that a dried-out, dewatered region forms around the waste emplacement holes in less than a year, so that the possibility for liquid transport of radionuclides is apparently reduced. The majority of mass transport of water at early time after emplacement is expected to occur in the vapor phase. Heated vapor will be introduced into the drifts, and ventilation requirements must be considered.

Field experiments in granite and tuff indicate that water movement is an induced response that can be expected upon heating a rock mass. In many instances, water has entered heater and instrumentation holes, thereby affecting instrumentation longevity as well as the temperatures resulting from simulated waste emplacement (Carlsson, 1978; Lappin et al., 1981; Johnstone et al., 1985). In tests in the Eleana argillite and in the water

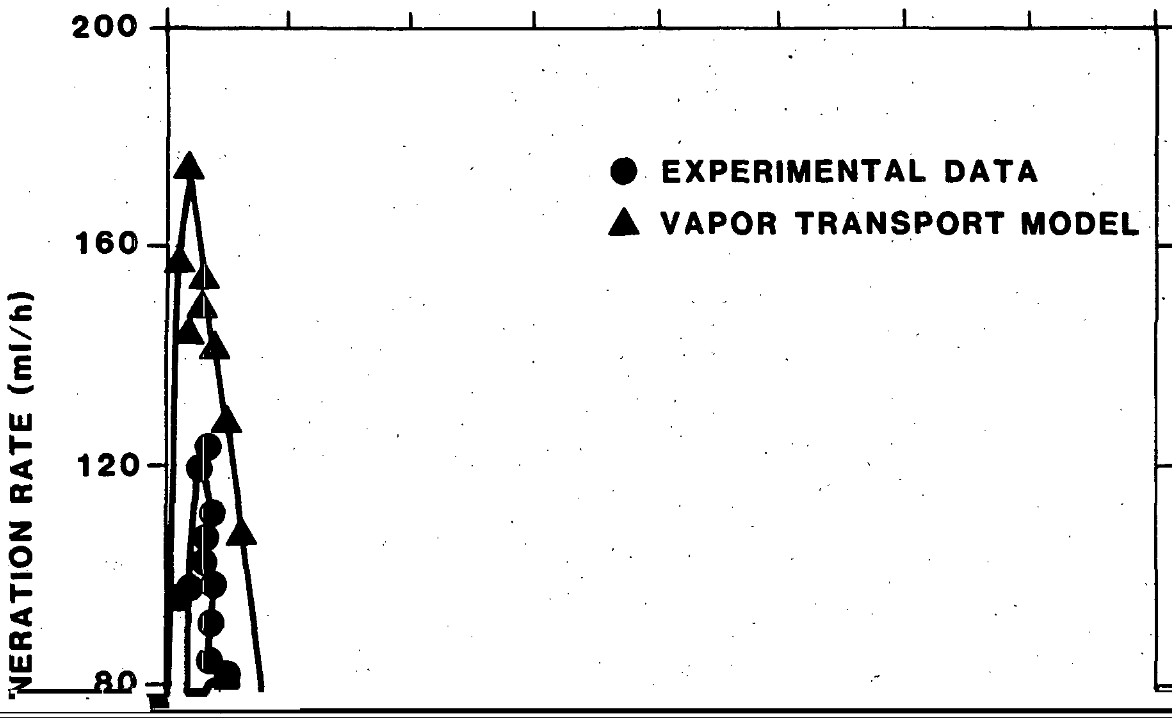
200
160
120
80
ERATION RATE (ml/h)
EXPERIMENTAL DATA
VAPOR TRANSPORT MODEL

(and that occurred only at the start of the test). Once the rock wall temperatures exceeded 94°C (the boiling temperature at ambient pressure in G-Tunnel), convective water transport mechanisms appeared to dominate. This was evidenced by the presence of vapor in the warmer air around the heater and condensate in the cooler region at the bottom of the boreholes. Differences between the two experiments in the quantities of water collected in cooler regions of the borehole suggest that some vapor may have moved through the fractures in the welded tuff.

Additional evaluations of water migration phenomena were made as part of the recently completed heated-block test, again carried out in G-Tunnel (Zimmerman et al., 1984a). Those measurements were intended primarily to evaluate changes in local saturations or pore pressures upon heating. Documentation of the saturations as a function of temperature is provided by Zimmerman et al. (1985). The moisture content as a function of temperature was monitored at one location for more than 8 months using a neutron moisture probe. The moisture content began to decrease at approximately 80°C and continued to decrease to the measurement limit of 15 percent saturation, attained at a temperature of approximately 150°C. When coupled with the temperature measurements, these results should aid in understanding thermally induced flow and its effect on material properties (primarily thermal conductivity).

From the results of heated-borehole experiments in a granitic rock mass monitored for nearly 2 yr, it was concluded that the induced temperature field caused stress in the rock mass that closed fractures and cracks (Nelson and Rachiele, 1982). The water contained in the openings was forced to migrate as pore and crack space was reduced. When the heat was turned off, the cracks ceased closing, and the flow of water into the instrumented boreholes was reduced or stopped. It should be noted that in a partially saturated, fractured rock mass like the Topopah Spring Member, the fractures are expected generally to be in a condition of very low saturation because of the strong capillary forces of the matrix (Montazer and Wilson, 1984). Therefore, the closing of fractures by thermal strain should not be a significant cause of water migration in the Topopah Spring Member.

Additional evaluations of thermally induced water migration phenomena are planned as part of laboratory testing (Section 8.3.4.2). Thermally induced water migration phenomena will also be observed in association with in situ testing in the exploratory shaft facility. These tests are intended to examine both the mechanisms of thermally induced water movement and the effect of thermal dewatering on the thermal and mechanical properties of the rock mass.

2.7.3 GEOENGINEERING PROPERTIES OF SURFACE MATERIALS

Ongoing studies to select a site for the major surface facilities of a repository at Yucca Mountain are concentrating on locations in which the surface material is alluvium (Neal, 1985). A general description of this material is provided in Chapter 1. A more site-specific description is given in this section, along with the available geoengineering data pertinent to the design of the surface facilities.

2.7.3.1 Lithologic description of alluvium

Limited preliminary investigations, consisting of surface observations and exploratory borings, were completed in six areas selected as potential sites for central surface facilities (Neal, 1985). Preliminary stratigraphic information has been developed from the exploratory boreholes. The total depth of the alluvium at the proposed location of the central surface facilities (designated site 3 by Neal (1985)) is about 90 ft (27.4 m); however, because the bedrock surface is sloping, the thickness of alluvium may be more or less than this value, depending on the final location of surface structures.

In general, the alluvium is a light tan-to-gray, silty-to-sandy gravel, with numerous blocky cobbles and boulders. These rock particles, which are derived from nearby bedrock sources, consist mostly of welded or partly welded volcanic ash-flow tuffs. Test pits excavated at several of the sites studied showed well-developed soil horizons in the upper portions of the alluvium. The top 1 or 2 ft (0.3 or 0.6 m) (A and B horizons) are loose and [illegible]

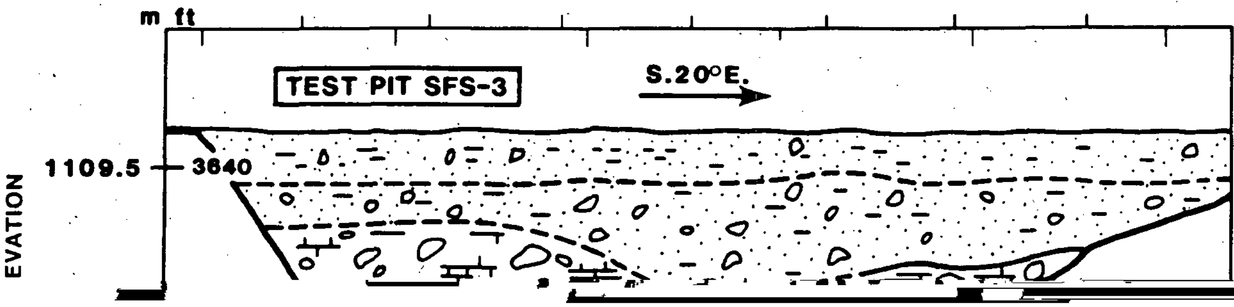
m ft
TEST PIT SFS-3
S.20°E.
1109.5
3640
EVATION

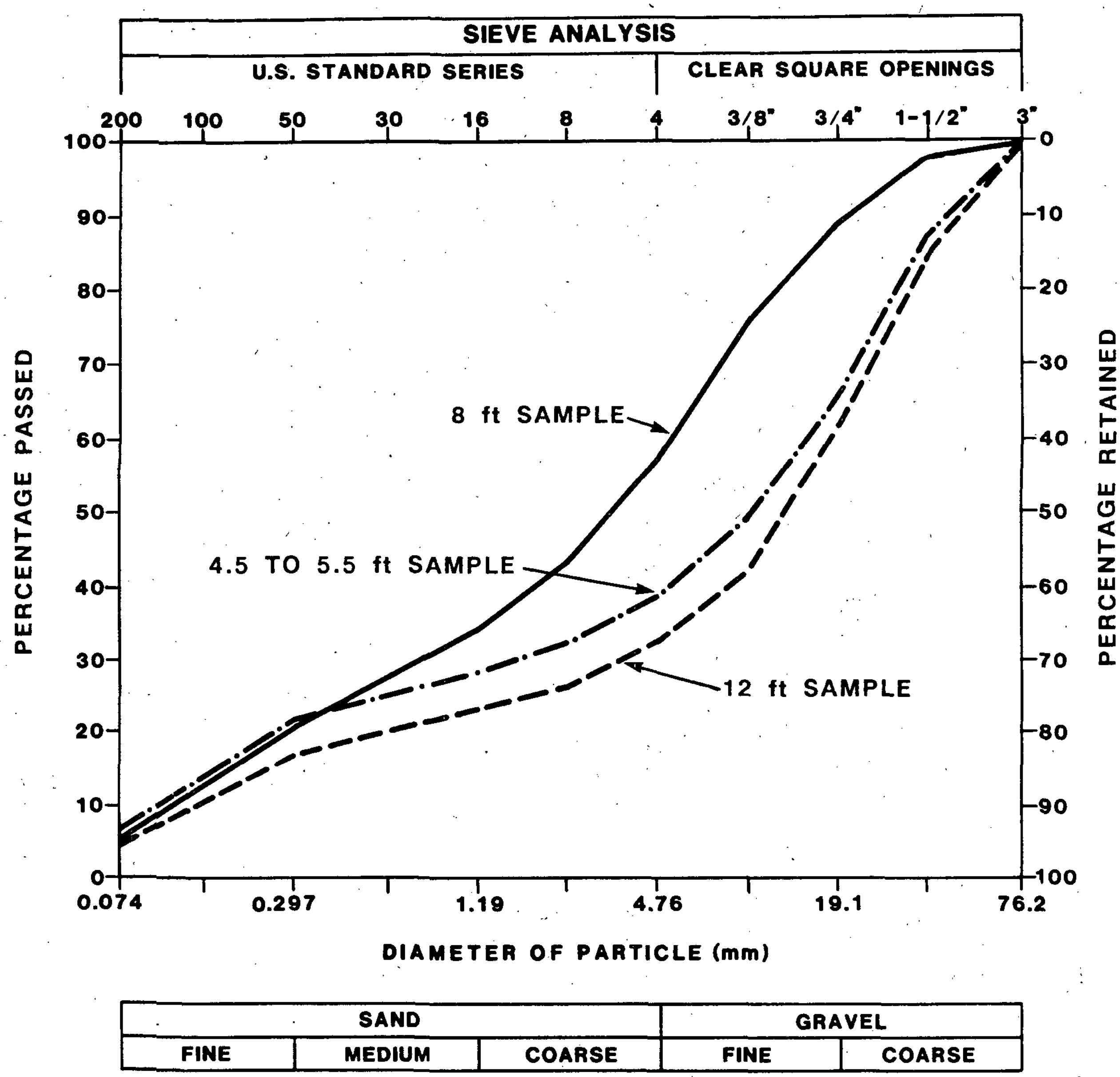

Figure 2-25. Gradation curves of samples from test pit SFS-3 at 4.5 to 5.5, 8, and 12-ft depths. Modified from Ho et al. (1986).

Compaction test results for the soils sampled from test pit SFS-3 show appreciable variation. The maximum dry density ranges from 108 to 114 lb/ft^3 (1.73 to 1.83 g/cm^3). The corresponding optimum moisture contents are 14.7

Table 2-15. Summary of physical and engineering properties of alluvium[a]

PHYSICAL PROPERTY[b]	
Soil classification	GP and GM present[c]
Natural moisture content	5.1-9.2%
In situ density	101-112 pcf (1.62-1.79 g/cm^3)
Percent of maximum dry density	93.5-100%
Specific gravity of soil solids	2.43
Void ratio	0.37
ENGINEERING PROPERTY[d]	
Young's modulus	10,000-20,000 psi (0.7-1.4 GPa)
Poisson's ratio	0.30-0.35
Modulus of subgrade reaction	200-300 pci (5,536-8,304 g/cm^3)
Cohesion	0
Angle of internal friction	33-37°C
Allowable bearing pressure[e]	6 ksf (0.3 MPa)

[a]Source: Ho et al. (1986).

[b]Values and ranges of physical properties are from samples taken from test pit SFS-3.

[c]GP classification is poorly graded gravels, gravel-sand mixtures, and

2.8.2 EXCAVATION CHARACTERISTICS OF ROCK AT THE SITE

2.8.2.1 G-Tunnel experience

For definition of the mining methods to be used in the repository, the most applicable data come from experience gained in the development of G-Tunnel at the NTS. G-Tunnel experience in the Grouse Canyon Member and planned excavations in Yucca Mountain are similar in many ways:

1. Overburden loadings, opening dimensions (up to 5-m span), and excavation methods will be similar.

2. The degrees of saturation are similar for geoengineering purposes (0.65 in the Topopah Spring Member (Montazer and Wilson, 1984) versus 0.6 to 0.9 in the Grouse Canyon Member (Zimmerman et al., 1984b)), however, for hydrologic purposes these differences may be

Table 2-16. Comparison of properties of Topopah Spring and Grouse Canyon members

Property	G-Tunnel Grouse Canyon Member	Yucca Mountain Topopah Spring Member
Matrix porosity (°°/0)	6-24[a]	6-19[a]
Grain density (g/cm^3)	2.57-2.63[b]	2.51-2.58[b]
Saturation	0.6-0.9[a]	0.65[c]
Saturated thermal conductivity (W/mK)	1.6-2.0[a]	2.1-2.5[a]
Dry thermal conductivity (W/mK)	1.0-1.6[b]	1.5-2.1[b]
Coefficient of linear thermal expansion (10^{-6} K^{-1})	7.8-10.6[a]	7.3-14.1[a]
Young's modulus (GPa)	22-28[a]	24-38[a]
Poisson's ratio	0.16-0.32[a]	0.12-0.32[a]
Unconfined compressive strength (MPa)	64-142[a]	55-287[a]

[a]Zimmerman et al. (1984b).
[b]Nimick and Lappin (1985).
[c]Montazer and Wilson (1984).

fractured than the nonwelded material, it is more difficult to assess whether damage to finished rock surfaces is the result of the mining technique. A mechanical miner was used successfully to cut the welded tuff and to level the floors, although relatively rapid wear of the picks attached to the rotating drum was noted. The spans of G-Tunnel openings in the welded material (Figures 2-2 and 2-3) range from 3.4 to 5 m. The experiment drift identified is 5 m wide and 5 m high, approximately the dimensions being considered for repository drifts. At one time during the excavation of the extensometer drift, miners were unavailable to install roof supports immediately after seven blasting rounds had been shot. This left a 14-m length of roof unsupported for 1 to 2 months. During this time no deterioration of roof material was evident. Following this hiatus, roof bolts and wire mesh were installed successfully in the roof. A nearly vertical fault with 1 m of

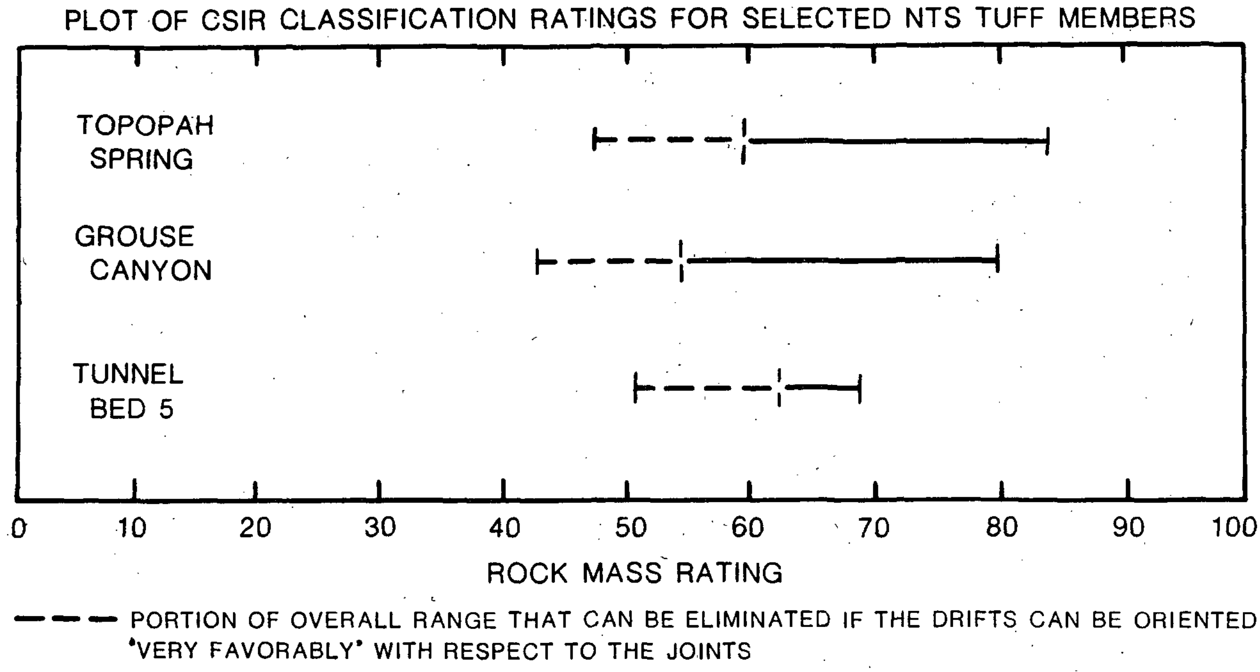

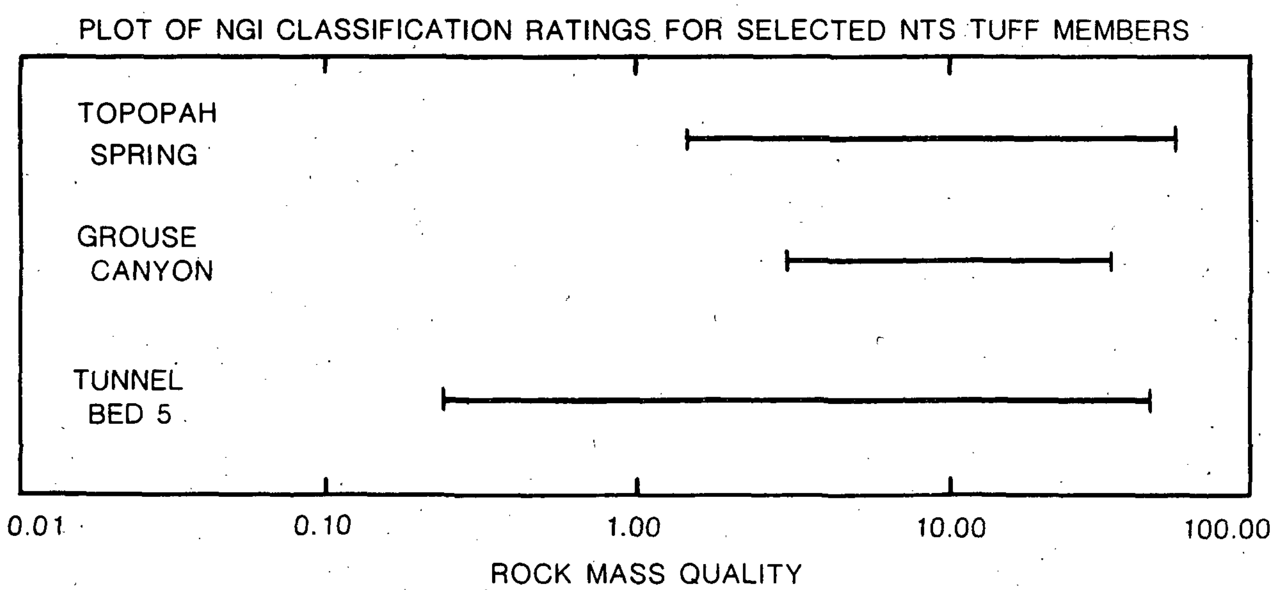

Figure 2-26. Rock mass classification values for various tuff units. (CSIR = South African Council for Scientific and Industrial Research Geomechanics. NGI = Norwegian Geotechnical Institute. NTS = Nevada Test Site) Modified from Lankopf and Gnirk (1986).

estimates of support requirements for excavations in tuff at Yucca Mountain and in G-Tunnel (Table 2-17). Despite the variation in rock mass classification for the various units, the support estimates indicate that either untensioned grouted rock bolts with shotcrete or tensioned grouted rock bolts with shotcrete should suffice in most instances. These estimates are based both on an assumed span width of 5 m and on an excavation support ratio (ESR) consistent with permanent support similar to that required for underground power stations, major road and railway tunnels, and civil defense chambers, which somewhat exceed the support required for a permanent mine opening. For the tunnel beds and the Grouse Canyon Member, the actual support requirements are at the lower end of the range of estimated support requirements. Actual support for these members consists of tensioned rock bolts (grouted) and wire mesh, without shotcrete being necessary.

More detailed studies and evaluations of requirements for permanent support systems will be made in the exploratory shaft facility. Additional discussion of support considerations in the design process is provided in Section 6.2.6.3.6.

Table 2-17. Estimated support requirements based on the Norwegian Geotechnical Institute (NGI) Rock Mass Classification System

Unit	Location	Classification value (Q)	Suggested support requirements
Nonlithophysal Topopah Spring Member	Yucca Mountain	53.3 to 1.46	(a),(b)
Tunnel bed 5	G-Tunnel	46.5 to 0.24	(c),(a),(b)
Welded Grouse Canyon Member	G-Tunnel	34.0 to 3.08	(c),(a),(b)

[a]Untensioned grouted rock bolts with unreinforced shotcrete.
[b]Tensioned grouted rock bolts with wire mesh-reinforced shotcrete.
[c]No support requirements.

2.8.2.4 Estimates of ground-water inflow

As expected above the water table, there is no spatially continuous flow of water into any of the drifts in G-Tunnel. An unmeasured but presumed small quantity is removed by the ventilation system. Observed water flow is limited to seepage from saturated faults or fractured zones oriented more or less vertically. The quantities of water are estimated to be approximately

15 gal/day (Fernandez and Freshley, 1984) and are removed by routine pumping of a small sump area.

It is expected that ground-water inflow in the Topopah Spring Member in Yucca Mountain will be even less than that at G-Tunnel and that dewatering requirements will be minimal. This conclusion is based on the lower degree [illegible] during the drilling of drillholes through the unsaturated zone at Yucca Mountain, and on the lesser precipitation and smaller frequency of snow cover on Yucca Mountain as compared with Rainier Mesa.

2.8.2.5 Excavation methods

The conclusions that are drawn from the observations made in G-Tunnel as related to repository design in the Topopah Spring Member are as follows:

1. Controlled drilling and blasting mining techniques can be used successfully for excavating welded tuff.

2. Because the welded tuff was cut successfully (during floor leveling) with a mechanical mining machine, tunnel-boring machines and mechanical miners could be used.

2.8.3 CHANGES IN GEOENGINEERING PROPERTIES RESULTING FROM EXCAVATION

Underground excavation causes changes in rock mass properties in the vicinity of the excavation. The changes result from stress changes caused by generally limited to within 1 m or less of the tunnel wall (Kelsall et al., 1982). The fracturing induced in more competent and uniform rock will extend a shorter distance away from the charge. Careful planning, careful shothole spacing, and proper selection of the charge-and-firing sequence can minimize the thickness of the zone of increased fracturing.

Mechanical mining machines cause fracturing for a distance of only several centimeters into the rock (Agapito et al., 1984). Slow, deep, and straight cuts with the mechanical miner minimize the specific energy of the process and also the collateral fracturing.

Tunnel-boring machines using disk cutters create a zone of increased fracturing in rock up to 30 cm thick (Nishida, 1982). Optimization of the specific energy for the specific in situ circumstances reduces the collateral fracturing.

Regardless of the excavation technique used, a zone of increased fracturing will exist in which rock properties will differ from those in the surrounding rock mass. This zone will be more intensely fractured than the remainder of the rock and may have reduced saturations resulting from the ventilation of the adjacent openings. The characterization of this zone is one of the goals of some tests planned for the exploratory shaft (Section 8.3.1.15).

The mechanical properties of the rock in the zone of increased fracturing, especially the strength and deformation modulus, will be reduced from values in the surrounding rock. The magnitude of the reduction will depend on the extent of fracturing in the zone. Section 2.3.3 discusses the qualitative effects of fracturing on mechanical properties.

The volumetric heat capacity in the zone of increased fracturing will be lower than rock mass values because of the higher porosity and the lower water content (Section 2.4.2.2). The coefficient of thermal expansion will be lowered by the presence of more fractures, but the deviation from the

2.9 SUMMARY

2.9.1 SUMMARY OF SIGNIFICANT RESULTS

This section summarizes the important results from Sections 2.1 through 2.8. Individual sections should be consulted for additional details.

2.9.1.1 Geoengineering properties

The development of the data base of geoengineering properties for use in technical decisions related to a repository at Yucca Mountain is well under way. At present, the data base consists primarily of the results of laboratory tests on core samples, but it is enhanced by initial results from field observations and tests being made in G-Tunnel at Rainier Mesa. The selection of the Topopah Spring Member as the target horizon for the repository was based mostly on the average thermal and mechanical properties (for each of the four horizons considered) defined from approximately 600 bulk-property measurements, 75 thermal conductivity tests, 95 thermal expansion tests, 35 mineralogic-petrologic analyses, 60 mechanical tests on jointed-rock samples, and 190 unconfined and 50 mechanical-property triaxial tests. Definition of the properties to be expected in the candidate repository horizons relied on combining the measured thermal and mechanical property data with the corresponding bulk properties (porosity and grain density) to produce average thermal and mechanical properties for thermal and mechanical units. The thermal and mechanical units can be defined in the exploration holes drilled to date, although individual layers vary in thickness and, in places, do not coincide with identified lithologic tuff units. The preliminary values of geoengineering properties for the thermal and mechanical units to be used in design and performance assessment work have been summarized in Tables 2-7, 2-9, and 2-14.

Studies of the mechanical properties of intact samples from Yucca Mountain indicate that observed variations between the four horizons studied for horizon selection depend mainly on porosity. Preliminary assessments have been performed of the effects of water, temperature, confining and fluid pressure, loading time, lithophysae, and anisotropy. Additional testing is being focused almost entirely on the Topopah Spring Member. Large-scale laboratory tests (sample diameters up to 30 cm) have been performed to evaluate lithophysae effects, and similar testing is under way to examine parameter effects (temperature, confining pressure, strain rate, saturation, and sample size) on mechanical properties. Assessment of the lateral variability of properties will rely partly on material from the lateral boreholes or drifts planned for the exploratory shaft facility.

Studies of the mechanical properties of discontinuities (e.g., joints, bedding planes, and faults) have focused on the mechanical properties of simulated joints precut in samples of tuffs from the Grouse Canyon and the Prow Pass members. These results are included in this report because of the physical and mechanical similarities of these units to the Topopah Spring Member. Variations in the mechanical properties of simulated joints resulting from the effects of displacement rate, water saturation, and time-dependent behavior have been quantified for use in predicting the mechanical response of the rock mass. Testing is under way to determine the properties of natural and artificial joints in samples of the Topopah Spring Member. In addition to providing data on the selected horizon, such testing will enable an evaluation of the application of results from other welded, devitrified tuff to the Topopah Spring Member. The type, spacing, orientation, and properties of discontinuities at the repository level will be characterized in the exploratory shaft facility.

To date there has been no large-scale testing of the tuffs from Yucca Mountain. The heated-block test performed in G-Tunnel has provided some data for the rock mass modulus of deformation. These data can be used with the laboratory results for the Grouse Canyon Member to estimate how much the intact rock Young's moduli of Yucca Mountain units need to be reduced to describe the rock mass. Currently, it is estimated that the in situ modulus of deformation will be about half the Young's modulus measured in the laboratory. The pressurized-slot tests fielded in G-Tunnel will provide additional data on the in situ modulus of deformation.

When underground access to the Topopah Spring Member becomes available, large-scale in situ tests will be performed to measure directly rock mass mechanical properties and to evaluate whether rock mass response can be predicted using numerical analysis codes. These tests will be designed and positioned to be representative of the rock mass, including discontinuities. Plate-bearing tests, strength tests, and the Yucca Mountain heated-block measurement will emphasize properties evaluations. Shaft and drift deformation monitoring during excavation along with the canister-scale heater test will assist in the design approach by evaluating the construction and thermal effects of waste emplacement on a larger scale than in the properties tests.

The thermal conductivities of saturated and dehydrated samples are variable and show dependence on variations in porosity and grain density (mineralogy). Studies indicate that the effects of layering (fabric anisotropy) on the thermal conductivity of welded and nonwelded tuffs are negligible. It appears that the effects on conductivity of air-filled lithophysae that occur within the Topopah Spring Member can be modeled as additional air-filled porosity. However, the distribution of these voids remains poorly defined, and the above assertion requires further confirmation. The presence of fractures is expected to have a negligible effect on in situ rock mass thermal conductivity.

The calculated values of volumetric heat capacity for the tuff strongly depend on porosity and degree of saturation and somewhat depend on mineralogy (grain density). A series of measurements of the heat capacity of some of the thermal and mechanical units at Yucca Mountain is planned to provide confirmation of the calculated values.

The laboratory measurements of the thermal expansion of samples from Yucca Mountain indicate that because of the presence of variable amounts of hydrous phases, three temperature ranges must be defined for the thermal-expansion behavior of Yucca Mountain tuffs: pretransitional, transitional, and posttransitional. Studies indicate that the effects of bedding and textural anisotropy on matrix thermal expansion behavior of densely welded tuffs are negligible. The presence of thermally induced or preexisting fractures is expected to reduce thermally induced rock mass stresses to below those predicted using thermal and mechanical properties measured in the laboratory, primarily because of the lower elastic moduli in the field.

An examination of in situ stress at the NTS and at Yucca Mountain indicates that measurements at Yucca Mountain are consistent with other measurements in the region. Measurements and calculations have provided reasonable bounds on the magnitudes of in situ stresses at Yucca Mountain.

For a repository in the Topopah Spring Member, analyses predict that the partial saturation, relatively low porosity, and the presence of prevalent fractures preclude thermally induced decrepitation of the rock mass. Laboratory tests of thermally induced water migration will be made to estimate its effect on ventilation requirements in a repository and on the effective thermal conductivity of the rock mass. In addition, these tests will provide a better understanding of the mechanisms and magnitude of water movement in tuff subjected to a changing temperature field. Observations of thermally induced water migration will also be made in engineered barrier system design tests planned for the exploratory shaft facility.

Because tuffs at Yucca Mountain and Rainier Mesa are similar, G-Tunnel experience indicates that controlled-blasting techniques can be used to excavate the welded tuff. In addition, roof bolts and wire mesh should be sufficient to stabilize the openings. Control of water flow should not be a significant factor in the repository design. The excavation characteristics of tuffs from Yucca Mountain have been evaluated by using several empirical approaches with borehole and core sample data. These empirical correlations suggest that no unusual support systems will be required during the excavation of the exploratory shaft or the repository in the Topopah Spring Member. Confidence in the predictions was gained by applying them to the nonwelded tuffs in tunnel bed 5 and the welded tuffs in the Grouse Canyon Member at Rainier Mesa.

2.9.1.2 Relationship of data to performance objectives

The data required to analyze the performance objectives have been identified through the definition of information needs. These information needs and their relationship to specific performance objectives are discussed in Section 8.2. The data in Chapter 2 that apply to performance objectives are presented in Section 2.9.3. The performance objectives to which the analysis of geoengineering data contribute are briefly discussed in this section.

Performance objectives for the geologic operations area are described in 10 CFR Part 60. Those objectives to which information in Chapter 2 are most relevant are discussed in the following paragraphs.

Part (b) of 10 CFR 60.111 (retrievability of waste) is the performance objective for which geoengineering data provide the most information. To satisfy this objective, the Yucca Mountain Project position is that all underground openings, including waste emplacement holes, drifts, and access ramps from the surface must remain stable through the retrievability period (Flores, 1986). For emplacement drillholes, there must be reasonable assurance that the walls will not deteriorate to an extent that would preclude removal of waste containers. The data summarized in this chapter demonstrate that both mechanical and thermal properties of the Topopah Spring Member are similar to correlative properties of the Grouse Canyon Member where, even at high temperatures, heater tests have not resulted in any damage to the heater-hole walls (Zimmerman, 1983).

A similar statement can be made about drifts in the Topopah Spring Member. G-Tunnel, which penetrates tuffs similar to the Topopah Spring Member, has required minimal support over its lifetime and has remained a stable opening. The additional factor of the elevated temperatures expected in the Topopah Spring Member, as a result of waste emplacement, must be treated with thermal and mechanical calculations such as those discussed in Chapter 6.

The data in Chapter 2 also may be used in an assessment of the performance objective for particular barriers after permanent closure (10 CFR 60.113). The analysis of the mechanical stability of the emplacement hole and of the expected environment (e.g., moisture content and temperature) must demonstrate that the waste package portion of the engineered barrier system will isolate the waste for the specified time (10 CFR 60.113(a)(1)(ii)(A)) and that radionuclide release rates from the engineered barrier system will be less than or equal to the limits specified in 10 CFR 60.113(a)(1)(ii)(B).

The conceptual models representing tuffs at Yucca Mountain were described briefly in the introduction to this chapter and are discussed in more detail in Chapter 6. Descriptions of alternative conceptual models for the process of heat transfer, and mechanical constitutive models for rheological behavior and material properties of the tuff units at Yucca Mountain, are presented in Section 8.3.1.15. All the data necessary to implement the models have been identified and either have been obtained or are part of the test program discussed in Chapter 8. Specific items that are either data or boundary conditions for which information is incomplete are presented in the following paragraphs.

The data summarized in Chapter 2 are insufficient for complete site characterization in the following specific areas:

1. The effects of the parameters (temperature, confining pressure, strain rate, saturation, and sample size) on the mechanical properties of welded, devitrified Topopah Spring Member.

2. The measurement of properties of joints in the Topopah Spring Member.

3. The confirmation that data obtained to date are representative of material to be characterized during underground testing in the exploratory shaft.

4. In situ measurement of geoengineering properties including thermal and mechanical rock mass properties, fracture properties, and in situ stress.

The data discussed in this chapter are of good quality (i.e., were obtained following detailed test procedures and using calibrated instruments

under controlled test conditions); the experimental uncertainties are
approximately 10 percent for thermal properties and 3 percent for mechanical

Table 2-18. Relationship of geoengineering data to issues, information needs and investigations (page 1 of 3)

Information need or investigation	Description	Pertinent geoengineering data	Relevant section of Chapter 2
1.1.1	Site information needed to calculate the releases of radionuclides to the accessible environment (Section 8.3.5.13.1)	Porosity	2.4.3
1.6.1	Site information and design concepts needed to identify the fastest path of likely radionuclide travel and to calculate the ground-water travel time along that path (Section 8.3.5.12.1)	Porosity	2.4.3
1.6.5	Boundaries of the disturbed zone (Section 8.3.5.12.5)	Effect of excavation methods on rock properties	2.8.3
1.7	Determination that the subsurface conditions encountered and the changes in those conditions during construction and waste emplacement operations are within the limits assumed in the licensing review [10 CFR 60.43(b), 60.74, 60.140(a)(1) and 60.141(b)] (Section 8.3.5.16)	Ambient stress conditions	2.6
		Porosity	2.4.3
		Density	2.4.3
		Thermal conductivity	2.4.2.1, 2.5.2
		Heat capacity	2.4.2.2, 2.5.2
		Thermal expansion	2.4.2.3, 2.5.2
		Compressive strength	2.1.2.3.1, 2.3.2, 2.3.3
		Tensile strength	2.1.2.3.2, 2.3.3
		Elastic moduli	2.1.2.2, 2.3.2, 2.3.3
		Joint properties	2.2
1.11.1	Site characterization information needed for design (Section 8.3.2.2.1)	All properties in Chapter 2	2.1-2.8
1.11.6	Predicted thermal and thermomechanical response of the host rock surrounding strata, and ground-water system (Section 8.3.2.2.6)	Ambient stress conditions	2.6
		Porosity	2.4.3
		Density	2.4.3
		Thermal conductivity	2.4.2.1, 2.5.2
		Heat capacity	2.4.2.2, 2.5.2
		Thermal expansion	2.4.2.3, 2.5.2
		Compressive strength	2.1.2.3.1, 2.3.2, 2.3.3
		Tensile strength	2.1.2.3.2, 2.3.3
		Elastic moduli	2.1.2.2, 2.3.2, 2.3.3
		Joint properties	2.2
		Thermally induced water migration	2.7.2

Table 2-18. Relationship of geoengineering data to issues, information needs and investigations (page 2 of 3)

Information need or investigation	Description	Pertinent geoengineering data	Relevant section of Chapter 2
8.3.1.2.2	Description of the unsaturated zone hydrologic system at the site	Porosity	2.4.3
8.3.1.2.3	Description of the saturated zone hydrologic system at the site	Porosity	2.4.3
8.3.1.3.4	Radionuclide retardation by sorption processes along flow paths to the accessible environment	Dry bulk density	2.4.3
8.3.1.3.6	Radionuclide retardation by dispersive/diffusive/advective transport processes along flow paths to the accessible environment	Porosity	2.4.3
8.3.1.15.1	Spatial distribution of thermal and mechanical properties	Thermal conductivity	2.4.2.1, 2.5.2
		Thermal expansion	2.4.2.3, 2.5.2
		Heat capacity	2.4.2.2, 2.5.2
		Compressive strength	2.1.2.3.1, 2.3.2, 2.3.3
		Elastic moduli	2.1.2.2, 2.3.2, 2.3.3
		Joint properties	2.2
		Tensile strength	2.1.2.3.2, 2.3.3
8.3.1.15.2	Spatial distribution of ambient stress and thermal conditions	Ambient stress conditions	2.6
8.3.1.6.4	Potential effects of erosion on the hydrologic and geochemical characteristics at Yucca Mountain	All of Chapter 2	2.1-2.8
8.3.1.8.5	Potential effects of igneous and tectonic activity on rock characteristics	All of Chapter 2	2.1-2.8
8.3.1.9.3	Potential effects of exploiting natural resources on hydrologic, geochemical, and rock characteristics	All of Chapter 2	2.1-2.8
2.4.1	Site and design data required to support retrieval (Section 8.3.5.2.1)	Thermal conductivity	2.4.2.1, 2.5.2
		Thermal expansion	2.4.2.3, 2.5.2
		Heat capacity	2.4.2.2, 2.5.2

Table 2-18. Relationship of geoengineering data to issues, information needs and investigations (page 3 of 3)

Information need or investigation	Description	Pertinent geoengineering data	Relevant section of Chapter 2
2.4.1 (continued)		Joint properties	2.2
		Compressive strength	2.1.2.3.1, 2.3.2, 2.3.3
		Tensile strength	2.1.2.3.2, 2.3.3
		Elastic moduli	2.1.2.2, 2.3.2, 2.3.3
2.7.1	Site information needed for design (Radiological protection) (Section 8.3.2.3.1)	All of Chapter 2	2.1-2.8
4.2.1	Site and performance assessment information needed for design (Section 8.3.2.4.1)	All of Chapter 2	2.1-2.8
4.4.1	Site and performance assessment information needed for design (Section 8.3.2.5.1)	All of Chapter 2	2.1-2.8
8.3.1.14.2	Soil and bedrock properties of potential locations of surface facilities	Geoengineering properties of surface materials	2.7.3
8.3.1.15.1	Spatial distribution of thermal and mechanical properties	Thermal conductivity	2.4.2.1, 2.5.2
		Heat capacity	2.4.2.2, 2.5.2
		Thermal expansion	2.4.2.3, 2.5.2
		Compressive strength	2.1.2.3.1, 2.3.2, 2.3.3
		Elastic moduli	2.1.2.2, 2.3.2, 2.3.3
		Joint properties	2.2
		Tensile strength	2.1.2.3.2, 2.3.3
8.3.1.15.2	Spatial distribution of ambient stress and thermal conditions	Ambient stress conditions	2.6

Regulatory Guide 4.17 requires that an analysis of elastic and inelastic behavior be included in the section on the mechanical properties of the rock matrix (NRC, 1987). As discussed in Section 2.1.2.3.1.4 of this report, inelastic deformation of the matrix of the Topopah Spring Member is considered unlikely at Yucca Mountain. However, linear creep and nonlinear creep have been identified as alternative hypotheses for conceptual mechanical constitutive models of rock mass behavior as described in Section 8.3.1.15 and Table 8.3.1.15-2. Additional experimental work is ongoing to examine the validity of this position, as discussed in Section 8.3.1.15.

A description of special geoengineering properties is required to be present in a site characterization plan. Of the examples of such properties listed in NRC Regulatory Guide 4.17 (NRC, 1987), brine migration is not relevant to the Yucca Mountain site. Section 2.7.1 has predicted that thermal degradation and thermally induced water migration will not be significant. The latter conclusion is being examined in more detail during in situ testing in the exploratory shaft.

 DOE/RW-0199

Nuclear Waste Policy Act
(Section 113)

Site Characterization Plan

Yucca Mountain Site, Nevada Research and Development Area, Nevada

Volume I, Part A

Chapter 2 References

December 1988

U. S. Department of Energy
Office of Civilian Radioactive Waste Management

REFERENCES FOR CHAPTER 2

ASTM (American Society for Testing and Materials), 1966. "True Specific Gravity of Refractory Material by Water Immersion," Standard Test Method, Reapproved 1976, ASTM C 135-66, Philadelphia, Penn.

ASTM (American Society for Testing and Materials), 1971. "Linear Thermal Expansion of Rigid Solids with a Vitreous Silica Dilatometer," Standard Test Method, ASTM E 228-71, Philadelphia, Penn.

ASTM (American Standard Test Methods), 1978. "Moisture-Density Relations of Soils and Soil-Aggregate Mixtures Using 10-lb (4.54-kg) Rammer and 18-in. (457 mm) Drop," Standard Test Methods, ANSI/ASTM D 1557-78, Philadelphia, Penn., pp. 270-276.

ASTM (American Society for Testing and Materials), 1979a. "True Specific Gravity of Refractory Materials by Gas-Comparison Pycnometer," Standard Test Method, ASTM C 604-79, Philadelphia, Penn.

ASTM (American Society for Testing and Materials), 1979b. "Unconfined Compressive Strength of Intact Rock Core Specimens," Standard Test Method, ANSI/ASTM D 2938-79, Philadelphia, Penn.

ASTM (American Society for Testing and Materials), 1980a. "Triaxial Compressive Strength of Undrained Rock Core Specimens without Pore Pressure Measurements," Standard Test Method, ASTM D 2664-80, Philadelphia, Penn.

ASTM (American Society for Testing amd Materials), 1980b. "Elastic Moduli of Intact Rock Core Specimens in Uniaxial Compression," Standard Test Method, ANSI/ASTM D 3148-80, Philadelphia, Penn.

ASTM (American Society for Testing and Materials), 1981a. "Density of Soil and Soil-Aggregate in Place by Nuclear Methods (Shallow Depth)," ASTM D 2922-81, Philadelphia, Penn.

ASTM (American Society for Testing and Materials), 1981b. "Splitting Tensile Strength of Intact Rock Core Specimens," Standard Test Method, ASTM D 3967-81, Philadelphia, Penn.

ASTM (American Society for Testing and Materials), 1982. "Density of Soil in Place by the Sand-Cone Method," ASTM D 1556-82, Philadelphia, Penn.

ASTM (American Society for Testing and Materials), 1984. "Thermal Conductivity of Refractory Brick," Standard Test Method, ASTM C 202-84, Philadelphia, Penn.

Agapito, J. F. T., H. N. Maleki, J. R. Aggson, and L. A. Weakly, 1984. "Impact of Excavation Technique on Strength of Oil Shale Pillars," International Journal of Mining Engineers, Vol. 2, pp. 93-105.

Bandis, S., A. C. Lumsden, and N. R. Barton, 1981. "Experimental Studies of Scale Effects on the Shear Behavior of Rock Joints," International Journal of Rock Mechanics, Mining Science, and Geomechanical Abstracts, Vol. 18, pp. 1-21.

Barton, N., 1973. "Review of New Shear-Strength Criterion for Rock Joints," Engineering Geology, Vol. 7, pp. 287-332.

Barton, N., R. Lien, and J. Lunde, 1974a. Analysis of Rock Mass Quality and Support Practice in Tunneling and a Guide for Estimating Support Requirements, Internal Report 54206, Norwegian Geotechnical Institute, Oslo, Norway.

Barton, N., R. Lien, and J. Lunde, 1974b. "Engineering Classification of Rock

Blanford, M. L., 1982. Heated Block Test Conceptual Design Calculations, SAND81-1841, Sandia National Laboratories, Albuquerque, N. Mex.

Board, M. P., M. L. Wilson, and M. D. Voegele, 1987. Laboratory Determination of the Mechanical, Ultrasonic and Hydrologic Properties of Welded Tuff from the Grouse Canyon Heated Block Site, SAND86-7130, Sandia National Laboratories, Albuquerque, N. Mex.

Broxton, D. E., D. T. Vaniman, F. Caporuscio, B. Arney, and G. Heiken, 1982. Detailed Petrographic Descriptions and Microprobe Data for Drill Holes USW-G2 and UE25b-1H, Yucca Mountain, Nevada, LA-9324-MS, Los Alamos National Laboratory, Los Alamos, N. Mex.

Byerlee, J., 1978. "Friction of Rocks," Pageoph (Pure and Applied Geophysics), Vol. 116, pp. 615-626.

Carlsson, H., 1978. A Pilot Heater Test in the Stripa Granite, Swedish-American Cooperative Program on Radioactive Waste Storage in Mined Caverns in Crystalline Rock, Technical Project Report No. 6, LBL-7086, Lawrence Berkeley Laboratory, Berkeley, Calif.

Carr, W. J., 1974. Summary of Tectonic and Structural Evidence for Stress Orientation at the Nevada Test Site, USGS-OFR-74-176, Open-File Report, U.S. Geological Survey.

Chen, E. P., 1987. A Computational Model for Jointed Media with Orthogonal Sets of Joints, SAND86-1122, Sandia National Laboratories, Albuquerque, N. Mex.

Cook, N. G. W., P. A. Witherspoon, E. L. Wilson, and L. R. Myer, 1983. "Progress with Thermomechanical Investigations of the Stripa Site," in Proceedings of the Workshop on the Geological Disposal of Radioactive Waste In Situ Experiments in Granite, Stockholm, Sweden, October 25-27, 1983, pp. 19-31.

Costin, L. S., 1983. "A Microcrack Model for the Deformation and Failure of Brittle Rock," Journal of Geophysical Research, Vol. 88, No. B11, pp. 9485-9492.

Dieterich, J. H., 1978. "Time-Dependent Friction and the Mechanics of Stick-Slip," Pageoph (Pure and Applied Geophysics), Vol. 116, pp. 790-806.

Dischler, S. A., and K. Kim, 1985. "Determination of Rock Mass Deformation Modulus during Hydraulic Fracturing," in Proceedings of the 26th U.S. Symposium on Rock Mechanics, Rapid City, South Dakota, June 26-28, 1985, E. Ashworth (ed.), A. A. Balkema, Boston, Mass., pp. 363-373.

Doe, T., K. Ingevald, L. Strindell, B. Haimson, and H. Carlsson, 1981. "Hydraulic Fracturing and Overcoring Stress Measurements in a Deep

Eaton, R. R., D. E. Larson, and C. M. Korbin, 1981. "Sensitivity of Calculated Pore-Fluid Pressure to Repository Fracture Geometry," Scientific Basis for Nuclear Waste Management, J. G. Moore (ed.), Vol. 3, Plenum Press, New York, pp. 591-598.

Ellis, W. L., and J. R. Ege, 1976. Determination of In Situ Stress in U12g Tunnel, Rainier Mesa, Nevada Test Site, Nevada, USGS-474-219, U.S. Geological Survey.

Ellis, W. L., and J. E. Magner, 1980. Compilation of Results of Three-Dimensional Stress Determinations Made in Rainier and Aqueduct Mesas, Nevada Test Site, Nevada, USGS-OFR-80-1098, Open-File Report, U.S. Geological Survey.

Ellis, W. L., and H. S. Swolfs, 1983. Preliminary Assessment of In Situ Geomechanical Characteristics in Drill Hole USW G-1, Yucca Mountain, Nevada, USGS-OFR-83-401, Open-File Report, U.S. Geological Survey.

Erickson, J. R., and R. K. Waddell, 1985. Identification and Characterization of Hydrologic Properties of Fractured Tuff using Hydraulic and Tracer Tests--Test Well USW H-4, Yucca Mountain, Nye County, Nevada, USGS-WRI-85-4066, Water-Resources Investigations Report, U.S. Geological Survey.

Fernandez, J. A., and M. D. Freshley, 1984. Repository Sealing Concepts for the Nevada Nuclear Waste Storage Investigations Project, SAND83-1778, Sandia National Laboratories, Albuquerque, N. Mex.

Fischer, F. G., P. J. Papanek, and R. M. Hamilton, 1972. The Massachusetts Mountain Earthquake of 5 August 1971 and Its Aftershocks, Nevada Test Site, USGS-474-149, U.S. Geological Survey, 20 p.

Flores, R. J., 1986. Retrievability: Strategy for Compliance Demonstration, SAND84-2242, Sandia National Laboratories, Albuquerque, N. Mex.

Goodman, L. E., and C. B. Brown, 1963. "Dead Load Stresses and the Instability of Slopes," in Journal of the Soil Mechanics and Foundations Divisions, Proceedings of the American Society of Civil Engineers, May 1963, pp. 103-134.

Goodman, R. E., 1980. Introduction to Rock Mechanics, John Wiley & Sons, Inc., New York.

Gregory, E. C., and K. Kim, 1981. "Preliminary Results from the Full-Scale Heater Tests at the Near-Surface Test Facility," in Proceedings of the 22nd U.S. Symposium on Rock Mechanics, Massachusetts Institute of Technology, Cambridge, Mass., pp. 137-142.

Gurr, C. G., T. J. Marshall, and J. T. Hutton, 1952. "Movement of Water in Soil Due to a Temperature Gradient," Soil Science, Vol. 74, No. 5, pp. 335-345.

Guzowski, R. V., F. B. Nimick, M. D. Siegel, and N. C. Finley, 1983. Repository Site Data Report for Tuff: Yucca Mountain, Nevada, NUREG/CR-2937, SAND82-2105, U.S. Nuclear Regulatory Commission, Washington, D.C.

Haimson, B. C., 1981. "Confirmation of Hydrofracturing Results Through Comparisons with Other Stress Measurements," in Proceedings of the 22nd U.S. Symposium on Rock Mechanics, Massachusetts Institute of Technology, Cambridge, Mass., pp. 379-385.

Haimson, B. C., J. Lacomb, A. H. Jones, and S. J. Green, 1974. "Deep Stress Measurements in Tuff at the Nevada Test Site," Advances in Rock Mechanics, Vol. II, Part A, National Academy of Science, Washington, D.C. pp. 557-561.

Handin, J., R. V. Hager, M. Friedman, and J. N. Feather, 1963. "Experimental Deformation of Sedimentary Rocks Under Confining Pressure: Pore Pressure Tests," Bulletin of the American Association of Petroleum Geologists, Vol. 47, No. 5, pp. 717-755.

Hardin, E., N. Barton, M. Voegele, M. Board, R. Lingle, H. Pratt, and W. Ubbes, 1982. "Measuring the Thermomechanical and Transport Properties of a Rockmass Using the Heated Block Test," in Proceedings 23rd U.S. Symposium on Rock Mechanics, Society of Mining Engineers, New York, pp. 802-813.

Hardin, E. L., M. D. Voegele, M. P. Board, and H. R. Pratt, 1985. "Development of a Test Series to Determine In Situ Thermomechanical and Transport Properties," Measurement of Rock Properties at Elevated Pressures and Temperatures, H. J. Pincus and E. R. Hoskins (eds.), ASTM STP 869, American Society for Testing and Materials, Philadelphia, Penn., pp. 128-153.

Hart, R. D., P. A. Cundall, and M. L. Cramer, 1985. "Analysis of a Loading Test on a Large Basalt Block," in Proceedings of the 26th Symposium on Rock Mechanics, Rapid City, South Dakota, 26-28 June, 1985, pp. 759-768.

Heuze, E. H., and A. Salem, 1977. "Rock Deformability Measured In Situ, Problems and Solutions," in Proceedings of the Field Measurements in Rock Mechanics, International Symposium, Zurich, Switzerland, April 4-6, 1977, Vol. 1, A. A. Balkema, Rotterdam, pp. 375-387.

Heuze, F. E., 1980. "Scale Effects in the Determination of Rock Mass Strength and Deformability," Rock Mechanics, Vol. 12, pp. 167-192.

Heuze, F. E., and B. Amadei, 1985. "The NX-Borehole Jack: A Lesson in Trials and Errors," International Journal on Rock Mechanics, Mining Science, and Geomechanical Abstracts, Vol. 22, No. 2, pp. 105-112.

Heuze, F. E., W. C. Patrick, R. V. De la Cruz, and C. F. Voss, 1981. In Situ Geomechanics, Climax Granite, Nevada Test Site, UCRL-53076, Lawrence Livermore National Laboratory, Livermore, Calif.

Ho, D. M., R. L. Sayre and C. L. Wu, 1986. Suitability of Natural Soils for Foundations for Surface Facilities at the Prospective Yucca Mountain Nuclear Waste Repository, SAND85-7107, Sandia National Laboratories, Albuquerque, N. Mex.

Holland, J., and S. J. Bauer, 1984. Calculation of Overburden-Induced Stresses at Rainier Mesa, Nevada, SAND84-1592A, Sandia National Laboratories, Albuquerque, N. Mex.

Hooker, V. E., and D. L. Bickel, 1974. Overcoring Equipment and Techniques Used in Rock Stress Determination, U.S. Bureau of Mines Information Circular 8618, Washington, D.C.

Hooker, V. E., J. R. Aggson, and D. L. Bickel, 1971. Report on In Situ Determination of Stresses, Rainier Mesa, Nevada Test Site, U.S. Bureau of Mines Report, Denver Mining Research Center, Denver, Colo.

Hubbert, M. K., and D. G. Willis, 1957. "Mechanics of Hydraulic Fracturing," Journal of Petroleum Technology, Vol. 210, pp. 153-168.

Hustrulid, W. A., 1976. "An Analysis of the Goodman Jack," Monograph 1 on Rock Mechanics Application in Mining, papers presented at the 17th U.S. Symposium on Rock Mechanics, Snowbird, Utah, August, 1976, W. S. Brown, S J. Green, and W. A. Hustrulid (eds.), pp. 4B10-4 to 4B10-8

ISRM (International Society for Rock Mechanics), 1978. "Suggested Methods for Determining Tensile Strength of Rock Materials," International Journal of Rock Mechanics, Mining Science, and Geomechanical Abstracts, Vol. 15, pp. 99-103.

ISRM (International Society for Rock Mechanics), 1979a. "Suggested Methods for Determining the Uniaxial Compressive Strength and Deformability of Rock Materials," International Journal of Rock Mechanics, Mining Science, and Geomechanical Abstracts, Vol. 16, pp. 135-140.

ISRM (International Society for Rock Mechanics), 1979b. "Suggested Methods for Determining Water Content, Porosity, Density, Absorption and Related Properties and Swelling and Slake-Durability Index Properties," International Journal of Rock Mechanics, Mining Science, and Geomechanical Abstracts, Vol. 16, pp. 141-156.

Jaeger, J. C., and N. G. W. Cook, 1979. Fundamentals of Rock Mechanics, Chapman and Hall, London, England, pp. 390-391, 405.

Jeffry, J. A., T. Chan, N. G. W. Cook, and P. A. Witherspoon, 1979. Determination of In-Situ Thermal Properties of Stripa Granite from Temperature Measurements in the Full-Scale Heater Experiments: Method and Preliminary Results, Swedish-American Cooperative Program on Radioactive Waste Storage in Mined Caverns in Crystalline Rock, Technical Information Report No. 24, LBL-8423, Lawrence Berkeley Laboratory, Berkeley, Calif.

Johnson, B., and A. F. Gangi, 1980. "Thermal Cracking of Nonuniformly Heated Thick-Walled Cylinders of Westerly Granite," in Proceedings of the 21st U.S. Symposium of Rock Mechanics, University of Rolla, Missouri, pp. 197-206.

Johnstone, J. K., R. R. Peters, and P. F. Gnirk, 1984. Unit Evaluation at Yucca Mountain, Nevada Test Site: Summary Report and Recommendation, SAND83-0372, Sandia National Laboratories, Albuquerque, N. Mex.

Johnstone, J. K., G. R. Hadley, and D. R. Waymire, 1985. In Situ Tuff Water Migration/Heater Experiment: Final Report, SAND81-1918, Sandia National Laboratories, Albuquerque, N. Mex.

Kelsall, P. C., J. B. Case, and C. R. Chabannes, 1982. A Preliminary Evaluation of the Rock Mass Disturbance Resulting from Shaft, Tunnel, or Borehole Excavation, ONWI-411, Office of Nuclear Waste Isolation, Columbus, Ohio.

Kim, K., and W. M. McCabe, 1984. "Geomechanics Characterization of a Proposed Nuclear Waste Repository Site in Basalt," in Proceedings of the 25th U.S. Symposium on Rock Mechanics, Evanston, Ill., pp. 1126-1135.

Kingery, W. D., H. K. Bowen, and D. R. Uhlmann, 1976. Introduction to Ceramics, Second Edition, John Wiley & Sons, New York, p. 608.

Kovari, K., A. Tisa, H. H. Einstein, and J. A. Franklin, 1983. "Suggested Methods for Determining the Strength of Rock Materials in Triaxial Compression: Revised Version," International Journal of Rock Mechanics, Mining Science, and Geomechanical Abstracts, Vol. 20, No. 6, pp. 283-290.

Kuszyk, J. A., and R. C. Bradt, 1973. "Influence of Grain Size on Effects of Thermal Expansion Anisotropy in MgTi205," Journal of the American Ceramic Society, Vol. 56, No. 8, pp. 420-423.

Lama, R. D., and V. S. Vutukuri, 1978. Handbook on Mechanical Properties of Rocks - Testing Techniques and Results - Volume II, Trans Tech Publications, Clausthal, Germany, pp. 231-236.

Langkopf, B. S., and P. R. Gnirk, 1986. Rock-Mass Classification of Candidate Repository Units at Yucca Mountain, Nye County, Nevada, SAND82-2034, Sandia National Laboratories, Albuquerque, N. Mex.

Lanigan, D. C., M. L. Cramer, and K. Kim, 1983. "Determination of Rock Mass Deformation Modulus in Closely Jointed Columbia River Basalt," EOS, Transactions American Geophysical Union, Vol. 64, No. 9, p. 87.

Lappin, A. R., 1980a. Preliminary Thermal Expansion Screening Data for Tuffs,

Neal, J. T., 1985. Location Recommendation for Surface Facilities for the Prospective Yucca Mountain Waste Repository, SAND84-2015, Sandia National Laboratories, Albuquerque, N. Mex.

Nelson, P. H., and R. Rachiele, 1982. "Water Migration Induced by Thermal Loading of a Granitic Rock Mass," International Journal of Rock Mechanics, Mineral Sciences and Geomechanical Abstracts, Vol. 19, No. 6, pp. 353-359.

Nimick, F. B. (comp.), 1987. Technical Correspondence in Support of the Site Characterization Plan, SAND87-0115, Sandia National Laboratories, Albuquerque, N. Mex.

Nimick, F. B., and A. R. Lappin, 1985. Thermal Conductivity of Silicic Tuffs from Yucca Mountain and Rainier Mesa, Nye County, Nevada, SAND83-1711/1J, Sandia National Laboratories, Albuquerque, N. Mex.

Nimick, F. B., and B. M. Schwartz, 1987. Bulk, Thermal, and Mechanical [illegible] Member of the Paintbrush Tuff, Yucca [illegible] Mountain, Nevada, SAND85-0762, Sandia National Laboratories, Albuquerque, N. Mex.

Nimick, F. B., R. H. Price, R. G. Van Buskirk, and J. R. Goodell, 1985. Uniaxial and Triaxial Compression Test Series on Topopah Spring Tuff from USW G-4, Yucca Mountain, Nevada, SAND84-1101, Sandia National Laboratories, Albuquerque, N. Mex.

Nishida, T., 1982. "Excavation of an Inclined Tunnel by Tunnel-Boring Machine," Tunnelling '82, M. J. Jones (ed.), Institution of Mining & Metallurgy, pp. 145-152.

Olsson, W. A., 1982. Effects of Elevated Temperature and Pore Pressure on the Mechanical Behavior of Bullfrog Tuff, SAND81-1664, Sandia National Laboratories, Albuquerque, N. Mex.

Olsson, W. A., 1987. Rock Joint Compliance Studies, SAND86-0177, Sandia National Laboratories, Albuquerque, N. Mex.

Olsson, W. A., and A. K. Jones, 1980. Rock Mechanics Properties of Volcanic Tuffs from the Nevada Test Site, SAND80-1453, Sandia National Laboratories, Albuquerque, N. Mex.

Ortiz, T. S., R. L. Williams, F. B. Nimick, B. C. Whittet, and D. L. South, 1985. A Three-Dimensional Model of Reference Thermal/Mechanical and Hydrological Stratigraphy at Yucca Mountain, Southern Nevada, SAND84-1076, Sandia National Laboratories, Albuquerque, N. Mex.

Paterson, M. S., 1978. Experimental Rock Deformation - The Brittle Field, Springer-Verlag, New York, pp. 90-92, 99-111.

Patton, F. D., 1966. "Multiple Modes of Shear Failure in Rock," in Proceedings of the First Congress of the International Society of Rock Mechanics, pp. 509-513.

Price, R. H., 1983. Analysis of Rock Mechanics Properties of Volcanic Tuff Units from Yucca Mountain, Nevada Test Site, SAND82-1315, Sandia National Laboratories, Albuquerque, N. Mex.

Price, R. H., 1986. Effects of Sample Size on the Mechanical Behavior of Topopah Spring Tuff, SAND85-0709, Sandia National Laboratories, Albuquerque, N. Mex.

Price, R. H., and S. J. Bauer, 1985. "Analysis of the Elastic and Strength Properties of Yucca Mountain Tuff, Nevada," in Proceedings of the 26th U.S. Symposium on Rock Mechanics, A. A. Balkema, Boston, Mass., pp. 89-96.

Price, R. H., and A. K. Jones, 1982. Uniaxial and Triaxial Compression Test Series on Calico Hills Tuff, SAND82-1314, Sandia National Laboratories, Albuquerque, N. Mex.

Price, R. H., and K. G. Nimick, 1982. Uniaxial Compression Test Series on Tram Tuff, SAND82-1055, Sandia National Laboratories, Albuquerque, N. Mex.

Price, R. H., A. K. Jones, and K. G. Nimick, 1982a. Uniaxial Compression Test Series on Bullfrog Tuff, SAND82-0481, Sandia National Laboratories, Albuquerque, N. Mex.

Price, R. H., K. G. Nimick, and J. A. Zirzow, 1982b. Uniaxial and Triaxial Compression Test Series on Topopah Spring Tuff, SAND82-1723, Sandia National Laboratories, Albuquerque, N. Mex.

Price, R. H., S. J. Spence, and A. K. Jones, 1984. Uniaxial Compression Test Series on Topopah Spring Tuff from USW GU-3, Yucca Mountain, Southern Nevada, SAND83-1646, Sandia National Laboratories, Albuquerque, N. Mex.

Price, R. H., F. B. Nimick, J. R. Connolly, K. Keil, B. M. Schwartz, and S. J. Spence, 1985. Preliminary Characterization of the Petrologic, Bulk, and Mechanical Properties of a Lithophysal Zone within the Topopah Spring Member of the Paintbrush Tuff, SAND84-0860, Sandia National Laboratories, Albuquerque, N. Mex.

Price, R. H., J. R. Connolly, and K. Keil, 1987. Petrologic and Mechanical Properties of Outcrop Samples of the Welded, Devitrified Topopah Spring Member of the Paintbrush Tuff, SAND86-1131, Sandia National Laboratories, Albuquerque, N. Mex.

Pruess, K., Y. W. Tsang, and J. S. Y. Wang, 1984. Numerical Studies of Fluid and Heat Flow Near High-Level Nuclear Waste Packages Emplaced in Partially Saturated Fractured Tuff, LBL-18552, Lawrence Berkeley Laboratory, Berkeley, Calif.

Richardson, A. M., W. Hustrulid, S. Brown, and W. Ubbes, 1985. "In-Situ Load-Deformation Characterization of the CSM/OCRD Jointed Test Block," in Proceedings of the 26th U.S. Symposium on Rock Mechanics, Rapid City, S.D., June 26-28, 1985, pp. 777-784.

Rocha, M., 1970. "New Techniques in Deformability Testing of In Situ Rock Masses," Determination of the In-Situ Modulus of Deformation of Rock, ASTM, ASTM STP 477, American Society for Testing and Materials, Philadelphia, Penn., pp. 39-57.

Scott, R. B. and M. Castellanos, 1984. Stratigraphic and Structural Relations of Volcanic Rocks in Drill Holes USW GU-3 and USW G-3, Yucca Mountain, Nye County, Nevada, USGS-OFR-84-491, Open-File Report, U.S. Geological Survey.

Shimamoto, T., and J. M. Logan, 1981. "Effects of Simulated Clay Gouges on the Sliding Behavior of Tennessee Sandstone," Tectonophysics, Vol. 75, pp. 243-255.

Smith, C., W. C. Vollendorf, and W. E. Warren, 1981. In-Situ Stress from Hydraulic Fracture Measurements in G-Tunnel, Nevada Test Site, SAND80-1138, Sandia National Laboratories, Albuquerque, N. Mex.

Somerton, W. H., 1982. "Porous Rock-Fluid Systems at Elevated Temperatures and Pressures," Recent Trends in Hydrogeology, T. N. Narasimhan (ed.), Geological Society of America Special Paper 189, pp. 183-197.

Spengler, R. W., and M. P. Chornack, 1984. Stratigraphic and Structural Characteristics of Volcanic Rocks in Core Hole USW G-4, Yucca Mountain, Nye County, Nevada, with a section on geophysical logs by D. C. Muller and J. E. Kibler, USGS-OFR-84-789, Open-File Report, U.S. Geological Survey.

Springer, J. E., R. K. Thorpe, and H. L. McKague, 1984. Borehole Elongation and Its Relation to Tectonic Stress at the Nevada Test Site, UCRL-53528, Lawrence Livermore National Laboratory, Livermore, Calif.

Stock, J. M., J. H. Healy, and S. H. Hickman, 1984. Report on Televiewer Log and Stress Measurements in Core Hole USW G-2, Nevada Test Site, October-November 1982, USGS-OFR-84-172, U.S. Geological Survey.

Stock, J. M., J. H. Healy, S. H. Hickman, and M. D. Zoback, 1985. "Hydraulic Fracturing Stress Measurements at Yucca Mountain, Nevada, and Relationship to the Regional Stress Field," Journal of Geophysical Research, Vol. 90, No. B10, pp. 8691-8706.

Sun, Z., C. Gerrard, and O. Stephansson, 1985. "Rock Joint Compliance Tests for Compression and Shear Loads," International Journal of Rock Mechanics, Mining Science, and Geomechanical Abstracts, Vol. 22, No. 4, pp. 197-213.

Svanholm, B. O., P. A. Persson, and B. Larsson, 1977. "Smooth Blasting for Reliable Underground Openings," in Proceedings of the First International Symposium Storage in Excavated Rock Caverns, Stockholm, 5-8 September 1977, M. Bergman (ed.), Vol. 3, Pergamon Press, New York, pp. 573-579.

Swolfs, H. S., and W. Z. Savage, 1985. "Topography, Stresses, and Stability at Yucca Mountain, Nevada," in Proceedings of the 26th Symposium on Rock Mechanics, Rapid City, South Dakota, 26-28 June, 1985, pp. 1121-1129.

Teufel, L. W., 1981. Frictional Properties of Jointed Welded Tuff, SAND81-0212, Sandia National Laboratories, Albuquerque, N. Mex.

Teufel, L. W., and J. M. Logan, 1978. "Effect of Displacement Rate on the Real Area of Contact and Temperatures Generated during Frictional Sliding of Tennessee Sandstone," Pageoph (Pure and Applied Geophysics), Vol. 116, pp. 840-865.

Thomas, R. K., 1982. A Continuum Description for Jointed Media, SAND81-2615, Sandia National Laboratories, Albuquerque, N. Mex.

Tibbs, H., 1985. Letter from H. Tibbs (F&S) to J. J. D'Lugosz (DOE/NVO), September 23, 1985; regarding mining experience through faulted welded tuff beds in U12G Tunnel "Rock Mechanics" drift.

Tillerson, J. R., and F. B. Nimick, 1984. Geoengineering Properties of Potential Repository Units at Yucca Mountain, Southern Nevada, SAND84-0221, Sandia National Laboratories, Albuquerque, N. Mex.

Tyler, L. D., and W. C. Vollendorf, 1975. Physical Observations and Mapping of Cracks Resulting from Hydraulic Fracturing In Situ Stress Measurements, Paper SPE-5542, Society of Petroleum Engineers of American Institute of Mechanical Engineers, Dallas, Tex.

USGS (U.S. Geological Survey) (comp.), 1984. A Summary of Geologic Studies through January 1, 1983, of a Potential High-Level Radioactive Waste Repository Site at Yucca Mountain, Southern Nye County, Nevada, USGS-OFR-84-792, Open-File Report, U.S. Geological Survey.

Van Buskirk, R., D. Enniss, and J. Schutz, 1985. "Measurement of Thermal Conductivity and Thermal Expansion at Elevated Temperatures and Pressures," Measurement of Rock Properties at Elevated Pressures and Temperatures, H. J. Pincus and E. R. Hoskins (eds.), ASTM STP 869, American Society for Testing and Materials, Philadelphia, Penn., pp. 108-127.

Warpinski, N. R., D. A. Northrop, R. A. Schmidt, W. C. Vollendorf, and S. J. Finley, 1981. The Formation Interface Fracturing Experiment: An In Situ Investigation of Hydraulic Fracture Behavior Near a Material Property Interface, SAND81-0938, Sandia National Laboratories, Albuquerque, N. Mex.

Waters, A. C., and P. R. Carroll (eds.) 1981. Preliminary Stratigraphic and Petrologic Characterization of Core Samples from USW-G1, Yucca Mountain, Nevada, LA-8840-MS, Los Alamos National Laboratory, Los Alamos, N. Mex.

Zimmerman, R. M., 1983. "First Phase of Small Diameter Heater Experiments in Tuff," in Proceedings of the 24th U.S. Symposium on Rock Mechanics, June 1983, pp. 271-282.

Zimmerman, R. M., and W. C. Vollendorf, 1982. Geotechnical Field Measurements, G-Tunnel, Nevada Test Site, SAND81-1971, Sandia National Laboratories, Albuquerque, N. Mex.

Zimmerman, R. M., M. P. Board, E. L. Hardin, and M. D. Voegele, 1984a. "Ambient Temperature Testing of the G-Tunnel Heated Block," in Proceedings of the 25th U.S. Rock Mechanics Symposium, Northwest University, Evanston, Ill., June 25-27, 1984, Society of Mining Engineers, New York, pp. 281-295.

Zimmerman, R. M., F. B. Nimick, and M. P. Board, 1984b. "Geoengineering Characterization of Welded Tuffs from Laboratory and Field Investigations," in Proceedings of the Material Resources Society Annual Meeting, Boston, Massachusetts, November, 1984.

Zimmerman, R. M., M. L. Wilson, M. P. Board, M. E. Hall, and R. L. Schuch, 1985. "Thermal Cycle Testing of the G-Tunnel Heated Block," in Proceedings of the 26th U.S. Symposium on Rock Mechanics, Rapid City, South Dakota, E. Ashworth (ed.), A. A. Balkema, Boston, Mass., pp. 749-758.

Zimmerman, R. M., R. L. Schuch, D. S. Mason, M. L. Wilson, M. E. Hall, M. P. Board, R. P. Bellman, M. L. Blanford, 1986. Final Report: G-Tunnel Heated Block Experiment, SAND84-2620, Sandia National Laboratories, Albuquerque, N. Mex.

Zoback, M. L., and M. D. Zoback, 1980. "State of Stress in the Conterminous United States," Journal of Geophysical Research, Vol. 85, No. B11, pp. 6113-6156.

CODES AND REGULATIONS

10 CFR Part 60 (Code of Federal Regulations), 1987. Title 10, "Energy," Part 60, "Disposal of High-Level Radioactive Wastes in Geologic Repositories," U.S. Government Printing Office, Washington, D.C., pp. 627-658.